

Oceans of Opportunity

**56th Annual Meeting
Radiation Research Society**

**September 25–29, 2010
Grand Wailea Resort Hotel and Spa
Maui, Hawaii**



Saturday September 25, 2010	Sunday September 26, 2010	ROOM	Monday September 27, 2010	ROOM	Tuesday September 28, 2010	ROOM	Wednesday September 29, 2010	ROOM
	8:00am - 8:50am Topical Reviews		8:00am - 8:50am Topical Reviews		8:00am - 8:50am Topical Reviews		8:00am - 8:50am Topical Reviews	
	TR1 Wendy Pogozelski- The Outsider's Guide to Understanding Radiation- Induced Damage to DNA	H5	TR5 Doug Boreham - Biological Responses to Low Dose Exposures from Natural, Medical and Occupational Sources	H4	TR9 Elaine Ron - Radiation epidemiology: from case series to global population studies	H4	TR13 Simon Powell - synthetic lethality and repair targeting	H2
	TR2 - Jackie Williams (chair) Meet the Federal Agencies - A Quick Guide to Open Federal Funding Mechanisms	H2	TR6 Takeo Ohnishi - Space Radiation Effects in ISS-Space Experiment of "RadGene"	H5	TR10 Herwig Paretzke - ICRU update - The relevance to radiation research	H5	TR14 Richard Wagner - Low energy electron induced DNA damage: from product analysis to possible mechanisms	H4
	TR3 Marianne Koritzinsky- Mechanisms of adaptation to hypoxia and their relevance in cancer	H3	TR7 Fiona Stewart - Late radiation damage in normal tissues; pathogenesis and strategies for intervention	H2	TR11 Hooshang Nikjoo - Radiation track, DNA damage-repair, and risk from low doses of radiation	H3	TR15 Wendy Kuhne - radio-ecology	PIK2
	TR4 Grigory Dianov - The Role of Phosphorylation and Ubiquitination of DNA Repair Enzymes in the Cellular Resistance to Radiation	H4	TR8 Dennis Hallahan - Radiation guided drug delivery systems	H3	TR12 Sandra Demaria - Effects of radiation on the interactions between immune system and normal or neoplastic self tissues	H2	TR16 Stratford - Targeted drugs with radiation. What is needed to get these agents into clinical trials?	H3
	9:00am - 10:00am Plenary Lecture	H1	9:00am - 10:00am Plenary Lecture	H1	9:00am - 10:00am Plenary Lecture	H1	9:00am - 10:00am SIT Plenary Lecture:	H1
	P1 Alan Balmain-Cancer Complexity: insights from Systems analysis of tumour susceptibility		P2 Tom Tullius - A radical perspective on the role of DNA structure in the functioning of the human genome		P3 Max Wicha - SIT 'What's Hot' (Ann) Clinical implications of the cancer stem cell hypothesis		P4 Penny Jeggo - A journey through DNA double strand break repair in the context of chromatin superstructure	
	10:00-10:15am Coffee Break		10:00-10:15am Coffee Break		10:00-10:15am Coffee Break		10:00-10:15am Coffee Break	
	10:15am - 12:15pm Symposia/Workshops/Mini-Symposium		10:15am - 12:15am Presidential Symposium		10:15am - 12:15pm Symposia/Workshops/Mini-Symposium		10:15am - 12:15pm Symposia/Workshops/Mini-Symposium	
SIT WORKSHOP 7:30am - 5:00pm	S1 Effects of ionizing radiation on nucleic acids: inspiration for analytical and mechanistic investigations Marc Greenberg and Paul Black	LIL	S7 President's Symposium Ionizing Particles in Space and Medicine Kathy Held	H1	RRS History Committee Presentation Pioneers of the Radiation Sciences: Historical Review By Bill Osborne Introduction by Eleanor Blakely	LIL	S13 Bridging the gap between track structure and stable end products Jay LaVerne and Ianik Plante	PIK2
	S2 The Role of MicroRNA in Radiosensitivity and Human Cancer Tom Hei and Nicole Simone	H2			S11 Radiation treatment factors: effects on immune and normal tissue responses Sandra Demaria and Jackie Williams	H2	S14 Risk from in utero radiation exposure Evan Douple and John Boice	H3
	S3 Limoli - Stem cells at the crossroads of basic and translational radiobiology Charlie Limoli and Frank Pajonk	H3			S12 Missing Links and New Pathways in DNA Double-Strand Break Repair Yoshihisa Matsumoto and Susan Lees-Miller	H3	S15 Telomeres and double-strand breaks: which end's which? Susan Bailey and John Murnane	H2
	MS1 Part I Experimental therapeutics and translational research	H4			MS5 Bystander effects/Epidemiology	H4	S16 Low dose radiobiology: the cross talk between adaptive responses, bystander effects and genomic instability Ed Azzam and Giuseppe Schettino	H1
	MS2 Mutagenesis / clastogenesis / carcinogenesis / stem cells	H5			MS6 Physico-chemical events / Radiation protection- Biodosimetry	H5	MS7 Radiation protection - protection, mitgators and treatment	H4
	12:15pm - 2:00pm Lunch Break		12:15pm - 2:00pm Business Meeting w/lunch on own	H1	12:15pm Free Afternoon		12:15pm - 2:00pm SIT Luncheon	H5
	2:00pm - 2:45pm Poster Session		2:00pm - 2:45pm Poster Session				2:00pm - 2:45pm Poster Session	
	PS1 Radiation protection - protection/mitgators/treatment		PS3 Physico-chemical events stem cells radiation protection - biodosimetry				PS5 Mutagenesis/clastogenesis/carcinogenesis Bystander effects/adaptive response Epidemiology	
	2:45pm - 3:30pm Poster Session		2:45pm - 3:30pm Poster Session					
	PS2 DNA damage induction, repair and DNA damage response		PS4 Cell and tissue kinetics / signaling / microenvironment					
	3:30pm - 5:30pm Symposia/Workshops/Mini-Symposium		3:30pm - 5:30pm Symposia/Workshops/Mini-Symposium				3:30pm - 5:30pm Symposia/Workshops/Mini-Symposium	
	S4 Heavy ions in space radiation and hadron therapy Michael Dingfelder and Zi-Wei Lin	LIL	S8 Elementary processes in DNA damage formation William Berhard and Amitava Adhikary	LIL			S17 Update: Auger emitters in Medicine and Biology Roger Martin and Katherine Vallis	PIK2
	S5 The Tumour Microenvironment: Exploiting Pathways for Targeted Therapies Robert Bristow and Ester Hammond	H2	S9 Dosimetry for radiation emergency Hal Swartz and Narayani Ramakrishnan	H5			S18 Novel High Throughput Screening to Identify Radiation Response Modulators for Mechanistic Understanding and Translational Application Howard Lieberman and Bill Morgan	H1
	S6 Studies of radiation susceptibility to cancer: where do we stand? Alice Sigurdson and Sally Admunson	H3	S10 When is low dose-rate radiation harmful to health? Pam Sykes and Ron Mitchel	H4			S19 A role of chromatin reorganization in genome stability after IR exposure Tsuyoshi Ikura and Satoshi Tashiro	H2
	WS1 Markers and Prevention of Radiotherapy-Induced Second Cancers Don Jones and David Brenner	H4	WS2 SIT Debate Moderator Andreea Simons-Burnett Hypo-fractionation: the available radiobiological models are adequate in predicting acute and late effects	H2			MS8 Part II Experimental therapeutics and translational research	H3
	MS3 DNA damage induction, repair and the DNA damage response	H5	MS4 High LET / space radiation effects / dose rate effects	H3			MS9 Cell and tissue kinetics/signaling/microenvironment	H4
	5:30-5:45pm Coffee Break		5:30-5:45pm Coffee Break				4:45pm - 6:15pm Poster Sessions with Reception	
							4:45pm - 5:30pm PS6 high LET/space radiation effects/dose rate effects	
REGISTRATION HOURS: SIT ONLY Sat: 7:00am-11:00am EARLY REG Sat: 3:00-7:00pm Sunday: 7:00am-6:00pm Monday: 7:00am-5:00pm Tuesday: 7:00am-12:15pm Wednesday: 7:00am-5:00pm	5:45pm - 6:45pm Failla Lecture James Mitchell (NIH, Bethesda) Introduction by Kathy Held	H1	5:45pm - 6:10pm Michael Fry Research Award David Kirsh (Duke University Medical Center) Introduction by Kathy Held	H1			5:30pm - 6:15pm PS7 Experimental therapeutics and translational research	
			6:10pm - 6:30pm Marie Curie Award Shichuan Zhang Introduction by Kathy Held	H1			6:15pm END OF MEETING	
6:30-8:30pm SIT Reception Tsunami	7:00pm-8:30pm Failla and Welcoming Reception Molokini Gardens		Evening on Own				7:00 pm Optional Closing Banquet Featuring a Hawaiian Luau	

Abstracts



**56th Annual Meeting
of the
Radiation Research Society**

**Grand Wailea Resort Hotel and Spa
Maui, Hawaii**

September 25th–September 29th, 2010

Failla Lecture

(AL01) Chasing free radicals in cells and tissues. James B. Mitchell, National Cancer Institute, Bethesda, MD

In the context of ionizing radiation, it has long been known that free radicals, which exist over a very brief time scale, set into motion a series of events that may lead to cell killing, mutation, and untoward normal tissue effects (acute and late). Interestingly, from research conducted over the past 2-3 decades, it has become apparent that even under normal circumstances cells and tissues must cope with free radicals. Oxidative stress imposed by free radicals and reactive oxygen species have been identified in a number of normal processes including intracellular oxygen metabolism, immune-mediated attack of pathogens, inflammatory responses, signal transduction/gene expression pathways, as well as being present and contributing to an ever-increasing number of human pathological conditions. A central theme of our research has been to better understand how cells and tissues cope with oxidative stress and how these responses can be modulated with the goal of translating our findings into clinical trials for cancer patients. Various attempts to enhance tumor cell radiosensitivity or to protect normal tissue damage will be discussed along with our experiences with a unique class of compounds called nitroxides. Nitroxides possess antioxidant and radiation protective properties, despite the fact that they are paradoxically stable free radicals. Nitroxides have become useful reagents to elucidate free radical mechanisms in biological systems. A number of practical and potentially therapeutic applications of nitroxides have emerged encompassing ischemia/reperfusion injury, obesity, neurodegenerative disorders, and cancer chemo-preventive agents. Because nitroxides are paramagnetic, they can also be used to interrogate the redox status of tissue using MRI. Application of other free radical spin probes makes it now possible to non-invasively assess tissue oxygen concentration. In this lecture I hope to highlight the thrill of the chase.

Michael Fry Lecture

(AL02) Using Genetically Engineered Mice for Radiation Research. David G. Kirsch, Duke University Medical Center, Durham, NC

The laboratory mouse has been utilized for many decades as a model system for radiation research. Recent advances in genetic engineering allow scientists to delete genes in specific cell types at different stages of development. The ability to manipulate genes in the mouse with spatial and temporal control opens new opportunities to investigate the role of genes in regulating the response of normal tissues and tumors to radiation. We are using the Cre-loxP system to delete genes, such as p53, in a cell-type specific manner in mice to study mechanisms of acute radiation injury and late effects

of radiation. As a complimentary approach, we are utilizing in vivo shRNA to reversibly knock down p53 to study radiation biology. Our results demonstrate that p53 is required in the GI epithelium to prevent the radiation-induced gastrointestinal (GI) syndrome and in endothelial cells to prevent late effects of radiation. We have also used these genetic tools to generate primary tumors in mice to study tumor response to radiation therapy. These advances in genetic engineering provide a powerful model system to dissect mechanisms of normal tissue injury and tumor cure by radiation.

Marie Curie Lecture

(AL03) Disabled DNA-PKcs phosphorylation impairs genomic stability in mice. Shichuan Zhang¹, Hirihiko Yajima¹, HoangDinh Huynh¹, Junke Zheng¹, Yu-Fen Lin¹, Elsa Callen², Hua-Tang Chen², Andre Nussenzweig², Cheng Cheng Zhang¹, David J. Chen¹, Benjamin Chen¹, ¹UT Southwestern Medical Center, Dallas, TX, ²National Cancer Institute, National Institutes of Health, Bethesda, MD

The catalytic subunit of DNA dependent kinase (DNA-PKcs) is well known for its role in DNA double strand break repair. In addition to its kinase activity, phosphorylation of DNA-PKcs is also indispensable for its proper functioning. We have previously shown that phosphorylation at the Thr2609 cluster (mouse equivalent Thr2605) is critical for DNA double strand break repair and this phosphorylation is mediated by ataxia telangiectasia mutated (ATM) and ATM and Rad3-related (ATR). To further understand the importance of phosphorylation of DNA-PKcs in DNA damage response, we generated mice carrying DNA-PKcs with three alanine substitutions at Thr2605, Thr2634, and Thr2643 in the Thr2605 cluster (3A mutant). Several lines of evidence from this newly-established mouse model strongly suggest an important role for DNA-PKcs in maintenance of genomic integrity. First, mouse embryonic fibroblast derived from homozygotic mice showed high sensitivity toward both ionizing radiation and DNA crosslinking reagents. Profound chromosome aberrations were observed in these cells after DNA-damage treatment. Second and most interesting, in sharp contrast to the normal life span of DNA-PKcs knockout mice, all homozygotic 3A mutant mice died of hematopoietic stem cell (HSC) failure at a premature age. Importantly, loss of HSCs happens between embryonic day 12.5 and 16.5 when HSCs are fast cycling, suggesting a pivotal role of DNA-PKcs phosphorylation in replication associated stress response for stem/progenitor cells. In addition to early and acute loss of HSCs, mice surviving anemia by bone marrow transplantation developed varied kinds of tumors including lymphoma, skin cancer, and breast cancer. The high tumor incidence and broad spectrum of tumor type suggested that phosphorylation of the Thr2609 cluster is critical in modulating DNA repair pathways and thus maintaining the mammalian genome.

CANCER COMPLEXITY: INSIGHTS FROM SYSTEMS ANALYSIS OF TUMOUR SUSCEPTIBILITY

(P001) Cancer Complexity: insights from systems analysis of tumour susceptibility. Alan Balmain, UCSF Helen Diller Family Comprehensive Cancer Center, San Francisco, CA

Quantitative genetics has identified polymorphisms within gene regulatory factors or their target genes which cause variation in phenotypes, such as inflammation and obesity, or responses to exogenous perturbation by carcinogens or radiation. Expression levels of individual genes can also be regarded as “phenotypes” under genetic control, some of which may influence susceptibility to cancers induced by environmental agents. Applying expression Quantitative Trait Locus (eQTL) approaches to mouse strains with differing susceptibility to diseases, such as obesity and cancer, has identified signaling hubs that may be important targets for drug development. We used network construction methods to analyze the genetic architecture of gene expression in normal mouse skin in a cross between tumor-susceptible *Mus musculus* and tumor-resistant *Mus spretus*. The data showed that gene expression motifs representing different constituent cell types within the skin such as hair follicle cells, haematopoietic cells, and melanocytes are under separate genetic control. Motifs associated with inflammation, epidermal barrier function, cell cycle control and proliferation are differentially regulated in mice susceptible or resistant to tumor development. The intestinal stem cell marker *Lgr5* is identified as a candidate master regulator of hair follicle gene expression, and the Vitamin D receptor (*Vdr*) links epidermal barrier function, inflammation, and tumor susceptibility. These gene expression networks undergo substantial rewiring during development of benign and malignant skin tumors. Motifs associated with inflammation may play a protective role in normal skin, but a promoting role in tumors themselves. This combination of genetics and gene expression approaches offers substantially greater power than classical methods for identification of genetic factors that contribute to cancer susceptibility and progression. Application of these approaches to radiation induced cancers in mouse models may identify the specific combinations of factors that contribute to radiation damage and tumor development.

A RADICAL PERSPECTIVE ON THE ROLE OF DNA STRUCTURE IN THE FUNCTIONING OF THE HUMAN GENOME

(P002) A radical perspective on the role of DNA structure in the functioning of the human genome. Tom Tullius, Boston University, Boston, MA

The hydroxyl radical is a key product of the interaction of ionizing radiation with water. Labs around the world have revealed the many deleterious effects of the hydroxyl radical on biological molecules. In this lecture I will describe how my laboratory has chosen to take the opposite tack, by exploiting the chemistry of the hydroxyl radical as a high-resolution chemical probe of DNA structure. Our early work focused on studies of purified DNA. We showed that the extent of hydroxyl radical-induced cleavage of DNA at a particular nucleotide depends sensitively on the solvent-accessible surface area of the deoxyribose, thus providing a chemistry-based map of the shape of DNA at single-nucleotide resolution. With the revolution in genomics that came with the sequencing of the human genome, my lab has turned to investigate how the molecular shape of DNA contributes to genome function. The basic idea is that DNA is not merely a string of letters, as it is invariably represented in genomics studies. DNA is a molecule, and its shape varies with nucleotide sequence. My lab has produced a database of DNA cleavage patterns (ORChID), and used this database to develop an algorithm to predict the hydroxyl radical cleavage pattern at high accuracy for any DNA sequence (including the 3 billion base pairs in the human genome). Recent work by several labs has uncovered a new mode for recognition of DNA by proteins that depends on DNA shape, and not strictly on nucleotide sequence. We have used ORChID to demonstrate that DNA shape is under evolutionary selection, a fundamentally new way to understand how information is encoded in the human genome. I also will describe new work from my lab that uses next-generation DNA sequencing to map the extent of

radiation-induced single-strand breaks at every nucleotide in the yeast genome. We thus have come full circle, to study the damaging effects of radiation-produced hydroxyl radical on an entire genome.

CLINICAL IMPLICATIONS OF THE CANCER STEM CELL HYPOTHESIS

(P003) Clinical implications of the cancer stem cell hypothesis. Max S. Wicha, University of Michigan Comprehensive Cancer Center, Ann Arbor, MI

There is accumulating evidence that many cancers are organized in a hierarchical fashion in which a cellular sub component displaying stem cell properties drives tumorigenesis. These stem cell properties include self renewal which drives tumorigenesis and differentiation which generates cellular heterogeneity. Cancer stem cells were first described in human leukemias and more recently in a variety of solid malignancies. These cancer stem cells have been shown to be relatively resistant to both radiation and chemotherapy. A number of mechanisms have been proposed to account for the relative radio resistance of a cancer stem cells. These include more efficient DNA repair, lower level of oxidants and changes in cell cycle kinetics. In addition cancer stem cells may express increased levels of anti apoptotic proteins. These mechanisms may also account for chemotherapy resistance. In addition cancer stem cells express increased levels of cellular transporters and metabolizing enzymes which may also contribute to their chemotherapy resistance. Both in vitro and mouse studies suggest that stem cells mediate a tumor invasion and metastasis. Since these cells contribute to treatment resistance and relapse, effective targeting of this cell population may be required to improve patient outcome.

A JOURNEY THROUGH DNA DOUBLE STRAND BREAK REPAIR IN THE CONTEXT OF CHROMATIN SUPERSTRUCTURE

(P004) A journey through DNA double strand break repair in the context of chromatin superstructure. Penny Jeggo¹, Aaron Goodarzi¹, Atsushi Shibata¹, Andrea Beucher², Markus Lobrich², ¹Genome Damage and Stability Centre, University of Sussex, East Sussex, United Kingdom, ²Darmstadt University of Technology, Radiation Biology and DNA Repair, Darmstadt, Germany

Studies on DNA double strand break (DSB) repair over many years have shown that ~ 85 % of X-ray induced DSBs are repaired with fast kinetics whilst 15 % are repaired more slowly. The slow DSB repair component in G1 phase represents the repair of DSBs located within heterochromatic DNA (HC-DNA DSBs) via a process involving ATM and the mediator proteins, H2AX, MRN, MDC1, RNF8, RNF168 and 53BP1. These and additional findings show that heterochromatin is a barrier to DSB repair. ATM's role in HC-DSB repair is to phosphorylate the heterochromatic protein, KAP-1, which causes local HC-DNA relaxation. The mediator hierarchy is required to localise 53BP1 at the site of the DSB. Via an interaction between 53BP1 and MRN, 53BP1 tethers ATM at the DSB, generating defined ATM foci. ATM-dependent KAP-1 phosphorylation occurs in a pan-nuclear manner and is 53BP1-independent, consistent with the notion that ATM activation is mediator-protein independent. Pan-nuclear KAP1 phosphorylation, however, rapidly dissipates after lower doses of radiation, allowing defined p-KAP1 foci to be visualised. p-KAP1 foci form uniquely at HC-DNA DSBs and, in contrast to pan-nuclear KAP1 phosphorylation, require 53BP1 and the downstream mediator proteins. We suggest that localised, concentrated p-KAP1 formation at HC-DSBs is required for efficient chromatin relaxation to allow repair at these DSBs. In G2, DSBs are also repaired with fast and slow kinetics. Fast DSB repair occurs by NHEJ as in G1 phase but the slow DSB repair process represents HR and requires BRCA2, RAD51 and CtIP-dependent resection. Importantly, this process also requires ATM and the nuclease Artemis. Moreover, DNA end-resection, the first step in HR, is substantially diminished, although not abolished in cells lacking ATM or Artemis. Thus, ATM and Artemis promote a form of NHEJ in G1 phase but HR in G2 phase. These findings suggest that HR predominantly repairs DSBs at HC-DNA in G2 phase whilst the majority of DSBs are repaired by NHEJ. Our current findings on the regulation of DSB repair pathway choice in G2 phase will be discussed.

THE OUTSIDER'S GUIDE TO UNDERSTANDING RADIATION INDUCED DAMAGE TO DNA

(TR001) The outsider's guide to understanding radiation induced damage to DNA. Wendy K. Pogozelski, State University of New York at Geneseo, Geneseo, NY

This talk is an overview of what is known about how radiation causes chemical changes to the sugars and bases of DNA. It is designed with the non-chemist in mind. It will include a historical background of the methods used to determine radiation-induced damage as well as a discussion of the significance of the various damage pathways.

MEET THE FEDERAL AGENCIES - A QUICK GUIDE TO OPEN FEDERAL FUNDING MECHANISMS

(TR002) Meet the federal agencies – a quick guide to open federal funding mechanisms. Chair Jacky P. Williams, James P. Wilmot Cancer Center, Rochester, NY

In the past few years, following the events of 9/11, the field of radiation research in the United States and elsewhere has found itself returning to an old "emphasis", namely that of developing real-time dosimetry and countermeasures targeted at nuclear or radiological events. Grant opportunities for such work are being made available through agencies with which we, as radiation scientists, have had little to no former contact. In addition, there have been substantial changes in the application and review system at the NIH. In order to provide RRS membership with the most up-to-date information on grant application processes, as well as promoting communication between the society members and both the "new" and "old" funding agencies, we are providing a forum in which members can meet with, hear from, and talk to representatives from NIAID and BARDA, as well as NIH, NASA and DOE.

MECHANISMS OF ADAPTATION TO HYPOXIA AND THEIR RELEVANCE IN CANCER

(TR003) Mechanisms of adaptation to hypoxia and their relevance in cancer. Marianne Koritzinsky, Ontario Cancer Institute, Toronto, ON, Canada

Human tumors are characterized by low levels of oxygen (hypoxia), which predicts for poor outcome. Cancer cells can tolerate the hostile tumor microenvironment due to two mechanisms; selection of cells with mutations that confer low sensitivity to death initiation (e.g. p53 mutations) and activation of adaptive biological responses. These responses include stabilization of the HIF family of transcription factors, inhibition of signaling through the mTOR pathway and activation of the unfolded protein response (UPR). Many common genetic alterations in cancer also affect these hypoxia response pathways, typically resulting in increased HIF expression and constitutive activation of mTOR signaling. Several of the biologically targeted agents that are emerging as novel cancer therapeutics hence influence the biological responses to hypoxia, which in consequence may lead to changes in the tumor microenvironment and responses to radiation.

THE ROLE OF PHOSPHORYLATION AND UBIQUITINATION OF DNA REPAIR ENZYMES IN THE CELLULAR RESISTANCE TO RADIATION

(TR004) The Role of Phosphorylation and Ubiquitination of DNA Repair Enzymes in the Cellular Resistance to Radiation. Grigory L. Dianov, Gray Institute for Radiation Oncology and Biology, Oxford, United Kingdom

Base excision repair (BER) is a frontline DNA repair system that is responsible for maintaining genome integrity, thus preventing

premature aging and cancer, by repairing DNA base lesions and single strand breaks caused by endogenous and exogenous mutagens. It is also the principal DNA repair system in cancer cells that counteracts the killing effect of the major cancer treatments e.g. chemotherapy (alkylating agents) and ionizing radiation (about 80 % of DNA damage induced by ionizing radiation are base lesions) and changes in BER most probably are responsible for many cases of cancer sensitivity or resistance to radiation. Although it is clear that an individual's BER capacity varies, the mechanism involved in regulation of BER and that which is responsible for such variations is still unknown. This significant gap in scientific knowledge is impeding both the discovery of new cancer therapy targets and the development of novel cancer treatment strategies. We have investigated the cellular mechanism regulating the levels of BER enzymes and found that the stability of BER enzymes in mammalian cells is linked to and controlled by the level of DNA lesions. We demonstrated that the stability of BER enzymes increases after formation of a repair complex on damaged DNA. We also found that the proteins which are not involved in a repair complex are polyubiquitinated by the E3 ubiquitin ligases and subsequently rapidly degraded by the proteasome and in several cases this process is controlled by phosphorylation status of the DNA repair protein. In contrast, we demonstrated that deubiquitination of DNA repair proteins is able to inhibit their degradation by the proteasome and thus elevate protein levels in response to DNA damage. I will discuss a novel dynamic model for the regulation of the steady state levels of BER enzymes and the role of posttranslational modifications in this process.

BIOLOGICAL RESPONSES TO LOW DOSE EXPOSURES FROM NATURAL, MEDICAL AND OCCUPATIONAL SOURCES

(TR005) Biological Responses to Low Dose Exposures from Natural, Medical and Occupational Sources. Douglas Boreham, McMaster University, Hamilton, ON, Canada

Humans have always been and will continue to be exposed to ionizing radiation from natural background radiation. In addition to natural radiation, man-made sources are now becoming prominent and include medical exposures from diagnostic and therapeutic procedures, and from occupational exposures. This topical review will summarize the types of natural and manmade sources of radiation exposure. Radiation quality, magnitude of doses, and dose rates will be discussed. The biological responses to the various exposure scenarios will be reviewed. Epidemiological evidence for low dose risk will be presented and laboratory studies investigating cellular mechanisms induced by low dose exposures will be addressed. An emphasis on medical radiation exposures will be presented given the current issues surrounding increased usage and occasional over-exposure of humans in the clinic. Cancer risk from low dose radiation exposure remains the primary concern and cancer-risk modification by low dose exposure will be reviewed. Finally, non-cancer endpoints influenced by low doses of ionizing radiation will be summarized. This talk is intended to give participants a better understanding of our current knowledge of low dose radiation and human health.

SPACE RADIATION EFFECTS IN ISS-SPACE EXPERIMENT OF "RADGENE"

(TR006) Space Radiation Effects in ISS-Space Experiment of "RadGene". Takeo Ohnishi, Nara Medical University School of Medicine, Nara, Japan

The space environment contains two major biologically significant influences of microgravity and space radiations at low dose with low dose-rate containing high linear energy transfer particles. (1) To identify DNA damage induced by space radiations, phospho-H2AX (γ H2AX) foci formation was analyzed in two human cultured lymphoblastoid cell lines of TSCE5 (a wild-type p53 gene) and WTK1 (a mutated p53 gene) frozen in a freezer of

International Space Station (ISS) for 133 days. Here, we show a track of the positive foci in them by immuno-cytochemical methods. We compared doses of space radiations between biological dosimetry by these frequencies and physical dosimetry by CR-39 and TLD. (2) To clarify the biological effects of space radiations and microgravity, gene and protein expression was analyzed from *p53*-dependent regulated manner by using DNA chips and protein chips, respectively. Under 1 gravity or microgravity condition, the cells were grown in a cell biology experimental facility of ISS for 8 days without the stresses during launching and landing. In addition, we analyzed the gene expression in the cells cultured on ground after space flight for 133 days with frozen condition. We report the results and discussion from the functions of the up-regulated and down-regulated genes after an exposure to space radiations and/or microgravity. (3) To clear the effect of space radiations on the radio-adaptive response, the cells kept at frozen state for 133 days in space were cultured for 6 h, and then exposed to challenging X-ray at 1.2 Gy or 2 Gy after landing. Cellular sensitivity, apoptosis, chromosome aberrations and mutation frequencies were scored. All of these radio-adaptive responses were found in *wtp53* cells, but not in the *mp53* cells. These results confirmed that the cells were exposed to space radiations with the specific low dose range (window; 20-100 mSv) which can lead to an adaptive response on ground-base experiments. The initial goal of "Rad Gene" space experiment was completely achieved. It is expected that data are useful in designing physical protection from the deleterious effects of space radiations during long term stays in space.

LATE RADIATION DAMAGE IN NORMAL TISSUES; PATHOGENESIS AND STRATEGIES FOR INTERVENTION

(TR007) Late radiation damage in normal tissues; pathogenesis and strategies for intervention. Fiona A. Stewart, The Netherlands Cancer Institute, Amsterdam, Netherlands

Earlier diagnosis and better treatment options have led to improvements in cancer specific survival for many tumor types, but this also results in an increased number of patients at risk for treatment related side effects. It is widely recognized that vascular damage is one of the major underlying causes of late radiation injury. In small vessels early endothelial cell (EC) damage initiates inflammatory and coagulation cascades which, combined with EC detachment and exposure of the sub-endothelium, leads to vascular leakage, microthrombus formation, vascular occlusion and secondary tissue ischemia. The over- production of inflammatory cytokines, TGF β and thrombin also drive smooth muscle cell proliferation and collagen production in fibroblasts, resulting in fibrosis. In large vessels, monocytes adhere to the damaged, irradiated endothelium and transmigrate into the intima. In the presence of high cholesterol, invading monocytes transform into activated macrophages (foam cells), which ingest lipids and form fatty streaks in the intima, thereby initiating the process of atherosclerosis. It has been shown that radiation both accelerates the development of atherosclerosis and predisposes to an inflammatory, thrombotic plaque phenotype, more likely to rupture and cause fatal heart attack or stroke. An increased understanding of the mechanisms whereby radiation vascular injury develops has led to research on strategies to intervene in these processes, to inhibit late radiation injury. These strategies will be discussed.

RADIATION GUIDED DRUG DELIVERY SYSTEMS

(TR008) Radiation guided drug delivery systems. Dennis E. Hallahan, Washington University School of Medicine, St. Louis, MO

Ionizing radiation induces gene expression and the presentation of sequestered proteins which in turn mediate the physiologic response to radiation. These molecular responses have been exploited in several ways to guide or activate drug delivery to cancer. First example is radiation inducible gene therapy which led to TNFerade clinical trials. Secondly, radiation induced receptors are

molecular targets for ligand binding. A proof of concept clinical trial showed radiolabeled peptides binding in irradiated cancers in patients. More recently, preclinical advocacy studies have demonstrated improved tumor control in mouse models of human cancer. These studies show conjugated peptide ligands to drug delivery systems such as Abraxane or Doxil to target chemotherapy to irradiated cancers. Finally, radiation induced neoantigens are induced in cancer during radiotherapy and provide novel antigens for the development of therapeutic antibodies. To discover radiation inducible receptors, we utilized phage-displayed peptide libraries injected into the circulation of mice bearing irradiating tumors. We prioritized a peptide with amino acid sequences HVGSSV and GIRLRG which maintain cancer specific binding when conjugated to drug delivery systems. We conjugated these peptides to nanoparticles and liposomes to guide drug delivery to irradiated cancers. This approach enhanced cancer response to radiation. Moreover, this approach increased the bioavailability of cancer drugs to tumors treated with radiation (2 Gy). To discover radiation inducible antigens, we utilized subtractive immunization. This approach allows us to discover mouse monoclonal antibodies that bind to radiation inducible neoantigens. The prioritized antibodies bind to proteins that translocate to the surface of cancer cells in response to radiation. In particular, antibodies to TIP-1, GRP78 and calreticulin show cancer specific binding to irradiated tumors in mouse models of human cancer. These IgG antibodies activate the Fc receptor on APCs and effector cells to initiate an immune response. Irradiated cancer cells are subsequently phagocytized following antibody binding to radiation inducible antigens. This new field in radiation oncology and radiation biology will be reviewed.

RADIATION EPIDEMIOLOGY: FROM CASE SERIES TO GLOBAL POPULATION STUDIES

(TR009) Radiation epidemiology: from case series to global population studies. Elaine Ron, NCI, NIH, Bethesda, MD

The field of radiation epidemiology aims to characterize and quantify the risk of disease in populations exposed to radiation, alone or in combination with other agents or risk factors. Epidemiologic studies provide human data needed to assess risks from occupational, environmental/accidental and medical radiation exposures. These data are used in formulating protection standards for workers and the general public and addressing issues of public health concerns. They also contribute to the understanding of individual susceptibility, factors that modify risk, and disease processes. In addition, results from epidemiologic studies of diagnostic and therapeutic radiation have led to improvement in clinical practice. Soon after the introduction of x-rays for medical use, excesses of skin cancer and leukemia were observed among highly exposed radiologists. Within a few years, multiple health problems, including bone sarcomas, were noted among radium dial painters. Reports of leukemia among A-bomb survivors, lung cancer among miners, and thyroid cancer among children exposed to medical radiation followed. Since the 1960s, large numbers of epidemiologic studies of human populations with diverse backgrounds and exposure characteristics have demonstrated that radiation can cause most cancers and that risk increases with increasing dose. Contemporary studies are clarifying the carcinogenic effects at low doses and dose rates from a variety of radiation sources, quantifying the risks for individual cancer sites and histological subtypes, describing the age and temporal patterns of risk, and identifying high-risk. Research also is focusing on evaluating radiation-related risks for non-malignant diseases (e.g. cardiovascular disease and cataracts) and understanding the role of genetics in radiation susceptibility. New statistical methods for analyzing pooled data from multiple studies and an emphasis on conducting multi-center international studies with sophisticated dosimetry have improved the ability to detect smaller risks and modifying effects. Better methods being developed for handling uncertainties in dose estimates and incorporating biologic data will further enhance risk quantification. The topical review will provide a brief overview of the history and the substantial advances made in the field of radiation epidemiology, highlight current methodologic issues, summarize major results from epidemiologic research, and note some remaining challenges and opportunities.

ICRU UPDATE - THE RELEVANCE TO RADIATION RESEARCH

(TR010) ICRU activities with relevance to radiation research. Herwig G. Paretzke¹, Leslie A. Braby², Hans Menzel³, ¹Helmholtz-Center Munich, Neuherberg, Germany, ²Texas A&M University, College Station, TX, ³CERN, Geneva, Switzerland

Measurements of and irradiations using ionizing radiations need international harmonization in field specification and reporting; otherwise such reports cannot be interpreted and understood worldwide in the same, correct, and satisfying way. As it is well-known: statement of just a value of the quantity "absorbed dose" is not sufficient for effect quantification. To this purpose the ICRU is e.g. in the status of issuing new recommendations regarding several possible approaches to the quantification and reporting of low dose and other heterogeneous exposures (report committee chairman: Les Braby). These recommendations have possible smaller or larger impacts e.g. on the reporting of radiation biological results, of personal dosimetry in radiation protection, and in radiation therapy, etc. This lecture will give an introduction into these recommendations, explain the underlying philosophy and give several simple, practical examples of how to apply these recommendations properly in these various fields mentioned above.

RADIATION TRACK, DNA DAMAGE-REPAIR, AND RISK FROM LOW DOSES OF RADIATION

(TR011) Radiation track, DNA damage-repair, and risk from low doses of radiation. Hooshang Nikjoo, Peter Girard, Reza Taleei, Thiansin Liamsuwan, Karolinska Institute, Stockholm, Sweden

A premise of research in radiation biology and biophysics is to understand the mechanism and consequences of damage, and quantify the emerging risk involved as a function of dose, dose rate and quality of radiation. After a half century of rapid advances, much information has been accumulated through experimental work, epidemiological studies and genomic knowledge. But there still remains a lack of coherent description of mutagenic processes, pathways to neoplastic changes and cancer induction, and models to quantify accurately risk to humans from acute and protracted exposures. The genomic analysis and reanalysis of human cancers show many genes are involved in most cancers. More than one thousand somatic mutations have been identified in over two hundred cancers. All of these show a complex picture which requires a combination of theoretical predictions and experimental confirmation to get a clearer picture. Traditionally, track structure simulated at molecular level have been applied to scrutinize aspects of radiation damage in biological molecules from a theoretical approach based upon fundamental physical and chemical principles to provide hypotheses which are testable experimentally. To this end track structure has provided a basis for understanding the mechanism of dose effect relationships. In particular it has provided predictions of frequencies of different types of DNA damage in terms of complexity and source of damage which otherwise is not possible to obtain experimentally. This presentation, reviews theoretical and computational approaches to characterize radiation track structure, DNA damage and DNA-repair produced from exposure of cells to radiations of varying qualities.

EFFECTS OF RADIATION ON THE INTERACTIONS BETWEEN IMMUNE SYSTEM AND NORMAL OR NEOPLASTIC SELF TISSUES

(TR012) How irradiated healthy and neoplastic tissues interact with the immune system. Sandra Demaria, New York Univ School Of Medicine, New York, NY

The immune system comprises two main components, innate and adaptive, that serve different functions but are highly inter-dependent. The innate immune system includes cells of the myeloid

(granulocytes, monocytes/macrophages, dendritic cells) and lymphoid lineage (natural killer and natural killer T cells), whereas T and B lymphocytes are the key members of the adaptive immune system. Innate immune cells are the first responders to tissue damage and serve a critical function as interpreters of the nature of the damage. Molecular signals released from damaged and dying cells, and from breakdown of the extracellular matrix are broadly defined as Damage-Associated Molecular Pattern (DAMP) molecules. DAMPs bind to a family of receptors called Toll-Like Receptors (TLR) that are expressed by innate immune cells. TLR signaling determines the response program that will be triggered. For example, radiation-induced tumor cell death is associated with release of the DAMP molecule HMGB-1, which binds to TLR4 and promotes the cross-presentation of tumor-derived antigens by dendritic cells, leading to activation of anti-tumor T cells. Thus, TLR engagement in the presence of additional inflammatory signals will lead to activation of adaptive immunity by innate immune cells, whereas tissue damage that is not perceived as "dangerous" will trigger a repair response, associated with production of anti-inflammatory cytokines. Depending on the dose and regimen of radiation, and on metabolic, genetic and physical parameters, cells that do not die show a range of responses to radiation. These include the upregulation of secreted factors, such as chemokines, that recruit specific subsets of immune cells, effectively altering the microenvironment. In addition, several cell surface receptors such as Major Histocompatibility Complex (MHC) molecules, ICAM-1, Fas/CD95, and NKG2D ligands, are increased following radiation. These molecules mediate the interactions between T cells and their targets, and may fuel and amplify the inflammatory process to the detriment or benefit of the host, depending on the tissue context. In this session we will review evidence in support of the concept that changes in the interactions between the irradiated tissue and the immune system are key determinants of the response to radiation of both healthy and neoplastic tissues.

SYNTHETIC LETHALITY AND REPAIR TARGETING

(TR013) DNA Repair Defects in Human Cancers: New Opportunities for Treatment. Simon Powell, Memorial Sloan Kettering Cancer Ctr, New York, NY

Defective DNA repair is well documented for heritable cancers, both in mismatch repair deficiency syndromes (MSH2,3,6, Pms1,2 and Mlh1,3) and in familial breast and ovarian cancer syndromes (BRCA1 and BRCA2). In these inherited conditions, there is germline autosomal dominant inheritance of a mutant allele of the repair gene, but the heterozygous cells usually have no clear genetically unstable phenotype that can be measured. However, there must be haplo-insufficiency to allow the subsequent development of tumors as a direct result of this inheritance. By the time the tumor develops, the second allele of the repair gene is inactivated in almost all cases, by genetic loss, by gene conversion of the wild-type to the mutant allele or by methylation of the functional allele. Paradoxically, loss of function of mismatch repair in Lynch Syndrome tumors has not resulted in sensitivity to DNA damaging agents, since the survival response is dominated by signaling to cell death pathways and therefore relative resistance to therapy. In familial breast cancer, one allele of BRCA1 or BRCA2 is germline mutant and the second allele is inactivated to allow tumor development, making the loss of function of BRCA1/BRCA2 a tumor-specific finding. The role of alternative repair pathways in the tumor cells therefore critical for their survival, revealing potential synthetic lethal relationships that are tumor specific. We have shown that loss of Rad52 function is synthetic lethal with BRCA2 deficiency, whereas there was no impact on cell growth in BRCA2-complemented cells. Rad52 can respond to DNA double strand breaks and replication stalling independently of BRCA2, which makes Rad52 a potential target for therapy in these tumors. Targeting DNA repair deficiencies in BRCA1 and BRCA2 deficient tumors has recently shown significant therapeutic opportunity: the use of poly-ADP-ribose polymerase (PARP) inhibitors have been shown to sensitize BRCA-deficient tumor cells. In addition, Fanconi Anemia patients are predisposed to leukemias and squamous cancers of the head and neck, and the cancers arising in these patients should also be vulnerable to DNA cross-linker therapy. More recently, there is increasing evidence that sporadic cancers have defects in DNA repair and the development

of functional assays of repair would allow better selection of the patients who would benefit from DNA repair based therapies. For example, there is evidence that homologous recombination involving the BRCA1-BRCA2 pathway can be functionally inactivated in sporadic breast cancer and perhaps other cancers, suggesting that the pool of patients amenable to PARP-inhibitor therapy is larger than initially expected. In addition, certain lymphomas and leukemias may have defects in non-homologous end-joining, which would make them particularly vulnerable to agents that induce DNA double-strand breaks. Understanding the status of DNA repair in human cancers could therefore open up therapeutic opportunities for not only inherited cancers but also a broader pool of sporadic cancers. The development of strategies to target deficiencies in DNA repair is now a major growth area in the search for targeted therapies of human cancer.

LOW ENERGY ELECTRON INDUCED DNA DAMAGE: FROM PRODUCT ANALYSIS TO POSSIBLE MECHANISMS

(TR014) Low energy electron induced DNA damage: from product analysis to possible mechanisms. J. Richard Wagner, Leon Sanche, Universite de Sherbrooke, Sherbrooke, QC, Canada

The transfer of energy from ionizing radiation to biological molecules generates a large number of secondary low-energy electrons (LEEs; ca. 3×10^4 /MeV; energy < 30 eV). LEEs likely contribute to DNA damage, as indicated by the formation of single and double strand breaks upon irradiation of plasmid DNA on condensed films under ultra high vacuum. The mechanism of LEE-induced damage has largely been investigated by the desorption of small anions from the surface (H^- , O/NH_2^- , CNO^- , etc.). These studies have established that LEEs initially form a transient anion state with DNA components (i.e., nucleobases, deoxyribose and phosphate groups). The transient anion state decays to reactive anions and radicals by dissociative electron attachment (DEA), or if the electron autodetaches, by a dissociative excited state of the molecule. To further understand the mechanism of LEE-induced DNA damage, we have focused on the chemical analysis of non-volatile products remaining on the surface of irradiated films. In these studies, products resulting from the reaction of LEEs with nucleosides, nucleotides, and short oligonucleotides (trimers and tetramers) have been examined using HPLC coupled to UV detection and mass spectrometry. These studies indicate (in agreement with theoretical predictions) that LEEs induce cleavage of the *N*-glycosidic (C-N) bond, leading to base release, and cleavage of the phosphodiester (C-O) bond, leading to the release of fragments bearing an intact terminal phosphate group. The latter pathways represent about 1/3 of the total damage. Interestingly, the total damage and the distribution of C-N and C-O bond cleavage are sensitive to the nature of neighboring DNA bases. This suggests that LEE-induced DNA damage depends on DNA sequence. In addition, there is increasing evidence from product analysis that single electron events induce more than one modification in the same molecule, suggesting that LEEs contribute to clustered damage. The chemical analysis of LEE-induced DNA damage together with mechanistic studies will help clarify the role of LEEs in radiation biology.

RADIO-ECOLOGY

(TR015) Radioecology: Historical overview, challenges and future research directions. Wendy Kuhne, Savannah River National Laboratory, Aiken, SC

Radioecology in the United States can be traced back to the early 1950s when small research programs were established to address the fate and effects of radionuclides released in the environment from activities at nuclear facilities. These programs focused primarily on local environmental effects, but global radioactive fallout from nuclear weapons testing and the potential for larger scale local releases of radioisotopes resulted in major concerns about the threat, not only to humans, but to other species, and ecosystems that support all life. These concerns were shared by other countries and it was quickly recognized that a multi-disciplinary approach would be required to address and understand the implications of anthropogenic radioactivity in the environment. This presentation will provide a historic overview of radioecology's contributions to science and society. A current challenge facing U.S. radioecologists is that much of the information used in today's critical decision making for remediation and management of contaminated lands, determination of human health risk, and emergency response planning for accidents and terrorists events was collected more than thirty years ago. Various data gaps have always existed in the area of radionuclide transport, which have sometimes led to extreme conservatism and unwise expenditures of money and resources. Improvements in cytogenetic, molecular and genetic techniques used in radiation biology to measure radiation effects at low doses, warrant examination of current radiation protection guidelines for plants and animals. The renewed commitment to nuclear power as part of the United States long-term energy strategy has the potential to increase activities in the nuclear fuel cycle, including uranium mining and processing, and in the nuclear power industry. Increasing societal concerns for the protection of humans living near nuclear power plants and processing facilities, and for non-human biota exposed to areas containing multiple stressors like radionuclides and heavy metals, which are often associated with these activities, confirm the need for continued training of future radioecologists and for increased funding levels to support research that has implications for protection of human health and the environment on a global scale.

TARGETED DRUGS WITH RADIATION. WHAT IS NEEDED TO GET THESE AGENTS INTO CLINICAL TRIALS?

(TR016) Targeted drugs with radiation. What is needed to get these agents into clinical trials? Ian J. Stratford, University of Manchester, Manchester, United Kingdom

The use of molecularly targeted drugs in combination with radiotherapy is receiving increasing attention as there are real prospects that such combined modality work could result in changes in the standard of care of the cancer patient. Many of these new chemotherapeutic agents may well have been into man in the context of monotherapy or combination chemotherapy. However, their subsequent use in early clinical trials when combined with radiotherapy requires substantial preclinical experimentation to give the necessary information to allow optimum drug use. The purpose of this review is to outline some of the considerations that need to be made when assessing the possibility of a new drug / radiation combination. These could include; scheduling, protection, sensitization, tumour or normal tissue model, endpoints, underlying mechanisms of the interaction etc. The goal is to illustrate how to gather sufficient information to prepare a pre-clinical package that will facilitate rational clinical evaluation of any new combination. Some examples will be given and an outline provided of the current UK strategy for promoting novel chemo/radiotherapy approaches.

WS1 MARKERS AND PREVENTION OF RADIOTHERAPY-INDUCED SECOND CANCERS

Chairs: George Don D. Jones, University of Leicester, Leicester, United Kingdom; David J. Brenner, Center for Radiological Research, New York, NY

Modern radiotherapy, such as IMRT, exposes larger amounts of normal tissue, but to lower doses. In term of second cancers, the risk-benefit balance here is still unclear, relative to larger doses to smaller volumes. The Workshop will focus on predictive models of second cancer, emphasising possible biomarkers and potential preventative strategies.

WS2 SIT DEBATE: HYPO-FRACTIONATION: THE AVAILABLE RADIOBIOLOGICAL MODELS ARE ADEQUATE IN PREDICTING ACUTE AND LATE EFFECTS

Moderator: Andreas L. Simons-Burnett, University of Iowa, Iowa City, IA

The Scholars In Training (SIT) Committee of the Radiation Research Society is proud to host their very first SIT Debate. The SIT Debate is intended to be a learning event and will be an ideal opportunity for SIT members to hear arguments on both sides of a particular issue and come to a balanced judgment based on the arguments heard. Overview: Radiation-induced death for mammalian cells is classically described according to the linear-quadratic (LQ) equation. According to this model, tumor cell survival rate depends on the overall radiation dose, the dose per fraction, and the overall treatment time. The dose response of tumors and normal tissues to fractionated irradiation can be described according to the alpha-beta ratio (α/β). The α/β ratio parameter is an indicator of the fractionation sensitivity of a particular cell type. In general, α/β is high (≥ 10 Gy) for most tumors and low (< 5 Gy) for late-responding normal tissues. Because of the different α/β values for tumor cells and normal tissue, it may be possible to increase local

tumor control and decrease normal tissue late effects by using unconventional fractionation schedules such as hypofractionation. Hypofractionation treatment schedules have been referred to as less arduous and less costly and have been shown in some studies to offer comparable local/regional tumor relapse and late adverse effects to standard radiotherapy schedules. However, some have questioned the use of hypofractionation schedules because of unacceptable late effects observed when large doses per fraction were administered. Additionally, the accuracy of the LQ model has been questioned at high doses. Therefore, in this year's SIT Debate, the proposition will be "Hypofractionation: the available radiobiological models are adequate in predicting acute and late effects." Arguing for the proposition will be Drs. Steven Lee, Steve Howard, Sylvia Formenti and David Gius. Arguing against the proposition will be Drs. Chandan Guha, Peter Schiff, John Buatti and Ashwatha Narayana. Persons participating in the SIT Debate are selected for their knowledge and communicative skill. Their positions for or against the proposition may or may not reflect their personal beliefs.

RRS HISTORY COMMITTEE PRESENTATION

Pioneers of the Radiation Sciences: Historical Review. J. W. Osborne, University of Iowa, Iowa City, IA

This presentation will be a tribute to honor the many pioneers who have contributed to our understanding of the usefulness and potential hazards of the various types of ionizing radiation from the perspective of physicists, chemists, biologists or clinicians. An historical review of key events in radiation sciences from the decision to establish the Radiation Research Society at the Oberlin Ohio Symposium in 1950 that led to Gino Failla's incorporation of the Society in Washington, D.C. on March 25, 1952, up to today's current scientific multidisciplinary contributions as evidenced at this year's 2010 meeting will be chronicled with historical images maintained by the Society's History Committee. Prominent pioneers will be featured along with a review of the several significant research themes addressed over the last 58 years, including the Society's emphasis on supporting and encouraging young investigators to become future pioneers.

S1 EFFECTS OF IONIZING RADIATION ON NUCLEIC ACIDS: INSPIRATION FOR ANALYTICAL AND MECHANISTIC INVESTIGATIONS

DNA is widely accepted to be the cytotoxic target of ionizing radiation. Consequently, a tremendous effort has been put forth to determine the products of DNA degradation and the mechanisms for their formation. The Max Planck Institut für Strahlenchemie in Mulheim Germany was a center of excellence for research on the effects of ionizing radiation on nucleic acids, their molecular components, and related molecules, such as carbohydrates. Leaders in the field such as Clemens von Sonntag utilized product analysis, spectroscopic measurements (e.g. EPR), and time resolved methods to provide fundamental understanding of the very complicated chemistry that ensues when nucleic acids are exposed to ionizing radiation. These ground breaking investigations and technological advancements have helped researchers develop a deeper understanding of the effects of ionizing radiation on nucleic acids, as well as to utilize this chemistry in a variety of applications. The presentations in this symposium will demonstrate how chemists continue to employ the most modern analytical methods (e.g. ESI-MS), spectroscopy (UV, EPR), chemical synthesis, and biochemistry to further our understanding of oxidative nucleic damage, place it in biological context, and utilize it as a means for understanding nucleic acid structure.

(S101) Repair of radiation-induced products of DNA by DNA glycosylases NEIL1 and NEIL3. Miral Dizdaroglu, National Institute of Standards & Tech, Gaithersburg, MD

DNA glycosylases are involved in the first step of the base excision repair of radiation-induced DNA base lesions. Mammalian DNA glycosylase NEIL1 was shown to be specific for 4,6-diamino-5-formamidopyrimidine (FapyAde) and 2,6-diamino-4-hydroxy-5-formamidopyrimidine (FapyGua); however, it exhibited no significant activity for 8-hydroxyguanine. Loss of NEIL1 resulted in significant biological consequences. Thus, knockout of *neil1* in mice led to symptoms of metabolic syndrome and several types of cancer. Murine cells with knockdown *neil1* were hypersensitized to killing effects of ionizing radiation. We observed significant accumulation of FapyAde and FapyGua in *neil1*^{-/-} mice, proving these lesions as *in vivo* substrates of NEIL1. Four known polymorphic variants of human NEIL1 were characterized. Two of them exhibited near wild-type enzyme specificity and excision kinetics, whereas the others were devoid of glycosylase activity. Furthermore, we showed significant accumulation of (5'R)- and (5'S)-8,5'-cyclo-2'-deoxyadenosines in *neil1*^{-/-} mice without exposure to oxidative stress. This finding suggests the involvement of NEIL1 in nucleotide excision repair of these tandem lesions. Another protein of the same family, NEIL3 was shown to be a glycosylase. Its glycosylase domain (NEIL3Δ324) preferentially removed FapyAde and FapyGua, and, to a lesser extent, some pyrimidine-derived lesions from γ -irradiated DNA. However, it exhibited no activity for 8-hydroxyguanine. *E. coli* triple mutant strain lacking Fpg, Nei and MutY glycosylase activities, which exhibited high Gua \rightarrow Thy transversion mutation frequency (up to 600-fold), accumulated 3-fold greater level of FapyGua than the wild type strain. Expression of NEIL1 and NEIL3Δ324 in these mutants significantly reduced both the spontaneous mutation frequency and the level of FapyGua, confirming this lesion to be mutagenic leading to Gua \rightarrow Thy transversions and to be *in vivo* substrates of these glycosylases.

(S102) Prototropic Equilibria in DNA Containing One-electron Oxidized GC: Intra-duplex vs. Duplex to Solvent Deprotonation. Amitava Adhikary, Oakland University, Rochester, MI

By use of ESR and UV-vis spectral studies, this work identifies the protonation states of one-electron oxidized G:C (viz. G^{•+}:C, G(N1-H)^{•+}:C(+H⁺), G(N1-H):C, and G(N2-H):C) in a DNA oligomer d[TGCGCGCA]₂. Benchmark ESR and UV-vis spectra

from one electron oxidized 1-Me-dGuo are employed to analyze the spectral data obtained in one-electron oxidized d[TGCGCGCA]₂ at various pHs. At pH ≥ 7 , the initial site of deprotonation of one-electron oxidized d[TGCGCGCA]₂ to the surrounding solvent is found to be at N1 forming G(N1-H^{•+}):C at 155 K. However, upon annealing to 175 K, the site of deprotonation to the solvent shifts to an equilibrium mixture of G(N1-H):C and G(N2-H):C. For the first time, the presence of G(N2-H):C in a ds DNA-oligomer is shown to be easily distinguished from the other prototropic forms, owing to its readily observable nitrogen hyperfine coupling ($A_{zz}(N2) = 16$ G). In addition, for the oligomer in H₂O, an additional 8 G N2-H proton HFCC is found. This ESR identification is supported by a UV-vis absorption at 630 nm which is characteristic for G(N2-H)^{•+} in model compounds and oligomers. We find that the extent of photo-conversion to the C1' sugar radical (C1'^{•+}) in the one-electron oxidized d[TGCGCGCA]₂ allows for a clear distinction among the various G:C protonation states which can not be easily distinguished by ESR or UV-vis spectroscopies with this order for the extent of photo-conversion: G^{•+}:C > G(N1-H)^{•+}:C(+H⁺) >> G(N1-H):C. We propose that it is the G^{•+}:C form that undergoes deprotonation at the sugar and this requires reprotonation of G within the lifetime of excited state.

(S103) Photoreactivity of 5-halopyrimidines in nucleic acids. Hiroshi Sugiyama, Graduate School of Science Kyoto University, Japan

5-Halouracils are analogues of thymine in which the methyl group of thymine has been replaced with a halogen atom. The photoreactive 5-halouracils, bromouracil (BrU) and iodouracil (IU), are widely used in medical applications and biological and chemical research. Because of the similarity in size of 5-halouracils and thymine, the thymine moiety of DNA can be replaced with a 5-halouracil without impairing the *in vivo* functionality of DNA. Such replacement enhances the UV sensitivity of the cell with respect to DNA-protein cross-linking, DNA strand breakage, and the creation of alkali-labile sites by forming uracil-5-yl radicals when exposed to UV irradiation. 5-Halouracil-based photocrosslinking and photo-footprinting methods have been used to investigate specific DNA-protein interfaces. The photoreactions of 5-halouracil-containing DNAs have been extensively studied using DNA oligonucleotides and DNA fragments with defined sequences. The reactivities of 5-halouracils in DNA differ significantly from those of monomeric model systems. It has been demonstrated that hydrogen (H) abstraction by uracil-5-yl is atom specific and is highly dependent on local DNA conformation. It has been suggested that the photoreactivity of 5-halouracils could be used to detect various DNA structures. Oxidative lesions generated by H abstraction and subsequent oxidation allow us to investigate stability and reactivity of these sites in DNA, which could provide useful information to understand molecular mechanisms of DNA damage. In addition to their H abstraction properties, 5-halouracil residues in DNA can be used as electron acceptors as they rapidly eliminate halide anions and generate uracil-5-yl radicals when reduced to an anion radical. The electron transfer and back electron transfer processes are highly dependent on DNA conformation. Specific H abstraction by uracil-5-yl radicals in various DNA conformations, and 5-halouracil studies on electron transfer in the B and Z forms of DNA and between DNA-protein interfaces will be discussed.

(S104) Nucleobase radical reactivity in DNA and RNA - oh what a difference a 2'-hydroxyl group makes. Marc M. Greenberg, Johns Hopkins University, Baltimore, MD

Seminal studies on radiation induced nucleic acid damage by Von Sonntag and others often utilize RNA homopolymers as substrates. More recent investigations have utilized DNA substrates. Although nucleobase radicals are the predominant species formed in DNA and RNA, the latter leads to direct strand breaks in significantly greater yield. We have used synthetic, nonnative nucleotides to independently generate nucleobase radicals at defined sites in DNA and RNA. Tandem lesions are the major family of products observed under aerobic conditions in DNA, and little if

any direct strand scission is detected. In contrast, direct strand scission is produced from an independently generated nucleobase radical in RNA. Strand break yields are greatest in double stranded RNA under anaerobic conditions. In addition, 5,6-dihydrouridin-6-yl radical is more proficient at producing direct strand breaks in duplex than single-stranded RNA. The reduction of the C2'-carbon-hydrogen bond dissociation energy in a ribonucleotide compared to a 2'-deoxyribonucleotide provides the driving force for direct strand scission in RNA via the nucleobase radical. A key step in direct strand scission involves C2'-hydrogen atom abstraction by the 5,6-dihydrouridin-6-yl radical. Mechanistic and product studies will be presented.

S2 THE ROLE OF MicroRNA IN RADIOSENSITIVITY AND HUMAN CANCER

MicroRNAs are a class of small, single stranded, non-coding RNA that has a profound effect in the regulation of a variety of cellular processes such as differentiation, apoptosis, cell cycle progression, motility and invasiveness. In this symposium, several leading investigators will discuss the role of microRNAs in modulating radiosensitivity, DNA repair and as diagnostic and therapeutic agents in cancer.

(S201) MicroRNAs as potential diagnostics and therapeutics in cancer. Frank Slack, Yale University, New Haven, CT

MicroRNAs are small non-coding RNAs that regulate gene expression to control important aspects of development and metabolism such as cell differentiation, apoptosis and lifespan. let-7 encodes a microRNA implicated in human cancer. Specifically, human let-7 is poorly expressed or deleted in lung cancer, and over-expression of let-7 in lung cancer cells radiosensitizes them and inhibits their growth, demonstrating a role for let-7 as a tumor suppressor in lung tissue. let-7 is expressed in the developing mammalian lung and regulates the expression of important oncogenes implicated in lung cancer, suggesting a mechanism for let-7's involvement in cancer. We are focused on the role of let-7 and other oncomirs in regulating proto-oncogene expression during development and cancer, and on using miRNAs to suppress tumorigenesis.

(S202) DNA Damage Induces Direct Repression of microRNAs let-7a and let-7b by p53. Nicole Simone¹, Anthony Saleh¹, Jason Savage¹, James B. Mitchell¹, David Gius², ¹NIH, Bethesda, MD, ²Vanderbilt, Nashville, TN

Cellular stress pathways allow cells to survive ionizing radiation or other cytotoxic cancer treatments. Radiation induces free radical damage to cells that results in a stress response involving large scale changes in gene expression including that of microRNAs (miRNA). Specifically, decreased expression of the let-7 family of miRNA has been reported, and increased expression of let-7b has been shown to increase radiation sensitivity in lung cancer cells. The precise mechanism by which let-7 increases sensitivity to radiation treatment and is repressed has yet to be elucidated. In this study, we demonstrate that p53 is required for the repression of let-7a and let-7b in response to radiation and other genotoxic agents. Using real time RT-PCR we showed that let-7a and b expression decreased in several cell types in response to irradiation, etoposide, UV, and H₂O₂. We also showed that this decrease in expression of let-7a and let-7b was dependent on p53, as the decrease was absent in HCT116 p53 knockout cells. Further analysis of the effect of p53 on let-7a3 and let-7b expression by CHIP showed an association of p53 with a predicted binding site in the host gene promoter. Total body irradiation of mice resulted in decreased let-7a and let-7b expression in radiation-sensitive tissues. However, no decrease was observed in tissues collected from p53-/- mice. Transfection of additional let-7a or let-7b into HCT116 cells decreased survival after radiation treatment, but survival is

unchanged by exogenous expression of let-7 in HCT116 p53 knockout cells. Radiation sensitivity is thought to result from a combination of altered cell cycle and proliferation pathways, DNA repair suppression, and the upregulation of apoptosis. FLOW cytometry performed on HCT116 cells transfected with let-7b showed an increase in the percentage of cells in G2/M as compared with their controls. Increased apoptosis can also be detected following IR and etoposide treatment in HCT116 and tera-1 cells transfected with let-7b. However, gamma-H2AX levels following IR treatment of transfected cells did not show a significant difference over time as compared with controls, suggesting that DNA repair was unaltered. These results suggest that p53 can directly repress let-7 expression. Also, alteration of cell cycle control and the apoptotic response suggests that let-7 may play an important role in the regulation and fine-tuning of cell fate decisions directed by p53. Furthermore, our data implies that therapeutics aimed at inducing overexpression of let-7 may be useful in augmenting cytotoxic cancer treatment.

(S203) MicroRNAs as biomarkers for exposure to low- and high-LET ionizing radiation. Lubomir Smilenov, Columbia University, New York, NY

MiRNAs are important regulators of gene expression. Their main property is the ability to target hundreds of genes resulting in modest downregulation of expression. While miRNAs are defined by this property, the exact mechanism by which they exert control over biological processes at the pathway and network level is unknown. miRNA regulation most probably results in shifts and synchronization of pathways in a normal cell state or in transition between different cell states. This aspect of miRNAs biology makes them very attractive in studying the effects of ionizing radiation. We investigated the changes of miRNA expression signatures in mouse and human blood in response to radiation. Mouse-related experiments involved irradiating mice with γ -radiation and high LET ⁵⁶Fe ions and protons. Our main finding is that miRNA expression signatures derived from mouse whole blood are specific for every irradiation condition we studied. Of 320 miRNAs examined, a total of 35 were differentially expressed in the studied irradiation conditions (FDR <0.07, p<0.001). The expression data were used to generate predictive classifiers. We developed radiation type and dose-related classifiers which correctly classified 75 to 100% of samples with unknown radiation status. The acquired miRNA expression data were also used to demonstrate that radiation induces changes in the miRNA control of intercellular pathways and networks. Remarkably, two groups of biological processes were with increased miRNA control after irradiation: a core group common for all irradiation conditions and a dose and time specific group of processes. For the human studies, we obtained blood under IRB-approved protocols from 8 patients that were subject to total body irradiation of 1.25 Gy for therapeutic purposes. Despite the genetic variation between the patients, 45 miRNAs (p<0.03, FDR=0.2) were differentially expressed 4 hours after irradiation. miRNA target analysis show increased miRNA control over several important cellular pathways and networks. miRNA based classifiers correctly predicted the irradiation conditions of unknown samples. The proper estimation of the role of miRNAs is ultimately dependent on the assessment of the effect on the expression of their target genes. This led us to test a methodology designed to identify all transcriptionally downregulated targets of the cell's endogenous miRNA. This was done by transfection of the complete set of miRNAs in parental cells. The results show that 24% of the expressed genes in the studied normal cells were under miRNA control and that miRNAs regulate very important biological processes including cell signaling, immunity and defense, and genetic disorders. Taken together, these results demonstrate the importance of miRNA studies in the cell's response to radiation and illustrate the power of miRNAs in biodosimetry.

(S204) MiR-210 is an integral component of the hypoxic response of tumor cells. Amato J. Giaccia, Stanford University School of Medicine, Stanford, CA

Untransformed and transformed cells have evolved sophisticated mechanisms of adapting to changes in oxygen. These mechanisms involve migration from a hypoxic to oxic regions of tissues, changing cellular metabolism to an anaerobic state, and increasing the expression of genes such as erythropoietin to increase the production of erythrocytes to provide increased oxygen to hypoxic tissues. Major regulators of the hypoxic response of cells are the HIF (Hypoxia Inducible Factor) family of transcription factors. Many of the genes that promote adaptation and survival to hypoxia are regulated by the HIF family. Recently, microRNAs (miRNAs) have emerged as a new class of genes that are regulated by HIFs in response to hypoxia. One of the miRNAs, miR-210 is consistently induced by hypoxia in a variety of different cell types. In this talk we will discuss the physiologic functions of miR-210 under hypoxic conditions and its role in tumor progression.

S3 STEM CELLS AT THE CROSSROADS OF BASIC AND TRANSLATIONAL RADIOBIOLOGY

Stem cells play critical roles in dictating normal tissue tolerances to irradiation and are integral to the maintenance of tissue health. The capability to regenerate damaged tissues provides a powerful tool to counteract the adverse effects of exposure to genotoxic and cytotoxic agents, disease and ageing. In most cases the success or failure of this regenerative therapy depends on the interplay between stem cells and the damaged microenvironment into which they must functionally integrate. Damaged incurred acutely or accumulated over chronic times can impact the capability of stem cells to proliferate and/or differentiate, and secondary reactive processes within the irradiated tissue bed can modulate the extent of tissue remodeling and grafting efficiency. While such factors have a significant influence on the radioresponse of normal tissues, the mechanisms regulating the behavior of tissue-specific stem cells and their immediate progeny in response to stress are diverse. This symposium will highlight certain critical aspects of fundamental stem cell biology involving DNA repair mechanisms, telomeres, oxidative stress, proteosomal regulation, and cell fate decisions. These basic research themes will then be translated to clinically relevant scenarios, as speakers will highlight the pros and cons of irradiating stem cell niches, unique cancer stem cells features, the capability of stem cells to be used in spinal cord injury, and the use of stem cells for the reconstitution of cognition after irradiation. Information from this symposium will provide insight into radiation effects on unique tissue compartments and if/how normal tissue damage can be spared for improving the recovery and function of compromised tissue.

(S301) Double-Strand Breaks Near Telomeres are Poorly Repaired and Result in Chromosome Instability in Mouse Embryonic Stem Cells. John P. Mumane, Univ. of Calif., San Francisco, San Francisco, CA

Telomeres play an important role in capping the ends of chromosomes to keep them from appearing as double-strand breaks (DSBs) and thereby prevent chromosome fusion. We have used plasmids integrated adjacent to telomeres to investigate the consequences of telomere loss for chromosome stability in mouse embryonic stem (ES) cells and human tumor cells. These plasmids contain selectable marker genes and a recognition site for I-SceI endonuclease to monitor the consequences of DSBs. Our results have demonstrated that the types of events occurring as a result of DSBs near telomeres are much different than the events observed as a result of DSBs at other (interstitial) locations. The most common events at interstitial DSBs are small deletion of a few base pairs, while large deletions and gross chromosome rearrangements (GCRs) are relatively uncommon. However, while the frequency of small deletions is similar at interstitial and telomeric DSBs, the frequency of large deletions and GCRs is greatly increased at DSBs near telomeres in both mouse ES cells and human tumor cells. Moreover, the GCRs resulting from DSBs near telomeres often lead to prolonged periods of chromosome instability in both the mouse ES cells and human tumor cells. Another type of rearrangement that

is unique to DSBs near telomeres is the addition of a new telomere to the site of the DSB, called chromosome healing. While chromosome healing is relatively rare in human tumor cells, it accounts for approximately one-third of the events at DSBs near telomeres in mouse ES cells. Our results show that chromosome healing results from the de novo addition of telomeric repeat sequences by telomerase, and that chromosome healing prevents degradation, GCRs, and chromosome instability. We propose that the reason for the difference in the types of events at interstitial and telomeric DSBs is twofold. The first reason is that regions near telomeres are highly sensitive to DSBs, which we have shown extends at least 100 kb from the telomere. In view of the fact that there are 92 telomeres in human cells, the telomeric regions constitute a relatively large target that is sensitive to DSBs. We are currently investigating the mechanism for this sensitivity by comparing the repair of I-SceI-induced DSBs at interstitial and telomeric sites using plasmids containing a gene for green fluorescent protein. Our results demonstrate that the frequency of repair of DSBs by both homologous recombination repair and nonhomologous end joining is significantly reduced near telomeres compared to interstitial sites. The second reason for the differences in the types of events at telomeric and interstitial DSBs is that chromosome healing is likely to be inhibited at interstitial sites. Studies in yeast have shown that this inhibition of chromosome healing is mediated by the PIF1 helicase, which binds directly to TERT, the catalytic subunit of telomerase. In yeast, PIF1 is phosphorylated in response to DSBs, which is necessary to prevent chromosome healing. We are currently investigating the mechanism of regulation of chromosome healing in mammalian cells. We hypothesize that the differential response of telomeric regions to DSBs is associated with the role of telomeres in preventing chromosome fusion, possibly through the inhibition of MRE11 and ATM by the telomeric protein TRF2. The inactivation of MRE11 and ATM would both inhibit DSB repair and prevent the activation of PIF1. This sensitivity of telomeric regions may play a role in spontaneous telomere loss and chromosome instability in human cancer cells, and in radiation-induced chromosome instability and cancer.

(S302) Cancer Stem Cells - Lessons learned from the needle in the haystack. Erina Vlashi, Chann Lagadec, Lorenza Della Donna, Patrick Evers, Carmen Dekmezian, Joseph Behjat, Frank Pajonk, UCLA, Los Angeles, CA

The cancer stem cell hypothesis is an old concept in oncology. However, until recently cancer stem cells (CSCs) in solid carcinomas could not be identified prospectively. Now, with marker profiles available for CSCs in a variety of different solid cancers, CSCs and their responses to established and novel treatments can be studied for the first time directly and in detail. In this presentation our most recent observations on maintenance of the breast cancer and glioma CSC phenotype, treatment responses, and the metabolic state of CSCs will be discussed.

(S303) Stem cell transplantation strategies for the rescue of radiation-induced cognitive dysfunction. Munjal M. Acharya, Lori-Ann Christie, Mary L. Lan, Charles L. Limoli, University of California Irvine, Irvine, CA

Out of 1.5 million cancers diagnosed in United States, 30% develops brain metastatic tumors. For majority of CNS tumors, cranial irradiation remains primary treatment modality (200,000 patients per year). For many of these patients cognitive dysfunction is inevitable, a serious complication that may be caused by the radiation induced depletion of neural stem and precursor cells. To explore the possibility of ameliorating radiation induced cognitive impairment, we transplanted human embryonic or neural stem cells (hESCs/hNSCs) into the hippocampal formation of rats after cranial irradiation. Two month old athymic nude rats (ATN) subjected to 10 Gy head only irradiation were grafted 2 days later with stem cells prelabeled with BrdU at 4 distinct hippocampal-sites (100,000 cells/site, 8×10^5 cells/animal). Control (CON) and irradiated (IRR) rats receiving vehicle (sterile conditioned medium)

served as sham surgery groups. At 1 and 4 months postgrafting, rats were tested using hippocampal-dependent novel place recognition task (NPR). Compared to controls, irradiated rats showed significant cognitive decrements. In contrast, IRR rats receiving either hESC or hNSC grafts did not differ from the CON group and spent more time than expected by chance exploring the novel place. To better understand these cognitive data, the total time spent exploring both objects during the familiarization phase of the task were analyzed. Significant differences between the groups were found; IRR animals spent less time exploring during familiarization compared to both CON and IRR+hESC/hNSC rats. These results suggested that hESC and hNSC transplantation attenuated radiation induced cognitive impairment by preserving hippocampal-dependent spatial information processing when analyzed 1- and 4-months postirradiation. Immunocytochemical analysis revealed extensive migration of grafted stem cells throughout the host hippocampus. Transplanted stem cells also exhibited significant homing to the neurogenic niche of the hippocampus. Unbiased stereology for the hESC group at 1 and 4 months postgrafting revealed 34 and 17% survival of transplanted cells respectively. Ongoing analyses using dual immunofluorescence and confocal microscopy has thus far revealed that the grafted hESCs differentiated into neurons, astrocytes and oligodendrocytes. These findings provide the first evidence that transplanted pluripotent (hESCs) and multipotent (hNSCs) human stem cells can survive, differentiate along neural lineages, and ameliorate cognitive impairments caused by cranial irradiation. These data also suggest that similar strategies can be tailored to minimize the adverse side effects associated with exposure to ionizing radiation. [Supported by CIRM grant RS1-00413-1 (CLL) and CIRM Training Grant TG2-01152 (MMA)]

(S304) Utilization of human fetal spinal stem cells and human embryonic stem cell-derived neural precursors for spinal grafting in models of spinal ischemic injury and amyotrophic lateral sclerosis. Martin Marsala, UCSD, La Jolla, CA

Several spinal neurodegenerative disorders, including spinal cord ischemic injury and amyotrophic lateral sclerosis (ALS), are characterized by a progressive loss of well defined neuronal populations including interneurons and/or A-motoneurons. The resulting neurological deficit is typically presented as increased muscle tone (i.e., spasticity and rigidity) or progressive development of motor weakness and flaccidity. In addition, it has been demonstrated that in ALS the release of toxic substances from SOD+ mutated astrocytes plays a key role in the evolution of upper- and lower-motor neuron lesion. In previous studies, we have characterized a potent therapeutic effect after spinal grafting of human spinal stem cells in rat spinal ischemic injury as validated by improvement in ambulatory motor function and correlative restoration of motor evoked potentials. The degree of functional recovery corresponded with robust cell survival and development of putative synapses with the host persisting neurons. Using SOD+ transgenic rats, we have shown significant protection in A-motoneuronal survival in the vicinity of grafted cells which correlated with transient protection of spinal monosynaptic stretch reflex. Using a preclinical minipig model, we have also defined the optimal cell dosing and volume of injections not associated with any significant side effects. A similar cell dosing/delivery regimen is currently used in a clinical ALS spinal cell-replacement trial (Neuralstem Inc.). In more recent studies, we have employed human embryonic-stem cells (ES-NPCs) and human induced pluripotent stem cell-derived neural precursors (iPS-NPCs) for spinal grafting in several models of spinal injury, including spinal air embolism, spinal ischemia or spinal trauma. Our initial data demonstrate a favorable safety profile with no tumor formation at 2 weeks to 3 months after grafting. In addition, if compared to fetal tissue-derived NPCs, ES-NPCs showed widespread migration in spinal gray and white matter and development of synaptic contacts with the host neurons. These data demonstrate that ES-derived NPCs can represent an important cell source to be used in CNS cell-replacement therapies.

S4 HEAVY IONS IN SPACE RADIATION AND HADRON THERAPY

Heavy ions are a radiation quality normally not found naturally on earth (except alpha particles). They differ significantly from beta and gamma radiation, both in physical properties as in biological response and effects. They are part of the Galactic Cosmic Rays and therefore important to NASA and mankind's dream of deep space travel. Furthermore, proton and carbon beams in cancer therapy become available and open new possibilities in treatment options. In this symposium we will explore heavy ion applications in radiation biology and radiation therapy, learn about the space radiation field and radiation protection on the moon, and get an overview over the NASA Space Radiation Laboratory at Brookhaven National Lab where relativistic heavy ion beams are available.

(S401) Monte Carlo simulation of NHEJ repair of DSB after ion irradiation. Werner Friedland, Pavel Kundrat, Peter Jacob, Helmholtz Zentrum Muenchen - Institute of Radiation Protection, Neuherberg, Germany

The combination of track structure calculations with sophisticated multi-scale DNA models in the biophysical simulation code PARTRAC allows reasonable estimation of initial yields and patterns of DNA damage after photon as well as ion irradiation. However, the capability of such calculations to predict late effects such as chromosomal aberrations or cell survival is limited since extrapolations in time over more than 12 orders of magnitude are necessary. In particular, the removal of DNA lesions by repair processes introduces non-linear responses of the biological system that call for explicit consideration in corresponding models. In the past years, knowledge on DNA repair processes has advanced from qualitative information on the involved repair enzymes towards quantitative data on the spatio-temporal dynamics of individual processes and DNA lesions. Based on such data, a stochastic model has recently been established for the NHEJ pathway of DNA repair (Friedland et al. 2010 Radiat Res 173:677). It describes step-by-step by Monte Carlo method the attachment and dissociation of Ku70/Ku80 and DNA-PKcs as well as the diffusive motion of DNA ends. Initial DNA lesion patterns from PARTRAC calculations represent DSB complexity; its influence on the repair process is implemented via cleaning steps required for dirty DNA ends of complex DSB. An adaptation of model parameters to DSB repair kinetics after γ -irradiation yielded, in parallel, correct results for the yield of misrejoined DSB, indicating the predictive power of the model. A first application of the repair model to DSB rejoining after ^{60}Co γ and nitrogen ion irradiation, however, has failed to reproduce the essential experimental results, namely (1) an almost identical kinetics during the initial fast repair phase, and in the later phase (2) very similar time constants but with LET increasing fractions (3) of slowly repairing DSB and (4) of eventually unrejoined DSB. A refined model setup for the post-synaptic phase of repair, addressing these issues, is currently under development. Consistency regarding (1) could be achieved by assuming, in parallel to the rejoining process, an ongoing induction of detectable DSB through enzymatic processing of heat-labile sites or other lesions induced predominantly by low-LET irradiation. Agreement concerning (2) and (3) has been improved by model calculations considering limited availability of repair enzymes needed for processing of complex lesions. Restriction of the movement of DNA ends contributes essentially to conformity regarding (4) and to rather dose-independent residual DSB after low-LET irradiation. By complementing the existing biophysical simulation tool PARTRAC by NHEJ pathway of DSB repair, the reported model represents a quantum leap towards systems radiation biology modeling. Acknowledgement: This work was partially supported by the EC within the 6th FP integrated projects 'RISC RAD' (F16R-CT2003-508842) and 'NOTE' (F16R 036465).

(S402) Stochastics in specific energy imparted to cells in radiation therapy. Hans Bichsel, Univ of Washington, Seattle, WA

In radiation treatment with C-ions the spectrum of the energies of ions as well as that of LET is quite broad. At average doses of 2

Gy, the number of ions crossing a cell is about ten, and the specific energies z in the cells will have a Poisson distribution from the random incidence of the ions. The random energies of the ions will cause further stochastics in z . The consequence is a broad spread in survival fractions in the tissue which is irradiated.

(S403) Transport model studies of the space radiation environment on the Moon. Zi-Wei Lin, East Carolina University, Greenville, NC

In human space missions, astronauts will be exposed to space radiation from both galactic cosmic rays (GCR) and solar particle events (SPE). For a habitat on the Moon, it is useful to know the variation of the space radiation exposure inside the habitat and locate the places with the lowest radiation exposure. It is also important to know how effectively a habitat of various thicknesses can reduce the space radiation exposure in the habitat. This talk will first present recent results on how a domed habitat of different thicknesses affects the radiation exposure in the habitat (Jia and Lin, *Radiat. Res.* 173, 238-244, 2010). The Monte Carlo code Geant4 is used to study the modified radiation environment in a lunar regolith habitat on the Moon in a GCR environment, where all primary GCR particles from protons up to Ni nuclei are included in the transport calculations. In particular, we will show how the effective dose from secondary and albedo particles, including neutrons, electrons, positrons, photons, and pions, change with the habitat thickness. We will also present results on the variation of the radiation exposure inside a domed habitat (Lin, Baalla and Townsend, *Rad. Meas.* 44, 369-373, 2009). A 1-dimensional radiation transport is used to calculate the space radiation exposure to blood-forming organs everywhere inside the habitat. We find that the center of the hemispherical dome has the largest radiation exposure while locations on the inner wall of the dome have the lowest exposure. This conclusion agrees with an earlier study on a spherical-shell shield but differs from another earlier study on a hemispherical dome, and we will show how the difference is resolved. We find that the reduction of the dose equivalent going from the center to the inner wall of the dome is especially large for SPE environments.

(S404) Overview of the NASA Space Radiation Laboratory. Adam Rusek, Brookhaven National Laboratory, Upton, NY

The NASA Space Radiation Laboratory (NSRL) at Brookhaven National Laboratory (BNL), an accelerator-based facility which provides ion beams for radiobiology, physics and instrumentation studies, is currently in its 8th year of operation. We will survey developments at NSRL since its commissioning in 2003, touching on developments in beam profiles, intensities, energies and time structure, beam imaging techniques, dose measurement methods, instrument calibration and quality assurance. The large beam and Solar Particle Event (SPE) simulation capabilities will be described, and additions to the NSRL instruments and methods which grew out of interactions with individual users will be highlighted. We will then discuss near and not so near future activities and plans, including the commissioning and usage of the new Electron Beam Ion Source (EBIS), which will provide ions unavailable from the source currently used, and a Galactic Cosmic Ray (GCR) simulator which involves upgrading NSRL to 1.5 GeV/n. Our working relationship with NASA and opportunities for additional usage of the facility will be discussed. *Work performed under the auspices of the U.S. National Aeronautics and Space Administration and the U.S. Department of Energy.

S5 THE TUMOUR MICROENVIRONMENT: EXPLOITING PATHWAYS FOR TARGETED THERAPIES

Altered metabolism within the tumor microenvironment can drive resistance to current chemotherapy protocols and radiother-

apy. However new knowledge regarding intratumoral signaling pathways pertaining to tumour hypoxia, tumor metabolism and the epithelial-mesenchymal transition (EMT) may be exploited for novel cancer therapies. This session will review microenvironmental effects on differential gene transcription and translation and microRNAs, EMT and TGF-beta signaling, DNA repair and cell cycle checkpoints and vascular stem cell biology. The session will synthesize this knowledge and discuss the implications for novel prognostic factors and cancer therapeutics.

(S501) Targeting pathways of hypoxia tolerance to improve tumour response to radiotherapy. Bradly G. Wouters, Princess Margaret Hospital/ontario Cancer Institute, Toronto, ON, Canada

Hypoxia is a common feature of tumors that contributes to malignancy and treatment resistance. The basis for these effects derives in part through a transcriptional response mediated by the hypoxia inducible factor (HIF) family of transcription factors. In addition, we have shown that hypoxia influences mRNA translation by activation of the PERK kinase as part of the unfolded protein response (UPR) and by inhibition of the eIF4F complex which is controlled by the mammalian target of rapamycin (mTOR). Although several studies implicate important roles for HIF, PERK and mTOR in hypoxic adaptation, the potential of targeting these pathways to modify hypoxia and therapy response has not been addressed. To this end, we established a new tumor model that allows therapeutic evaluation of targeting these pathways within an identical genetic background. Cell lines were engineered to accept transgenes at a single genomic location encoding dominant negative or mir30 based RNAi targeting various components of these three hypoxic pathways. To closely mimic the clinical situation, transgene expression is regulated by doxycycline such that tumors can be established with a wild type phenotype and subsequently induced to inactivate the pathway of interest. In tissue culture, knockdown of HIF-1 α resulted in decreased proliferation under hypoxic conditions, whereas interference with UPR and/or mTOR signaling had no effect. Conversely, cells defective in UPR activation, mTOR-signaling and HIF-expression were significantly sensitized to hypoxia induced cell death. In vivo, targeting the HIF, UPR or mTOR pathways after tumor establishment had little or no effect on overall tumor growth, but substantially changed the tumor-microenvironment and decreased the level of hypoxic cells. However, if targeted prior to irradiation, only targeting the UPR and mTOR pathways resulted in a significant increase in tumor growth delay in comparison to wild type tumors or tumors induced to inactivate HIF. When targeted after irradiation, a significant increase in tumor growth delay was observed in HIF-deficient tumors, but not in UPR or mTOR targeted tumors. Neither targeting UPR, mTOR nor HIF resulted in changes in the intrinsic radiosensitivity of the cells under normoxic or hypoxic conditions. These data suggest that the UPR and mTOR contribute to hypoxic tolerance of radioresistant cells in vivo and could be an interesting therapeutic target in combination with radiotherapy.

(S502) Cell cycle checkpoints and DNA repair in hypoxic conditions. Ester M. Hammond, Stanford University, Stanford, CA

Severe levels of hypoxia (<0.1% O₂) lead to a rapid and robust induction of the DNA damage response. Interestingly, this occurs in the absence of DNA damage detectable by comet assay or formation of 53BP1 foci but does involve H2AX. Specifically, H2AX is both phosphorylated and forms nuclear foci in response to severe hypoxia. DNA combing studies demonstrate that severe hypoxia induces a replication arrest which includes both stalled forks and the inhibition of new origin firing. This correlates with a rapid decrease in available nucleotides during exposure to hypoxia. Both ATR and ATM are active in these conditions and phosphorylate numerous targets including p53, Chk 1, Chk2 and RPA. Replication re-start does not occur unless hypoxic cells are reoxygenated during a certain time frame (acute exposure), after this point the cells remain replication incompetent regardless of oxygen tension. We have attributed this to the collapse of the replication

fork, which includes the loss of essential factors such as the MCM complex. Recent studies from us and others have demonstrated that essential components of the DNA repair machinery are also repressed in hypoxic conditions. This, combined with the replication arrest induced by severe hypoxia, results in sensitivity to agents such as PARP and Chk1 inhibitors.

(S503) Targeting TGFβ in Radiotherapy. Mary H. Barcellos-Hoff, NYU School of Medicine, New York, NY

Transforming growth factor beta (TGFβ) is a pleiotropic cytokine that we have shown is induced by radiation and regulates ATM kinase activity and the DNA damage response (DDR). In addition, TGFβ promotes malignancy via well-defined roles in immune function, invasion, and metastasis. We propose that inhibiting TGFβ during radiotherapy (RT) could improve efficacy by increasing cell kill, impeding invasion/metastasis, and priming anti-tumorigenic immunity. To better mimic the clinic, we designed an experiment in which tumors were established and treatment started at a time when most animals had developed measurable lung metastases. The highly metastatic 4T1 mouse mammary carcinoma was injected s.c. in the flank of syngeneic mice to evaluate the efficacy of RT in conjunction with a monoclonal pan-specific TGFβ neutralizing antibody, 1D11.16 (Genzyme, Inc.), that was administered the day before treatment. γH2AX foci immunostaining, an index of ATM kinase activity, were reduced in irradiated tumors treated with 1D11 compared to irradiated tumors treated with isotype control mAb. Consistent with reduction of DDR, tumor growth delay was reduced in RT- and 1D11-treated mice compared to mice unirradiated and compared to RT and isotype mAb. Furthermore, animals receiving TGFβ neutralizing antibody and RT exhibited few metastatic lesions. These preclinical studies of 4T1 tumors, which are similar to triple negative breast cancer, support the use of a TGFβ inhibitor to increase the response to RT, inhibit metastatic growth by possibly promote radiation-induced anti-tumor immunity. The findings are timely since TGFβ inhibitors are already in PHASE I-II clinical assessment. Supported by funding from the NYU Cancer Center and the NYU Department of Radiation Oncology. Antibodies were a gift by Genzyme, Inc.

(S504) Targeting the tumor vasculature: It's the circulating cells that count. Martin Brown, G-one Ahn, Mitomu Kioi, Stanford University, Stanford, CA

There is an increasing controversy in radiotherapy as to whether the important target for cell killing are the tumor cells or the endothelial cells lining the blood vessels of the tumor. Much of this controversy can be resolved by taking into account the fact that there are circulating cells from the bone marrow and elsewhere that can reconstitute the tumor vasculature after irradiation, a process known as vasculogenesis. However, if this process could be blocked it is likely that tumors would be much more sensitive to irradiation. We have tested this hypothesis using two human tumors (FaDu and U251 glioma) transplanted into nude mice and have used a variety of bone marrow transplantation studies to identify bone marrow derived cells in tumors. We show that an essential contributor to vasculogenesis in irradiated tumors are CD11b+ myelomonocytic cells expressing MMP-9, that these are recruited to the irradiated tumors by stromal derived factor 1 (SDF-1) induced by increased levels of HIF-1 in the irradiated tumors. Importantly, a variety of ways of blocking this process (neutralizing antibodies to CD11b, inhibition of the interaction of CXCR4 with SDF-1, antibodies against CXCR4 and inhibition of HIF-1) render tumors more radiosensitive. Our data suggest that although the sensitivity of the tumor vasculature affects the growth delay of irradiated tumors it does not affect the TCD50 because bone marrow derived cells can "rescue" the tumor vasculature. However, if the bone marrow contribution is inhibited, tumors can be permanently controlled by considerably lower radiation doses.

S6 STUDIES OF RADIATION SUSCEPTIBILITY TO CANCER: WHERE DO WE STAND?

The symposia session will cover genotyping, statistical, phenotypic and functional challenge assays as means to determine radiation susceptibility to cancer.

(S601) Molecular epidemiology of radiation susceptibility to cancer among atomic-bomb survivors. Tomonori Hayashi, Kei Nakachi, Kengo Yoshida, Kazue Imai, John B. Cologne, Seishi Kyoizumi, Yoichiro Kusunoki, Evan B. Douple, Roy E. Shore, Radiation Effects Research Foundation, Hiroshima, Japan

RERF epidemiological studies have reported that atomic-bomb (A-bomb) radiation exposure resulted in long-term health effects in the survivors, particularly enhanced risks of various cancers with increased radiation dose. Our molecular epidemiology study's aim is to evaluate genetic susceptibility of individuals to radiation-associated cancers and other diseases on the basis of results obtained from our parallel and long-term immunobiology study. Recent research has revealed significant radiation effects on immune responses in A-bomb survivors, in terms of radiation-associated attenuation of T-cell functions (e.g. CD4 and CD8 naïve T-cell frequencies, PHA response, and IL-2 production) and elevation of plasma inflammatory markers (e.g. IL-6, TNF-α, IL-10, and CRP). These effects may potentially be potent mechanisms underlying increased risk for various diseases. The immunobiology study, with measurement of numerous biomarkers among the RERF cohort members, indicated that host immunology and somatic mutability (i.e., glycophorin A mutant fraction) status generally were altered by prior radiation exposure in a dose-dependent manner, but that this radiation response varied among individuals. A follow-up survey of this cohort showed that inter-individual variation observed in selected biomarkers was associated with occurrence of cancers. Therefore, we initiated the molecular epidemiology study to identify the origins of such individually differing radiation responses through an immunogenome approach. The approach comprises analyses of 1) radiation effects on immunological and somatic mutability biomarkers (phenotype study); 2) identification of genetic polymorphisms responsible for inter-individual variation of the biomarkers (genotype-phenotype association study); and 3) risk estimation of cancers on the basis of gene/radiation interactions (genotype study). In this presentation, we will review our current progress along these lines, including research into relationships between *IL-10*, *CD14*, and *EGFR* gene polymorphisms and risks of radiation-associated cancers of the stomach, colon, and lung, respectively. The aim of our study is to delineate the relationship between radiation dose and cancer risk for groups with different genetic backgrounds on the basis of long-term follow-up data of A-bomb survivors exposed to a wide-range of radiation doses, with the potential for contributing to individualized risk estimation in the future.

(S602) Radiosensitivity and other challenge assays: promise and peril for detecting susceptibility to radiation-associated cancers. Alice Sigurdson, National Cancer Institute, Bethesda, MD

After mutagen challenge assays were introduced in the early 1980's, several hundred case-control study results have reported various measures of chromosome instability, DNA damage or functional tests of DNA repair capacity that were associated with two- to 10-fold increased cancer risk at several sites, including breast, lung and brain. These cancers share radiation exposure as a factor that increases their risk. Consequently, the mutagen challenge tests incorporated bleomycin (a radiomimetic agent) and x- or γ-radiation as the test mutagen because radiation was thought to be one of the causative agents. But, these studies have been criticized because they share the design limitation of measuring both the host's response to cancer and the underlying genetic susceptibility, a bias termed "reverse causation". Indirect evidence from family and twin studies have found that mutagen sensitivity has a high heritable component, suggesting the assay may be measuring a host susceptibility factor.

However, even if the challenge assays are shown to be unbiased, if their sensitivity and specificity remain low, this would reduce their utility for screening for radiation-related cancer risk. Despite design limitations, these phenotypic assays are capturing aspects of the end result of a cellular cascade of processes to initiate and complete repair to damaged DNA, among other functions. The ability to measure subtle deficiencies can provide information about individual human variation. Such variation clearly exists, and certain defects such as in the *ATM* and *PTCH* genes are associated with radiation-related increased breast and basal cell carcinoma risks. More subtle deficiencies also exist, such as increased radiosensitivity in the apparently normal parents of children with retinoblastoma. But, not all hereditary retinoblastoma patients (or cell lines from them) show genomic instability, suggesting other mechanisms play a role. A heightened ability to detect more subtle human variation is reasoned to occur when the radiation challenge can be delivered at a low dose rate as opposed to a high dose rate. Individuals with proficient systems can process the damage more easily than individuals with variably impaired systems, thereby creating a more easily detected disparity. But such experiments with low dose rates are even more time consuming and may not be easily scalable to large numbers. Advancements with assays using γ -H2AX could be promising, but will require validation in large human studies. Tests using peripheral blood samples that are economical in cost and scale may be a side benefit of measures being developed for triage after radiation accidents. For concerted efforts to be undertaken using mutagen challenge assays, prospective studies with blood collected well before cancer outcomes will need to be done. One small cohort study using the bleomycin sensitivity assay of 220 patients with Barrett's esophageal cancer, but nested studies with stored samples or larger cohorts will need to be followed before the assays will be more largely accepted. The challenge assays with test mutagens like bleomycin or radiation do hold promise for potentially identifying susceptible individuals for radiation-related cancer outcomes, but more work needs to be done on several fronts before they will be widely used.

(S603) Discovery of Gene by Radiation Interactions. Daniel Stram, Univ of Southern California, Los Angeles, CA

Genome-wide association scans (GWAS studies) of cancer have by now led to a number of highly reproducible findings regarding the influence of common alleles on cancer risk for many cancers. Broadening GWAS studies to encompass alleles that are involved in gene-environment interactions is one of the most important tasks leading to understanding the full range of genetic influence on cancer risk and for adding to our basic knowledge of cancer etiology. In radiation epidemiology the discovery of alleles that modify individual genetic sensitivity to the carcinogenic effects of radiation exposure have potential consequences for radiation protection policy. At present the evaluation of gene environment interactions in GWAS studies is just beginning, and there are a number of methodological as well as biological issues to be considered, both generally, and specifically for radiation. These issues include 1) The scale upon which "interactions" are to be defined. More generally: what is the synergy between radiation exposure and genetic variation? In some approaches to risk estimation exposures that affect risk multiplicatively are not considered to be interactions, and some statistical techniques for detecting interactions are not sensitive to multiplicative effects. 2) The relative impact of rare and common risk alleles on cancer risk generally and upon individual susceptibility to radiation specifically. 3) The suggestion (at least in certain cancers) that many hundreds of common risk alleles may ultimately be found to be involved in disease risk: with many more genes having small effects on risk rather than large effects. 4) Whether the influence of many risk alleles with small effects can be combined when addressing susceptibility to radiation. 5) Whether gene x gene interactions need to be taken into account when evaluating gene x radiation interactions. 6) Whether results from studies of genetic susceptibility to high doses (e.g. therapeutic) of radiation can be interpolated to low doses. Consider for example problems (1) and (4). For any specific allele it may be difficult, because of sample size and power concerns, to evaluate the relationship between inheritance of a risk allele and its synergy with radiation, e.g. whether excess cancer risks due to both are additive, super-additive, multiplicative or super

multiplicative. However if individuals who (by virtue of their combined inherited risk alleles) are highly susceptible to cancer are also more susceptible to the effects of radiation, then statistical techniques exist that are both very powerful for detecting gene by radiation interactions [1] and for defining the "synergy" between radiation exposure and genetic susceptibility. Such analysis is based upon defining an appropriate risk score from known genetic variants and its power depends partly upon the range of susceptibility that this risk score encompasses. For some cancers very simple (log-additive) risk scores produce up to four-fold risk differences between individuals carrying "high" and "low" numbers of risk alleles (c.f. [2]). Evaluation of the synergy between such a risk score and radiation is feasible in many studies, even studies that are not large or powerful enough to support genome-wide efforts by themselves. Studies of the relationship between single alleles and radiation, and specifically the problem of discovering alleles that increase radiation-related risk but don't show strong effects in the absence of radiation exposure, is a difficult discovery problem. Even in a highly radiation exposed cohort, such as the WECARE Study [3], a much larger number of cases is required to detect such interactions than to detect main effects with comparable relative risks. The sample size requirements for interaction testing can be reduced by using exposure stratified matching such as counter-matching [4] in the design of the study and this has been done in the WECARE study specifically. The number of required cases can also be reduced (by approximately one half) if it can be assumed that exposure to radiation is independent of the genetic variant of interest so that a case-only analysis [5] can be relied on to provide a valid test for interaction. The assumption of independence of genes and radiation exposure may not always hold, but case only analyses should be used when it is deemed unlikely that genes directly affect the exposure probability. The main issue involved in using the case-only approach is probably not direct actions of genes on radiation exposure (possibly moderated by tumor type, in the therapeutic setting for example), which would seem to be rare events, but rather the potential confounding of genes with hidden population structure related to exposure probability. Control for hidden population structure can be accommodated in case-only analyses of GWAS data, perhaps with less loss of power than reverting to a case-control test. Empirical Bayes and Bayes model averaging approaches for combining case control and case only analyses to provide intermediately powered analyses is also a current topic in genetic epidemiology [6,7]. Another approach appropriate in the GWAS context entails a two-step analysis using a test of gene-environment independence in the combined case-control set to scan for possible interactions, following by conventional case-control testing of this subset; this can greatly improve power by requiring multiple testing correction only for the number of tests performed in the second step [8]. Regarding point (6) studies of high dose therapeutic radiation certainly have their place, and should be extended to other populations such as childhood cancer survivors. Clearly, however, the interpolation of high-dose to low-dose effects requires a leap of faith, specifically there may be alleles that interact with low-dose but not high-dose radiation that are undiscoverable in therapeutic studies: Overcoming the limitations involved in mounting a GWAS aimed at detecting new alleles that interact with low-dose exposure will be difficult, even the most feasible such studies - perhaps of CT radiation - requiring extremely large sample sizes and decades of follow-up. Evaluation in the low dose setting of interactions between radiation and genetic risk scores using alleles having important cumulative effects on individual susceptibility is much more feasible since the risk score approach (if appropriate) gives much more power than testing individual alleles for interactions. It may be possible to use high-dose data to get an appreciation of whether interactions without main effects seem common. If they appear to be highly unusual for high doses then this could have relevance for low-dose studies as well. References: 1. Chatterjee N, Kalaylioglu Z, Moslehi R, Peters U, Wacholder S. Powerful multilocus tests of genetic association in the presence of gene-gene and gene-environment interactions. *Am J Hum Genet* 2006; 79: 1002-16 [PMID: 17186459]. 2. Haiman CA, Patterson N, Freedman ML, Myers SR, Pike MC, Waliszewska A, Neubauer J, Tandon A, Schirmer C, McDonald GJ, Greenway SC, Stram DO, Le Marchand L, Kolonel LN, Frasco M, Wong D, Pooler LC, Ardlie K, Oakley-Girvan I, Whittemore AS, Cooney KA, John EM, Ingles SA, Altshuler D, Henderson BE, Reich D. Multiple regions within 8q24 independently affect risk for prostate cancer. *Nat Genet* 2007; 39: 638-44 [PMID: 17401364]. 3. Bernstein JL, Langholz B, Haile RW, Bernstein L, Thomas DC, Stovall M, Malone KE, Lynch CF, Olsen

JH, Anton-Culver H, Shore RE, Boice JD, Jr., Berkowitz GS, Gatti RA, Teitelbaum SL, Smith SA, Rosenstein BS, Borresen-Dale AL, Concannon P, Thompson WD. Study design: evaluating gene-environment interactions in the etiology of breast cancer - the WECARE study. *Breast Cancer Res* 2004; 6: R199-214 [PMID: 15084244]. 4. Andrieu N, Goldstein AM, Thomas DC, Langholz B. Counter-matching in studies of gene-environment interaction: efficiency and feasibility. *Am J Epidemiol* 2001; 153: 265-74 [PMID: 11157414]. 5. Piegorsch WW, Weinberg CR, Taylor JA. Non-hierarchical logistic models and case-only designs for assessing susceptibility in population-based case-control studies. *Stat Med* 1994; 13: 153-62 [PMID: 8122051]. 6. Li D, Conti DV. Detecting gene-environment interactions using a combined case-only and case-control approach. *Am J Epidemiol* 2009; 169: 497-504 [PMID: 19074774]. 7. Mukherjee B, Chatterjee N. Exploiting Gene-Environment Independence for Analysis of Case-Control Studies: An Empirical Bayes-Type Shrinkage Estimator to Trade-Off between Bias and Efficiency. *Biometrics* 2007 [PMID: 18162111]. 8. Murcay CE, Lewinger JP, Gauderman WJ. Gene-environment interaction in genome-wide association studies. *Am J Epidemiol* 2009; 169: 219-26 [PMID: 19022827].

(S604) Radiation-related contralateral breast cancer: genetic sources of susceptibility. Jonine Bernstein, Memorial Sloan-Kettering Cancer Center, New York, NY

Of the nearly 185,000 US women expected to develop breast cancer in 2009 and the over 2.4 million breast cancer survivors currently residing in the US, five to ten percent will develop a subsequent primary in the contralateral breast (CBC) (www.cancer.org). Epidemiologic studies have identified factors associated with an increased risk of developing CBC, including family history of breast cancer, early age at diagnosis, hormonal factors, tumor characteristics of the first primary, and mutations of specific genes including *BRCA1*, *BRCA2*, and *CHEK2*. Importantly, the treatment a woman receives for her first primary breast cancer can also influence her risk of developing a second breast cancer; chemotherapy reduces the risk of developing CBC, while the radiation received to the contralateral breast during radiotherapy increases the risk of CBC. We previously reported a 3-fold increase in risk of CBC associated with radiation dose of 1Gy or more to the contralateral breast among women under age 40 who survived at least 5 years from treatment. Despite the number of established risk factors for increased CBC risk, their combined effect accounts for only a small portion of the CBCs that develop each year. It is unclear whether, and to what extent, genetic factors and radiation, individually or via interaction, contribute to the development of radiation-induced CBC. A key unresolved question is whether individuals who carry defects in DNA repair genes and who are exposed to radiation are especially susceptible to radiation-induced breast cancer. To address this question, we initiated the WECARE (for Women's Environmental Cancer and Radiation Epidemiology) Study, a population-based nested case-control study, designed specifically to evaluate the possible interaction between genetic variation and radiation exposure on breast cancer risk. Recently, we initiated a two-stage genome-wide association study (GWAS) within the WECARE Study in order to identify novel causal genetic markers of both CBC and radiation-related CBC risk, factors that may also increase risk for breast cancer in general. Our hypothesis is that young women who carry particular genetic variants will be more susceptible to CBC and/or to radiation-induced breast cancer than are non-carriers. Our goal is to understand genetic and environmental factors that influence susceptibility to breast cancer. In this talk, I will describe our approach to building a comprehensive model of DNA damage response genes using candidate gene, pathway driven and GWAS approaches for gene discovery, validation, and gene characterization. Our findings will be discussed in the context of what is known about human susceptibility to radiation and the public health implications for the long-term clinical management of women with breast cancer and for targeting prevention efforts.

S7 IONIZING PARTICLES IN SPACE AND MEDICINE

In recent years, interest in and research into the biological effects of energetic charged particles has increased significantly on

two fronts: studies of possible effects of galactic cosmic rays and solar particle events on astronauts in space and investigations of the cell, tissue and organism responses to protons and carbon ions in radiation oncology. Although these enterprises encompass diverse research interests, there are also commonalities in terms of basic radiation chemical, biochemical and biological processes. This symposium will spotlight some of the cutting-edge work in radiation chemistry, physics, biology and medicine related to ionizing particles currently in internationally. The symposium will start off with a speaker discussing innovative approaches and results on basic DNA and cellular responses to ion irradiation (Taucher-Scholz). This will be followed by two speakers who will highlight research findings of relevance to astronauts in space – namely, potential for normal tissue damage (Blakely) and for induction of carcinogenesis (Shay). Subsequently, two speakers will address radiation oncology-related issues – predicting risk for second cancers from particle therapy (Paganetti) and clinical outcomes in patients treated with carbon ions (Mizoe). Together, the talks in this symposium should highlight the many opportunities for cross-fertilization between the space radiation and charged particle radiation oncology research communities and identify important research questions of relevance to both groups.

(S701) Spatiotemporal dynamics of DNA double-strand breaks in the context of chromatin. Gisela Taucher-Scholz¹, Burkhard Jakob¹, Joern Splinter¹, Kay-Obbe Voss¹, Marco Durante^{1,2}, ¹GSI Helmholtz Center for Heavy Ion Research, Darmstadt, Germany, ²Technical University, Darmstadt, Germany

Charged particles induce highly localized DNA damage including spatially correlated double-strand breaks (DSBs) that are related to the effectiveness of carbon ions in tumor therapy but also to the biological risks of charged particles during space travel. Heavy ion damage tracks have proved useful to study the spatiotemporal dynamics of radiation-induced foci during lesion processing. DSB markers (e.g. gamma-H2AX, 53BP1) and micro-foci forming repair proteins (RPA or XRCC1) were analyzed in immunostained or living cells. Live cell imaging over 40h revealed a restricted mobility of damaged chromatin, independent of lesion density and irradiation. This positional stability of DSBs points out the need of lesion proximity for the induction of chromosomal translocations. The pattern of foci along tracks however not always reflected DSB numbers, but depended on chromatin structure. The repair proteins were mostly found at intermediate DNA densities or adjacent to DNA intensity maxima. Mouse embryonic fibroblast cells containing highly compacted heterochromatin (HC) regions (chromocenters) were irradiated with linear ion tracks to compare the damage response in euchromatic and heterochromatic chromatin. We found (at 1h postirradiation) most of the gammaH2AX streaks bending around HC compartments, with only few weaker signals within HC, suggesting a relocation of damage sites from the initially induced linear track to the periphery. The fraction of gammaH2AX streaks bent around HC increased with time, as did HC-associated streaks, due to the slower repair of ion-induced damage within HC. To address the early damage response in HC we used single ion microbeam irradiation to produce localized DSBs directly within murine chromocenters. Unexpectedly, at early times H2AX was indeed phosphorylated within this highly compacted chromatin, demonstrating the accessibility to repair proteins. Remarkably, the damage site was subsequently expelled from the centre to the periphery of chromocenters within ~20 min. A local chromatin decondensation measured at the ion-hit sites could give rise to physical forces potentially involved in heterochromatic damage movement. This dynamics reconciles the previously observed lack of H2AX phosphorylation within heterochromatin and the here reported DNA damage response.

(S702) Charged particles and the crystalline lens. Eleanor A. Blakely, Lawrence Berkeley National Laboratory, Berkeley, CA

The lens is the most radiosensitive structure of the eye and can be at risk for late effects from radiotherapy treatments for cancer, or due to occupational exposures including air and space

travel. Cataract has been the late radiation effect of concern and has long been recognized as distinct from senile cataracts experienced by most individuals in their 6th or 7th decade of life. The distinction between aging- and radiation-induced cataract has been made primarily based on the anatomical location of the opacities, without a complete understanding of the different mechanisms underlying their different etiologies. There is an extensive literature evaluating cataract prevalence or incidence after exposure to a staggering array of biological models, radiation types and doses, and dose-fractionation regimes, but little has been understood about the molecular and cellular events occurring during the “latency” period preceding the appearance of the cataract. The availability of cultured human lens epithelial cells grown *in vitro* on extracellular matrix derived from bovine corneal endothelial cells and able to differentiate to lens fiber cells opened the possibility to investigate early molecular and cellular events that occur following radiation exposure. Supported by NASA these studies focused on the effects of charged particle beams. Studies on particle beam-induced changes in gene and protein expression as detected in this cultured model have also been investigated in both mice and rats to demonstrate the link to lenticular opacifications *in vivo*. Emerging epidemiological evidence is pointing to the need to reevaluate the present guidelines for radiation exposures to the lens, and it is hoped that a more complete understanding of underlying molecular and cellular events that lead to the appearance of mixed cataract phenotypes after radiation exposure will allow the development of biological countermeasures to prevent cataract. In addition, recent published clinical work has also linked lenticular opacities to Alzheimer’s Disease and Down’s Syndrome. More basic research is needed to understand how radiation alters normal lens homeostasis and the molecular links to aging and disease. This work was supported by NASA Grant #NNJ07HC791 and the US Department of Energy Grant DE-AC02-05CH11231.

(S703) Human Epithelial Cell Cultures and Mouse Models of Cancer to Assess Cancer Risk from Charged Particle Irradiation. Jerry W. Shay, University of Texas Southwestern Medical Center, Dallas, TX

Most previous studies on human cells and mice to assess risks of cancer initiation and progression from exposure to space radiation have utilized normal cells and mice. To see carcinogenesis affects, scientists have often resorted to using very large single doses and energies, but this is unlikely to represent the reality of irradiation exposure on long-term space missions. It is believed that much lower doses of mixed field charged particles will be present. Also, since the average age of a typical astronaut is well over 40 years of age, there is a high probability that some initiated but not cancer progressed cells will be present and subject to irradiation induced damage in space. To better assess risks, we have used hTERT immortalized human cells expressing well defined loss and gain of function changes in 2D and 3D culture to determine DNA damage and repair as well as cancer progression using well established biological cell transformation assays. In addition, we have used mouse models that are susceptible to cancer to determine if the incidence of cancer initiation or cancer progression is affected by single acute compared to fractionated/protracted doses of irradiation. An update on our human cell and mouse experiments will be presented. In addition, we have been investigating barodoxyline methyl (BARD) a putative biological countermeasure and mitigator of radiation-induced neoplastic transformation of normal human epithelial cells. BARD (also termed RTA402 and CDDO-Me) is able to partially protect immortalized human colonic (HCEC) and bronchial (HBEC) epithelial cells against radiation-induced DNA double-strand damage and transformation. Immortalized HCECs can be experimentally transformed with exposure to 2 Gy of Proton (1 GeV/n) followed 24 hours later by 50 cGy of ⁵⁶Fe (1GeV/n). After approximately two months of continuous culture following irradiation, cells showed an increase in proliferation rate and in both anchorage-dependent and anchorage-independent colony formation ability. Pre-treatment of cells with 50nM BARD which has been shown to activate Nrf2 (which controls the production of over 250 antioxidant and detoxification enzymes) significantly reduced radiation-induced neoplastic transformation. BARD also mitigates radiation-induced cell transformation by

treatment within 30 minutes after gamma-irradiation. BARD is an oral available non toxic compound that is currently in Phase IIB clinical trials in patients with diabetic nephropathy and has been shown to improve renal function. An update on these experiments will be presented. Research support by NASA grants, NNJ05HD36G, NNX08BA54G & NNX09AU95G

(S704) Predicting the risk of developing a radiation-induced second cancer when treating a primary cancer with radiation. Harald Paganetti, Basit S. Athar, Massachusetts General, Boston, MA

There is a growing concern regarding radiation-induced cancers among long-term survivors of radiation therapy. This risk pertains to tissues adjacent, near, and distant from the target receiving high, intermediate, and low doses, respectively. It has been cautioned that, compared with conventional radiation therapy, the use of IMRT or proton therapy could result in a higher incidence of radiation-induced second cancers. The overall dose distributions between IMRT and proton therapy are quite different. Typically, IMRT treatment plans require more fields than proton treatment plans to reach comparable dose conformity. In addition, photon beams do not stop in the patient. However, while proton therapy allows a lower integral dose compared to photon therapy, it can potentially cause neutron-generated dose outside of the treatment field. This presentation will outline the dosimetric characteristics of scattered and secondary radiation as a function of various treatment parameters. As dose distributions within the human body are not directly measurable one must rely to a large extent on Monte Carlo radiation transport simulations. Furthermore, absorbed doses have to be converted into equivalent doses despite considerable uncertainties in neutron radiation weighting factors. Simulations to determine organ-specific equivalent doses as well as models to translate organ-specific equivalent doses into cancer risks will be outlined. Different risk models need to be applied in order to estimate the risk in high or intermediate dose regions as compared to the risk in low dose regions. Finally, the latest modeling results on radiation induced cancer estimations for pediatric patients will be presented. It seems that there is a distinct advantage of proton beams in high and intermediate dose regions while in low dose areas scattered doses in IMRT might be comparable to secondary doses in passive scattered proton therapy. Data will be presented that demonstrate how the treatment plan and the patient’s age influences the risk for a second cancer.

(S705) Carbon ion radiotherapy for skull base chordoma. Jun-etsu Mizoe¹, Hirohiko Tsujii², Azusa Hasegawa², Roberto Orecchia¹, ¹Fondazione CNAO (Centro Nazionale de Adroterapia Oncologica), Pavia, Italy, ²NIRS, Chiba, Japan

Skull base chordomas are rare tumors originating from ectopic remnants of the embryonal notochord at the sphenoid-occipital synchondrosis. Because the tolerance doses of surrounding normal tissues are lower than the doses needed for tumor control, the required high local doses are often difficult to apply by conventional XRT. It is clear that the charged particle therapy is a more appropriate radiotherapy for the skull base chordoma than XRT because of excellent dose distribution. Clinical evidence of proton therapy, alone or combined with photon therapy, showed excellent tumor control and minimized normal tissue morbidity. However, it has been pointed out that in certain patient groups it is difficult to achieve local control with proton radiotherapy even at elevated doses. The high biological effectiveness of carbon ion radiotherapy has therefore a promising potential for these intractable skull base and paracervical chordomas. Between June 1995 and June 2007, a total of 34 cases in 33 patients with the chordoma of the skull base (27 cases) and the paracervical spine (7 cases) were treated by CIRT at the National Institute of Radiological Sciences (NIRS) in Chiba, Japan. During the past period, there were three protocols historically (a pilot study, a phase I/II dose escalation study and a phase II study). All of the patients were treated by 16 fractions for four weeks with a total dose of 48.0, 52.8, 57.6 and 60.8 GyE respectively. There was no grade 3 or higher grade acute skin and

mucosal reactions. Also there was no grade 2 or higher grade late skin and mucosal reactions. The 5 year local control rate of 19 cases treated with 60.8 GyE showed 100% and that of 15 cases treated by 48.0 ~ 57.6 GyE showed 78% (SE; 11%) (p=.2664). The 5 year overall survival rate of 19 cases treated with 60.8 GyE showed 94% (SE; 5%) and that of 14 cases treated by 48.0 ~ 57.6 GyE showed 86% (SE; 9%) (p=.7399). As a result of the dose escalation study of CIRT for skull base tumors, a dose fractionation of 60.8 GyE/16 fractions/4 weeks was decided as the recommended dose because of acceptable normal tissue reactions and good local tumor control. Preliminary results of the phase II clinical study of CIRT for skull base chordoma showed that the 5 year local control is 100% and normal tissues showed a mild reaction without any severe morbidity of important organs.

S8 ELEMENTARY PROCESSES IN DNA DAMAGE FORMATION

A large fraction of ionizing radiation events are deposited in clusters, even for low LET radiation. The degree to which the track expands, and, thereby, whether or not the final damage in DNA is clustered, depends on elementary processes that occur in under a second. Key processes include electron, hole, proton, and excitation transfer reactions.

(S801) Various modes of DNA damage formation by the direct effect of radiation. Akinari Yokoya, Japan Atomic Energy Agency, Ibaraki, Japan

Ionizing radiation induces a variety of molecular changes in genomic DNA through both direct ionization of DNA and indirect reactions with diffusible OH radicals. These reactions are often deleterious, resulting in strand breaks, base lesions, apurinic/apyrimidinic (AP) sites and inter- or intra-strand cross-linkages. Numerous studies have verified the yield and the induction mechanisms of strand breaks, particularly double-strand breaks, as it is thought that they represent one of the major types of damage that are involved in cell lethality. Recently, base lesions and AP sites have also been considered to play an important role as constituent lesions of clustered DNA damage sites. Biochemical experiments using synthetic oligonucleotides containing specific base lesions, AP sites, or single-strand breaks (SSBs) transformed into *Escherichia coli* cells have revealed that certain configurations strongly inhibit the base excision repair activity of cells. Here, we attempted to clarify whether the yields of base lesions and strand breaks were dependent on ionization modes by subjecting dry DNA films to monochromatic soft X-rays and high LET ion beams generated from accelerator facilities. It was revealed that the yields of induced base lesions, as measured using base excision glycosylases as enzymatic probes, at the oxygen K-edge (560 eV) were approximately 10- to 30-fold higher than the yields observed at energy levels below the nitrogen K-edge (380 eV). In addition, the yield of SSBs was also enhanced at the oxygen K-ionization edge, but was only two-fold higher than the controls. We also found that base lesions induced in fully hydrated DNA by irradiation with He ions at ~ 120 keV/μm are only processed to a limited extent by base excision glycosylases. The experimental evidence presented here was used to evaluate and determine the various modes of radiation-induced base lesions and strand breaks. New methods developed for the visualization of clustered SSBs and base lesions, which are poorly detected by conventional plasmid DNA assays, are also presented. Finally, the preliminary data obtained from DNA denaturation treatments using these new techniques are also discussed in comparison with the relative data from previous studies.

(S802) Ionization and excitation induced free radical pathways in DNA radiation damage processes. Michael D. Sevilla, Amitava Adhikary, Anil Kumar, Deepti Khanduri, Oakland University, Rochester, MI

Direct type effects of high energy radiation induce ionizations and excitations within DNA that result in cation and anion radical intermediates and their excited states. The chemical reaction pathways of the initial ion radicals are now increasingly well understood. Especially significant is the role of the protonation state of one-electron oxidized or reduced DNA as it is critical to subsequent processes such as charge transfer and reactivity. The detailed understanding of prototropic equilibria in one electron oxidized and reduced oligos is of substantial importance. In our recent efforts, we have identified four protonation/deprotonation states of the one-electron oxidized GC base pair : G^{•+}:C, G(N1-H):C(+H⁺), G(N1-H):C, and G(N2-H):C in oligos, e.g., in d[TGCGCGCA]₂. Employing selective deuteration of the H-atom at C8 in the guanine moiety, both the site of localization of the hole and the protonation state of the hole at that site can be determined. These results provide valuable insights into the chemical pathways involved in the formation of damaged products involving G. However, reactions of ion-radical in their ground state do not fully account for the DNA products formed and ion radical excited states are now increasingly implicated in the mechanisms of radiation-induced DNA damage. Excited states of DNA base cation radicals have been shown to lead to sugar radicals that result in strand breaks. Further, the interaction of low energy electrons with DNA produces anion excited states which are now understood to be highly reactive and have been experimentally found to result in strand breaks in DNA. These pathways will also be discussed with emphasis on the mechanisms of action and their relative significance and with the latest experimental and theoretical evidences. Supported by NIH NCI RO1CA045424.

(S803) The spork. Not exactly the cutting edge of DNA damage. Trinh T. Do, Vicky J. Tang, Joseph A. Aguilera, Jamie R. Milligan, University of California at San Diego, La Jolla, CA

The direct effect of ionizing radiation results in electron removal from DNA itself. The resulting electron deficient sites (called holes) exhibit a preference to relocate to guanine bases (to form a guanyl radical), because these are the most easily oxidized sites and therefore the most stable location available in DNA for the holes. However other even more favorable locations exist in several functional groups which are present in chromatin in close proximity to the DNA. One important example appears to be tyrosine residues present in DNA binding proteins. The tyrosine side chain has a phenolic structure. In donating an electron to a DNA guanyl radical a phenol must also lose its hydroxylic proton. These electron and proton transfer steps appear to be mechanistically linked, reminiscent of the spoon fork hybrid the spork. Nearby proton acceptors might be expected to increase the rate of proton loss and therefore of electron transfer to DNA. We have tested this hypothesis by comparing the reactivity of the phenol derivatives 2- and 4-hydroxybenzoate with DNA guanyl radicals. When compared with suitable control compounds, the faster reaction of the former confirms the hypothesis. The implication is that tyrosine residues with their hydroxyl groups hydrogen bonded to proton acceptors such as aspartate or glutamate may be kinetically competitive in scavenging or repairing the hole in DNA before it can be trapped to form DNA damage. Supported by PHS grant CA46295.

(S804) Fast chemical repair of radiation damage to DNA by bound and unbound antioxidants. Robert F. Anderson¹, Sujata S. Shinde¹, Andrej Maroz¹, Roger L. Martin², ¹University of Auckland, Auckland, New Zealand, ²Peter MacCallum Cancer Centre, Melbourne, Australia

The radiolysis of aqueous solutions leads to the formation of reactive oxygen species (ROS) as well as certain radical anions, e.g. the carbonate radical (CO₃^{•-}); species which are also formed by continual oxidative stress. Such oxidising species/radicals react with DNA by electron transfer and create what are known as 'holes,' either directly on guanine (G), or through hole transfer from other base radicals as the neutral guanyl radical, G(-H); possesses the lowest radical reduction potential, E(1)R, of all the DNA bases. Changes in the structure of G(-H) (formed upon the rapid

deprotonation of the initial guanyl radical cation in the GC pair) with time, have been investigated by comparing experimental UV-VIS spectra with DFT calculated spectra. Other radicals can react with DNA by an inner sphere mechanism, e.g. by H-atom abstraction by the $\cdot\text{OH}$ radical. As radical species formed on DNA are relatively long-lived (seconds), this opens up the possibility for the fast chemical repair of such radicals by small concentrations of antioxidants. Intramolecular electron transfer from DNA-bound antioxidants to G(-H) \cdot , and the bimolecular reaction between unbound antioxidants and radical sites on DNA need to be considered. The driving force for such antioxidant reactions is the ΔE between the $E(1)R$ value of G(-H) \cdot and those of the antioxidant radicals. Using pulse radiolysis we have determined the $E(1)R$ values of G(-H) \cdot in DNA and for a series of Hoechst-type, bisbenzimidazole ligands bound in the minor groove of DNA. By observing electron transfer from these ligands to G(-H) \cdot (hole transfer to the ligands), we find that such a reaction is barrier controlled with the rate, k , being best described by the relationship $k = k_0 \exp(\text{constant}/R)$, where k_0 is the rate constant for surmounting the barrier in the absence of perturbation by the ligands and R is the average distance between the bound ligands and G(-H) \cdot . The fast chemical repair of DNA radicals by freely diffusing antioxidants is influenced by steric and electrostatic factors as well as the $E(1)R$ of the antioxidant radicals. Flavonoid compounds are found to act as antioxidants in the repair of $\cdot\text{OH}$ radical-damaged sites on DNA, reducing the amount of base damage and strand breakage, whereas vitamin C does not. The concept of flavonoid compounds being 'pivotal' antioxidants will be discussed.

S9 BIODOSIMETRY FOR UNPLANNED RADIATION EXPOSURES TO LARGE POPULATIONS

An adequate response to events where large numbers of people are potentially exposed to levels of radiation sufficient to cause the ARS requires the rapid and efficient identification of individuals with clinically significant exposures. The session considers the likely key to this problem, Biodosimetry based on direct measurements of individuals.

(S901) Overview of biosimetry and the niches in which it is utilized. Harold M. Swartz, Benjamin B. Williams, Ann B. Flood, Dartmouth Medical School, Hanover, NH

The need for biosimetry arises from the great need for information on radiation doses to individuals following the potential exposure of large numbers of individuals, combined with the lack of methods to obtain this estimate by other means. This information is needed for acute exposures that may be sufficient to lead to the acute radiation syndrome and also for lower doses that may result in long term consequences. The information is needed for dealing with the potential consequences to individuals and also for understanding the probability of long term effects from the "natural experiments" resulting from the exposures of populations to radiation. The needs for the measurements of acute exposures include for triage to enable the response system to cope with the large numbers of individuals effectively and efficiently, and also for management of individual patients. Depending on the circumstances in the use for triage there may be a need for rapid screening in the field or, if there is not severe local disruption, it may be possible to proceed more deliberately and obtain the results from samples that are processed elsewhere. There are two types of biosimetry: 1) based on physical changes in tissues (detected by techniques such as EPR or luminescence). 2) based on changes in biological parameters such as gene activation or chromosomal abnormalities. The biologically based parameters are potentially very sensitive, but may require time for the changes to occur via biological processing and may be affected by other perturbations that may be associated with an acute event including stress, wounds, and burns. The physically based methods are not subject to these limitations but may not fully reflect the biological implications of some of the biologically based methods. Characteristics of types biosimetry include differences in capacity, requirements for specially trained personnel, field

deployability, interval before measurement can be made, interval before results are available, precision, applicability to the population, response to the energy of photons, response to neutrons, determination of dose distribution, and variation in response among individuals. Considering all of the above, several conclusions can be drawn: 1. The applicability of a particular type of biosimetry will depend on the characteristics of the particular event. 2. It is unlikely that any single type of biosimetry will be the method of choice for most situations. 3. Some types of biosimetry may be the method of choice for particular situations. 4. The best approach is likely to be the use of more than one type of biosimetry. 5. Decisions on the use of particular types of biosimetry methods will be facilitated by knowledge of their detailed characteristics. 6. The employment of biosimetry should be integrated into other types of information that bear on the exposure doses of the particular event. Research Support by NIH (U19AI067733) and DARPA (HR0011-08-C-0022 and HR0011-08-C-0023)

(S902) High-throughput radiation biosimetry using gene expression signatures. Sally Amundson, Columbia Univ. Medical Center, New York, NY

Gene expression is extremely responsive to many types of stress, including ionizing radiation exposure. There is also accumulating evidence that it may be possible to define gene expression signatures that are stress type specific. Lymphocytes are an extremely sensitive tissue in terms of gene expression responses. This, coupled with the relative ease of obtaining blood specimens compared with other tissues, makes gene expression in peripheral blood an attractive potential method for biosimetry. Our laboratory has been developing gene expression signatures of radiation exposure as potential biosimeters. We have also been collaborating in the development of self-contained automated assay systems suitable for making rapid gene expression measurements in the field. Together, these approaches could provide a biosimetry solution for large-scale triage in a radiological or nuclear event. This presentation will cover some of the key developments in this research, including a basic radiation dosimetric signature that correctly classifies samples by dose with up to 98% accuracy, and which performs with similar accuracy when transported to new data sets derived from different donors, dose ranges, disease states, and *in vivo* exposures. The performance of the radiation response appears to be robust against such potential confounders as smoking status and gender, and we are continuing to explore other conditions that may interfere with accurate biosimetry using this approach. Although many challenges remain in this field, progress continues to be extremely encouraging.

(S903) In vivo EPR radiation biosimetry: Overview and progress towards field deployment. Benjamin B. Williams¹, Ruhong Dong¹, Roberto J. Nicolalde¹, Tim Reynolds¹, Piotr Lesniewski¹, Oleg Grinberg², Jason Sidabras³, James Hyde³, Harold M. Swartz¹, ¹Dartmouth Medical School, Hanover, NH, ²Clin-EPR, LLC, Lyme, NH, ³Medical College of Wisconsin, Milwaukee, WI

In order to meet the potential need for emergency large-scale radiation biosimetry following an accident or attack, we have developed *in vivo* EPR instrumentation and methodology for the quantification of radiation-induced radicals within intact teeth and fingernails. These techniques have several very desirable characteristics for triage, including: independence from confounding biologic factors; non-invasive measurement procedures; the capability to make measurements over wide periods in time after the event; providing immediate estimation of the dose; and the ability to perform measurements with non-expert operators at the site of an event. Throughout development there has been a particular focus on the need for a deployable system, including instrumental requirements for transport and field use, the need for high throughput, and use by minimally trained operators. We have produced and tested an operational and deployable L-band (1200 MHz) system for tooth dosimetry based on a 60 lb dipole permanent-magnet with a 17 cm gap which was designed to minimize weight, while maintaining

adequate accessibility, and having a suitably sized region of magnetic field homogeneity. The electronics for EPR detection and sweeping of the magnetic field are contained in a single deployable instrument rack which can be powered using the public electric supply or a generator. The fully integrated software and hardware components of the instrument allow for complete automation of the data acquisition procedure and enable reliable use by operators without specialized training. The collection and analyses of sets of three serially-acquired spectra with independent placements of the resonator in a data collection process lasting approximately five minutes provides dose estimates with standard errors of prediction in the range of 0.5 - 1 Gy. Numerous measurements have been performed using this system in clinical and other non-laboratory settings. *In vivo* measurements have been performed using all types of teeth in normal, unexposed populations as well as patients undergoing radiation therapies. As an example, measurements were performed on incisor teeth of subjects who had either received no irradiation or 2 Gy total body irradiation for prior bone marrow transplantation; this exercise provided a direct and challenging test of our capability to identify subjects who would be in need of acute medical care. Additional studies performed to evaluate the effects of cosmetic whitening and UV illumination during dental procedures indicate that the effects of common dental and environmental exposures will not significantly confound dose estimation at the levels of interest. Based on ROC analysis and a projected distribution of exposures following a nuclear detonation, the system appears to be capable of providing the sensitivity and specificity needed for effective screening for exposures associated with acute radiation syndrome. Instrumentation and methodology for *in vivo* fingernail dosimetry at X-band are also being developed for measurements of intact nails. *In vivo* measurements of intact nails have been enabled through the development of novel resonator structures where the microwave field is restricted to the nail volume. Together with biologically based radiation biodosimetry methods, as well as EPR measurements of isolated fingernail clippings, these approaches would help enable a rational response to a catastrophic radiation event. Supported by NIH U19AI067733 and R43AI081495, DARPA HR0011-08-C-0023 and -0022

(S904) Ex Vivo Radiation Biodosimetry: Assays Based on an Internal and External Biomarker. Steven G. Swarts¹, Yansong Guo², Xiaoming He³, Paul Okunieff¹, Harold Swartz³, Dean Wilcox³, Lurong Zhang¹, Stephen Zhang¹, ¹University of Florida, Gainesville, FL, ²University of Rochester, Rochester, NY, ³Dartmouth College, Hanover, NH

The challenge in a radiological mass exposure event is estimating the dose that each individual in this population has received within 1-3 days post-exposure. In such an exposure scenario, standard dosimetry methods will not be available for estimating dose. Instead, individual dosimetry estimates will need to be calculated on the basis of dose-dependent changes either on or within the exposed individual. These methods must be portable and capable of either rapid (< 15 min) measurement times from sampling to dose estimate or provide high throughput sample processing capabilities. To this end, a number of methods are in various stages of development that rely on dose dependent chemical alterations in biomaterials or biological responses. Two examples of *ex vivo* biodosimetry assays for measuring dose dependent changes in an internal and external marker will be presented here. A measure of dose-dependent radiation-related toxicity is the release of dsDNA into plasma as a consequence of IR-induced cell death is one internal marker with potential of functioning as the basis of a rapid biodosimetry assay. Radiation-induced cell death is influenced by both apoptotic and non-apoptotic mechanisms. It is postulated that during cell death, cells release DNA into the circulation system. Methods for measuring the dose dependent changes in the IR-induced plasma DNA concentration have been developed and include PCR, DNA binding fluorescent probes, and nucleotide binding that incorporate B-DNA technology for signal amplification. The differing quantitative methods will be compared and discussed within the context of meeting the needs of field deployable and rapid biodosimetry assays. Likewise, a complimentary but external biodosimetry approach will be discussed in the same context which relies on IR-induced chemical changes in keratin and other proteins in finger or toe nails. Of specific interest

are the electron paramagnetic resonance (EPR) measurements of the signal produced from the quasi-stable IR-induced free radicals formed in these proteins. The radiation-induced signal (RIS) is predominantly a singlet. The intensity of the singlet shows a linear dose dependence at doses under 10 Gy. Because the EPR method uses *ex vivo* measurements of RIS in nail clippings, there is a signal from mechanically-induced radicals (MIS) generated at the shear edge of the clipping. The MIS signal contains spectral features that overlap with the RIS signal. To measure the RIS in clipped nails, several approaches have been examined and will be described for removing the MIS without adversely affecting the RIS. The combination of the two biodosimetry methods provides an ability to independently estimate dose in an individual exposed to IR, and may also provide assessment of additional damage in the individual, for example from combined injury (i.e. radiation exposure and trauma and/or burns).

(S905) Protein biomarkers as a complementary approach to conventional biodosimetry for radiation injury and exposure dose assessment. Natalia I. Ossetrova, David J. Sandgren, Arifur Rahman, William F. Blakely, AFRRRI/USUHS, Bethesda, MD

Terrorist attacks or nuclear accidents could expose large numbers of people to ionizing radiation. Optimal medical management of radiological terrorism and accidental irradiation situations would include use of validated biomarkers of radiation injury and exposure dose received by victims with an extremely high precision in order to distinguish non-exposed vs. exposed individuals, as well as to provide rapid diagnostic information for triaging of exposed individuals. We recently reported results from a murine total-body irradiation (TBI) model demonstrating for the first time that a protein expression profile (GADD45 α , IL-6, and SAA) measured in samples collected 1 and 2 d after exposure can predict mice exposed to radiation but also can distinguish the level of radiation exposure, ranging from 1 to 7 Gy ⁶⁰Co γ rays (0.1 Gy/min). The SAS-based algorithm was established for early (1 and 2 d) dose assessment and dose-dependent discrimination of study animal groups. Effect of combination of SAA and hematological biomarkers demonstrated: (1) an enhanced separation of 1-Gy irradiated animals from controls and also between different combinations of doses, and (2) an improvement of the threshold for γ -exposure detection compared to the selected protein profile only. Here in, we present similar results from the on-going nonhuman primate TBI radiation model using 30 rhesus macaques irradiated to a broad dose range of 1 to 8.5 Gy with ⁶⁰Co γ -rays (0.55 Gy/min) dose- and time-dependent changes in blood proteins CRP, Flt-3 ligand, IL-6, and GADD45 α measured by enzyme linked immunosorbent assay (ELISA). The combination of biomarkers provides greater accuracy than any one biomarker alone. The results also show that the dynamics and content of CRP and Flt-3 ligand levels reflect the course and severity of the acute radiation sickness (ARS) and may function as prognostic indicators of ARS outcome. These results demonstrate proof-in-concept that these radiation-responsive proteins show promise as a complimentary approach to conventional biodosimetry for early assessment of radiation exposures and as may also contribute as diagnostic indices in the medical management of radiation accidents. [AFRRRI supports this research under project RBB4AR; DARPA under MIPR entitled: "Nonhuman Primate Testing for Biodosimetry"].

S10 WHEN IS LOW DOSE-RATE RADIATION HARMFUL TO HEALTH?

Protective adaptive responses have been demonstrated for health outcomes after low dose radiation exposure. Dose and dose-rate thresholds are crucial for the type of biological responses elicited. This symposium will focus on very low doses as well as upper and lower dose thresholds which do, and do not, induce adaptive responses *in vitro* and *in vivo*.

(S1001) Dose and dose-rate thresholds for radiation-induced neoplastic transformation *in vitro*. J. Leslie Redpath, Eugene Elmore, Univ of California Irvine, Irvine, CA

Neoplastic transformation *in vitro* has proven to be a useful assay with which to explore the effects of low doses of ionizing radiation in the context of cancer induction. The fact that there is a baseline level of spontaneous neoplastic transformation has allowed for the detection of hormetic effects resulting in the suppression of transformation frequencies to levels below that seen spontaneously resulting in a J-shaped dose-response curve. It is thought that this is due to low dose induction of an adaptive response. Such an adaptive response can be the consequence of multiple mechanisms. Threshold doses for induction of transformation can be delineated as a function of dose-rate. The data indicate that such thresholds can range from ca. 100 mGy to > 1000 mGy as dose-rate is decreased from 100 mGy/min to 0.2 mGy/min. An interesting question is whether there is a dose-rate below which no adaptive response is induced. Preliminary evidence suggest this may be the case when the dose-rate is reduced below 1 mGy/day of low-LET radiation, a dose-rate that is of the order of 300 to 3000-fold greater than the range for natural background radiation. Many of the low dose and dose-rate effects seen *in vitro* have also been seen *in vivo*, including in epidemiologic data. Supported by the U.S. Department of Energy and N.A.S.A.

(S1002) Upper and lower dose thresholds for risk. Ron E. Mitchel, Atomic Energy of Canada Limited, Chalk River, ON, Canada

The current radiation protection system assumes that any radiation exposure can only increase risk, in a manner directly proportional to dose, without a threshold. While founded on well established risk outcomes from high dose exposures, the radiation protection system is assumed to also predict and protect against risks from low dose exposures. However, extensive *in vitro* and *in vivo* evidence indicates that at low doses this assumption is incorrect. Low doses induce protective responses that can reduce, rather than increase risk. A transition between increased risk at high doses and reduced risk at lower doses implies the existence of an upper dose threshold for risk. Since the protective responses induced by low doses are part of a general response to stress, a dose too low to induce this stress response may not induce protective effects, implying that lower dose thresholds for risk can also exist. This presentation will describe evidence for the existence of both upper and lower dose thresholds for risk *in vivo*, and examine some factors that influence those thresholds.

(S1003) Radiation Dose Dose-Rate Effectiveness Factor (DDREF) and Dose-Rate Effectiveness Factor (DREF): How big should they be? Antone L. Brooks, Washington State University Tri-Cities, Richland, WA

The slope of the dose-response relationship for cancer induction from the A-bomb data is non-linear. To estimate the risk in the low dose and dose-rate region the slope in the high dose region is multiplied by a Dose, Dose-rate, Effectiveness Factor (DDREF). Currently the recommended values of this factor are from 1.5-2.0. This paper evaluates the molecular, cellular, animal and human data to evaluate the magnitude of the DDREF and the DREF. Molecular, cellular and animal data suggest that the Dose-Rate Effectiveness Factor (DREF) may be large and variable. This paper evaluates life time data from dogs exposed to low LET radiation and the influence of dose-rate on the responses. Following high doses delivered at low dose-rate that the survival and cancer responses are much lower than observed following high dose rate exposures. It was noted that the adaptive response is present following both high and low dose-rate exposures and that in many cases the response is decreased below that in the controls. The DREF for cancer in dogs with protracted exposures in the high dose region was high as 35. The data suggest a need to reevaluate the current values used for the DDREF and illustrated that the DREF is very high following protracted exposure from internally-deposited radioactive materials.

(S1004) The relevance of bystander effects at the low dose-rates relevant to human exposure. Benjamin J. Blyth, Flinders University and Medical Centre, Adelaide, South Australia, Australia

The potential for communication from irradiated cells to neighbouring or distant cells has been firmly established. Within tissues irradiated at high dose-rates, the only communication is from irradiated cells to other irradiated cells, since no unirradiated cells remain. Bystander effects (effects transmitted from irradiated to neighbouring unirradiated cells) are thus by definition, a low dose, low dose-rate issue. Systemic or long-range effects originating from high dose irradiated tissues following partial body exposures are a distinct phenomenon, and such abscopal effects should not be considered interchangeably with bystander effects. Having shown that irradiated cells can communicate with their unirradiated neighbours, the question now turns to 'Do bystander effects induced in unirradiated cells alter carcinogenic risk *in vivo*?' For both low- and high-LET radiations the relevant human exposure scenarios for which bystander effects are applicable, are at dose-rates/fluences low enough to spare a significant number of cells within an irradiated tissue from ionising track traversal. Most high-LET bystander experiments work in this range (1 particle per hit cell, <100% of cells hit). However there have been few low-LET bystander experiments where cellular absorbed doses commensurate with single electron track traversals have been studied, and few experiments where only a small fraction of the cells receive energy depositions. Very few bystander experiments have been conducted *in vivo*. Although the effects of cell-cell communication in high dose irradiated tissues and abscopal effects in partial body irradiations are important scenarios to explore, the potential for bystander effects to alter carcinogenic risk after low dose exposures must be evaluated in the context of relevant human exposure scenarios. This paper will discuss the human exposure scenarios that should be the focus of future research, and *in vivo* models that could be utilised to further investigate bystander effects after low dose radiation exposures. This work is funded by the Low Dose Radiation Research Program, BER, US Dept of Energy, Grant # DE-FG02-05ER64104.

S11 RADIATION TREATMENT FACTORS: EFFECTS ON IMMUNE AND NORMAL TISSUE RESPONSES

There is a growing appreciation that tissue responses to radiation are the result of a complex cross-talk between parenchymal, stromal and inflammatory/immune cells. Clearly, based on the extent of parenchymal cell death and potential ability of a tissue to regenerate, some predictions can be made about the likelihood of functional recovery in normal tissue following lethal doses of radiation. However, the range of adaptive responses that take place under conditions of less severe damage is not well understood. Importantly, acute as well as chronic tissue responses to radiation are largely the result of activation of canonical pathways of response to damage: damage is perceived by the innate immune system as any loss of integrity by a tissue that results in release of damage-associated molecular pattern (DAMP) molecules. The aim of the ensuing inflammatory reaction is to restore homeostasis. However, micro-environmental cues, such as cytokine and chemokine expression, that are released by parenchymal, stromal and immune cells play an important role in shaping the direction of the response and can promote different outcomes. More importantly, treatment variants, such as dose, regimen of delivery, radiation intensity and quality (high versus low-linear energy transfer (LET) particles), have been found to also affect tissue response. Improved understanding of not only the molecular mechanisms that regulate tissue responses to radiation, but also how these mechanisms are affected by conditions found in the clinic, will provide new and well reasoned therapeutic targets to prevent undesirable outcomes such as carcinogenesis and fibrosis, and improve functional recovery. The four speakers in this symposium will discuss the complex interactions between the parenchymal, stromal and inflammatory cells that take place following radiation therapy, including the response to tissue damage and its regulation by the immune system, the radiation

biology of the hemopoietic tissues, and the effects of proton radiation on the immune system.

(S1101) Radiation treatment factors and cellular response.

Richard P. Hill, Ontario Cancer Institute/Princess Margaret Hospital, Toronto, ON, Canada

The early success of the linear-quadratic model in predicting the fractionation response of many normal tissues led to the hypothesis that the survival and recovery of parenchymal cell populations was the predominant factor in the functional outcome of irradiation of normal tissues. However, it is now recognized that such responses are more complex, involving interactions and contributions of the parenchymal cells, the stromal cells, inflammation and infiltrating immune cells. The functional outcome of radiation treatment of normal tissues depends on these interactions and on the ability of the parenchymal cell populations and stroma to recover and retain/regain appropriate functional activity over time. In this presentation I will discuss how different treatment factors can affect tissue response with a primary emphasis on the response of parenchymal cell populations. Much of the work to date has been focussed on cell survival in these populations but functional outcome also depends on the lifetime of the cells in the tissue and on their biochemical function. Relatively little is known about the effect of treatment factors on the function of infiltrating immune cells and even stromal cell populations. Understanding how the underlying parenchymal cells respond to the radiation insult can provide a baseline to address the critical role of immune cells and inflammatory reactions in tissue response. Determining how/whether these latter effects differ with different treatment factors will be important in helping to understand their role in normal tissue response to irradiation.

(S1102) Does the immune system regulate radiation-induced tissue damage? Dörthe Schae¹, Evelyn L. Kachikwu², Yu-Pei Liao¹, Josephine A. Ratikan¹, Keisuke S. Iwamoto¹, William H. McBride¹, ¹David Geffen School of Medicine at UCLA, Los Angeles, CA, ²City of Hope National Medical Center, Duarte, CA

There is increasing evidence that tumor irradiation has a spectrum of immune-modulating effects ranging from enhancing immunity to favoring immune tolerance. Our experience with animal tumor models and in cancer patients is that RT increases anti-tumor immune responses in some cases, but not all, while increasing immunosuppressive T regulatory cells (Treg) representation. It seems that the production of immunosuppressive cytokines and the rise in Tregs seen after radiation may be linked to the expression of extracellular ectonucleotidases that catabolize nucleotides such as ATP in sites of damage to produce adenosine. In fact, adenosine has long been known to play a critical and non-redundant role in the protection of normal tissues from collateral damage during inflammation. Perhaps Treg cells form an important homeostatic mechanism for tissues injured by radiation, and in a tumor context may assist in immune evasion during therapy. Targeting this population or appropriate treatment scheduling might allow enhancement of radiotherapeutic benefit through immune modulation.

(S1103) Proton versus photon radiation effects on immune and other normal tissues. Daila S. Gridley, Xian Luo-Owen, Asma Rizvi, Adeola Y. Makinde, Jian Tian, Xiao Wen Mao, James M. Slater, Michael J. Pecaut, Loma Linda University & Medical Center, Loma Linda, CA

Radiation damage to immune and other normal tissues is a concern in at least four scenarios: 1) patients receiving radiotherapy, 2) crewmembers on space missions, 3) workers in medical and other occupations that involve radiation and 4) nuclear/radiological terrorist acts. Although immune system cells are highly radiosensitive, protons and photons (γ -rays, x-rays) are different forms of

radiation with different biological effects. Likewise, total radiation dose, dose rate, animal species, body compartment, cell type, endpoint evaluated and time post-exposure can make a difference. Immune system studies with total-body irradiated (TBI) mice have shown that the impact of low-dose/low-dose-rate (LDR) exposure to total doses of 0.01 and 0.1Gy is dependent on radiation quality, dose and time of assessment. Differences have been noted in major and subset leukocyte population counts and gene expression patterns in CD4+ T cells that play critical roles in both adaptive and innate immunity. Priming with 0.01Gy LDR γ -rays prior to simulated solar particle event (sSPE) protons modified the levels of certain signaling/survival proteins (NF- κ B, p38MAPK, JNK, Lck) in CD4+ T cells compared to sSPE protons alone, as well as their capacity to secrete immunomodulating cytokines (IL-2, IL-4, TGF- β 1). Comparisons of acutely delivered protons and γ -rays with sSPE protons, all delivered to the same total dose, showed differential effects on bone marrow-derived cell populations, including the highly immunosuppressive CD4+CD25+Foxp3+ T regulatory cells. Changes have also been quantified in non-immune, sub-lethally irradiated cells, especially at the molecular level. Gene expression and other assays of liver, lungs, brain and skin have shown dramatically different patterns after TBI related to radiation quality, as well as variations in regimen and time after exposure. These and other data clearly demonstrate that protons and photons, even at very low doses, can modify many cellular and molecular responses. It is also clear that results obtained with photons frequently do not correlate with results obtained with protons. Although LDR irradiation has sometimes "normalized" the effect of a subsequent high dose event, suggesting radioadaptation, identification of safe and effective countermeasures remains important.

(S1104) Inflammatory responses and the radiation biology of hemopoietic tissue. Eric Wright, University of Dundee, Dundee, United Kingdom

The major adverse consequences of radiation exposures are attributed to DNA damage, arising as a consequence of deposition of energy in the cell nucleus at the time of exposure that has not been correctly restored by metabolic repair processes. However, so called, non-targeted effects, including bystander effects demonstrated in non-irradiated cells that have communicated with irradiated cells, indicate that genetic lesions are not necessarily restricted to directly irradiated cells. At present, most information has been obtained using *in vitro* systems and the *in vivo* significance of bystander effects is not clear. However, it has been known for many years that clastogenic factors capable of causing chromosome breaks in unirradiated cells can be detected in blood plasma after radiation exposures and there is a body of clinical and experimental radiotherapy data concerning absopal or out of field effects where responses are detected in tissues or organs that are not irradiated. These various effects also highlight additional mechanisms distinct from the conventional model of radiation-induced genotoxicity. We have investigated the radiation responses of haemopoietic tissues using mouse models and current findings are consistent with non-targeted effects *in vivo* not being due to direct signalling between irradiated and non-irradiated cells but reflecting genotype-dependent tissue responses in which inflammatory mediators are produced in response to the effects of the initial irradiation. The findings have implications for extrapolating from *in vitro* to *in vivo* situations, for mechanistic understanding of the body's radiation responses and for investigating the development and prevention of associated pathologies.

S12 MISSING LINKS AND NEW PATHWAYS IN DNA DOUBLE-STRAND BREAK REPAIR

DNA double-strand breaks (DSBs) are repaired mainly through non-homologous end joining (NHEJ) or homologous recombination (HR) pathways. This session presents recent advances in critical, but still unsettled, issues in DSB repair mechanisms and also discusses possible new repair pathways or emerging connection with other cellular processes.

(S1201) XRCC4: a bona fide substrate of DNA-PK in DNA Double-Strand Break Repair. Yoshihisa Matsumoto, Tokyo Institute of Technology, Tokyo, Japan

DNA-dependent protein kinase (DNA-PK) is considered the “sensor” of DNA double-strand breaks (DSBs) and thought to play an essential role in DSB repair and recombination through non-homologous end-joining (NHEJ) pathway. It is shown that the protein kinase activity of DNA-PK is required for its function and that DNA-PK is capable of phosphorylating a number of proteins in vitro. However, the substrate(s) in vivo and the significance of phosphorylation have remained to be clarified for many years. We have shown that XRCC4 undergoes DNA-PKs-dependent phosphorylation in response to radiation (Matsumoto et al., FEBS Lett., 2000). The phosphorylation sites were first explored in in vitro experiments using recombinant XRCC4 protein generated in E.coli and DNA-PK purified from cultured human cells. We have so far identified four phosphorylation sites in XRCC4 by DNA-PK in vitro. To examine in vivo phosphorylation, the phosphorylation-specific antibodies were generated corresponding to respective sites. By use of these antibodies, we found all of them indeed phosphorylated in cultured human or murine cell lines. Finally, the mutant cDNA of XRCC4 lacking these phosphorylation sites were introduced into XRCC4-deficient cell line M10 to examine radiosensitivity and other characteristics. Disruption of two sites resulted in elevated radiosensitivity and also in reduced proliferation rate. These results collectively indicated that the phosphorylation of XRCC4 by DNA-PK play an essential role in the repair of radiation-induced and spontaneous DNA DSBs. Supported by Grant-in-Aid for Scientific Research from JSPS and MEXT, Japan. A part of this study is the result of “Study on Initiating Events in the Recognition and Repair of DNA Double-Strand Breaks” carried out under the Strategic Promotion Program for Basic Nuclear Research, MEXT, Japan.

(S1202) Structural and functional insights into the roles of DNA-PKcs in the DNA damage response. Susan Lees Miller, University of Calgary, Calgary, AB, Canada

The protein kinase activity of the DNA-dependent protein kinase catalytic subunit (DNA-PKcs) is required for repair of ionizing radiation (IR)-induced DNA double-strand breaks (DSBs) by non-homologous end joining (NHEJ). DNA-PKcs is recruited to DSBs through its interaction with DNA-bound Ku heterodimer, where it undergoes autophosphorylation, resulting in release from Ku and DNA, thus facilitating pathway progression. Using small angle X-ray scattering (SAXS), molecular modeling and biochemical approaches, we show that the C-terminal region of Ku80 forms a flexible extension for recruitment of DNA-PKcs and that autophosphorylation causes a large conformational change that opens up the central, DNA-binding region of DNA-PKcs. Together, these studies provide a structural basis for regulation of complex assembly and disassembly in the initial stages of NHEJ. We have also examined the role of protein dephosphorylation in the DNA damage response. By immunoprecipitation and mass spectrometry, we find that DNA-PKcs interacts with the catalytic subunit of protein phosphatase PP6. Significantly, siRNA depletion of PP6c prolonged gamma-H2AX phosphorylation after exposure to IR, induced radiation sensitivity and delayed release from the G2/M checkpoint after IR. These studies suggest that DNA-PKcs recruits PP6 to sites of DNA damage where it contributes to the dephosphorylation of gamma-H2AX, dissolution of foci and regulation of the G2/M checkpoint. The implications of these results for NHEJ and the cellular response to IR will be discussed.

(S1203) Real-time imaging reveals a novel view of protein assembly in the non-homologous end-joining pathway. Ken-ichi Yano¹, Keiko Morotomi-Yano¹, David J. Chen², ¹Kumamoto University, Kumamoto, Japan, ²University of Texas Southwestern Medical Center, Dallas, TX

Non-homologous end-joining (NHEJ) is the major repair pathway for DNA double-strand breaks (DSBs) in mammalian

species. Upon DSB induction, a living cell quickly activates the NHEJ pathway comprising of multiple molecular events. However, it has been difficult to analyze the initial phase of DSB responses in living cells, primarily due to technical limitations. Recent advances in real-time imaging and site-directed DSB induction using laser microbeam allow us to monitor the spatiotemporal dynamics of NHEJ factors in the immediate-early phase after DSB induction. Using these new approaches, together with the use of cell lines deficient in each essential NHEJ factor, we analyzed the dynamic behavior of NHEJ factors in living cells. We observed that XLF is quickly recruited to DSBs in the absence of XRCC4 or DNA-PKcs. The recruited XLF molecules constantly exchange at DSBs, and XRCC4 modulates the exchange rate of the recruited XLF. XRCC4 can be recruited to DSBs without DNA-PKcs, but DNA-PKcs stabilizes the recruited XRCC4. These observations are inconsistent with the prevailing concept that NHEJ proteins are sequentially recruited to DSBs, which is mainly supported by in vitro evidence. Based on our imaging data, we propose a novel two-phase model for the assembly of NHEJ factors at DSBs in vivo. XLF, XRCC4, and DNA-PKcs are independently recruited to Ku-bound DSBs. The recruited factors are assembled into a large complex, in which the protein interactions observed in vitro define the stability of the recruited factors. This new model provides important mechanistic insights into the protein assembly at DSBs and the regulation of DSB repair.

(S1204) Novel role for RNA binding proteins in DNA repair. William S. Dynan^{1,2}, Shuyi Li¹, Hairong Xiong^{1,3}, Kyungsoo Ha^{1,2}, Durga Udayakumar¹, ¹Institute of Molecular Medicine and Genetics, Augusta, GA, ²Cancer Center, Medical College of Georgia, Augusta, GA, ³Institute of Virology, Wuhan University School of Medicine, Wuhan, China

Recent work provides evidence for the novel involvement of a small family of human RNA binding proteins in DNA double-strand break (DSB) repair. In humans, the family has three members-PSF, p54^{nrb}, and PSPC1. These three proteins are core components of paraspeckles, which are nuclear structures that are organized around a long noncoding RNA scaffold and that regulate gene expression by retaining adenosine-to-inosine hyper-edited mRNAs. Separate experiments indicate, however, that members of this protein family participate in both homologous recombination and nonhomologous end joining, which are the two main pathways of DSB repair in human cells. Biochemical data suggest that a PSF-p54^{nrb} complex binds to internal DNA sites (rather than directly to DNA ends) and may be involved in maintaining pairing, or synapsis, of broken DNA strands. Knockdown of p54^{nrb} expression in human cells leads to a delay in DSB repair in a γ -H2AX focus assay, to a significant increase in ionizing radiation-induced chromosomal aberrations, and to increased radiosensitivity in a clonogenic survival assay. Laser microirradiation experiments reveal that PSF and p54^{nrb} (and under some conditions PSPC1) rapidly relocalize to sites of induced DNA damage, suggesting the existence of a molecular switch that controls RNA versus DNA interaction. Thus, a combination of biochemical, genetic, and cell biological data together support a hypothesis that PSF and its partners are mediators of gene regulation and DNA repair that switch rapidly between RNA and DNA interaction modes following the induction of DNA damage. It is possible that therapeutic RNAs could be developed to influence switching between RNA biogenesis and DNA repair modes and thus alter clinical radiation response.

S13 BRIDGING THE GAP BETWEEN TRACK STRUCTURE AND STABLE END PRODUCTS

Track structure is at the heart of many of the observed effects induced by the passage of ionizing radiation in condensed media. Ionizing radiation deposits energy along its path in localized regions of the medium as determined by radiation type, energy, and other parameters. The geometry of this localized energy deposition makes up the track structure and it is responsible for much of the subsequent radiation chemistry and biology. Furthermore, the track

structure is not static, but evolves in time with diffusion and reaction of the energetic species produced by the medium decomposition. Even though track structure is extremely important, it is rarely directly observed in condensed media. Track structure is usually inferred from comparison of model predictions with specifically measured end products. End product formation can be complex and thereby difficult to interpret with respect to track structure. The probability of observing certain end products is dependent on the evolution of the track, which again complicates the interpretation of the track structure. In this symposium, the correlation between track structure and observed end products will be shown for a variety of systems ranging from basic water decomposition to DNA damage. The presentations will highlight some of the techniques used to interpret product formation and stress how understanding the track structure and its effects are crucial to predicting radiation damage.

(S1301) Radical yields in the radiolysis of water with different types of radiation. Jay A. LaVerne¹, Simon M. Pimblott², ¹University of Notre Dame, Notre Dame, IN, ²University of Manchester, Manchester, United Kingdom

The hydrated electron and the OH radical are the primary species produced in the decomposition of water by ionizing radiation. These reducing and oxidizing species, respectively, are produced within a few picoseconds following the passage of the radiation and they are responsible for most of the subsequent radiation chemistry in irradiated aqueous media. Track structure effects are manifested in the temporal variation of the radical yields. Competition between radical reactions and radical diffusion is dependent on the evolution of the track structure, which ultimately determines the amount of radiation damage. Since hydrated electrons and OH radicals are formed on such a short time scale they are a particularly good measure of the initial track structure due to energy deposition by the incident radiation. Measurements of the temporal evolution of the hydrated electron and OH radical will be compared to predictions of stochastic track model calculations. Track structure can then be inferred from the model calculations. Comparisons between the observed and calculated yields for the hydrated electron and the OH radical will be shown for a variety of particle types and particle characteristics such as energy and linear energy transfer, LET.

(S1302) Water radiolysis with high-energy heavy ions: conversion of transient water radicals into stable product inside heavy-ion tracks. Shinichi Yamashita¹, Yosuke Katsumura², Jintana Meesungnoen³, Jean-Paul Jay-Gerin³, Mingzhang Lin¹, Yusa Muroya², Takeshi Murakami⁴, ¹Japan Atomic Energy Agency, Ibaraki, Japan, ²School of Engineering, University of Tokyo, Bunkyo-ku, Tokyo, Japan, ³University of Sherbrooke, Sherbrooke, QC, Canada, ⁴National Institute of Radiological Sciences, Inage-ku, Chiba, Japan

Deaerated aqueous solutions of 0.25 mM methyl viologen (MV) containing various concentration of sodium formate (HCOONa) were irradiated with He, C, Ne, Si, Ar and Fe ions of 135-500 MeV/u provided from HIMAC (Heavy Ion Medical Accelerator in Chiba) at NIRS, Japan. Water radicals such as hydrated electron (e_{aq}^-), hydroxyl radical (OH) and hydrogen atom (H) are scavenged by the solutes, leading to reduction of MV cation (MV^{2+}) into MV radical (MV^+), which is stable without oxygen and easily quantifiable by commonly-used off-line absorption spectroscopy. $HCOO^- + OH/H \rightarrow \cdot COO^- + H_2O/H_2$, $MV^{2+} + \cdot COO^- \rightarrow MV^+ + CO_2$, $MV^{2+} + e_{aq}^- \rightarrow MV^+$. These scavenging reactions occur approximately at time scales estimated as the inverse of scavenging capacities, which are defined as the product of scavenger concentration and bimolecular rate constant for scavenging reaction. By changing formate concentration, yield of MV^+ was measured for the abovementioned heavy-ion beams. Then, the yield of MV^+ increased with decreasing LET and with increasing formate concentration. Specifically, $G(MV^+)$ for He ions of 2.2 eV/nm in LET increased from 5.7 to 7.1 and that for Fe ions of 185 eV/nm in LET did from 2.2 to 4.1 (100 eV)⁻¹ with increasing formate concentration from 0.01 to 2 M. This fact shows that consumption of water radicals in intra-track

reactions with time occurs and becomes more and more significant with increasing LET. In order to discuss more quantitatively, Monte-Carlo simulation code for water radiolysis with heavy ions named IONLYS-IRT, which has been developed by a group of University of Sherbrooke, was employed to reproduce our experimental results. Although a few reactions, which have not been reported yet, were needed to be added in the simulation, the experimentally measured MV^+ yields were well reproduced for wide ranges of ion-types, LET values and formate concentrations. Further, contribution of each elemental reaction in the simulation was separated from the others, and characteristics of intra-track dynamics were discussed, and possibility of non-negligible amount of "unexpected" reactions in heavy-ion tracks is indicated.

(S1303) Monte-Carlo simulation of radiation tracks and calculation of dose deposition in nanovolumes. Ianik Plante^{1,2}, Francis A. Cucinotta², ¹USRA/DSLS, Houston, TX, ²NASA Johnson Space Center, Houston, TX

The radiation track structure is of crucial importance to understand radiation damage to molecules and subsequent biological effects. Of great importance in radiobiology is the induction of double-strand breaks (DSBs) by ionizing radiation, which are likely caused by clusters of lesions in DNA, and oxidative damage to cellular constituents leading to aberrant signaling cascades. DSB can be visualized in cell nuclei with immunofluorescence measurements of DNA repair proteins. The distribution of DSB is weakly dependent on the LET, however endpoints resulting from DSB misrepair such as chromosomal aberrations and mutations are strongly LET dependent. DSB produced by high-LET radiation are more difficult to repair than those resulting from low-LET radiation. To investigate DSB distributions and chromosomal aberrations, models of radiation tracks are used with chromosome geometry models. The DSB induction probability can be calculated by using the local dose obtained from the radial dose profile of a heavy ion track or by more CPU expensive models utilizing detailed Monte-Carlo scoring within atomistic representations of DNA structures. In the present work, a new approach is proposed to calculate the local dose deposited by ionizing radiation. The irradiated volume is divided in 3D pixels (voxels) of 20 nm x 20 nm x 20 nm. Then, tracks are simulated with the Monte-Carlo track structure code RITRACKS and the dose is calculated in each voxel. The number of tracks is chosen such as the irradiated volume received 1 Gy. For high-LET ions, very high local dose is found in voxels corresponding to direct ion traversal. Voxels of high doses are also found distributed apparently as uncorrelated points around the path of the track, but corresponding, as expected, to electron track ends. In some cases, they may be found a few millimeters away from the track core. Voxels which receive very high dose are not found for low-LET ions. The appearance of the calculated dose distribution in 3D looks very similar to DSBs seen in γ -H2AX experiments, both for low and high-LET ions. This calculation also shows that very high dose voxels are found only in high-LET tracks and may explain the difference in the nature and reparability of DSBs induced by high and low-LET radiation.

(S1304) Using Monte Carlo DNA damage simulations and deterministic repair models to examine the putative mechanisms of radiation-induced cell death. David J. Carlson¹, Victor K. Yu², Robert D. Stewart², ¹Yale University, New Haven, CT, ²Purdue University, West Lafayette, IN

The physical advantage of protons and more massive ions over conventional x-rays provides potential for a higher level of local tumor control and improvement in normal tissue sparing. The initial kinetic energy of the incident particle can also be adjusted to modulate the relative biological effectiveness (RBE) for cell killing. The purpose of this work is to develop an approach that uses the Monte Carlo DNA damage simulation (MCDS) and the deterministic repair-misrepair-fixation (RMF) model to explore the putative mechanisms underlying RBE and oxygen effects in proton and carbon ion radiotherapy. The MCDS, which reproduces DNA damage yields from more detailed track structure simulations, has

been modified to estimate initial yields and complexity of the double-strand breaks (DSB) produced by protons and carbon ions under varying oxygen concentrations. Linear-quadratic (LQ) model parameters linking radiosensitivity to DSB induction and repair are derived from the RMF model. The formulas explicitly account for unrejoinable DSB, misrepaired and fixed DSB, and exchanges formed through intra- and intertrack DSB interactions. The MCDS and RMF models are used in combination to (1) predict trends in radiosensitivity parameters derived from cell survival data with increasing particle LET and oxygen concentration and (2) determine more accurate estimates of RBE and oxygen enhancement ratios (OER) for protons and carbon ions. Estimates of RBE values for protons and carbon ions are shown to increase as particle energy and tissue α/β decrease. RBE also decreases as the width of the spread out Bragg peak (SOBP) and the fraction size increases. RBE in the distal edge of the SOBP is higher than at the proximal edge. For protons, the entrance RBE at the patient skin is close to unity and RBE values range from 1.05 to 1.8 from the proximal to distal edge of the SOBP, respectively. Carbon ions are more biologically effective than protons and similar trends are observed. The radioprotective effect of hypoxia becomes less significant as particle LET increases. The proposed approach results in an enhanced understanding of the biophysical mechanisms underlying DSB induction and cell killing and the determination of more accurate RBE and OER values that can be practically used in particle radiotherapy.

S14 RISK FROM IN UTERO RADIATION EXPOSURE

Recent epidemiology and radiobiology studies following in utero radiation exposures to the atomic bombs in Japan, I-131 after Chernobyl, and occupational radiation will be summarized. Risk estimates will be compared with those for cancer, non-cancer, and chromosome aberrations following radiation exposures to children and adults.

(S1401) Are those exposed *in utero* the most radiosensitive population? - the Japanese A-bomb experience. Roy Shore, Kotaro Ozasa, Fumiyoshi Kasagi, Misa Imaizumi, Yoshimi Tatsukawa, Radiation Effects Research Foundation, Hiroshima, Japan

Studies have been conducted from 1950 to the present of persons exposed *in utero* (IU) to the atomic bombs in Hiroshima and Nagasaki. Early studies clearly demonstrated effects on the developing brain among those exposed during 8-25 weeks post-conception. Radiation effects on childhood leukemia or other childhood malignancies were equivocal and only marginally compatible with the findings by Alice Stewart and others which had suggested large childhood-cancer risks from diagnostic medical irradiation IU. Risk of solid cancers in adulthood associated with IU radiation exposure is evident but is not larger than that seen among those irradiated in early childhood, and there is some indication of a different temporal pattern in risk between IU and childhood exposure. New data suggest differences in leukemia and noncancer mortality risks between the IU and childhood-exposure cohorts as well. Additional new findings pertain to thyroid disease, cardiovascular disease and cataract following IU radiation exposure. A number of gaps still remain in our knowledge about the lifetime effects of IU radiation exposure; the A-bomb studies will probably continue to be our most important source of information to fill those gaps as the RERF studies are extended.

(S1402) Incidence of Cancer among Individuals Exposed *in Utero* to Iodine-131 from the Chernobyl Fallout in Ukraine. Alina V. Brenner¹, Maureen Hatch¹, Mykola Tronko², Valeriy Tereshchenko², Tetyana Bogdanova², Victor Shpak², Olexandr Zvinchuk², Anna Derevyanko², Zoya Fedorenko³, Evgeniy Gorokh³, Kiyohiko Mabuchi¹, ¹DCEG, NCI, NIH, Bethesda, MD, ²Institute of Endocrinology and Metabolism, Kiyv, Ukraine, ³National Cancer Institute, Kiyv, Ukraine

Background: As a result of the 1986 Chernobyl nuclear accident, residents of northern Ukraine were exposed to radioactive fallout of which iodine-131 (I-131) was the major component. The subsequent increase in risk of thyroid cancer among those exposed in early childhood has been well established. Data on the effects of exposure of I-131 to the embryo/fetus are very limited, yet important, because the fetal thyroid may receive appreciable doses of I-131 via maternal circulation, other organs might be exposed to lower doses, and developing tissues are thought to be very susceptible to radiation. The primary objective of our study was to evaluate risk of thyroid cancer and other thyroid diseases from *in utero* exposure to I-131; a second goal was to explore the incidence of other cancers. Methods: We identified 2,582 mother-child pairs from Ukraine in which the mother was pregnant at the time of the Chernobyl accident or two months following when I-131 fallout was still present. Individual I-131 dose estimates to the fetal thyroid (mean=72 mGy; range: 0-3,230 mGy) were estimated from I-131 activity in the mother's thyroid. No dose estimates to other fetal organs are presently available. From 2003 to 2006, the *in utero* cohort was screened to identify a range of thyroid diseases including thyroid cancer. To evaluate incidence of other cancers, we linked the *in utero* cohort with the Ukrainian National Cancer Registry (UNCR) to ascertain cancers that occurred between 1997 (the earliest year for which national electronic records are available) and 2008, and estimated the standardized incidence ratio (SIR). Findings: There were 7 cases of thyroid carcinoma and 1 case of Hurthle cell neoplasm identified by screening. While the estimated excess odds ratio per Gy for thyroid carcinoma was elevated (EOR/Gy =11.7), it was not statistically significant (P=0.12). No radiation risks were identified for other thyroid diseases. Based on preliminary results of record linkage with the UNCR, we identified 6 cases of cancer (2 in males and 4 in females) including 2 brain gliomas, 3 Hodgkin's diseases, and 1 choriocarcinoma. The SIR was 0.9 (95% CI: 0.11-3.28) for males and 1.8 (95% CI: 0.49-4.66) for females. Interpretation: Our results suggest that *in utero* exposure to radioiodines may have increased the risk of thyroid carcinoma approximately 20 years after the Chernobyl accident. The preliminary results for cancer incidence at other sites need to be interpreted cautiously as they are based on small numbers. Possible approaches to improve ascertainment of childhood cancers in the first 11 years following the accident will be discussed. It will be important to follow this cohort further to evaluate the incidence of thyroid and non-thyroid cancers and to determine if an increase of radiation-related cancer risks occurs when the cohort approaches ages at which background cancer rates increase.

(S1403) Cancer mortality following *in utero* exposure to occupational radiation among offspring of the Mayak Worker Cohort. Sara J. Schonfeld¹, Yulia V. Tsareva², Dale L. Preston³, Pavel V. Okatenko², Ethel S. Gilbert¹, Elaine Ron¹, Mikhail E. Sokolnikov², Nina A. Koshurnikova², ¹Division of Cancer Epidemiology and Genetics, National Cancer Institute, Bethesda, MD, ²Epidemiology Laboratory, Southern Urals Biophysics Institute, Ozersk, Russian Federation, ³Hirosoft International Corporation, Eureka, CA

Case-control studies have indicated that *in utero* radiation exposure increases the risk of childhood cancer but prospective epidemiological data regarding long-term cancer risk following *in utero* exposure are scarce. The Ozersk offspring study provides a unique setting in which to evaluate cancer mortality among a large cohort of individuals exposed to gamma and/or plutonium radiation *in utero* as a result of their mothers' employment during pregnancy at the Mayak nuclear weapons facility in Ozersk, Russia while taking into account offspring cohort members' own adulthood occupational exposure. The offspring study includes approximately 53,000 individuals who were born in Ozersk between 1948 and 1988. Based on currently available dosimetry information derived from mothers' occupational histories, over 4,000 cohort members were exposed *in utero*. Doses were highest between 1948 and 1952, the earliest years of Mayak's operation. Similar to the methods used in the atomic bomb survivors' study, mother's gamma uterine dose is used as a surrogate for *in utero* external radiation dose. Mean mothers' uterine dose during pregnancy was approximately 45 mGy, with over 600 mothers having doses exceeding 100 mGy. The referent group includes 49,000 offspring of Mayak workers whose

mothers were not exposed during pregnancy as well as individuals born in Ozersk to mothers not employed at Mayak. Cancer deaths through December 31, 2008 were ascertained from review of death certificates. Cancer was reported as the cause of death for approximately 60 individuals exposed *in utero*. Solid cancers accounted for approximately 80% of all cancer deaths. Cancer deaths primarily occurred during adulthood although 10 deaths were reported before age 19. The results from dose-response analyses of *in utero* radiation exposure and cancer mortality will be presented and compared with results from other studies.

(S1404) Fetuses are not little children: just ask their hematopoietic stem cells. Nori Nakamura¹, Mimako Nakano¹, Kazuo Ohtaki¹, Yoshiya Shimada², Yoshiaki Kodama¹, ¹Radiation Effects Research Foundation, Hiroshima, Japan, ²National Institute of Radiological Sciences, Chiba, Japan

Cytogenetic tests of blood lymphocytes from atomic bomb survivors have long been conducted at RERF for better understanding radiation doses received by individual survivors. Curiously, however, those who were exposed to radiation as fetuses (in utero survivors) did not indicate any dose effect when they were examined at about 40 years old, which was quite counterintuitive as fetuses are believed to be hypersensitive to radiation. The results were confirmed by mouse experiments (fetal irradiation followed by cytogenetic tests at 20 weeks of age). In addition, we found that irradiated neonates also showed the refractory characteristics of recording radiation effects when examined at 20 weeks of age while mice irradiated at a young age started to record radiation effects with the increase of age at the time of irradiation. Animals irradiated at 6 weeks old or older gave the same results as adults. *P53* gene status (and hence *P53*-dependent apoptosis) did not affect the results. The results indicate that in mice some critical events occur during 3 to 4 weeks after birth when hematopoietic stem cells (HSC) start to record radiation damage permanently. It is well known that HSC reside in liver at the time of birth. And a recent report showed that a drastic shift of the niche occurs at around 3-4 weeks of age from liver to bone marrow (Bowie et al, 2006). Remarkably, this transition is accompanied by a sharp increase of ATM gene expression by 10 to 100 times; that is, the level is very low in HSC in fetal liver and at 3 weeks of age (Bowie et al, 2007). Thus, DNA repair system is not probably operating in HSC of immature animals. We then asked if the present results are general characteristics of fetal cells or HSC is the exception. Our preliminary data of mammary epithelial cells in rats showed that mammary gland stem cells in fetuses are not less sensitive than those in adults in recording cytogenetic damage. Therefore, the fate of cytogenetically aberrant cells in fetuses largely differ depending on the tissue. It is not yet understood the relationship between the fate of cytogenetic damage and cancer risk.

S15 TELOMERES AND DOUBLE-STRAND BREAKS: WHICH END'S WHICH?

Telomeres represent the natural DNA ends of linear chromosomes. In order to maintain genomic stability, chromosomal termini must be protected from degradation and loss, as well as from end-joining events. In striking contrast, broken DNA ends, damaged for example by exposure to ionizing radiation, must be correctly and rapidly rejoined. Recent years have witnessed increasing evidence that these seemingly contradictory requirements trigger a highly integrated cellular response, and in the process have been redefining traditional roles for protein players more commonly regarded as acting in a particular pathway, or at a specific type of DNA end. Such observations return us to a fundamental question first recognized by Muller and McClintok, how does a cell know which end's which? The sometimes surprising answers have important implications in the study of not only telomeres, but also of DNA repair, cancer and aging.

(S1501) Ku86 Represses Lethal Telomere Deletion Events in Human Somatic Cells. Yongbao Wang, Eric A. Hendrickson, University of Minnesota Medical School, Minneapolis, MN

Classic non-homologous end joining (C-NHEJ), a form of DNA double-strand break (DSB) repair, is conserved from bacteria to humans. One essential NHEJ factor is Ku, which consists of a heterodimer of Ku70 and Ku86. In a plethora of model systems, null mutations for Ku70 or Ku86 present with defects in DNA DSB repair, V(D)J recombination and/or telomere maintenance. The complete loss of Ku from bacteria to mice is, however, compatible with viability. In striking contrast, human patients with mutations of either Ku subunit have never been described. We have utilized recombinant adeno-associated virus mediated gene targeting to produce a human somatic cell line that expresses a conditionally null allele of Ku86. The induced loss of Ku86 results in cell death accompanied by massive telomere loss in the form of t-circles. One unusual feature of this Ku-induced telomere dysfunction is the lack of chromosome:chromosome fusions and a high incidence of apparent sister chromatid fusions or associations. To genetically address this issue, we have created a compound double mutant cell line that is null for ligase IV (LIGIV) and conditionally null for Ku86. The apparent incidence of sister chromatid fusions or associations was unaffected by the absence of LIGIV, suggesting that they are mediated by a pathway different from C-NHEJ. Lastly, to demonstrate whether the Ku-induced t-circle formation is truly mediated by homologous recombination (HR) as has been predicted by numerous laboratories, we have constructed an additional compound double mutant cell line that is null for an important HR factor, radiation 54B (RAD54B), and conditionally null for Ku86. The impact of the absence of RAD54B on t-circle formation will be described. Importantly, these studies demonstrate that Ku86 is an essential gene in human somatic cells due to its requirement _ not in C-NHEJ or V(D)J recombination, but _ in telomere maintenance.

(S1502) Telomere instability in the progeny of irradiated human cells. Laure M. Sabatier, CEA- life Sciences Division, Fontenay-aux-roses, France

Many studies have described the presence of dysfunctional (too short) telomeres as a universal mechanism in the early phase of cancer development (Rudolph et al, 1999; O'Hagen et al, 2002; Meeker et al, 2004; Raynaud et al, 2008). It has been proposed that short telomeres will contribute to genomic instability in the aged progeny of irradiated cells (Sabatier et al, 1992, 1994; Martins et al, 1993; Ayouaz et al, 2008). Moreover, dysfunctional telomeres are involved in radiation-induced genomic instability and radiosensitivity (Goytisolo et al, 2000; McIlrath et al, 2001; Williams et al, 2009). Even after telomerase activation, the loss of telomeres can generate most of the types of chromosomal rearrangements detected in cancer cells such as gene amplification and chromosome imbalances (Murnane et al, 2004, Bioassays; Sabatier et al, 2005). Our running hypotheses on the mechanism of radiation-induced tumours combine the transmission of radiation-induced damages and the cellular senescence that will happen though cell proliferation. After irradiation, the large majority of the induced mutations are recessive, i.e. they will remain silent until the occurrence of a mutation on the second allele, such an event is highly improbable in view of the fact that the target is one gene among tens of thousands. However efficient unmasking of recessive mutations could occur through or LOH on the second allele resulting from telomere dysfunction. The work presented here is the characterization of karyotypes and telomere loss in non-irradiated fibroblast and keratinocyte populations from the same donor during the different stages of proliferation *in vitro* (Gosselin et al, 2009) and results for long term transmission of radiation-induced damage in keratinocytes. An increase in the incidence of telomere loss with doublings *in vitro* was noted; however, it followed different kinetics in the two cell types. An increase in clonal and *de novo* chromosomal aberrations was observed in both fibroblasts and keratinocytes as proliferation progressed into senescent phases. Clonal emergence from the second senescent plateau, characterized by progressive instability of the genome and different kinetics of telomere maintenance, was observed in keratinocytes. Using a keratinocyte cell culture set-up (Fortunel et al, 2010), we studied

the follow-up of the post-irradiation progeny of single cells. We observed that chromosomal instability can occur during the proliferation of irradiated human keratinocytes, i.e. 20-25 population doubling after 2 Gy γ -rays. This de novo chromosomal instability can be characterized by the accumulation of non-reciprocal translocations (NRTs) induced after one telomere loss and cycles of breakage-fusions-breakage. Such instability is rarely observed in human fibroblasts and has been described only after high-LET exposure (Sabatier et al, 1992). The radiosensitivity of each cell type and the transmission of radiation-induced damage could largely differ according to the cell type status at irradiation (fibroblasts/keratinocytes, young/senescent) and their role in the long-term occurrence of radiation-induced tumours will be discussed.

(S1503) Endogenous DNA double-strand damage in aging and cancer. Asako J. Nakamura, William M. Bonner, Olga A. Sedelnikova, Laboratory of Molecular Pharmacology, Bethesda, MD

Accumulation of DNA damage is a hallmark of genome instability and is associated with both aging and cancer. DNA double-strand break (DSB)-specific foci, which contain phosphorylated histone H2AX (γ -H2AX), 53BP1, Mre11, Rad50 and Nbs1 accumulate in senescent human cells as well as in germ and somatic cells of aged mammals. The level of endogenous γ -H2AX foci per cell increases with donor age in human lymphocytes and primary fibroblasts. Fibroblasts taken from patients with Werner syndrome, a disorder associated with premature aging, genomic instability and cancer predisposition, exhibited considerably higher levels of γ -H2AX foci than those taken from normal donors of comparable age. Further increases in γ -H2AX foci occurred in culture as both normal and Werner syndrome fibroblasts progressed toward senescence. Similarly, cancer cell cultures and tumors are characterized by elevated levels of DNA damage which vary substantially among different tumors and cell lines, and by heterogeneity of γ -H2AX foci numbers in tumor cell populations. These endogenous γ -H2AX foci can result from two types of DNA double-strand damage, eroded telomeres and non-telomeric frank DSBs, which may result from oxidative stress, compromised DNA repair, cell cycle checkpoint defects, and inappropriate gene amplification. Utilizing combined γ -H2AX and telomere-FISH staining of metaphase chromosomes, we found that both telomeric and non-telomeric DNA lesions accumulated during mammalian senescence with telomeric lesions predominating in human cells. This technique also revealed that critically short telomeres may account for the majority of the increased DNA damage in human tumors as well as for the heterogeneity of γ -H2AX foci numbers in tumor cell populations.

(S1504) Tankyrase 1 influences telomeric recombination and stability of the NHEJ protein DNA-PKcs. Ryan C. Dregalla, Rupa R. Idate, Christine Battaglia, Junqing Zhou, Howard L. Liber, Susan M. Bailey, Colorado State University, Fort Collins, CO

Intrigued by the dynamics of the seemingly contradictory yet integrated cellular responses to the requisites of preserving telomere integrity while also efficiently repairing damaged DNA, we investigated roles of the telomeric PARP tankyrase 1 in telomere function and the DNA damage response. Utilizing siRNA knockdown of tankyrase 1 in human cells, we found its reduction resulted in increased levels of telomeric recombination, specifically telomere sister chromatid exchange (T-SCE), in telomerase negative backgrounds. Consistent with defective DNA damage response, we also observed increased sensitivity to ionizing radiation-induced cell killing, mutagenesis and chromosome aberrations. Most unexpected however, was the finding that tankyrase 1 depletion also led to rapid reduction of DNA-PKcs protein levels, while Ku86 and ATM levels remained unchanged; DNA-PKcs mRNA levels were also unaffected. We demonstrate that depletion of tankyrase 1 results in rapid DNA-PKcs proteasome-mediated degradation, likely explaining the associated

radiosensitivity phenotype. Our results also suggest that the requirement of tankyrase 1 for DNA-PKcs protein stability reflects the necessity of PARP enzymatic activity (PARsylation). While reciprocal interactions between PARP1 and DNA-PKcs have been reported, we provide the first evidence to our knowledge for tankyrase 1 - DNA-PKcs interaction, and in so doing reveal a novel aspect of DNA-PKcs regulation.

S16 LOW DOSE RADIOBIOLOGY: THE CROSS TALK BETWEEN ADAPTIVE RESPONSES, BYSTANDER EFFECTS AND GENOMIC INSTABILITY

Adaptive responses, bystander effects and genomic instability are experimental radiation biology phenomena that have been confirmed in many systems. The radiation-induced adaptive response has been recognized as the expression of mechanisms that protect cells and organisms against damage generated from normal endogenous processes or from subsequent challenge exposure to ionizing radiation or other exogenous stressors. Conversely, radiation-induced bystander effects refer to the propagation of biological signals from irradiated to neighboring non-targeted cells, which induces biological changes in the latter cells. On the other hand, radiation-induced genomic instability leads to an enhancement in the rate of expression of spontaneously induced mutations and chromosomal aberrations. It has been suggested that the expression of these phenomena may amplify or moderate the basic molecular changes/stress responses that are induced upon the interaction of radiation with targeted cells. Recently, significant advances in our understanding of the underlying molecular mechanisms have occurred. Similar and distinct biochemical events have been shown to mediate the three phenomena. In some cases the same biological endpoints have been used to examine expression of either of the phenomena. The current advances in cross-talk between the three phenomena, with particular emphasis on the mediating role of oxidative metabolism, and relevance to radiation protection and radiotherapy, will be discussed by leaders in the field.

(S1601) Interactions between targeted and non-targeted effects elicited by combinations of low doses of energetic protons and iron ions. Kathryn D. Held, Nicole Magpayo, Hongying Yang, Massachusetts General Hospital/Harvard Medical School, Boston, MA

In space, astronauts are exposed to mixed radiation fields consisting of energetic protons and high atomic number, high energy (HZE) particles at low dose rates, such that particle traversals through individual cells in an astronaut's body may be well separated in tissue location and time. These studies were designed to assess possible interactions between two types of radiation in cells when the irradiations are separated in time or when an individual cell is traversed by an ion and also is a "bystander" cell, exposed to signals from another cell that was traversed by a particle. AG01522 human skin fibroblasts were exposed to iron ions or protons, and a transwell insert co-culture system was used to study bystander signaling. DNA damage endpoints were micronuclei (MN) formation and 53BP1 foci induction. Sequential exposures to 1 cGy 1 GeV protons (~350 proton traversals/cell) and 1 GeV/n Fe ions (~0.45 traversals/cell) caused the same magnitude of DNA damage in irradiated cells as seen with either protons or Fe ions alone. The same magnitude of DNA damage was also observed in non-irradiated bystander cells sharing medium with cells exposed to either 1 cGy protons or iron ions or protons plus iron ions. However, when the "bystander" cells were exposed to 1 cGy protons up to 3 h before co-culture with Fe ion-irradiated cells, no DNA damage in the "bystander" cells was observed. Because persistent induction of reactive oxygen species (ROS) has been shown in irradiated mammalian cells and ROS are implicated in bystander signaling, we investigated whether ROS could mimic the effect of prior proton irradiation in the reduction of the medium-mediated Fe-induced bystander response. However,

pre-treating cells with a low level of hydrogen peroxide prior to co-culture with Fe-irradiated cells did not modulate the “bystander” cells’ ability to exhibit increased MN after sharing medium with irradiated cells. Together, the data provide evidence for interactions between targeted and non-targeted effects in DNA damage caused by dual exposure to low doses of energetic protons and iron ions, but imply that ROS may not be involved in decreasing Fe-induced medium-mediated bystander effects caused by a low prior proton dose. (Supported by NASA grant #NNX07AE40G.)

(S1602) The signaling pathways in radiation-induced bystander effects: COX-2 and beyond. Hongning Zhou, Vladimir Ivanov, Tom K. Hei, Columbia University, New York, NY

Although radiation-induced bystander effects have been well studied in the past decade, the precise mechanisms are still unclear. In sub-confluent cultures or medium transfer studies, there is evidence that reactive oxygen/nitrogen species and cytokines are involved in mediating the process. On the other hand, gap junction-mediated cell-cell communications have been shown to be critical for bystander effects in confluent cultures of either human or rodent origins. It is likely that a combination of pathways is involved in producing a bystander response. Recently, we reported mitochondria played an important role in radiation-induced bystander effect, partially via mitochondria-dependent regulation of iNOS and cyclooxygenase-2 (COX-2) signaling pathways, which are under NF- κ B regulation. To continue the studies, we found that expression of several early NF- κ B dependent genes including *IL8*, *COX-2*, *TNF*, and *IL33* in directly irradiated human skin fibroblasts produced cytokine signals, which activated pathways and targeted NF- κ B dependent gene expression in bystander cells. As a result, bystander cells also started to express and produce of IL8, COX-2-generated prostaglandin E2 and IL33 followed by autocrine and paracrine stimulation of the NF- κ B and MAPK pathways. In addition, the IGF-1/IGF-1-Receptor controlled the PI3K-AKT pathway in both directly irradiated and bystander cells. A pronounced and prolonged up-regulation of AKT activity after irradiation appeared to be a signature feature of bystander cells. Subsequently, AKT mediated inactivation of GSK3 β resulted in stabilization of β -catenin protein levels in bystander cells. A better understanding of the mechanism of bystander effect is pivotal in assessing the potential health consequence of this stress-associated phenomenon.

(S1603) Radioadaptive response can be induced even after priming irradiation of a limited number of cells with charged heavy particles. Hideki Matsumoto¹, Masanori Tomita², Kensuke Otsuka², Masanori Hatashita³, ¹Division of Oncology, Biomedical Imaging Research Center, University of Fukui, Fukui, Japan, ²Radiation Safety Research Center, Nuclear Technology Research Laboratory, Central Research Institute of Electric Power Industry, Komae-shi, Tokyo, Japan, ³Biology Group, Research and Development Department, The Wakasa Wan Energy Research Center, Tsuruga-shi, Fukui, Japan

A classical paradigm of radiation biology asserts that all radiation effects on cells, tissues and organisms are due to the direct action of radiation. The risks of exposure to low dose ionizing radiation (below 100 mSv) are estimated by extrapolating from data obtained after exposure to high dose radiation, using a linear no-threshold model (LNT model). However, the validity of using this dose-response model is controversial because evidence accumulated over the past decade has indicated that living organisms, including humans, respond differently to low dose/low dose-rate radiation than they do to high dose/high dose-rate radiation. In other words, there are accumulated findings which cannot be explained by the classical “target theory” of radiation biology. Of these responses to low dose/low dose-rate radiation, the radiation-induced adaptive and bystander responses seem to be particularly important. In order to define the radiation-induced adaptive and bystander responses to provide a basis for the understanding of non-targeted events and to elucidate the mechanisms involved, recent sophisticated research has been conducted with X-rays and charged heavy particles, and these studies

have produced many new observations. Based on these observations, the associations have been suggested to exist between them. The presentation focuses on these phenomena, and summarizes observations supporting their existence, and discusses the linkage between them in light of recent our results obtained from experiments utilizing broad- and micro-beams of charged heavy particles.

(S1604) Low dose radiation enhances intercellular ROS signaling through multiple and distinct amplification steps. Georg Bauer, Universität Freiburg, Freiburg, Germany

Our studies are based on three biochemically defined stages during multistep carcinogenesis: nontransformed, transformed (pre-malignant) and tumor cells. Transformed cells generate extracellular superoxide anions and are therefore subject to control by intercellular induction of apoptosis, a TGF- β -triggered, ROS-mediated control mechanism that is mediated by the HOCl and the NO/peroxynitrite signaling pathway. Nontransformed cells are insensitive for intercellular induction of apoptosis due to their lack of extracellular superoxide anion generation. Tumor cells show superoxide anion generation, but are resistant to intercellular ROS signaling due to the establishment of resistance controlled by membrane-associated extracellular catalase. Catalase destroys hydrogen peroxide as well as peroxynitrite and thus protects tumor cells against both intercellular signaling pathways. Abrogation of this resistance mechanism renders tumor cells sensitive for intercellular ROS signaling. Low dose gamma irradiation modulates apoptosis in transformed cells due to a remarkable increase in superoxide anion generation by the transformed cells and a strong increase in peroxidase release by neighbouring nontransformed cells as well as in the transformed cells themselves (autocrine signaling). Low dose radiation does not induce apoptosis in tumor cells when it is applied by itself. However, the combination of low dose radiation with a variety of secondary plant compounds (including established chemotherapeutics) leads to a massive synergistic effect and a very efficient apoptosis induction in tumor cells. Reconstitution experiments in combination with inhibitors and specific small interfering RNAs allowed to define several amplification steps involved in establishment of intercellular apoptotic signaling. It seems that mitochondrial functions are required to amplify the effect of low dose radiation within the minority of cells that are originally hit by radiation. The actually hit cells then transfer signal molecules to neighbouring unaffected cells. Within few hours of incubation this intercellular signal amplification causes the majority of cells to release peroxidase and to increase superoxide anion production though only a minority had been actually experienced radiation. TGF- β thereby represents a crucial signal and contributes to the speed of signaling through its potential for autoinduction. In the case of low dose radiation-treated tumor cells in the presence of certain secondary plant compounds, a complex, but and well-defined sequence of chemical interactions leads signal amplification and finally to singlet oxygen generation and subsequent catalase inactivation. Tumor cells with inactivated catalase trigger catalase inactivation in neighbouring tumor cells through specific ROS interactions and thus amplify the original biochemical effect. These data demonstrate how very low doses of radiation trigger ROS-dependent signaling reactions with amplificatory potential and thus can finally lead to a strong and specific biological effect. Low dose radiation triggered ROS-dependent signaling effects may have a substantial impact on the control of oncogenesis and a possible therapeutic potential.

S17 UPDATE: AUGER EMITTERS IN MEDICINE AND BIOLOGY

The nanometer range of high LET radiochemical damage from Auger emitters is a remarkable phenomenon. The early “suicide” experiments involving incorporation of 125I into cellular DNA foreshadowed potential therapeutic applications, but also lead to more fundamental contributions. The approximate one-to-one association between 125I decay events and DNA dsb induction not only illuminated the relationship between DNA dsbs and lethality, but

also provided the basis to calibrate assays for DNA dsb, such as neutral elution and gamma-H2AX foci. At the molecular level, DNA sequencing gel analysis of strand breaks from decay events in isolated DNA provided a geometrical map of the range of damage, which in turn contributed to the refinement of microdosimetry models. A more obtuse exploitation of the damage map is its reversal; rather than delineating the relationship between distance and damage, patterns of damage are analyzed to infer spatial relationship between the decaying isotope and the target of damage. This so-called radio-probing is the subject of the first talk in this symposium. Igor Panyutin will describe its application to investigating the structure of telomeres, captured in their "native" state, as distinct from the "frozen" poise reflected by X-ray crystallography. Returning to the exploitation of Auger emitters in cancer therapy, the 60-day half-life of the archetypical Auger emitter ^{125}I is frankly impractical, prompting interest in ^{123}I (half-life 13 hours). Ralf Kriehuber will describe the consequences of the somewhat "weaker" Auger decay of ^{123}I , on cellular endpoints such as apoptosis, micronucleus formation, cell cycle arrest and mutagenicity. Also on therapeutic potential, the established observation that DNA ligands can be used to target Auger-induced damage to DNA, needs to be supplemented with targeting at the cellular level. This is the subject of the talk by Pavel Lobachevsky, who will describe the use of labeled DNA ligand/transferrin conjugates, which exploit the specificity of receptor mediated endocytosis. The clinical success of such approaches will rely on the efficacy of targeting *in vivo*. Although in theory this could be done by imaging techniques that utilize the gamma-emission associated with Auger emitters, sensitivity is a challenge. This is addressed in the final presentation in the symposium, by Katherine Vallis. She will describe a novel approach to imaging DNA damage *in vivo* which could be applied to Auger therapy. The innovation takes advantage of the phosphorylation of histone H2AX. Considering DNA damage from Auger emitter, an impressive feature of the innovation is the signal amplification. Thousands of molecules of gamma-H2AX are phosphorylated in response to a single DNA dsb, each with the potential to be bound by a labeled antibody molecule.

(S1701) Radioprobing of telomeric DNA; prediction of DNA structure based on I-125 decay produced strand breaks. Igor Panyutin, Timur Gaynutdinov, Ronald Neumann, National Institutes of Health, Bethesda, MD

Decay of an Auger electron emitter, such as I-125, incorporated into a DNA molecule results in strand breaks with highest frequency within one helical turn (10 base pairs) around the decay site. The probability of DNA breaks caused by decay of I-125 is inversely related to the distance between the radionuclide and a nucleotide sugar moiety in the DNA backbone where the break occurs; therefore, by measuring the frequencies of breaks in an I-125-labeled nucleic acid molecule one can gain information on the conformation of this molecule. We called this method radioprobing. With radioprobing, as with NMR, it is possible to obtain information about the interatomic distances; and, in principle, to reconstruct the 3D-structure of DNA. Radioprobing was first tested on a DNA-protein complex with well-known 3D structure. Iodine-125 was incorporated in iododeoxycytosine at a single position of a short DNA duplex containing the E. coli cyclic AMP receptor binding sequence. The frequencies of breaks produced by decay of I-125 in the complementary strand of the duplex were in good agreement with the distances to the corresponding sugars calculated from the 3D structure in the range from 10 to 30 Å. These frequencies were also sensitive to the few angstrom changes in the distances caused by the binding of CRP to that duplex. Since then radioprobing was applied to study the spatial arrangement of DNA strands within several complexes of DNA with RNA and/or proteins. Recently we applied this technique to assess the conformation of the human telomeric DNA. Human telomeres contain numerous copies of (TTAGGG)_n-(AATCCC)_n repeated sequence with multiple TTAGGG repeats in the 3' single-stranded overhangs. We showed that single-stranded oligonucleotides consisting of four TTAGGG repeats can fold into various intramolecular quadruplexes structures stabilized by quartets of guanines. This quadruplex structures are believed to play a role in telomere function and considered as targets for anticancer drugs design. In an effort to create a more realistic model of telomeric

DNA we designed oligonucleotides containing a duplex region at the 5' end and four telomeric repeats in the 3' overhang. We found that the conformation of quadruplex dramatically changed upon 5' duplex formation, and depended on the position of the duplex/overhang interface. Obtained structural data may help to understand the role of G-quadruplex conformation in telomere functions and in design of telomere-specific anticancer drugs.

(S1702) Cyto- and genotoxicity of ^{123}I - and ^{125}I -UdR *in vitro*: Apoptosis induction, micronucleus formation and chromatin damage in three human cell lines. Ralf Kriehuber, Marcus Unverricht, Eberhard Kümmerle, Ekkehard Pomplun, Forschungszentrum Jülich, Jülich, Germany

The Auger electron emitters (AEE) ^{123}I and ^{125}I are characterized by different half-lives (13.2 h vs. 59.4 d) and by different average numbers of Auger electrons emitted per decay (8 vs. 15). The biological response in synchronized mammalian cells labelled with various activity concentrations of ^{123}I - and ^{125}I -UdR were investigated and compared in respect to accumulated decays and dose rate to further elucidate the biological effectiveness of Auger electrons. SCL-II, Kidney-T1 and Jurkat cells were synchronized in G1-phase, subsequently labelled with ^{123}I - respectively ^{125}I -UdR and the cellular up-take and DNA-incorporation of I-UdR were determined. Chromatin damage was quantified by the alkaline Comet-assay, apoptosis induction was assessed by the Annexin V/PI assay employing flow cytometry and micronucleus formation was quantified using the Cytochalasin-B-micronucleus assay at various times post-labelling. ^{137}Cs gamma rays served as reference radiation. ^{123}I -UdR induced overall a slightly stronger response in human cell lines than ^{125}I -UdR regarding micronucleus formation and chromatin damage. Apoptosis induction was much more profound in ^{125}I -UdR-labelled cells immediately after labelling in comparison to ^{123}I -UdR. Both AEE induced a pronounced long-lasting G2/M phase arrest which was not observed after external gamma irradiation. Albeit of a lower dose rate, ^{125}I -UdR is 1.2 to 1.5 times more genotoxic than ^{123}I -UdR. On average one decay (^{125}I -UdR) every 120 seconds per DNA/cell is sufficient to induce a permanent cell cycle arrest.

(S1703) Studies with DNA ligand conjugates for tumour PET imaging and Auger endoradiotherapy. Pavel Lobachevsky, Roger Martin, Trescowthick Research Laboratories Peter MacCallum Cancer Centre, Melbourne, Australia

Induction of cytotoxic DNA double strand breaks (DSB) by DNA ligands labelled with Auger electron emitters such as ^{125}I (0.8 DSB/decay in plasmid DNA) suggests a therapeutic potential that could be realised by targeting such ligands to tumour cells as protein conjugates. Accumulation of the radiolabelled ligand in cell nucleus and its binding to DNA can be achieved following internalisation of the conjugate via receptor-mediated endocytosis, intracellular degradation of the conjugate and consequent release of the labelled DNA ligand. Use of another Auger-emitter ^{124}I , introducing the additional feature of positron-emission, opens the opportunity for combined tumour therapy and PET imaging. To explore this potential, we synthesised and evaluated conjugates of ^{124}I - and ^{125}I -labelled DNA ligands and transferrin as a model tumour targeting protein. Previously, we established that the unconjugated ^{124}I -ligands, when associated with plasmid DNA, induce 0.6 DNA DSB per decay thus confirming its therapeutic potential. We obtained PET images and compared biodistribution following injection of the conjugate, the directly labelled ^{124}I - or ^{125}I -transferrin or unconjugated labelled DNA ligand into nude mice bearing a subcutaneous human K562 lymphoma tumour that overexpresses transferrin receptors. Our results demonstrated accumulation of the radioactive label in tumour and liver with much higher uptake following injection of the conjugate of the DNA labelled ligand compared to the directly labelled transferrin. We attribute this to accumulation of the labelled DNA ligand bound to nuclear DNA following internalisation and degradation of the conjugate. High uptake of the radiolabelled ligand in the liver is consistent with the high expression of transferrin receptors on mouse hepatocytes.

(S1704) Auger electron radiation therapy: targeting the DNA damage response. Katherine Vallis, Bart Cornelissen, University of Oxford, Oxford, United Kingdom

Auger electron-emitting radiopharmaceuticals that track to the nuclei of cancer cells and target molecular components of the DNA damage response have the potential to amplify pre-existing DNA damage caused by anticancer therapies. Prototypic agents that target the DNA signaling protein, γ H2AX, which accumulates at the sites of DNA double-strand breaks, have been synthesized. These are antibody-based and incorporate the cell penetrating peptide, TAT. TAT-modified radioimmunoconjugates (RIC-TAT) have been fluorophore- or ^{111}In -labeled and shown, unlike non-specific IgG-TAT control RICs, to be extensively retained in the nuclei of cancer cells in which DNA damage has been induced. In clonogenic assays, the combination of ^{111}In -RIC-TAT plus 4 Gy ionizing radiation (IR) was significantly more cytotoxic than either agent alone and more cytotoxic than ^{111}In -IgG-TAT plus IR. The enhancement by ^{111}In -RIC-TAT of IR-induced cell death was found to be dose-dependent over a specific activity range of 0.5-6.0 MBq. The combination index (CI) of IR (4 Gy) plus ^{111}In -RIC-TAT was 0.86 in MDA-MB-468 breast cancer cells and the CI of IR (10 Gy) plus ^{111}In -RIC-TAT was 0.31 in H2N cells, a HER2-transfected subclone of MDA-MB-231 cells (CI <0.9 indicates superadditivity). In mice, the growth of MDA-MB-231/H2N tumor xenografts was significantly inhibited by the combination of a single dose of IR (10 Gy) plus ^{111}In -RIC-TAT, compared to either treatment alone and to control treatments consisting of IR plus ^{111}In -IgG-TAT. Auger electron emitting radiopharmaceuticals that target γ H2AX effectively stimulate the formation of their own target and convert sublethal DNA lesions into irreparable damage. This strategy therefore holds promise as a new cancer treatment.

S18 NOVEL HIGH THROUGHPUT SCREENING TO IDENTIFY RADIATION RESPONSE MODULATORS FOR MECHANISTIC UNDERSTANDING AND TRANSLATIONAL APPLICATION

The advent of high throughput screens to identify molecules of interest has impacted on a variety of fields, including radiation research. This symposium concerns the use of this strategy to reveal novel genes and pathways involved in radiosensitization or radioprotection, to gain insight into relevant mechanisms and to develop anti-cancer agents.

(S1801) Functional genomics and signaling in bystander and alpha particle irradiated fibroblasts. Shanaz A. Ghandhi, Columbia University Medical Center, New York, NY

The existence of a radiation bystander effect, in which non-irradiated cells respond to signals from irradiated cells, is well established. To understand early signaling and gene regulation in bystander cells, we used a bio-informatics approach, measuring global gene expression at time points ranging from 30 minutes to 24 hours after irradiation and bystander exposure. We also studied signaling pathways within a few hours after exposure to alpha-particles in lung and skin fibroblasts. The results of signaling studies indicated that a rapid inflammatory response to irradiation was observed in exposed and neighboring cells and mRNA levels of signaling molecules such as interleukin-8, interleukin-1 β and cyclooxygenase-2 were induced as early as half hour after exposure. We also used a clustering approach to study gene expression patterns across the time series and network analysis to predict common regulatory modules that control gene expression. Our studies indicated that in addition to transcription factor signaling, epigenetic control of gene expression may be a major player in the bystander response.

(S1802) Discovery of Novel Mitochondria-Targeted Radioprotectors/Radiomitigators: Oxidative Lipidomics Approach. Valerian E. Kagan, University of Pittsburgh, Pittsburgh, PA

One of the consequences of the symbiogenic origin of eukaryotic cells is the unique presence of one particular class of phospholipids, cardiolipin (CL), in mitochondria. In normal cells, CL is predominantly confined to the inner mitochondrial membrane where it is essential for many mitochondrial functions. Recently, we have identified CL and its oxidation products as important participants and signaling molecules in apoptosis induced by irradiation. Early in apoptosis, transmembrane redistribution of CL results in its appearance in the outer mitochondrial membrane. Consequently, significant amounts of CL become available for interactions with cytochrome c (cyt c), one of the major proteins of the intermembrane space. Cyt c/CL complexes act as a CL-specific peroxidase. Using mass-spectrometry based oxidative lipidomics, we discovered selective CL peroxidation early in apoptosis and identified and characterized its oxidation products. The catalytic mechanisms of CL peroxidation include the formation of protein-derived (tyrosyl) radicals detectable by low-temperature EPR as well as by immuno-spin trapping. Oxidized CL (CLOx) is essential for the release of pro-apoptotic factors - including the central "lethal" signal, cyt c itself - from mitochondria into the cytosol. Based on these findings, we developed new classes of mitochondria-targeted inhibitors of cyt c/CL peroxidase activity effectively preventing CL oxidation and protecting/mitigating against irradiation induced apoptosis.

(S1803) What high throughput screening tells us about radioprotectors and mitigators. William McBride¹, Andrew Norris¹, Robert Damoiseaux¹, Brendan Price², Yingli Sun², James Sayre¹, Kwanghee Kim¹, ¹UCLA, Los Angeles, CA, ²Dana-Farber Cancer Institute, Harvard Medical School, Boston, MA

High throughput screening is generally performed with bioactive or chemically defined small molecule libraries. The former have the advantage that they have known biological properties and examining classes of bioactive agents can inform as to pathways that might be utilized to prevent or deal with radiation damage. We have used radiation-induced apoptosis of a T lymphocyte cell line as an assay, with this aim. By giving agents 3hrs before or 1hr after radiation exposure we were able to compare radioprotective and radiomitigating activities. In general, few of 36,000 compounds that were tested were effective in both situations, but some, such as cyclopiazonic acid (CPA), had dual action. Two classes of antibiotics, tetracycline analogs and fluoroquinolones, clearly emerged as being radioprotective and, less strikingly, as mitigators of radiation damage. Interestingly, CPA, tetracyclines and fluoroquinolones have a common planar cyclic/aromatic ring structure that binds divalent cations and that may be the active pharmacophore. On the basis of Tip60 activation, we hypothesize that the activity of these agents in part stems from their ability to intercalate within DNA and affect chromatin structure, a novel mechanism by which radiation damage may be mitigated. Another class of mitigating agents that came from our HTS was the purinoreceptor agonists, such nucleosides deoxyadenosine and adenosine, and the analogue vidarabine. Adenosine production by extracellular nucleotidases is a known mechanism of tissue protection and indicates a possibly major pathway of radiomitigation. Finally, fatty acids, in particular linoleate, had radiomitigating activity. In conclusion, HTS has identified classes of bioactive agents that inform on pathways affecting radiation responses. This work was supported by UCLA's Center for Biological Radioprotectors U19 AI067769/NIAD.

(S1804) Using Cell-Based High-Throughput Assays and Novel Animal Model Systems to Identify and Characterize Effective Radiosensitizers. Constantinos Koumenis, University of Pennsylvania, Philadelphia, PA

Agents with the ability to preferentially increase the cytotoxic effects of ionizing radiation (IR) toward tumor cells have the

potential to significantly alter the therapeutic ratio and improve patient survival. Using a high throughput, cell-based approach to screen a chemical library of compounds with high Lipinski scores, we identified two nitrophenone compounds with similar structures (NS-123 and NS-160) which act as true radiosensitizing agents in various solid tumor cell lines *in vitro* and *in vivo*. NS-123 radiosensitized U251 glioma cells in a dose- and time-dependent manner, with dose enhancement ratios (DERs) ranging from 1.3 to 2.0. NS-123 did not increase the radiation sensitivity of normal human astrocytes or cause developmental abnormalities or lethality of irradiated Zebrafish embryos. In a novel xenograft model of U251 cells implanted into Zebrafish embryos, NS-123 enhanced the tumor growth-inhibitory effects of IR with no apparent effect on embryo development. Similar results were obtained in a mouse model in which NS-123 sensitized U251 xenograft tumors to IR while exhibiting no overt toxicity. Mechanistic studies showed that pretreatment with NS-123 resulted in accumulation of unrepaired IR-induced DNA strand breaks and prolonged phosphorylation of the surrogate markers of DNA damage following IR, suggesting that NS-123 inhibits a critical step in the DNA repair pathway. Further analysis revealed that NS-123 inhibits Akt kinase activation by IR in glioma and prostate carcinoma cells. In "hit-to-lead" optimization studies, we have identified two analogs of NS-123 with with substantially enhanced DERs due to better cellular uptake. These compounds are currently in animal testing. These results show the potential of a cell-based, high-throughput screening method to identify novel radiosensitizers and suggest that NS-123 and similar nitrophenol compounds may be effective in anti-tumor modalities.

S19 A ROLE OF CHROMATIN REORGANIZATION IN GENOME STABILITY AFTER IR EXPOSURE

DNA repair should be regulated in chromatin context after ionizing irradiation. It is, however, still unclear how the dynamic organization of chromatin after ionizing irradiation regulates DNA repair system. In this session, we will present our perspective on recent progress about the role of chromatin dynamics in DNA repair and DNA damage response.

(S1901) Mechanism of the DNA damage-induced focus formation of RAD51. Satoshi Tashiro, Hiroshima University, Hiroshima, Japan

DNA damage-induced foci are higher order nuclear architectures formed by the accumulation of proteins associated with DNA repair at sites containing DNA damage. We previously found that RAD51, a key protein involved in the recombinational repair of DNA double strand breaks (DSBs), forms nuclear foci during S phase, and also accumulates at sites containing DNA damage. We also found that TIP60, a histone acetylase, plays a role in the regulation of RAD51 focus formation at sites containing DSBs. However, the molecular mechanism involved in the regulation of RAD51 focus formation is still unclear. Recently, covalent binding of SUMOs to target proteins, or SUMOylation, has been shown to be implicated in the cellular response to DSBs. RAD51 is known to interact with SUMO-1. Here we show that SUMO-1 is required for the recruitment of RAD51 at damaged sites. We also found that interaction of RAD51 with SUMO-1 is essential for the RAD51 accumulation at sites containing DSBs. These findings suggest the involvement of SUMO modification system in the DNA damage-induced focus formation of RAD51. Regulation of DNA damage-induced nuclear domain formation by protein modifications will be discussed.

(S1902) Autophosphorylation of ATM at Serine 1981 mediates the interaction with MDC1 and stabilizes ATM at sites of DNA-double-strand breaks. Anthony Davis, David J. Chen, UT Southwestern Medical Center, Dallas, TX

The cellular response to DNA damage is a complex process that includes recognition of the DNA damage, activation of signaling pathways, including cell cycle checkpoints, and repair of the damage. An important protein in the cellular response to DNA damage is the ataxia telangiectasia mutated (ATM) protein. In response to DNA double strand breaks (DSBs), ATM is autophosphorylated at serine 1981. Although this autophosphorylation is widely considered a sign of ATM activation, it is still not clear if autophosphorylation at serine 1981 is required for ATM functions including localization to DSBs and activation of ATM kinase activity. In this study, we show that localization of ATM to DSBs is differentially regulated with the initial localization requiring the MRE11-RAD50-NBS1 complex and sustained retention at the chromatin requiring autophosphorylation of ATM at serine 1981. Autophosphorylated ATM interacts with MDC1 and the latter is required for the prolonged association of ATM to the chromatin. Ablation of ATM autophosphorylation or knock-down of MDC1 protein affects the ability of ATM to phosphorylate downstream substrates and confer radioresistance, suggesting that the stabilization of ATM at DSBs by MDC1 allows ATM to phosphorylate its substrates at sites of the damage or the damage-flanking chromatin. Together, these data suggest that autophosphorylation at serine 1981 stabilizes ATM at the sites of DSBs and damage-flanking chromatin and this is required for a proper DNA damage response.

(S1903) Chromatin reorganization and modification required for amplification of ATM-dependent DNA damage signal. Keiji Suzuki, Division of Radiation Biology, Nagasaki, Japan

Ionizing radiation causes DNA double strand breaks, which stimulate ATM-dependent DNA damage checkpoint. Upon irradiation, activated ATM through dimer dissociation and autophosphorylation phosphorylates various downstream mediators and effectors. These factors are recruited to the sites of chromatin surrounding DNA double strand breaks to form the initial foci. Previously, we demonstrated that residual foci persistent for over 24 hours became quite large in size, and the foci growth was essential for amplifying DNA damage signals. Although recent studies have shown that multiple modifications of histones are involved in DNA damage signal amplification, the molecular mechanisms underlying the persistent DNA damage signal amplification has not been fully understood yet. Therefore, in the present study, we examined growth of foci of DNA damage checkpoint factors in normal human diploid cells and DNA repair-defective rodent cells exposed to ionizing radiation. We found that decreased acetylation of histone H3 and di-methylation of histone H3 at lysine 9 did not affect the initial foci formation but they ablated persistent foci formation observed 24 hours after irradiation. We also found that foci growth was coupled with DNA repair. Thus, these results indicate that chromatin reorganization and modification are indispensable for proper response to DNA damage, by which stability of the genome is maintained.

(S1904) Checkpoint activation regulated by DNA damage-induced H2AX eviction. Tsuyoshi Ikura, Kyoto University, Kyoto, Japan

Chromatin reorganization involving histone modifications, histone variant exchange, histone eviction and nucleosome remodeling is required for DNA repair factors to access DNA damage sites. We previously showed that histone H2AX is rapidly evicted from chromatin after induction of DNA damage. Analysis of purified H2AX complex revealed that DNA damage induced the acetylation and ubiquitination of H2AX in addition to the phosphorylation. Interestingly, the eviction of H2AX depends not on phosphorylation, but rather on acetylation by TIP60 histone acetylase, an enzyme involved in DNA repair, and ubiquitination. However, it remains unclear how such chromatin reorganization is coupled with the initiation of DNA repair process and/or the activation of checkpoint machinery after DNA damage. Here we found that H2AX evicted from damaged chromatin was associated with the checkpoint proteins, NBS1 and ATM. Thus, we

investigated the effect of the eviction of H2AX regulated by the TIP60 complex on the binding of NBS1 with damaged chromatin. As a result, depletion of TIP60 reduced the binding of NBS1 and ATM with damaged chromatin. It suggested that the TIP60 complex is required for the binding of NBS1 and ATM with damaged chromatin. Since TIP60 acetylates the Lys 5 (K5) of H2AX upon DNA damage, we next examined whether the acetylation of K5 of H2AX is necessary for the binding of NBS1 and ATM with damaged chromatin. Mutation of K5 in the H2AX acetylation site reduced the binding of NBS1 and ATM with chromatin, suggesting that the acetylation of K5 of H2AX is required for the binding of NBS1 and ATM with chromatin. Thus, the eviction of H2AX regulated by the TIP60 complex may function as a molecular link between DNA damage sensing and chromatin remodeling. We will discuss about the role of the eviction of H2AX upon DNA damage in chromatin remodeling and checkpoint activation.

(MS101) Microarray analysis of mRNA and miRNA after single-dose and fractionated radiation in LNCAP human prostate carcinoma cells. Molykutty J. Aryankalayil, Sanjeevani T. Palayoor, Charles B. Simone, II, Adeola Y. Makinde, David Cerna, C. Norman Coleman, National Cancer Institute, Bethesda, MD

MicroRNAs (miRNAs) are an important class of non-coding small RNAs capable of regulating gene expression at the translation level. To explore the role of miRNAs in cellular response to ionizing radiation, in addition to the gene expression analysis by mRNA microarray, we examined radiation-induced changes in miRNAs. Methods: LNCAP cells were exposed to 5Gy and 10Gy either as a single-dose radiation or multi-fractionated (0.5Gyx10 and 1Gyx10) radiation. RNA was extracted at 24h after the final dose of radiation and miRNA and mRNA microarray analyses were done using Agilent human miRNA Microarray Kit (V2) and CodeLink whole genome bioarray (55,000 probes), respectively. Data were analyzed using GeneSpring software (Agilent technologies). Results: Of the total 723 miRNAs represented in the array, 91 miRNAs were differentially expressed (> 1.5 fold change) by the 4 radiation protocols and more than 70% of these miRNAs were induced by the 2 fractionated radiation protocols. mRNA microarray analysis revealed a total of 978 differentially expressed genes (> 2 fold change, $p < 0.05$) and 69% of these genes were altered by single-dose radiation. The most prominently altered genes were PIG3, SULF2, SERPINB5 and cyclin A2 (single dose radiation) and CES1, ANGPT2, NOS3 and CYP3A43 (fractionated radiation). Cell cycle regulatory genes AURKA, AURKB, CDKN2C, CCNB2, PLK4, E2F2 and E2F8 were significantly down regulated after single and fractionated radiation. Interestingly, the miRNA microarray analysis revealed significant upregulation of p53 inducible miR-34a, a known cell cycle regulator, after both single and fractionated radiation. Thus, the present data revealed an inverse correlation between miR-34a and cell cycle regulatory genes. This study also demonstrated significant changes in the let-7 family of miRNAs by radiation; 7 of the 9 let-7 miRNAs were significantly upregulated after fractionated radiation whereas none of them were altered after single dose radiation. Conclusion: We are currently in the process of evaluating radiation-induced differential gene expression changes by a combined approach of mRNA, miRNA and protein array analysis to identify radiation induced molecular targets for cancer therapy. Modulation of miR-34a in cancers with mutated p53 may affect tumor radioresponsiveness.

(MS102) H6CAHA, a stable and potent hydroxamate-based histone deacetylase inhibitor, enhances the therapeutic efficacy in prostate cancer radiotherapy. Zacharoula Konsoula, Mira Jung, Georgetown University, Washington, DC

Structurally diverse histone deacetylase inhibitors (HDACIs) have emerged as an important class of anti-cancer agents and have shown to cause differentiation, cell cycle arrest and apoptosis. Here, we present evidence that a hydroxamate-based HDACI, H6CAHA, has favorable physicochemical properties, including lipophilicity, solubility and permeability. In addition, plasma pharmacokinetics in male nude mice revealed that the peak concentration (C_{max}) of H6CAHA was $6.88 \pm 0.71 \mu\text{M}$ and the area under the curve (AUC) was $8.08 \pm 0.91 \mu\text{M} \times \text{h}$, indicating good plasma distribution. Peak plasma levels were observed at 2 h post-administration of H6CAHA and the half-life was calculated to be $11.17 \pm 0.87 \text{ h}$. Furthermore, H6CAHA was tested to determine whether it influences survival and DNA damage-repair in irradiated human prostate cancer and normal cells. *In vitro* clonogenic assays revealed that H6CAHA decreased the survival in prostate cancer cells and promoted the survival in normal cells. Additionally, immunofluorescence analysis displayed that H6CAHA caused an accretion in the radiation induced phospho-H2AX (γH2AX) and RAD51 foci beyond 24 h in prostate cancer cells and a decline in normal cells. Taken together, H6CAHA has been shown to enhance the therapeutic potential in cancer radiotherapy by killing cancer cells and still protecting normal cells from radiation-induced damage. Thus, the results provide a rationale for clinical investigation of the therapeutic efficacy of H6CAHA in combination with radiotherapy.

(MS103) Gemcitabine and 5-fluorouracil as radiosensitizers of low dose rate radiation in the treatment of liver cancer. Theodore S. Lawrence, Mary A. Davis, University of Michigan, Ann Arbor, MI

Treatment options for diffuse hepatocellular carcinoma (HCC) are extremely limited; the only established therapy is sorafenib, which improves survival by only 2 months. Therefore, the use of low dose rate radiation delivered by ^{90}Y trium labeled glass microspheres administered directly into the hepatic artery, from which HCC derives most of its blood supply, is being investigated as a treatment option. As we have successfully combined radiosensitizers with external beam radiation (Ben Josef, et al *J Clin Oncol*, 34:8735-8739, 2005), we hypothesized that sensitizers could improve the response of HCC to low dose rate radiation as delivered by ^{90}Y trium microspheres. We used a custom built device which is housed in a cell culture incubator and which delivers gamma radiation (^{137}Cs) at a dose rate of 0.18 Gy/h. Exposing HepG2 or Hep3B cells for 16 h to low dose rate radiation resulted in surviving fractions of 0.35 ± 0.06 and 0.22 ± 0.06 , respectively. We then examined the effects of gemcitabine, 5-fluorouracil (5-FU), and sorafenib on radiation sensitivity. Gemcitabine was added at nontoxic doses for 2 hours, 24h before the cells were placed in the low dose rate device. For 10 nM gemcitabine, the enhancement ratios were 1.99 ± 0.39 in HepG2 cells, and in Hep3B cells, for 30 nM gemcitabine, was 1.52 ± 0.31 . Likewise, 5-FU was added 24 h prior to the start of radiation but was left on throughout the 16h of radiation treatment. Under these conditions, 1 μM 5-FU (nontoxic) treatment resulted in enhancement ratios of 1.91 ± 0.04 in Hep G2 and 4.79 ± 0.62 in Hep3B cells. At clinically achievable doses, sorafenib did not sensitize either cell line to low dose rate radiation. Experiments are underway to confirm these results in mice and at other, lower dose rates. These data suggest that radiosensitizers may be useful in combination with treatment with ^{90}Y microspheres and will form the preclinical rationale for a proposed clinical trial to treat HCC.

(MS104) Mechanism of action of an imidopiperidine inhibitor of human polynucleotide kinase/phosphatase. Gary K. Freschauf, Rajam S. Mani, Todd R. Mereniuk, Mesfin Fanta, Dennis G. Hall, Michael Weinfeld, University of Alberta, Edmonton, AB, Canada

The small molecule, 2-(1-hydroxyundecyl)-1-(4-nitrophenylamino)-6-phenyl-6,7a-dihydro-1H-pyrrolo[3,4-b]pyridine-5,7(2H,4aH)-dione (A12B4C3), is a potent inhibitor of the phosphatase activity of human polynucleotide kinase/phosphatase (PNKP) *in vitro*. Cellular studies revealed that A12B4C3 sensitizes A549 human lung cancer cells to the topoisomerase I poison, camptothecin, but not the topoisomerase II poison, etoposide, in a manner similar to siRNA against PNKP. A12B4C3 also inhibits the repair of DNA single and double-strand breaks following exposure of cells to ionizing radiation, but does not inhibit two other key strand break repair enzymes, DNA polymerase beta or DNA ligase III, providing additional evidence that PNKP is the cellular target of the inhibitor. Kinetic analysis revealed that A12B4C3 acts as a non-competitive inhibitor, and this was confirmed by fluorescence quenching, which showed that the inhibitor can form a ternary complex with PNKP and a DNA substrate, i.e. A12B4C3 does not prevent DNA from binding to the phosphatase DNA binding site. Conformational analysis using circular dichroism, UV-difference spectroscopy and fluorescence resonance energy transfer all indicated that A12B4C3 disrupts the secondary structure of PNKP. Investigation of the potential site of binding of A12B4C3 to PNKP using site directed mutagenesis pointed to interaction between Trp⁴⁰² of PNKP and the inhibitor. A12B4C3 is thus a useful reagent for probing hPNKP cellular function and will serve as the lead compound for further development of PNKP-targeting drugs.

(MS105) miRNA response in endothelium and tumors in response to angiogenesis inhibitors and radiation. Peter E. Huber¹, Ramon Lopez¹, Mechthild Wagner¹, Sebastian Schölich², Nuh Rabari², Moritz Koch², Ute Wirkner¹, ¹Radiation Oncology, dkfz and University Hospital, Heidelberg, Germany, ²Surgery, University Hospital, Heidelberg, Germany

The interdependencies between tumor and tumor microenvironment are critical for tumor therapy. Increasingly, for many tumors, combination therapy regimens that include new targeted biologicals e.g. angiogenesis inhibitors and radiotherapy are being pursued. Noncoding RNA has been shown to be important regulators for cancer and endothelial cells. Here we have systematically investigated the roles of noncoding RNA in response to cancer therapies including small molecule VEGF/PDGF RTKI (Sutent), TGF-beta RKI, integrin inhibitors (Cilengitide), and EGFR AB (Cetuximab) alone and in combination with ionizing radiation in human microvascular endothelial (HDMEC) and pancreatic carcinoma cells (BXPC3) in vitro and in vivo using a balb c nude mouse model. RNA was isolated from 2 - 72 h after treatments, and the Exiqon V9.2 microarray expression profiling platform was used along with qRT-PCR to measure differentially regulated miRNA. To functionally analyze the roles of the differentially regulated miRNAs, cell proliferation, migration and clonogenic survival assays were performed after transfection with miRNA precursor or inhibitor constructs. We found that both drugs and radiation significantly regulated the expression of many miRNAs (~5-20 miRNA/modality) with distinct similarities between the in vitro and in vivo situation, e.g. Cetuximab and Cilengitide reduced miR-558 expression in BxPC3 which was further enhanced by their combination. In HDMEC, Cetuximab decreased e.g. miR-571, Cilengitide increased miR-335, and TGF-beta RKI increased let-7g and miR-214 levels. Radiation up-regulated let-7g, miR-16, miR-20a, miR-21 and miR-29c, while miR-18a, miR-125a, miR-127, miR-148b, miR-189 and miR-503 were down-regulated. Overexpression of let-7g, miR-127, and miR-20a increased radiation-induced cell toxicity, while e.g. overexpression of miR-189 and miR-125a reduced radiosensitivity. The data show that microRNA in endothelium and tumor cells are regulated upon treatment with specific signaling inhibitors of VEGF/PDGF, TGF-beta, integrins and EGF. The data also suggest that miRNA are critically involved in a complex regulation of endothelial and tumor cell response to these specific drugs and radiation which may have important implications for choosing optimal tumor therapy combinations.

(MS106) Transforming growth factor β (TGF β) inhibition uncovers radiation-induced anti-tumor immunity in a mouse breast cancer model. Karsten A. Pilonis, Sophie Bouquet, Mary Helen Barcellos-Hoff, Sandra Demaria, New York University, New York, NY

Prior studies have shown that radiation triggers the activation of transforming growth factor β 1 (TGF β 1) and that TGF β 1 is a potent inhibitor of effector functions of CD8 T cells. While testing the potential for TGF β neutralizing 1D11.16 monoclonal antibody (generously provided by Genzyme, Inc.) to block the DNA damage response (see abstract by Bouquet et al, this meeting), we examined whether inhibition of TGF β 1 would also release immunosuppressive networks in the tumor microenvironment that prevent effective anti-tumor immunity. Employing the highly metastatic mouse breast cancer model 4T1, we have previously shown that local ionizing radiation therapy (RT) to the primary tumor induces tumor-specific CD8 T cells capable of inhibiting lung metastases as well as the irradiated tumor when combined with immunotherapy (*Clin Cancer Res* 11, 728, 2005, *Clin Cancer Res* 15, 597, 2009). Groups of 5 mice were treated with (1) isotype control monoclonal antibody (mAb), (2) RT, (3) 1D11.16, (4) RT + 1D11.16. Antibodies were given i.p. on day 13 post 4T1 tumor cell injection at 5mg/kg. RT was delivered exclusively to the primary tumor as a single non-ablative dose of 8 Gy on day 14. Mice were followed for tumor growth until day 22 or 30 when animals were euthanized for analysis of tumor-infiltrating T cells (TILs) and lung metastases, respectively. RT or 1D11.16 as single treatment did not significantly inhibit the growth of the primary tumor or lung metastases. In contrast, mice receiving 1D11.16 + RT had significantly smaller tumors ($p < 0.05$ on day 22), presumably due in part to increased radiation sensitivity, and concomitant with increased infiltration by CD8 but not CD4 T cells. The ratio of CD8+NKG2D+ effector to CD4+ T cells was significantly increased ($p = 0.04$), which suggests that TGF β inhibition also alters the immunological environment. Consistent with this, the number of pulmonary metastases evaluated on day 30 was significantly reduced only in mice given 1D11.16 +

RT (median = 2, $p < 0.05$) compared to control (median = 8) or single agent RT or 1D11.16 (median = 7, $p > 0.05$) groups. These data suggest that inhibition of TGF β 1 is an effective strategy to improve radiation response by increasing both tumor radiation sensitivity and increased immunogenic response. Supported by NYU Cancer Center pilot funding.

(MS107) Effectiveness of the combined treatment of Hsp90 inhibitor 17AAG with gamma-rays or carbon ions in a tumor xenograft model. Ryuichi Okayasu¹, Dong Yu¹, Miho Noguchi², Momoko Takahashi¹, Akira Fujimori¹, ¹National Institute of Radiological Sciences, Chiba, Japan, ²Japan Atomic Energy Agency, Tokai-mura, Japan

Hsp 90 inhibitor 17AAG has been shown to be an effective radio-sensitizer in vitro using several tumor cell lines. One attractive point of using this chemical with radiation is its sensitizing effectiveness in normal cells being significantly smaller than that in tumor cells. We have shown that inhibition of DNA double strand break (DSB) repair by 17AAG is one of the causes for this sensitization in X-irradiated tumor cells. (Noguchi et al 2006). Inactivation of proteins associated with homologous recombination repair was also described in the publication. In this report, in vivo studies of 17AAG combined with radiation are presented using a mouse xenograft model with human tumor cells. SQ5 lung carcinoma cells were transplanted into the leg of nude mice, and the mice were treated with either 17AAG alone, radiation alone (gamma-rays or carbon ions), or the combined 17AAG and radiation treatment. 17AAG doses of 80 mg/kg body weight was given i.p. for 3 consecutive days. With 17AAG treatment or 10 Gy of gamma-ray alone, tumor growth was delayed in comparison to the control. The combination of 17AAG (pre-treatment for 3 days) and gamma-rays caused further delay in tumor growth. With 5 Gy dose of carbon ions, the combined treatment showed a significant delay in tumor growth, but by 25 days after irradiation, the tumor growth became similar in 5 Gy carbon treatment alone and in the combined treatment. These data indicate that 17AAG is effective in enhancing radiation response in gamma-irradiated tumors in vivo. Furthermore, carbon ion irradiation alone is very effective in controlling tumors in vivo even at low radiation doses.

(MS108) Inhibition of SDF-1/CXCR7 radiosensitizes ENU-induced glioblastomas in the rat. Diane Tseng, Fred Lartey, Shie-Chau Liu, Mitomu Kioi, Milton Merchant, Matthew Walters, Juan Jean, Tom Schall, Lawrence Recht, Martin Brown, Stanford University, Stanford, CA

Radiation therapy is the standard therapy for patients with glioblastoma (GBM) after maximal surgical excision. However, recurrences invariably occur within the radiation field. Recently we have shown that inhibition of the CXCR4-SDF-1 axis with AMD3100 can sensitize U251 glioblastomas to local irradiation in an orthotopic mouse xenotransplant model by preventing the influx into the irradiated tumor of proangiogenic CD11b+ bone marrow derived myelomonocytes. In the present study we tested the hypothesis that similar radiosensitization could be achieved by blocking post-irradiation endothelial cell influx by inhibiting the interaction of CXCR7, which is highly expressed on activated endothelial cells, with its ligand SDF-1. To test the hypothesis, we chose an extremely refractory tumor model that closely mimics human GBM. In this model pregnant rats are given a single dose of ENU on day 17 of gestation. The rats born to these mothers reliably die from brain tumors from day 120 - day 200. We monitored survival of rats following whole brain irradiation (WBI) in combination with blocking CXCR7 with CCX2066 (ChemoCentryx Inc.), or CXCR4 (with AMD3100) or the combination of the two after irradiation. Rats were irradiated with 15 or 20 Gy to the whole brain on day 112 and were randomized into 5 treatment groups: CCX2066 alone, WBI alone, WBI plus AMD 3100, WBI plus CCX2066, and WBI plus AMD 3100 + CCX2206. The drugs were administered for 4 weeks following irradiation. At 224 days the survival of rats given CCX2206 with WBI was significantly longer

by > 50 days ($P < 0.01$) compared to the control and irradiation alone groups. Because SDF-1 is released from an irradiated tumor and is a ligand for CXCR4 and CXCR7, we examined whether serum SDF-1 levels would be a suitable biomarker to define the period after irradiation over which the drugs should be delivered. We found that serum SDF levels were $>3 \times$ higher in the irradiated rats compared to the control rats at 10 days but had fallen to control levels by 17 days after irradiation. In conclusion, inhibition of SDF-1/CXCR7 in combination with local tumor irradiation significantly increased the survival of ENU-induced GBM in rats. In ongoing studies we are comparing the efficacy of inhibiting either SDF-1/CXCR4 or SDF-1/CXCR7 or the combination of the two following irradiation.

(MS201) Genetic dissection of the temporal role of p53 in regulating radiation-induced carcinogenesis. Chang-Lung Lee¹, Yongbaek Kim², Julie M. Sullivan³, Laura B. Jeffords³, Scott W. Lowe⁴, David G. Kirsch^{1,3}, ¹Department of Pharmacology and Cancer Biology, Duke University Medical Center, Durham, NC, ²Department of Population Health and Pathobiology, North Carolina State University, Raleigh, NC, ³Department of Radiation Oncology, Duke University Medical Center, Durham, NC, ⁴Cold Spring Harbor Laboratory, Cold Spring Harbor, NY

Suppression of p53 function during irradiation (IR) ameliorates short-term hematopoietic injury but may exacerbate long-term carcinogenesis as p53 heterozygous knockout mice show accelerated lymphomagenesis post-IR. By utilizing transgenic mice in which an shRNA to p53 can be induced temporally *in vivo* by doxycycline, we propose to 1) investigate if short-term inhibition of p53 during radiation promotes carcinogenesis and 2) elucidate the temporal role of p53 in eliminating damaged cells in hematopoietic tissues post-IR. Our results show that temporary induction of p53.shRNA prevented radiation-induced apoptosis in the thymus and protected mice from the hematopoietic syndrome caused by exposure to total body irradiation (TBI) of 7.5 Gy, indicating that short-term inhibition of p53 by RNA interference ameliorates acute radiation injury. To investigate the temporal role of p53 in regulating radiation-induced carcinogenesis, mice in which p53.shRNA were induced either short-term (during IR) or long-term (during and after IR) after exposure to a daily fraction of 1.8 Gy TBI every 24 hours for four days have been followed for tumor development. The mice in which p53.shRNA were induced permanently post-IR show significantly shorter latency of carcinogenesis compared to their littermate controls which did not express p53.shRNA. These results show that suppression of p53 expression permanently by RNA interference can recapitulate the tumor-prone phenotype of p53^{-/-} mice. We are utilizing this *in vivo* p53.shRNA model to investigate the effects of temporary inhibition of p53 during IR on long-term carcinogenesis.

(MS202) Vitamin E and the active green tea agent EGCG suppress radiation-induced carcinogenesis by different molecular mechanisms. Marc S. Mendonca, Anthony Borgman, Ryan Dhaemers, Helen Chin-Sinex, Indiana University School of Medicine, Indianapolis, IN

Treatment induced secondary malignancies after successful radiation and/or chemotherapy cure of primary tumors is a growing area of concern. The identification of chemopreventive compounds that reduce radiation-induced secondary malignancy but are both nontoxic and tolerated with long-term use is a critical need. We investigated the chemopreventive potential and mechanism of action of Vitamin E and EGCG (the active agent in green tea) with the human CGL1 radiation neoplastic transformation assay. The molecularly characterized CGL1 assay allows both alterations of the quantitative neoplastic transformation as well the potential underlying molecular processes of the chemoprevention to be determined. We found long-term treatment with 15 microM EGCG or 50 microM Vitamin E beginning 72 hours after 7 Gy irradiation, significantly reduce radiation-induced neoplastic transformation frequency by a factor of 2.3. We determined that Vit E suppressed radiation-induced carcinogenesis by the induction of a p53 and pro-

apoptotic Bax dependent apoptosis in the progeny of the irradiated cells. In addition, we demonstrated that EGCG does not reduce radiation-induced carcinogenesis by increased apoptosis, but rather by the onset of p16 dependent senescence in the irradiated CGL1 progeny. Vit E and EGCG are excellent candidate nontoxic chemopreventive agents for radiation-induced carcinogenesis that work by two distinct molecular mechanisms. We propose that this information should also aid in the development of next generation chemopreventive compounds. These studies were supported by a grant from the DOD awarded to MSM.

(MS203) Genome-wide profiling of histone acetylation in breast-cancer cells in response to histone deacetylase inhibitors. John H. Miller¹, Seema Verma¹, Julie Stanton², John Wyrick², Rajiv Prasad³, David Springer³, ¹Washington State University Tri-Cities, Richland, WA, ²Washington State University, Pullman, WA, ³Pacific Northwest National Laboratory, Richland, WA

Acetylation of lysine residues in core histones is a well characterized reversible posttranslational modification of chromatin that affects gene expression. Recent studies have suggested that histone deacetylase (HDAC) inhibitors de-repress genes involved in cell differentiation, growth arrest, and apoptosis of cancer cells and, because of these features, HDAC inhibitors are currently being used as anti-cancer agents. HDAC inhibitors have also been shown to enhance DNA repair. To gain more direct evidence of histone modification in the activities of HDAC inhibitors, genome-wide histone H3 acetylation patterns were measured in estrogen receptor positive MCF-7 breast cancer cells treated with 1 mM valproic acid (VPA) or 300 nM trichostatin-A (TSA) for 12 hours. ChIP-chip analysis was performed using affymetrix human promoter tiling arrays to identify genomic regions associated with acetylation of histone H3 at Lys 9 and Lys 14. Raw data was analyzed using the MAT algorithm and the affymetrix probes were mapped on the human assembly 18 to identify ChIP enriched peaks. Untreated control cells exhibited 1739 chromosome regions of significant antibody binding compared to 16,298 and 5822 significantly acetylated chromosome regions of VPA and TSA treated cells, respectively. These results clearly show that the HDAC-inhibitor properties of VPA and TSA led to extensive H3 acetylation in MCF-7 cells under our exposure conditions. MAT scores were used to compare treated and control cells at common acetylated regions. Analysis of hyperacetylated ChIP regions among significantly acetylated regions common to treated and control cells revealed 65 and 42 genes whose expression is likely to be up-regulated by VPA and TSA, respectively, due to chromatin remodeling. The MetaCore software was used to identify pathways significantly enriched in these genes. The top-ranked network included genes with functions in DNA replication, recombination and repair as well as regulation of cell-cycle, apoptosis and differentiation. These preliminary results suggest that HDAC inhibitors VPA and TSA up-regulate transcriptional targets of p53 that regulate DNA damage response, apoptosis, and cell differentiation.

(MS204) Tie2⁺ bone marrow endothelial cells regulate hematopoietic reconstitution following total body irradiation. Phuong L. Doan, J. Lauren Russell, Heather A. Himburg, Sarah K. Meadows, Pamela Daher, Julie M. Sullivan, Nelson J. Chao, David G. Kirsch, John P. Chute, Duke University Medical Center, Durham, NC

Radiation causes myelosuppression via damage to bone marrow (BM) hematopoietic stem cells (HSCs). HSCs reside in association with BM endothelial cells (ECs), but the function of BM ECs in regulating HSC regeneration after injury is not well understood. We hypothesize that BM ECs regulate hematopoietic reconstitution following stress. To test this hypothesis, we compared the hematopoietic response to total body irradiation (TBI) of Tie2Cre;Bak^{-/-};BaxFl^{-/-} mice with Tie2Cre; Bak^{-/-};BaxFl^{+/+} mice which have constitutive *Bak* deletion but retain *Bax* in Tie2⁺ BM ECs. Two hours after 300 cGy TBI, Tie2Cre;Bak^{-/-};BaxFl^{-/-} mice displayed an increase in viable BM cells ($p=0.03$), total ckit+sca+ lineage- (KSL) progenitor cells ($p=0.001$), CFU-Spleen day 12

($p=0.005$), and a 2.5-fold increase in 12-week competitive repopulating units (CRUs, $p=0.009$) compared to Tie2Cre;Bax $^{-/-}$; BaxFl/+ mice. Since Tie2 is expressed by BM ECs and, to a lesser extent, HSCs, we asked whether radioprotection of Tie2Cre;Bax $^{-/-}$; BaxFl $^{-/-}$ mice was caused by protection of Tie2 $^{+}$ BM ECs or Tie2 $^{+}$ HSCs. We transplanted 4×10^6 BM cells from Tie2Cre;Bax $^{-/-}$; BaxFl $^{-/-}$ mice into lethally irradiated wild type (WT) B6.SJL mice to generate mice that retained *Bax* and *Bax* deletions in HSCs while having a wild type BM ECs (HSC- BaxFl $^{-/-}$;EC-WT), verified by qRT-PCR. At 16 weeks post-transplant, we exposed the chimeric mice to 300 cGy TBI and observed a significant decrease in total KSL cells ($p=0.02$), CFU-Spleen day 12 ($p=0.03$), and 12-week CRUs ($p=0.04$) in chimeric mice compared to Tie2Cre;Bax $^{-/-}$; BaxFl $^{-/-}$ mice. After exposure to 750 cGy TBI, we observed 100% survival in Tie2Cre;Bax $^{-/-}$; BaxFl $^{-/-}$ mice compared to 10% survival in Tie2Cre;Bax $^{-/-}$; BaxFl/+ mice and wild type C57Bl6 mice at 30 days. Interestingly, the HSC-BaxFl $^{-/-}$;EC-WT mice demonstrated 40% survival, which was significantly less than the Tie2Cre;Bax $^{-/-}$; BaxFl $^{-/-}$ mice, indicating that BM ECs regulated the survival of mice following high dose TBI ($p=0.005$). These results demonstrate that the hematopoietic response to ionizing radiation is governed by the function of BM ECs. BM ECs are a novel therapeutic target to facilitate hematopoietic reconstitution *in vivo* following radiation injury.

(MS205) The development of stem cell therapy to reduce radiation-induced hyposalivation. Robert P. Coppes, Lalitha S. Y. Nanduri, Marianne van der Zwaag, Mirjam Baanstra, Jielin Feng, Monique A. Stokman, Ronald P. van Os, University Medical Center Groningen, Groningen, Netherlands

Salivary glands are often exposed to radiation, during radiotherapy for head and neck cancers. This may result in life-long salivary gland impairment severely reducing the post-treatment quality of life of the patients. In a culture of dissociated salivary glands both mice and human cells are able to form salispheres. In mice, we showed that transplantation of salisphere derived c-Kit $^{+}$ stem/progenitor cells rescued the salivary glands from radiation-damage⁽¹⁾. In a similar manner c-Kit $^{+}$ cells could be isolated from human salivary glands⁽¹⁾. Currently we are investigating the potency of these cells. To compare human and murine salisphere c-Kit $^{+}$ cells we determined the co-expression of several adult tissue stem cell markers and their growth characteristics. Human salivary gland cells grow steadily and are able to generate new salispheres after digestion and further culturing in matrigel. Human and murine salispheres cultures were tested for the presence of several stem cell markers on c-Kit $^{+}$ salisphere cells. Next, the differentiation potential of human and murine salisphere cells was investigated in 3D culture and in a NODscid/beige kidney capsule transplantation model. Both human and murine salispheres contain CD133 $^{+}$ and CD24 $^{+}$ /CD29 $^{+}$ cells. Transplantation of 10.000 mice CD133 $^{+}$ or CD24 $^{+}$ /CD29 $^{+}$ cells could reduce radiation-induced hyposalivation. Within c-Kit $^{+}$ cells between 50-85% also expressed CD133 $^{+}$. However, whereas mice c-Kit $^{+}$ cells clearly co-expressed both CD24 and CD29, human c-Kit $^{+}$ cells hardly expressed these markers. In 3D-differentiation culture a mixture of collagen and matrigel with medium containing R-Spondin, both human and murine salispheres gave rise to similar morphological structures, such as ducts and acinar cells. Moreover, human salivary gland cell like-structures were formed under the kidney capsule, most potently after implantation of c-Kit $^{+}$ cells. In conclusion, human and murine salivary gland c-Kit $^{+}$ co-express a different subset of stem cell markers but exhibit similar potencies. (1) Lombaert IM et al. *PLoS One* 2008;3(4):e2063. Supported by the Dutch Cancer Society and The Netherlands Organisation for Health Research and Development.

(MS206) Activation of hematopoietic stem cells attenuates radiation-induced genetic instability by stimulating the repair of DNA double-strand breaks. Senthil Kumar Pazhanisamy¹, Ningfei An², Yong Wang², Daynna J. Wolff², Daohong Zhou¹, ¹University of Arkansas for Medical Sciences, Little Rock, AR, ²Medical University of South Carolina, Charleston, SC

Safeguarding the genomic integrity of hematopoietic stem cells (HSCs) is crucial for the maintenance their function and prevention of genomic instability and leukemia. Unfortunately, little is known on why HSCs are highly susceptible to the induction of genomic instability by various genotoxic agents including ionizing radiation (IR). In the present study, we investigated the DNA damage and repair process in both HSCs and hematopoietic progenitor cells (HPCs) isolated from adult mouse bone marrow (BM) by using γ -H2AX immunofluorescent staining and neutral comet assay. The results from our study showed that HSCs repaired IR-induced DNA double-strand breaks (DSBs) less efficiently than HPCs. Intriguingly, this phenomenon is likely attributable to the quiescence of HSCs, because HSCs from both the embryonic day 14.5 (E14.5) mice fetal livers (FL) and adult mice BM 5 days after injection of 5-fluorouracil (5-FU) were proficient in repair of IR-induced DSBs. Further studies revealed that quiescent HSCs were deficient in repair of DSBs because they were unable to effectively activate the homologous recombination (HR) and non-homologous end joining DSB repair pathways even though they were capable of sensing and signaling the damage. However, activation of quiescent HSCs with stem cell factor (SCF) and thrompoietin (TPO) *in vitro* and with polyinosinic:polycytidylic acid (PolyI:C) *in vivo* stimulated DSB repair function in HSCs. More importantly, it was found that a single iv injection of PolyI:C after total body irradiation (TBI) significantly attenuated IR-induced accumulation of DSBs in HSCs and increase in the number of unstable chromosomal aberrations in the progeny of HSCs. Taken together, these findings suggest that transient activation of HSCs may represent a novel mechanism-based approach for the prevention of genotoxic stress-induced hematopoietic genetic instability by stimulating the repair of DSBs in HSCs.

(MS207) Effect of ionizing radiation on the differentiation responsible for transforming mouse iPS cells into the three germ layers. Naoki Hayashi¹, Kenji Takahashi¹, Satoru Monzen¹, Tsuyoshi Fujioka², Yukio Nakamura², Ikuo Kashiwakura¹, ¹Department of Radiological Life Sciences, Hirosaki University Graduate School of Health Sciences, Hirosaki, Japan, ²RIKEN BioResource Center, Tsukuba, Japan

Objective: iPS cells are generated by transfer of suitable genes such as *Nanog*, *Oct4*, *c-myc*, and *Klf4*. Although iPS cells have the potential to differentiate into various cells, detailed information with regard to their radiosensitivity is limited. This study aimed to examine the effects of ionizing radiation on the differentiation responsible for transforming mouse iPS cells into the three germ layers. Materials and Methods: Mouse iPS cells were purchased from RIKEN BioResource Center (Tsukuba, Japan). iPS cells were derived from mouse embryonic fibroblasts and cultured in DMEM containing 15% FBS and 1000 U/ml LIF. Embryoid body (EB) formation was performed in a conical tube with a loose cap in a culture medium of α -MEM containing 10% FBS. EB diameter was measured on culture day 5. The expression of various genes was analyzed by quantitative real-time RT-PCR. mRNA expression for the differentiation of the endoderm marker *Afp*, early mesoderm marker *brachyury*, and ectoderm marker *Nestin* was analyzed. X-irradiation was performed using an X-ray generator with 0.5-mm Al and 0.2-mm Cu filters at 150 kV, 20 mA, and a dose rate of 3.3-3.4 Gy/min in the range of 1-7.5 Gy. Results and Discussion: The surviving curve of mouse iPS cells showed D_0 and n values of 2.09 Gy and 1.02, respectively. The EB formation efficiency of nonirradiated and X-irradiated iPS cells was almost 100%, but EB diameter decreased in a dose-dependent manner. The mRNA expression of the pluripotent stem cell markers, *Nanog* and *Oct4*, detected in EBs derived from nonirradiated iPS cells was downregulated compared with iPS cells. No difference was observed in these markers detected in EBs derived from irradiated iPS cells. The expression of *Afp* was downregulated in EBs derived from irradiated iPS cells in a dose-dependent manner in comparison to that seen in nonirradiated control cells. Furthermore, no significant difference was observed in other two markers at 2-7.5 Gy irradiation. These results suggest the possibility that iPS cells are relatively radioresistant, but radiosensitive differences may be observed among differentiation pathways that transform iPS cells into the three germ layers.

(MS208) Nf- κ B-her2, a new biomarker to target radioresistant breast cancer stem cells. Nadire Duru, Ming Fan, Jian Jian Li, UC Davis Medical Center, Radiation Oncology, Sacramento, CA

Acquired tumor resistance to chemo and radiation therapy, especially in recurrent and metastatic lesions, has been the challenge in improving the efficacy of tumor control and overall cancer patient survival. Cancer stem cells (CSCs), consisting less than 1% of total tumor cells, are defined as specific tumor cells with a unique capacity to self-renew and give rise to heterogeneous lineages of cancer cells within the tumor. Recent data show that CSCs are more radioresistant than cancer cells without the feature of CSCs. Therefore, identifying CSCs and their roles in tumor repopulation may generate valuable information for developing new therapeutics to control the aggressiveness of recurrent and metastatic tumors. In clinic, breast cancer patients with HER2/nue (a ErbB family member) over-expressing in a tumor are shown to live one-third shorter than HER2 negative patients due to the aggressive tumor growth, resistance to treatment and high risk of local relapse and recurrence. We reported that some cancer cell lines isolated from the survival fraction of cancer cells after exposure to multiple doses of therapeutic radiation show a resistant phenotype to radiation due to HER2 overexpression that is regulated by the transcription factor NF- κ B. HER2 protein levels, not gene copy number, are found to be elevated in the recurrent tumors compared with the primary breast cancer. Thus, radiation-induced repopulation of breast cancer cells appear to be related to activation of a specific pro-survival pathway with a novel set of radioresistant breast cancer stem cell marker, i.e., NF- κ B/HER2/CD44⁺/CD24^{-/low}. The radioresistant MCF7 clones with high HER2 level or MCF7 cells overexpressing HER2 show a significant enhancement in cell invasiveness and aggressiveness compared with wild type MCF7 cells. Furthermore, with FACS live-sorted MCF7 cells we find that HER2⁺/CD44⁺/CD24^{-/low} cells are more radioresistant, aggressive and invasive than the HER2/CD44⁺/CD24^{-/low} cells. These results demonstrate a novel feature of tumor repopulation with radioresistant breast CSCs and a potentially effective therapeutic target for imaging and inhibiting radioresistant CSCs.

(MS301) High-throughput screens for small molecule inhibitors of DNA mismatch repair and novel repair-associated genes. Nicholas M. Pedley, Thomas Helleday, Gray Institute for Radiation Oncology & Biology, University of Oxford, Oxford, United Kingdom

The exploitation of tumour genetic abnormalities through the drugging of synthetic lethal targets has been shown to be an effective and selective new therapeutic strategy in the treatment of cancer. Defects in one or more DNA repair pathways have been shown to be a common feature of cancer, whilst loss of function mutations in 'stability' genes that normally maintain the integrity of the genome are likely a key rate-limiting step in carcinogenesis. Since even genetically unstable cells require some repair functionality to maintain viability, these cancers probably exhibit an over-reliance on other DNA repair pathways. An in-depth knowledge of the genetic basis of repair processes in combination with a suite of DNA repair inhibitors to knock out these backup pathways may therefore prove extremely useful tools in the development of the next generation of cancer chemotherapeutics. To this end, we present the results of a small molecule high-throughput screen to detect novel inhibitors of the DNA mismatch repair (MMR) pathway, together with results of a small interfering RNA (siRNA) screen for novel MMR-associated genes. Key to both screening strategies are the resistance of cells with a dysfunctional mismatch repair pathway to a range of cytotoxic drugs, including the alkylating agent N-methyl-N'-nitro-N-nitrosoguanidine (MNNG). By exploiting this MMR-dependent toxicity we have assayed for small molecules and siRNA that permit the survival of MNNG-treated MMR-proficient cells to levels comparable to MMR-deficient cells, and which therefore represent putative MMR modulating agents. Specific MMR activity assays that monitor the repair of a G:T mismatch in nuclear extracts and live cells were subsequently applied to verify our screen results. In summary, we are presenting small molecule structures that inhibit MMR activity in Human cells, together with the identification of novel genes that are involved in the MMR DNA repair pathway.

(MS302) Characteristics of DNA binding proteins determine the biological sensitivity to high linear energy transfer radiation. Hongyan Wang¹, XiangMing Zhang¹, Ping Wang¹, Xiaoyan Yu¹, Jeroen Essers², David Chen³, Roland Kanaar², Shunichi Takeda⁴, Ya Wang¹, Emory University, Atlanta, GA, ²Erasmus Medical Center, Rotterdam, Netherlands, ³UT Southwestern Medical Center, Dallas, TX, ⁴Kyoto University, Kyoto, Japan

Non-homologous end-joining (NHEJ) and homologous recombination repair (HRR), contribute to repair ionizing radiation (IR)-induced DNA double strand breaks (DSBs). Mre11 binding to DNA is the first step for activating HRR and Ku binding to DNA is the first step for initiating NHEJ. High-linear energy transfer (LET) IR (such as high energy charged particles) killing more cells at the same dose as compared with low-LET IR (such as x or γ rays) is due to inefficient NHEJ. However, these phenomena have not been demonstrated at the animal level and the mechanism by which high-LET IR does not impact the efficiency of HRR remains unclear. In this study, we showed that although wild type and HRR deficient mice or DT40 cells are more sensitive to high-LET IR than to low-LET IR, NHEJ deficient mice or DT40 cells are equally sensitive to high- and low-LET IR. We also showed that Mre11 and Ku respond differently to shorter DNA fragments in vitro and to the DNA from high-LET irradiated cells in vivo. These findings provide strong evidence that the different DNA DSB binding properties of Mre11 and Ku determine the different efficiencies of HRR and NHEJ to repair high-LET radiation induced DSBs. (This work was supported by NASA grant NNX07AT40G.)

(MS303) Targeting BRCA1 localization to augment tumor cell susceptibility to poly (adp-ribose) polymerase-1 (PARP1) inhibition. Eddy S. Yang, Somaira Nowsheen, Fen Xia, Vanderbilt University, Nashville, TN

Purpose: Agents which target cancers deficient in DNA double strand break (DSB) repair, such as poly (ADP-ribose) polymerase-1 (PARP1) inhibitors, have gained recent attention due to their highly selective killing of BRCA-mutated familial breast and prostate tumors while maintaining minimal toxicity in normal tissues. However, the majority of sporadic breast and prostate cancers possess wild-type (WT) BRCA1 and maintain proficient DSB repair. In this study, we investigated whether the targeting of BRCA1 localization away from its nuclear repair substrates can transiently induce BRCA1 dysfunction in DSB repair, and thus subsequently augment sporadic breast and prostate tumor cell susceptibility to PARP1 inhibition. Methods: To generate a DSB repair defect, WT BRCA1 was targeted to the cytoplasm away from its nuclear repair substrates using irradiation (IR) or ectopic expression of the small peptide tr-BRCA1, a truncated form (1-301aa) of BRCA1 that can effectively shift BRCA1 to the cytosol. Immunohistochemistry for BRCA1 localization was performed following IR or tr-BRCA1 to confirm cytosolic BRCA1 redistribution. DSB repair capacity was assessed via a GFP-based repair assay. Cell survival as measured by colony formation assays was performed. The dependence on p53 was also investigated. Results: IR or ectopic tr-BRCA1 expression efficiently targeted BRCA1 to the cytosol and subsequently inhibited DSB repair by more than 3 fold compared to control in human breast and prostate cancer cells independent of cell cycle redistribution. Consequently, these cancer cells exhibited exquisite susceptibility to PARP1 inhibition (maximal 30 fold reduction in cell survival). Interestingly, the anti-tumor effects of PARP1 inhibition following IR were p53-dependent, while p53 was dispensable for PARP1 inhibition-mediated cell death following tr-BRCA1 expression. Conclusions: By transiently inducing a DSB repair defect via targeting BRCA1 localization away from its nuclear repair substrates, augmenting breast and prostate cancer cell susceptibility to PARP1 inhibitors can be an innovative strategy to enhance therapeutic index. Furthermore, this strategy may also be feasible for other tumor types, including lung, pancreas, and brain cancers.

(MS304) The effects of alpha particle radiation on gene transcripts associated with apoptosis in a human monocytic cell-line. Vinita Chauhan¹, Matthew Howland¹, James P. McNamee¹, Trevor J. Stocki¹, Trevor Burn², Lindsay A. Beaton², Ruth Wilkins¹, ¹Health Canada, Ottawa, ON, Canada, ²Carleton University, Ottawa, ON, Canada

Radon (²²²Rn) gas is a naturally occurring radioactive carcinogen which, in humans, accounts for more than forty percent of radiation exposure. When inhaled, ²²²Rn decays into products that pass into the lungs and emit alpha- α particles. These α -particles can damage cells and may have the potential to induce lung cancer. An understanding of the mechanisms associated with these carcinogenic effects remains limited. Apoptosis is a critical component of cellular homeostasis and dysregulation of this process can often lead to tumourgenesis. This study was designed to examine the effects of α -particle radiation on apoptosis and the associated changes in gene expression. Exponentially growing human monocytic cells (THP-1) were exposed to α -particle radiation at a dose range of 0-1.5 Gy. The expression of a focused panel of 84 genes related to apoptosis was analyzed for differential expression 72 h following α -particle radiation using real-time PCR. Concurrently, apoptosis was measured in these cells using flow cytometry by annexin V conjugate staining and a multi-caspase detection assay. A total of 15 genes were shown to be differentially expressed at all three doses tested and approximately 30% of the transcripts were shown to be upregulated. Among these genes, expression levels of two key initiators of apoptosis, tumour necrosis factor alpha (TNF α) and fas were markedly elevated ($p \leq 0.05$). The majority of the genes that were differentially expressed at all three doses were shown to be downregulated. Specifically, expression levels of transcripts associated with anti-apoptotic functions (BCL2, BCLAF1, IGFIR and BIRC2) were significantly downregulated by two fold ($p \leq 0.05$). These transcript modulations were correlated to increases in apoptosis as measured by flow cytometry using a multi-caspase detection kit and annexin V conjugate staining. On average, 35% of the cells were shown to be apoptotic at the highest dose of α -particle radiation tested relative to only 2% in the untreated controls ($p \leq 0.05$). This data suggests that α -particle radiation may induce apoptosis through the activation of TNF α and fas, and through the modulation of key anti-apoptotic genes.

(MS305) The XLF C-terminal region is required for DNA binding and interaction with Ku in vitro but not for repair of double-strand breaks in vivo. Brandi L. Mahaney, Yaping Yu, Shujuan Fang, Susan P. Lees-Miller, University of Calgary, Calgary, AB, Canada

DNA double strand breaks (DSBs) are one of the most detrimental DNA lesions in the cell. DSBs can be induced by ionizing radiation (IR) and in mammalian cells these DSBs are primarily repaired by the non homologous end-joining pathway (NHEJ) which involves several core proteins including the DNA-PK complex which is composed of the Ku70/80 heterodimer and the DNA-PKcs catalytic subunit; the XRCC4-DNA ligase IV complex; and the XRCC4-like factor (XLF) which has been shown to stimulate XRCC4-DNA ligase IV mediated DNA end-joining. Crystal structures of XLF confirm that it is structurally similar to XRCC4 yet contains noticeable differences in the C-terminal region. Previously, we have shown that the C-terminal region of XLF binds DNA *in vitro* and is phosphorylated by DNA-PK *in vivo*. Here we show that this region, which is predicted to be unstructured, is also required for the DNA-dependent interaction between XLF and the DNA-PK complex in cell extracts and for interaction with purified Ku70/80 in pull-down assays. Interestingly, the highly conserved penultimate amino acid F298 is absolutely required for the interaction between XLF and Ku as well as for DNA binding in electrophoretic mobility shift assays. However, C-terminal truncation of XLF or mutation of F298 does not significantly alter the kinetics of gamma-H2AX foci resolution following IR *in vivo*. These results suggest that although the C-terminal region of XLF is important for DNA binding and interaction with Ku *in vitro* these interactions may not be necessary for double-strand break repair *in vivo*.

(MS306) Kinetics of *in vivo* formation and reduction of γ H2AX in bone marrow cells after exposure of mice to 100 MeV/n protons. Paiboon Reungpatthanaphong¹, Louise Honikel¹, Marc Golightly¹, Carl A. Anderson², Kanokporn Rithidech¹, ¹Stony Brook University, Stony Brook, NY, ²Brookhaven National Laboratory, Upton, NY

Very little is known about the rate of production and loss of γ H2AX after *in vivo* exposure to radiation. To date, there is no information on the kinetics of *in vivo* formation and reduction of γ H2AX levels in bone marrow (BM) cells, the target for radiation-induced leukemia. Our research project is the first to fill in this knowledge gap. We gave BALB/cJ mice a whole-body exposure to 0.5 or 1.0 Gy of 100 MeV/n protons, delivered at 0.5 or 1.0 cGy/min. For each dose and dose rate of 100 MeV/n protons, mice exposed to 0 Gy of protons served as sham controls. After irradiation, BM cells were collected at 1.5, 3, and 24 hr for analyses. There were four mice per treatment group per harvest time. We used a well-established flow cytometry method for determining the level of γ H2AX in each phase of the cell cycle of BM cells. For each mouse, at least 20,000 cells were analyzed. We incubated BM cells with antibody against mouse γ H2AX, Ser-139, followed by Alexa Fluor 488 (AF488, goat anti-mouse IgG) and propidium iodide (PI) to identify cells in different stages of the cell cycle. As an internal control, we also used PI to stain cells from each sample without AF488. At 1.5 hr post-irradiation, significant increases ($p < 0.05$, Student's t-test) in levels of γ H2AX were found in all phases of the cell cycle in BM cells collected from mice exposed to 1.0 Gy of 100 MeV/n protons, in relation to those in their corresponding sham controls, regardless of the dose rate. However, these increases were more pronounced when the higher dose rate, *i.e.* 1 cGy/min, was used. Subsequently, the levels of γ H2AX declined towards the level detected in non-irradiated cells within 24 hr. Further, the ability of BM cells to rejoin/repair damage was found to decrease when the dose rate increased, suggesting dose-rate effects of proton-irradiation. With respect to mice exposed to 0.5 Gy, there was no increase in γ H2AX levels in BM cells of exposed mice as compared to those found in sham controls at any time points included in the study, regardless of the dose rate. This finding may indicate that BM cells are capable of repairing/rejoining the damage induced by 0.5 Gy of 100 MeV/n protons delivered at these two low-dose rates and that the repair/rejoin processes completed before 1.5 hr post-irradiation (the first time point included in the study). Research funded by NASA Grant #NNX07AP88G.

(MS307) DNA Mismatch repair protein MSH2 may dictate cellular survival in response to low dose radiation. Lynn M. Martin¹, Brian Marples², Mary Coffey¹, Mark Lawler¹, Thomas Lynch³, Donal Hollywood¹, Laure Marignol¹, ¹Trinity College Dublin, Dublin, Ireland, ²William Beaumont Hospital, Royal Oak, MI, ³St. James's Hospital, Dublin, Ireland

We have previously shown that exposure to low dose radiation (0.05-0.3Gy) induces a hypersensitive response (HRS) in prostate cells that is associated with the response of cells to O6-methylguanine lesions. HRS was associated with a DNA mismatch repair (MMR) proficient phenotype. To explore the specific role of MMR protein MSH2 in HRS, we used isogenic cell lines proficient and deficient in MSH2 (endometrial carcinoma: HEC59, HEC59+chr2). Using cell sorter clonogenic assays we found that HRS is expressed solely in MMR+ cells with greatest sensitivity in the low dose range observed following 0.2Gy. HRS+ glioma cells have previously been demonstrated to bypass the early G2 checkpoint following such a dose. To gain deeper insight into the role of MSH2 in the mechanism underlying HRS we examined the activation of the early G2 phase checkpoint 0-3 hours after 0.2Gy, using cellular staining with phospho-histone H3 (ph-h3) and PI. Strikingly, flow cytometry revealed that only MSH2+ cells arrested efficiently at this checkpoint. This was confirmed using high content screening (HCS) image analysis for ph-H3. Western blotting and use of the inhibitor UCN-01 in flow cytometry studies revealed that efficient activation of the arrest was chk2 dependent. MMR proteins are known to suppress homologous recombination (HR) via regulation of RAD51 which may also influence chk2 phosphorylation. To explore the role of HR in the activation of the early G2 arrest, we used HCS image analysis to compare basal

RAD51 expression and the induction of RAD51 foci after 0.2 Gy. HCS revealed that MSH2+ cells expressed lower basal levels of RAD51 and increased RAD51 foci after 0.2 Gy. Using the RAD51 stimulator RS-1 and Hsp-90 inhibitor 17-aag, preliminary results suggest that differential RAD51 regulation may be responsible for the activation of the early G2 checkpoint and induction of HRS in MSH2+ cells. Collectively these data reveal the complexity of the low dose DNA damage response and indicate that an MSH2-RAD51-chk2 dependent mechanism may be responsible for HRS which is consistent with the concept that HRS is enhanced in G2 phase cells as has been reported. This is the first report of an MSH2-mediated hypersensitive response to low doses of radiation. MSH2 may therefore represent an excellent biomarker for radiation sensitivity in the low dose range.

(MS308) Processing and biological consequences of clustered DNA damage containing a single strand break and an AP site. Naoya Shikazono¹, Miho Noguchi¹, Ayumi Urushibara¹, Peter O'Neill², Akinari Yokoya¹, ¹Japan Atomic Energy Agency, Tokaimura, Japan, ²University of Oxford, Oxford, United Kingdom

Clustered DNA damage, defined as two or more lesions within one to two helical turns of DNA by a single radiation track, is a unique feature of ionizing radiation. Although extensive work has been carried out on how non-dsb type of clustered damage is processed *in vitro*, the processing of clustered damage *in vivo* still needs further investigation. Using a bacterial plasmid-based assay, we have studied the biological consequences of bistranded clustered damage sites which consist of a single strand break (SSB) and an apurinic/apyrimidinic (AP) site. Plasmids were ligated with oligonucleotides containing clustered lesions. Following transformation of the ligated plasmids into the wild type strain of *Escherichia coli*, we found significantly lower transformation frequencies for the clustered SSB + AP lesions (separated by 1bp) than that for either a single SSB or a single AP site. When the two lesions were placed further apart (10-20bp), both transformation efficiency and mutation frequency are comparable to those of the single lesions. The lesion separation required for plasmid recovery is dependent on the relative orientation of the clustered SSB + AP lesions. The efficiency of plasmid recovery, in part, required PolI activity. We suggest that a double strand break or a replication block is formed during the processing of the SSB + AP clusters and that DNA synthesis plays a significant role in determining its biological consequences. These results indicate that the biological consequences of clustered DNA damage strongly depend on the separation and relative orientation of the lesions.

(MS401) Design and testing of compact tissue equivalent proportional counters for astronauts during extra vehicular activity and inside spacecraft. Thomas B. Borak¹, Leslie Braby², Lawrence Heilbronn³, Yoshi Iwata⁴, Terry Lusby⁵, Takeshi Murakami⁴, David Oertli¹, Tore Straume⁵, David Warner¹, ¹Colorado State University, Ft. Collins, CO, ²Texas A&M University, College Station, TX, ³University of Tennessee, Knoxville, TN, ⁴National Institute of Radiological Sciences, Chiba, Japan, ⁵NASA Ames Research Center, Moffett Field, CA

A compact real-time dosimeter will be required for astronauts during prolonged extra vehicular activities (EVA) and could be configured to serve as a portable radiation monitor inside transport spacecraft. It must be capable of measuring the dose rate and quality factor from galactic cosmic rays during ambient conditions. It must also record the dose and issue a warning to the astronaut during the initiation of a high intensity solar particle event (SPE). General specifications outlined by NASA are that the detectors should be tissue equivalent, omni-directional and capable of accurately measuring ambient dose rates on the order of 300 μ Gy/d for particles with LET ranging from 0.2 to 300 keV/ μ m. At the onset of a solar particle event the system must be capable of signaling an alarm at 0.05 mGy/min and at 10 mGy/min. We have designed several prototype dosimeters to satisfy these requirements based on spherical tissue equivalent proportional counters. The directional response to HZE particles has been measured for several detector

assemblies and electronic configurations. We are developing a version of the variance-covariance method, using a single detector, that can accommodate the large dynamic range of particles and dose rates. This work is supported by NSBRI-NASA, RE01301 (TB) and RE01302 (TS).

(MS402) LET is a critical factor in accelerating development of lymphoma in irradiated Bax transgenic C57/B6 mice. James Jacobus, Chester Duda, Sean Martin, Mitchell Coleman, Kranti Mapuskar, Michael Knudson, Douglas Spitz, University of Iowa, Iowa City, IA

A major risk during exposure to both low and high linear energy transfer (LET) radiation is the development of lymphoma. Both occupationally and therapeutically exposed individuals are at risk for lymphoma development induced by low LET radiation, while deeply penetrating high LET radiation is a significant concern for those planning and undertaking long duration missions in space where a high degree of uncertainty on actual risk exists due to the lack of epidemiologically-based datasets. The C57/B6 transgenic mice used in this study have been genetically engineered to possess either one (Bax 1) or two (Bax 38/1) extra copies of the pro-apoptotic Bax gene under the T cell specific Lck promoter. Bax expression causes reduced cellularity of the thymus, increased relative cell proliferation, genomic instability, and development of T cell lymphoma, with an average age to death of 28 weeks in untreated Bax 38/1 animals and > 60 weeks for Bax 1 animals. Using these model systems we tested the hypothesis that overexpression of Bax would significantly affect lymphoma development in response to low (10 cGy) and high (100 cGy) dose radiation from either low LET or high LET sources. Mice were whole body irradiated using low LET radiation from a cesium-137 source or high LET irradiated with iron nuclei accelerated at Brookhaven National Laboratory, NASA Space Radiation Laboratory. Our results indicate that 100 cGy of 1 GeV iron in whole body irradiated double transgenic Bax 38/1 mice is significantly more potent at accelerating lymphoma development in the thymus than 100 cGy of low LET gamma rays. While this study is currently ongoing, at twenty-four weeks of age 80% (16/20) of 100 cGy high LET Bax 38/1 mice have died from lymphoma, versus 40% (5/12) of control Bax 38/1 mice. Low LET 10 and 100 cGy exposed Bax 38/1 and Bax 1 mice show a trend toward accelerated lymphoma development that is not dose-dependent nor statistically significant at this time. In contrast, there appears to be a dose response for accelerated lymphoma development using high LET radiation, with 10 cGy being less effective than 100 cGy in the Bax 38/1. These results suggest that the effects of high LET radiation on T cell lymphoma development may be greater than expected based on our low LET epidemiological data. (supported by a joint grant from DOE/NASA, DE-SC0000830).

(MS403) Distinct transcriptome profiles associated with HZE particle radiation of different energy and LETs. Lianghao Ding, Michael D. Story, UT Southwestern, Dallas, TX

The objective of this study is to characterize cell responses to HZE particle radiation of different energy and LETs. We used immortalized human bronchial epithelial cells (HBEC-3KT) to perform microarray analysis to study whole genome profiles of mRNA and miRNA expression. Radiation exposures were provided by the NASA Space Radiation Lab (NSRL) using 1 GeV Fe, 1 GeV Si, 1 GeV O, 200 MeV O and γ -rays. Experiments were carried out from 5 NSRL beam runs so that at least two independent radiations were received for each particle type. Cells were irradiated at 0.5 Gy and 1 Gy for HZE particles, 1 Gy and 3 Gy for γ -rays. Total RNA was isolated from cells that were harvested at 0hr (control), 1 hour, 4 hours, 12 hours and 24 hours after each irradiation. Whole genome expression Illumina BeadChips were used to perform microarray analysis. Raw signal intensities were background-subtracted and quantile-normalized using the MBCB algorithm. Results of principal component analysis showed segregation of gene expression profiles based on different particle types. Significantly changed genes after radiation were determined by applying a time

course analysis model (maSigPro). A signature of 20 genes was used to build a model to predict Fe, Si and γ -ray exposures. The models were built using Support Vector Machine. The best model was chosen by repeatedly partitioning sample groups for building and cross-validation of the models. The cross-validating results showed 98% accuracy in predicting the three radiation types. An independent testing set was collected in the latest BNL run and the prediction results are being analyzed. We have now collected data from 200 MeV O exposures (LET equivalent to 1 GeV Si) as we intend to study whether LET is the dominant factor that defines the different expression profiles from different particles. This initial analysis is ongoing. Expression changes for miRNA are also being investigated using the same cell samples. The preliminary data suggested that the most robust miRNA responses happen at 1 hour after radiation, which is earlier than mRNA responses. MiRNAs associated with the p53 pathway and cell cycle regulation were found significantly changed. More functional analysis of significantly changes mRNAs and miRNAs are underway and will be revealed at the time of the meeting.

(MS404) Prolonged lifespan, decreased thymic lymphoma incidence, and activated immune-regulated genes in low-dose-rate irradiated AKR/J mice. Hee-sun Kim, Suk-Chul Shin, Yu-Mi Kang, Kwang-Hee Yang, Cha-Soon Kim, Ji-Young Kim, Seon-Young Nam, Seung-Jin Choi, Young-Woo Jin, Radiation Health Research Institute, Seoul, Republic of Korea

To evaluate the effect of low-dose-rate radiation on cancer incidence, we reared AKR/J mice in a Long-term Low-dose-rate Irradiation Facility (^{137}Cs , 0.7 mGy/h). We compared the thymic lymphoma incidence and lifespan of high-dose-rate (^{137}Cs , 0.8 Gy/min, total dose of 4.5 Gy) irradiated mice with those of non-irradiated mice. Previously, we reported that the incidence of thymic lymphoma in low-dose-rate irradiated mice was decreased (15%, $P < 0.01$) and the average lifespan of low-dose-rate irradiated mice was extended (35 days, $P = 0.02$). We collected normal-sized thymuses at 130 days after irradiation and performed whole genome microarray analysis. In all, 17,625 genes were expressed. We classified expressed genes associated with the carcinogenesis pathways (DNA repair, DNA damage signaling, cell cycle, cancer pathway finder, p53 signaling, apoptosis, and T-cell and B-cell activation). In this study, we focused on the expression of immune-related genes. We found the expression of immune-regulated genes (*Lilrb3*, *Igh6*, *Fcgr2b*, *Fcgr3*, *MGC60843*, and *Jag 2*) in low-dose-rate irradiated mice. The results suggested that cells with incompletely repaired DNA and cancer cells are removed by the stimulation of apoptosis and activation of NK and T and B cells, which contribute to the decreased thymic lymphoma incidence and elongated lifespan. We also observed that the expressed down-regulated immune genes (*Il15*, *Cd3e*, *Sp3*, *Traf6*, *Itra2*, *Rag2*, *CD28*, and *Chfb*) in high-dose-rate irradiated mice. These data suggested that apoptotic pathway and immune related cells (NK cells and lymphocytes) and autoimmunity are suppressed by high-dose-rate radiation. Functional studies for identifying the role of the other genes associated with thymic lymphoma incidence that were expressed in low-dose-rate irradiated mice are currently in progress.

(MS405) Irradiation of immortalized human fibroblasts with high energy protons at both high and low dose rates. Bradford D. Loucas, Richard L. Eberle, Michael N. Cornforth, University of Texas Medical Branch, Galveston, TX

One characteristic of low LET radiations are dose rate effects. By lowering the dose rate, the magnitude of many radiation-induced effects is lessened. One such change is the flattening of chromosome aberration dose responses. These are thought to result from a reduction in the frequency of multi-track exchanges with decreasing dose rates. The rate below which no further reduction in effect is observed has been defined as the limiting low dose rate. When this is achieved, in theory, only single-track exchanges are formed which should produce linear dose responses. While this phenomenon has been well studied with X- and gamma-rays, it is unclear to what extent such an effect will be observed following

irradiation with high energy, low LET protons which are of concern to NASA with regard to solar particle events. To test the presence and extent of dose rate effects for high energy protons, we irradiated plateau phase hTERT immortalized BJ-1 human fibroblasts at NSRL with 1 GeV, 150 MeV and 50 MeV protons at a low dose rate of about 0.5 cGy/min which is near the limiting low dose rate for gamma photons and at a high dose rate of about 100 cGy/min. Cells were subcultured 72-96 hours post-irradiation and mitotic cells were collected 32-36 hours later. These were fixed, spread onto slides and examined using mFISH to measure the frequency of chromosome aberrations. The scoring of cells irradiated with 1 GeV is nearing completion and results thus far indicate that the frequency of aberration break-points produced by 3 Gy at low dose rate is about 1/3 of that observed at the higher dose rate. Part of this difference seems to have resulted from a greater relative reduction in the frequency and size of complex exchanges forming from three or more chromosome breaks as compared to simple exchanges. The inspection of cells irradiated at the two lower energies is on going but preliminary evidence suggests that results will be similar to those of the 1 GeV experiments. The authors gratefully acknowledge support from the National Aeronautics and Space Administration, Office of Biological and Physical Research NASA/OBPR; NNJ07ZSA001N. Special thanks also to Adam Rusek and the NSRL support staff for their expertise during proton irradiations.

(MS406) Effects of radiation on blood cell numbers in mice exposed to whole body irradiation from gamma and electron radiation. Ana L. Romero-Weaver, Jeffrey H. Ware, Ann R. Kennedy, University of Pennsylvania, Philadelphia, PA

As part of the activities of the NSBRI Center of Acute Radiation Research (CARR), the effects of solar particle event (SPE) radiation on peripheral blood cell counts are being evaluated to determine the risks to astronauts from blood cell loss. From the data obtained, Relative Biological Effectiveness (RBE) values are being determined in which the results from SPE radiation are compared to those from a reference radiation. In these studies, both electrons and gamma radiation are being utilized in different experiments as the reference low Linear Energy Transfer (LET) radiations. Whole body irradiation can cause a decrease in the number of blood cells which can be due to killing of the circulating cells and/or loss of precursor cells and/or loss of cells from the circulation by hemorrhage. The doses of SPE (primarily proton) radiation that astronauts can be exposed to during extravehicular activity (EVA) include doses as high as 2 Gy (deep dose). The methods used for determining the numbers of blood cells in irradiated animals have been established. Two methods utilized to determine White Blood Cell (WBC) differential counts in mice (manual and automated cell counts) exposed to 0.25, 0.5, 1 and 2 Gy of 6-MeV electrons at a dose rate of 0.5 Gy/minute or 0.5 Gy/hour were compared. The results demonstrated a close correlation and a high degree of agreement between manual cell counts determined in our laboratory and those determined from automated counts at Antech Diagnostics. In experiments performed with gamma (2 Gy) or electron radiation (6 MeV, 1 Gy), the effects on whole body irradiation were evaluated utilizing a single high dose rate at numerous time points out to 30 days post-irradiation. At periods of time within the first day post-irradiation, WBC counts and lymphocyte counts were significantly reduced. Both neutrophil and lymphocyte counts reached their lowest numbers by day 2 post-irradiation. By 30 days post-irradiation the levels of these blood cells returned to normal levels. These results indicate that with a single acute dose as high as 2 Gy, blood cell numbers are significantly reduced for short time periods post-irradiation, but that there is no long-term effect on blood cell numbers for either electron or gamma radiation exposure.

(MS407) Effects of fractionated irradiation with carbon ions on gut crypt survivals and tumors. Koichi Ando¹, Sachiko Koike², Akiko Uzawa³, Ryoichi Hirayama², Yoshitaka Matsumoto³, Yoshiya Furusawa³, Nobuhiko Takai⁴, Takeshi Fukawa³, Yukari Yoshida¹, ¹Gunma University, Maebashi, Japan, ²Natl Inst.Radiol.Sci., Chiba, Japan, ³Natl.Inst.Radiol.Sci., Chiba, Japan,

⁴Nagasaki International University, Sasebo, Japan, ⁵Josai International University, Togane, Japan

Purpose: We have previously reported that RBE values of carbon-ion beams for skin reaction and tumors increases with an increase of fractionation in a different way so that therapeutic gain is maximally obtained at around 4 fractions. Purpose of present study is to compare survivals of crypts and tumor cells after multiple 1 Gy per fraction followed by top-up doses. **Materials and Methods:** C3H male and female mice at age 8-12 week old were used. NFSa fibrosarcoma was subcutaneously transplanted to ventral skin of male mice 10 days before irradiation. Carbon ions with 290 MeV/u were accelerated by HIMAC synchrotron, and LET of 20 keV/μm at entrance plateau of a Spread-Out Bragg peak (6 cm width) was used. Mice were immobilized by placing in Lucite holders without anesthesia, and received horizontal beams every 4 hr. Tumors were removed shortly after final irradiation, and preceded to single cell preparation. Cell suspensions were intravenously injected to recipient mice that were pretreated with cyclophosphamide, and lung colony assay was conducted. Jejunum of female mice was removed 3.5 days after final irradiation and served for histology preparation. **Results:** Survival curves for crypts and tumor cells were obtained after single doses, 1 Gy x 5 fractions plus top-up doses and 1 Gy x 11 fractions plus top-up doses. The NFSa tumor showed biphasic curves after single doses, suggestingoxic and hypoxic cells included. Slopes of survival curves fit by single hit model were not significantly different between single doses and fractionated doses, even though single doses showed a lightly shallower curve than the fractionated doses. Crypt survivals plot against total doses clearly shifted to the right after fractionated doses: 1 Gy x 5 fractions moved survival curves parallel to single doses while 1 Gy x 11 fraction not only moved further to the right but also showed a shallower slopes that either single or 1 Gy x 5 fractions. **Conclusion:** Repair of damage caused by 1 Gy of low-LET carbon ions was different between the NFSa tumor and gut crypts. Therapeutic gain was apparently larger for 11 fractions than 5 fractions.

(MS408) Gap-junction communication and oxidative metabolism mediate the propagation of toxic effects between alpha-particle irradiated human cells. Narongchai Autsavaprompong¹, Sonia M. de Toledo¹, John B. Little², Jean-Paul Jay-Gerin³, Andrew L. Harris⁴, Edouard I. Azzam¹, ¹New Jersey Medical School-Cancer Center, UMDNJ, Newark, NJ, ²Harvard School of Public Health, Boston, MA, ³University of Sherbrooke, Sherbrooke, QC, Canada, ⁴New Jersey Medical School, UMDNJ, Newark, NJ

Coordinated interactions of specific molecular and biochemical processes are likely involved in the cellular stress response to different types of ionizing radiation. Here, we investigated the roles of gap-junction intercellular communication and oxidative metabolism in modulating cell killing and repair of potentially lethal damage (PLDR) in confluent normal human fibroblasts exposed to ²⁴¹Am α particles or ¹³⁷Cs γ-rays at doses by which all cells in the exposed cultures are irradiated. As expected, α particles were more effective than γ-rays at inducing cell killing. Whereas PLDR occurred in γ-irradiated cells, holding α particle-irradiated cells in the confluent state for various times resulted in increased cell killing, which was associated with increased DNA damage, protein oxidation and lipid peroxidation. Inhibiting gap junction communication with 18-α-glycyrrhetic acid or knockdown of the level of connexin43, a constitutive protein of junctional channels, by siRNA, promoted protective effects in α particle-irradiated cell cultures; it decreased induced DNA damage and enhanced clonogenic survival. Using human adenocarcinoma cells in which specific connexins can be expressed in the absence of endogenous connexins, we found that permeability aspects of gap junctions affect the response to radiation. Whereas connexin26 and connexin43 channels mediated the propagation of toxic effects among irradiated cells, connexin32 channels conferred protective effects. We also investigated the role of oxidative metabolism: Up-regulation of antioxidant defense, by ectopic overexpression of glutathione peroxidase, protected against toxic effects expressed during the incubation period post α particle-irradiation. Together, these data show that the damaging effect of α particles, a high linear energy transfer radiation, is amplified by junctional communication

among the irradiated cells and results in enhanced oxidative stress. Supported by Grant NNJ06HD91G from NASA

(MS501) Transcriptional activity dictates susceptibility to stress-induced bystander DNA damage. Jennifer S. Dickey¹, Brandon J. Baird¹, Christophe E. Redon¹, Alexei Kondratyev², Valeriya Avdoshina², Guillermo Palchik², William M. Bonner¹, Olga A. Sedelnikova¹, ¹NIH, Bethesda, MD, ²Georgetown University, Washington, DC

The radiation-induced bystander effect (RIBE) is a well-known consequence of exposure to ionizing radiation (IR). An early event in this effect is the induction of DNA double-strand breaks (DSBs) in bystander cells that initiate downstream pathways leading to increased genomic instability and decreased viability. Measuring DNA DSB formation by monitoring γ-H2AX induction is an extremely sensitive way to detect this bystander damage. Similar to the RIBE, a distinct DNA DSB response is seen in bystander cell populations proximal to or when exposed to media from stressed, transformed, senescent, or damaged cells. Similar mechanistic pathways, involving NO, TGF-β, and other inflammatory cytokines seem to be responsible for bystander effects generated from all forms of stress. Bystander DNA damage seems to mainly be induced in cells during S-phase. However it remains unclear whether cell cycle state alone confers bystander effect vulnerability. Therefore, primary human lymphocytes and primary rat neurons were examined. Bystander DNA damage induction was monitored in response to UVC, 0.2 Gy, and 20 Gy IR. Both media transfer and co-culture protocols were utilized. We found that while quiescent lymphocytes did not display a bystander response, activated lymphocytes were able to both transmit and respond to bystander signals. Lymphocytes one day post-activation were responsive to bystander signals though they have yet to reach S-phase. Additionally, while rat cortical and hippocampal neurons were unresponsive to bystander signaling, neurons derived from the cerebellum were susceptible, despite being non-replicating. Bystander effect vulnerability correlated with the ability of TGF-β and NO to induce DNA DSBs in these cell populations. Analysis also revealed that high transcription rates in cells conferred bystander signaling vulnerability regardless of cell cycle stage. Blocking transcription with α-amanitin eliminated bystander-induced DNA damage in both lymphocytes and neurons. Taken together, these results indicate for the first time that cellular signaling of stress to bystander populations is closely linked to transcriptional activity as well as cell cycle stage, and confirms that bystander effects are mediated through reactive oxygen species as well as inflammatory cytokines.

(MS502) Hypersensitivity of human and rodent Fanconi anemia (FA) cells to bystander effect-induced DNA damage. Paul F. Wilson¹, Hatsumi Nagasawa², Ayano C. Kohlgruber¹, Salustra S. Urbin¹, John R. Brogan², Matt A. Coleman¹, John M. Hinz³, ¹Lawrence Livermore National Laboratory, Livermore, CA, ²Colorado State University, Fort Collins, CO, ³Washington State University, Pullman, WA

Fanconi anemia (FA) is a chromosomal instability and cancer predisposition syndrome characterized by developmental defects, progressive bone marrow failure, and cellular hypersensitivity to agents that induce DNA interstrand crosslinks and oxidative stress. Previously, we reported on the hypersensitivity of the isogenic *Fancg*-deficient CHO mutant KO40 for sister chromatid exchange (SCE) induction following low dose plutonium-238 α-particle irradiation where <1% of cell nuclei are hit. Compared to wild-type AA8 and *CgFancg*-complemented KO40 cells (40BP6) in which SCE frequencies increased ~30% over background levels in irradiated cultures, SCE frequencies in KO40 *fancg* cells increased ~50% over background levels in irradiated cultures. More recently, this hypersensitivity was also observed when KO40 cells were grown for two cell cycles in medium transferred from 2 Gy γ-irradiated AA8 cultures or medium to which a 1:10 dilution of Hank's balanced salt solution (HBSS) from 2 Gy γ-irradiated AA8 cultures was added (indicating bystander molecules can be released

when cells are maintained and irradiated in simple isotonic buffers). Together, this data supports our hypothesis that DNA damage induced in non-irradiated bystander cells consists primarily of single-stranded oxidative lesions that interfere with replicative DNA polymerases and require FA proteins to direct repair using translesion polymerases or homologous recombinational repair (HRR). We are investigating bystander effect-mediated SCE induction in other CHO mutants, including UV40 and NM3 *fancc* cells and EM9 *xrcc1* cells, and *fanca*, *fancc*, *fancd2*, and *faneg* primary human fibroblasts and their complemented controls. Bystander effect-mediated transcriptional responses in the human FA fibroblasts grown in bystander medium are being assessed by quantitative RT-PCR and microarray analyses following a recent report from our group demonstrating significant induction of Tp53-responsive genes in *fanca* lymphoblastoid lines following treatment with mitomycin C and hydroxyurea. The hypersensitivity of FA cells to bystander effect-mediated DNA damage makes them attractive candidates for identifying associated signaling mechanisms that are likely important factors modulating low dose IR cancer risk following low and high LET exposures.

(MS503) Investigations into out-of-field cell survival and radiation induced bystander responses following exposure to intensity-modulated radiation fields. Karl T. Butterworth¹, Conor K. McGarry², Colman Trainor¹, Joe M. O'Sullivan², Alan R. Hounsell², Kevin M. Prise¹, ¹Queens University Belfast, Belfast, United Kingdom, ²Northern Ireland Cancer Centre, Belfast, United Kingdom

Intensity-modulated radiation therapy (IMRT) is an advanced radiotherapy approach in which highly modulated fields are used to achieve high dose conformity across a target tumor volume. Recent in vitro studies have suggested cell survival following exposure to modulated fields may not be accounted for using a traditional linear quadratic (LQ) model as non-local dose effects may have an important role in determining radiobiological response both within and outside of the primary radiation field. Cell survival was determined by clonogenic assay in human prostate cancer (DU145) and transformed fibroblast (AGO1552) cells following exposure to different field configurations delivered using a 6 MV photon beam produced with a Varian clinical linear accelerator at the Northern Ireland Cancer Centre. Delivery of uniform dose distributions as modulated or non-modulated fields showed no significant difference in cell survival with the exception of DU-145 cells at 8 Gy ($p = 0.024$). Non-uniform dose distributions were delivered using a multileaf collimator (MLC) in which half of the cell population was shielded. Clonogenic survival in the shielded region was significantly lower than that predicted from the LQ model and for DU145 cells saturated at 40% survival at scattered radiation doses above 0.7 Gy. In contrast, cells in the exposed part of the field showed increased survival. These observations were abrogated by inhibition of cellular communication. Additional studies have shown the proportion of cells irradiated and dose delivered to the shielded and exposed regions of the field have an impact on response. These data demonstrate out of field effects as important determinants of cell survival following exposure to modulated irradiation fields with cellular communication between differentially irradiated cell populations playing an important role. This highlights the need for refinement of existing radiobiological models to incorporate non-targeted effects and modulated dose distributions. This work is supported by Cancer Research UK (Grant C1513 / A7047).

(MS504) Radio-adaptive response of *hprt* mutation in normal human fibroblasts induced by proton microbeams. Masao Suzuki, Chizuru Tsuruoka, Teruaki Konishi, Masakazu Oikawa, Cui H. Liu, Yumiko Kaneko, Yoshiya Furusawa, National Institute of Radiological Sciences, Chiba, Japan

Recently we have investigated that the mutation frequency at the hypoxanthine-guanine phosphoribosyltransferase (*hprt*) locus, which was detected with measuring 6-thioguanine resistant clones, in normal human fibroblasts induced by the 200kVp X-ray challenging dose (1.5Gy) was reduced at 0.15 times in cells pre-

treated with low-dose-rate neutrons (1mSv/8h) as a priming dose compared to unpre-treated cells. Furthermore, the reduced mutation frequency was returned to the control level, when using a specific inhibitor of gap-junction mediated cell-cell communication (40 μ M lindane). We set up a hypothesis that recoiled protons emitted by the interaction between primary neutrons and surroundings near irradiated cells induce radio-adaptive response in irradiated cell population via gap-junction mediated bystander effect. To examine the hypothesis around 1.5% of total cells were irradiated with single 3.4MeV proton before irradiating the X-ray challenging dose using the microbeam irradiation system, Single Particle Irradiation system to Cell (SPICE) in National Institute of Radiological Sciences, Japan. The result clearly showed that the X-ray induced mutation frequency of *hprt* locus was suppressed in cells pre-treated with proton microbeams and returned to the control level, when using a specific inhibitor of gap-junction mediated cell-cell communication. The result suggests that neutron-induced adaptive response is caused by recoiled protons and gap-junction mediated bystander effect plays an important role to induce such cellular response.

(MS505) SIRT3 regulates mitochondrial antioxidant enzyme activity following exposure to ionizing radiation. Mitchell C. Coleman¹, James A. Jacobus¹, David Gius², Douglas R. Spitz¹, ¹University of Iowa, Iowa City, IA, ²Vanderbilt University School of Medicine, Nashville, TN

Members of the sirtuin family of deacetylases can be found within many compartments of the cell and have been hypothesized to play critical roles in cell maintenance and repair. Recent work has demonstrated that the mitochondrially-located sirtuin 3 (SIRT3) is crucial in maintaining normal mitochondrial physiology and functions as a tumor suppressor in mouse embryonic fibroblasts (MEFs) as well as *in vivo*. SIRT3^{-/-} MEFs also demonstrate increased superoxide levels and increased genomic instability following exposure to ionizing radiation (*Cancer Cell* 17:41-52). Since the tumor-permissive phenotype seen in SIRT3^{-/-} MEFs was ameliorated by addition of superoxide dismutase and manganese superoxide dismutase (MnSOD) is a potential SIRT3 target, it was hypothesized that SIRT3^{-/-} mice may have deficiencies in mitochondrial MnSOD regulation in response to stress. When SIRT3^{-/-} mice were exposed to 2 x 2 Gy fractions of whole body ionizing radiation over 48 hours, SIRT3^{-/-} liver mitochondria showed no increase in MnSOD activity in contrast to a two-fold increase in control mice. Also, SIRT3^{-/-} heart mitochondria showed a 25-30% decrease in MnSOD activity following IR relative to control. In addition SIRT3^{-/-} heart and liver mitochondria demonstrated a slight 10-15% increase in glutathione peroxidase-1 (GPx-1) activity following IR while control mice showed a slight 15-20% decrease in GPx-1 activity following IR. These data support the hypothesis that SIRT3 may be a crucial factor in determining antioxidant enzyme responses in mouse mitochondria following exposure to ionizing radiation. (supported by a grant from DOE DE-SC0000830)

(MS506) The European NOTE project: A commentary on current research in non-targeted effects of ionising radiation. Munira A. Kadhim, Oxford Brookes University, Oxford, United Kingdom

The discovery / elucidation of non-DNA targeted effects of ionizing radiation, which include genomic instability (GI), and a variety of bystander effects (BE) including abscopal effects and bystander mediated adaptive response (BE/AR), has raised concerns for their implications in the radiation protection of the public, especially for quantification of human risk at low doses. Genomic instability, bystander effects and adaptive responses are defined by the experimental procedures used to study them. As such, they are not basic biological processes like transcription or DNA synthesis. Although these operational definitions serve a useful purpose, they constrain our thinking. Despite excellent research in this field from eminent research groups, there are still gaps in our understanding of the likely mechanisms associated with non-DNA targeted effects, particularly with respect to systemic (human health) consequences

at low and intermediate doses of ionising radiation. Other outstanding questions include the direct / indirect cross mechanistic links between the different NOTE responses and if the variation in non-targeted response observed between individuals and cell lines is linked to sex, genetic background, epigenetic effects or phenotype. This presentation is a contribution from a European Integrated Research Project on non-targeted effects (NOTE) which will aim to provide a commentary on the current state of the field. It will explore the background to the development of the concept of NOTE with respect to key radiobiological aspects, as well as critically examine how the evidence for non-targeted effects emerged from radiation biology research. It will also include discussion regarding terminology, some apparently contradictory results in the field and consider the implications of the effects for health effects, and therefore whether they would require revision of the approach to assessing radiation risk.

(MS507) The association of inbreeding with lung fibrosis incidence in beagle dogs that inhaled $^{238}\text{PuO}_2$ or $^{239}\text{PuO}_2$. Dulaney A. Wilson, Andrea Brigantic, William F. Morgan, Pacific Northwest National Laboratory, Richland, WA

Studies of the biological behavior and subsequent health effects from internally deposited plutonium in beagle dogs were intended to predict likely health effects in humans. Although care was taken to ensure 'random' mating, the beagle dog gene pool was limited compared with human populations. The relationship between plutonium inhalation and lung fibrosis was evaluated to determine if there was a genetic or familial component that would explain the relationship. The genetic or familial component is described by the inbreeding coefficient, the probability that a dog has two identical alleles for any gene. The inbreeding coefficient ranged from zero to 9.4 with a mean of 2.5 (SD 2.3). Dogs given plutonium-238 dioxide ($^{238}\text{PuO}_2$) had lower inbreeding coefficients than dogs given plutonium-239 dioxide ($^{239}\text{PuO}_2$) or control dogs. A previous analysis of data from life-span studies of beagle dogs given a single exposure to $^{238}\text{PuO}_2$ or $^{239}\text{PuO}_2$ generated estimates of the cumulative hazard of lung fibrosis. In dogs exposed to $^{238}\text{PuO}_2$ the addition of an inbreeding coefficient to the model did not improve the model fit. However, the inbreeding coefficient did affect the modeling in dogs given $^{239}\text{PuO}_2$. The best model of lung fibrosis after exposure to $^{239}\text{PuO}_2$ incorporated a linear dose-response function. When the inbreeding coefficient was added to the model, the best-fitting model included a linear dose-response function modified by the inbreeding coefficient, an interaction term between inbreeding coefficient and sex and the age at exposure. An increase in inbreeding coefficient was associated with decreased probability of lung fibrosis in females (RR 0.87; 95% CI 0.79-0.96) but a slightly increased probability in males (RR 1.14; 95% CI 1.04-1.25). These differences by sex probably reflect the make-up of the breeding population. However, the protective effect of increased inbreeding in dogs exposed to $^{239}\text{PuO}_2$ is surprising. This work was supported by Radiation Biology and Biophysics, U. S. Department of Energy, Pacific Northwest National Laboratory's Laboratory Directed Research and Development Program and funding from a pilot project awarded by the National Institutes of Health, National Institute for Allergy and Infectious Disease grant U19 AI 067770, Centers for Medical Countermeasures against Radiation.

(MS508) Localization of lens opacity and model fitting analysis by UV substitution in cataract of A-bomb survivors. Kazuo Neriishi¹, Eiji Nakashima¹, Atsushi Minamoto², ¹Radiation effects Research Foudation, Hiroshima, Japan, ²Minamoto Eye Clinic, Hiroshima, Japan

For evaluation of radiation-induced ocular lens damage, accurate assessment of risk factor characteristics is extremely important. Since a significant city difference was found to exist between Hiroshima and Nagasaki in terms of cataract prevalence in the previous study, we analyzed the localization of lens opacities and fit a model incorporating the variable impact of UV on the eye, assuming that the city difference in cataract prevalence was due to a difference in UV radiation between the two cities. The results

suggest that cataracts among Nagasaki residents were more frequently located at the inferior nasal portion of the lens than among Hiroshima residents, with no radiation-specific localization observed. Based on incidence angles, UV was suggested as a possible cause of the city difference. We therefore analyzed the fit of the model by modeling city differences in terms of levels of UVA and UVB irradiation. The UVB model, compared with the UVA model, provided a better fit. The evidence suggests that UVB may be the cause of the city difference. The current study suggests that the location of residence and investigation period, as well as outdoor activities, are important as surrogate factors for UVB in evaluation of radiation-induced cataract, and that the superior temporal portion of the lens may be suitable for the evaluation of ionizing radiation effects because of the minor amount of interference at that site.

(MS601) Cross sections for bare and dressed carbon ions in water: a classical trajectory Monte Carlo calculation. Thiansin Liamsuwan, Hooshang Nikjoo, Karolinska Institutet, Stockholm, Sweden

We present a model calculation for the interaction cross sections for bare and dressed carbon ions 1keV/u - 1MeV/u in water. Cross sections are needed for the description of track, interaction by interaction, in irradiated media. At the investigated energies, the stopping power of ions exhibits a maximum. Therefore, understanding of energy-loss processes is of particular interest for the investigation of radiation effectiveness. When ion slows down under the Bragg peak, charge transfers give rise to the fraction of dressed projectiles in the ion track, and should be included for the precise determination of energy loss of track. We use the three-body Classical Trajectory Monte Carlo (CTMC) method to calculate the interaction cross sections. Two-center effect is automatically incorporated in the model. Two separated collision schemes were simulated: these are projectile-target electron-target core and; projectile core-projectile electron-target molecule. The radial and momentum distributions of the active electron to the core are determined from the binding energy, and used for sampling of the initial condition of the electron before the collision. Electron-electron interactions within a core are simplified using the model potential, taking into account the distance-dependent screening of the core. The total and differential cross sections for ionization, electron capture, and electron loss will be presented and compared to the existing experimental data. We aim to implement the calculated cross sections in a Monte Carlo track structure code for simulation of carbon ion tracks, and characterize radiation therapy beams using microdosimetry and biophysical modeling.

(MS602) The influence of amino acids on the fragmentation of oligonucleotides exposed to low energy electrons. Sylwia Ptasinska¹, Zejun Li², Nigel J. Mason¹, Leon Sanche², ¹The Open University, Milton Keynes, United Kingdom, ²University of Sherbrooke, Sherbrooke, QC, Canada

The majority of interactions between amino acids and nucleobases can be applied across all protein-DNA complexes [1]. Therefore investigating the effect of amino acids on DNA analogues can mimic the phenomena observed in the cell exposed to ionizing radiation and provide a better understanding of protein-DNA radiolysis at the molecular level. In our approach, we have studied tetramer oligonucleotides (GCAT) containing all four nucleobases: adenine (A), cytosine (C), guanine (G) and thymine (T) with glycine (Gly) and arginine (Arg), both amino acids can be found in natural proteins. The amino acid - GCAT pairs were irradiated with electrons of 1 eV. This electron energy was chosen to simplify the effects of multiple electron scattering in our samples. Moreover, one eV electrons can induce single strand breaks in DNA only via dissociative electron attachment [2]. Irradiated samples were analyzed by high performance liquid chromatography and the total fragmentation yields were measured for different molar ratios of Arg:GCAT and Gly:GCAT. Our experimental studies have shown that at higher molar ratios of glycine and arginine, both amino acids protect DNA from the direct action of electrons. Whilst at low ratios, mainly in the case of glycine, an increase in the total

fragmentation yield was observed. This additional damage of oligonucleotides can be attributed to interaction of the H^+ radicals produced from glycine. As it has been shown in the gas phase studies on dissociative electron attachments to glycine the formation of dehydrogenated molecule and hydrogen radical appears with a huge cross section for this reaction [3]. In addition, the computational modelling has revealed binding energies and sites for particular amino acid-nucleobase/nucleotide pairs. Both amino acids interact relatively strongly with nucleotides via van der Waals and electrostatic interactions, however the average value for the binding energy for Arg-nucleotide ($-1.633 \text{ kcal mol}^{-1}$) is higher than those for Gly-nucleotide pairs ($-1.228 \text{ kcal mol}^{-1}$). Thus arginine interacts more strongly, which is in good agreement with our experimental results. [1] N.M. Luscombe et al., Nucl. Acids Res. 29, 2860 (2001). [2] F. Martin et al., Phys. Rev. Lett. 93, 068101 (2004). [3] S. Ptasinska et al., Anal. Bioanal. Chem. 377, 1115 (2003).

(MS603) Simulation of secondary electron yields from thin metal foils after fast proton impact. Anderson Travia, Michael Dingfelder, East Carolina University, Greenville, NC

Accurate particle interaction cross sections are the fundamental input data of event-by-event Monte Carlo track structure codes used in the simulation of radiation effects on materials. The track structure simulation consists of recording the energy loss, interaction type, and classical path of the primary particle and all the induced secondaries from the first interaction to total stop. Tests on thin metal foils with well known physical properties are performed to assess the accuracy of these codes that can be used with complex targets such as water and biological tissues. We have simulated secondary electron yields from thin aluminum, copper, and gold foils after proton impact using the Monte Carlo track structure code PARTRAC. Energy- differential cross sections and total inverse mean free paths have been calculated using the first Born approximation and the dielectric response theory. The target is described by a generalized oscillator strength constructed with optical oscillator strengths obtained from photo-absorption data employing a delta oscillator dispersion algorithm. The shell separation method has been applied to determine the inner atomic shells in which the ionization event originated. Electron exchange effects have also been incorporated. Comparisons with previous results will be presented. This work is supported in part by the National Institute of Health, National Cancer Institute Grant No. 2R01CA093351.

(MS604) Studying the effects of temperature on the mechanism of iodine-125 decay induced DNA damage. Thabisile Ndebe, Igor Panyutin, Ronald Neumann, National Institute of Health, Bethesda, MD

Targeted radiotherapy is an alternative cancer therapy that utilizes a tumor-localizing agent with a radioactive atom attached. This results in more localized damage primarily at the tumor cells. Gene targeted radiotherapy combines both gene manipulation and targeted radiotherapy. Our group has previously developed triplex-forming oligonucleotides, which target genes of interest and selectively cleave these genes by using an attached iodine-125 radionuclide. Understanding the DNA damaging mechanism of the Auger electron emitter, iodine-125, is relevant for the therapeutic potential of this method. Auger electron emitters produce highly localized damage in DNA. This highly localized damage primarily proceeds through three mechanisms; 1) direct damage by the emitted Auger electrons, 2) indirect damage by diffusible free radicals produced by Auger electrons in water, and 3) charge neutralization of the highly positively charged tellurium daughter atom. An additional intermediate charge transport mechanism has also been proposed as a factor in iodine-125 decay induced DNA damage. Charge transport is a mechanism that describes how charge travels along DNA and subsequently leads to damage in DNA. Our earlier work showed that charge transport was not a factor in iodine-125 induced DNA damage at 193K. The purpose of our current work was to determine whether the charge transport mechanism

along DNA contribute to iodine-125 decay produced damage at more elevated temperatures. This was achieved by using charge transport inhibitors, such as BrdU, 8-oxo-G, and GpG steps, to probe for charge transport in iodine-125 decay induced DNA damage. These charge transport inhibitors were each incorporated proximal to the iodine-125 in different DNA hairpins. Their effect on the distribution of DNA breaks produced by iodine-125 decay was analyzed by polyacrylamide gel electrophoresis. We found that the inhibitors had no measurable effect on the distribution of DNA breaks at the elevated temperatures of 253K, 277K and 298K. Our results, therefore, suggest that charge transport is not a factor in iodine-125 decay-induced DNA damage at these temperatures.

(MS605) Yields of oxidative damage produced in puc18 by the direct effects of 70kV x-rays at 4 K and room temperature.

Anita R. Peoples¹, Jane Lee², Michael Weinfeld², Jamie R. Milligan³, William A. Bernhard¹, ¹University of Rochester, Rochester, NY, ²Cross Cancer Institute, Edmonton, AB, Canada, ³University of California at San Diego, La Jolla, CA

Our mechanistic understanding of damage formation in DNA by the direct effect relies on what is known of free radical intermediates studied by EPR spectroscopy. Bridging this information to stable product formation requires analytical methods with comparable detection sensitivities, a criterion met by the 32P-postlabelling assay developed by Weinfeld and Soderlind [Biochemistry 30, 1091(1991)]. When applied to the indirect effect, this technique detected thymine glycol (Tg) and phosphoglycolate (pg). Other base damage products were evident but not identified (called X). Importantly, X must be due to oxidation but is not 8-oxo-Gua, or 8-oxo-Ade. We used this assay to determine yields of products in pUC18 films with hydration levels (Γ) of 2.5, 15 or 22 waters per nucleotide and X-irradiated at either 4 K or RT. Results from the first set of experiments gave chemical yields of pg (G(pg)) close to zero; e.g., for $\Gamma = 2.5$, $G(\text{pg}) = 4 \pm 1 \text{ nmol/J}$ (RT) and $3 \pm 1 \text{ nmol/J}$ (4 K). Given that formation of pg requires O₂ attack at the C4'-deoxyribose radical, this is evidence that the C4' radical contributes little to the total deoxyribose damage, which from the previously measured unaltered free base release is $134 \pm 4 \text{ nmol/J}$. The yield of detectable base damage (G(Tg+X)) at $\Gamma = 2.5$ was found to be $35 \pm 4 \text{ nmol/J}$ (RT) and $19 \pm 3 \text{ nmol/J}$ (4 K). Given the paucity of water in these samples, formation of Tg appears unlikely, raising the possibility of other oxidation products similar to but different than Tg. Supported by PHS Grant 2-R01-CA32546 of the NCI.

(MS606) Radiation dose-response for induction of γ -H2AX foci in tissues: use of new automatic counting software.

Alesia Ivashkevich¹, Olga A. Sedelnikova², Christophe E. Redon³, Andrea J. Smith¹, William M. Bonner², Roger F. Martin¹, Pavel N. Lobachevsky¹, ¹Peter MacCallum Cancer Centre, Melbourne, Australia, ²National Cancer Institute, Bethesda, MD, ³National Cancer Institute, Melbourne, MD

The γ -H2AX foci endpoint is extremely useful in many aspects of radiation biology, as well as other scenarios associated with oxidative damage to DNA. γ -H2AX foci are generally counted manually, but it is time consuming and fatiguing. One of us (PL) has developed a new computer program (TGR_IMG) for automatic counting of foci to address this problem. The software incorporates standard image analysis algorithms in sequences designated for focal analysis, while still allowing the flexibility in selecting or rejecting a particular algorithm and in optimizing the analysis parameters. It offers fast optimizing of focus identification and counting parameters based on test counts for a few images, and allows also user-independent parameter optimization. Automation requires minimum user input and allows batch processing of a range of images. The program also calculates focus area, total intensity, distribution of cells with respect to focus number etc. TGR_IMG has been initially validated using images of human lymphocytes collected from 4 different donors and irradiated *ex vivo* with various doses (0.02-1.5 Gy), in which γ -H2AX foci were also manually counted. In this validation exercise, which involved 50 images with an average of 30 cells per image, the respective times for manual

and TGR_IMG analysis were 12-14 and 4 hrs. This study demonstrated a high degree of correlation between average values for each group (radiation dose/donor) obtained from manual and automatic counting ($R^2 = 0.973$). The automatic versus manual counting comparison was then extended to radiation dose response studies with various mouse tissues, by examination of touch prints (duodenum) or sections (oral mucosa, duodenum), after whole body irradiation (0.5-5 Gy). A correlation coefficient $R^2 = 0.773$ was obtained in the analysis of average numbers of foci per image comparing manual and automatic counting, and $R^2 = 0.952$ for average values per group (radiation dose). The results confirm the general utility of the automatic counting program coupled with significant time saving.

(MS607) High-Throughput processing and analysis of micronucleus and γ -H2AX assays in ex vivo irradiated human samples. Antonella Bertucci, Helen C. Turner, Guy Garty, Olekandra V. Lyulko, Maria Taveras, David J. Brenner, Columbia University, New York, NY

At the Center for High-Throughput Minimally Invasive Radiation Biodosimetry we have developed the Rapid Automated Biodosimetry Tool (RABIT). The RABIT is a dedicated and ultra-high throughput robotically based biodosimetry system to quantify DNA damage and estimate individual past radiation exposures using a very small volume of blood. During the past year we have adapted established protocols for both γ -H2AX and cytokinesis-block micronucleus assays (CBMN) to be entirely performed in the RABIT. Histone H2AX phosphorylation on a serine four residues from the carboxyl terminus (producing γ H2AX foci) is a sensitive marker for DNA double-strand breaks (DSBs). The γ -H2AX assay measures DNA damage directly by immuno-staining the phosphorylated H2AX histones which localize DSBs. The *in vitro* micronucleus test is widely used to assess cytogenetic damage. In this system, chromosome fragments or whole chromosomes become detectable in the cytoplasm of cells that have undergone mitotic division as micronuclei (MN). Whole blood samples, from twelve healthy donors, were irradiated with γ -rays: 1, 2, 3, 4, 5, 7.5 and 10 Gy. After exposure, 30 μ l samples are placed into heparin-coated PVC capillaries containing 50 μ l of lymphocyte separation media. The separated lymphocyte bands are released into filter bottomed multi-well plates where the cells were either cultured for the MN assay or incubated for γ -H2AX assay. For the MN assay, isolated lymphocytes were cultured in complete RPMI 1640 medium containing phytohemagglutinin (PHA) to stimulate mitosis followed by the addition of cytochalasin B to block cytokinesis and obtain binucleate cells. Cells then were stained with DAPI. For the immunodetection of γ -H2AX foci, lymphocytes were incubated with an anti-human γ -H2AX monoclonal antibody and visualized using an Alexa Fluor 555 secondary antibody and nuclei were counterstained with Hoechst 33342. We will present dose response curves for both assays processed and imaged in the RABIT. Work supported by NIAID grant 5 U19-AI067773.

(MS608) Early-response biological dosimetry using hematological profile - NHP dose response. William F. Blakely¹, Natalia Ossetrova¹, Arifur Rahman¹, Melanie V. Cohen², Ann Farese², David J. Sandgren¹, Thomas J. MacVittie², ¹AFRRI, Bethesda, MD, ²University of Maryland, School of Medicine, Baltimore, MD

Medical management of suspected radiation casualties necessitates use of multiple parameter biological dosimetry assessment. Radiation causes changes in peripheral blood (PB) counts that are useful for both dose- and acute radiation syndrome (ARS) - hematological system severity assessments. The ability to discriminate individuals exposed to radiation from controls by their hematological profile at an early time point is important in mass-casualty radiological incidents where repeated blood counts may not be possible. We are pursuing research activities to develop and enhance an integrated, multiple-parameter biodosimetric system for both triage and reference laboratory applications. We recently

reported results from nonhuman primate (NHP) total-body irradiation (TBI) study demonstrating that combination of total lymphocytes with the neutrophil to lymphocyte ratio improved the discrimination index between 7.2 Gy and 8.4 Gy cohorts from 44% to 81% and 44% to 69% for 1 and 2 days post irradiation, respectively. Herein, we characterize the utility of changes in the hematological profiles for early (<4 days) radiation dose and injury assessment based on pooled data from NHP TBI studies over a broad dose range. Baseline and radiation time- and dose-dependent changes have been measured in the PB of NHP (males and females *Macaca mulata*) irradiated between the dose range of 1 to 13 Gy with ⁶⁰Co γ -rays (0.55 Gy/min) and 6 MV LINAC (0.8 Gy/min). A dose-dependent early-phase (1-3 d) demonstrated: a) decline in lymphocytes, b) abortive rise at 1d followed by a decline in neutrophils, c) increase in the neutrophil to lymphocyte ratio, and d) negligible changes in platelets. Lymphocyte depletion and increases in the neutrophil to lymphocyte ratios were most robust as diagnostic indices spanning the broad dose ranges from 1-3 d after irradiation, however, these two bioindicators plateau with progressive increases in radiation doses >6.5 Gy. These data support the development of an integrated and multiparameter biodosimetric software analysis system that provides diagnostic indices for medical management of radiation casualties. [Research was supported under AFRRI work units RBB4AR; DARPA under MIPR entitled: "Nonhuman Primate Testing for Biodosimetry", and NIAID contract number HHSN266200500043C.]

(MS701) Radioprotection and Radiomitigation Properties of Ex-RAD™ Upon Oral Administration. Ramesh Kumar, Onconova Therapeutics, Inc., Princeton, NJ

Onconova Therapeutics has discovered a novel small molecule kinase inhibitor Ex-RAD™ which has demonstrated significant protection against radiation damage, at lethal doses of radiation *in vitro* and *in vivo*, with remarkable margin of safety. At present, Ex-RAD is being developed as a subcutaneous injectable product for first responders for prophylactic use. Onconova has completed several clinical trials with subcutaneous (SC) administration of drug. The oral route of administration of ExRAD would provide significant benefit of use in civilian population especially children and elderly. Preclinical pharmacokinetics studies in rats, dogs, rabbits and monkeys reveal that ExRAD is well absorbed, and has a relative bioavailability ranging from 47 to 91%. Here we report effectiveness of Ex-RAD™ upon oral administration in a mouse whole body irradiation (WBI) model. Methods: Ex-RAD was administered SC or orally (PO) to 6-8 weeks old male C3H/Hen or female C57BL/6J mice (N=10) at 24h and 15 minutes prior to 7.5 Gy whole body irradiation (WBI). C3H/Hen mice (N=10) were also dosed 24h and 36h after WBI. Irradiation was done using a 137-Cs source. Survival was monitored for 30 days. Results: We saw significant survival advantage with Ex-RAD administered pre- and post-radiation. Radioprotection results were similar with PO and SC administration of Ex-RAD at 500 mg/Kg. Significant radioprotection was also observed with lower oral dose (200 mg/Kg) of Ex-RAD. Oral formulation (500 mg/Kg) when administered +24h and +36h after radiation showed 90% survival compared to 50% in vehicle administered group. Conclusions: Ex-RAD™ is equally effective when administered either orally or subcutaneously. Orally administered Ex-RAD™ offers the benefit of convenient dosing options to the civilian population for either prophylaxis or the treatment of Acute Radiation Syndrome.

(MS702) Transplantation of bone marrow-derived adherent stem cells provide support to the intestinal stem cell niche and mitigate radiation induced gastrointestinal syndrome (RIGS) in mice. Subhrajit Saha¹, Payel Bhanja¹, Rafi Kabarriti², Laibin Liu¹, Alan Alfieri¹, Emily Chen³, Chandan Guha², ¹Albert Einstein College of Medicine, Bronx, NY, ²Albert Einstein College of Medicine and Montefiore Medical Centre, Bronx, NY, ³Stony Brook University Medical Center, Stony Brook, NY

RIGS is the result of direct cytotoxic effects on intestinal crypt cells with subsequent loss of the mucosal barrier. This manifests as

electrolyte imbalance, systemic infection (sepsis) and death. The stromal cells surrounding the intestinal stem cell (ISC) provide the niche and supply critical growth factors for stem cell regeneration. We hypothesized that supplement of bone marrow-derived adherent stem cells (BMASCs) as source of ISC niche component including mesenchymal stem cells (MSCs), endothelial progenitor cells (EPCs) and macrophages may restore ISC and its niche to mitigate RIGS. C57Bl/6 mice BM was cultured for 4 dys, followed by collection of adherent cells (BMASCs). Mice receiving BMASCs (2×10^6 cells i.v. at 24 and 72hrs post irradiation) containing 48±2% MSC (CD105⁺CD45⁻), 7.1±0.5% EPC (CD133⁺ Flk⁺) and 17.3±1.8% myeloid/macrophages (CD11b⁺F480⁺) survived (100%) lethal doses of whole body irradiation (WBI) (10.4Gy) and abdominal irradiation (AIR) (18Gy), $p < 0.002$ and $p < 0.004$ respectively. Transplantation of either CD11b⁺ myeloid cells or CD11b⁻ and CD105⁺ MSCs could mitigate 30-40%, indicating cooperative role of MSCs and macrophages for RIGS survival. Histopathology of jejunum demonstrated significant increases in proliferation ($p < 0.004$), crypt depth ($p < 0.001$) & decrease in apoptotic crypt cells ($p < 0.003$) with BMASC transplant after irradiation (IR). Immunohistological analysis showed restoration of intestinal subepithelial myofibroblast (α SMA +ve & desmin -ve) (major ISC niche component) with BMASC transplant. Xylose absorption was greater in these mice indicating functional integrity following BMASC transplantation. To study the possible radio-mitigating factor secreted from BMASC, concentrated culture supernatant was administered to irradiated mice at 24hr and 72 hr after either, WBI (10.4 Gy) or AIR (16Gy). 50% of mice survived for up to 30 days indicating the presence of mitigating factors in culture supernatants. Proteomic analysis was performed to identify potential mitigating agents present in the culture supernatant. So far, this is the first demonstration that supplementation of stromal component / factors could mitigate supra-lethal doses of IR. Studies are ongoing to identify the cellular and molecular mechanisms responsible for radiation mitigation.

(MS703) Abscopal bone marrow suppression is the direct cause of acute death in mice following abdominal irradiation.

Peter Corry, Sue Theus, Katie Steed, Leah Hennings, Dan Jia, University of Arkansas for Medical Sciences, Little Rock, AR

Acute death in humans 5-10 days after a large dose ionizing radiation is also known as “gastrointestinal (GI) death” since the histological destruction of the GI tract is the predominant radiation tissue injury within this period. Whether GI injury is the direct cause of acute radiation death, however, has not been settled. To address this issue, we developed a mouse abdominal irradiation (AI) model. Ten-wk-old male C57BL/6 mice were irradiated with a single fraction of 20 Gy x-rays to the abdomen only. The mice were given a single injection of saline or syngeneic bone marrow cells (10^7 - 10^8 cells) via tail vein 24h after AI. In some experiments, the mice were monitored daily for body weight change and survival. In separate experiments, mice were sacrificed at post-AI day 7 for peripheral blood cell count, *ex vivo* bone marrow clonogenicity assay, and histological assessment of jejunum, spleen, and bone marrow cellularity. AI alone caused a 90% decrease in peripheral white blood cell count, white pulp area of the spleen, and bone marrow stromal cells in mice 7 days after AI, a collective evidence of bone marrow suppression. Bone marrow transplantation (BMT) led to the recovery of these parameters to 70% of the levels in sham-irradiated mice at post-AI day 7, indicating a restoration of the hematopoietic capacity. Moreover, BMT dose-dependently increased the 10-day survival rates of the irradiated mice to 40-80%, as compared with 0% in saline-treated group. The increased animal survival was accompanied by dose-dependent recovery of mouse body weight. Interestingly, at post-AI day 7 the extent of jejunum edema as well as the loss of jejunum villi, crypts, and epithelial cells enveloping the villi in mice receiving BMT were all comparable to that in saline-treated abdominally irradiated mice. Our results demonstrate that GI injury alone is not sufficient to cause GI death and that BMT mitigation of acute death after AI is independent of the restoration of jejunum structure. Abscopal suppression of bone marrow, presumably mediated by signals from radiation GI injury, is the direct cause of acute death after AI.

(MS704) The bisphosphonate risedronate prevents deterioration of bone in rats at directly irradiated sites after modeled radiotherapy. Jeffrey S. Willey¹, Michael E. Robbins², J. D. Bourland², Ted A. Bateman¹, ¹Clemson University, Clemson, SC, ²Wake Forest University, Winston Salem, NC

Radiation therapy for pelvic tumors in postmenopausal women increases pelvic-bone fracture rates by ~65-200%. One-year after a hip fracture mortality is nearly 20% in women. The cause of these fractures is not well understood. Recent work has demonstrated that radiation rapidly activates osteoclasts, leading to acute bone loss. However, mouse studies showing damaged bone after irradiation have used whole-body exposures. It is unclear if bone loss occurs primarily as a direct response at irradiated sites or from systemic factors. The purpose of this study was to apply a clinically relevant fractionated dose to determine direct radiation effects. Twenty-one-week old Sprague-Dawley rats were divided into 3 groups: non-irradiated; irradiated; and irradiated + risedronate (an osteoporosis therapy; 0.1 mg/kg/wk) treated rats. Over a 2-week period, right hind limbs were exposed to a total dose of 16 Gy of 6 MV X-rays delivered in 4 fractions using a LINAC. A cervical cancer treatment regimen was modeled using the Fowler equation assuming an α/β ratio of 3 for human and rat bone. For these women 30 x 1.8 Gy fractions (M-F for 6 weeks) are delivered, applying 54 Gy to the tumor. Hips receive ~50% of each fraction totaling 27 Gy, resulting in a BED of 35.1 Gy. We modeled this with 4 fractions of 4 Gy each over 2 weeks (BED = 36.8). At 2, 4 and 6 weeks after the last fraction, microCT evaluated trabecular bone in the proximal tibia 3mm distal to the growth plate. Severe deterioration of bone in the irradiated right limb relative to the non-irradiated left limb was observed at all time points. Reduced trabecular connectivity and fewer trabeculae were present at directly irradiated sites relative to the non-irradiated limbs ($p < 0.05$). Quality of the trabeculae was reduced as struts became rod-like ($p < 0.05$). Thickness of the trabeculae, however, was increased by 2 weeks ($p < 0.05$), mitigating loss of volume despite loss of structural integrity. Atrophy of irradiated limbs was entirely prevented with risedronate administration. Local irradiation resulted in deterioration of bone relative to a non-irradiated site on the opposite limb. An antiresorptive osteoporosis therapy mitigated local bone atrophy. While systemic factors cannot be excluded, radiation appears to induce bone loss primarily within the irradiated volume (supported by AR054889).

(MS705) Minozac mitigates rat brain radiation injury following whole brain irradiation. Kenneth A. Jenrow, Stephen L. Brown, Karen Lapanowski, Andrew Kolozsvary, Jae Ho Kim, Henry Ford Hospital, Detroit, MI

Whole brain irradiation (WBI) doses of 10 Gy or less are sufficient to impair neurogenesis within the rat dentate gyrus, along with hippocampal plasticity and cognitive function. Impaired neurogenesis reflects both the acute loss of neural progenitors via apoptosis and a more gradual disruption of neurogenic signaling via inflammation. Anti-inflammatory drugs can partially prevent these deleterious effects when administered prior to irradiation. Here we have investigated whether minozac, a selective inhibitor of pro-inflammatory microglial cytokines, can mitigate these deleterious effects when administered post-irradiation. Male Fischer 344 rats received WBI doses of 0 (control) and 10 Gy using a Cs-137 irradiator. Minozac (5 mg/kg/day, IP) therapy was initiated 24 hours post-WBI and continued in separate withdrawal cohorts for 1 or 4 weeks post-WBI. Rats were sacrificed at 8 weeks post-WBI. Three weeks prior to sacrifice, rats received once daily BrdU injections (50 mg/kg/day, i.p.) for 5 days to label mitotically active cells. Rats were sacrificed by transcardial perfusion/fixation. Tissues were subsequently processed for paraffin embedding, thin sectioned at 5 μ m, and immunohistochemically stained for BrdU, Ki67, double cortin (DCX), NeuN, CD-68, and Ox-6. Volume densities of cells expressing these markers were quantified within the dentate gyrus in multiple sections along the anterior-posterior axis. Minozac, administered for either 1 or 4 weeks post-WBI, significantly reduced the expression of Ox-6⁺ microglia and significantly preserved/restored granule cell DCX⁺ neurons within the dentate gyrus at 8 weeks post-WBI. The mitigating effects of minozac in this context are consistent with reduced inflammation and a preservation/

restoration of neurogenic signaling integrity within the dentate gyrus. Remarkably, these mitigating effects persisted for several weeks after therapy withdrawal, suggesting that inhibiting the actions of pro-inflammatory microglial cytokines for as little as 1 week post-WBI is sufficient to produce a lasting, and perhaps permanent, benefit. Funded by NIAID Cooperative Agreement U19 AI067734.

(MS706) The effect of amifostine and ionizing radiation on apoptosis and chromosomal inversion responses. Rebecca J. Ormsby¹, Mark D. Lawrence¹, Benjamin J. Blyth¹, Eva Bezak², David J. Grdina³, Pamela J. Sykes^{1,4}, ¹Flinders University & Medical Centre, Adelaide, Australia, ²Royal Adelaide Hospital, Adelaide, Australia, ³University of Chicago, Chicago, IL, ⁴SA Pathology, Adelaide, Australia

Low dose radiation (LDR) and the chemical radioprotector amifostine can both mitigate some of the harmful effects of radiation exposure. They display a number of distinct similarities including their ability to protect cells against radiation-induced DNA damage and cell death, and metastases formation. We previously demonstrated that LDR protects from radiation-induced chromosomal inversions when delivered *after* high dose radiation. The ability to retrospectively protect from a prior radiation exposure is common to only a few agents, including amifostine. Subsequent studies examining chromosomal inversion responses have revealed further similarities between amifostine and LDR suggesting that there are common mechanisms associated with low dose radioprotective responses and amifostine-mediated cytoprotection. We hypothesized that chromosomal inversion changes induced by amifostine are mediated via changes in apoptosis frequency. To test this, amifostine was administered to mice alone or in conjunction with X-rays. Mice were euthanized at various timepoints and spleen tissues analysed for apoptosis. We observed that high doses of amifostine administered alone and in combination with radiation, which previously reduced inversions, induce apoptosis. However, no significant changes in apoptosis were found at lower doses of amifostine to support our hypothesis. The observation that amifostine potentiates radiation-induced apoptosis is contrary to published reports which attribute amifostine's cytoprotection to apoptosis inhibition. Normal cells are considered to have a greater apoptosis threshold following amifostine treatment due to the active import of amifostine providing greater defence against radiation. Our results indicate that this is not true in spleen and indicates that different tissues have different apoptosis responses to radiation in the presence of amifostine. We are currently analysing bone marrow which has been reported to be protected from radiation-induced apoptosis by amifostine. These results show that amifostine does not protect all tissues from radiation-induced apoptosis, and may have implications for the clinical use of amifostine. This research was supported by the U.S. Department of Energy, Low Dose Radiation Research Program grant #DE-FG02-05ER64104.

(MS707) Mitigation of Acute Radiation Injury by Interleukin-12. Dolph D. Ellefson¹, Tim Gallaher¹, Joseph Miller², Lena Basile¹, ¹Neumedicines, Inc., Pasadena, CA, ²University of Southern California, Los Angeles, CA

We have previously demonstrated that IL-12, a much characterized mediator of innate and adaptive immune responses, is also a potent regulator of hematopoiesis. IL-12 stimulates hematopoietic reconstitution in mice following exposure to 625 cGy total body irradiation (TBI) when administered 24 hr pre-exposure or 2 hr post-exposure. Because of the demonstrated effectiveness of IL-12 post-exposure, we employed a more challenging model of radiation exposure to examine the ability of IL-12 to mitigate survival and recovery. In a murine pre-clinical model of myeloablation, a single, low-dose injection of IL-12 administered up to 48 hrs after lethal exposure stimulates hematopoietic recovery and enhances survival. Single administration of an optimized low-dose formulation of IL-12 administered 24 hrs post-TBI mitigated morbidity and increased survival to 70% in mice exposed to levels corresponding to the LD_{100/30} relative to vehicle-treated controls. When irradiated at levels of exposure

corresponding to the LD_{100/10}, 100% of mice treated with IL-12 at 6 hrs post-exposure survived relative to non-treated controls, suggesting that IL-12 may also mitigate death attributable to the GI syndrome. Mitigation of radiation exposure and restoration of homeostasis requires therapeutics capable of stimulating repair through the proliferation, expansion, and differentiation of regenerative cells in the body. These data suggest that IL-12 could be an effective mitigant against intentional release of radiation as well as a potent tool for accelerated recovery following therapeutic application of radiation. Ongoing pre-clinical efficacy studies of recombinant human IL-12 (rhIL-12) in non-human primates (*Macaca mulatta*) will establish the effective dose range required for mitigation of acute radiation syndrome in humans. This project has been funded in whole or in part with Federal funds from the Biomedical Advanced Research and Development Authority, Office of the Assistant Secretary for Preparedness and Response, Office of the Secretary, Department of Health and Human Services, under Contract No. HHSO100200800060C.

(MS708) Alxn4100tpo, a tpo agonist, ameliorates radiation-induced injury by stimulating proliferation and differentiation of multi-lineage hematopoietic progenitors. Merriline M. Satyamitra¹, Eric Lombardini², Conor Mullaney³, John Graves III³, London Harrison³, Krista Johnson⁴, Jeffrey Hunter⁴, Paul Tamburini⁴, Yi Wang⁴, Jeremy P. Springhorn⁴, Venkataraman Srinivasan¹, ¹SRD, AFRR, Bethesda, MD, ²VSD, AFRR, Bethesda, MD, ³SRD, AFRR, Bethesda, MD, ⁴Alexion Pharmaceuticals, Inc, 352 Knotter Drive, Cheshire, CT

Previously, a single dose of 1 mg/kg Alxn4100TPO (4100TPO), a thrombopoietin agonist, administered sc 12 h after a LD-90 dose (9.25 Gy at 0.6 Gy/min, cobalt 60 gamma source, AFRR) of total body irradiation (TBI) demonstrated significant mitigation in CD2F1 mice. The current study investigated the mechanism of prophylactic (24 h before) or therapeutic (12 h after TBI) 4100TPO-treatment in 7 Gy irradiated mice using (1) Peripheral blood indices, (2) *In vitro* colony forming units (3) Histopathology and (4) Micronuclei formation in mouse bone marrow. 4100TPO alone, increased mouse peripheral blood platelet levels 5-fold, which peaked 8 days later and remained elevated for 3 weeks thereafter, demonstrating the thrombopoietic nature of the agonist. Irradiation severely depleted peripheral blood WBCs, lymphocytes, neutrophils and platelets (p<0.001); 4100TPO treatment resulted in earlier reconstitution of WBCs, neutrophils and megakaryocytes in blood (day 10, compared to no changes in blood indices on day 21 for TBI alone group). 4100TPO also increased the number of multipotent (GEMM) colonies compared to vehicle or irradiated controls, denoting a multi-lineage recovery of the hematopoietic tissue. This effect on recovery was further validated using surface markers for committed myeloid (CD117), megakaryopoietic (CD45), and erythropoietic (CD71) progenitors; drug-treated groups showed rapid repopulation of the progenitors (day 7, p<0.01) compared to the irradiated control. Further, histopathological analyses of sternum showed that 4100TPO treatment significantly increased cellularity (100% and 30% for pre- and post-TBI drug-treatment, respectively, compared to 5% for irradiated controls), regenerative foci and megakaryocytes assessed on day 7. 4100TPO reduced the number of micronucleated reticulocytes observed following 7 Gy (p<0.001 compared to vehicle) and facilitated faster restoration of erythropoiesis by normalizing the polychromatic to normochromatic erythrocyte (P/N) ratio by days 7 and 10, for pre- and post-drug treatment, respectively. We conclude that 4100TPO acted as a radiation countermeasure by stimulating multi-lineage hematopoietic recovery and reconstitution of the radiation-ablated hematopoietic organ.

(MS801) Topical TLR-7 agonist imiquimod inhibits tumor growth and synergizes with local radiotherapy in a mouse model of breast cancer. M. Zahidunnabi Dewan¹, Tze-Chiang Meng², James S. Babb¹, Silvia C. Formenti¹, Sylvia Adams¹, Sandra Demaria¹, ¹New York University School of Medicine, New York, NY, ²3Graceway Pharmaceuticals, Martin Luther King Jr Blvd Bristol, TN

Toll-like receptor (TLR) agonists are attractive agents for the active immunotherapy of cancer. TLR7 activation stimulates innate immune responses and directs the adaptive arm towards a Th1 profile. Local administration of TLR7 activator imiquimod (IMQ) creates an inflammatory environment suitable for tumor antigen cross-presentation and infiltration by effector T cells and dendritic cells (DC). Like IMQ, radiotherapy (RT) is a local modality that can alter the tumor microenvironment and enhance tumor immunogenicity, and we have previously shown its ability to synergize with immunotherapy. To test the therapeutic potential of topical IMQ alone or in combination with local RT for the treatment of subcutaneous (s.c.) breast cancer we employed the poorly immunogenic TLR7-negative TSA mouse breast carcinoma model injected into syngeneic immunocompetent mice. TSA cells (1×10^5) were injected s.c. into Balb/c mice at the right flank. On day 10 when tumors became palpable, mice were randomly assigned to 4 groups ($N=5-10/\text{group}$): topical IMQ 5% or placebo cream 3x per week for up to 4 weeks with or without local RT (8 Gy x 3 fractions, days 12, 13 and 14). Treatment response was determined by measuring tumor growth and survival of mice. In some experiments, mice were injected in both flanks with TSA cells, and only one of the tumors was irradiated. Tumor-bearing mice treated with IMQ alone showed delayed tumor progression in comparison with control mice ($p < 0.0001$ on day 25) and increased infiltration by DC, CD4 and CD8 T cells. RT as single modality delayed tumor growth; however, neither treatment by itself was able to induce complete tumor regression. When IMQ was given in combination with RT, there was enhanced tumor inhibition ($p < 0.05$) and complete tumor regression in 4/6 mice at day 35. Analysis of regressing tumors at day 25 showed a marked enhancement over the baseline in untreated tumors in CD8 and CD4 T cell infiltration by IMQ + RT (5 to 10-fold) as compared to IMQ alone (2 to 3-fold). Remarkably, local treatment with RT + IMQ to one tumor resulted in significant inhibition of a second tumor outside of the radiation field only when the latter also received topical IMQ. Overall, results indicate that synergistic anti-tumor effects are obtained when local RT is administered coincident with TLR7 activation.

(MS802) Down-regulation of human DAB2IP gene expression in prostate cancer cells results in resistance to ionizing radiation. Zhaolu Kong, Daxing Xie, Thomas Boike, Pavithra Raghavan, Sandeep Burma, David Chen, Jer-Tsong Hsieh, Debabrata Saha, UT Southwestern Med Center, Dallas, TX

DAB2IP (DOC-2/DAB2 interactive protein) is a member of the RAS-GTPase activating protein family. In metastatic prostate cancer, DAB2IP is often down-regulated and has been reported as a possible prognostic marker to predict the risk of aggressive prostate cancer. We observed that a metastatic human prostate cancer PC3 cells deficient in DAB2IP (shDAB2IP) exhibit increased clonogenic survival in response to ionizing radiation (IR) compared to control cells expressing endogenous level of DAB2IP (shVector). Radioresistance was also observed in normal prostate cells that are deficient in DAB2IP. This enhanced resistance to IR in DAB2IP-deficient PCa cells is primarily due to faster DNA double strand break (DSB) repair kinetics. More than 90% of DSBs were repaired in DAB2IP deficient cells by 8 hrs after 2 Gy radiation whereas only 60% of DSB repair was completed in DAB2IP proficient cells at the same time. Secondly, upon irradiation, DAB2IP-deficient cells enforced a robust G_2/M cell cycle checkpoint compared to control cells. Finally, DAB2IP deficient cells showed resistance to IR-induced apoptosis that could result from a striking decrease in the expression levels of pro-apoptotic proteins caspase 3, 8, and 9 and significantly higher levels of anti-apoptotic proteins Bcl-2 and STAT-3 than those in DAB2IP proficient cells. In order to radiosensitize the DAB2IP deficient prostate cancer cells we have used a microtubule stabilizing agent Etoposide B in cell culture and in animal study. We noticed significant radiation dose enhancement and tumor growth delay in response to the combined treatment of EpoB and radiation in DAB2IP deficient prostate cancer cells. This radiosensitization can be attributed to delayed DSB repair, prolonged G_2 block and increased apoptosis in cells entering the cell cycle after G_2/M arrest. In summary, DAB2IP plays a significant role in prostate cell survival following IR exposure due to enhanced DSB repair, robust G_2/M check-point control and

resistance to IR-induced apoptosis. Therefore, it is important to identify patients with dysregulated DAB2IP for (i) assessing prostate cancer risk and (ii) alternative treatment regimens.

(MS803) The small molecule inhibitor QLT0267 radiosensitizes human head and neck squamous cell carcinoma cells in an ILK independent manner. Iris Eke, Franziska Leonhardt, Katja Storch, Stephanie Hehlhans, Nils Cordes, OncoRay - Radiation Research in Oncology, Dresden, Germany

As cancer cell resistance to radio- and chemotherapy constantly increases, novel targeting approaches are required to improve patient survival. Integrin-Linked Kinase (ILK) has been reported as potent cancer target, which promotes survival and tumor growth. However, our previous findings using genetic models clearly showed that ILK transduces antisurvival signals in cells exposed to ionizing radiation. To evaluate the impact of the putative ILK inhibitor QLT0267 on the cellular radiation survival response, FaDu and UTSCC45 human head and neck squamous cell carcinoma (hHNSCC) cells as well as ILKflox/flox (fl/fl) and ILK-/- mouse fibroblasts growing either two-dimensionally (2D) on or three-dimensionally (3D) in laminin-rich extracellular matrix were treated with QLT0267 alone or in combination with irradiation (X-rays, 0-6 Gy single dose). Additionally, FaDu cells were stably transfected with a constitutively active ILK mutant (FaDu-IH) or empty vector. ILK knockdown was performed using small interfering RNA transfection. ILK kinase activity, clonogenic survival, number of residual DNA double strand breaks (rDSB; gammaH2AX/53BP1 foci assay), cell cycle distribution, protein expression and phosphorylation (e.g. Akt1, ERK1/2) were determined. Besides inhibition of ILK activity, treatment with QLT0267 resulted in dephosphorylation of several signaling molecules. Thus, QLT0267 seems to have a broad inhibitory spectrum. QLT0267 significantly reduced survival and radioresistance of all tested cell lines (including ILK-/- cells) independent of ILK status. In parallel, the number of gammaH2AX/53BP1 positive foci was increased. While in 2D treatment of QLT0267 led to an accumulation of cells in G_2 , the cell cycle distribution was not altered when cells grew in 3D. ILK knockdown had no effect on radiation survival of hHNSCC cells. Our results clearly show that the small molecule inhibitor QLT0267 has potent cytotoxic and radiosensitizing capability in hHNSCC cells, which could not be attributed to the effect on ILK. Further in vitro and in vivo studies are necessary to clarify the potential of QLT0267 as a novel approach in the clinic.

(MS804) A Study of Biodistribution and Imaging of Radioiodinated HVGGSSV in Irradiated Glioma-bearing Nude Mice. Charles A. Phillips¹, Dennis Hallahan², Jerry J. Jaboin¹, ¹Vanderbilt University, Nashville, TN, ²Washington University, St. Louis, MO

Background: Utilizing biopanning with the T7 bacteriophage system, we previously demonstrated that among screened phage-displayed peptides, the HVGGSSV peptide binds with high sensitivity and specificity to irradiated allograft and xenograft glioma tumors. When bound to near infrared imaging agents, this peptide selectively binds to responding irradiated tumors differentiating responding from non-responding tumors. Our objective was to develop a system for imaging tumor response in humans. Methods: We bioconjugated streptavidin-labeled HVGGSSV to iodine radionuclides (I^{125} and I^{131}) utilizing Iodogen[®] pre-coated tubes. Radiolabeling was obtained in 74-89% yield for I^{131} and 37-52% yields for I^{125} . Final radiochemical purity after gel chromatography was >98%. Constructs were injected via jugular catheters into mice 4 hours following irradiation of $\sim 1 \text{ cm}^3$ GL261 (murine glioma) tumors grafted in the hind limb of nude mice. We used a SPECT/CT scanner to record localization of labeled constructs within the mice over time. For near infrared imaging experiments, cold iodide was bioconjugated to a streptavidin-labeled scrambled peptide and streptavidin-labeled HVGGSSV. These constructs were subsequently labeled on tyrosine residues with Alex Fluor 750, and near infrared imaging was performed on a Xenogen IVIS scanner. Results: I^{131} -labeled

HVGGSSV had poor signal resolution with SPECT-CT imaging revealing diffuse uptake on day 0 followed by clearance within 24 hours with limited tumor binding. The ^{123}I -labeled HVGGSSV had improved signal resolution over ^{131}I , but again rapidly cleared the mice. The streptavidin-labeled constructs had similar findings. In the near infrared imaging experiments, the streptavidin-HVGGSSV (positive control) demonstrated robust tumor-specific uptake within 24 hours, which persisted through 142 hours. The streptavidin-HVGGSSV conjugated to iodide, however, had mild tumor uptake similar to that of the negative control (streptavidin-labeled scrambled peptide). Conclusions: Direct conjugation of iodide or its radionuclides abrogates tumor-specific targeting of HVGGSSV, suggesting that peptide radioiodination is not a feasible approach for noninvasive monitoring of tumor response.

(MS805) A small molecule screen to identify novel inhibitors of the Unfolded Protein Response and hypoxia tolerance in tumor cells. Lori S. Hart¹, Andrew T. Segan¹, Ioanna Papandreou², Albert Koong², Constantinos Koumenis¹, ¹University of Pennsylvania, Philadelphia, PA, ²Stanford University School of Medicine, Palo Alto, CA

Hypoxia arguably represents the most thoroughly characterized of microenvironmental factors in tumor pathogenesis. Clinical evidence identifies hypoxia as a contributor of therapeutic resistance, as well as an indicator of an aggressive tumor phenotype. The adaptation of tumor cells to hypoxia is largely due to activation of HIF1 and HIF2; however, other mechanisms also play a part. The Unfolded Protein Response (UPR) represents such a mechanism and contributes to tumor cell survival. Inactivation of the UPR results in reduced hypoxia tolerance and slower tumor growth in animal models. Our studies have focused on the role of PERK, a kinase that responds to unfolded proteins by phosphorylating eIF2 α , downregulating global protein synthesis, and specifically inducing the translation of ATF4. Loss of ATF4 sensitizes tumor cells to hypoxia, validating the importance of identifying ATF4 inhibitors. We have employed a small molecule screen to identify inhibitors of ATF4 via overexpression of a reporter construct with the 5'-UTR of ATF4 fused to the luciferase gene in HT1080 cells. When ATF4 reporter cells were treated with Thapsigargin, we observed more than a four-fold induction of luciferase over control cells in a PERK-dependent manner. Using the Stanford University chemical library of over 160,000 diverse small molecules and the NIH Molecular Libraries Small Molecule Repository at the University of Pennsylvania, we performed a primary screen on the HT1080 ATF4-luciferase cells. We identified 5 small molecules based on the inhibition of ATF4, with Z-values above 3 and low μM or high nM IC50 values. The compounds are currently undergoing validation in secondary screens for the specific inhibition of ATF4 but not CMV-luciferase or XBP-1-luciferase reporters. We plan to identify structural families and perform structure-activity relationship (SAR) analysis to identify related compounds. Validated compounds will be assessed for the ability to reduce hypoxic tolerance through cell proliferation, cell survival, and *in vitro* and *in vivo* tumorigenicity assays. Tumor cells exploit normal cellular processes for their own survival and propagation. The identification of UPR inhibitors represents an opportunity to abolish one such process, and represents a novel therapeutic strategy for the treatment of solid tumors.

(MS807) Comparative evaluation of liposomal and non-liposomal platinum drugs combined or not with concomitant radiation to improve treatment of glioblastoma implanted in rat brain. Gabriel Charest, David Fortin, David Mathieu, Léon Sanche, Benoit Paquette, Université de Sherbrooke, Sherbrooke, QC, Canada

Despite recent advances, the radiotherapy and chemotherapy protocols only marginally improve the overall survival of patients bearing glioblastoma (GBM). In our study, the anticancer efficiency with and without radiation combination of five platinum compounds

was tested: cisplatin, oxaliplatin, their liposomal formulation LipoplatinTM (cisplatin), LipoxalTM (oxaliplatin) and carboplatin. The liposomal formulations were included since they can potentially reduce the toxicity of cisplatin and oxaliplatin. The tumor F98 glioma implanted in the brain of Fischer rats was used as model to mimic the human glioblastoma. Although intra venous (i.v.) injection is the usual way to administrate the chemotherapeutic agents, the blood brain barrier (BBB) largely limits drug uptake to brain tumor. To improve the efficiency of chemotherapeutic agents, the BBB was temporarily disrupted (BBBD) and the drugs were injected via carotid artery (i.a.). The post-administration time corresponding to the maximal tumor drug uptake was determined to optimize the concomitant treatment with radiotherapy delivered by Gamma Knife. Up to now, only studies using the i.a. route of drug administration treatment were completed. The i.a. route allows preferential uptake (up to 30X) into the tumor volume compared to the healthy brain tissue. Our study confirms that the liposomal formulations allowed bypassing the toxicity and considerably improving the life span of the animals. The anticancer efficiency of oxaliplatin was increased when incorporated in LipoxalTM resulting in a considerable improvement of the life span of animals implanted with a GBM. The efficiency of LipoxalTM, LipoplatinTM and carboplatin were similar with a median survival times of 29-32 days, compared to 22 days for untreated rats. Concomitant treatment with radiotherapy further extend the median survival times with the highest efficiency obtained with LipoxalTM (37 days) and carboplatin (47 days), compared to 34 days with radiation only. We expect that i.v. administration should reduce the tumor uptake compare to i.a. whereas i.a. plus BBBD should increase the tumor uptake. The aim of this study is to find a better route of administration, a better chemotherapy formulation and a better post-administration time to combine ionizing radiation in clinical GBM therapy.

(MS808) Radioresistant melanoma cells show defective G1 arrest in response to IR and are radiosensitized by inhibition of B-RAF. Janiel M. Shields, Craig C. Carson, Maria J. Sambade, Nancy E. Thomas, University of North Carolina, Chapel Hill, NC

While advanced melanoma is often reported to be relatively resistant to conventional radiotherapy, stereotactic radiosurgery (SRS) is increasingly used to treat melanoma brain metastases with 1-year local control rates ranging from 75-40% depending on tumor size. However, melanoma brain metastases tend to be multifocal with disparate SRS responses seen among brain metastases in individual patients resulting in high morbidity rates. Thus, there is a critical need to improve the therapeutic radioresponsiveness of melanoma. Mutational activation of the B-RAF oncogene occurs in approximately 50% of melanoma patients. B-RAF, a serine/threonine kinase, leads to constitutive activation of MEK1/2>ERK1/2. Activation of Raf>MEK1/2>ERK1/2 has previously been shown to promote radioresistance. Here, a large collection of melanoma cell lines (n=37) were treated with 0 - 8 Gy IR and clonogenic survival assays used to generate survival curves to rank relative radiosensitivities among the cell lines. Treatment of highly radioresistant *B-Raf+* cells with the B-RAF inhibitor PLX-4032 in combination with radiation provided enhanced inhibition of proliferation in both colony formation (ER average 9.7; range 1.2 - 29.3) and invasion assays, and radiosensitized cells through an increase in G1 arrest. In addition, while p53 mutations are uncommon in melanoma, radioresistance in melanoma cell lines correlated with a defective G1 checkpoint and loss of p21 expression suggestive of loss of p53 function. Agilent 4 x 44k RNA microarrays were used to identify genes associated with radioresistance vs radiosensitivity by Quantitative Trait Analyses. Using the ranked radiation sensitivities of the cell lines and highly stringent filtering parameters 20/44,000 genes were found to be associated with either radioresistance or sensitivity (p<0.001) with increased expression of genes associated with DNA repair and regulation of histone acetylation in the radioresistant cell lines. These data suggest radioresistance in melanoma is mediated, in part, through loss of p53 function and increased DNA repair and that pharmacologic inhibition of BRAF could provide improved radiotherapeutic response in B-Raf+ melanoma patients.

(MS901) Role of bradykinin in a rat model of radiation-induced heart disease. Marjan Boerma¹, Sunil Sharma¹, Eduardo G. Moros¹, Peter M. Corry¹, Kerrey A. Roberto¹, Elena Kaschina², Thomas Unger², Martin Hauer-Jensen¹, ¹University of Arkansas for Medical Sciences, Little Rock, AR, ²Charite - University Medicine, Berlin, Germany

Background: Radiation-induced heart disease (RIHD) is a potentially severe side effect after radiation therapy of thoracic and chest wall tumors. We have previously shown that mast cells protect against cardiac function loss and adverse myocardial remodeling after local heart irradiation in the rat. Mast cells may play this protective role via bradykinin, a peptide hormone with cardioprotective effects. The current studies begin to address the role of bradykinin in a rat model of RIHD. Methods: Male Sprague-Dawley rats received localized fractionated heart irradiation with 9 Gy for 5 consecutive days. The effects of radiation on the expression of the bradykinin receptors B1 and B2 and on the cardiac *ex vivo* functional response to bradykinin perfusion were assessed. A breeding colony of Brown Norway Katholiek (BNK) rats, which are deficient in the precursor of bradykinin, was established. Kininogen-deficient BNK and wild-type BN rats received localized fractionated heart irradiation with 9 Gy on 5 consecutive days. At different time points after irradiation, *in vivo* cardiac function was assessed with small animal echocardiography. Results: Local heart irradiation resulted in a significant increase in the expression of both the B1 and B2 receptor in the rat heart. In addition, irradiated hearts showed a functional response to bradykinin similar to sham-irradiated hearts, as shown by a significant reduction in coronary pressure after *ex vivo* perfusion with bradykinin in the Langendorff apparatus. The effects of localized heart irradiation on echocardiographic parameters of cardiac function in BNK rats and BN rats are presented. Conclusions: These studies start to unravel the mechanistic role of bradykinin in functional and structural changes in the rat heart after localized irradiation.

(MS902) MKP1-mediated radioresistance in breast cancer cells. Demet Candas, Ming Fan, Jian Jian Li, University of California, Davis, Sacramento, CA

Mitochondria are considered the powerhouses of cells, essential for keeping the cells alive and functional. They play an additional and yet very crucial role in the regulation of cell death, namely apoptosis. Cancer specific mitochondrial alterations have gained more attention as cancer cells have been shown to have enhanced resistance to mitochondria-mediated apoptosis. The changes occurring in the mitochondrial membrane potential modulate vital functions including: ion transport, protein influx, biogenesis and energy conservation. Although many nuclear-encoded proteins have been identified in mammalian mitochondria, the exact mechanism underlying mitochondrial protein influx is unknown. We were able to show that mitogen activated protein kinase phosphatase 1 (MKP1), overexpressed upon radiation in a NF- κ B-mediated manner, translocates to mitochondria in response to radiation and potentially results in the inhibition of mitochondria-mediated apoptosis in breast cancer cells. Although the apoptosis inhibiting function of MKP1 is well-defined, its role in mitochondria has not been studied. We proposed that radiation-induced MKP1 mitochondria localization is responsible for the inhibition of apoptosis, causing adaptive tumor radioresistance. The mechanisms of MKP1-mediated inhibition of apoptosis in radioresistant cells and the downstream molecules involved are of great interest as they might offer new therapeutic targets for breast cancer. Among the MAPKs that are induced in response to radiation, JNK has been shown to be affected by MKP1 activation, indicating that radiation-induced MKP1 is likely to play an anti-apoptotic role via the inhibition of JNK-mediated apoptosis. Furthermore, JNK has been shown to localize to mitochondria upon radiation to initiate mitochondria-mediated apoptosis via the phosphorylation of Bcl-xL, suggesting that MKP1-mediated inactivation of JNK takes place in mitochondria and functions to block radiation-induced apoptosis, leading to increased cell survival. Therefore, suppression of MKP1 activity may enable the pro-apoptotic signals from JNK in radioresistant breast cancer cells. Elucidation of mechanisms of

MKP1-mediated inhibition of apoptosis may provide novel drug targets to re-sensitize radioresistant tumors.

(MS903) Detection of the radio-sensitivity of oxygenated cell fractions in quiescent cell populations within solid tumors. Shin-ichiro Masunaga¹, Hideko Nagasawa², Yong Liu¹, Yoshinori Sakurai¹, Hiroki Tanaka¹, Genro Kashino¹, Minoru Suzuki¹, Yuko Kinashi¹, Akira Maruhashi¹, Koji Ono¹, ¹Research Reactor Institute, Kyoto University, Osaka, Japan, ²Laboratory of Pharmaceutical Chemistry, Gifu Pharmaceutical University, Gifu, Japan

Purpose: To detect the radio-sensitivity of oxygenated tumor cells not labeled with pimonidazole among intratumor quiescent (Q) cells. Methods and Materials: C57BL mice bearing EL4 tumors received 5-bromo-2'-deoxyuridine (BrdU) continuously to label all proliferating (P) cells in the tumors. They received gamma-ray irradiation at a high dose-rate (HDR) or reduced dose-rate (RDR) one hour after the administration of pimonidazole. The responses of Q and total (= P + Q) cell populations were assessed based on frequencies of micronucleation and apoptosis using immunofluorescence staining for BrdU. Meanwhile, the response of pimonidazole unlabeled tumor cell fractions was assessed by apoptosis frequency using immunofluorescence staining for pimonidazole. Results: The cell fraction not labeled with pimonidazole showed significantly greater radio-sensitivity than the whole tumor cell fraction more remarkably in the Q than total cell population. However, the pimonidazole unlabeled cells showed a significantly clearer decrease in radio-sensitivity through a delayed assay or decrease in irradiation dose-rate than the whole cell fraction, again more markedly in the Q than total cell population. Conclusion: Pimonidazole unlabeled, probably oxygenated, Q tumor cells are thought to be a critical target in the control of solid tumors as a whole, based on a significantly greater radio-resistance and capacity to recover from radiation-induced damage in the Q than total cell population within solid tumors.

(MS904) Temporal expression signature of hypoxia associated genes in irradiated mouse lung. Isabel L. Jackson, Xiuwu Zhang, Zahid Rabbani, Yu Zhang, Zeljko Vujaskovic, Duke University Medical Center, Durham, NC

Tissue hypoxia in the irradiated lung is associated with the development of normal tissue injury. However, direct evidence of hypoxia-mediated signaling in irradiated tissue has not been fully investigated. C57BL/6J mice were sacrificed at 1-day, 3-day, 1-week, 3-week, 6-week, and 6-month after giving a single fraction of 15 Gy to the whole thorax. The mRNA expression of 113 hypoxia-associated genes was tested using the hypoxia signaling pathway specific Oligo DNA microarray and further verified by RT-PCR. In total, 44 hypoxia-related genes were found to be upregulated after radiation. These genes participate in a variety of physiological and pathological functions including cell signaling transduction, tissue regeneration and cell proliferation (Dr1, Dctn2, CdC42, Gap43) and apoptosis (DapK) as well as inflammation, oxidative stress (Cygb) and extracellular matrix synthesis (Agtbbp1, Mmp14, Adm, Angpt14, CTGF, leptin, and Plod3). In this study, expression of genes involved in lipid, carbohydrate, and protein metabolism, such as Agpat2, Angpt4, Car12, Eef1a1, Fabp4, Lipe, Man2b1, Ppar α , Prkaz1, Rps7, Slc2a1, Slc2a8, Tub α 1, and Tub β 3 were upregulated at various time points post-radiation. The temporal expression of these genes suggest that following the initial ionizing event, genes are upregulated that result in sustained oxidative stress, cell apoptosis, and tissue repair. At later time points genes associated with inflammation and fibrogenesis begin to be expressed. During the period following radiation exposure and extending throughout the follow-up period, several genes involved in vascular function, lipid, protein, and carbohydrate metabolism, and angiogenesis remain upregulated. The expression profile provides insight into the hypoxia associated genes involved in lung injury beginning 24 hours after radiation exposure and extending throughout the time to disease progression. Although, the physiological processes highlighted by the genes identified herein are not novel, the transcriptome profile does provide a clear view of those genes involved

in these processes and the timeline of events. Improved understanding of hypoxia-driven gene expression could lead to improved understanding of the pathophysiological mechanisms underlying radiation-induced lung injury.

(MS905) A mouse model to study the skin complication following hypo-fractionation for SBRT. Juong G. Rhee, Jonathan Ha, Zhendong Whang, William F. Regine, Cedric X. Yu, University of Maryland at Baltimore, Baltimore, MD

Stereotactic body radiation therapy (SBRT) is a recent innovation that offers high tumor cure rates which are superior to the outcome of conventional radiotherapy. However, its toxicity to normal tissues appears to be clinically unacceptable in many cases; the nature of hypo-fractionation necessitates the use of high doses per fraction. We have established a mouse model to study the skin complication associated with hypo-fractionation. The dorsal skin of C3H/HeJ mice were sutured to a home-made metal chamber which has an open window (16 x 14 mm, oblique) for irradiation. NE cells (nullipotent embryonic teratocarcinoma) were implanted subcutaneously in the middle of the chamber. This chamber allowed us to secure the skin with or without tumor tissues at the same position for repeated irradiation, in a manner equivalent to stereotactic positioning. The skin and tumors were subjected to a hypo-fractionation (13 Gy, 4 times daily) or a grid-fractionation (52 Gy each quarter, 4 times daily). The purpose of the former setup was to simulate SBRT while the intent of the latter was to integrate spatial fractionation through the use of a grid (20 x 20 mm), which has 25 openings (2 x 2 mm) that are aligned 2 mm apart in both the horizontal and vertical directions in order to expose 1/4th of the intended field to each exposure. There were 4 observation groups: 2 control groups (hypo-fractionation; 13 Gy x 4 days) for the skin or skin having tumor tissues and 2 variable groups (grid-fractionation; 52 Gy each quarter x 4 days for different quarter areas) for the skin or skin having tumor tissues. Our preliminary results from 12-14 mice for each group showed that the amount of hair re-growth (a late effect) in the grid-fractionation group was almost double the amount of hair re-growth in the hypo-fractionation group, suggesting a clear skin protection. In addition to this, tumor curability was reduced by only 1/5th (92% to 75%) due to the use of the grid. Our observation for the skin protection is stimulating and may implicate the possibility that migrating and repopulating skin stem cells are better saved when the skin is subjected to spatially fractionated radiation using a grid, and that skin complications in SBRT may be reduced to a clinically acceptable level by using the grid.

(MS906) The TGF β /smad repressor TG-interacting protein (TGIF) plays a role in radiation-induced intestinal injury. Mohammad Hneino, Agnès François, Valérie Buard, Georges Tarlet, Marc Benderitter, Fabien Milliat, Institute for radiobiological protection and nuclear safety, Fontenay aux roses, France

TGF β is a key mediator involved in radiation-induced normal tissue damage. The TGF β signal is mediated through serine/threonine kinase receptors and activation of its downstream signaling mediators Smads. Smad signaling is controlled by various mechanisms including co-activators and co-repressors. Intestinal injury in patients treated with radiotherapy is associated with the activation of TGF β mediators (Smad) and target genes (PAI-1) in vascular compartment. TGIF (TG-Interacting factor) is a transcriptional repressor that has been reported to repress expression of TGF β /Smad target genes, antagonizing TGF β /Smad pathway. In this work, we hypothesized that TGIF could play a role in minimizing TGF β -dependent deleterious effects in irradiated tissues. Immunohistochemical labeling of TGIF was performed in patients treated with pre-operative radiotherapy for rectal adenocarcinoma. *In vitro*, influence of TGIF overexpression in transcriptional activation of TGF β /Smad pathway and target genes was investigated in endothelial cells. *In Vivo*, in a model of radiation enteropathy (19 Gy localized single dose), survival was monitored and intestinal radiation injury was assessed in wild-type, TGIF +/- and TGIF mice -/- mice (n=13 to 15 mice/group). In rectum from patients treated with radiotherapy TGIF immunoreactivity is observed in vascular

compartment and especially in the endothelium. Using a gene reporter approach and after transfection of a TGF β /smad responsive reporter (CAGA9 luciferase) in HUVECs, we demonstrate that overexpression of TGIF completely inhibits SMAD-dependent transcriptional activation showing that TGIF is a key regulator of TGF β signaling in endothelial cells. Interestingly, *in vivo*, TGIF genetic deficiency is associated with increased sensitivity to intestinal irradiation. At 10 days after irradiation, 64% of TGIF +/- mice are alive compared with 35% for TGIF +/- and only 20% for TGIF -/- mice. Fifty days after irradiation, no TGIF -/- mice survive whereas 57 % of TGIF +/+ and 23 % of TGIF +/- are alive. This study demonstrates that TGIF plays a role in radiation-induced intestinal damage and suggests that strategies aimed to strengthen TGIF activity could be a powerful way to control TGF β -dependent damages observed in normal tissues after radiation therapy.

(MS907) Manganese superoxide dismutase 3'-untranslated region: sensor for cellular responses to environmental stress. Leena Chaudhuri, Amanda L. Kalen, Maneesh G. Kumar, Prabhat C. Goswami, The University of Iowa, Iowa City, IA

In recent years, there is a growing interest in understanding the role of 3'-untranslated region (UTR) in regulating mRNA turnover and translation. The 3'-UTR harbors the poly(A) signal and post-transcriptional regulatory sequences like miRNA and AU-rich elements. The presence of multiple poly(A) sites often results in multiple transcripts; shorter transcripts correlating with more protein abundance. Manganese superoxide dismutase (SOD2) is a nuclear encoded and mitochondrial localized antioxidant enzyme that converts mitochondrial generated superoxide to hydrogen peroxide. A decrease in SOD2 activity increases the steady state levels of superoxide leading to oxidative stress. Humans have two transcripts of SOD2, 1.5 and 4.2 kb. We hypothesize that the preferential abundance of SOD2 transcripts regulates its activity during quiescent and proliferative growth states, and in response to environmental stress. Results from a quantitative RT-PCR assay showed that the shorter transcript (1.5 kb) is more abundant in quiescent cultures of normal human skin fibroblasts, non-malignant (MCF-10A) and malignant (MB-231) human mammary epithelial cells. Conversely, the longer transcript (4.2 kb) was more abundant in the proliferative state of all three cell lines. MCF-10A cells exposed to 2-(4-chlorophenyl)benzo-1,4-quinone (4-Cl-BQ), a metabolite of the environmental pollutant polychlorinated biphenyl 3, showed a significant decrease in the abundance of the 4.2 kb transcript due to a faster mRNA turnover, 14 h compared to 20 h in untreated control cells. Interestingly, the same treatment did not result in any change in the abundance of the shorter transcript. The decrease in the 4.2 kb transcript levels was associated with a corresponding decrease in SOD2 protein levels and activity, which resulted in a significant inhibition of quiescent cells entry into the proliferative cycle. A preferential abundance of the SOD2 transcripts was also observed in irradiated cells compared to controls. A better understanding of the 3'-UTR regulating gene expression in irradiated cells could lead to the development of new molecular biology-based radiation therapy. (NIH RO1 CA111365 and NIEHS P42 ES 013661).

(MS908) The role of p53 in hypoxia-induced apoptosis. Rachel Poole, Ester M. Hammond, Gray Institute for Radiation Oncology and Biology, Oxford, United Kingdom

Tumour hypoxia contributes to both chemo- and radio-resistance and is associated with poor prognosis. Severe hypoxia has been shown to select for the loss of the tumour suppressor p53, which induces apoptosis in these conditions. Despite this the mechanism by which p53 induces apoptosis in response to hypoxia remains unclear. In this study we have investigated the post translational modifications of p53 in hypoxic conditions. Previously, phosphorylation of p53 at serine 46 was shown to be important for apoptotic signalling in response to agents such as UV. We have shown that p53 is robustly phosphorylated at this residue in response to hypoxia but that this does not appear to contribute to hypoxia-induced apoptosis. We hypothesise that this relates to the lack of transactivation by p53 in hypoxia as serine 46 has been

described as being essential for the induction of p53-regulated apoptosis inducing protein 1 (p53AIP1). Micro-array data suggest that in hypoxic conditions p53 acts primarily as a trans-repressor although few targets have been described. Recently p53 was shown to contribute to hypoxia-induced apoptosis through the repression of

a specific miR. We have compared the effect of wild type and mutant (in the DNA binding region) p53 on miR expression using miR arrays. Expression arrays were also carried out in order to identify potential targets of p53-regulated miRs in hypoxia. These results will be discussed.

(PS1.01) Mitochondrial targeting peptide isostere bound 4-amino-tempo (JP4-039) mitigates against the ionizing irradiation induced hematopoietic syndrome. Xichen Zhang¹, Joel Greenberger¹, Tracy Dixon¹, Darcy Franicola¹, Peter Wipf², Michael Epperly¹, ¹University of Pittsburgh Cancer Institute, Pittsburgh, PA, ²University of Pittsburgh, Pittsburgh, PA

Stabilization of the mitochondria following irradiation has been shown to be important in cellular irradiation protection against apoptosis. The small molecule (JP4-039) mitochondrial targeted nitroxide has been shown to have a 32 fold increased localization to the mitochondria compared to Tempol. JP4-039 both protects and mitigates 32D cl 3 murine hematopoietic progenitor cellular radiation damage by clonogenic survival curve assay. Addition of drug to 32D cl 3 cells before irradiation produced an increased shoulder on the survival curve (\bar{n} 9.4 \pm 1.7) compared to control 32D cl 3 cells (1.7 \pm 0.2, $p = 0.0101$). JP4-039 added after irradiation mitigated against irradiation with an increased shoulder as shown by an increased \bar{n} of 5.8 \pm 2.4 compared to 2.5 \pm 0.5 for the control 32D cells ($p = 0.0025$). We tested whether JP4-039 had protective and mitigative effects in vivo. JP4-039 was dissolved in 10% cremphor el, 10% ethanol, and 80% water. C57BL/6NHsd mice were injected intraperitoneally with JP4-039 (10 mg/kg) either 10 min before irradiation or at several time points after LD50/30, 9.5 total body irradiation. Administration both before or immediately after irradiation increased survival compared to control C57BL/6NHsd mice ($p = 0.0125$ or 0.0285 , respectively). There was a significantly increased survival when drug was administered 4 hours after irradiation ($p = 0.0214$). Concentrations as low as 0.5 mg/kg resulted in significant mitigation with increased survival ($p = 0.0021$) compared to the control irradiated mice. These results indicate that JP4-039 is both an effective radioprotector and radiomitigators against the hematopoietic syndrome.

(PS1.02) Efficacy of structurally-different angiotensin converting enzyme (ACE) inhibitors for mitigation of radiation pneumonitis. Meetha Medhora^{1,2}, Swarajit N. Ghosh^{1,2}, Brian L. Fish², Feng Gao^{1,2}, Ying Gao^{1,2}, Lakhan Kma^{1,2,3}, Stephanie Gruenloh^{1,2}, Jayashree Narayanan², Elizabeth R. Jacobs¹, John E. Moulder², ¹Pulmonary and Critical Care Division, Department of Medicine, Medical College of Wisconsin, Milwaukee, WI, ²Department of Radiation Oncology, Medical College of Wisconsin, Milwaukee, WI, ³Department of Biochemistry, North-Eastern Hill University, Shillong, India

Aim: To test the potential of 3 structurally-different angiotensin converting enzyme (ACE) inhibitors as mitigators of radiation-pneumonitis induced by total body irradiation (TBI). **Methods:** Rats (adult, female, WAG/RijCmcr) were exposed to a single dose of 11Gy TBI followed by a syngeneic bone marrow transplant. Three structurally-different ACE inhibitors (captopril, enalapril and fosinopril) were provided in drinking water; therapy started 4 hours to 49 days after irradiation. Rats were assessed for up to 120 days to determine morbidity through the pneumonitis phase (occurring from 40-80 days). Endpoints included breathing rate, wet:dry weight ratio and histology. **Results:** Captopril (100-200 mg/m²/day), enalapril (10-30 mg/m²/day) or fosinopril (10-50 mg/m²/day) decreased morbidity. Enalapril improved outcomes at all doses tested, while captopril and fosinopril were more effective at the higher doses. **Conclusions:** Structurally-different ACE inhibitors mitigate experimental radiation pneumonitis. Efficacy varied with dose and schedule of each drug. Our findings support the therapeutic potential of inhibiting ACE activity since this is a shared property of all three drugs we tested. This work was funded by RC1 AI 81294 and NIH/NIAID agreements U19-AI-67734. Dosimetry was done by the CMCR Irradiation Core at MCW; histology was done in the Children's Research Institute at MCW under direction of Dr. Paula North.

(PS1.03) Single injection of novel medical radiation countermeasure CBLB502 rescues non-human primates within broad time window after lethal irradiation. Vadim Krivokrysenko¹, Ilya Toshkov¹, Anatoli Gleiberman¹, Andrei Gudkov^{1,2}, Elena Feinstein¹, ¹Cleveland BioLabs, Buffalo, NY, ²Roswell Park Cancer Institute, Buffalo, NY

Introduction: Protection of the human organism from ionizing radiation is a key problem in nuclear safety, radiation therapy, and space travel. CBLB502 is a Cleveland BioLabs, Inc. proprietary radiation countermeasure that is being developed for biodefense and medical applications. It is a rationally designed recombinant protein derivative of *Salmonella enterica* flagellin. CBLB502 acts via interaction with Toll-like receptor 5 and subsequent NF- κ B mediated induction of multiple protective mechanisms. CBLB502 is an effective radioprotectant and radiomitigator: in mice, with a dose modifying factor (DMF) of 1.5-1.8, an effective administration window of -24 to +50 hrs relative to irradiation, and a therapeutic index of \sim 100x. **Methods:** In multiple non-human primate (NHP) experiments, rhesus monkeys (*Macaca mulatta*) received a single i.m. injection of 0.01-0.04 mg/kg CBLB502, given as a monotherapy at different times relative to 6.5-6.75 Gy (LD_{70/40}) or 5 Gy (LD_{20/40}) bilateral total-body gamma irradiation (TBI). **Results:** Single-dose protective injection of 0.04 mg/kg CBLB502 45' before 6.5 Gy TBI increased survival of NHPs from 25% in control group (n=8) to 64% (n=11). Single-dose mitigative injections of 0.01-0.04 mg/kg CBLB502 at 1, 16, 25 or 48 hrs after 6.5-6.75 Gy TBI increased survival of NHPs from 20-40% in the control groups (n=8-10) to 70-100% in treated groups (n=10-12). CBLB502 treatment reduced the severity of damage and/or promoted regeneration of the GI tract, spleen, thymus and bone marrow. The severity and duration of radiation-induced thrombocytopenia and neutropenia were significantly decreased by CBLB502 treatment. Thrombocytopenia (PLT \leq 20,000/ul) was reduced from 7 to 2.0-4.5 days and neutropenia (NEU \leq 500/ul) was shortened from 11.5 to 9.5-11 days when CBLB502 was injected 16-48 hrs after 6.5Gy TBI. **Conclusions:** Single administration of CBLB502 dramatically improves NHP survival following lethal irradiation, reduces the severity of thrombocytopenia and neutropenia, and enhances protection/regeneration of bone marrow, small intestine, thymus and spleen. We conclude that CBLB502 is a non-toxic and effective radioprotectant/radiomitigator that reduces radiation damage to the HP and GI systems and, therefore, has great potential as a life-saving treatment for ARS.

(PS1.04) Radiation injury treatment network: health care professionals preparing for mass casualty radiological and nuclear incidents. Joel R. Ross¹, Cullen Case², John Chute¹, Mark Dewhirst¹, Nelson Chao¹, ¹Duke University, Durham, NC, ²National Marrow Donor Program, Minneapolis, MN

The Radiation Injury Treatment Network® (RITN) is a cooperative effort of the National Marrow Donor Program (NMDP) and The American Society for Blood and Marrow Transplantation (ASBMT). The goals of RITN are to educate hematologists, oncologists, and stem cell transplant practitioners about their potential involvement in the response to a radiation event and provide treatment expertise in the aftermath of a radiation event. This focus leverages the expertise of these specialists who are used to providing the intensive supportive care required by patients with a suppressed marrow function. Following a radiological event, RITN centers may be asked to: accept patient transfers to their institutions; provide treatment expertise to practitioners caring for victims at other centers; travel to other centers to provide medical expertise; or provide data on victims treated at their centers. Moving forward it is crucial that we develop a coordinated interdisciplinary approach in planning for and responding to radiological and nuclear incidents. The ongoing efforts of radiation biologists, radiation oncologists, and health physicists can and should complement the efforts of RITN and government agencies.

(PS1.05) MnTnHex-2-PyP5+ provides protection in non-human primate lungs after whole-thorax exposure to ionizing irradiation. Mark Cline¹, Greg Dugan¹, Donna Perry¹, Ines Batinic-Haberle², Zeljko Vujaskovic², ¹Wake Forest University School of Medicine, Winston-Salem, NC, ²Duke University Medical Center, Durham, NC

The goal of this project was the development of an effective and practical medical countermeasure (MCM) to mitigate and/or

treat radiation-induced lung injury using a metalloporphyrin-based SOD mimic. The rationale for SOD mimics as MCM arises from well-characterized pathophysiological pathways, which rely on redox signaling, that underly the development of radiation-induced lung injury. We have developed a highly efficacious SOD mimic, MnTnHex-2-PyP⁵⁺ (hexyl), that in preliminary studies in rodents mitigates radiation-induced lung injury when given at a low 0.05 mg/kg dose 2 hours after irradiation. In this study, sixteen Rhesus monkeys (NHP) received sham irradiation (IR), sham IR with hexyl at 0.05 mg/kg, 10 Gy whole thorax irradiation (WTI), or 10 Gy WTI with hexyl treatment. Hexyl was given after irradiation, subcutaneously daily for the first 2 months. Blood counts and serum chemistry panels were collected weekly for the first 60 days and thereafter once per month. Respiratory rates (RR), arterial blood gases, and correlative pulse oximetry were measured weekly. Bronchoalveolar lavage was performed monthly. CT scans were performed prior to treatment, at 2 months after treatment when elevated respiratory rates were seen, and terminally at 4 months post-irradiation. Supportive fluid therapy, corticosteroids, analgesics, antibiotics, and symptomatic care were given as needed based on clinical pathology and clinical signs in this IACUC-approved study. Increases in CT abnormalities and RR were seen at 2 and 4 months post-radiation, requiring euthanasia at 4 months. There was no difference in RR between treated and untreated animals after thoracic irradiation. Histologic changes included pneumonitis and fibrosis. Treated NHPs showed a delay in the onset of CT abnormalities, and significantly ($p < 0.05$) lower lung injury at necropsy than non-treated, irradiated primates. These results show (1) the development of a NHP model of radiation-induced lung injury and (2) a statistically significant protective effect by hexyl treatment, with no toxicity. Future studies will focus on determining the maximum tolerated dose in NHPs, followed by efficacy studies to evaluate whether hexyl can achieve similar mitigation of injury in primates as was observed in our rodent model of radiation-induced lung damage.

(PS1.06) γ -tocotrienol and/or pentoxifylline attenuates DNA and lipid oxidative damage in mice intestine after total body irradiation. Li Cui¹, Qiang Fu¹, K.Sree Humar², Martin Hauer-Jensen^{1,3}, ¹University of Arkansas for Medical Sciences, Little rock, AR, ²Armed Forces Radiobiology Research Institute, Bethesda, MD, ³Central Arkansas Veterans Healthcare System, Little rock, AR

Background: Oxidative stress increases in the intestine after exposure to total body irradiation (TBI). Two facts are known: gamma-tocotrienol (GT3) exhibits remarkable antioxidant ability and pentoxifylline (PTX) attenuates radiation-induced intestinal permeability and tight junction breakdown by improving local blood flow. The present study is to investigate whether or not there is a synergistic effect combining GT3 and PTX against intestinal oxidative stress after TBI. Methods: Male CD2F1 mice were randomly assigned to four groups treated with GT3, PTX, GT3+PTX or vehicle. Administration of 100 μ l of GT3 (400 mg/kg), PTX (200 mg/kg), GT3 (400mg/kg) + PTX (200 mg/kg) or vehicle (a mixture of polyethylene glycol) was performed on each group before exposure to TBI (12 Gy). Animals were euthanized at baseline (0 day), 1 day, 3.5 days and 7 days after TBI. The levels of 8-hydroxy-2'-deoxyguanosine (8-OHdG) and malondialdehyde (MDA) in the intestine were semi-quantitatively determined by immunofluorescence microscopy. Results: Intestinal baselines of 8-OHdG and MDA were similar in all 4 treatment groups. Exposure to TBI caused significant increases in 8-OHdG and MDA levels at Day 1 and Day 3.5 but not at Day 7. Administration of GT3, PTX, or GT3 + PTX reduced the 8-OHdG and MDA levels as compared with vehicle-treatment ($p < 0.05$). Significant differences between 3 treatment groups: GT3 treatment, PTX treatment, or GT3+PTX, were noticed by means of the 8-OHdG assay, indicating that GT3 was more effective in reduction of the 8-OHdG than the GT3 + PTX treatment. Conclusions: Administration of GT3, PTX, or GT3 + PTX attenuates TBI-induced oxidative damage in the intestine. 8-OHdG assay detects a subtle difference between GT3 treatment and GT3+ PTX treatment in terms of their efficacy against intestinal oxidative stress after TBI. The phenomenon may be attributable to an involvement of blood flow increasing effect of PTX.

(PS1.07) PHY906 as a potential adjunct to radiotherapy: Preliminary studies. Sara Rockwell¹, Yanfeng Liu¹, Susan A. Higgins¹, Yung-Chi Cheng², Carmen J. Booth³, ¹Department of Therapeutic Radiology, Yale University School of Medicine, New Haven, CT, ²Department of Pharmacology, Yale University School of Medicine, New Haven, CT, ³Department of Comparative Medicine, Yale University School of Medicine, New Haven, CT

PHY906, a state-of-the-art adaptation of Huang-Qin-Tang, a traditional Chinese medicine prepared from a combination of 4 herbs, has been used for over 1800 years in the treatment of a variety of gastrointestinal ailments. PHY906 has been developed by PhytoCeutica as a standardized, well-characterized pharmaceutical product and is subjected to quality-control procedures that include chemical fingerprinting by LC/MS, individual target bioassays, and comprehensive bioresponse profiling. PHY906 was shown in preclinical studies to decrease intestinal injury from anticancer drugs including CPT-11 and VP16, and is currently being evaluated in Phase II clinical trials as an adjunct to chemotherapy. The goals of this pilot project were to test the hypothesis that PHY906 would also be effective in reducing the intestinal toxicity of whole-abdomen irradiation and to begin to assess the potential value of PHY906 as an adjunct to abdominal radiotherapy. Cell culture studies showed that PHY906 in the medium did not alter cell growth and did not act as a radioprotector when present during irradiation. SPF BALB/cRw mice were irradiated with fractionated whole-abdomen irradiation using 250 kV x-rays. Injury to the intestine was assayed by physiological observations and by quantitative histological studies. PHY906 decreased the toxic effects of fractionated abdominal irradiation. Treatment with PHY906 alone did not alter the growth or metastatic spread of EMT6 tumors in BALB/cRw mice. In addition, tumor growth studies showed that PHY906 increased the antitumor effect of single-dose and fractionated irradiation. Overall, in preliminary studies in this mouse model system PHY906 decreased the toxicity of abdominal irradiation but increased the response of tumors to radiation, suggesting that further studies of PHY906 as an adjuvant to radiotherapy regimens involving pelvic or large-field abdominal irradiation are warranted. Supported by a pilot grant from the Yale Cancer Center.

(PS1.08) Thoracic irradiation influences the immune response to a subsequent influenza a virus infection. Casey M. Manning, Christina K. Reed, Jennifer L. Head, Carl J. Johnston, B. Paige Lawrence, Jacky P. Williams, Jacob N. Finkelstein, University of Rochester, Rochester, NY

It is well established irradiation of the lung alters homeostasis of the pulmonary environment and can cause the development of pulmonary fibrosis. Additionally, because the pulmonary environment is continuously in contact with the outside air, we are at risk for exposure to airborne pathogens and respiratory infections. The objective of our research is to determine if prior irradiation of the lung alters its immune response to a subsequent pulmonary challenge. In this study, we tested the hypothesis that thoracic irradiation will cause an attenuation of the immune response to influenza A virus and impair resolution of infection. Adult, C57Bl/6 mice were subjected to 15 Gy thoracic irradiation. At 10 weeks post irradiation, mice were intra-nasally infected with a sub-lethal dose of influenza A virus. At this time post irradiation, the lung has recovered from the acute effects of radiation and no morphological changes are evident. Animal weight loss following infection was recorded daily. At 3, 6, 9, and 14 days post-infection (p.i.) mice were sacrificed for endpoint analyses. Initially following infection, irradiated mice demonstrated similar patterns of weight loss to the sham controls, dropping to approximately 70% of their initial weight by day 7 p.i. However, by day 14 p.i., the sham controls recovered to 90% of their initial weight, whereas the irradiated mice only recovered to 75% of their initial body weight. Quantification of neutrophils, natural killer cells, CD8+ T cells, and virus-specific CD8+ T cells in the lung at each time post-infection was done using flow cytometry. Irradiated animals demonstrated reduced numbers of CD8+ T cells at days 9 and 14 p.i. and had reduced virus-specific CD8+ T cells at day 9 p.i. In contrast, irradiated mice had increased neutrophils at day 9 p.i. compared to sham mice and natural killer cells were increased at

days 3 and 6 p.i. Furthermore, irradiated and sham-infected mice showed no differences in survival and both groups cleared the virus by day 9 p.i. From this data, it is concluded that the normal immune response to influenza A virus is altered with irradiation. Our data further suggests this alteration may in part be due to affects on the adaptive immune response, thereby impairing resolution and recovery from a viral infection. Supported by U19 AI-067733, ES01247, and T32 ES07026.

(PS1.10) Recovery from radiation-induced hematopoietic and gastrointestinal sub-syndromes by Ex-RAD™ in murine model.

Sanchita P. Ghosh¹, Shilpa Kulkarni¹, Michael W. Perkins², Kristen Gambles¹, Kevin Hieber¹, Manoj Maniar³, Thomas M. Seed⁴, K. Sree Kumar¹, ¹AFRRI/USUHS, Bethesda, MD, ²US Army Medical Research, Institute of Chemical Defense, Aberdeen Proving Ground, MD, ³Onconova Therapeutics Inc., Newton, PA, ⁴TMS Incorporation, Bethesda, MD

We tested the efficacy of a new chemical entity, ON01210.Na (Ex-RAD™) in collaboration with Onconova Therapeutics to protect mice from radiation injury. Exposure to total body irradiation (TBI) results in hematopoietic and gastrointestinal (GI) sub-syndromes depending on the radiation dose. We reported that administration of Ex-RAD™ 24 h and 15 min before TBI protected mice from lethality with a dose reduction factor of 1.16. Ex-RAD™ accelerated recovery of peripheral blood elements in sublethally irradiated mice. In this study, we report amelioration of radiation-induced bone marrow suppression, protection of GI crypt cells, and inhibition of p53-mediated apoptosis in spleen. C3H/HeN mice were injected subcutaneously with various doses of Ex-RAD™ 24 h and 15 min prior to radiation (7 Gy @ 0.6 Gy/min). Bone marrow cells were isolated on 4, 8, and 14 days post-radiation and granulocyte macrophage colony forming units (GM-CFUs) were found to be maintained at higher levels in drug-treated relative to vehicle-treated controls (*p<0.01). Crypt cell analysis was performed to assess GI injury in irradiated mice (exposed to 13 and 14 Gy). Numbers of crypts regenerated per circumference in the jejunum of mice treated with drug were significantly higher compared to vehicle alone on 12 h and 3.5 days post-radiation (*p<0.001). Expression of phosphorylated p53 was down-regulated in spleen from mice irradiated and treated with Ex-RAD™. These data suggest that the mechanisms of radiation protection by Ex-RAD™ involve protection from hematopoietic and gastrointestinal sub-syndromes and down-regulation of phosphorylated p53. (This work was supported by a grant (DAMD17-03-2-0027 to KSK) from the U.S. Army Medical Research Acquisition Activity, 82D Chandler St., Fort Detrick, MD 21702-5014, United States Army Medical Research and Materiel Command, administered by the The Henry M. Jackson Foundation for the advancement of Military Medicine, Rockville, MD).

(PS1.11) Alxn4100tpo, a tpo agonist, ameliorates radiation-induced injury by stimulating proliferation and differentiation of multi-lineage hematopoietic progenitors. Merriline M. Satyama¹, Eric Lombardini², Conor Mullaney³, John Graves III³, London Harrison³, Krista Johnson⁴, Jeffrey Hunter⁴, Paul Tamburini⁴, Yi Wang⁴, Jeremy P. Springhorn⁴, Venkataraman Srinivasan¹, ¹SRD, AFRRI, Bethesda, MD, ²VSD, AFRRI, Bethesda, MD, ³SRD, AFRRI, Bethesda, MD, ⁴Alexion Pharmaceuticals, Inc, 352 Knotter Drive, Cheshire, CT

Previously, a single dose of 1 mg/kg Alxn4100TPO (4100TPO), a thrombopoietin agonist, administered sc 12 h after a LD-90 dose (9.25 Gy at 0.6 Gy/min, cobalt 60 gamma source, AFRRI) of total body irradiation (TBI) demonstrated significant mitigation in CD2F1 mice. The current study investigated the mechanism of prophylactic (24 h before) or therapeutic (12 h after TBI) 4100TPO-treatment in 7 Gy irradiated mice using (1) Peripheral blood indices, (2) *In vitro* colony forming units (3) Histopathology and (4) Micronuclei formation in mouse bone marrow. 4100TPO alone, increased mouse peripheral blood platelet levels 5-fold, which peaked 8 days later and remained elevated for 3 weeks thereafter, demonstrating the thrombopoietic nature of the

agonist. Irradiation severely depleted peripheral blood WBCs, lymphocytes, neutrophils and platelets (p<0.001); 4100TPO treatment resulted in earlier reconstitution of WBCs, neutrophils and megakaryocytes in blood (day 10, compared to no changes in blood indices on day 21 for TBI alone group). 4100TPO also increased the number of multipotent (GEMM) colonies compared to vehicle or irradiated controls, denoting a multi-lineage recovery of the hematopoietic tissue. This effect on recovery was further validated using surface markers for committed myeloid (CD117), megakaryopoietic (CD45), and erythropoietic (CD71) progenitors; drug-treated groups showed rapid repopulation of the progenitors (day 7, p<0.01) compared to the irradiated control. Further, histopathological analyses of sternum showed that 4100TPO treatment significantly increased cellularity (100% and 30% for pre- and post-TBI drug-treatment, respectively, compared to 5% for irradiated controls), regenerative foci and megakaryocytes assessed on day 7. 4100TPO reduced the number of micronucleated reticulocytes observed following 7 Gy (p<0.001 compared to vehicle) and facilitated faster restoration of erythropoiesis by normalizing the polychromatic to normochromatic erythrocyte (P/N) ratio by days 7 and 10, for pre- and post-drug treatment, respectively. We conclude that 4100TPO acted as a radiation countermeasure by stimulating multi-lineage hematopoietic recovery and reconstitution of the radiation-ablated hematopoietic organ.

(PS1.12) Modulation of NF-κB and cytokine expression by radioprotective TLR agonists in hematopoietic cells. Rupak Pathak¹, Therese Barber², Alexander Shakhov², Elena Feinstein², Vijay K. Singh^{1,3}, ¹Armed Forces Radiobiology Research Institute, Bethesda, MD, ²Cleveland BioLabs, Inc., Buffalo, NY, ³Edward Hebert School of Medicine, Uniformed Services University of the Health Sciences, Bethesda, MD

The potential threat of acute radiation exposure to civilian and military personnel necessitates the development of a radiation countermeasure capable of providing protection against detrimental effects of ionizing radiation in case of a mass casualty scenario. Recent studies on Toll-like receptors (TLR), which play a crucial role in immunodulation, have shown the efficacy of TLR agonists in protection against radiation injury. The present study has been designed to understand the signaling pathway of different TLR agonists identified as promising radiation countermeasures in hematopoietic cells. The presence of different TLR was investigated by flow cytometry using specific antibodies in human fetal osteoblast (hFOB) cells. hFOB cells were exposed to different concentrations (5, 10, 50, 100, and 200 ng/ml) of three different TLR agonists (CBL502 - TLR5, CBL612 - TLR2/TLR6, and CBL613 - TLR2/TLR6) for 24 h and expression of various cytokines was measured by multiplex Luminex. Expression of NF-κB in hFOB cells was investigated by Western blot analysis after treating the cells with different TLR agonists for 24 h before irradiation. Flow cytometric analysis confirmed the presence of TLR2, TLR3, TLR4, TLR5, and TLR9 in hFOB cells. TLR9 was detected by exposing cells to TLR9 antibody conjugated to FITC. All other TLR were identified only after permeabilization of cells. Our results demonstrate significant induction of interleukin-6 (IL-6) and interleukin-8 (IL-8) by all three TLR agonists. The optimal concentration of CBL502 for cytokine induction was 10 ng/ml and for CBL612 and CBL613 50 ng/ml. Levels of IL-8 were higher compared to IL-6 in response to TLR agonists. Expression of NF-κB p65 and p50 was elevated by treatment with TLR ligands in the presence or absence of cobalt-60 gamma-irradiation. Our findings will help to better understand the radioprotective mechanism of TLR ligands in hematopoietic cells.

The potential threat of acute radiation exposure to civilian and military personnel necessitates the development of a radiation countermeasure capable of providing protection against detrimental effects of ionizing radiation in case of a mass casualty scenario. Recent studies on Toll-like receptors (TLR), which play a crucial role in immunodulation, have shown the efficacy of TLR agonists in protection against radiation injury. The present study has been designed to understand the signaling pathway of different TLR agonists identified as promising radiation countermeasures in hematopoietic cells. The presence of different TLR was investigated by flow cytometry using specific antibodies in human fetal osteoblast (hFOB) cells. hFOB cells were exposed to different concentrations (5, 10, 50, 100, and 200 ng/ml) of three different TLR agonists (CBL502 - TLR5, CBL612 - TLR2/TLR6, and CBL613 - TLR2/TLR6) for 24 h and expression of various cytokines was measured by multiplex Luminex. Expression of NF-κB in hFOB cells was investigated by Western blot analysis after treating the cells with different TLR agonists for 24 h before irradiation. Flow cytometric analysis confirmed the presence of TLR2, TLR3, TLR4, TLR5, and TLR9 in hFOB cells. TLR9 was detected by exposing cells to TLR9 antibody conjugated to FITC. All other TLR were identified only after permeabilization of cells. Our results demonstrate significant induction of interleukin-6 (IL-6) and interleukin-8 (IL-8) by all three TLR agonists. The optimal concentration of CBL502 for cytokine induction was 10 ng/ml and for CBL612 and CBL613 50 ng/ml. Levels of IL-8 were higher compared to IL-6 in response to TLR agonists. Expression of NF-κB p65 and p50 was elevated by treatment with TLR ligands in the presence or absence of cobalt-60 gamma-irradiation. Our findings will help to better understand the radioprotective mechanism of TLR ligands in hematopoietic cells.

(PS1.13) Protonix (Pantoprazol Sodium), a proton pump inhibitor, potentiates radiation lethality. Prabh G. Biju¹, Sarita Garg¹, Wenze Wang¹, Prem K. Gupta¹, Marjan Boerma¹, Martin Hauer-Jensen^{1,2}, Alexander F. Burnett³, ¹Department of Pharmaceutical Sciences, University of Arkansas for Medical Sciences, Little Rock, AR, ²Departments of Surgery and Pathology, University of Arkansas for Medical Sciences and Surgery Service, Central Arkansas Veterans Healthcare System, Little Rock, AR,

agonist. Irradiation severely depleted peripheral blood WBCs, lymphocytes, neutrophils and platelets (p<0.001); 4100TPO treatment resulted in earlier reconstitution of WBCs, neutrophils and megakaryocytes in blood (day 10, compared to no changes in blood indices on day 21 for TBI alone group). 4100TPO also increased the number of multipotent (GEMM) colonies compared to vehicle or irradiated controls, denoting a multi-lineage recovery of the hematopoietic tissue. This effect on recovery was further validated using surface markers for committed myeloid (CD117), megakaryopoietic (CD45), and erythropoietic (CD71) progenitors; drug-treated groups showed rapid repopulation of the progenitors (day 7, p<0.01) compared to the irradiated control. Further, histopathological analyses of sternum showed that 4100TPO treatment significantly increased cellularity (100% and 30% for pre- and post-TBI drug-treatment, respectively, compared to 5% for irradiated controls), regenerative foci and megakaryocytes assessed on day 7. 4100TPO reduced the number of micronucleated reticulocytes observed following 7 Gy (p<0.001 compared to vehicle) and facilitated faster restoration of erythropoiesis by normalizing the polychromatic to normochromatic erythrocyte (P/N) ratio by days 7 and 10, for pre- and post-drug treatment, respectively. We conclude that 4100TPO acted as a radiation countermeasure by stimulating multi-lineage hematopoietic recovery and reconstitution of the radiation-ablated hematopoietic organ.

³Department of Gynecology and Obstetrics, University of Arkansas for Medical Sciences, Little Rock, AR

Background: Protonix (pantoprazole sodium) is a proton pump inhibitor widely used to treat peptic ulcer and gastroesophageal reflux due to its ability to inhibit gastric acid secretion. Moreover, acid suppression with proton pump inhibitors is often considered for supportive therapy after exposure to total body irradiation (TBI). We investigated the effect of Protonix on TBI-induced lethality in mice. **Methods:** Male CD2F1 mice were exposed to various doses of uniform TBI using a ¹³⁷Cs irradiator. Protonix (Wyeth Pharmaceuticals, 16mg/Kg body weight) was administered by twice daily subcutaneous injection in saline from 4 days before to 5 days after irradiation. Effects on gastric pH, and gastrointestinal and hematopoietic toxicity (post-TBI survival, intestinal crypt colonies, mucosal surface area, plasma citrulline levels, gut bacterial translocation, peripheral blood cell counts, and number of spleen colonies) were evaluated. **Results:** Protonix administration significantly exacerbated 30 day lethality, gastrointestinal toxicity, and hematopoietic toxicity. An adverse effect of Protonix was observed both in terms of intestinal crypt survival as well as hematopoietic recovery. In contrast, preliminary results suggest that equivalent doses of a histamine type 2 receptor blocker, another commonly used class of acid-suppressing drugs, was not associated with similar detrimental effects. **Conclusion:** The adverse effect of Protonix on TBI-induced lethality is highly important because of the widespread use of proton pump inhibitors in the general population, as well as the potential use of these drugs for acid suppression in individuals exposed to TBI. Further studies of the mechanisms underlying the adverse effect of proton pump inhibitors after exposure to TBI are clearly warranted. Until results from such studies are available, other acid-suppressing strategies should be preferred in the context of radiation exposure.

(PS1.14) The protective effects of SB203580 on mice exposed to total body irradiation. Zhibin Zhai, Jianhui Chang, Heng Zhang, Lu Lu, Yan Wang, Deguan Li, Hongying Wu, Yueying Wang, Yong Wang, Daohong Zhou, Aimin Meng, Chinese Academy of Medical Science, Tianjin, China

Purpose The present study was to analyze the protective effects of SB203580(SB), an inhibitor of p38 MAPK signal pathway, to inhibit total body irradiation (TBI) -induced injury in mice. **Materials and Methods:** All mice received TBI from a Cesium-137 gamma irradiation and the radioprotective effects of the SB203580 was determined by measuring 30-day survival rate, intestinal crypt cell apoptosis at 7.2Gy, bone marrow hemopoietic cell survival at 6 Gy. Mice were intraperitoneal injected SB (15 mg/kg)30 mins ahead of TBI and then given every 2 days for 5 times after the TBI. **Results** The mean survival time of SB administered mice was 13.6 days after radiation, but the mean survival time of irradiated alone mice was only 7.5 days. Consistent with this result, the 30-day survival rate of SB administered mice was significant higher than that of radiation alone group (40% and 0%, respectively). In the intestinal crypt cell apoptosis experiment, mice were given SB(15 mg/kg)30min before the TBI at a dose of 7.2Gy. These mice were sacrificed at 24th hour after TBI and intestine was obtained for biopsy. Results showed that there were 1.83 ± 0.41 apoptotic cells per intestinal crypts in radiation alone group, but after SB administration the number decreased to 1.13 ± 0.20 . Comparing with the irradiated alone mice, the Caspase-3 positive cells in SB treated mice also decreased. In the bone marrow damage protection assay, the peripheral white blood cells and platelet were significantly decreased in radiation group after TBI and the reduction attenuated by SB treatment significantly ($p < 0.05 \sim 0.01$). The femoral bone marrow cellularity and CFU-GM in SB203580 treated group were significantly higher than those of irradiation mice ($p < 0.05$). **Conclusion:** The results showed that SB203580 exhibit a certain degree of protection from TBI injury in mice. **Key words:** SB203580, irradiation, protective effect, mouse

(PS1.15) The increased stability of p16 mRNA in murine hematopoietic stem cell after irradiation was mediated by p38

signal pathway. Xiao-Chun Wang, Zhi-bin Zhai, Hong-ying Wu, Li-qing Du, Jian-hui Chang, Yue-ying Wang, Lu Lu, Heng Zhang, Dao-hong Zhou, Ai-min Meng, Institute of Radiation Medicine, Tianjin, China

Purpose: The present study was undertaken to examine the expression level of p16 mRNA in mouse hematopoietic stem cell after irradiation and to explore its molecular mechanism. **Methods and Materials:** Bone marrow mononuclear cells was isolation from 30 C57 male mice and then lineage negative hematopoietic (Lin⁻) cells was sorted using magnetic bead. The hematopoietic stem cell was divided into 5 groups, including control group, radiation group, p38 inhibition group (SB203580 (5 umol) was added into culture medium 30 minutes before radiation) and transcription inhibition group. Except the control group, the other four groups were exposed to γ ray at a dose of 4 Gy. The expression status of p16 mRNA was examined using Real-time PCR after 5 days. For the transcription inhibition group, actinomycin D (5ug/ml) was added into culture medium 3 hours before RNA extraction. **Results:** Comparing with the control group, the expression of p16 in radiation group was significant increased, showing radiation can induce the expression of p16 in hematopoietic stem cell. In contrast, the p16 expression level in SB203580 group was not increased after irradiation. These data suggested that the increased p16 expression in hematopoietic stem cell after irradiation was mediated by p38 signal pathway. Comparing with control group, the p16 expression level in transcription inhibition group was still increased, suggesting the stability of p16 mRNA was increased. **Conclusion:** These data showed that the increased expression of p16 in mouse hematopoietic stem cell was mediated by p38 signal pathway. Moreover, this kind of increasing was partly due to the increased stability of p16 mRNA. **Keywords:** p16 mRNA, stability, p38, HSC 1.

(PS1.16) The bisphosphonate risedronate prevents deterioration of bone in rats at directly irradiated sites after modeled radiotherapy. Jeffrey S. Willey¹, Michael E. Robbins², J. D. Bourland², Ted A. Bateman¹, ¹Clemson University, Clemson, SC, ²Wake Forest University, Winston Salem, NC

Radiation therapy for pelvic tumors in postmenopausal women increases pelvic-bone fracture rates by ~65-200%. One-year after a hip fracture mortality is nearly 20% in women. The cause of these fractures is not well understood. Recent work has demonstrated that radiation rapidly activates osteoclasts, leading to acute bone loss. However, mouse studies showing damaged bone after irradiation have used whole-body exposures. It is unclear if bone loss occurs primarily as a direct response at irradiated sites or from systemic factors. The purpose of this study was to apply a clinically relevant fractionated dose to determine direct radiation effects. Twenty-one-week old Sprague-Dawley rats were divided into 3 groups: non-irradiated; irradiated; and irradiated + risedronate (an osteoporosis therapy; 0.1 mg/kg/wk) treated rats. Over a 2-week period, right hind limbs were exposed to a total dose of 16 Gy of 6 MV X-rays delivered in 4 fractions using a LINAC. A cervical cancer treatment regimen was modeled using the Fowler equation assuming an α/β ratio of 3 for human and rat bone. For these women 30 x 1.8 Gy fractions (M-F for 6 weeks) are delivered, applying 54 Gy to the tumor. Hips receive ~50% of each fraction totaling 27 Gy, resulting in a BED of 35.1 Gy. We modeled this with 4 fractions of 4 Gy each over 2 weeks (BED = 36.8). At 2, 4 and 6 weeks after the last fraction, microCT evaluated trabecular bone in the proximal tibia 3mm distal to the growth plate. Severe deterioration of bone in the irradiated right limb relative to the non-irradiated left limb was observed at all time points. Reduced trabecular connectivity and fewer trabeculae were present at directly irradiated sites relative to the non-irradiated limbs ($p < 0.05$). Quality of the trabeculae was reduced as struts became rod-like ($p < 0.05$). Thickness of the trabeculae, however, was increased by 2 weeks ($p < 0.05$), mitigating loss of volume despite loss of structural integrity. Atrophy of irradiated limbs was entirely prevented with risedronate administration. Local irradiation resulted in deterioration of bone relative to a non-irradiated site on the opposite limb. An antiresorptive osteoporosis therapy mitigated local bone atrophy. While systemic factors cannot be excluded, radiation appears to induce bone loss primarily within the irradiated volume (supported by AR054889).

(PS1.17) Radioprotective efficacy of gamma-tocotrienol and pentoxifylline combination in murine model. Shilpa S. Kulkarni¹, Sanchita Ghosh¹, Kevin Hieber¹, Lyudmila Romanyukha¹, Martin Hauer-Jensen², Sree Kumar¹, ¹AFRRI, Bethesda, MD, ²University of Arkansas for Medical Sciences, Little Rock, AR

Ionizing radiation causes multi-organ dysfunction syndrome (MODS) that can lead to mortality. We reported that gamma tocotrienol (GT3) is a good radiation countermeasure in the murine model. Pentoxifylline (PTX) in combination with vitamin E has been shown to ameliorate radiation-induced fibrosis in clinical trials. We report here that combinations of GT3 and PTX enhance radioprotection provided by GT3 alone in murine model. Mice pretreated with GT3 and PTX were irradiated and monitored for 30-day survival and the data was used to calculate the dose reduction factor (DRF). Hematology studies were conducted on mice treated with GT3 and PTX, and irradiated at 4 and 8 Gy. Colony forming units were also calculated in 14 day CFU assays performed on bone marrow from all groups. The combination of GT3 (200 mg/kg, -24 hr) and PTX (200 mg/kg, -15 min) increased the 30-day survival in lethally irradiated mice significantly over the GT3 controls. The LD_{50/30} was calculated to be 11.31 for GT3 alone and, 12.23 for GT3-PTX combination. The DRF was calculated to be 1.45 for GT3-PTX and 1.3 for GT3. GT3 and GT3-PTX combination groups showed similar accelerated recovery in neutrophils, WBC, platelets, and monocytes, and a similar CFU efficiency, compared to vehicle controls. PTX did not provide any additional protection to the hematopoietic tissue. However, it is important to note that PTX significantly improved the survival in mice at radiation doses (12 Gy) that lead to mortality related to GI injury. More experiments are being conducted to analyze the protective effect of PTX on the GI tract.

(PS1.18) Over expression of miR-100 is responsible for the low expression of ATM in the human glioma cell line: M059J. Wooi Loon Ng¹, Dan Yan¹, Xiangming Zhang¹, Yin-Yuan Mo², Ya Wang¹, ¹Emory University, School of Medicine, Atlanta, GA, ²Southern Illinois University, School of Medicine, Springfield, IL

M059J and M059K cells were isolated from different portions of the same human malignant glioma. M059J cells are more radiosensitive than M059K cells due to the absence of DNA-PKcs and low-expression of ATM. The mechanism concerning the absence of DNA-PKcs in M059J is involved in the frameshift mutation in *PRKDC* (DNA-PKcs gene); however, the reason for the low expression of ATM in M059J cells remains unclear. We report here that ATM is a target of *miR-100* that is highly-expressed in M059J cells, about 4-fold greater than in M059K cells. The 3'-UTR of ATM contains a *miR-100*-binding site. Knocking-down *miR-100* promotes ATM expression in M059J cells, while up-regulating *miR-100* in M059K cells reduces ATM expression and sensitizes M059K cells to ionizing radiation. These results indicate that the low-expression of ATM in M059J cells is due to the high-expression of *miR-100* and suggest that *miR-100* could be a useful tool to target ATM and sensitize cells to ionizing radiation.

(PS1.19) Combined injury treated with COX-2 inhibitors: Acute effects on immunity. Wan Jiao, L.H. Cary, B.F. Ngudiankama, T.B. Elliott, G.D. Ledney, J.G. Kiang, AFRRI, Bethesda, MD

Aim: A nuclear detonation will cause combined injuries (CI) decreasing the immune responses. At Hiroshima and Nagasaki, 60% to 70% of casualties sustained CI. In this study, Th1/Th2-related cytokine concentrations in splenocytes and sera, and bone-marrow stem-cell regeneration were determined after treatment with COX-2 enzyme inhibitors. Methods: B6D2F1/J female mice, 20 wk and 25g, were given 9.75 Gy ⁶⁰Co γ radiation at 0.4 Gy/min and, within 1 h after RI, a 15% total-body skin-area dorsal wound was inflicted under anesthesia. Serum and splenocyte Th1/Th2 cytokine concentrations, including IFN- γ , IL-2, 12, and TNF- α (Th1-related) and IL-4, 5, 10, and 13 (Th2-related) were determined 2 days after RI or CI with kits from Bio-Plex and RayBio, respectively. Bone marrow

(BM) stem-cell CD^{34+/117+} were measured by flow cytometry. Results: Sham-treated control mice were given only vehicle (no radiation or wounding). RI or CI mice were given COX-2 inhibitors, celecoxib or meloxicam, or vehicle. Th1/Th2 cytokines in test groups were normalized to sham values. RI decreased Th1/Th2-related cytokine expression more than CI. Celecoxib increased Th1-related IFN- γ and IL-2, Th2-related IL-5 and 10 secretions; meloxicam increased Th2-related IL-5 secretion after RI. CI generally suppressed Th1/Th2-related cytokine secretions. Serum Th1/Th2-related cytokine concentrations varied after RI or CI compared to splenocyte concentrations. In both RI and CI, CD^{34+/117+} stem cells increased about 50% compared to sham values. These results may be explained by our previously reported elevation of Flt-3 ligand (FL) and G-CSF concentrations in the serum, especially after CI (Jiao W, et al. Radiat Res. 2009; 172(6):686-97). COX-2 inhibitors did not change CD^{34+/117+} stem cells after RI. Conclusion: Th1/Th2 cytokines have important immunoregulatory roles. An imbalance of these cytokines could be a critical determinant of immune responses observed after RI or CI. Our preliminary data show for the first time that RI or CI changed splenocyte and serum Th1/Th2-related cytokine concentrations, and these changes were affected by COX-2 enzyme inhibitors. (This work was funded by NIH/NIAID: YI-AI-5045-04)

(PS1.20) Mitigation of Acute Radiation Injury by Interleukin-12. Dolph D. Ellefson¹, Tim Gallaher¹, Joseph Miller², Lena Basile¹, ¹Neumedicines, Inc., Pasadena, CA, ²University of Southern California, Los Angeles, CA

We have previously demonstrated that IL-12, a much characterized mediator of innate and adaptive immune responses, is also a potent regulator of hematopoiesis. IL-12 stimulates hematopoietic reconstitution in mice following exposure to 625 cGy total body irradiation (TBI) when administered 24 hr pre-exposure or 2 hr post-exposure. Because of the demonstrated effectiveness of IL-12 post-exposure, we employed a more challenging model of radiation exposure to examine the ability of IL-12 to mitigate survival and recovery. In a murine pre-clinical model of myeloablation, a single, low-dose injection of IL-12 administered up to 48 hrs after lethal exposure stimulates hematopoietic recovery and enhances survival. Single administration of an optimized low-dose formulation of IL-12 administered 24 hrs post-TBI mitigated morbidity and increased survival to 70% in mice exposed to levels corresponding to the LD_{100/30} relative to vehicle-treated controls. When irradiated at levels of exposure corresponding to the LD_{100/10}, 100% of mice treated with IL-12 at 6 hrs post-exposure survived relative to non-treated controls, suggesting that IL-12 may also mitigate death attributable to the GI syndrome. Mitigation of radiation exposure and restoration of homeostasis requires therapeutics capable of stimulating repair through the proliferation, expansion, and differentiation of regenerative cells in the body. These data suggest that IL-12 could be an effective mitigant against intentional release of radiation as well as a potent tool for accelerated recovery following therapeutic application of radiation. Ongoing pre-clinical efficacy studies of recombinant human IL-12 (rhIL-12) in non-human primates (*Macaca mulatta*) will establish the effective dose range required for mitigation of acute radiation syndrome in humans. This project has been funded in whole or in part with Federal funds from the Biomedical Advanced Research and Development Authority, Office of the Assistant Secretary for Preparedness and Response, Office of the Secretary, Department of Health and Human Services, under Contract No. HHSO100200800060C.

(PS1.21) Mitochondria-targeted ligands of heme-iron in cytochrome c as novel radioprotectors/radiomitigators. Jeffrey Atkinson¹, Alexandr Kapralov², Zhenhai Huang², Natalia A. Belikova², Naveena Yanamala², Jianfei Jiang², Judith Klein-Seetharaman², Michael W. Epperly², Detcho A. Stoyanovsky², Joel S. Greenberger², Valerian E. Kagan², ¹Brock University, St. Catharines, ON, Canada, ²University of Pittsburgh, Pittsburgh, PA

Irradiation induced apoptosis is executed via the mitochondria-dependent pathway. The early events are transmigration of cardiolipin (CL) from the inner to the outer mitochondrial membrane, the formation of cytochrome (cyt) c-CL peroxidase complex leading to accumulation of CL peroxidation products that are essential for the release of pro-apoptotic factors into the cytosol. Therefore, quenching of the peroxidase activity of cyt c-CL complex may be a promising strategy to reduce irradiation injury. We developed a series of compounds with Fe-liganding capacity that bind with cyt c/CL complex and position themselves such that they are capable effective inhibition of the peroxidase activity. Conjugation of these compounds with a mitochondria-targeting group (triphenylphosphonium cation, TPP) resulted in their accumulation in mitochondria of cells and inhibition of the peroxidase activity, CL peroxidation as well as irradiation-induced apoptosis (as revealed by externalization of phosphatidylserine on the cell surface, caspase 3/7 activation and inhibition of cytochrome c release from mitochondria). The radioprotective activity was also confirmed *in vivo*. We conclude that mitochondria-targeted cyt c-CL peroxidase inhibitors represent a new promising class of radiomitigators. Supported by NIH NIAID U19 AI 068021.

(PS1.22) Treatment with r-spondin 1 and toll-like receptor 9 ligands improve the therapeutic ratio of abdominal irradiation.
 Payel Bhanja, Albert Einstein College of Medicine, Bronx, NY

RIGS is the result of direct cytotoxic effects on intestinal crypt cells with subsequent loss of the mucosal barrier. This manifests as electrolyte imbalance, systemic infection (sepsis) and death. The stromal cells surrounding the ISC provide the niche and supply critical growth factors for stem cell regeneration. We hypothesized that supplement of bone marrow-derived adherent stem cells (BMASCs) as source of ISC niche component including mesenchymal stem cells (MSCs), endothelial progenitor cells (EPCs) and macrophages may restore ISC and its niche to mitigate RIGS. C57Bl/6 BM was cultured for 4 days, followed by collection of adherent cells (BMASCs). Mice receiving BMASCs (106 cells *i.v.* at 24 and 72hrs post IR) containing 48±2% MSC (CD105+CD45-), 7.1±0.5% EPC (CD133+ Flk+) and 17.3±1.8% myeloid/macrophages (CD11b+F480+) survived (100%) lethal doses of WBI (10.4Gy) and AIR (18Gy), *p*<0.002 and *p*<0.004 respectively. Transplantation of either CD11b+ myeloid cells or CD11b- and CD105+ MSCs could mitigate 30-40%, indicating cooperative role of MSCs and macrophages for RIGS survival. Histopathology of jejunum demonstrated significant increases in proliferation (*p*<0.004), decrease in crypt depth (*p*<0.001) & apoptotic crypt cells (*p*<0.003) with BMASC transplant after IR. Immunohistological analysis showed restoration of ISMEF (α SMA +ve & desmin -ve) (major ISC niche component) with BMASC transplant. Xylose absorption was greater in these mice indicating functional integrity following BMASC transplantation. To study the possible radiomitigating factor secreted from BMASC concentrated culture supernatant was administered to irradiated mice at 24hr and 72 hr after either, WBI (10.4 Gy, n=5) or AIR (16Gy, n=5). 50% of mice survived for up to 30 days indicating the presence of mitigating factors in culture supernatants. Proteomic analysis of culture supernatant using mass spectrometry followed by Ingenuity Pathway Analysis identified potential mitigating agents including angiogenic factors, antiapoptotic factors, epithelial mitogens, smooth muscle proliferating agents. This is the first demonstration that supplement of stromal component / factors could mitigate supra-lethal doses of IR. Studies are ongoing to identify the cellular and molecular mechanisms responsible for radiation mitigation.

(PS1.23) Gene Expression Profiling in Irradiated Skin. A. Lopez, X. Wu, E. B. Olasz, J. Lazar, R. Sells, B. L. Fish, M. Mader, A. M. Schock, B. J. Althouse, J. E. Moulder, Zelmira Lazarova, Medical College of Wisconsin, Milwaukee, WI

Skin exposure to ionizing radiation generates reactive oxygen and nitrogen species (ROS, RNS). These highly-reactive species may oxidize constitutive proteins, DNA and lipids. When the intrinsic repair and free radical scavenger systems are not able to

neutralize these insults, acute severe oxidative damage occurs. Chronic oxidative stress has been suggested as a contributor to the progression of radiation-induced late effects. Since the specific genes or pathways involved in this process are ill-defined, we obtained results from microarrays 30 days after 30 Gy single-dose local irradiation of rat skin. Male WAG/RijCmcr rats (n=10) were divided into irradiated and non-irradiated groups (5 rats per group). The dorsal skin was exposed to a 15kVp x-ray beam with a steep dose gradient. Rats were irradiated without anesthesia and control rats were sham irradiated. 30 days after irradiation, when rats developed severe radiation dermatitis, the animals were euthanized. Total RNA was isolated using RNeasy Mini Kit (Qiagen, Valencia, CA), pooled and RT² Profiler PCR Arrays on Oxidative Stress and Antioxidant Defense (SA Biosciences, Frederick, MD) were performed. Analysis of the gene expression showed upregulation of 19 genes and downregulation of 7 genes in irradiated skin compared to controls. Classification of these genes revealed that upregulated genes were the key antioxidant enzymes involved in detoxification of ROS and RNS. Interestingly, the downregulated genes were involved in immune defense and DNA repair. These preliminary results demonstrate the critical role of oxidative stress in the late stages of radiation-induced skin injury. This work was supported by NIAID cooperative agreement AI067734.

(PS1.24) Cytokine responses after combined pulmonary exposures to low-dose low-LET radiation and fungal spores.
 Laura Downing¹, Kara Sawarynski¹, Jacqueline P. Williams², Jacob Finkelstein², Matthew Sims¹, Brian Marples¹, ¹William Beaumont Hospital, Royal Oak, MI, ²University of Rochester, Rochester, NY

The effects of whole-body X-irradiation and *Aspergillus fumigatus* inoculation were determined in C57BL/6 female mice. Animals were either exposed to spores and immediately irradiated with 2 Gy, or the inoculation and irradiation were separated by 8 weeks. Pulmonary injury was assessed at 24 and 48 hrs, and 1, 2, 4, 8, and 24 wks post-irradiation. A 5 Gy dose was also examined at 8 wks. Lungs were examined histologically and immunohistochemically (IHC) and compared with sham-treated, age-matched controls. Alveolar septal thickness and tissue architecture were evaluated. Quantitative IHC for invasive inflammatory cells (macrophages [CD68], neutrophils [771G], and B [CD79a] and T [CD3] lymphocytes) and cytokines (*e.g.*, IL6, IL β) was performed. Circulating cytokines were assessed from harvested blood by a BIO-RAD Bio-Plex Pro™ Assay (IL1 β , IL1 α , IL10, IL6, MCP1, MIP2, TGF β). Individual radiation-induced and fungal-induced changes in lung architecture were evident at 24h-2 wks and 24h-4 wks, respectively. When radiation and spores were given concurrently, lung damage was still evident 8 wks post-treatment, indicating that simultaneous combined exposures increased the duration of pulmonary damage. An increase in damage intensity was also evident. Separating the two insults by 8 weeks did not lead to combined measures of injury. Radiation exposure alone was associated with early elevated levels of circulating MCP1 (48 hrs; 407±155 pg/ml compared with sham 169±118 pg/ml) and late TGF β (24 wks; 7.2±1.98 pg/ml compared with sham 0.6±1.35 pg/ml), and fungal exposure alone increased circulating levels of IL1 α and IL6, but not IL10, compared with sham-treated controls. Elevated levels of IL1 α , IL1 β (1-7 days) and IL6 (2-24 wks) were seen after combined treatments. These data indicate that the circulating cytokine response to combined exposures of low-dose low-LET radiation and fungal spores are dominated by the fungal component of injury. In the event of an explosive radiological attack, pulmonary injury from the inhalation of radioactive particles should be considered in combination with damage from environmentally ubiquitous fungal spores or bioterrorism-related microbial agents. Supported by NIAID-U19AI067733, University of Rochester, NY and Department of Radiation Oncology, William Beaumont Hospital, MI

(PS1.25) Effectiveness of DF-1, a nontoxic carbon fullerene based antioxidant, as a biomedical countermeasure against radiation. Corey A. Theriot¹, Rachael Casey¹, Jodie Conyers²,

Honglu Wu¹, ¹NASA Johnson Space Center, Houston, TX, ²University of Texas Health Science Center, Houston, TX

A long-term goal of radiation research is the mitigation of inherent risks of radiation exposure. Thus the study and development of safe agents, whether biomedical or dietary, that act as effective radioprotectors is an important step in accomplishing this long-term goal. Some of the most effective agents to date have been aminothiols and their derivatives. Unfortunately, most of these agents have side effects such as nausea, vomiting, hypotension, weakness, and fatigability. For example, nausea and emesis occur in most patients treated with WR-2721 (Amifostine), requiring the use of effective antiemetics, with hypotension being the dose-limiting side effect in patients treated. Clearly, the need for a radioprotector that is both effective and safe still exists. Development of biocompatible nano-materials for radioprotection is a promising emerging technology that could be exploited to address the need to minimize biological effects when exposure is unavoidable. Testing free radical scavenging nanoparticles for potential use in radioprotection is exciting and highly relevant. Initial investigations presented here demonstrate the ability of a particular functionalized carbon fullerene nanoparticle, (DF-1), to act as an effective radioprotector. DF-1 was first identified as the most promising candidate in a screen of several functionalized carbon fullerenes based on lack of toxicity and antioxidant therapeutic potential against oxidative injuries (i.e. organ reperfusion and ionizing radiation). Subsequently, DF-1 has been shown to reduce chromosome aberration yield and cell death, as well as overall ROS levels in human lymphocytes and fibroblast after exposure to gamma radiation and energetic protons while demonstrating no associated toxicity. The dose-reducing factor of DF-1 at LD50 is 2.0 for gamma radiation. In addition, DF-1 treatment also significantly prevented cell cycle arrest after exposure. Finally, DF-1 markedly attenuated COX2 upregulation in cell culture after irradiation thus preventing an inflammatory response to irradiation. Taken together, these results suggest that DF-1 provides potent protection against several deleterious cellular consequences of irradiation in mammalian systems including oxidative stress, DNA damage, inflammation and cell death.

(PS1.26) Radioprotective and therapeutic effects of delta-tocotrienol in mouse bone marrow hematopoietic tissue (*in Vivo* study). Mang Xiao, Xiang Hong Li, Dadin Fu, Nabil H. Latif, Cam T. Ha, Armed Forces Radiobiology Research Institute, USUHS, Bethesda, MD

Exposure to γ -radiation causes rapid hematopoietic cell apoptosis, bone marrow suppression, and even animal death. Recent report from Dr. Srinivasan at AFRRRI demonstrated that natural delta-tocotrienol (DT3), one of the isomers of vitamin E, significantly enhanced 30-day survival in lethally irradiated mice. In the present study, we have explored the protective and therapeutic effect of DT3 on mouse bone marrow (BM) hematopoietic cell survival after 8.75 Gy total body γ -irradiation (TBI). Pathological study using HE-stained mouse sternum slides showed DT3 administration 24 h before TBI suppressed red blood cell congestion in sinus and protected mouse BM from radiation-induced hemorrhage. DT3 increased BM myeloid cell viability by 3.5 fold and regenerative microfoci with significant megakaryocyte restoration 8 days post-irradiation. Furthermore, an enhanced granulocyte colony-stimulating factor (G-CSF) level in DT3-treated mouse serum was shown 24 h after irradiation. Most importantly, DT3 treatment 6 h post-irradiation resulted in a 2.6 fold increase of mouse BM progenitor cell clonogenicity and two fold increase of Lin⁻c-kit⁺Sca-1⁺ HSPCs compared with BM from vehicle control-treated mice. In a study of mechanisms by which DT3 induced mouse BM hematopoietic cell survival, we found DT3 induced Erk1/2 phosphorylation and significantly inhibited formation of the DNA-damage marker γ -H2AX foci in mouse bone marrow after irradiation, as determined by immuno-fluorescence staining and confirmed by immunoblotting studies. DT3 upregulated mTOR activation and subsequently released the mTOR downstream target, cap-dependent mRNA translation factor eIF4E, from 4EBP1 inhibition in mouse BM myeloid cells. Most mRNAs are translated in mammalian cells through a cap-dependent mechanism, and translational control allows for more rapid protein regulation in

response to positive or negative stimuli, including cell growth, cell cycle progression, and apoptosis. One of the major upstream signaling components that control mTOR activity is the MAPK/Erk pathway. Thus, our data suggest that the protective and therapeutic effects of DT3 in irradiated mouse BM are through the regulation of stress and survival signal pathways including Erk and mTOR signaling.

(PS1.27) The impact of a metalloporphyrin antioxidant on radiation response in two tumorigenically distinct lung cell types. Xian Luo-Owen¹, Tanya L. Freeman¹, Celso Perez¹, James D. Crapo², Mike J. Pecaut¹, James M. Slater¹, Daila S. Gridley¹, ¹Loma Linda University & Medical Center, Loma Linda, CA, ²National Jewish Medical and Research Center, Denver, CO

Radiation therapy (RT) is an important therapeutic modality in the treatment of cancers, but potential for cure is often limited by concern for normal tissue tolerance in sensitive areas such as lungs. Lung injury from radiation is believed to be a consequence of oxidative stress and a cascade of cytokine activity. Recent data suggest that broad-spectrum catalytic antioxidants, such as MnTE-2-PyP5 [manganese (III) mesotetakis (N-ethylpyridinium-2-yl) porphyrin], may be especially useful in protecting normal tissues from radiation-induced injury. However, a drug that protects normal tissues must not also protect the tumor cells against radiation damage. The purpose of this study was to evaluate the response of Lewis lung carcinoma cells (LLC) and human lung epithelial cells (HLE) when subjected to radiation in the presence of MnTE-2-PyP5. LLC and HLE cells were irradiated in OptiCellTM plates using a ⁶⁰Co source delivered in a single fraction at a dose rate of ~0.7 Gy/min. MnTE-2-PyP5 (6 μ g/ml) was added 60 min before gamma-irradiation. The cells were exposed to 0 and 2 gray (Gy) and harvested post-irradiation, dispensed into 96-well microtiter plates (4 x 10⁴/well for HLE, 1 x 10⁴/well for LLC) and analyzed after 48h incubation at 37°C for DNA synthesis (³H-thymidine incorporation), caspase3/7 and lysosomal acid phosphatase activity (PAC) analyses. LLC cells exhibited significantly low cpm values for DNA synthesis in presence of MnTE-2-PyP5 at both 0 and 2 Gy compared to their counterparts irradiated without drug (P<0.01). In contrast, there was no significant difference between HLE cells irradiated with and without drug. Furthermore, significantly higher caspase 3/7 activities and lower PAC activities (P<0.01) were found in LLC cells treated with MnTE-2-PyP5 compared to non-drug-treated cells in both 0 and 2 Gy groups at 48h. These data suggest that MnTE-2-PyP5 may interact with normal and tumor tissues via totally different mechanisms during radiotherapy. The drug may also possess anti-tumor properties that could be attributed partly to its inhibition of cell proliferation, induction of mitochondria-initiated apoptosis in cancer cells through caspase activation, and enhancement of lysosomal damage. The findings warrant further evaluation of metalloporphyrin antioxidants in combination with radiation.

(PS1.28) Mitigation of radiation-induced pneumonitis and pulmonary vascular injury using combined therapy: angiotensin converting enzyme inhibitors and super oxide dismutase (SOD) mimetics. Robert C. Molthen^{1,2,3}, QingPing Wu^{1,4}, Brian L. Fish⁴, Elizabeth R. Jacobs¹, John E. Moulder⁴, Susan R. Doctrow⁵, Meetha Medhora^{4,1}, ¹Medical College of Wisconsin, Department of Medicine: Pulmonary and Critical Care, Milwaukee, WI, ²Marquette University, Department of Biomedical Engineering, Milwaukee, WI, ³Zablocki VA Medical Center, Milwaukee, WI, ⁴Medical College of Wisconsin, Department of Radiation Oncology, Milwaukee, WI, ⁵Boston University School of Medicine, Department of Medicine, Pulmonary Center, Boston, MA

Aim: To investigate potential therapies for radiation-induced lung injury. In this study we examine the effectiveness of independent and combined treatment using angiotensin converting enzyme (ACE) inhibitors and a super oxide dismutase (SOD) mimetic as mitigators of radiation injury after total body irradiation (TBI). **Methods:** Rats (WAG/RijCmcr) were irradiated with a single dose (11Gy, TBI) followed by a syngenic bone marrow transplant.

Rats were then treated with captopril (100 mg/m²/day) or enalapril (10 mg/m²/day) in their drinking water or with the super oxide dismutase (SOD) catalase mimetic EUK-207 (1.8 mg/m²/day) alone or in combination starting at approximately one wk after TBI, continuing until the endpoint. Rats were studied 6 wks after TBI and indices of health as well as heart and lung structure and function were measured. Results: Body weight was significantly decreased by TBI and not improved by any treatment schedule. Hematocrit tended to be decreased, but not significantly, in TBI rats and mostly unchanged by treatment. Right ventricular hypertrophy (RVH) was significantly increased by TBI. RVH was mitigated by captopril and EUK alone or in combination, but not by enalapril + EUK. Total lung ACE activity was significantly decreased by TBI, this effect was significantly mitigated by treatment with EUK alone or in combination with either ACE inhibitor. Pulmonary vascular resistance (PVR) was significantly increased by TBI. PVR was significantly decreased by treatment with captopril and EUK alone or in combination, but not by enalapril + EUK. Conclusions: Radiation induced injury appears to be mitigated by treatment with EUK and/or captopril, but not enalapril + EUK. This work was funded by RC1 AI 81294 and NIH/NIAID agreements U19-AI-67734. Dosimetry was done by the CMC Irradiation Core at MCW; histology was done in the Children's Research Institute at MCW under direction of Dr. Paula North.

(PS1.29) Triptolide reduces radiation-induced cytokines in lung inflammation model. Chun Chen, Shanmin Yang, Mei Zhang, Steven B. Zhang, Xiaohui Wang, Yansong Guo, Jun Ma, Alexandra Litvinchuk, Steven Stwartz, Paul Okunieff, Lurong Zhang, UF Shands Cancer Center, Gainesville, FL

Triptolide (TPL), a compound purified from *Tripterygium wilfordii*, has been shown to reduce both ionizing radiation (IR) induced pneumonitis and lung fibrosis in our previous animal studies. The induction of numerous cytokines due to the interaction between the activated macrophages and apoptotic type I and type II pneumocytes is likely to be the basis of IR pneumonitis and lung fibrosis. The aim of this study is to establish a viable *in vitro* model of IR acute alveolar inflammation to evaluate the effect of TPL on multi-cytokines. The murine lung MLE-15 cells were irradiated with 3Gy, then to co-culture with Raw264.7 cells that were seeded in transwell inserts, in which the direct cell-cell contact was prevented but a transfer of factors was permitted. The MLE-15 cells were irradiated with 3Gy, then added to transwell inserts to co-culture with Raw264.7 cells, in which the direct cell-cell contact was prevented but a transfer of factors was permitted. The levels of IL-1 α , IL-6, TNF- α , MIP-2 and TGF- β 1 in the co-culture medium were measured. Each factor had its own secretion pattern during 48 hr post IR. TNF- α reached a peak level at 6 hr after IR, and then rapidly dropped; IL-6 and MIP-2 were secreted continuously and accumulated over 48 hours, especially MIP-2 which obtained a level of 5.6ng/ml at 48hr; IL-1 α and TGF- β 1 levels declined to a nadir at 12 hr followed by a peak between 24-48 hr. To determine the TPL effect, TPL was added to a co-culture of Raw264.7/MLE-15 1 hr after MLE-15 irradiation to 3Gy. After 24 hr, the levels of cytokines and TGF- β 1 in the supernatant were measured. TPL at 5 ng /ml achieved a significant reduction in the levels of IL-6, TNF- α , MIP-2 and TGF- β 1. All these cytokines are believed to be involved in the IR-induced pneumonitis and lung fibrosis. In summary, a unique co-culture system was used to test TPL in an *in vitro* model of the cell-cell interaction of type II pneumocyte and macrophage. The anti-pneumonitis and anti-fibrosis effect of TPL was due to down-regulation of the levels of IL-6, TNF- α , MIP-2 and TGF- β 1.

(PS1.30) Radiosensitization by celastrol is mediated by modification of antioxidant thiol molecules. Haeng Ran Seo¹, Woo Duck Seo², Tae-Hee Kim¹, Byong Won Lee², Yeung Bae Jin¹, Ki Hun Park³, Yun-Sil Lee¹, ¹Korea Institute of Radiological & Medical Science, Seoul, Republic of Korea, ²National Institute of Crop Science, Miryang, Republic of Korea, ³Gyeongsang National University, Jinju, Republic of Korea

The several quinone methide containing triterpenes (QMT) enhanced the cytotoxic effect of IR, but 6-(2-oxopropyl)-22- β -hydroxyingenol, which does not contain the quinone methide moiety, did not. Of the QMTs, celastrol had the greatest enhancing effect in IR induced cell death *in vitro* and *in vivo* nude mouse xenografting system, when compared to celastrol or IR alone treated cells. Furthermore, the quinone methide moiety of celastrol was found to be essential for celastrol-mediated radiosensitization because dihydrocelastrol, which does not contain the quinone methide moiety, did not show a radiosensitizing effect. Reactive oxygen species (ROS) production by IR was augmented by combination with celastrol which was responsible for celastrol-mediated radiosensitization. Celastrol induced thiol reactivity to antioxidant enzymes such as thioredoxin reductase and total glutathione activity induced the inhibition of these antioxidant enzyme activities, which resulted in increased ROS production. Our results suggest that celastrol, one of QMT synergistically enhanced the effects of IR in lung cancer cells. These results suggest the novel anticancer therapeutic use of celastrol in combination with radiation therapy.

(PS1.31) Efficacy of "single-shot" SOM230-LAR as a mitigator of total-body irradiation-induced lethality: comparison with SOM230. Wenze Wang¹, Qiang Fu¹, Prabath Biju¹, Sarita Garg¹, Herbert Schmid², Martin Hauer-Jensen¹, ¹UAMS, Little Rock, AR, ²Novartis Institutes for BioMedical Research, Basel, Switzerland

Background: The somatostatin analog SOM230 (pasireotide), administered by twice daily subcutaneous (sc) injection for 2 weeks, potentially mitigates lethality after total-body irradiation (TBI). This study tested the potential for improved logistics with a long-acting release form of SOM230, SOM230-LAR. Methods: Male CD2F1 mice were exposed to 9-10 Gy TBI. Beginning 24 hrs after irradiation, SOM230 or vehicle was administered by twice-daily sc injections for 14 days and compared with SOM230-LAR or vehicle administered as single subcutaneous injections. Animals were monitored up to 30 days post-TBI. Plasma concentrations of SOM230 after injection of SOM230-LAR were monitored, intestinal proteolytic activity was assessed using a protease fluorescent detection kit, and plasma levels of growth hormone and insulin-like growth factor 1 were determined. Results: Twice-daily administration of SOM230 (1 or 4 mg/kg/d) begun 24 h post-TBI for 14 days significantly enhanced animal survival. Measurement of plasma concentration of SOM230-LAR after a single injection (8-320 mg/kg, sc) showed that the concentration of SOM230 increased in a dose-dependent manner and was maintained for at least 28 days. The survival benefit of SOM230-LAR was mainly evident during the early post-TBI period. Hence, while SOM230-LAR prolonged median survival time, 30-day lethality was not different from that of control animals. Conclusions: These results suggest that (1) both SOM230 and SOM230-LAR enhances the survival when administered 24 h after TBI; (2) however, the survival benefit of SOM230-LAR is predominantly during the initial two weeks after TBI; (3) the long-lasting action of SOM230-LAR may not confer an additional survival benefit and may, in fact, be detrimental; (4) the use of "single-shot" SOM230-LAR as a radiation mitigator requires further study, for example, with SOM230-supplementation during the first few days post-TBI.

(PS1.32) High-throughput CT imaging for quantitative evaluation of radiation induced lung injury in small animals. Ross McGurk, Puting Xu, Zeljko Vujaskovic, Duke University, Durham, NC

Purpose: Currently, small-animal imaging is accomplished using dedicated small-animal CT, MRI and/or SPECT/PET systems. Such systems provide very high resolution images but are limited to imaging one animal at a time. This restricts their usefulness in studies that require high-throughput imaging of many animals, for example, in drug screening/efficacy studies. The purpose of this study was to evaluate whether a clinical CT scanner has the ability to image multiple small-animals simultaneously with the sensitivity required to detect changes in lung volume and average lung density.

Such parameters can provide useful metrics for radiation induced lung injury small animal models. **Material & Methods:** Three strains of mice, C57L/BL6, CBA and C57/L strains were exposed to a 12.5 Gy whole-thorax radiation dose. A novel high-throughput CT imaging platform was used to position and subsequently image 5 irradiated animals and 5 age-matched control (no radiation) animals from each strain at time-points of 10 weeks and 14 weeks. Image acquisition parameters of 0.625 mm axial resolution, with in-plane resolution of ~200 μm were acquired using the high-resolution mode on the GE Lightspeed multi-detector CT (Waukesha, WI). Tube voltage was 80 kVp and tube current was 300 mA. Total lung volumes were contoured and exported for density and volume analysis. Unpaired two-tailed student t-tests were used to determine the null hypothesis that lung volume and density values are the same between irradiated and control animals for each strain. **Results:** No significant ($p=0.05$) differences in density or volume were observed between the control and irradiated animals for any strain at the ten week time-point. Differences in lung density were significant ($p=0.003$) for the CBA strain at the fourteen week time-point. No significant differences in density or volume were seen for the other strains. **Conclusions:** Our CT imaging and analysis protocol offers advantages in the ability to increase the number of animals. Significant differences were observed at the 14 week time-point in the CBA strain. Volume and density changes in the other strains were not significant. This could be due to these differences manifesting later in time for these strains and later time-points may reveal significant differences in the BL6 and 57L strains.

(PS1.33) Precise mapping of entrance skin dose during neurointerventional procedure: what is the most effective method to avoid radiation-induced skin injury? Takashi Moritake¹, Mikito Hayakawa², Yuji Matsumaru², Yasuhiro Koguchi³, Yuka Miyamoto³, Yusuke Mizuno⁴, Koichi Chida⁵, Keiichi Akahane⁶, Koji Tsuboi¹, Takeji Sakae¹, Hideyuki Sakurai¹, ¹Proton Medical Research Center, University of Tsukuba, Tsukuba, Japan, ²Department of Endovascular Neurosurgery, Toranomon Hospital, Tokyo, Japan, ³Oarai Research Center, Chiyoda Technol Corporation, Oarai-machi, Japan, ⁴Department of Anesthesiology, Yokohama City University, Yokohama, Japan, ⁵Department of Radiological Technology, Tohoku University, Sendai, Japan, ⁶Radiological Protection Section, National Institute of Radiological Sciences, Chiba, Japan

Purpose Although several cases of radiation-induced skin injury (RSI) have been reported in association with neurointerventional procedures, the absorbed doses to these regions are not measured directly in most cases. We therefore first built a direct measurement system so that the ideal dosimetry for entrance skin dose (ESD) during neurointerventional procedures can be easily determined. This system was then applied to a patient to establish the efficacy of precise mapping of ESDs using a number of radiophotoluminescent glass dosimeters (RPLDs) to avoid RSI. Finally, we determined the most useful method to predict the maximum ESD (Max ESD) in real time. **Methods and Materials** Using RPLDs, the ESDs were measured in 47 patients. Angiographic parameters including procedure time, exposure time, dose-area product (DAP), total ESD were recorded. The patient was measured for ESDs wearing the fitted dosimetry cap throughout the procedures. We then compared the correlations between Max ESD and these angiographic parameters. **Results Case Illustration:** A 55-year-old man underwent two transvenous embolizations for dural arteriovenous fistula in the right cavernous sinus with an interval of 2 months. After the first procedure, temporal epilation occurred in the occipital region that was exposed to 4.2 Gy. In the second procedure, to prevent further RSI, we intermittently used the second best position. As a result, Max ESD was 1.0 Gy in the right posterior-temporal region, and the epilation site was exposed to ≤ 0.7 Gy. The patient thus did not develop any further epilation. **Max ESD and Parameters:** The correlations between a patient's Max ESD and the total procedure time, the total exposure time, the DAP, and the total ESD were $r = 0.5086$, $P = 2.62 \times 10^{-4}$; $r = 0.6205$, $P = 3.28 \times 10^{-6}$; $r = 0.5835$, $P = 1.67 \times 10^{-5}$; and $r = 0.7328$, $P = 4.74 \times 10^{-9}$, respectively. **Conclusions** We showed the information regarding ESD distribution could assist the physician to prevent further RSIs in subsequent procedures. We also showed the total ESD is the most useful parameter to predict the Max ESD. Taken

together, a combination of different viewing-angle and real-time monitoring of the total ESD could prevent from excessive radiation, thereby reducing the risk of skin injury.

(PS1.34) Survival and cancer induction of C3H mice protected from lethal whole body radiation by Amifostine. James B. Mitchell¹, Miriam Anver², Anastasia Sowers¹, Maria Figueroa¹, Angela Thetford¹, Kristin Fabre¹, Murali C. Krishna¹, John A. Cook¹, ¹National Cancer Institute, Bethesda, MD, ²SAIC Frederick/NCI-Frederick, Frederick, MD

Amifostine is a potent protector against radiation-induced lethality in mice. It was hypothesized that mice surviving lethal whole body radiation (WBR) with Amifostine would experience an elevated risk of cancer post-exposure and a shortened lifespan compared to unirradiated mice. Female C3H mice were injected with Amifostine (i.p., 400 mg/kg) 30 min prior to a lethal WBR dose of 10.8 Gy. Another set of mice was exposed to 5.4 Gy (without Amifostine) ($n = 150$, for both groups). The selection of 5.4 Gy was derived from LD50/30 data for Amifostine, which exhibits a dose-modifying factor (DMF) of approximately 2. Animals were followed for their entire lifespan. The endpoint for the study was tumor formation or until the animal reached a humane endpoint at which time the animal was euthanized (pathology evaluated on all animals). The median survival for mice receiving 0, 5.4 or 10.8 Gy were 706, 460, and 491 days, respectively. There was no difference between the 5.4 and 10.8 Gy groups ($p = 0.42$); however, the median survival of both irradiated groups was significantly shorter compared to unirradiated mice ($p < 0.0001$). Cancer incidence (hematopoietic plus solid tumors) was similar between the 5.4 and 10.8 Gy groups and was significantly greater than for unirradiated controls. However, the ratio of hematopoietic to solid tumors differed between the two groups, with the 5.4 Gy group having a higher incidence of hematopoietic neoplasms compared to the 10.8 Gy group (1.8 fold). A greater incidence of solid tumors was observed in the 10.8 Gy group. A comprehensive analysis of cancer incidence for all the groups will be presented. Overall, the qualitative similarities of lifespan reduction and total cancer incidence between the 5.4 Gy and 10.8 Gy groups were consistent with an Amifostine DMF of approximately 2. The results of this study demonstrate that mice protected from lethal WBR have a shortened lifespan, due in large part, to cancer induction post-radiation compared to unirradiated controls. Further, the results emphasize the need for more research and identification of countermeasures for radiation-induced carcinogenesis post-radiation exposure. Currently, there are no safe and effective interventions to reduce this risk to humans.

(PS1.35) Oral Ca- and Zn-DTPA: A novel tablet formulation with improved decorporation of americium-241. Gita N. Shankar¹, Waylon Weber², Melanie Doyle-Eisele², Naveen Bejugam¹, Shravan Mutyam¹, Raymond A. Guilmette², ¹SRI International, Menlo Park, CA, ²Lovelace Respiratory Research Institute, Albuquerque, NM

The goal of this project was to develop orally bioavailable formulation of Ca- and Zn-DTPA for treatment of radionuclide exposure. Currently administered intravenously or by nebulizer, Ca- and Zn-DTPA have poor oral bioavailability. Our initial studies, reported at this meeting in 2008, evaluated pharmacokinetic and efficacy studies of a new oral capsule formulation in rats. The current studies evaluate rat decorporation (efficacy studies) on a novel tablet formulation (SRI-DTPA) of Ca- and Zn-DTPA. Pilot batches of the SRI-DTPA were made by compression, under optimized conditions. The optimized tablet formulation included a liquid permeation enhancer known to improve oral bioavailability. The efficacy of SRI-DTPA was tested in groups of six young adult F344 rats (3 male and 3 female) injected intravenously with a soluble Am(241)-citrate complex. A single dose of SRI-DTPA (60 mg) was given by gavage at 1 hr, 1, 5, or 14 days after the Am-241 injection. Each rat was placed in a metabolism cage for complete and separate collection of urine and feces, and the treated animals were euthanized 7 days after DTPA administration (8, 12, or 21

days after the Am-241 injection). Saline-treated control groups were also euthanized at the same times post Am-241 injection. SRI-DTPA was shown to significantly increase the excretion of Am-241 for all treatment times. Statistically significant decreases in liver and bone content of Am-241 were also observed. For example, for SRI-DTPA treatment at 1 hr, the total body content of Am-241 was reduced to 39% of the injected dose, compared to 74% in the untreated controls. We concluded that this formulation is very effective in decorporating Am-241 in rats, even with a single-dose administration. This work is being supported by the NIAID contracts HHSN266200500043C, awarded to the University of Maryland School of Medicine, and HHSN26620050047C.

(PS1.36) Inhibition of the Integrin-TGFβ axis potentiates acute radiation-induced pneumonitis. Simon K. Cheng, Silvia Formenti, John Munger, New York University School of Medicine, New York, NY

Purpose Radiation therapy for thoracic neoplasms is limited by the risk of lung radiation injury. Acute pneumonitis is thought to result in a perpetual cascade of cytokines production post-irradiation which eventually leads to pulmonary fibrosis. TGFβ is a key cytokine in the response to radiation injury. We have previously shown that anti-integrin β6 (dominant TGFβ activator in the lung) therapy prevents and reverses radiation-induced late phase lung fibrosis. Interestingly TGFβ can have both pro-inflammatory function and immunosuppressive effects depending on the cellular context. It is not known which opposing activities of TGFβ predominate in radiation-induced acute pneumonitis. Methods Pneumonitis-susceptible C3HBe/FeJ mice were selectively treated to the whole thorax with a 15 Gy single fraction, and were injected weekly with either anti-integrin β6 mAb (6.3G9, Biogen; 3mg/kg/wk), soluble TGFβ type II receptor (sTGFR, 5 mg/kg), or control PBS starting 1 day prior to irradiation. At 9 weeks, we assessed the extent of pneumonitis by histopathological changes on lung sections, and alveolar inflammation was determined by differential cell count from BAL fluid. Survival curves were generated by Kaplan-Meier analysis. Results Kaplan-Meier survival curve analysis showed significant decreased survival in irradiated mice injected with anti-integrin β6 mAb (median survival 59.5d) or sTGFR (MS 77d) compared with irradiated controls (MS 94.5d, P<0.05). At 9 weeks post-irradiation, the lungs of the irradiated mice treated with anti-integrin β6 mAb showed substantially more alveolar wall edema and thickening, and increased infiltration of inflammatory cells compared with radiation only controls. Differential cell count from BAL revealed significant increased alveolar inflammation in irradiated mice injected with anti-integrin β6 mAb (lymphocyte 308 ± 73 SEM, neutrophil 606 ± 118) compared with irradiated controls (lymphocyte 9 ± 5, neutrophil 7 ± 2). Conclusions Our results show that TGFβ signaling has an unexpected and novel immunosuppressive function in radiation-induced acute pneumonitis. This suggests that TGFβ is not a key mediator of radiation-induced pneumonitis unlike in the late fibrosis phase, and that inhibiting TGFβ signaling during therapeutic thoracic radiation maybe detrimental.

(PS1.37) Technical and Operational Feasibility of Integrating WebEOC within the Hospital Incident Command Structure for Crisis Management of a Nuclear Detonation. Joseph Albanese^{1,2}, Bruce Pantani¹, Lynette Lines¹, Noelle Gallant¹, Eileen Blake¹, James Paturas¹, Domenico Delli Carpini³, Michael Bohan⁴, Edward Wilds⁵, Sara Rockwell², Nicholas Dainiak^{6,7}, ¹Yale New Haven Health Center for Emergency Preparedness and Disaster Response, New Haven, CT, ²Department of Therapeutic Radiology, Yale University School of Medicine, New Haven, CT, ³Department of Radiation Services, Greenwich Hospital, Yale New Haven Health, Greenwich, CT, ⁴Department of Radiation Physics, Yale-New Haven Hospital, Yale New Haven Health, New Haven, CT, ⁵Connecticut Department of Environmental Protection, Hartford, CT, ⁶Department of Medicine, Bridgeport Hospital, Yale New Haven Health, Bridgeport, CT, ⁷Yale University School of Medicine, New Haven, CT

Objective: A functional exercise involving the simulated detonation of a 1 kT nuclear device was developed and implemented to assess the Yale New Haven Health System (YNHHS) and its associated hospitals' (Delivery Networks, DNs) emergency management response capabilities. Of several objectives, one was designed to evaluate each hospital's Emergency Operation Center's (EOC) capability to integrate WebEOC, a web-based application that compiles real-time data inputs from multiple terminals and allows administrators to formulate operational decisions for mitigating crises, within the Hospital Incident Command Structure (HICS). Method: The week preceding the exercise, representative members of each EOC attended a 1 hour training session that provided a synopsis of the WebEOC application, and instructions on reading and posting to WebEOC event boards, creating position logs and completing situation reports. A qualitative evaluation of the extent to which WebEOC was utilized for the exchange of crisis information among YNHHS and its DNs was performed according to Homeland Security Exercise and Evaluation Program standards. Results: Observational data recorded by subject matter expert evaluators at each exercise location during the exercise, feedback from participants collected immediately following the exercise (hot-washes), as well as that provided in the exercise debrief surveys revealed that participants were facile with WebEOC functionality at all HICS positions, and utilized WebEOC efficiently to obtain real-time situational awareness of available resources within each hospital and the System, and reallocate these resources appropriately according to the unfolding scenario. Further, the use of WebEOC was preferred over other means for communicating critical information among exercise locations. Recommendations included: 1) integration of a HICS position dedicated to data input into WebEOC; and 2) delivery of WebEOC training to all HICS positions. Conclusions: WebEOC offers flexible coordination of emergency management data within the EOC environment. Its integration within HICS may potentially confer added capability for reallocation of resources and efficient communication, and decreased administrative burden during mass casualty incident management within a hospital system.

(PS1.38) Minozac mitigates rat brain radiation injury following whole brain irradiation. Kenneth A. Jenrow, Stephen L. Brown, Karen Lapanowski, Andrew Kolozsvary, Jae Ho Kim, Henry Ford Hospital, Detroit, MI

Whole brain irradiation (WBI) doses of 10 Gy or less are sufficient to impair neurogenesis within the rat dentate gyrus, along with hippocampal plasticity and cognitive function. Impaired neurogenesis reflects both the acute loss of neural progenitors via apoptosis and a more gradual disruption of neurogenic signaling via inflammation. Anti-inflammatory drugs can partially prevent these deleterious effects when administered prior to irradiation. Here we have investigated whether minozac, a selective inhibitor of pro-inflammatory microglial cytokines, can mitigate these deleterious effects when administered post-irradiation. Male Fischer 344 rats received WBI doses of 0 (control) and 10 Gy using a Cs-137 irradiator. Minozac (5 mg/kg/day, IP) therapy was initiated 24 hours post-WBI and continued in separate withdrawal cohorts for 1 or 4 weeks post-WBI. Rats were sacrificed at 8 weeks post-WBI. Three weeks prior to sacrifice, rats received once daily BrdU injections (50 mg/kg/day, i.p.) for 5 days to label mitotically active cells. Rats were sacrificed by transcardial perfusion/fixation. Tissues were subsequently processed for paraffin embedding, thin sectioned at 5 μm, and immunohistochemically stained for BrdU, Ki67, double cortin (DCX), NeuN, CD-68, and Ox-6. Volume densities of cells expressing these markers were quantified within the dentate gyrus in multiple sections along the anterior-posterior axis. Minozac, administered for either 1 or 4 weeks post-WBI, significantly reduced the expression of Ox-6⁺ microglia and significantly preserved/restored granule cell DCX⁺ neurons within the dentate gyrus at 8 weeks post-WBI. The mitigating effects of minozac in this context are consistent with reduced inflammation and a preservation/restoration of neurogenic signaling integrity within the dentate gyrus. Remarkably, these mitigating effects persisted for several weeks after therapy withdrawal, suggesting that inhibiting the actions of pro-inflammatory microglial cytokines for as little as 1 week post-WBI is sufficient to produce a lasting, and perhaps

permanent, benefit. Funded by NIAID Cooperative Agreement U19 AI067734.

(PS1.39) Ionizing radiation and genetic risks - prediction of genetic risks using the human genome as the starting point. Hooshang Nikjoo, K Sankaranarayanan, Karolinska Institute, Radiation Biophysics Group, Stockholm, Sweden

Efforts to estimate genetic risks of exposure of human populations to ionizing radiation began in the 1950s and still continue. The risk estimates considered 'recent' are the ones published by the BEIR Committee of the US National Academy of Sciences in 2006. Owing to the continued absence of directly usable human data on radiation-induced adverse effects, estimates of risk are obtained indirectly using mouse data on radiation-induced mutations but are expressed as predicted increases in the frequencies of genetic diseases relative to the baseline frequencies in the population. Two core concepts incorporated in this report set the stage for research in the field in the 21st century: (1) most radiation-induced mutations are DNA deletions, often encompassing multiple genes; however, because of structural and functional constraints only a proportion of induced deletions may be compatible with offspring viability and (2) viability-compatible deletions induced in human germ cells are more likely to manifest themselves as multi-system developmental abnormalities rather than as single gene disorders as has been assumed until now. This presentation will examine how a synthesis of mechanistic insights gained from studies of DNA DSB repair and from those of the origin of human genomic disorders can be forged to pursue these concepts further to make a paradigm change and 'interrogate' the human genome directly for adverse genetic effects of radiation.

(PS1.40) Novel agents for mitigation of radiation-induced pulmonary injury. Leo E. Gerweck, Pierre Leblanc, Peter Biggs, Mark C. Poznansky, Kathryn D. Held, Massachusetts General Hospital, Boston, MA

The efficacy of two novel therapeutic agents is being evaluated for mitigation of radiation-induced pulmonary injury. NOV-002 has shown efficacy as a mitigator of radiation-induced hematopoietic damage in rodents and decreases chemotherapy-induced toxicity in humans. NOV-205 is an anti-inflammatory and anti-fibrosis agent with efficacy in hepatotoxicity studies in rodents and is in clinical trials in hepatitis patients. Both agents are proprietary formulations of oxidized glutathione. In ongoing experiments, C57BL/6 mice, which exhibit both pneumonitis and fibrosis upon irradiation, were irradiated in specially designed micro-isolator cassettes and housed in a barrier facility until end of life. Adult anesthetized mice were treated with single doses of 0 and 10 to 19 Gy 60Co radiation in 3 Gy increments, with 20-22 mice per dose of radiation alone, or plus drug, per treatment group. The proper positioning and alignment of the mice, definition of the thorax and alignment of field defining 10 cm thick lead blocks, were established and confirmed by radiographic thoracic simulation. Extensive dosimetry under build-up conditions was achieved with miniature ionization chambers, film and TLD. The superior inferior (apex base) dimensions of the field were 17 mm at full width half-max and the 90:50 penumbra was 1.3 mm. Animals were irradiated at a nominal dose rate of 2 Gy/min at 70 cm SAD. Within 4 hours following irradiation, and then thrice weekly until death, 10 or 11 randomly selected mice at each radiation dose level for each drug, and for radiation or drug alone, were subcutaneously injected with drug in saline or saline alone. Endpoints being evaluated to assess drug efficacy at intervals following irradiation include: weight, breathing rate, arterial oxygen saturation, heart rate, overall lifespan and LD50. Subsequent studies will evaluate changes in lung weight, quantification of pleural effusions, histopathology, including histopathologic evaluation for lung fibrosis, and alternate post radiation drug administration schedules. This work was supported by NIAID grant # 1RC1 AI081282.

(PS1.41) Understanding the Mechanism of Mitigation of Radiation Nephropathy by ACE Inhibitors. Brian L. Fish, John E. Moulder, Marylou M. Mader, Ashley M. Schock, Meetha M. Medhora, Medical College of Wisconsin, Milwaukee, WI

We have shown that the ACE inhibitor captopril is effective in the mitigation of radiation-induced renal injury in humans and rodents. However, the mechanism of action remains unknown. Captopril is the only ACE inhibitor containing a reducing sulphhydryl (-SH) group, which may be effective against oxidative stress induced by radiation. We are therefore testing 3 other ACE inhibitors (ramipril, fosinopril and enalapril) with different side groups, head-to-head against captopril for the mitigation of radiation nephropathy. If the four ACE inhibitors are equally effective, it would imply that their mitigation efficacy is directly tied to ACE inhibition. Using a rat model of total body irradiation (TBI) we are monitoring renal injury for up to 200 days. Drugs are provided in the drinking water starting immediately or 1 week after TBI and continued for 8 weeks or until the end of the experiment. Rats are followed serially using a surrogate marker of nephropathy, uremia as measured by blood urea nitrogen (BUN). Preliminary data show that irradiated rats receiving captopril or enalapril, but not fosinopril, started immediately or one week after irradiation, have a significantly lower BUN than those receiving irradiation with no intervention. Rats receiving captopril or enalapril for only 8 weeks also have significantly lower BUN. Ramipril is still being tested. We will monitor drug dose equivalency by serum AcSDKP levels, a hematopoietic cytokine that is degraded by ACE and is used clinically to monitor compliance in patients on ACE inhibitors. Our results suggest that ACE inhibition, rather than reduction by the -SH group of captopril, is responsible for mitigation of experimental radiation nephropathy. Also, the longer lasting ACE inhibitor enalapril may be preferred over captopril, which has an in vivo half-life of only 2 hours. Understanding the mechanism of mitigation is important since it will support FDA approval of the use of these mitigators for radiation nephropathy. This work was supported by NIAID, 1RC1A181294 and cooperative agreement AI067734.

(PS1.42) Abscopal bone marrow suppression is the direct cause of acute death in mice following abdominal irradiation. Peter Corry, Sue Theus, Katie Steed, Leah Hennings, Dan Jia, University of Arkansas for Medical Sciences, Little Rock, AR

Acute death in humans 5-10 days after a large dose ionizing radiation is also known as "gastrointestinal (GI) death" since the histological destruction of the GI tract is the predominant radiation tissue injury within this period. Whether GI injury is the direct cause of acute radiation death, however, has not been settled. To address this issue, we developed a mouse abdominal irradiation (AI) model. Ten-wk-old male C57BL/6 mice were irradiated with a single fraction of 20 Gy x-rays to the abdomen only. The mice were given a single injection of saline or syngeneic bone marrow cells (10^7 - 10^8 cells) via tail vein 24h after AI. In some experiments, the mice were monitored daily for body weight change and survival. In separate experiments, mice were sacrificed at post-AI day 7 for peripheral blood cell count, *ex vivo* bone marrow clonogenicity assay, and histological assessment of jejunum, spleen, and bone marrow cellularity. AI alone caused a 90% decrease in peripheral white blood cell count, white pulp area of the spleen, and bone marrow stromal cells in mice 7 days after AI, a collective evidence of bone marrow suppression. Bone marrow transplantation (BMT) led to the recovery of these parameters to 70% of the levels in sham-irradiated mice at post-AI day 7, indicating a restoration of the hematopoietic capacity. Moreover, BMT dose-dependently increased the 10-day survival rates of the irradiated mice to 40-80%, as compared with 0% in saline-treated group. The increased animal survival was accompanied by dose-dependent recovery of mouse body weight. Interestingly, at post-AI day 7 the extent of jejunum edema as well as the loss of jejunum villi, crypts, and epithelial cells enveloping the villi in mice receiving BMT were all comparable to that in saline-treated abdominally irradiated mice. Our results demonstrate that GI injury alone is not sufficient to cause GI death and that BMT mitigation of acute death after AI is independent of the restoration of jejunum structure. Abscopal suppression of bone

marrow, presumably mediated by signals from radiation GI injury, is the direct cause of acute death after AI.

(PS1.43) Does ethyl pyruvate act as a radioprotectant in macrophage cell lines? Michael J. Pecaut, Erben Bayeta, Cory Pan, Celso P. Perez, Daila S. Gridley, Loma Linda University, Loma Linda, CA

Exposure to radiation is known to cause inflammation, a process that sometimes leads to complications in patients undergoing radiotherapy. Ethyl Pyruvate (EP) has proven to be an effective countermeasure against damage incurred during sepsis, ischemia/reperfusion injury, and hemorrhagic shock. Because of its anti-inflammatory properties, this low molecular weight compound is being considered as a potential radioprotectant. Indeed, preliminary work by others indicates that EP can impact measures of apoptosis *in vitro* and increases survival in mice after whole-body irradiation (Epperly, *et al*, *Radiation Research* **168**:552-559, 2007). With this in mind, we characterized the efficacy of EP in mitigating the effects of radiation on several measures of oxidative stress in macrophage cell lines (including RAW264.7 & J774.A1). Cells were treated with 0-10 μ M EP for 60 minutes and subsequently exposed to 0-4 Gy γ -irradiation (^{60}Co) in a single fraction at a dose rate of 0.8 Gy/min. After a 24 hour incubation period, we assessed cell survival, background reactive oxygen species (ROS) levels, oxidative burst capacity, total protein and glutathione (GSH) levels. Each experiment was repeated five times to ensure repeatability. Data from all five experiments were normalized to controls and combined for the final analysis. Although we found very reliable main effects of both radiation and EP ($P < 0.001$ for most endpoints), there were no significant radiation x EP interactions on any characterized parameter. This would seem to indicate the protective nature of EP does not directly involve changes in reactive oxygen metabolism within macrophages.

(PS1.44) The role of NF- κ B-activation in radioprotection by flagellin in mice. Lyudmila Burdelya¹, Tomas Tallant², Semra Aygun-Sunar¹, Bojidar Kojouharov¹, Gary Haderski³, Joseph DiDonato², Andrei Gudkov¹, ¹Roswell Park Cancer Institute, Buffalo, NY, ²Cleveland Clinic Foundation, Cleveland, OH, ³Cleveland Biolabs, Inc, Buffalo, NY

The Toll-like receptor 5 (TLR5) agonist *Salmonella* flagellin is a powerful radioprotectant against both the hematopoietic and gastro-intestinal components of acute radiation syndrome (ARS) in mice. We hypothesized that flagellin-mediated radioprotection involves activation of the anti-apoptotic pro-survival NF- κ B pathway. To investigate the relevance of NF- κ B activation in the radioprotection mediated by flagellin, we constructed a series of rationally designed flagellin derivatives that contained different portions of the N- and C-terminal sequences known to be essential for TLR5 activation, which were connected by artificial linkers. Ten flagellin variants from this series were tested for their ability to activate NF- κ B in vitro using the cell-based reporter system and in vivo using reporter mice carrying luciferase cDNA under the control of a NF- κ B-responsive promoter. Flagellin derivatives with only a few amino acid differences in their structures but significant differences in their NF- κ B activating capacities were tested for radioprotection in mice subjected to lethal doses of total body irradiation (TBI), inducing either HP (10 Gy) or combined HP and GI (13 Gy) ARS. A strong correlation was observed between dose dependence of NF- κ B activation in vitro by these flagellin derivatives and their in vivo radioprotection from both HP- and GI-inducing radiation doses. To determine whether this correlation reflected a functional role for NF- κ B in the radioprotection mediated by these TLR5 agonists, we tested whether pharmacological inhibition of NF- κ B prevented radioprotection by these flagellin derivatives. We found that treatment with the NF- κ B inhibitor ketamine led to both lack of reporter activation and radioprotection by otherwise effective flagellin derivatives. Thus, NF- κ B mediates TLR5-dependent radioprotection.

(PS1.45) The effects of γ -tocotrienol and pentoxifylline on total body irradiation-induced injury and lethality. Maaiké Berbée¹, Qiang Fu¹, K. Sree Kumar², Martin Hauer-Jensen^{1,3}, ¹University of Arkansas for Medical Sciences, Little Rock, AR, ²Armed Forces Radiobiology Research Institute, Uniformed Services University, Bethesda, MD, ³Central Arkansas Veterans Healthcare System, Little Rock, AR

Background: The vitamin E analog γ -Tocotrienol (GT3) has potent radioprophylactic properties. This study was performed to a) determine whether treatment with GT3 together with pentoxifylline (PTX) has more powerful radioprotective effects than treatment with GT3 only, and b) to obtain information about the mechanism of action. Methods: Male CD2F1 mice were exposed to 8.5-13 Gy uniform total body irradiation (TBI) in a cesium irradiator. Mice were randomly assigned to one of the 4 following treatment groups: vehicle control; PTX; GT3; and GT3 with PTX. Mice received a single dose of GT3 (400 mg/kg) and/or PTX (200mg/kg) 24 hours and 30 minutes before radiation exposure respectively. Overall lethality as well as markers of radiation-induced intestinal and hematopoietic injury were assessed. To study the effect of the different treatments on the bone marrow microenvironment, cytokine levels were determined the bone marrow plasma, i.e. the medium used to collect the bone marrow cells from the femurs. Results: GT3 combined with PTX significantly improved survival compared to GT3 only. Both GT3 and GT3 with PTX reduced radiation-induced intestinal injury. GT3 with PTX improved post-irradiation bone marrow CFUs, spleen colonies counts as well as platelet recovery compared to GT3 only. Both GT3 and GT3 with PTX caused an increase in bone marrow plasma G-CSF levels. GT3 with PTX also increased the availability of Il-1 α and Il-6 in the early post-irradiation phase. Conclusion: Combined treatment with GT3 and PTX is a promising strategy to reduce radiation injury and subsequent lethality. The mechanism of action likely involves protection against intestinal radiation injury and modulation of the hematopoietic radiation response by the induction of hematopoietic stimuli.

(PS1.46) Treatment with MnTE-2-PyP⁵⁺ mitigates total body irradiation-induced long-term bone marrow suppression. Hongliang Li^{1,2,3}, Yong Wang², Senthil K Pazhanisamy^{1,2}, Lijian Shao^{1,2}, Aimin Meng³, Ines Batinic-Haberle⁴, Daohong Zhou^{1,2}, ¹Division of Radiation Health, Department of Pharmaceutical Sciences and Winthrop P. Rockefeller Cancer Institute, University of Arkansas for Medical Sciences, Little Rock, AR, ²Department of Pathology, Medical University of South Carolina, Charleston, SC, ³Department of Biochemistry and Molecular Biology, Institute of Radiation Medicine, Chinese Academy of Medical Science and Peking Union Medical Collage, Tianjin Key Laboratory of Molecular Nuclear Medicine, Tianjin, China, ⁴Department of Radiation Oncology, Duke University, Durham, NC

Our recent study showed that total body irradiation (TBI) induces long-term bone marrow (BM) suppression by induction of hematopoietic stem cell (HSC) senescence through the ROS-p38MAPK-p16^{Ink4a} pathway. The superoxide dismutase mimetic MnTE-2-PyP⁵⁺ is a potent antioxidant and we examined if it can be used to ameliorate TBI-induced long-term BM injury by inhibiting IR-induced oxidative stress and HSC senescence in a mouse model. Specifically, male C57BL/6-Ly-5.2 mice were exposed to a sublethal dose (6.5 Gy) of TBI. Six hours after TBI, they were treated with vehicle (PBS) or MnTE-2-PyP⁵⁺ (6 mg/kg) by s.c. injection and then the injection was repeated every day for 30 days. Immediately after the last injection, BM cells were harvested from normal control mice and irradiated mice receiving vehicle or MnTE-2-PyP⁵⁺ treatment after euthanization. The cells were analyzed for ROS production by flow cytometry after DCF staining, oxidative DNA damage by 8-OHdG and γ -H2AX immunofluorescent microscopy, clonogenic function by colony-forming cell (CFC) and cobblestone area-forming cell (CAFC) assays, frequencies of HSCs and hematopoietic progenitor cells (HPCs) by flow cytometry after immunostaining with antibodies against lineage markers, c-kit and Sca1, and expression of p16^{Ink4a} by real-time RT-PCR. The results showed that MnTE-2-PyP⁵⁺ treatment significantly inhibited TBI-induced increases in ROS production and oxidative DNA damage in HSCs and HPCs. The reduction of oxidative stress was

associated with a significant increase in HSC frequency and clonogenic function. In fact, the clonogenic function of HSCs from irradiated mice after MnTE-2-PyP⁵⁺ treatment was comparable to that of HSCs from normal controls on a per HSC basis, suggesting that MnTE-2-PyP⁵⁺ treatment abrogated IR-induced HSC senescence. This suggestion is supported by the finding that MnTE-2-PyP⁵⁺ treatment also reduced IR-induced expression of p16^{Ink4a} mRNA in HSCs. Therefore, our results from this study demonstrated that MnTE-2-PyP⁵⁺ has the potential to be used as therapeutic agent to mitigate TBI-induced long-term BM suppression by inhibition of IR-induced HSC senescence through the ROS-p38MAPK-p16^{Ink4a} pathway. * These authors contributed equally to this work. **To whom correspondence should be addressed. E-mail: dzhou@uams.edu.

(PS1.47) Substance P enhances cell proliferation and the anti-apoptotic responses of γ -irradiated stem cells in bone marrow. You Sun An¹, Mi-Hyun Kang¹, Hyun Sook Hong², EunAh Lee², Mi-Ra Kim¹, Youngsook Son², Jae Youn Yi¹, ¹Korea Institute of Radiation and Medical Sciences, Seoul, Republic of Korea, ²Kyung Hee University, Seoul, Republic of Korea

The therapeutic use of ionizing radiation (*e.g.*, X-rays and γ -rays) needs to inflict minimal damage on non-target tissue. Recent studies have shown that substance P (SP) mediates multiple activities in various cell types, including cell proliferation, anti-apoptotic responses, and inflammatory processes. The present study investigated the effects of SP on γ -irradiated bone marrow stem cells (BMSCs). In mouse bone marrow extracts, SP prolonged activation of Erk1/2 and enhanced Bcl-2 expression, but attenuated the activation of apoptotic molecules (*e.g.*, p38 and cleaved caspase-3) and down-regulated Bax. To determine how SP affects bone marrow stem cell populations, mouse bone marrow cells were isolated and colony forming unit (CFU) of mesenchymal stem cells (MSCs) and hematopoietic stem cells (HSCs) was estimated. SP-pretreated ones showed higher CFUs of MSC and HSC than untreated ones. Furthermore, when SP was pretreated in cultured human MSC (Human MSCs), it significantly decreased apoptotic cells 48 and 72 hours after γ -irradiation. Compared with untreated cells, SP-treated human MSCs showed reduced cleavage of apoptotic molecules such as caspase-8, caspase-9, caspase-3, and poly ADP-ribose polymerase (PARP). Thus, our results suggest that SP alleviates γ -radiation-induced damage to mouse BMSCs and human MSCs via regulation of the apoptotic pathway.

(PS1.48) Early life exposure to radiation sensitizes mice to later life pulmonary inflammatory challenges. Jacob N. Finkelstein, Jacqueline P. Williams, Eric Hernady, Carl J. Johnston, University of Rochester Medical Center, Rochester, NY

Rationale: Processes occurring during postnatal development appear to be critical in the ability of the lung to cope with external stress. In the course of our ongoing investigation into radiation effects on the lung and development of models to evaluate potential mitigators, we identified significant differences between the response of the immature, neonatal lung to radiation, compared to the adult, and a significant interaction between prior irradiation and subsequent respiratory infection. Studies of this interaction are critical in developing successful mitigation strategies for this special population. Our hypothesis is that exposure to radiation is likely to alter the developmental processes resulting in long-term consequences including altered susceptibility to respiratory infection. Methods: C57Bl/6 mice ages: 4 days of age received total body irradiations of 2.5 or 5.0 Gy. Mice were examined 3 month or 6 months post irradiation (PI). At these time points mice were then re-challenged with a priming dose of LPS by inhalation and examined 24 hours later or received a challenge dose of LPS and examined at 3 days post inhalation. Tissue injury was determined by histological examination and analysis of epithelial and inflammatory markers. Proinflammatory, chemokine, antioxidant and early response genes were analyzed for changes in message abundance by RNase Protection Assay and immunohistochemical analysis. Results: Sensitization of response to a secondary challenge: Irradiated

neonatal mice exposed to a priming dose of inhaled LPS (~10 ng deposition) as adults and examined 24 hours post-inhalation exhibited an augmented response to inflammatory challenge. Resolution of the inflammatory response. Irradiated mice exposed to a challenge dose of LPS (~20 ng deposition) as adults and examined 3 days post-inhalation showed a delayed ability to resolve the inflammatory response associated with this challenge. Conclusions: These results demonstrate that early life radiation injury subjected tissues to a greater injury resulting in long term alterations in structure and function and sensitized the lung to inflammatory challenge. Supported by By: U19 AI-067733-05S1, P30 ES-01247 and EPA Star PM Center R-827354.

(PS1.49) Pathophysiological changes in normal rat brain following single high dose radiation. Stephen L. Brown, Kenneth A. Jenrow, Andrew Kolozsvary, Jae Ho Kim, Henry Ford Health System, Detroit, MI

The brain is the most critical tissue necessary for survival and its normal function is adversely affected by radiation exposure. A need exists for a well-characterized, reproducible animal model to study the three interlinked compartments identified to explain the pathogenesis of brain radiation injury: 1) parenchymal cell loss that involves demyelination of white matter, encephalomalacia, gliosis, and neural cell loss, 2) vascular endothelial damage that may cause altered permeability due to breakdown of the blood-brain barrier, and teleangiectasia, hyalinosis and fibrinoid deposits in the vessel walls in the late phase, and 3) depletion of neural progenitor cells in the subgranular zone of the dentate gyrus. We measured an array of structural and functional endpoints at various times in adolescent Fischer rats after 20 Gy whole brain irradiation (WBI). Structural brain endpoints included gross changes assessed by MRI and immunohistochemistry (IHC), markers of myelin basic protein (MBP), immature neurons (DCX), mature neurons (NeuN), mature astrocytes (GFAP) and microglial (CD68). Functional endpoints included blood flow and vascular permeability assessed by MRI and electrophysiological measures of visual evoked potential (VEP reflecting leukoencephalomalacia) and IHC markers of proliferation (BrdU, Ki67). Rats that received WBI appeared normal, gained weight and required no special care (other than bi-weekly teeth clipping), even up to 12 months after radiation except for some fur thinning and excessive upper teeth growth (probably due to radiation-induced reduced growth of lower teeth). No changes in MBP or GFAP were observed even 1 year post-WBI. Although a statistically significant VEP change was measured after WBI, the magnitude of the change was minimal. No change in MRI assessed blood flow or vascular permeability was measured, however steady increases in ventricular volume and contrast enhancement were observed starting at 3 months post-WBI. IHC gave evidence of cell loss; BrdU, Ki67, DCX, NeuN and CD68 positive stained cells decreased with time after WBI. Further studies continue with refinements to MRI measures of contrast agent distribution volumes using Logan plots and electrophysiological measures of long-term potentiation (LTP) reflecting learning, memory and plasticity.

(PS1.50) Angiotensin converting enzyme (ACE) inhibitors in combination with EUK-207 for mitigation of radiation pneumonitis. Feng Gao^{1,2}, Swarajit N. Ghosh^{1,2}, Lakhon Kma^{1,2,3}, Qingping Wu^{1,2}, Robert Molthen², Brian L. Fish¹, John E. Moulder¹, Susan R. Doctrow⁴, Meetha Medhora¹, ¹Department of Radiation Oncology, Medical College of Wisconsin, Milwaukee, WI, ²Pulmonary and Critical Care Division, Department of Medicine, Medical College of Wisconsin, Milwaukee, WI, ³Department of Biochemistry, North-Eastern Hill University, Shillong, India, ⁴Pulmonary Center, Department of Medicine, Boston University School of Medicine, Boston, MA

Aim: Because doses of ACE inhibitors required to mitigate radiation pneumonitis are high and may be poorly tolerated by some individuals, we tested the potential of combining low dose ACE inhibitors with antioxidant reagents as mitigators of radiation pneumonitis after total body X-irradiation (TBI). The approach of combinational therapy can also help to understand the mechanism

of mitigation. Methods: Rats (WAG/RijCmcr) were exposed to a single dose of 11 Gy TBI followed by a syngeneic bone marrow transplant. Two ACE inhibitors, captopril and enalapril were provided in drinking water starting 7-10 days after irradiation; they were given alone or in combination with the super-oxide dismutase (SOD) catalase mimetic EUK-207. Drug therapy continued for 8 weeks. Rats will be followed up to 120 days. Results: Studies with captopril (100 mg/m²/day) or enalapril (10 mg/m²/day) each combined with EUK-207 (1.8 mg/m²/day) are ongoing. While captopril + EUK-207 shows promise as a mitigating combination when compared to either drug alone, enalapril + EUK-207 does not appear to decrease morbidity, lung structural injury or pulmonary dysfunction. Unlike enalapril, captopril has a reducing -SH moiety which may compliment EUK-207 to diminish oxidative injuries. Conclusions: Captopril but not enalapril, given at low dose in combination with EUK-207, may be effective in mitigating radiation pneumonitis in rats, suggesting a complementary mechanism of -SH and SOD to mitigate oxidative stress. This treatment combination may provide an efficacious alternative to persons experiencing side effects such as severe hypotension with high dose ACE inhibitors alone. This work was funded by RC1 AI 81294 and NIH/NIAID agreements U19-AI-67734. Dosimetry was done by the CMCR Irradiation Core at MCW; histology was done in the Children's Research Institute at MCW under direction of Dr. Paula North.

(PS1.51) Transplantation of bone marrow-derived adherent stem cells provide support to the intestinal stem cell niche and mitigate radiation induced gastrointestinal syndrome (RIGS) in mice. Subhrajit Saha¹, Payel Bhanja¹, Rafi Kabarriti², Laibin Liu¹, Alan Alfieri¹, Emily Chen³, Chandan Guha², ¹Albert Einstein College of Medicine, Bronx, NY, ²Albert Einstein College of Medicine and Montefiore Medical Centre, Bronx, NY, ³Stony Brook University Medical Center, Stony Brook, NY

RIGS is the result of direct cytotoxic effects on intestinal crypt cells with subsequent loss of the mucosal barrier. This manifests as electrolyte imbalance, systemic infection (sepsis) and death. The stromal cells surrounding the intestinal stem cell (ISC) provide the niche and supply critical growth factors for stem cell regeneration. We hypothesized that supplement of bone marrow-derived adherent stem cells (BMASCs) as source of ISC niche component including mesenchymal stem cells (MSCs), endothelial progenitor cells (EPCs) and macrophages may restore ISC and its niche to mitigate RIGS. C57Bl/6 mice BM was cultured for 4 dys, followed by collection of adherent cells (BMASCs). Mice receiving BMASCs (2x10⁶ cells i.v. at 24 and 72hrs post irradiation) containing 48±2% MSC (CD105⁺CD45⁺), 7.1±0.5% EPC (CD133⁺ Flk⁺) and 17.3±1.8% myeloid/macrophages (CD11b⁺F480⁺) survived (100%) lethal doses of whole body irradiation (WBI) (10.4Gy) and abdominal irradiation (AIR) (18Gy), p<0.002 and p<0.004 respectively. Transplantation of either CD11b⁺ myeloid cells or CD11b⁻ and CD105⁺ MSCs could mitigate 30-40%, indicating cooperative role of MSCs and macrophages for RIGS survival. Histopathology of jejunum demonstrated significant increases in proliferation (p<0.004), crypt depth (p<0.001) & decrease in apoptotic crypt cells (p<0.003) with BMASC transplant after irradiation (IR). Immunohistological analysis showed restoration of intestinal subepithelial myofibroblast (αSMA +ve & desmin -ve) (major ISC niche component) with BMASC transplant. Xylose absorption was greater in these mice indicating functional integrity following BMASC transplantation. To study the possible radio-mitigating factor secreted from BMASC, concentrated culture supernatant was administered to irradiated mice at 24hr and 72 hr after either, WBI (10.4 Gy) or AIR (16Gy). 50% of mice survived for up to 30 days indicating the presence of mitigating factors in culture supernatants. Proteomic analysis was performed to identify potential mitigating agents present in the culture supernatant. So far, this is the first demonstration that supplementation of stromal component / factors could mitigate supra-lethal doses of IR. Studies are ongoing to identify the cellular and molecular mechanisms responsible for radiation mitigation.

(PS1.52) The Gottingen Minipig as a Model for Acute Radiation Syndrome (ARS). Maria Moroni¹, Thea Coolbaugh¹,

Eric Lombardini², Jennifer Mitchell², Krinon Moccia², Larry Shelton², Vitaly Nagy³, Mark Whitnall¹, ¹Radiation Countermeasure Program, Scientific Research Department, AFRR, Bethesda, MD, ²Veterinary Science Department, AFRR, Bethesda, MD, ³Radiation Sources Department, AFRR, Bethesda, MD

The best studied animal models for ARS are mice, canines, and non-human primates (NHP). An alternative large animal model would be advantageous for countermeasure development, to provide flexibility in matching compounds to a suitable species in terms of pharmacological parameters. Swine are increasingly used in drug development because of the similarity of their anatomy and physiology to those of humans. We demonstrate here the Gottingen minipig is a viable model in terms of practicality of whole-body gamma-irradiation, reliability of serial blood sampling from unanesthetized animals, and responses to ionizing radiation similar to what is observed in canines, NHP, and humans. Methods: Vascular access ports were implanted subcutaneously in 20 minipigs. Animals were bilaterally irradiated with Cobalt-60 (0.6 Gy/min) at 1.6, 1.7, 1.8, 1.9, or 2 Gy. Clinical signs, complete blood counts, clinical chemistry, acute-phase proteins, circulating hematopoietic progenitor cells, histopathology, microbiology, and survival were assessed. Results: Our preliminary estimate of the LD50/30 is 1.7-1.9 Gy. ARS was characterized by a 2-48 h prodromal phase, with mild fever, mild disorientation (from behavioral observation), and transient erythema. Severe lymphopenia and granulocytosis were evident within the first few h. A latent phase followed the prodromal phase, lasting approximately 12-14 days. Manifest illness had a rapid course; skin changes and signs of internal bleeding became evident. Hematological changes consisted of rapid loss of lymphocytes, initial granulocytosis followed by a progressive decline in neutrophils, and a 7-day shoulder in platelets followed by progressive thrombocytopenia. Time to start of recovery for lymphocytes, platelets, and neutrophils was around days 14, 20, and 23, respectively. Changes in blood elements were in agreement with bone marrow aplasia and loss of circulating progenitor cells. CRP was induced by irradiation. Histopathological data suggest death was caused by critical multi-organ dysfunction. Extensive hemorrhages were present in the majority of tissues. Impairment of physiological function in animals prior to death was confirmed by biochemical analysis of organ-specific enzymes.

(PS1.53) Radioprotection by the Histone Deacetylase Inhibitor Phenylbutyrate. Alexandra Miller, AFRR, Bethesda, MD

The histone deacetylase inhibitor (HDAC), phenylbutyrate (PB), is a novel anti-tumor agent. Studies have demonstrated that HDAC inhibitors can suppress cutaneous radiation syndrome and stimulate hematopoiesis in clinical studies. The objective of this study was to test the ability of PB treatment to protect against acute radiation-induced lethality *in vivo*. Western blot studies showed that PB acetylated histones in DBA/2 mouse bone marrow. PB (100 mg/kg) was administered to DBA/2 mice i.p. at -24 or +24 hrs relative to ⁶⁰Co gamma radiation. Survival was monitored for 30 days post-radiation. Prophylactic administration of PB (10-500 mg/kg) provided radioprotection against (8-9.5 Gy) and PB demonstrated a DRF of 1.31 [p = 0.001; 95% confidence interval: 1.27, 1.36]. When PB was administered post-radiation (0 and 12 hr) it provided significant radioprotection at 8.0 Gy radiation (P = 0.01 and 0.022 respectively), but not at 8.5 Gy in comparison to saline-treated controls. PB treatment was associated with significant elevations in neutrophils and platelets following radiation. These results indicate that an HDAC inhibitor like PB has potential as both a radiation protector and a radiation injury mitigator. PB is being assessed for its ability to protect against gastrointestinal acute radiation syndrome.

(PS1.54) The effect of amifostine and ionizing radiation on apoptosis and chromosomal inversion responses. Rebecca J. Ormsby¹, Mark D. Lawrence¹, Benjamin J. Blyth¹, Eva Bezak², David J. Grdina³, Pamela J. Sykes^{1,4}, ¹Flinders University & Medical Centre, Adelaide, Australia, ²Royal Adelaide Hospital,

Adelaide, Australia, ³University of Chicago, Chicago, IL, ⁴SA Pathology, Adelaide, Australia

Low dose radiation (LDR) and the chemical radioprotector amifostine can both mitigate some of the harmful effects of radiation exposure. They display a number of distinct similarities including their ability to protect cells against radiation-induced DNA damage and cell death, and metastases formation. We previously demonstrated that LDR protects from radiation-induced chromosomal inversions when delivered after high dose radiation. The ability to retrospectively protect from a prior radiation exposure is common to only a few agents, including amifostine. Subsequent studies examining chromosomal inversion responses have revealed further similarities between amifostine and LDR suggesting that there are common mechanisms associated with low dose radioprotective responses and amifostine-mediated cytoprotection. We hypothesised that chromosomal inversion changes induced by amifostine are mediated via changes in apoptosis frequency. To test this, amifostine was administered to mice alone or in conjunction with X-rays. Mice were euthanized at various timepoints and spleen tissues analysed for apoptosis. We observed that high doses of amifostine administered alone and in combination with radiation, which previously reduced inversions, induce apoptosis. However, no significant changes in apoptosis were found at lower doses of amifostine to support our hypothesis. The observation that amifostine potentiates radiation-induced apoptosis is contrary to published reports which attribute amifostine's cytoprotection to apoptosis inhibition. Normal cells are considered to have a greater apoptosis threshold following amifostine treatment due to the active import of amifostine providing greater defence against radiation. Our results indicate that this is not true in spleen and indicates that different tissues have different apoptosis responses to radiation in the presence of amifostine. We are currently analysing bone marrow which has been reported to be protected from radiation-induced apoptosis by amifostine. These results show that amifostine does not protect all tissues from radiation-induced apoptosis, and may have implications for the clinical use of amifostine. This research was supported by the U.S. Department of Energy, Low Dose Radiation Research Program grant #DE-FG02-05ER64104.

(PS1.55) Oral administration of multiple antioxidants reduced damage in lethally gamma-irradiated animals. Kedar N. Prasad¹, William C. Cole¹, Gerald M. Haase¹, Jeffrey A. Jones², Rachael C. Casey³, ¹Premier Micronutrient Corporation, Novato, CA, ²NASA-Johnson Space Center, Houston, TX, ³Universities Space Research Association, Houston, TX

This study evaluated the efficacy of an antioxidant mixture administered orally before and/or after gamma-irradiation with doses that produced bone marrow syndrome (mice), gastrointestinal (GI) syndrome (sheep) and GI-central nervous system (CNS) syndrome (rabbits) on survival rate (mice), survival time (sheep) and lung damage (rabbits). Antioxidant mixture was administered orally before (1 day) in mice or before (daily for 7 days) and after (daily for 7 days) irradiation in sheep and rabbits. Animals received whole-body gamma-irradiation delivered in a single dose 7.5 to 9.5 Gy to mice, 4.41Gy to sheep and 9.011 Gy to rabbits. An antioxidant mixture increased the 30-day survival rate from 0 to 40% in irradiated mice, the survival time from 7 to 38 days in irradiated sheep without any supportive care. All rabbits died irrespective of treatment. About 25% of rabbits receiving 9.011 Gy died of CNS syndrome in 4 hours with or without antioxidant treatment. Necropsy of these animals showed that the lungs of irradiated control rabbits were dark, necrotic and without a lobular architecture. However, the lungs of antioxidant treated animals exhibited minimal pulmonary hemorrhage while maintaining the lobular architecture. These levels of radiation protection after an oral administration of antioxidants have never been demonstrated.

(PS1.56) Radioprotection and Radiomitigation Properties of Ex-RAD™ Upon Oral Administration. Ramesh Kumar, Onconova Therapeutics, Inc., Princeton, NJ

Onconova Therapeutics has discovered a novel small molecule kinase inhibitor Ex-RAD™ which has demonstrated significant protection against radiation damage, at lethal doses of radiation in vitro and in vivo, with remarkable margin of safety. At present, Ex-RAD is being developed as a subcutaneous injectable product for first responders for prophylactic use. Onconova has completed several clinical trials with subcutaneous (SC) administration of drug. The oral route of administration of ExRAD would provide significant benefit of use in civilian population especially children and elderly. Preclinical pharmacokinetics studies in rats, dogs, rabbits and monkeys reveal that ExRAD is well absorbed, and has a relative bioavailability ranging from 47 to 91%. Here we report effectiveness of Ex-RAD™ upon oral administration in a mouse whole body irradiation (WBI) model. Methods: Ex-RAD was administered SC or orally (PO) to 6-8 weeks old male C3H/Hen or female C57BL/6J mice (N=10) at 24h and 15 minutes prior to 7.5 Gy whole body irradiation (WBI). C3H/Hen mice (N=10) were also dosed 24h and 36h after WBI. Irradiation was done using a 137-Cs source. Survival was monitored for 30 days. Results: We saw significant survival advantage with Ex-RAD administered pre- and post-radiation. Radioprotection results were similar with PO and SC administration of Ex-RAD at 500 mg/Kg. Significant radioprotection was also observed with lower oral dose (200 mg/Kg) of Ex-RAD. Oral formulation (500 mg/Kg) when administered +24h and +36h after radiation showed 90% survival compared to 50% in vehicle administered group. Conclusions: Ex-RAD™ is equally effective when administered either orally or subcutaneously. Orally administered Ex-RAD™ offers the benefit of convenient dosing options to the civilian population for either prophylaxis or the treatment of Acute Radiation Syndrome.

(PS1.57) An animal model to study the effect of radiation on wound healing. M. Waleed Gaber¹, Janice A. Zawaski¹, Charles R. Yates², Omaima M. Sabek², Yunzhi Yang⁴, Duane D. Miller², ¹Baylor College of Medicine, Houston, TX, ²UTHSC, Memphis, TN, ³Methodist Research Institute, Houston, TX, ⁴University of Texas HSC, Houston, TX

In the case of a nuclear detonation a considerable number of the casualties are projected to suffer from combined radiation exposure and burn or wound injury. In normal circumstances wound healing starts almost immediately with the onset of inflammation followed by proliferation and finally remodeling. Impaired wound healing can occur as a result of immune suppression, pathological inflammation, and inadequate blood supply; radiation induces all of these factors. Full-thickness wounds with a diameter of 8 mm were introduced on the mouse dorsal region (open-wound model) and wounds monitored by taking digital photographs at 0, 10, 12, 14, and 16 days post wounding. The wound areas (wound area normalized to post-operative area (day 0), percent closure) were calculated and used to characterize wound closure rate and time to healing. An abdominal dermal and muscular closed-wound was used to study wound tensile strength (Newton/ m²) at point of rupture. Blood tests were carried out and animal survival and body weight monitored. Animals received a whole body irradiation (WBI) dose of 6Gy. Radiation delayed open-wound healing. Wounds in sham animals achieved 98% and 100% healing by days 12 and 14, respectively. In irradiated animals, wounds achieved only 33% and 86% healing at the same time points. There was no difference between wounds in irradiated and sham animals by day 16. In the abdominal closed-wound no significant difference in wound strength was observed at day 10 post combined injury. Blood chemistry showed a depletion of white blood cells at day 1 (decreased by 90%) that persisted up to day 15 post irradiation, and a significant decrease in platelet count from day 6 (74%) to day 15 (90%). Irradiated animals suffered a steep decline in body weight that reached its minimum value (13% loss) by day six and then climbed 4% by day 30 post irradiation plus injury, compared to sham animals that achieved a net gain of 16% at day 30. In conclusion, we have developed an animal model to characterize changes in response to WBI and wound injury. Our objective is to use this model to test anti-inflammatory drugs and radiomitigators to increase survival and enhance wound repair.

(PS1.58) Plasma B1 DNA as a potential index of radioprotective effect in mouse. Lei Zhang¹, Liangjie Yin², Mei Zhang², Bingrong Zhang², Yongbing Cao², Yeping Tian², Shanmin Yang², Lurong Zhang², Okunieff Paul², ¹Department of Laboratory Medicine, West China Hospital of Sichuan University, Chengdu, China, ²Department of Radiation Oncology, University of Rochester School of Medicine and Dentistry, Rochester, NY

The worldwide upsurge in screening radioprotective agents through animal experiments makes it necessary to explore additional rapid and sensitive method to determine radioprotective efficacy other than the mere confirmatory method of taking death as end point. The present study tried to utilize the cell free B1 DNA in plasma as an indicator to evaluate radioprotective effect of candidate agents in mice exposed to total-body gamma irradiation (TBI) with comparison to the method of survival analysis. BALB/c mice received 6 Gy TBI were randomly divided into groups, and then treated with different agents: 1. saline as vehicle control; 2. Amifostine (200 mg / kg i.v. 30min prior IR, only once) 3. Lipopolysaccharide (LPS) 250 µg / kg i.p. 30min post IR, only once; 4. FGF-p (20 mg / kg i.m 4 hour and 5 daily, then qod). Blood was collected in 0.5 ml EDTA-treated polypropylene tubes from the mouse lateral saphenous vein at 3, 6, 9, 12, and 24 hours after irradiation. Quantitative detection of plasma B1 DNA was conducted by a previously established branched DNA technology-based method. Following 6 Gy TBI, plasma B1 DNA concentration increased with time, peaked at 6 hours, and then declined rapidly toward baseline levels at 24 hours. The same dynamic change over time was identified in all groups. And significantly higher levels of plasma B1 DNA were observed at 6 hours post IR in the Amifostin (3394 ± 208 ng/ml) and LPS (14982 ± 4511 ng / ml) treatment groups compared with that in the FGF-P (1956 ± 663 ng / ml) treatment group and vehicle control group (2034 ± 106 ng / ml) (P < 0.01). The individual survive rate for each group were identified as 100%, 80%, 40% and 40% at 12 days post IR for the Amifostin, LPS, FGF-P and vehicle group, respectively. The upsurge of plasma B1 DNA may have special meaning in post-radiation adaptogenic response and favorably motivating biological repair systems to help survive the extreme physiological stress. Also, a correlation between the increased radioresistance and the elevated peak level of plasma B1 DNA in different mouse strains was found in our other studies. However, further research is warranted to better define the value of plasma B1 DNA as an index for radioprotective effect and understand the underlying mechanisms.

(PS1.59) The influence of bone marrow transplantation on recovery of intestinal mucosal immune cell populations after total body irradiation. Sarita Garg¹, Junru Wang¹, K. Sree Kumar², Martin Hauer-Jensen³, ¹University of Arkansas for Medical Sciences, Little Rock, AR, ²Armed Forces Radiobiology Research Institute, Uniformed Services University, Bethesda, MD, ³University of Arkansas for Medical Sciences and Central Arkansas Veterans Healthcare System, Little Rock, AR

Background: Bone marrow transplantation (BMT) substantially reduces 10-day lethality after total body irradiation (TBI), consistent with an effect on intestinal radiation death (Terry & Travis, IJROBP 1989;17:569). However, because BMT does not influence post-TBI crypt survival, the mechanism is likely unrelated to epithelial injury. TBI, in addition to injuring the intestinal epithelium, also perturbs the mucosal immune system, one of the largest and most complex in the body. The present study investigated the effect of bone marrow transplantation on restitution of specific intestinal immune cell populations. **Methods:** Male CD2F1 mice were exposed to uniform sublethal TBI (8.0 Gy) in a cesium irradiator and transplanted with bone marrow cells derived from the same strain within 4 hours. Groups of mice with and without BMT were euthanized at 0h (no irradiation), 4h, 1day (d), 3.5d, 7d, 14d, 21d and 30d and segments of proximal jejunum along with peripheral blood samples were procured. Changes in intestinal immune cell populations (granulocytes, macrophages, T lymphocytes, and B lymphocytes), peripheral blood cell counts, and cytokine transcripts and protein levels were assessed. **Results:** BMT accelerated the recovery of circulating white blood cells, erythrocytes, and platelets. In the intestine, BMT was associated with significant early recovery of mucosal granulocytes coinciding with

circulating granulocytes counts. By day 30 post-TBI both groups with/without BMT had reached the baseline level. BMT did not affect the numbers of mucosal macrophages, B and T lymphocytes at early time points, but recovery of these cells in BMT animals was enhanced from day 14 onwards. **Conclusion:** BMT, in addition to enhancing general hematopoietic and immune system recovery, also restores specific local intestinal immune cell populations. This may help explain the reduction in 10-day lethality associated with BMT.

(PS1.60) Eltrombopag enhances megakaryopoiesis of human bone marrow in 3D bioreactors after radiation exposure. Yuhchayou Chen¹, Irena Nowak¹, Ying Tsai¹, Jennifer Pietrusz¹, Hongliang Sun^{1,2}, JH David Wu², ¹University of Rochester Medical Center, Department of Radiation Oncology, Rochester, NY, ²University of Rochester, Department of Chemical Engineering, Rochester, NY

Purpose: Thrombocytopenia after acute radiation exposure is associated with the risk of bleeding. Apart from frequent platelet transfusions, there is no safe and effective therapy for the treatment of thrombocytopenia, due in part to autoantibody formation of recombinant thrombopoietin (TPO) against host platelets. Eltrombopag is a nonpeptide small molecule, agonist of the TPO receptor (c-Mpl), expressed on the hematopoietic stem cells and progenitor/precursor cells involved in thrombopoiesis. Eltrombopag binds to the transmembrane domain of the c-Mpl receptor and has strict species specificity to only humans and chimpanzees. The species specificity limits the options for the investigation of eltrombopag effects on human hematopoietic system after acute radiation exposure. Here we describe the investigation of eltrombopag effect on enhancing megakaryopoiesis after radiation exposure in a human bone marrow culture system established in 3D bioreactors. **Methods:** Human bone marrow cultures were established in the 3D bioreactors to support long-term growth and differentiation of all lineages of hematopoiesis. Megakaryocyte proliferation was enriched by TPO (10 ng/mL) and interleukin-11 (IL-11) (5 ng/mL) in the serum free IMDM medium. Cultures were irradiated on Day 11 using a Cs-137 source at a dose rate of 3.2 Gy/min. After removal of TPO in the medium, two doses of eltrombopag 8 and 12 µg/mL were added to the cultures 24 h after radiation and daily thereafter. Cultures were scored for cell viability and megakaryocytes on days 1, 7, 14 and 21. Flow cytometry analysis of CD41+/CD34- cells was also performed as markers of megakaryopoiesis. **Results:** Our assessment of megakaryocytosis by microscopic analysis of the bone marrow cultures shows good agreement with CD41+/CD34- cells analyzed by flow cytometry. In non-irradiated cultures, megakaryocyte proliferation between day 1 and day 14 was enhanced by eltrombopag to the same extent as TPO. In cultures irradiated with 2 and 3 Gy, eltrombopag enhanced megakaryocyte proliferation to the same level as TPO as well. **Conclusions:** In our bone marrow culture radiation model using 3D bioreactors, eltrombopag is as effective as TPO in sustaining long-term human 3D bone marrow cultures and in enhancing megakaryopoiesis after radiation bone marrow damage.

(PS1.61) A combined therapeutic approach to pulmonary mitigation following a radiological event. Jacqueline P. Williams¹, Richard P. Hill², Christina Haston³, Carl Johnston⁴, Jen-nie Miller¹, Cathy Zimmermann¹, Eric Hernady¹, Christina Reed⁴, Jacob N. Finkelstein⁴, ¹James P. Wilmot Cancer Center, Rochester, NY, ²University of Toronto, Toronto, ON, Canada, ³McGill University, Montreal, QC, Canada, ⁴University of Rochester, Rochester, NY

In this era of heightened terrorism risk, easily distributed countermeasures are urgently required following a mass radiological or nuclear event. However, survivors of the immediate crises that result from whole body exposure may be susceptible to late morbidities that may occur as part of a multi-organ dysfunction syndrome. Therefore, the down-stream roles played by such organs as the lung in the context of TBI are of concern. Although the overall progression to lung late effects (pneumonitis and fibrosis) is well recognized, the complex nature of the pathways leading to their

development, which includes cellular, molecular and temporal components, has led to our group's contention that no single agent or strategy is likely to be an effective measure against these potentially lethal endpoints. We have therefore devised a systematic experimental design to test agents, using a pertinent "2-strain" murine model with a TBI + lung irradiation schedule. We have assessed therapies that include a broad-based anti-inflammatory agent (simvastatin) administered in combination with a number of complementary agents, including G31P (a high affinity antagonist of CXCL8), anakinra (an interleukin-1 receptor antagonist), and EUK-207 (an SOD-catalase mimetic); all agents were assessed using combinations of acute and chronic administration regimens. Currently, EUK-270 appears to hold significant promise since, whether administered acutely or chronically, this agent led to improved survival in both murine strains, particularly when given in combination with simvastatin. Survival was associated with a reduction in infiltrating inflammatory cells (as determined by image analysis) and downregulation of proinflammatory cytokines (e.g. IL-1 β , MCP-1). Interestingly, an unanticipated response to simvastatin alone was seen compared to our earlier data (using an alternative statin). The current data suggest that although simvastatin induces dysregulation in the IL1-MCP1 signaling, as anticipated, this effect may only be transitory, delaying but not altering the downstream inflammatory response. These findings may have profound implications on the treatment of victims following a likely accident or terrorism event and are currently undergoing further testing. Supported by U19 AI-06773-5 and RC1 AI081244-01

(PS1.62) Deficiency of proteinase-activated receptor 1 (PAR1) exacerbates early, but attenuates delayed intestinal radiation injury in mice. Junru Wang¹, Ashwini Kulkarni¹, Martin Hauer-Jensen^{1,2}. ¹University of Arkansas for Medical Sciences, Little Rock, AR, ²Central Arkansas Veterans Healthcare System, Little Rock, AR

Background: The thrombin receptor, PAR1, is a member of a G protein-coupled receptor sub-family that is activated by specific proteinases. PAR1 mediates pro-coagulant, inflammatory, and fibrogenic responses to injury. Previous work from our laboratory has shown that PAR1 is upregulated in early and delayed intestinal radiation injury (radiation enteropathy) and that direct inhibition of thrombin (the main biologically relevant activator of PAR1) ameliorates injury. This study assessed the role of PAR1 in acute and delayed radiation enteropathy using a PAR1 deficient mouse model. Methods: PAR1 knockout mice and control mice underwent localized single dose irradiation (18.5 Gy) of a 5-cm loop of small intestine. Various aspects of radiation enteropathy were assessed at 2 weeks (acute toxicity), 12 weeks (subchronic toxicity) and 26 weeks (chronic toxicity) using quantitative histology, morphometry and immunohistochemistry. Results: Two weeks after irradiation, PAR1 knockouts had more severe intestinal mucosal injury (p=0.002) and increased intestinal serosal thickening (p=0.004) compared to wild-type control mice. In contrast, at the 26-week time point, PAR1 knockouts exhibited reduced overall structural injury of the irradiated intestine (p=0.02), less intestinal wall (p=0.03) and serosal thickening (p=0.004), and diminished collagen I deposition (p=0.04), and intestinal smooth muscle cell proliferation (p=0.02). Mice euthanized at 12 weeks exhibited "intermediate" changes in that intestinal mucosal injury (p=0.01) and collagen I deposition (p=0.04) were exacerbated, while intestinal serosal thickening (p=0.04) and intestinal smooth muscle proliferation (p=0.007) were attenuated in PAR1 knockouts. Conclusion: Deficiency of PAR1 exacerbates early, but attenuates delayed intestinal radiation injury. Thus, it appears that, while PAR1 plays a predominantly protective role during the early phase of radiation enteropathy, it may contribute to the subsequent development of delayed intestinal radiation fibrosis.

(PS1.63) Time course of radiation protection in mice following oral administration of genistein. Michael R. Landauer¹, Lynette J. Lowery¹, Thomas A. Davis², ¹AFRRRI, Bethesda, MD, ²Naval Medical Research Institute, Silver Spring, MD

Medical radiation countermeasures have applications in clinical oncology, space travel, radiation site cleanup and radiological terrorism. In the present studies, mice were pre-treated orally with the isoflavone genistein and exposed to a lethal dose (8.75 Gy) of cobalt-60 gamma radiation. Mice were gavaged with genistein (200 mg/kg) for either 1, 2, 4 or 6 days, twice a day (BID) (every 12 hours). When genistein was orally administered BID for 1, 2, 4 or 6 days, survival rates were 30%, 55%, 75% and 85%, respectively. Mice dosed for 4 or 6 days had survival rates significantly (p < 0.02) higher than vehicle-treated animals (30%). Based on the survival data, separate groups of mice were administered vehicle or genistein (200 mg/kg, BID) for 6 days prior to a sublethal dose of radiation (6 Gy) and evaluated for hematological recovery. Mice treated with genistein had an increase in bone marrow cellularity and a more rapid recovery of white blood cells, neutrophils, platelets, red blood cells, and reticulocytes than time-matched vehicle-treated mice. These data indicate that oral administration of genistein prior to irradiation protects mice from lethal doses of radiation by resulting in accelerated recovery of bone marrow and reducing the severity of pancytopenia in irradiated mice.

(PS1.64) Drug Combinations to Mitigate Radiation Nephropathy. John E. Moulder¹, Eric P. Cohen¹, Meetha M. Medhora¹, Susan R. Doctrow², Marylou L. Mader¹, Bryan J. Althouse¹, Brian L. Fish¹, ¹Medical College of Wisconsin, Milwaukee, WI, ²Boston University, Boston, MA

We have shown that FDA-approved ACE inhibitors and ATI blockers can be used to mitigate radiation nephropathy. The SOD catalase mimetic EUK-207 also mitigates radiation nephropathy. However none of these drugs are completely effective. We have now tested combinations of four different drugs in an effort to maximize efficacy. In the rat total body irradiation (TBI) model of radiation nephropathy we tested drugs started 10 days after irradiation and continued or started 7 days after irradiation and continued for 12 weeks. The combinations tested were captopril plus EUK-207, enalapril plus EUK-207, captopril plus a 4% salt diet and captopril plus atorvastatin. ACE inhibitors were given in the drinking water, atorvastatin and 4% salt in the chow and EUK-207 by subcutaneous mini-pump. Rats were followed to uremia as measured by blood urea nitrogen (BUN), a surrogate marker for radiation nephropathy. Preliminary data show, that irradiated rats receiving both atorvastatin and captopril have significantly less azotemia (as BUN) than irradiated rats receiving atorvastatin or captopril alone. The combination EUK-207 and ACE inhibitors is still being evaluated. When irradiated rats are given both 4% salt diet and captopril there is no added benefit compared to the captopril alone. These results advance our previous work and demonstrate that ACE inhibitors can be combined with other agents to further improve mitigation of radiation nephropathy. This work was supported by NIAID, 1RC1AI81294 and cooperative agreement AI067734.

(PS1.65) Preclinical development of a bridging therapy for radiation casualties. Vijay K. Singh¹, Darren S. Brown¹, Thomas M. Seed², ¹Armed Forces Radiobiology Research Institute, Bethesda, MD, ²Tech Micro Services, Bethesda, MD

Victims of a terrorist attack presenting with the hematopoietic syndrome resulting from exposure to excessive levels of ionizing radiation will succumb to sepsis if not adequately treated. The probability of survival is increased substantially if the victim's immune system is allowed to recover before sepsis sets in. We report here preclinical development of a new bridging therapy which will allow the victim's immune system to recover from damage caused by ionizing radiation. The hematopoietic progenitor cells in blood from tocopherol succinate (TS)-injected mice were analyzed quantitatively by standard in vitro soft matrix colony procedures. CD2F1 mice were irradiated with lethal, whole-body doses (9.2 Gy) of ⁶⁰Co γ -rays and then transfused intravenously (iv, peri-orbital sinus, venous plexus behind the eye) with whole blood, peripheral blood mononuclear cells (PBMC) or plasma from TS-

injected mice 2 and 24 h post irradiation. Survival was monitored for 30 days after transfusion of whole blood, PBMC or plasma. Progenitor cell analyses revealed that hematopoietic progenitors were mobilized into the peripheral blood of TS-injected mice. Our results demonstrated that infusions of whole blood or PBMC from TS-injected mice greatly improved chances of extended survival of lethally irradiated mice. TS-stimulated granulocyte-colony stimulating factor (G-CSF) mobilizes high numbers of progenitors into the peripheral circulation; in turn, this blood- these progenitors- can be used upon subsequent transfusion to effectively mitigate and repair primary acute radiation injury. The transfused cells act secondarily as a bridging therapy for irradiated mice while their own immune system recovers from the radiation induced damage. Further preclinical work and refinements may provide a simpler, improved protocol in clinical management of individuals suffering from high ionizing radiation dose-mediated acute radiation syndrome.

(PS1.66) Effect of Lovastatin on oral mucositis (mouse) after single dose or during daily fractionated irradiation. Wolfgang Doerr, Stefanie Buettner, Caroline Wildermuth, Margret Schmidt, University of Technology Dresden, Dresden, Germany

Oral mucositis is a severe and frequent early side effect of radio(chemo)therapy of head and neck tumours. Statins, by inhibition of HMG-CoA-reductase, change the metabolism of mevalonate, rhoA- and ras-associated signal transduction. Consequently, radiosensitivity, cell proliferation and differentiation as well as inflammatory changes can be modulated by statins. The present study was initiated to determine an influence of Lovastatin on oral mucositis (mouse tongue) induced by single dose (SD) or daily fractionated irradiation (Fract). In all experiments, mucosal ulceration, equivalent to confluent mucositis grade 3 RTOG/EORTC, was analysed as the quantal endpoint. Local single dose (graded doses) or daily fractionated irradiation with 5x3 Gy/week over 1 or 2 weeks, followed by graded test doses, were applied generate full dose-effect curves. Isoeffective doses indicate the residual mucosal tolerance at the time of single dose or test irradiation. Lovastatin (8 mg/kg (SD) or 16 mg/kg (SD, Fract) was given daily via gavage over various intervals. With SD, a significant increase in isoeffective doses by ca. 15% was consistently found if Lovastatin was administered for 3 days before irradiation until healing of all ulcers. With one week of fractionated irradiation, Lovastatin from days -3 to 7 significantly increased the ED50-value for the test irradiation (17%); Lovastatin given from day -3 until healing of the ulcerations caused an increase to 35%. With fractionation over two weeks Lovastatin on days -3 to 4, 7 to 14, 0 to 14 or from day 0 until healing of the ulcerations significantly increased the ED50-values in all treatment protocols (50-80%). In histological studies, treatment with Lovastatin alone over 15 days resulted in an increase of cell numbers in the epithelium to 140 %. With fractionated irradiation a clear reduction of the radiation-induced cell depletion by 50% was observed. This decrease was markedly less pronounced, with a minimum of ca. 70% of the control value, when Lovastatin was administered. In conclusion, daily administration of Lovastatin resulted in a clear increase in oral mucosal tolerance after one and two weeks of fractionated irradiation. This indicates involvement of rhoA- and/or ras-mediated signal transduction in the radiation response of oral mucosa.

(PS1.67) Glycogen synthase kinase-3 beta inhibitors protect hippocampal neurons from radiation-induced apoptosis by regulating MDM2/p53 pathway. Dinesh Thotala¹, Eugenia Yazlovitskaya², Dennis Hallahan¹, ¹Washington University, Saint Louis, MO, ²Vanderbilt University, Nashville, TN

Cranial irradiation is essential for the management of brain tumors. However, many of these patients will exhibit neurocognitive deficits due to radiation-induced apoptosis in hippocampal neurons. We have recently shown that inhibition of glycogen synthase kinase 3 β (GSK-3 β) resulted in significant protection from radiation-induced apoptosis in hippocampal neurons leading to the improved cognitive function in irradiated animals. Similar anti-

apoptotic effects were observed in irradiated cultured hippocampal neurons HT-22 pretreated with GSK-3 β small molecule inhibitors SB216763 or SB415286. While radiation alone led to elevated accumulation of p53, pretreatment of HT-22 with GSK3- β inhibitors prior to irradiation resulted in increased levels of MDM2 and prevented radiation-induced p53 accumulation. To determine the role of MDM2 in molecular mechanisms of the neuronal radioprotection mediated by GSK-3 β inhibition, we knocked down MDM2 in HT-22 neurons using shRNA. As expected, MDM2 knockdown led to increased protein level of p53. This up-regulation desensitized p53 to radiation and prevented radiation-induced p53 accumulation. In combined treatment, knockdown of MDM2 abrogated the effects of GSK-3 β inhibitors on irradiated HT-22 cells leading to increased accumulation of p53 and to decreased cell survival. The observed effect was confirmed in an alternative approach utilizing GSK-3 β knockdown by shRNA and MDM2 chemical inhibition by RITA or Nutlin-3a. These results suggest that while radiation responses in hippocampal neurons mostly involve GSK-3 β and p53, the radioprotective effects of GSK-3 β inhibitors engage interaction of all three proteins, GSK-3 β , p53 and MDM2. The uncovering of an essential role of MDM2 in radioprotection of hippocampal neurons by GSK-3 β inhibitors presents novel opportunities for therapeutic interventions for protection of CNS from radiation-induced neurocognitive deficiencies.

(PS1.68) Consumption of a high antioxidant diet decreases life shortening in mice after total body irradiation. Joel S. Greenberger¹, Michael Epperly¹, Jeffrey Jones², Carlos Montesinos³, Tracy Dixon¹, Hong Wang¹, ¹University of Pittsburgh Cancer Institute, Pittsburgh, PA, ²NASA, Houston, TX, ³AmeriSciences, Houston, TX

We tested the hypothesis that the mechanism of ionizing irradiation-induced life shortening is mediated by persistent oxidative stress in the microenvironment of self-renewing stem cell populations. Previous studies have demonstrated that adult mice receiving intravenous MnSOD-PL treatment prior to 9.25 Gy total body irradiation have increased survival from the acute hematopoietic syndrome (Epperly, et al., *Radiation Research*, 170(4):437-444, 2008). To determine whether continuous administration of dietary antioxidants ameliorated life shortening, groups of 100 mice maintained on a NASA antioxidant diet were compared to a Purina house diet. Female C57BL/6NHsd mice were fed either regular house diet or diet supplemented with antioxidants for one week prior to irradiation and continued for over a year. Twenty-four hours before irradiation half of the mice from each group were injected intravenously with MnSOD-PL (100 μ g plasmid DNA in 100 μ l). Mice were then irradiated to the LD50/30 dose of 9.25 Gy TBI and followed for the development of the hematopoietic syndrome. All mice which survived the hematopoietic syndrome were followed for development of late effects. There was no significant difference in non-irradiated mouse survival between the MnSOD-PL treated mice if kept on the house diet compared to the antioxidant diet. Mice on the antioxidant diet alone had no significant decrease in death following irradiation. Mice on either diet treated with MnSOD-PL before irradiation had a significant decrease in death from the hematopoietic syndrome compared to the control irradiated mice (p = 0.0009). The surviving MnSOD-PL treated mice on the antioxidant diet had a significant increase in survival over 1 year compared to mice on house diet or on antioxidant diet only with no MnSOD-PL (p < 0.0001). Comparing the mice surviving past 50 days after irradiation, those on the antioxidant diet had a significant increase in survival compared to the mice on the regular diet (p = 0.045). Mice on the antioxidant diet plus MnSOD-PL had the best overall survival compared to mice receiving MnSOD-PL alone (p = 0.060). The data supports the hypothesis that chronic oxidative stress survivors of acute irradiation-induced hematopoietic syndrome have life shortening which can be ameliorated by continuous antioxidant administration.

(PS1.69) Development of medical counter measures for radiation injury: identification of the etiology leading to

lethality as part of efficacy analysis. Simon Authier^{1,2}, Julie Gervais^{1,2}, Eric Troncy², ¹LAB Research, Laval, QC, Canada, ²University of Montreal, Faculty of Veterinary Medicine, St-Hyacinthe, QC, Canada

The hematopoietic acute radiation syndrome (ARS) is associated with pancytopenia. The etiology leading to lethality in the hematopoietic ARS may generally be attributed to hemorrhages, infections, chronic anemia or a combination. ARS lethal infections can be divided into sepsis or severe local infection. Sepsis can result from a systemic infection with a gram positive (e.g. cutaneous bacterial flora) or gram negative (e.g. gastrointestinal bacterial flora) bacteria. In-depth diagnostic procedures such as gross pathology, histopathology and microbiology are useful to identify the etiology leading to lethality in animal model of hematopoietic ARS. The incidence of these categories of pathologies in the non human primate hematopoietic ARS model was reviewed after doses from 4 to 12 Gy. Medical counter measures (MCMs) under development for the treatment of the hematopoietic ARS are aimed to prevent the occurrence of radiation-induced pathologies. Each MCM provides beneficial effects against susceptible pathologies which depend on the mechanism of action (e.g. anti-infective, thrombopoiesis stimulant, etc.). Our results suggest radiation dose-dependent changes to the incidence of the lethal pathologies. This translates into different proportions of MCM susceptible deaths at various exposure levels. No deaths were noted at 400 cGy. At 6 cGy, lethal pathologies were attributed to sepsis (28%), hemorrhages (22%), pneumonia (22%) and deep tissue infections (7%). At 6.34 cGy, lethal pathologies were ascribed to hemorrhages (38%), sepsis (13%) and pneumonia (13%), hemorrhage combined with sepsis (25%). At 12 Gy, hemorrhage represented 89% of lethal pathologies before Day 12. Supportive cares that can be used in ARS models differ between animal species which could result into different proportions of lethal pathologies with each model. In some cases, survival improvement in a model without supportive cares may be more easily achieved than with supportive cares as a result of competing effects between the MCM and supportive cares. The use of supportive cares in patients mandates the use of clinically relevant supportive cares during MCM development with animal models. Identification of lethal pathologies in models of ARS appears to be important for interpretations of survival data in efficacy studies.

(PS1.70) Protection of mice against irradiation injuries by the post-irradiation combined administration of p38 inhibitor and G-CSF. deguan Li¹, Yueying Wang¹, Hongying Wu¹, Lu Lu¹, Heng zhang¹, Jianhui Chang¹, Zhibin Zhai¹, Junling Zhang¹, Yong Wang², Daohong Zhou^{3,2}, Aimin Meng¹, ¹Institute of Radiation Medicine, Chinese Academy of Medical Science and Peking Union Medical Collage, Tianjin, China, ²Department of Pathology, Medical University of South Carolina, Charleston, SC, ³Division of Radiation Health, Department of Pharmaceutical Sciences and Winthrop P. Rockefeller Cancer Institute, University of Arkansas for Medical Sciences, Little Rock, AR

p38 mitogen-activated protein kinases (MAPKs) can be overactivated in hematopoietic stem and progenitors cells after ionizing radiation. In the present study, we examined if combined therapy with p38MAPK inhibitor SB203580(SB) and Granulocyte colony-stimulating factor (G-CSF) is more effective than individual agent alone against ionizing radiation(IR)-induced BM suppression. Mice were divided into five equal groups and designated as I-non-irradiated, non-treated control mice(control), II-total body gamma-irradiated mice(IR), III- total body gamma- irradiated mice treated with G-CSF by ip injection twice every day (1ug/each mouse) for six successive days, IV- total body gamma- irradiated mice administered SB (15mg/kg) by ip injection every other day after TBI for 10 days and V- total body gamma- irradiated mice undertaken combined therapy with SB and G-CSF. On the 30th day after 7.2Gy irradiation, 6.7% and 40% of mice remained alive in G-CSF and combined therapy groups, respectively. Bone marrow cell damage were assayed at 2Gy, 4Gy and 6Gy, respectively. The femoral bone marrow cells (BMs), peripheral white blood cells (WBC) in SB, G-CSF and SB+G-CSF groups exposed to different doses irradiation were all higher than those in IR group. In addition, the CFU-GM and CAFC were also determined. Bone marrow CFU-

GM in SB, G-CSF and SB+G-CSF groups were higher than those in IR group. In conclusion, these data indicated that post-irradiation administration of p38 inhibitor and/or G-CSF may protect the TBI-induced acute bone marrow injury, the combined therapy with SB and G-CSF exhibit more efficiency in some degree. Key words: p38 MAPK inhibitor, irradiation, acute bone marrow injury.

(PS1.71) Angiotensin converting enzyme (ACE) inhibitors mitigate pulmonary fibrosis in rats. Elizabeth R. Jacobs¹, Lakhani Kma^{1,2,3}, Feng Gao^{1,2}, Swarajit N. Ghosh^{1,2}, Brian L. Fish², Jayashree Narayanan², John E. Moulder², Meetha Medhora^{1,2}, ¹Pulmonary and Critical Care Division, Department of Medicine, Medical College of Wisconsin, Milwaukee, WI, ²Department of Radiation Oncology, Medical College of Wisconsin, Milwaukee, WI, ³Department of Biochemistry, North-Eastern Hill University, Shillong, India

Aim: To test the potential of angiotensin converting enzyme (ACE) inhibitors for mitigation of pulmonary fibrosis in survivors of a single dose of whole thorax irradiation (WTI). **Methods:** Rats (WAG/RijCmcr) were exposed to a single dose of 13 Gy of X-irradiation to the thorax only, at the dose rate of 1.43 Gy/min. Three structurally-different ACE inhibitors (captopril, enalapril and fosinopril) were provided in drinking water beginning 1 week after irradiation. Rats were assessed for up to 7 months for effects on the lung. Endpoints included breathing rate, wet:dry weight ratio, collagen content and histology. **Results:** Treatment with captopril (200 mg/m²/day) or enalapril (25 mg/m²/day), but not fosinopril (25 mg/m²/day), starting 1 week after WTI decreased morbidity during the pneumonitis phase (40 to 80 days). Based on histological indices and measurement of lung collagen at 7 months, all three ACE inhibitors attenuated the onset of radiation-induced lung fibrosis in animals that survived the pneumonitis phase. **Conclusions:** After whole-thoracic irradiation, three structurally- different ACE inhibitors mitigated radiation-induced pulmonary fibrosis. These treatments were effective even when started one week after irradiation. Our findings support the therapeutic potential of ACE inhibitors against long-term radiation-induced lung injuries. The mechanism of mitigation of radiation-induced pulmonary fibrosis appears to be a class effect of inhibition of ACE activity, since structurally different ACE inhibitors has similar efficacy. This work was funded by RC1 AI 81294 and NIH/NIAID agreements U19-AI-67734. Dosimetry was done by the CMCR Irradiation Core at MCW; histology was done in the Children's Research Institute at MCW under direction of Dr. Paula North.

(PS1.72) CBLB600: a novel class of radioprotective drugs acting via activation of TLR2 receptor complexes. Alexander Shakhov¹, Frederick Bone¹, Eugene Kononov¹, Alec Cheney¹, Peter Krasnov¹, Troitzta Toshkova¹, Vera Shakhova¹, Vijay Singh¹, Elena Elena Feinstein¹, ¹Cleveland BioLabs, Inc., Buffalo, NY, ²Armed Forces Radiation Research Institute, Bethesda, MD

Lipoproteins from different bacteria stimulate cell surface TLR2-containing complexes. Both synthetic and natural bacterial lipopeptides were previously shown to activate B-cells, monocytes, neutrophils, and platelets and to act as potent immunoadjuvants *in vivo* and *in vitro*. We have investigated the properties of one the well-known synthetic lipopeptides, R,R-Pam₂Cys-SKSKK, designated CBLB601, as a radiation countermeasure in mouse model system. This drug was the first in the CBLB600 series of radioprotectors developed by optimization of the peptide portion of lipopeptides. CBLB600 drugs show outstanding radioprotective efficacy rescuing 100% of mice from mortality elicited by 10 Gy total body irradiation (LD_{100/30} for ICR mice) when injected 24 hrs prior to irradiation. DMF₃₀ for CBLB600s obtained in optimal administration conditions is ~1.6. Significant radioprotection was also observed when the drugs were administered at any time between 48 hrs and 30 minutes prior to irradiation. At irradiation dose of LD_{90/30}, CBLB600s administered between 15 minutes and 9 hrs after irradiation also mitigate radiation injury rescuing up to 70% of mice. One of the possible mechanisms of radioprotection/radiomitigation action of CBLB600s is via activation of multiple

cytokines such as G-CSF, KC (murine analog of human IL-8), IL-6, IL-12, SCF, IP-10, IL-1b, TNF α and GM-CSF. Some of these cytokines are known to be powerful radioprotectors themselves and are involved in hematopoiesis. Radioprotection by CBLB600s is TLR2-dependent since the drugs are ineffective in TLR2 KO mice. Notably, not only CBLB600 efficacy but also the toxicity of the drugs in mice was TLR2-dependent as well. Using radiation bone marrow chimeric mice, we have demonstrated that TLR2 expression on the non-bone marrow derived (radioresistant) cells was essential for the ability of CBLB600s to exert their radioprotection potential. This was also correlated with the ability of CBLB600s to induce cytokine response in chimera mice.

(PS1.73) Radioprotection of human bone marrow by ON 01210.Na (Ex-RADTM) through AKT mediated signaling pathway. Anthony D. Kang^{1,2}, Stephen C. Cosenza¹, MV Ramana Reddy¹, E Premkumar Reddy^{1,3}, ¹Fels Institute For Cancer Research and Molecular Biology, Philadelphia, PA, ²Present address: Armed Forces Radiobiology Research Institute, Bethesda, DC, ³Present Address: Department of Oncological Sciences, New York, NY

Background: Limited availability of non-toxic radioprotective agents prompted us to identify a small molecule compound ON01210.Na (Ex-Rad) from our small molecule chemical library using a high throughput cell based assay screening system. If successfully evaluated, this radioprotective agent could be used by military personnel and civilians during a nuclear-radiological disaster or radiation therapy. ON01210.Na is a novel benzyl styryl sulfone that protects mice from ionizing radiation through the prevention of radiation-induced DNA damage and inhibition of apoptosis. The purpose of the current studies was to evaluate the radioprotective efficacy of the drug in human bone marrow cells and identify the mechanism of protection. **Methods:** Human bone marrows (hBM) cells were grown in methylcellulose semi-solid medium and colony forming units (CFU) determined after treatment with various doses of ON01210.Na and ionizing radiation. Toxicity of the drug was determined following 2 and 24 hr of incubation in the presence of 0 to 50uM of the drug. Efficacy of various concentrations of the drug was tested after exposure of cells to 2-4 Gy and was compared with amifostine for its dose reduction factor (DRF) and toxicity. An antibody array was used to identify the signaling pathway responsible for radioprotection. **Results and Discussion:** Treatment with varying doses of ON01210.Na for 2 and 24 hr did not inhibit the growth and differentiation of normal hBM. The drug radioprotected normal hBM cells irradiated with 2, 3, and 4 Gy and had a DRF of 1.6. This DRF is comparable to FDA-approved, amifostine. Incubation of lysates from vehicle or drug treated HFL-1 cells to the Phospho-MAPK Array comprising of 21 different anti-kinase antibodies and 7 different controls printed in duplicate showed that ON01210.Na activates the phosphorylation of AKT and GSK3 α/β following irradiation. Activation of AKT and inhibition of GSK3 β has been directly correlated with cytoprotection from ionizing radiation. Thus it was concluded that ON01210.Na is a safe and non-toxic alternative radioprotective drug with a novel mechanism of action by activating the AKT signaling survival pathway in the presence of radiation.

(PS1.74) The evaluation of piceatannol, a metabolite of resveratrol, as a potential anti-leukemic agent *in vitro* and *in vivo*. Kristin M. Fabre, Rajani Choudhuri, Anastasia L. Sowers, Askale Mathias, John A. Cook, James B. Mitchell, National Cancer Institute, Bethesda, MD

Piceatannol (PIC) is one of the major metabolites of resveratrol (RSV). PIC has been shown *in vitro* to be a potent inhibitor of spleen tyrosine kinase (Syk), a cell-surface protein expressed on B- and T-cells. Clinical data suggests a link between abnormalities in Syk function and hematopoietic cancers. In support of this observation, *in vitro* studies have shown PIC to have anti-leukemic properties such as blocking cell cycle, inhibiting NF κ B nuclear translocation and inducing apoptosis. We have shown that RSV sensitizes normal human cells to both ionizing radiation (IR)

and hydrogen peroxide while PIC protects against hydrogen peroxide. However, neither of these compounds affects survival *in vivo* after exposure to lethal doses of IR. We are now testing two human hematopoietic cancer cell lines (HL-60 acute promyelocytic leukemia (normal Syk expression) cells and Jeko-1 mantle cell lymphoma (over-expression of Syk) cells) with differing Syk expression to determine the efficacy of RSV and PIC as potential anti-leukemic agents *in vitro* and *in vivo*. End-points to evaluate potential anti-leukemic properties in HL-60 and Jeko-1 are Syk protein expression, apoptosis, cell proliferation, cell cycle analysis, NF κ B activity and xenograft/tumor growth delay. We have confirmed that Syk is indeed over-expressed in Jeko-1 cells compared to HL-60 cells and that PIC, but not RSV, inhibits its expression. Preliminary data demonstrates that pretreatment with RSV or PIC on both cell lines inhibit cell proliferation, with significantly more growth arrest observed in Jeko-1 cells when treated with PIC. Apoptosis and inhibition of NF κ B activity was enhanced in both cell lines after exposure to hydrogen peroxide, again with a more significant response in cell death and NF κ B activity inhibition in Jeko-1 cells treated with PIC. The combination of RSV or PIC with IR and their effects on apoptosis, cell cycle, NF κ B activity and cellular proliferation will be presented. HL-60 and Jeko-1 xenograft/tumor delay studies are also underway to determine if the anti-leukemic effects observed *in vitro* can be translated to an *in vivo* model.

(PS1.75) Small molecule inhibitors of p53/MDM2, MDM4 mitigate against ionizing irradiation damage *in vitro* and *in vivo*. Michael W. Epperly¹, Jean-Claude Rwigema¹, Donna Shields¹, Darcy Franicola¹, Tracy Dixon¹, Alexander Doemling², Joel Greenberger¹, ¹University of Pittsburgh Cancer Institute, Pittsburgh, PA, ²University of Pittsburgh, Pittsburgh, PA

Binding of irradiation induced p53 to its inhibitors MDM2 and MDM4 can limit cell cycle checkpoint associated repair and induce apoptosis. We reasoned that inhibition of binding of p53 to MDM2 and MDM4 would stabilize higher p53 reparative functions. BEB55 is one of a family of small molecules which have been demonstrated to both block p53 binding to MDM2/MDM4 and also separate bound complexes. To determine whether BEB55 mitigated irradiation damage *in vitro* and *in vivo*, BEB55 (10 μ M) was added to IL-3 dependent 32D cl 3 murine hematopoietic progenitor cells immediately after irradiation to doses ranging from 0 to 8 Gy. Cells were plated in semisolid methylcellulose containing medium, incubated for 7 days at 37°C, colonies of greater than 50 cells counted and data analyzed using linear quadratic and single-hit, multi-target models. The addition of BEB55 after irradiation resulted in a clear mitigation with an increased shoulder on the survival with a Dq of 4.3 ± 0.4 compared to 1.6 ± 0.4 ($p = 0.039$) for control 32D cl3 cells. To determine the effect of drug *in vivo*, BEB55 was dissolved in 10% cremphor el, 10% ethanol and 80% water. C57BL/6NHsd female mice were injected intraperitoneally with BEB55 (10 mg/kg) either 10 min before or 10 min after 9.5 Gy total body irradiation. Increased survival was observed both when BEB 55 was given before irradiation ($p = 0.0036$) or after irradiation ($p = 0.0051$) compared to control irradiated mice. Furthermore BEB55 was effective as a mitigator at a lower dose of 1.0 mg/kg. Thus, BEB 55 represents a new class of potentially effective radiation damage mitigators.

(PS1.76) Targeting the endothelial Thrombomodulin- Protein C pathway to mitigate radiation lethality. Snehalata A. Pawar¹, Qiang Fu¹, Junru Wang¹, Karl-Uwe Petersen², Hartmut Weiler³, Louis Fink⁴, Martin Hauer-Jensen¹, ¹University of Arkansas for Medical Sciences, Little Rock, AR, ²PAION Deutschland GmbH, Aachen, Germany, ³Blood Research Institute, Medical College of Wisconsin, Milwaukee, WI, ⁴Nevada Cancer Institute, Las Vegas, NV

Background: Radiation injury of normal tissues is associated with loss of vascular thrombo-resistance, from deficiency of endothelial thrombomodulin (TM) and consequent impaired Protein C activation by radiation-induced oxidation of Met388 in TM.

Therefore, interventions targeting the TM-Protein C system may be an attractive strategy to ameliorate the adverse effects of radiation in normal tissues. Methods: 1) The mitigating effect of mouse recombinant activated Protein C (APC) on 30-day survival of male CD2F1 mice exposed to 9.0 Gy total body irradiation (TBI) was assessed *in vivo* by intravenously administering APC or vehicle controls 30min after TBI. 2) Radiation studies were performed on mice lacking TM on one allele and the other allele containing a single amino acid substitution (Glu404Pro) in the TM gene to test the importance of the Protein C activating function of TM. 8-10 mice per group of TM +/+ and TM^{Pro/-} mice were exposed to TBI (7-11 Gy) and monitored for 30-day survival. 3) A modified human recombinant TM peptide, Solulin, was assessed *in vitro* as well as *in vivo*. a) Solulin and "wild-type" recombinant TM were exposed to increasing radiation doses (0-80 Gy) in a cell-free system, followed by assessment of Protein C activation *in vitro* assay. b) Solulin as a radiation mitigator was assessed by sub-cutaneous administration of Solulin or vehicle 30min after exposure of male CD2F1 mice to 8.5 Gy and or 9.5 Gy TBI with monitoring of 30-day survival. Results: Administration of APC, 30min after exposure to TBI, increased 30-day survival as compared to vehicle-treated mice. TM^{Pro/-} mice, an *in vivo* model of deficient protein C activation, exhibited a highly statistically significant increase in post-TBI lethality. Solulin, a modified recombinant soluble human TM resistant to oxidation and metabolic degradation, exhibited robust activation of Protein C *in vitro* after irradiation as compared to "wild-type" TM. Administration of Solulin *in vivo*, 30min after exposure to TBI, increased survival compared to vehicle-treated controls. Conclusions: These results strongly support a role for the vascular endothelium as a regulator of normal tissue radiation responses and highlight the importance of the TM-protein C system. APC and/or Solulin hold promise as possible medical countermeasures against radiation.

(PS1.77) Considerations of a "Bulk-Head Theory" to Dose-Volume Effects in Radiation Lung Damage: Does Fibrosis Matter? Julian Down, Harvard-MIT Division of Health Sciences and Technology, Massachusetts Institute of Technology, Cambridge, MA

The effects of ionizing radiation on the lung remain an active area of pre-clinical and clinical research and there is the increasing trend for investigators to focus their attention on the generation and prevention of chronic pulmonary fibrosis. The role of exposed lung volume in determining overall tolerance is well-recognized from the clinical experience where the preceding acute inflammatory pneumonitis reaction becomes life-threatening when the entire lung is exposed in wide-field radiation therapy (e.g. in patients receiving total body irradiation prior to stem cell transplants) as well as in accident victims. Long-term concerns of fibrosis do not appear to be an issue in this scenario. Exclusion of most of the lung in standard localized RT for thoracic malignancies enables much higher doses to be delivered and fibrosis based either in histological or radiological criteria is commonly reported although symptomatic incidences are still mostly attributed to pneumonitis. The events that follow the resolution of pneumonitis are particularly important and the part played by the unexposed lung should not be underestimated. The "Bulk-Head Theory" encompasses a compartmental and adaptive response of the lung to maintain a ventilation-perfusion balance such that blood is diverted away from the site of injury. In the extreme case the resultant ischemia causes atrophic loss of cellular elements and an increase in connective tissue that remains. Thus "fibrosis" as defined by regional accumulation of collagen may not be an active process but the remnants of lung tissue shrinkage. The overall effect may be considered as a "radiation pneumonectomy" where the compensatory growth of unirradiated lung largely determines long-term pulmonary function. These considerations have implications for the usefulness of strategies designed to target fibrosis (e.g. by inhibiting pro-fibrogenic cytokines) and may necessitate more attention in searching for ways to prevent earlier inflammation associated with pneumonitis.

(PS1.78) Medical management of acute radiation syndrome: first international consensus and evidence-based recommenda-

tions. Nicholas Dainiak¹, Robert N. Gent², Zhanat Carr³, Judith Bader⁴, Elena Buglova⁵, Norman Coleman⁴, Claude Gorin⁶, Martin Hauer-Jensen⁷, Patricia Lillis-Hearne⁸, David Weinstock⁹, Viktor Meineke^{10,11,12,8,13}, ¹Yale New Haven Hospital, Bridgeport Hospital, Center for Emergency Preparedness and Disaster Response and Yale University School of Medicine, New Haven, CT, ²Health Protection Agency, Porton Down, Wiltshire, United Kingdom, ³World Health Organization, Geneva, Switzerland, ⁴National Cancer Institute, Rockville, MD, ⁵International Atomic Energy Agency, Vienna, Austria, ⁶Hospital Saint-Antoine, Paris, France, ⁷University of Arkansas for Medical Science, Little Rock, AR, ⁸Armed Forces Radiobiology Research Institute, Bethesda, MD, ⁹Dana-farber Cancer Institute, Boston, MA, ¹⁰Bundeswehr Institute of Radiobiology, Munich and University of Ulm, Ulm, Germany, ¹¹Kanto Central Hospital, Tokyo, Japan, ¹²Karolinska Institute and National Board of Health and Welfare, Stockholm, Sweden, ¹³Centers for Disease Control and Prevention, Atlanta, GA

The risk for a high-casualty radiological/nuclear incident is perceived by governmental authorities to have increased. The World Health Organization (WHO) convened a panel of experts to rank the evidence for medical countermeasures for management of acute radiation syndrome (ARS) in a hypothetical scenario involving the hospitalization of 100-200 victims. The purpose was to assess the quality of evidence and classify recommendations as strong or weak for various treatment strategies for hospitalized patients with ARS. English-language articles were identified in MEDLINE and PubMed. Reference lists of retrieved articles were distributed to conferees prior to and updated during the meeting. Case series, case reports, publications of randomized, controlled trials of relevant interventions used to treat non-irradiated individuals, reports of studies in irradiated animals and prior recommendations of subject matter experts, were selected. Studies were extracted using the GRADE system. In cases where data were limited or incomplete, a narrative review of the observations was made. No randomized, controlled trials of medical countermeasures have been completed for individuals with ARS. The use of GRADE analysis of countermeasures for injury to hematopoietic tissue was restricted by the lack of comparator groups in man. Reports of countermeasures for non-hematopoietic system injury were often incompletely described, making the use of the GRADE system even more difficult. Reliance on data generated in non-irradiated humans and in experimental animals was necessary. Depending on resource availability and projected survival, a strong recommendation is made for use of cytokines for hematopoietic toxicity; a serotonin receptor antagonist when the suspected dose is > 2 Gy; surgical excision and grafting for skin necrosis; supportive care for neurovascular toxicity; mechanical ventilation for respiratory failure; and administration of fluids, electrolytes and sedatives for significant burns, hypovolemia and/or shock. Parenteral steroids should be used only for a specific medical indication. A weak recommendation is made for nine other clinical practices.

(PS1.79) Preparation, Quality Control and Biodistribution evaluation of ¹⁷⁷Lu-EDTMP for Bone Pain Palliation. Akbar Anvari, Shahid Beheshti University, Tehran, Iran, Islamic Republic of Iran

Currently, various radiopharmaceuticals such as ³²P ⁸⁹SrCl₂ ¹⁵³Sm-EDTMP and ¹⁸⁶Re-HEDP are recommended in order to cure skeletal metastases. ¹⁷⁷Lu-EDTMP complex is proposed as a proper alternatives to other radiopharmaceuticals as the relatively long half-life (T_{1/2}=6.71days), maximum energy β⁻ particle [E_β=498keV (78.6%)], low abundance gamma emission [208keV (11%), 111keV (6.4%)] and easy production are considered advantageous in the wider use of this product. In this study, ¹⁷⁷Lu was produced by thermal neutron bombardment on ¹⁷⁶Lu₂O₃ target in the 5MW Tehran Research Reactor. Radionuclide purity of the ¹⁷⁷Lu was ascertained by recording the gamma ray spectra using a gamma spectrometer with an HPGe detector. ¹⁷⁷Lu-EDTMP complex was prepared at room temperature. The radiochemical purity of the preparation was determined by thin layer chromatography which showed high purity of more than 98% for the resulted complex. The quality control and biodistribution studies of ¹⁷⁷Lu-EDTMP were performed in wild-type rats. The result showed favorable biodistribution features of ¹⁷⁷Lu-EDTMP, indicating significant accumu-

lation in bone. Also, it was observed that clearance of the activity from other organs happens after 7 days. This research presents ^{177}Lu -EDTMP as a suitable therapeutic radiopharmaceutical with proper half-life and low dose for bone palliation of skeletal metastases. Keywords: Bone metastases, Lutetium-177, EDTMP, Radiopharmaceutical, Biodistribution.

(PS1.80) C3 deficiency protects against impairment of hippocampal growth and learning induced by irradiation to the young brain. Marie Kalm, Ulf Andreasson, Thomas Björk-Eriksson, Milos Pekny, Kaj Blennow, Marcela Pekna, Klas Blomgren, University of Gothenburg, Göteborg, Sweden

Radiotherapy is used in the treatment of pediatric brain tumors and is often associated with debilitating late effects, such as intellectual impairment. Areas in the brain harboring stem cells are particularly sensitive to irradiation (IR) and loss of these cells may contribute to cognitive deficits. It has been demonstrated that IR-induced inflammation negatively affects neural progenitor differentiation. In this study, we used mice lacking the third complement component (C3^{-/-}) to investigate the role of complement activation in a mouse model of IR-induced injury to the dentate gyrus (DG) of the hippocampus. C3^{-/-} and wild type (WT) mice received a single dose of 8 Gy to the brain on postnatal day 10. Six hours after IR, IL-1 β and IL-6 were increased in C3^{-/-} but not in WT brains. Seven days after IR, WT but not C3^{-/-} mice displayed a smaller DG with fewer proliferating, phospho-histone H3-positive cells. The number of neuroD-positive neural progenitors in the DG was approximately 80% lower after IR, but there was no difference between C3^{-/-} and WT mice. Microglia density decreased 40% in the hilus of WT, but not C3^{-/-} mice. Astrocyte density increased 72% after IR in the granule cell layer in WT but not in C3^{-/-} mice. Importantly, months after IR the C3^{-/-} mice made fewer errors than WT mice in place learning and reversal learning tests. Together, these results indicate that the complement system contributes to IR-induced injury in the young hippocampus.

(PS1.81) Monte Carlo study of depth dose calculation for low energy clinical electron beams. Hamid Jafari¹, Hosein Chooan², Reza Taleei¹, ¹Shahid Beheshti University, Tehran, Islamic Republic of Iran, ²Amir Kabir University, Tehran, Islamic Republic of Iran

Monte Carlo method is the most accurate calculation method commonly used in clinical simulations. Although this method is worldwide used for treatment planning and dose calculation, there are still some debating problems due to the accuracy and calculation time of each code. Monte Carlo codes like MCNP and EGS has been calibrated with experimental data. In this work we have compared recent multipurpose FLUKA code with EGSnc, MCNP4C, and ETRAN Monte Carlo codes for understanding their limitations, and to avoid systematic errors in the simulation, and to suggest further improvement for the codes. The electron depth dose obtained from each code has been compared with energy interval between 10keV to 20MeV in the water phantom. There are minor disagreements between the codes, the physics and cross section of each code has been compared to evaluate the results. Their timing and further capabilities of each code has been compared. All codes show great agreement in predicting the depth dose rise up and fall out, with energy increase. The depth dose peak shifts toward the deeper depths, and spreads with energy increase. The codes show difference in regard to the slope of rise and fall, which is more observable at energies above 10 MeV.

(PS1.82) Effects of combined thermal and radiation burn injuries on skin. Sachin Jadhev¹, Colin K. Hill², Christopher Meeks², Theresa Espinoza², Norma Roda², Stan Louie¹, Kathy Rodgers², ¹USC School of Pharmacy, Los Angeles, CA, ²USC Keck School of Medicine, Los Angeles, CA

The renin angiotensin system (RAS) plays an important role in wound repair. However, little is known about RAS expression in response to thermal and combination thermal/radiation injury. In the event of a nuclear disaster, the population found within the immediate blast radius will suffer from radiation exposure accompanied by thermal injuries. It is well documented that radiation delays wound healing. We thus hypothesize that the combination of thermal and radiation injuries will lead to a delay and decrease in RAS expression which will correlate with a delay in wound healing. This study evaluates the changes in expression of various components of RAS in response to a thermal injury and compares this to thermal plus radiation (CRBI). The IHC data for AT₁ expression, a marker of proliferative activity, confirm there is a delay and decrease in the number of fibroblasts positively stained for AT₁. The injury sites demonstrated a decrease in collagen deposition for animals receiving combined injury when compared to thermal injury. When we studied the extent of wound healing by observing keratinocyte infiltration into the wounded area (all expressing AT₁ after injury), a significant decrease in wound healing in the CRBI groups was observed as compared to the thermal injury only. All of this data, and evidence from published studies that blockage of AT₁ delays dermal healing, support the notion that delayed wound healing observed in subjects suffering from radiation exposure and the temporal relationship with RAS expression is correlated. The expression of AT₂ and Mas in these models is currently undergoing evaluation. Another aspect of radiation injury is the level of cellular apoptosis. Apoptotic cells were determined by TUNEL staining in the wound site sections. Data suggest that mice receiving radiation alone show no marked increase in apoptosis. In mice treated with 100 cGy radiation + thermal injury a similar pattern of apoptosis was seen as in the thermal injury only group. However, mice receiving 600 cGy radiation + thermal injury reveal a delay and an increase in the number of apoptotic cells as compared to the thermal or radiation injury only. The gene expression data for apoptotic markers shows increased expression of TNFR1 suggesting that apoptosis induced is through the extrinsic pathway. Supported by IRC1AI080976-01.

(PS1.83) Recovery from Radiation Induced Thrombocytopenia by Angiotensin 1-7. Christopher M. Meeks¹, Colin K. Hill¹, Theresa Espinoza¹, Norma Roda¹, Stan L. Louie², Gere S. diZerga¹, Kathleen E. Rodgers¹, ¹USC Keck School of Medicine, Los Angeles, CA, ²USC School of Pharmacy, Los Angeles, CA

Angiotensin 1-7 (A(1-7)) has been shown to accelerate hematopoietic recovery after myelosuppression. Studies were undertaken to optimize A(1-7) administration schedule following total body irradiation (TBI). A study was performed where groups of animals were euthanized at various times after receiving 500 cGy TBI. A(1-7) accelerated recovery of both platelets and white blood cells. The nadir for myeloid and erythroid progenitor numbers was at day 3 with the recovery beginning by the next time point measured. Further, there was an early increase (up to 5 fold by day 7) in progenitors that continued to expand more rapidly than in control animals through day 14. The number of megakaryocytes in the bone marrow was measured by CD41+ (platelet glycoprotein IIb of IIb/IIIa complex) expression. In contrast to myeloid and erythroid progenitors, the nadir for megakaryocyte number after TBI was at day 8. In control animals, recovery was not observed until day 14 and plateaued at day 22. In animals treated with A(1-7), megakaryocyte number doubled by day 14 and continued to increase throughout the observation period. The recovery of CD41lo (immature megakaryocytes) versus CD41hi (mature megakaryocytes) did not change between the controls and A(1-7) treated animals. Megakaryocyte ploidy was also measured. As with total megakaryocytes, the nadir of ploidy found in the control animals occurred at day 8 with no recovery until day 10. In the A(1-7) treated animals, the nadir was not as low as seen with control animals, where recovery was seen at day 10. However, the recovery was more pronounced in the megakaryocytes with higher ploidy suggesting A(1-7) can increase megakaryocyte number, DNA synthesis and endomitosis. By day 14, the ploidy histogram in the treated animals was comparable to that observed in the control animals at day 22. Again, in control animals, after day 22, recovery reached a plateau, but recovery continued to increase through day 30 in the animals treated with A(1-7). In summary, A(1-7)

accelerated progenitor and platelet recovery after TBI. Supported by 1RC1A1080223.

(PS1.84) Mitigation of radiation-induced lung injury with Genistein or Euk-207. Javed Mahmood, Salomeh Jelveh, Richard P. Hill, Ontario Cancer Institute/Princess Margaret Hospital, Toronto, ON, Canada

Lung injury is a significant hazard for people accidentally exposed to radiation to the thoracic region. We previously found that Genistein, a soy isoflavone and Euk-207, a superoxide dismutase/catalase mimetic show promising mitigating effects on radiation-induced lung damage when administered starting immediately after irradiation. However, starting treatment in accident victims immediately after exposure may be difficult, so we have examined whether these drugs can provide effective mitigation if administered starting later after whole lung irradiation (WLR). Six-eight week old female Fisher 344 rats were irradiated with 12 Gy (225 KVp X-rays) to the whole lung. Rats were injected subcutaneously daily with Genistein (50 mg/kg) and Euk-207 (8 mg/kg) starting 2 weeks after irradiation. We found that both Genistein and Euk-207 shifted and reduced the peak of breathing rate increase (indicative of pneumonitis) at 4-8 weeks after irradiation relative to the radiation only groups. In contrast to our previous studies with Sprague-Dawley rats no elevation in breathing rate was observed at later times after irradiation but fibrosis was observed. Both Genistein and Euk-207 significantly decreased this fibrosis (soluble collagen content and Masson Trichrome staining) and also decreased levels of oxidative damage (8-OHdG staining and malondialdehyde concentration) and activated macrophages (ED-1) when measured at 48 weeks after irradiation. To further simulate possible accident scenarios we also examined whether exposure to a low dose of whole body irradiation (WBR) in combination with WLR influences the overall outcome of such treatment. Fisher rats were given two different doses of Genistein (750 or 3750 mg/kg/day in their diet) starting 1 week after 12Gy WLR or combined 4 Gy WBR plus 8 Gy WLR. The Genistein diet again caused a shift and reduction in breathing rate increase at 6-12 weeks after irradiation compared to the irradiated only groups and showed significant mitigation of radiation-induced fibrosis, oxidative damage and activated macrophages levels in surviving rats at 36 weeks but there was no benefit to increasing the dose. The combined WBR+WLR treatment caused more severe morbidity in the rats than WLR alone during the early pneumonitis phase. This was not mitigated by the Genistein treatment.

(PS1.85) Inhibition of p53 activation and its interaction with hsp90 limits apoptosis after ionizing irradiation in human peripheral blood cells. Risaku Fukumoto, Juliann G. Kiang, AFRRI, Bethesda, MD

17-DMAG, an Hsp90 inhibitor, protects human T-cells from ionizing irradiation-induced apoptosis by inhibiting inducible-nitric oxide synthase (iNOS) and its downstream caspase activation. It is also known that ionizing irradiation induces p53, whose inhibition improves mouse survival. Herein, we tested the effect of 17-DMAG on p53 expression and function after ionizing irradiation. In *ex vivo* human peripheral blood mononuclear cells, we found that ionizing irradiation increased p53 overexpression, acute p53 phosphorylation, Bax expression and caspase activation in an irradiation-dose and post-duration dependent manner. 17-DMAG inhibited these increases in a concentration-dependent manner. Similar to these drug effects, we confirmed in *in vitro* models that inhibition of p53 either by transient siRNA treatment or by genetic knock-out resulted in lower level of caspase activity 1 day and enhanced survival 10 days after irradiation, respectively. The analysis of p53-Hsp90 interaction in *ex vivo* cell lysates indicated that the binding between two molecules occurred after irradiation, which was ablated in the presence of 17-DMAG. Taken together, these results suggest the presence of Hsp90-dependent p53 stabilization upon acute irradiation and the potential use of Hsp90 inhibitors in radioprotection.

(PS1.86) Characterization of an ARS animal model of whole-body irradiation in the minipig. Karla D. Thrall¹, Laurie Staska², Sam Harbo², Mark Murphy¹, Jamie Lovaglio², ¹Pacific Northwest National Laboratory, Richland, WA, ²Battelle Toxicology Northwest, Richland, WA

In vivo efficacy studies are necessary to support development of medical countermeasures against radiation injuries. The minipig is an attractive large animal model with a number of physiological characteristics similar to humans. An LD50/30 study was conducted to characterize the dose-response survival and time-course change in hematological and clinical chemistry parameters resulting from whole-body radiation in the Göttingen minipig. Animals were exposed bilaterally to Co-60 at a dose rate of 0.08 Gy/min for doses of 1.5, 1.7, 1.9, 2.1 and 2.3 Gy. Supportive medical management was not provided, although analgesics were provided. Body weight and temperature were measured daily. Blood was collected from animals daily for hematological analyses and twice a week for clinical chemistry evaluations. Necropsy and histopathology was conducted on all animals at termination. The expected decline in blood components was observed across all exposure groups. Over the 30-day period post-irradiation, all animals at the lowest dose (1.5 Gy) were able to recover, whereas no animal survived whole-body irradiation at the highest level (2.3 Gy). All mortalities occurred between post-irradiation days 17 and 22.

(PS1.87) Characterization of pancytopenia and blood chemistry in a partially irradiated mouse model. Omaima M. Sabek¹, Janice A. Zawaski², Charlotte H. Ahern², M. W. Gaber², ¹The Methodist Research Institute, Houston, TX, ²Baylor College of Medicine, Houston, TX

It is widely accepted that in the aftermath of a nuclear detonation soldiers or civilians who survive the acute ionizing radiation exposure will suffer the deleterious effects of radiation injuries. The majority of those affected would receive partial body irradiation (PBI). We are developing a partial irradiated model to study the changes in kinetics and magnitude of pancytopenia and blood chemistry. Male C57BL6 mice, 8-10 weeks of age, received either whole body irradiation (WBI) or PBI of 6Gy (Radsourse 2000) with lead shielding of the femur. Blood was drawn from a cardiac puncture at 1, 5, 10, 20, and 30 days post-irradiation (n=3-4 animals per group). The complete blood counts were performed using an Advia 120 hematology system enabled with species specific software. Blood chemistry to test electrolytes, kidney & liver function, and cardiac markers were also run on a Roche Cobas Integra 400 plus. Our results indicate that white blood cell (WBC) counts were the lowest at 5 days post-irradiation in both WBI and PBI groups. The WBC counts in the PBI group were significantly higher than that in the WBI on day 20 and 30 (P=0.035 & P=0.001 respectively). At 20 days the red blood cell (RBC) counts and cholesterol levels were significantly higher in the PBI compared to the WBI group (P<0.001). Also at 20 days, the chemistry values of total protein, globulin, alkaline phosphatase (ALP), and calcium levels for PBI and WBI were significantly lower than in the unirradiated group. In addition, only in the WBI group alanine aminotransferase, blood urea nitrogen (BUN), and cholesterol levels were lower than normal levels. At 30 days PBI and WBI chemistry levels were compared to normal, the data showed a significant decrease in the PBI levels of sodium, osmolality, and BUN. In addition to these, the WBI levels of albumin, total protein, and ALP were significantly lower than normal. Also at 30 days, albumin levels were significantly higher in the PBI group compared to the WBI (P=0.040), which could be indicative of liver disease. In conclusion we have found that the partial shielding of the femur changed the WBC levels but had a lesser impact on the RBC and platelet levels. The damage to the organs also appears to be less severe with the shielding of the femur even though they received the same doses as the WBI group.

(PS1.88) Radiation mitigators: yeast-based screen identifies drug candidates. Yelena O. Rivina, Robert H. Schiestl, University of California, Los Angeles, Los Angeles, CA

There is an impending need for therapeutic agents that could ameliorate immediate and late effects of radiation-induced damage to cells and the organism as a whole. Immediate damage manifestation in this is cell and tissue death by necrosis or apoptosis, while the late manifestation is carcinogenesis. Thus, an ideal radiation mitigation agent should be able to not only reduce exposure-associated cell and tissue death, but also decrease genetic instability and prevent neoplastic development. To identify such therapeutic agents we have adopted the well-established DEL assay to a sensitive high throughput screening (HTS) assay with two phenotypic readouts: affect of the tested compound on cell survival and the affect on genetic stability. Additionally, we have modified the same DEL assay to specifically test chemical entities for their mitigation properties in an agar-based method. Using these assays we have identified six small, biologically-active molecules from the Asinex library of kinases, GPCRs, etc. Two of these molecules, Yel001 and Yel002, have been successfully tested in vivo in C3H mice with great efficacy in reducing radiation-related death and carcinogenesis following lethal radiation exposures. 63 to 75% of mice treated five times at 24,48,72,96, and 120hrs post LD100/30 exposure (8Gy) survive up to 180 days. We suggest that our novel screening methodology has the ability to identify pharmacologically-relevant molecules with radiation mitigation qualities.

(PS1.89) Dosimetry and dose uniformity techniques for irradiation of live animals, and the importance of including detail in published data. Mark K. Murphy, Roman K. Piper, Battelle-Pacific Northwest Laboratory, Richland, WA

There have been countless important studies involving irradiation of laboratory animals over the years, but only a small percentage of non-rodent studies have been published outside of the university or government laboratory in which they were performed. For those larger animal studies that have been published, there is often minimal information regarding the dosimetric characteristics of the irradiation delivery; especially regarding such parameters as the field characteristics, irradiation geometry, dosimetry methods, and depth dose distribution. In addition, the units of the delivered radiation quantity are inconsistent (e.g., Roentgen, absorbed dose to air, tissue kerma, etc.). This lack of reported dosimetric information and inconsistent radiation quantities compound to make it difficult to make valid comparisons of studies performed under potentially variant conditions, and impairs the ability of new investigators to reproduce or evaluate the influence of modified conditions (e.g., dose rate). Hence, performing animal studies to evaluate the efficacy of radio-sensitizer or radio-protectant compounds may be hampered. With the goal to improve the control of radiobiology studies, this poster describes methods for measurement of radiation dose and techniques to improve dose uniformity within the animal that are consistent with ICRU Report 30, *Quantitative Concepts and Dosimetry in Radiobiology* (1979). Included are the recommended minimum information on material and methods to be published for future investigators.

(PS1.90) Methods for estimating and minimizing uncertainty of radiation dose delivered to irradiated animals. Roman K. Piper, Mark K. Murphy, Pacific Northwest National Laboratory, Richland, WA

The estimated uncertainty for dosimetric information provided in the course of performing animal irradiation often is inadequately descriptive and inconsistent among various studies with respect to the constituents and the manner in deriving individual error components. Ignoring or under-appreciating contributors to uncertainty may lead to obvious underestimates of the overall uncertainty of calculated dose and may skew the conclusions or decisions made as a result of the study. Recent studies performed at the Pacific Northwest National Laboratory included thorough evaluation of uncertainties with respect to the delivered dose determined following guidance provided by ICRU Report 30, *Quantitative Concepts and Dosimetry in Radiobiology*. This presentation details the assessment of the dose delivered to two different types of specimens, processes used to enhance the uniformity of the

delivered dose, irradiation monitoring methods and the assessment of the affiliated expanded, combined uncertainty according to the method described by the ISO Guide to the Expression of Uncertainty in Measurement.

(PS1.91) Pharmacokinetic and pharmacodynamic studies of the radiomitigant OTP in Non-human Primates. Karin E. Thompson¹, Hui He¹, Gabor J. Tigy¹, Koen VanRompay², Veeressa Gududuru³, Duane D. Miller¹, Charles R. Yates¹, ¹The University of Tennessee HSC, Memphis, TN, ²California National Primate Research Center, University of California, Davis, CA, ³RxBio, Inc., Memphis, TN

Purpose: OTP is a small molecule that has proven efficacy as a radiomitigant in murine models of Acute Radiation Syndrome (ARS). A thorough understanding of the pharmacokinetics and pharmacodynamics is essential for drugs seeking licensure under the so-called "Animal Rule". Our purpose was to two-fold: 1) Characterize OTP pharmacokinetics (PK) in non-human primates (NHPs) and 2) Perform a biomarker discovery study in irradiated NHPs. Methods: Plasma protein binding of OTP was determined in NHP plasma using equilibrium dialysis. OTP was administered to NHPs (Macaca mulatta n = 5-6/group) either intravenously (0.3 mg/kg) or subcutaneously (0.3, 1, and 3 mg/kg). Serial plasma drug concentrations were measured by LC-MS/MS and plasma pharmacokinetic parameters estimated by noncompartmental analysis. For biomarker discovery studies, blood was collected from a separate group of NHPs prior to and 7 days after irradiation (12.5 Gy; 5% bone marrow shielding). Multiplex cytokine/chemokine analysis was performed using the Luminex platform. Results: OTP binds to plasma proteins (>99%) in a concentration-independent manner. Approximately 90% of the extravascular OTP dose was absorbed. Following s.c. administration, OTP exhibited linear pharmacokinetics with a half-life of approximately 15 hours. Multiple analytes have been targeted for validation as biomarkers. Conclusions: We have characterized the plasma PK of OTP in NHPs. In addition, we have identified potential biomarkers for radiation injury which require further validation.

(PS1.92) Understanding the biodistribution of actinides and lanthanides for the development of therapeutic decorporation agents. Rebecca J. Abergel¹, Polly Y. Chang², Eleanor A. Blakely¹, David K. Shuh¹, Kenneth N. Raymond¹, ¹Lawrence Berkeley National Laboratory, Berkeley, CA, ²SRI International, Menlo Park, CA

Because of the continuing use of nuclear fuel sources and heightened threats of nuclear weapon use, the amount of produced and released radionuclides is increasing daily, as is the risk of environmental contamination and larger human exposure to fission product lanthanides and actinides. In the past few years, the challenge of limiting such exposure to radiations, contamination with radionuclides, and subsequent deleterious effects has given rise to unprecedented interest in developing therapeutic actinide and lanthanide decorporation agents, as well as cost-effective bioremediation approaches for environmental decontamination. The preclinical development of two siderophore-inspired multidentate hydroxypyridonate ligands, 5-LIO(Me-3,2-HOPO) and 3,4,3-LI(1,2-HOPO), is currently underway at the Lawrence Berkeley National Laboratory. While these compounds are unrivaled in terms of actinide-affinity, selectivity and removal efficiency, a better understanding of the biodistribution and biochemistry of actinides, lanthanides, and the corresponding metal complexes formed with the prospective therapeutic chelating agents, is a critical asset to this program. A rodent model was used to follow the *in vivo* distribution of the representative radionuclides ¹⁵²Eu(III), ²³⁸Pu(IV), ²⁴¹Am(III), ²³⁷Np(V), and ²³³U(VI), administered as free metal ions or complexed with the ligands 5-LIO(Me-3,2-HOPO), 3,4,3-LI(1,2-HOPO) and diethylenetriaminepentaacetic acid (DTPA). In addition, the dose-dependent and time-dependent decorporation efficiencies of these chelating agents were assessed. Different metabolic pathways for the different metal ions were evidenced, resulting in intricate ligand- and metal-dependent

decorporation mechanisms. While both experimental chelators show unparalleled actinide and lanthanide decorporation effectiveness, the corresponding metal complexes may undergo *in vivo* decomposition and release metal ions in various biological pools. This study sets the basis to further explore the metabolism and *in vivo* coordination properties of internalized radionuclides for the future development of viable therapeutic actinide and lanthanide chelating agents.

(PS2.01) Characteristics of DNA binding proteins determine the biological sensitivity to high linear energy transfer radiation. Hongyan Wang¹, XiangMing Zhang¹, Ping Wang¹, Xiaoyan Yu¹, Jeroen Essers², David Chen³, Roland Kanaar², Shunichi Takeda⁴, Ya Wang¹, ¹Emory University, Atlanta, GA, ²Erasmus Medical Center, Rotterdam, Netherlands, ³UT Southwestern Medical Center, Dallas, TX, ⁴Kyoto University, Kyoto, Japan

Non-homologous end-joining (NHEJ) and homologous recombination repair (HRR), contribute to repair ionizing radiation (IR)-induced DNA double strand breaks (DSBs). Mre11 binding to DNA is the first step for activating HRR and Ku binding to DNA is the first step for initiating NHEJ. High-linear energy transfer (LET) IR (such as high energy charged particles) killing more cells at the same dose as compared with low-LET IR (such as x or γ rays) is due to inefficient NHEJ. However, these phenomena have not been demonstrated at the animal level and the mechanism by which high-LET IR does not impact the efficiency of HRR remains unclear. In this study, we showed that although wild type and HRR deficient mice or DT40 cells are more sensitive to high-LET IR than to low-LET IR, NHEJ deficient mice or DT40 cells are equally sensitive to high- and low-LET IR. We also showed that Mre11 and Ku respond differently to shorter DNA fragments *in vitro* and to the DNA from high-LET irradiated cells *in vivo*. These findings provide strong evidence that the different DNA DSB binding properties of Mre11 and Ku determine the different efficiencies of HRR and NHEJ to repair high-LET radiation induced DSBs. (This work was supported by NASA grant NNX07AT40G.)

(PS2.02) Disabled DNA-PKcs phosphorylation impairs genomic stability in mice. Shichuan Zhang¹, Hirohiko Yajima¹, HoangDinh Huynh¹, Junke Zheng¹, Yu-Fen Lin¹, Elsa Callen², Hua-Tang Chen², Andre Nussenzweig², Cheng Cheng Zhang¹, David J. Chen¹, Benjamin Chen¹, ¹UT Southwestern Medical Center, Dallas, TX, ²National Cancer Institute, National Institutes of Health, Bethesda, MD

The catalytic subunit of DNA dependent kinase (DNA-PKcs) is well known for its role in DNA double strand break repair. In addition to its kinase activity, phosphorylation of DNA-PKcs is also indispensable for its proper functioning. We have previously shown that phosphorylation at the Thr2609 cluster (mouse equivalent Thr2605) is critical for DNA double strand break repair and this phosphorylation is mediated by ataxia telangiectasia mutated (ATM) and ATM and Rad3-related (ATR). To further understand the importance of phosphorylation of DNA-PKcs in DNA damage response, we generated mice carrying DNA-PKcs with three alanine substitutions at Thr2605, Thr2634, and Thr2643 in the Thr2605 cluster (3A mutant). Several lines of evidence from this newly-established mouse model strongly suggest an important role for DNA-PKcs in maintenance of genomic integrity. First, mouse embryonic fibroblast derived from homozygotic mice showed high sensitivity toward both ionizing radiation and DNA crosslinking reagents. Profound chromosome aberrations were observed in these cells after DNA-damage treatment. Second and most interesting, in sharp contrast to the normal life span of DNA-PKcs knockout mice, all homozygotic 3A mutant mice died of hematopoietic stem cell (HSC) failure at a premature age. Importantly, loss of HSCs happens between embryonic day 12.5 and 16.5 when HSCs are fast cycling, suggesting a pivotal role of DNA-PKcs phosphorylation in replication associated stress response for stem/progenitor cells. In addition to early and acute loss of HSCs, mice surviving anemia by

bone marrow transplantation developed varied kinds of tumors including lymphoma, skin cancer, and breast cancer. The high tumor incidence and broad spectrum of tumor type suggested that phosphorylation of the Thr2609 cluster is critical in modulating DNA repair pathways and thus maintaining the mammalian genome.

(PS2.03) Role of NHEJ DNA repair proteins in the DNA damage response probed with a proteolytic fragment of Cyclin E. Alex Almasan¹, Jean Boutros¹, Dragos Plesca¹, Suparna Mazumder¹, Kamini Singh¹, Mekki Bayachou², ¹Cleveland Clinic, Cleveland, OH, ²Cleveland State University, Cleveland, OH

Exposure to genotoxic agents, such as ionizing radiation (IR) can initiate double strand breaks (DSBs) that in mammalian cells are predominantly repaired by nonhomologous end-joining (NHEJ). NHEJ requires the Ku70-Ku80 heterodimer, DNA-PK catalytic subunit (DNA-PKcs), XRCC4, Ligase IV and accessory factors, such as XLF/Cernunnos. We have identified Ku70 as a novel interacting partner of a proteolytic fragment of Cyclin E, p18CycE, that is produced during IR-induced apoptosis in hematopoietic tumor cells. Low non-toxic levels of p18CycE sensitize HEK 293T and H1299 cells to IR and etoposide. Neutral comet assays (tail length and tail moment) and gamma-H2AX foci formation, two DSB indicators, showed a marked difference in p18CycE-expressing cells as compared to parental cells following IR indicative of an ineffective NHEJ. In addition, the timing of DNA damage foci loss revealed a slower DNA repair kinetics in p18CycE-expressing cells, with the number of foci in parental cells decreased to 50% after 30 min while it took the p18CycE-expressing cells > 1 hour. Surprisingly, DNA pull-down assays demonstrated that the assembly of Ku70-Ku80 and DNA-PKcs on DSBs was not affected by the presence of p18CycE. However, the recruitment of XRCC4, Ligase IV, & XLF was significantly impaired by p18CycE. Similarly, the number of DNA-PKcs foci observed was affected as an indicator of the protein complex activity. Likewise, the phosphorylations of 53BP1 (S1778) and Kap-1, known to be mediated by DNA-PK, were highly attenuated in p18CycE-expressing cells. The activity of DNA-PKcs was diminished by the presence of p18CycE, to an extent similar to its pharmacological inhibition by Nu7441, while ATM phosphorylation maintained the same pattern with or without p18CycE. These data indicate a profound effect of p18CycE on NHEJ that is most likely dependent on its interaction with Ku70 and probably caused by interference with the activity of DNA-PKcs and subsequent recruitment of XRCC4-Ligase IV heterocomplex to the sites of DSBs. Interaction of p18CycE with nuclear Ku70 interferes with the NHEJ making the p18CycE-expressing cells more sensitive to IR. Therefore, these studies provide mechanistic insights into NHEJ activation, its role in the DNA damage response, and the choice between cell death and DNA repair following a genotoxic insult.

(PS2.04) DNA damage responses in glioma stem cells. Mariella Mannino¹, Evelyn Amoah-Buahin², Colin Watts³, Roger Phillips¹, Anthony J. Chalmers², ¹University of Sussex, Brighton, United Kingdom, ²Brighton and Sussex Medical School, Brighton, United Kingdom, ³University of Cambridge, Cambridge, United Kingdom

Objectives: Poor treatment outcomes associated with glioblastoma multiforme (GBM) have been attributed to the existence of 'glioma stem cells' (GSC) that are capable of self-renewal and tumour initiation. Published data derived from *in vitro* systems has shown wide variation in radiosensitivity of GSC, whereas substantial consistency is noted *in vivo*. Since GSC reside preferentially in niches, we hypothesized that the microenvironment is particularly important in modulating GSC radiosensitivity. In this study we compared a neurosphere formation assay (NFA) with conventional clonogenic survival as a measure of radiosensitivity, compared radiation responses of populations enriched or depleted for GSC and evaluated the feasibility of interrogating GSC in a 3D culture system. Methods: For NFA, single cells per well were plated by serial dilution or FACS sorting and sphere formation quantified at specific time points. For 3D culture, GSC enriched or depleted

populations were plated on a polystyrene scaffold (Reinnervate™) coated with extracellular matrix components and examined by immunofluorescence confocal microscopy for morphology and expression of stem cell markers. Results: NFA generated more accurate and reproducible radiosensitivity data than conventional clonogenic survival assays, and differences between GSC enriched and depleted populations were more pronounced. GSC enriched populations were resistant to radiation-induced apoptosis. No significant difference was noted in induction or repair of radiation induced DNA damage measured by comet assay, but γ H2AX foci analysis showed reduced induction of double strand breaks in GSC. Unlike differentiated cells, GSC cells maintained a neurosphere growth pattern in 3D culture. Conclusion: GSC enriched populations exhibit radioresistance, but this varies according to cell line and culture conditions. 3D culture systems support growth of GSC as neurospheres in the presence of various components of the tumour microenvironment. Future work will test the effect of modulators of the radiation response on radiosensitivity of GSC enriched and depleted populations by NFA and study molecular radiation responses of GSC in 3D systems that more closely resemble the tumour microenvironment.

(PS2.05) BRCA1 role in the repair of oxidative clustered DNA damage and chromosomal instability. Alexandros G. Georgakilas¹, Jessica M. Hair¹, Georgia I. Terzoudi², Vasiliki I. Hatziz², Katie A. Lehockey¹, Devika Srivastava¹, Weixin Wang³, Gabriel E. Pantelias², ¹Biology Department, East Carolina University, Greenville, NC, ²Radiobiology and Cytogenetics, National Center for Scientific Research 'Demokritos', Aghia Paraskevi, Athens, Greece, ³Department of Laboratory Medicine, Clinical Center, National Institutes of Health, Bethesda, Maryland, MD

To evaluate the role of BRCA1 deficiencies in the repair of radiation-induced DNA injury and generation of chromosomal instability we have used two human breast cancer cell lines, the BRCA1 deficient HCC1937 cells and as a control the BRCA1 wild type MCF-7 cells. As an additional control for the DNA damage repair measurements, the HCC1937 cells with partially reconstituted BRCA1 expression were used. Since clustered DNA damage is considered the signature of ionizing radiation, we have measured the repair of double strand breaks (DSBs), non-DSB bistranded oxidative clustered DNA lesions (OCDLs) as well as single strand breaks (SSBs) in cells exposed to radiotherapy-relevant γ -ray doses (3-5 Gy). Parallel measurements were performed in the accumulation of chromatid and isochromatid breaks. For the measurement of OCDL repair, we have used a novel adaptation of the denaturing single cell gel electrophoresis (Comet assay) and pulsed field gel electrophoresis with *E. coli* repair enzymes (Fpg and EndoIII) as DNA damage probes. Independent monitoring of the γ -H2AX foci was also performed while metaphase chromatid lesions were measured as an indicator of chromosomal instability. HCC1937 cells showed a significant accumulation of all types of DNA damage (DSBs, SSBs and OCDLs) even after 24 hrs repair as well as chromatid breaks compared to MCF-7. Wild-type BRCA1 partial expression in the HCC1937 cells contributed significantly in the overall repair of OCDLs. The current results suggest an important role of BRCA1 protein in the processing of oxidative DNA lesions. In addition, they further support the biological significance of repair resistant clustered DNA damage leading to chromosomal instability under a BRCA1 repair deficiency.

(PS2.06) NUCKS, a RAD51AP1 paralog, protects human cells from the cytotoxic effects of X-rays. Claudia Wiese¹, Alex Kuo¹, Ruyan Rahnama¹, Eloise Dray², Anne Carine Ostvold³, Patrick Sung², David Schild¹, ¹Lawrence Berkeley National Laboratory, Berkeley, CA, ²Yale University School of Medicine, New Haven, CT, ³University of Oslo, Blindern, Norway

RAD51 associated protein 1 (RAD51AP1) is a RAD51-interacting protein that is essential for homologous recombinational DNA repair (HRR; [1]), a pathway indispensable for genomic stability and tumor suppression [2]. RAD51AP1 shares extensive sequence homology with nuclear ubiquitous casein and cyclin-

dependent kinases substrate 1 (NUCKS), a 27 kD chromosomal protein of previously unknown function. NUCKS was discovered in 1985 as a high-mobility-group (HMG)-like protein present in human cells [3], is widespread in vertebrates, abundant in rapidly growing cells and over-expressed in a variety of cancers. Notably, *NUCKS* is located on human chromosome 1q32.1, a genomic region that is commonly gained in breast cancer [4], indicating that this protein could represent a potential target for future cancer therapy. We show that, similar to RAD51AP1, NUCKS is essential for DNA repair by HRR. However, unlike RAD51AP1, NUCKS also appears to be involved in DNA repair by non-homologous end-joining (NHEJ). NUCKS was found to be epistatic with the HRR proteins RAD51AP1 and XRCC3 in mitomycin C cell survival assays and, similar to cells with RAD51C or RAD51AP1 knockdown, NUCKS-depleted human cells show persistent phosphorylation of both RPA and CHK1 in response to camptothecin treatment. Functional loss of NUCKS greatly reduces the levels of gene conversion after induction of a site-directed DNA double-strand break by *I-SceI*, providing further support for a role of NUCKS in HRR. In addition, NUCKS-depleted cells in S-phase show enhanced sensitivity to X-rays, as expected for an HRR protein. However, different from proteins solely functioning in HRR, NUCKS-depleted cells show enhanced sensitivity to X-rays in G1-phase and epistasis with XRCC4. These results suggest that NUCKS may also function in NHEJ. Our findings are the first evidence for a biological function of *NUCKS*, an apparent vertebrate-specific gene that also may represent a new cancer susceptibility locus. A model will be presented, in which we anticipate delineating NUCKS function based on the specificity of its highly abundant posttranslational modifications. [1] Wiese C. *et al.*, Mol Cell, 28(3), 2007. [2] Schild D. and Wiese C. NAR, 38(4), 2010. [3] Østvold A.C. *et al.*, Eur J Biochem, 153(3), 1985. [4] Naylor T.L. *et al.*, Breast Cancer Res, 7(6), 2005.

(PS2.07) Excess of RAD51 affects replication initiation and elongation after DNA-damage induction. Ann C. Parplys¹, Eva Petermann², Horst-Werner Stuerzbecher³, Ekkehard Dikomey¹, Kerstin Borgmann¹, ¹Laboratory of Radiobiology and Radio-Oncology, University Medical Center Eppendorf, Hamburg, Germany, ²Gray Institute for Radiation Oncology, Oxford, United Kingdom, ³Institute of Human Genetics, Luebeck, Germany

Maintenance of genomic stability, especially in S/G2 phase is mediated by active Homologous recombination (HR). From this perspective it seems to be obvious that lesions primarily single strand breaks (ssb) or damaged bases (BD) will be converted to double strand breaks (dsbs) at replication forks and become substrates for HR. Changes in RAD51 expression strongly affects the genomic stability. Early RAD51 overexpression results in an increased spontaneous instability indicating a failure of DNA repair at replication forks in the presence of an excess of RAD51. To test the effect of RAD51 overexpression on replication initiation and elongation after dsb, ssb and base-damage induction was analyzed to allow the examination of broad spectrum of different lesions normally caused by irradiation, separately. Experiments were carried out on U2OS-cells transfected with Rad51 under control of a ponasterone inducible promoter. Replication fork progression and origin firing were analyzed by fibre assay. To estimate the effect after damage, 200 μ M H2O2 (dsbs) 10 μ M Topotecan (dsbs), 10 μ M H2O2 (ssb) and MMS (BD) were used. The activation of the Intra-S-Phase Checkpoint was analyzed by phosphorylation of ATR and Chk1 using Western blotting. A reduced fork progression was found in unperturbed cells overexpressing Rad51 resulting in 0.68 kb/min compared to 0.77 kb/min in controls. After damage induction the strongest effect on fork progression was seen after 200 μ M H2O2 and 10 μ M Topotecan (0.33 to 0.44 and 0.29 to 0.39 kb/min), to a lesser extent after 10 μ M H2O2 with 0.43 to 0.6 kb/min and after MMS with 0.46 to 0.64 kb/min. Further analysis of latent replication origins showed a strong activation only in cells overexpressing Rad51 after all agents employed. This increased perturbation indicates a defective intra-S-phase Checkpoint in cells overexpressing RAD51 which was confirmed by a reduced activation of ATR and Chk1 compared to controls. Overexpression of Rad51 leads to an increased sensitivity to endogenous and exogenous damage, which is evident in decreased replication fork

progression, an increased activation of latent origins due to a defect in Intra-S-Phase Checkpoint.

(PS2.08) Mitochondrial gene copy number variations in tissues from irradiated mice. Gayle Woloschak, Qiong Wang, Sumita Raha, Beau Wanzer, Tatjana Paunesku, Northwestern University, Chicago, IL

A large collection of paraffin tissues was accumulated from an extensive series of irradiation experiments conducted on 49,000 mice at Argonne National Laboratory. Paraffin embedded tissues from these animals represent a unique resource: large numbers of animals were exposed to different qualities of radiation, different doses and dose rates. In many cases these animals have been allowed to live out their entire life span after irradiation and at the time of death (in many cases years after completion of irradiation) tissues from these animals were embedded in paraffin and preserved for later studies. These samples are currently investigated using different types of imaging and quantitative real time PCR. To study effects of different radiation dose-rates on genomic and mitochondrial DNA, we isolated DNA from tissue sections from archived samples and performed Q-RT-PCR amplification. This study revealed variations in mitochondrial gene copy numbers in different tissues and samples. Gene copy number variations produced by gamma ray versus neutron irradiation showed distinctly different patterns. Moreover, among the gamma irradiated animals the highest dose rate was the most effective in causing mitochondrial gene copy number changes.

(PS2.09) Alternative splicing and alternative promoters induced by radiation. Carl N. Sprung, Monash University, Clayton, Australia

Understanding the molecular mechanisms underlying the response to radiation is essential to enable optimization of medical procedures such as X-ray imaging and radiotherapy for which nearly every person is subjected to in some form during their life. Furthermore, the many other occupations, including research, product development and safety quality control, also involve exposure or potential exposure to radiation and will benefit from this research. Alternative transcripts are used by over 80% of all genes and radiation can induce some of these transcripts. We have investigated the whole genome for alternative exon usage in response to radiation. Regulation at this level is just now starting to be fully appreciated. We have recently completed investigations using exon arrays to comprehensively track gene expression with a high degree of sensitivity, interrogating all known and predicted exons in human cell lines. This platform has also enabled us to identify alternatively spliced transcripts as well as use of alternative transcriptional start sites in response to radiation. We found an unusually large number of genes that utilize alternative transcription start sites in response to ionizing radiation, and therefore, have discovered a fundamental regulatory transcriptional radiation response. Further, we are investigating the factors responsible for this response including DNA sequences that may be important for protein binding and regulation. These investigations ultimately are likely to result in more effective treatment strategies by paving the way to optimizing and producing new types of radioprotectors, radiosensitizers and biodosimeters. Additionally, these investigations could contribute to identification of radiosensitivity and other diseases, such as cancer, which involve mis-regulation of alternative splicing and alternative transcriptional start sites in response to radiation.

(PS2.10) IKK β but not NF- κ B regulates cancer cell radiosensitivity by regulation of the repair of ionizing radiation (IR)-induced DNA double-strand breaks (DSBs). Lixian Wu^{1,2}, Lijian Shao^{1,2}, Ningfei An², Senthil Pazhanisamy^{1,2}, Daohong Zhou^{1,2}, ¹Department of Pharmaceutical Sciences, College of Pharmacy, University of Arkansas for Medical Sciences, Little rock, AR,

²Department of Pathology and Laboratory Medicine, Medical University of South Carolina, Charleston, SC

Activation of the NF- κ B pathway has been implicated in regulation of cancer cell sensitivity to IR. This effect has been largely attributed to the induction of anti-apoptotic proteins by NF- κ B. Since efficient repair of IR-induced DSBs is a pre-requirement for the survival of irradiated cells, we investigated if activation of the NF- κ B pathway also regulates the repair of DSBs induced by IR. It was found that pharmacological inhibition of IKK with the IKK β selective inhibitor BMS-345541 significantly reduced the repair of IR-induced DSBs in MCF-7 cells. Inhibition of DSB repair was also observed in MCF-7 cells and several other cancer cells treated with BMS-345541 or other IKK β specific inhibitors prior to IR. To determine which component(s) of the NF- κ B pathway is important for the regulation of DSB repair, we selectively inhibited the transcriptional factor activity of NF- κ B by ectopic expression of an I κ B α mutant or down-regulation of RelA (p65) expression using a RelA specific siRNA and found that DSB repair was not affected by the inhibition. Down-regulation of IKK α expression with IKK α shRNA had no effect on DSB repair as well. However, down-regulation of IKK β expression with IKK β shRNA significantly reduced DSB repair, indicating that IKK β is mainly responsible for the regulation of DSB repair in response to IR. This finding was confirmed by the analysis of DSB repair in IKK α or IKK β knockout mouse embryonic fibroblasts (MEFs), which also demonstrated that only IKK β knockout MEFs were deficient in repair IR-induced DSBs. More importantly, the survival of MCF-7 cells after IR is regulated by IKK β but not by IKK α and NF- κ B, since only IKK β knockdown cells exhibited a higher sensitivity to IR whereas cells expressing mutated I κ B α or IKK α shRNA were equally sensitive to IR as wild-type cells. In addition, activation of NF- κ B bypassing IKK β by transfection of *her2* gene also failed to promote the repair of DSBs and survival of MCF-7 cells after IR. In summary, these findings identify IKK β as a novel regulator of DSB repair and activation of IKK β but not IKK α and NF- κ B is primarily responsible for promoting tumor cell survival after IR by up-regulation of DSB repair. As such, specific inhibition of IKK β represents a novel approach in sensitizing cancer cells to IR.

(PS2.11) The atm kinase inhibitor ku-60019 quickly, completely, and reversibly inhibits the dna damage response at sub-micromolar concentrations. Sarah E. Golding¹, Elizabeth A. Rosenberg¹, Shayalini Wignarajah¹, Mark J. O'Connor², Timothy van Meter¹, Kristoffer Valerie¹, ¹Virginia Commonwealth University, Richmond, VA, ²KuDOS Pharmaceuticals Ltd – AstraZeneca, Cambridge, United Kingdom

Since the discovery of ataxia telangiectasia (A-T) mutated (ATM), there has been a great deal of interest in developing small molecule inhibitors that would specifically inhibit this critical regulator of the DNA damage response (DDR). The notion of mimicking the extreme radiosensitivity of A-T cells to sensitize radioresistant tumors with a drug is significant and exciting. ATM kinase activity is absolutely necessary for conferring cellular radioresistance so focus has been on targeting this entity. Until now research efforts and human testing have been hampered by a lack of such inhibitors that are specific and effective at clinically relevant doses. We recently reported on the superior radiosensitizing ability of a second generation ATM kinase inhibitor, KU-60019, that was active on cells in the low micromolar range. Our more recent results now show that sub-micromolar concentrations of KU-60019, provide quick, reversible, and complete inhibition of the DDR in human glioblastoma cells. KU-60019 at 300 nM inhibited the activation of major DNA damage effectors p53 (95%), H2AX (80%) and KAP1 (92%). This inhibition was detected as early as 15 min after application of the drug and remained effective for at least 72 h in tissue culture media when p53 ser-15 phosphorylation was examined (93% inhibition at 72 h). Inhibition was reversible with complete p53 ser-15 phosphorylation observed 1 h or earlier after fresh media was applied. Colony forming experiments showed that continuous exposure to KU-60019 effectively radiosensitized U1242 glioblastoma cells (DER [D37] 300 nM = 1.9; 600 nM = 2.1). In addition, when U1242 cells were co-treated with KU-60019 and Temozolomide (TMZ) – a drug used as standard treatment of

glioma-, we observed a slight additive effect (DER [D37] KU-60019 600 nM = 2.6; KU-60019 600 nM + TMZ 100 μ M = 2.9) with TMZ alone unable to significantly radiosensitize these cells. These data provide encouraging results for possible future clinical application of an ATM inhibitor as a radiosensitizer for glioblastoma. Supported by NIH P01CA72955, R01NS064593, R21ES016636, T32CA085159, and the American Brain Tumor Association.

(PS2.12) The effects of Bcl-2 and Bcl-X_L expression on long term radiation-induced genomic instability. Caitlin E. Mills, David W. Andrews, Douglas R. Boreham, McMaster University, Hamilton, ON, Canada

The effects of Bcl-2 and Bcl-X_L expression on the initial radiation sensitivity and long term stability of MCF-10A cells have been investigated. The stable, near diploid, non-tumorigenic MCF-10A cells were transfected to over express anti-apoptotic Bcl-2 or Bcl-X_L tagged with fluorescent protein venus. Overexpression was confirmed by Western blot. The cell lines were treated with doses ranging from 10 mGy to 4 Gy of gamma radiation from the Taylor radiobiology Cs-137 source at McMaster University. Immediate damage was assessed using automated MN and 53BP1 foci formation assays. Fully automated, image based micronucleus (MN) and 53BP1 foci formation assays were developed. The complete assays were performed in 384 well plates using a Thermo Scientific SP-WorkCell, a fully contained cell handling robotic workstation. The plates were imaged using a Perkin Elmer Opera confocal microplate imager and the data were analyzed using Acapella software. There were no significant differences between the Bcl-2 and Bcl-X_L over expressing cells and controls immediately following irradiation. The manifestation of 53BP1 foci following radiation exposure was independent of Bcl-2 and Bcl-X_L expression. Array comparative genomic hybridization (aCGH) and spectral karyotyping (SKY) were used to verify that the wildtype MCF-10A cells matched the known karyotype of the cell line. Array CGH and SKY were also employed to ensure that the transfections did not alter the karyotype of the cells. Furthermore, both techniques were used to evaluate the progression of genomic instability and accumulated mutations in the cell lines up to twenty passages following irradiation.

(PS2.13) Screening for inhibitors of and key players within the homologous recombination pathway of dna repair. Guy L. Kingham, Gray Institute of Radiation Oncology and Biology, Oxford, United Kingdom

The homologous recombination (HR) DNA repair pathway mediates the high fidelity repair of DNA double strand breaks. We are currently conducting (a) RNA interference screens to identify key players in HR and (b) chemical library screens to identify small molecule HR inhibitors. Studies in our lab have suggested that knockdown of proteins involved in homologous recombination is toxic to the Du145 prostate cancer cell line, whilst other labs have shown that compounds active against HR can be used as radiosensitisers. Inhibition of HR has also been shown in our lab to cause selective toxicity to poly-ADP-ribose polymerase 1 (PARP1) knockout mouse embryonic fibroblasts which are deficient in the single strand break DNA repair pathway, suggestive of a synthetic lethal interaction. These observations suggest HR inhibitors may have the potential to selectively kill cancer cells. We aim to use high throughput screening to identify specific small molecule inhibitors of HR to explore this hypothesis. In addition to identification of HR inhibitors, siRNA screens are being employed in an effort to characterise the HR network and to identify new targets for inhibition.

(PS2.14) Poly (ADP-ribose) polymerase protects neural cells from clustered DNA damage induced by ionizing radiation. Minli Wang^{1,2}, Linlin Tian¹, Xiaobing Tang¹, Huichen Wang¹,

¹Department of Radiation Oncology, Emory University, Atlanta, GA, ²Division of Space Life Sciences, USRA, Houston, TX

PARP-1 catalyzes poly (ADP-ribose) ation on DNA and proteins as an immediate response to DNA damage induced by ionizing radiation or following oxidative stress. Studies on neurodegenerative diseases have revealed that PARP-1 plays a critical role in strand break repair and base damage repair in the central nervous system (CNS). Inhibition of PARP-1 is lethal to cells when they are deficient in DNA double strand break (DSB) repair, such as BRCA1 and BRCA2. Previous data has shown that PARP-1 is also involved in DSB repair as a back-up pathway of classical non homologous end joining (NHEJ). In this study, we used an *in vitro* system based on cultures of mouse embryo neuronal progenitor cells (neurospheres) from PARP-1 knockout mice as well as immortalized mouse hippocampal neuronal precursor cells to study the function of PARP-1 on the protection of neural cells from DNA damage induced by low linear energy transfer (LET) radiation and high LET radiation. Using a mouse NeuroCult neural colony-forming cell assay, we found the proliferative potential of neural cells from PARP-1 knockout mice to be greatly impaired, and the deletion of PARP-1 in neuron stem cells caused highly radiation sensitive to killing. PARP inhibitor sensitizes neural cells to radiation. Deficiency of PARP-1 and inhibition of PARP activity also increased DNA single and double strand breaks, and delayed DNA repair detected by a modified single cell electrophoresis under alkaline and neutral conditions, respectively, and the decay of γ H2AX foci in neuronal cells. Treatment with Endonuclease III (Nth) significantly increased strand breaks in PARP-/- cells, which suggests that NthI recognizes oxidative damage and that radiation induced clustered DNA damage in neuronal progenitor cells. Compared with X-ray radiation, PARP-1 inhibitor induced more DNA damage in neuronal progenitor cells following ⁵⁶Fe particles and proton irradiation. Proliferating neural cells are more sensitive to radiation than differentiated neural cells. Inhibition of PARP increased ATM activity and induced its downstream signaling. These suggest that PARP-1 may play a role in DSB repair in the CNS and protect neuronal cells following ionizing radiation. This work is supported by NASA space radiation program NNX08BA08G.

(PS2.15) Radiosensitizing effects of Gimeracil. Masanori Someya¹, Masaru Takagi¹, Koh-ichi Sakata¹, Hiroshi Tauchi², Yoshihisa Matsumoto³, Masato Hareyama¹, Masakazu Fukushima⁴, ¹Department of Radiology, Sapporo Medical University, School of Medicine., Sapporo, Japan, ²Ibaraki University, Ibaraki, Japan, ³Tokyo Institute of Technology, Research Laboratory for Nuclear Reactors, Tokyo, Japan, ⁴Pharmacokinetics Research Laboratory, Taiho Pharmaceutical Co., LTD., Tokushima, Japan

[Purpose] Gimeracil was invented as a component of S-1 that is a new oral anticancer drug. S-1 contains Gimeracil and tegafur (prodrug of 5-FU) in a molar ratio of 0.4 : 1. Gimeracil competitively inhibits dihydropyrimidine dehydrogenase, which degrades 5-FU. Gimeracil is originally added to S-1 to yield prolonged 5-FU concentrations in tumor tissues. Recently, concurrent chemoradiotherapy using S-1 has been performed with promising results, suggesting that Gimeracil has the radiosensitizing effect. We aimed to clarify its mechanism of Gimeracil. [Material and Methods] DLD-1 is a human colorectal carcinoma cell line. M059J, XR-V15B, and xrs-5 lack DNA-PKcs expression whether M059K, V79, and CHO-K1 are normal counterpart, respectively. GM7166VA7 is a cell from a Nijmegen breakage syndrome patient. To measure cell-cycle-phase specific radiation sensitivity, cells were synchronized with nocodazole. [Result] The surviving fraction was significantly reduced after pretreatment with Gimeracil in all examined various kinds of rodent and human cell lines but cells deficient in HR (GM166VA7). Radiosensitizing effects of Gimeracil reached a plateau at 48h in its exposure times and 1mM in its concentrations on all examined cell lines. Gimeracil effectively sensitized cells deficient in NHEJ (M059J, XR-V15B, and xrs-5) compared to parent cell lines. Radiation-induced focus assay in DLD-1 indicated that Gimeracil inhibits loss of gamma-H2AX foci and reduces RPA and Rad51 foci formation at DSB sites. In cell cycle synchronization experiments, Gimeracil sensitized the cell population rich in S phase more than that rich in G0/G1 or G2/M.

These results suggested that Gimeracil may partially inhibit HR. [Conclusion] Gimeracil may partially inhibit HR in the DNA double strand breaks repair mechanism. Gimeracil is applicable to clinical radiotherapy. Since Gimeracil is administered orally and less toxic even in high concentration of 1mM, it can be given on a daily basis during fractionated radiotherapy.

(PS2.16) Use of zinc finger nucleases (ZFNs) in the evaluation of leukemogenic translocations in MLL 11q23. To Uyen T. Do¹, Shyh-Jen Shyh², Sheetal Singh², Andrew Vaughan², ¹University of California, Davis Graduate Group in Immunology, Davis, CA, ²University of California, Davis Dept of Radiation Oncology, Sacramento, CA

Objective(s): Certain types of leukemia process double stranded breaks (DSB) into chromosomal translocations within the 11q23 region of the Mixed Lineage Leukemia (*MLL*) gene. Radiation treatment or chemotherapy has been linked with a higher risk of secondary cancers such as therapy related Acute Myeloid Leukemia (tAML). Due to the random nature of radiation-induced DNA damage, we used ZFNs to cut at specific DNA sequences within *MLL* as a surrogate for the damage introduced by cancer treatment. Our goal was to analyze leukemogenic chromosomal rearrangements caused by DSB mis-repair. Materials/Methods: Site specific DSB introduced into exon 13 of the *MLL* gene and successful repair was measured by co-transfection of a specific ZFN and a homologous recombination (HR) reporter construct into lymphoblastic K562 cell line, human bone marrow (BM) and PBMC. Cells were also pre-treated with the DNA-PK inhibitor NU7026. Site specific DNA damage was analyzed by ligation-mediated PCR (LM-PCR). The Surveyor assay was used to quantitate non-homologous end joining (NHEJ) mis-repair. Specific DNA rearrangements were also measured using inverse PCR (IPCR) coupled to parallel sequencing and FISH analysis. Results: A *MLL* exon 13 targeted ZFN in K562 cells resulted in detectable activation of the HR reporter construct at 12h, reaching a maximum at 48h. Levels of HR reporter activity returned to baseline by 1 week. Interestingly, suppression of NHEJ function using NU7026 increased the rate of HR repair by two fold. DNA breaks at the target site were detected within the genome as early as 6h. Errors in DNA repair were observed via the Surveyor assay 12 h after transfection, reaching a peak of 22% after 48h. Conclusions: We demonstrate that a ZFN efficiently targets a known site of leukemogenic recombination in K562 cells. In K562 cells at least, rejoining of this break is biased towards mis-repair events. Manipulation of alternative repair pathways (NHEJ) with NU7026 enhances the recombination repair of these lesions indicating a possible route for the suppression or pre-leukemic lesions. Given that K562 cells were derived from a CML patient and potentially deficient in accurate repair, a 22% mis-repair is not surprising. We expect this to be quantitatively lower and DNA repair to be effectively more accurate in normal human BM and PBMC samples.

(PS2.17) The XLF C-terminal region is required for DNA binding and interaction with Ku in vitro but not for repair of double-strand breaks in vivo. Brandi L. Mahaney, Yaping Yu, Shujuan Fang, Susan P. Lees-Miller, University of Calgary, Calgary, AB, Canada

DNA double strand breaks (DSBs) are one of the most detrimental DNA lesions in the cell. DSBs can be induced by ionizing radiation (IR) and in mammalian cells these DSBs are primarily repaired by the non homologous end-joining pathway (NHEJ) which involves several core proteins including the DNA-PK complex which is composed of the Ku70/80 heterodimer and the DNA-PKcs catalytic subunit; the XRCC4-DNA ligase IV complex; and the XRCC4-like factor (XLF) which has been shown to stimulate XRCC4-DNA ligase IV mediated DNA end-joining. Crystal structures of XLF confirm that it is structurally similar to XRCC4 yet contains noticeable differences in the C-terminal region. Previously, we have shown that the C-terminal region of XLF binds DNA *in vitro* and is phosphorylated by DNA-PK *in vivo*. Here we

show that this region, which is predicted to be unstructured, is also required for the DNA-dependent interaction between XLF and the DNA-PK complex in cell extracts and for interaction with purified Ku70/80 in pull-down assays. Interestingly, the highly conserved penultimate amino acid F298 is absolutely required for the interaction between XLF and Ku as well as for DNA binding in electrophoretic mobility shift assays. However, C-terminal truncation of XLF or mutation of F298 does not significantly alter the kinetics of gamma-H2AX foci resolution following IR *in vivo*. These results suggest that although the C-terminal region of XLF is important for DNA binding and interaction with Ku *in vitro* these interactions may not be necessary for double-strand break repair *in vivo*.

(PS2.18) Distributions of low- and high-LET radiation-induced breaks in chromosomes are associated with inter- and intrachromosome exchanges. Megumi Hada, Ye Zhang, Alan Feiveson, Francis Cucinotta, Honglu Wu, NASA Johnson Space Center, Houston, TX

In a series of experiments, we studied low- and high-LET radiation-induced chromosome aberrations using the multicolor banding *in situ* hybridization (mBAND) technique with Chromosome 3 painted in 23 different colored bands. Human epithelial cells (CH184B5F5/M10) were exposed *in vitro* to Cs-137 γ rays at both low and high dose rates, secondary neutrons with a broad energy spectrum at a low dose rate, and 600 MeV/u Fe ions at a high dose rate. We report here the results of the location of the chromosome breaks along the length of Chromosome 3 of the cells after exposures to each of the four radiation scenarios. In comparison to the expected breakpoint distribution based on the length of the bands, the observed distributions were non-random for both the low- and high-LET radiations. The distributions were remarkably similar between γ rays of low and high dose rates, and between the two high-LET radiation types. In particular, a hot spot towards one end of the chromosome was found after low-LET irradiations of both low and high dose rates. Detailed analysis of the chromosome break ends involved in inter- and intrachromosome exchanges revealed that only the break ends participating in interchromosome exchanges contributed to the hot spot found for low-LET. For break ends participating in intrachromosome exchanges, the distributions for all four radiation scenarios were similar with clusters of breaks found in three regions of the chromosome. Analysis of the location of the two break ends in Chromosome 3 that joined to form an intrachromosome exchange further demonstrated non-randomness in rejoining between two breaks. Our data showed that two breaks with a greater genomic separation along the chromosome may be more likely to rejoin than two breaks with a closer genomic separation, demonstrating that chromatin folding can play an important role in the rejoining of chromosome breaks. In addition, comparisons of the breakpoint distribution to the distribution of protein coding genes along Chromosome 3 illustrated correlations between the two distributions. Our study demonstrated that the breakpoint distribution depends upon both the location of the genes in the chromosome, as well as the likelihood that a break will join with another break in the same chromosome or in a different chromosome.

(PS2.19) Computed tomography scans modify biological consequences of prior high dose radiation exposures in Trp53 heterozygous mice. Nghi Phan, Mary-Ellen Cybulski, Lisa Laframboise, Nicole McFarlane, Douglas R. Boreham, McMaster University, Hamilton, ON, Canada

We tested if computed tomography (CT) scans could modify the consequences of a prior high dose exposure in cancer-prone Trp53 heterozygous female mice. Mice (7-8 weeks old) were exposed to a whole-body 4 Gy dose of γ -radiation (Cs-137, 0.349 Gy/min). Four weeks after the high dose exposure, mice were then given weekly single whole-body CT scans (10 mGy/scan, 75 kVp) for ten consecutive weeks [n=10]. Five days after the last CT scan, bone marrow and blood were collected and challenged *in vitro* with 0, 1, and 2 Gy (Cs-137, 0.188 Gy/min). The corresponding age-

matched control groups were: i) non-irradiated controls [n=5] ii) 4 Gy-only at 7-8 weeks of age [n=5] and iii) weekly CT scans only [n=5]. The biological endpoints examined were flow cytometric micronucleated reticulocytes (MNRET), histone H2AX phosphorylation (γ H2AX), DNA oxidative stress (8-OHdG), and apoptosis (Annexin V + 7AAD). There were no differences in MNRET levels between the various mouse groups ($p > 0.05$). When challenged with 1 and 2 Gy *in vitro*, all groups exhibited significant increases in γ H2AX foci formation in bone marrow cell populations ($p < 0.01$). Following a 2 Gy challenge, there was a 9% reduction in γ H2AX foci in bone marrow lymphocytes of mice receiving only the weekly CT scans as compared to controls ($p = 0.014$). Furthermore, basal levels of DNA oxidation in bone marrow lymphocytes decreased 14% in mice treated with weekly CT scans relative to the controls and 4Gy-only cohorts ($p = 0.007$). DNA oxidative stress levels were also diminished by 10% after a 2 Gy challenge in CT scanned mice as compared to control mice ($p = 0.038$). Similarly, mice that received weekly CT scans demonstrated 20% lower spontaneous levels of apoptosis in peripheral blood lymphocytes than mice not CT scanned ($p = 0.006$). Reduced levels of apoptosis in CT scanned mice were also evident following a challenge dose of 1 Gy ($p = 0.011$) and 2 Gy ($p = 0.041$) relative to controls. In conclusion, repeated CT scans can modify the biological responses of a previous high dose acute 4 Gy total body exposure in cancer-prone Trp53+/- mice. The observed reduction in both levels of DNA oxidative stress and apoptosis in mice treated with weekly CT scans supports the contention that mice can adapt to repeated low dose exposure. Overall, repeated CT scans seem to confer resistance to larger doses in Trp53+/- female mice.

(PS2.20) USP7 phosphorylation is required for the cellular response to radiation induced DNA damage. Svetlana V. Khoronenkova, Irina I. Dianova, Jason L. Parsons, Grigory L. Dianov, Gray Institute for Radiation Oncology and Biology, University of Oxford, Oxford, United Kingdom

The ubiquitin specific protease USP7 or HAUSP (herpes virus-associated ubiquitin-specific protease) cleaves ubiquitin molecules from proteins that have been modified with either mono- or polyubiquitin chains. This protein is well known as a major regulator of Mdm2 stability, which is an important negative regulator of the p53 tumor suppressor protein. USP7 thus indirectly takes part in the regulation of cell cycle progression and apoptosis in response to DNA damage. It has previously been shown that USP7 is phosphorylated at serines 18 and 963 but a physiological role for this phosphorylation is unknown. We have found that overexpression of wild type USP7, but not phosphorylation deficient mutants, in HeLa cells resulted in an increased repair of radiation induced DNA damage. We also demonstrated that in human cells about 50-60 % of cellular USP7 is constitutively phosphorylated and that the phosphorylation status of USP7 does not affect protein stability or subcellular localization, but modulates its deubiquitylation activity. We propose that phosphorylation of USP7 plays an important role in the cellular response to DNA damage.

(PS2.21) Mof is critical for DDR and post mitotic cell survival. Rakesh Kumar¹, Arun Gupta¹, Thomas Ludwig², Tej Pandita¹, ¹UT Southwestern Medical Center, Dallas, MO, ²Columbia University, New York, NY

The human MOF gene encodes a protein that specifically acetylates histone H4 at lysine 16 (H4K16ac). We will discuss the significance of H4K16ac for DNA damage response (DDR) to ionizing radiation (IR) and post mitotic "Purkinje cell" survival. We demonstrated that decreased levels of H4K16ac, due to hMOF depletion, can alter DDR at several stages of DNA DSB repair and abrogate both the non-homologous end joining (NHEJ) and homologous recombination (HR) pathways of DNA repair. Depletion of MOF results in the death of Purkinje cells.

(PS2.22) Regulation of ionising radiation induced DSB repair is dependent on DSB complexity. Pamela Reynolds¹, Jane V. Harper¹, Stanley W. Botchway², Anthony W. Parker¹, Mark A. Hill¹, Peter O'Neill¹, ¹CR-UK/MRC Gray Institute for Radiation Oncology & Biology, University of Oxford, Oxford, United Kingdom, ²Lasers For Science Facility, Rutherford Appleton Laboratory, STFC, Didcot, Oxfordshire, United Kingdom

When cells are subjected to ionising radiation (IR), a variety of damage is induced within the DNA. Double strand breaks (DSB) are one of the most deleterious lesions. IR induces a spectrum of DSB ranging from simple to complex DSB, the latter with lesion(s) in close proximity to the termini are thought to be difficult to repair. In mammalian cells, non-homologous end joining (NHEJ) is the main pathway to repair radiation-induced DSB. We have used ultrasoft X-ray (USX) micro-irradiation to partially irradiate a cell nucleus as a comparison to NIR laser microbeam irradiation, to investigate if the repair of DSB of different complexity involve different sub-pathways of NHEJ through real time visualisation of Ku80-EGFP (a gift from D. Van Gent) and DNA-PKcs-YFP (a gift from D. Chen) to DSB induced in mammalian cells. We have previously shown that ~80% of the DNA DSB induced by USX irradiation are simple, whereas NIR laser microbeam irradiation produces mainly complex DSB. Following USX irradiation, Ku80-EGFP is recruited rapidly to sites of DNA DSB in the cellular dose range used of 2-100 Gy whereas DNA-PKcs-YFP, a protein downstream of Ku80, is visualised at DSB only at doses >20 Gy. From this dose difference, it is proposed that Ku80 is recruited to all DSB whereas DNA-PKcs-YFP is recruited to a sub-set of DSB. NIR laser microbeam irradiation studies have similarly shown that the recruitment of DNA-PKcs-YFP requires higher laser powers than for the recruitment of Ku80-EGFP. The real time repair kinetics following laser irradiation show that repair of DSB involving Ku80-EGFP occur by a fast ($T_{1/2} \sim 1$ min) and slow ($T_{1/2} \sim 70$ min) process whereas the repair of those DSB involving DNA-PKcs-YFP occur mainly via a slow process with half-life similar to the slow process seen with Ku80-EGFP. These observations occur independent of the cell cycle phase. Co-localisation studies have also shown that Ku80-EGFP is recruited in all cells whereas RAD51, a key component of HR, co-localises with Ku80-EGFP only in S- and G2/M-phase cells suggesting that RAD51 is predominantly involved in the repair of replication induced DSB. It is therefore concluded that Ku70/80 is required for the repair of all promptly formed DSB whereas DNA-PKcs may only facilitate the repair of simple DSB (fast process), but is required for the repair of complex damage (slow process).

(PS2.23) Radiation induced changes in histone gene expression. Jarah Meador, Shanaz Ghandhi, Sally Amundson, Columbia University, New York, NY

DNA synthesis and histone gene expression are tightly coordinated during S-phase of the cell cycle and both processes are regulated by cell cycle checkpoints in response to DNA damage caused by ionizing radiation. In this study we used microarrays to analyze differential gene expression as a function of p53 status and radiation quality, specifically high and low LET exposure. We observed a robust down-regulation of a large set of histone genes in TK6 and its p53-null derivative, NH32, following exposure to equitoxic doses of high (1.67 Gy ⁵⁶Fe ions) or low LET (2.5 Gy) irradiation and confirmed this pattern with qRT-PCR for specific histone subtypes from each of the core (H2A, H2B, H3 and H4) and linker (H1) categories at 3 and 24 hr after exposure. In TK6 we observed similar levels of decreased histone gene expression following equitoxic high and low LET radiation exposure. Although we also observed decreased histone gene expression for both high and low LET exposed NH32 cells, the decrease was not as low as in TK6. Interestingly, in both TK6 and NH32 greater variability in expression among the different histones was observed after 2.5 Gy gamma compared to the relatively consistent expression patterns of the 1.67 Gy ⁵⁶Fe exposed samples. Expression changes of histones were confirmed at the protein level with Western blotting. Taken together, the data indicates that p53 is involved in histone gene expression but that, in the absence of p53, other factors also play a role in the regulation of histone expression.

(PS2.24) Investigating NHEJ: a biochemical assay to study protein recruitment to double-strand DNA breaks. Tracey A. Dobbs, Ruiqiong Ye, Susan P. Lees-Miller, University of Calgary, Calgary, AB, Canada

DNA is continually exposed to endogenous and exogenous agents that cause a plethora of different types of DNA damage which affect the integrity of the DNA. One of the major forms of damage is that of double-strand DNA breaks (DSBs), which if mis- or un-repaired may be mutagenic or cytotoxic. Ionising radiation (IR)-induced DSBs which are characterized by the presence of base lesions, abasic sites or single-strand breaks (SSBs) in close proximity to the DSB termini, are believed to be a major cause of the biological effects of radiation exposure. The type, yield and spatial orientation of IR-induced DSBs can be extremely diverse and as such require intense co-ordination of the repair machinery. Non-homologous end joining (NHEJ) is the predominant pathway utilised by mammalian cells in the repair of DSBs. The key steps of the pathway include recognition and signaling of the break including histone modification of the surrounding chromatin, recruitment of repair factors, processing of the DNA and ultimately ligation of the break. Although, the 'core' components of NHEJ have been widely studied and identified, little is currently known about the order of recruitment, interaction and structural conformations that these components adopt during the repair process. Furthermore, even less is currently known about the interplay between different repair pathways (such as base excision repair) or the resolution and dissociation of repair factors from the DNA. Here, we have developed an *in vitro* assay to study the interaction of repair factors with modeled radiation-induced DSBs. In this assay, synthetic biotinylated oligonucleotides, coupled to magnetic beads, are incubated with extracts from unirradiated or irradiated human cells. Recruitment of proteins to the breaks is studied by western blot and mass spectrometry, with the aim of studying the effect of DNA structure on protein recruitment and the potential role of phosphorylation on both recruitment and repair processing. Furthermore, through transient knock-down of known repair factors such as Ku80 or XRCC4, the requirement for NHEJ factors in repair can be assessed and new insights gained into possible hierarchies of protein recruitment, back-up repair pathways and interchangeability of repair proteins in the absence of classic NHEJ.

(PS2.25) DNA Mismatch repair protein MSH2 may dictate cellular survival in response to low dose radiation. Lynn M. Martin¹, Brian Marples², Mary Coffey¹, Mark Lawler¹, Thomas Lynch³, Donal Hollywood¹, Laure Marignol¹, ¹Trinity College Dublin, Dublin, Ireland, ²William Beaumont Hospital, Royal Oak, MI, ³St. James's Hospital, Dublin, Ireland

We have previously shown that exposure to low dose radiation (0.05-0.3Gy) induces a hypersensitive response (HRS) in prostate cells that is associated with the response of cells to O⁶-methylguanine lesions. HRS was associated with a DNA mismatch repair (MMR) proficient phenotype. To explore the specific role of MMR protein MSH2 in HRS, we used isogenic cell lines proficient and deficient in MSH2 (endometrial carcinoma: HEC59, HEC59+chr2). Using cell sorter clonogenic assays we found that HRS is expressed solely in MMR+ cells with greatest sensitivity in the low dose range observed following 0.2Gy. HRS+ glioma cells have previously been demonstrated to bypass the early G2 checkpoint following such a dose. To gain deeper insight into the role of MSH2 in the mechanism underlying HRS we examined the activation of the early G2 phase checkpoint 0-3 hours after 0.2Gy, using cellular staining with phospho-histone H3 (ph-h3) and PI. Strikingly, flow cytometry revealed that only MSH2+ cells arrested efficiently at this checkpoint. This was confirmed using high content screening (HCS) image analysis for ph-H3. Western blotting and use of the inhibitor UCN-01 in flow cytometry studies revealed that efficient activation of the arrest was chk2 dependent. MMR proteins are known to suppress homologous recombination (HR) via regulation of RAD51 which may also influence chk2 phosphorylation. To explore the role of HR in the activation of the early G2 arrest, we used HCS image analysis to compare basal RAD51 expression and the induction of RAD51 foci after 0.2 Gy. HCS revealed that MSH2+ cells expressed lower basal levels of RAD51 and increased RAD51 foci after 0.2 Gy. Using the RAD51

stimulator RS-1 and Hsp-90 inhibitor 17-aag, preliminary results suggest that differential RAD51 regulation may be responsible for the activation of the early G2 checkpoint and induction of HRS in MSH2+ cells. Collectively these data reveal the complexity of the low dose DNA damage response and indicate that an MSH2-RAD51-chk2 dependent mechanism may be responsible for HRS which is consistent with the concept that HRS is enhanced in G2 phase cells as has been reported. This is the first report of an MSH2-mediated hypersensitive response to low doses of radiation. MSH2 may therefore represent an excellent biomarker for radiation sensitivity in the low dose range.

(PS2.26) Dynamics of ATM and DNA-PKcs in response to DNA double strand breaks. Anthony J. Davis, UT Southwestern Medical Center, Dallas, TX

Of the different types of DNA damage that occur in human cells, DNA double strand breaks (DSBs) are the most deleterious. The inability to repair DSBs can result in genomic instability, carcinogenesis, or cell death. The cellular response to DSBs is a complex process that includes recognition of the DNA damage, activation of signaling pathways including cell cycle checkpoints, and repair of the DNA lesions. Two important proteins that are required for the cellular response to DSBs are the DNA-dependent protein kinase catalytic subunit (DNA-PKcs) and the ataxia telangiectasia mutated (ATM) protein. DNA-PKcs and ATM belong to the PI3K-like family of serine/threonine protein kinases. Both kinases are rapidly activated in response to DSBs and play important roles in transducing the damage signal and for the repair of the DNA damage. In this study, we compared and contrasted the recruitment and retention of each protein to DSBs. Both proteins were shown to rapidly localize to DSBs, but DNA-PKcs reached its maximal level faster (10 min) than ATM (20 min). Although DNA-PKcs and ATM both rapidly associate to DSBs, their dissociation from DSBs is markedly different. DNA-PKcs rapidly dissociates from DSBs with only 20% of the protein still at DSBs 2 hours following introduction of the damage while 60% of ATM is still present at DSBs 2 hours later. Fluorescence after photobleaching data shows that the DNA-PKcs-DSB interaction is much tighter than that of ATM-DSB. Previous studies have shown that the phosphorylation status of ATM and DNA-PKcs play an important role in the dynamics of each protein at DNA DSBs. We found that autophosphorylation of ATM is not required for localization to DSBs as a kinase dead and a serine 1981 mutant form of ATM localizes to DSBs. But unlike wild-type ATM, both the 1981 mutant and kinase dead version of ATM rapidly dissociated from DSBs. Similar to ATM, phosphorylation of DNA-PKcs does not play a role in the ability of the protein to localize to DSBs. However, unlike ATM, ablation of phosphorylation of DNA-PKcs results in sustained retention of the protein to DSBs. These data show that although DNA-PKcs and ATM share many characteristics, including being recruited to and activated by DSBs, overall their dynamics at DSBs are clearly different with the phosphorylation status of the protein playing an important role.

(PS2.27) Mathematical evidence of non-linear DNA damage response for normal human cells exposed to ionizing radiation. Teresa Neumaier¹, Brian Yang², James Chen², Aris Polyzos², Mary Helen Barcellos-Hoff³, Sylvain V. Costes², ¹Helmholtz Zentrum München, Neuherberg, Germany, ²Lawrence Berkeley National Laboratory, Berkeley, CA, ³New York University School of Medicine, New York, NY

DNA damage induced by ionizing radiation elicits formation of microscopically visible nuclear domains (i.e. radiation-induced foci, RIF). These foci are an accumulation of proteins that can sense double strand breaks (DSBs). RIF have raised much interest over the past 10 years as a way to validate and measure DNA damage on a cell by cell basis. There are however confounding factors regarding their quantification, which makes interpretation challenging. We introduce here a novel imaging approach for quantifying foci in cells using chemically modified object slides integrated with image analysis and biophysical modeling to screen the response of

human cells over a wide range of ionizing radiation doses and time following exposure. Normal human breast and skin cells cultivated in 5 μ l microwells were used to optimize and accelerate immunostaining of DNA damage markers. By including a mathematical kinetic model of foci formation and resolution, we could evaluate unambiguously the RIF yield at various doses. Instead of being constant as it had been previously assumed, 53BP1 and γ H2AX RIF yield decreased with dose, with the number of RIF/cell/cGy three times lower at 400 cGy than at 15-50 cGy. In addition, kinetic constants were also dose dependent, suggesting a faster RIF formation but slower RIF loss as the dose went from 15 cGy to 400 cGy. Higher doses increase the probability of more complex lesions as well as clustering of damages. These clusters would be more rapidly detected but would be repaired more slowly. In agreement with this hypothesis, RIF along high energy ions, known to generate streaks of dense and complex DNA DSB, show a 10 to 20 fold increase for foci kinetic induction, where as RIF generated by secondary electrons outside these tracks had a kinetic comparable to the ones observed for X-rays. These results disprove the general well accepted concept that the DNA damage response can be scaled linearly from high to low dose. The microcell array platform and the mathematical model used to fit a full dose and time response opens the door for rapid and accurate screening for multiplexing DNA damage markers that could be used to quantify the influence of different factors on DNA repair, screen radiosensitivity, and study heterogeneity among populations. Supported by NASA Specialized Center of Research and low dose DOE Program.

(PS2.28) Selective inhibition of DNA dependent protein kinase by novel hypoxia activated prodrug HAPI3. Jordan D. Cran, Kirstin E. Lindquist, Andrew I. Minchinton, BC Cancer Research Centre, Vancouver, BC, Canada

Hypoxia is a distinct and potentially exploitable characteristic of many solid tumours. Hypoxic cells exhibit aggressive tumour behavior, displaying increased metastatic potential and genetic instability compared to oxygenated tumour cells, in addition to having increased expression of angiogenic factors associated with tumour progression. These cells are not only resistant to killing by ionizing radiation (IR), but to many chemotherapeutic agents as well. The DNA-dependent protein kinase, DNA-PK, is a logical choice as a radiosensitizing drug target as DNA double strand breaks (DSBs) are the primary means by which IR kills cells. Two models for DSB repair are currently supported: non-homologous end joining (NHEJ) and homologous recombination (HR). The DNA-PK holoenzyme is central to the NHEJ process and is comprised of several proteins: DNA-PKcs, the catalytic subunit; and the Ku heterodimer, composed of Ku70 and Ku80. Ku serves to bind and tether the broken ends of DSBs together and importantly, recruit DNA-PKcs to the site of the DSB. Inhibition of DNA-PKcs has shown not only to decrease NHEJ in cells, but HR as well, indicating multiple roles for DNA-PK in DSB repair. HAPI3 is a candidate prodrug designed to inhibit DNA-PKcs selectively under hypoxic conditions. The enzymatic metabolism of HAPI3 was investigated under hypoxic and aerobic conditions using isolated mouse liver microsomes in the presence or absence of the cofactor NADPH. Quantification of reduction products by HPLC displays that reduction of HAPI3 in to an active DNA-PK inhibitor is greatly enhanced under hypoxic conditions. Hypoxia selective activity in cells was confirmed by clonogenic survival. Cell viability was assessed to determine cytotoxicity. Our results indicate that targeting DNA repair through selective inhibition of DNA-PK is a promising approach to sensitizing radioresistant hypoxic cells. Future studies to elucidate the clinical potential of this class of prodrug will include pharmacokinetic characterization in mouse models of human cancer, characterization of reductase enzymes predominately involved the metabolism of HAPI3, and importantly, an investigation into the ability of hypoxia activated DNA repair inhibitors to penetrate tumour tissue.

(PS2.29) Radiosensitization of gliomas through inhibition of DNAPK. Amol Hosing, Nicholas Valerie, Jaroslaw Dziegielewski, David Brautigam, James Lamer, University of Virginia, Charlottesville, VA

Glioblastoma multiforme (GBM) is a primary brain tumor with a poor prognosis, characterized by an exceptionally high degree of radioresistance. The radioresistance of GBMs has been attributed to both the presence of glioma tumor stem cells which resist apoptosis and to the highly efficient repair of damaged DNA via the non homologous end joining pathway (NHEJ). A critical player in the NHEJ pathway is DNA-dependent protein kinase (DNA-PK). Previous work in our lab has shown that DNA-PK activity and DNA repair in response to radiation requires protein phosphatase 6 activity (PP6c) and its regulatory subunit PP6R1. Inhibition of DNA-PK activity through knockdown of PP6c or PP6R1 results in radiosensitization of GBM tumors in vitro. We hypothesize that expression of a PP6R1 mutant which disrupts the DNA-PK-PP6c interaction will prevent radiation induces DNA-PK activation and result in radiosensitization. To test this hypothesis, various PP6R1 deletion mutants were generated and tested for their binding to DNAPK and PP6c by co-precipitation from transiently transfected cells. The ability of these mutants to compete for the DNA-PK-PP6c interaction and to inhibit DNA-PK activation in response to radiation was tested by the ability to radiosensitize glioma cells. Results from these experiments will be presented.

(PS2.30) Characterizing low-dose ionizing radiation responsive genes and pathways. Matthew A. Coleman¹, Cindy Thomas¹, Shalini Mabery¹, Paul F. Wilson¹, Leif E. Peterson², ¹Biosciences, LLNL, Livermore, CA, ²The Methodist Hospital Research Institute, Houston, TX

Genome-scale microarray expression data in conjunction with DNA sequence/pattern databases were used to identify and validate gene regulatory elements that influence cellular responses to low dose ionizing radiation. Using expression data, we identified over 500 radiation responsive genes. Computational tools were then used to identify genes that showed a pronounced pattern of expression that correlated with low and high doses of ionizing radiation (IR). Pathway analysis suggested that chromatin structure, as well as transcription control, plays a large role in linking gene regulation to DNA damage and stress responses in humans for pathways associated with the TP53 (DNA damage) and NF- κ B (cell survival) signaling axes. The high degree of transcriptional variability was seen across individual samples irradiated both in vivo and ex vivo. Interestingly, as the dose increased, the level of transcriptional variation in these DNA damage signaling and cell survival pathways decreased, and was observed in multiple cell and tissue types. These results have led us to hypothesize that human population-level variation in the kinetics of chromatin modification and transcriptional regulation play a large role in understanding the low dose IR response curve across multiple tissue types. Thus, differences in the kinetics of DNA damage signaling and chromatin modification, and the subsequent upregulation of DNA repair may influence the susceptibility of individuals to low dose IR-induced carcinogenesis. This information will provide the basis for reducing the uncertainty of assessing risk at low dose levels for specific genes and pathways and may ultimately prove important for identifying susceptibility factors involved in individual responses to low dose IR. This work was performed under the auspices of the U.S. Department of Energy by Lawrence Livermore National Laboratory under contract DE-AC52-07NA27344 and supported by grant FWP SCW-0551 from the Low Dose Radiation Research Program.

(PS2.31) The effects of alpha particle radiation on gene transcripts associated with apoptosis in a human monocytic cell-line. Vinita Chauhan¹, Matthew Howland¹, James P. McNamee¹, Trevor J. Stocki¹, Trevor Burn², Lindsay A. Beaton², Ruth Wilkins¹, ¹Health Canada, Ottawa, ON, Canada, ²Carleton University, Ottawa, ON, Canada

Radon (²²²Rn) gas is a naturally occurring radioactive carcinogen which, in humans, accounts for more than forty percent of radiation exposure. When inhaled, ²²²Rn decays into products that pass into the lungs and emit alpha (α) particles. These α -particles can damage cells and may have the potential to induce lung cancer. An understanding of the mechanisms associated with these

carcinogenic effects remains limited. Apoptosis is a critical component of cellular homeostasis and dysregulation of this process can often lead to tumorigenesis. This study was designed to examine the effects of α -particle radiation on apoptosis and the associated changes in gene expression. Exponentially growing human monocytic cells (THP-1) were exposed to α -particle radiation at a dose range of 0-1.5 Gy. The expression of a focused panel of 84 genes related to apoptosis was analyzed for differential expression 72 h following α -particle radiation using real-time PCR. Concurrently, apoptosis was measured in these cells using flow cytometry by annexin V conjugate staining and a multi-caspase detection assay. A total of 15 genes were shown to be differentially expressed at all three doses tested and approximately 30% of the transcripts were shown to be upregulated. Among these genes, expression levels of two key initiators of apoptosis, tumour necrosis factor alpha (TNF α) and fas were markedly elevated ($p \leq 0.05$). The majority of the genes that were differentially expressed at all three doses were shown to be downregulated. Specifically, expression levels of transcripts associated with anti-apoptotic functions (BCL2, BCLAF1, IGFIR and BIRC2) were significantly downregulated by two fold ($p \leq 0.05$). These transcript modulations were correlated to increases in apoptosis as measured by flow cytometry using a multi-caspase detection kit and annexin V conjugate staining. On average, 35% of the cells were shown to be apoptotic at the highest dose of α -particle radiation tested relative to only 2% in the untreated controls ($p \leq 0.05$). This data suggests that α -particle radiation may induce apoptosis through the activation of TNF α and fas, and through the modulation of key anti-apoptotic genes.

(PS2.32) MicroRNA-21 involves radiation-promoted liver carcinogenesis. Yun Zhu¹, Xiaoyan Yu², Hanjiang Fu³, Hongyan Wang¹, Ping Wang¹, Xiaofei Zheng³, Ya Wang¹, ¹Emory University, Atlanta, GA, ²Jilin University, Changchun, China, ³Beijing institute of radiation medicine, Beijing, China

Ionizing radiation (IR) promotes carcinogenesis by affecting multi-pathways, but the whole picture remains unclear. MicroRNAs (miRNAs) involve multi-functions including carcinogenesis through posttranscriptional modification; however, there is no report to link miRNA and IR-induced carcinogenesis. Here we show that miR-21 (over-expressed in many different types of human cancer) is up-regulated in IR-promoted mouse hepatocellular carcinoma. IR stimulates miR-21 expression in human/mouse hepatocytes in vitro, and mouse liver tissues in vivo. Such stimulation depended on IR-induced up-regulation of AP-1 (at an earlier time, < 4 hours) and ErbB/Stat3 (at a later time, > 4 hours), which was also IR-dose-dependent (up to 5 Gy). We over-expressed miR-21 in human hepatocytes that were never exposure to IR, survived low-linear energy transfer (LET) IR (0.5 Gy) or survived high-LET IR (0.5 Gy), which resulted in these cells becoming tumorigenesis in mice. Interestingly, the size of the tumors derived from the cells survived low-LET IR was bigger and even bigger from the cells survived high-LET IR than that from non-irradiated counterpart. These results demonstrate for the first time that IR-induced up-regulation of miR-21 plays an important role in IR-promoted carcinogenesis and suggest that irradiated (especially high-LET) cells, provide an environment that facilitates miR-21-induced tumorigenesis. (This work is supported by the NASA grant NNX09AF24G).

(PS2.33) Kinetics of *in vivo* formation and reduction of γ H2AX in bone marrow cells after exposure of mice to 100 MeV/n protons. Paiboon Reungpatthanaphong¹, Louise Honikel¹, Marc Golightly¹, Carl A. Anderson², Kanokporn Rithidech¹, ¹Stony Brook University, Stony Brook, NY, ²Brookhaven National Laboratory, Upton, NY

Very little is known about the rate of production and loss of γ H2AX after *in vivo* exposure to radiation. To date, there is no information on the kinetics of *in vivo* formation and reduction of γ H2AX levels in bone marrow (BM) cells, the target for radiation-induced leukemia. Our research project is the first to fill in this knowledge gap. We gave BALB/cJ mice a whole-body exposure to 0.5 or 1.0 Gy of 100 MeV/n protons, delivered at 0.5 or 1.0 cGy/

min. For each dose and dose rate of 100 MeV/n protons, mice exposed to 0 Gy of protons served as sham controls. After irradiation, BM cells were collected at 1.5, 3, and 24 hr for analyses. There were four mice per treatment group per harvest time. We used a well-established flow cytometry method for determining the level of γ H2AX in each phase of the cell cycle of BM cells. For each mouse, at least 20,000 cells were analyzed. We incubated BM cells with antibody against mouse γ H2AX, Ser-139, followed by Alexa Fluor 488 (AF488, goat anti-mouse IgG) and propidium iodide (PI) to identify cells in different stages of the cell cycle. As an internal control, we also used PI to stain cells from each sample without AF488. At 1.5 hr post-irradiation, significant increases ($p < 0.05$, Student's t-test) in levels of γ H2AX were found in all phases of the cell cycle in BM cells collected from mice exposed to 1.0 Gy of 100 MeV/n protons, in relation to those in their corresponding sham controls, regardless of the dose rate. However, these increases were more pronounced when the higher dose rate, *i.e.* 1 cGy/min, was used. Subsequently, the levels of γ H2AX declined towards the level detected in non-irradiated cells within 24 hr. Further, the ability of BM cells to rejoin/repair damage was found to decrease when the dose rate increased, suggesting dose-rate effects of proton-irradiation. With respect to mice exposed to 0.5 Gy, there was no increase in γ H2AX levels in BM cells of exposed mice as compared to those found in sham controls at any time points included in the study, regardless of the dose rate. This finding may indicate that BM cells are capable of repairing/rejoining the damage induced by 0.5 Gy of 100 MeV/n protons delivered at these two low-dose rates and that the repair/rejoin processes completed before 1.5 hr post-irradiation (the first time point included in the study). Research funded by NASA Grant #NNX07AP88G.

(PS2.34) Evidence for a transgenerational transcriptome response to chronic low-dose irradiation in a medaka fish model system. Oleksandr Moskalenko¹, Dmytro Grygorovych², Thomas Hinton³, John D. Zimbrick⁴, ¹University of Minnesota, Minneapolis, MN, ²Oregon Health and Science University, Portland, OR, ³Savannah River Ecology Laboratory, Aiken, SC, ⁴Colorado State University, Fort Collins, CO

In this project one of our major goals is to understand how gene expression and DNA damage in a model organism, Japanese medaka fish (*Oryzias latipes*), change in response to low doses of gamma rays delivered continuously through a number of generations. Further, we seek to establish mechanistic relationships between these changes and cellular processes such as DNA repair. We have studied whole-body muscle tissue samples from medaka irradiated over four generations to obtain the data reported here. Fish specimens were irradiated at the Low-Dose Irradiation Facility (LoDIF) at the Savannah River Ecology Laboratory (SREL). Gene expression analysis and quantitation of DNA damages were carried out at Colorado State University (CSU). We performed large-scale transcriptional profiling using medaka oligonucleotide microarrays. The results of clustering, biological pathway, and gene ontology analyses as well as QPCR analyses of the selected transcripts will be presented. Out of 8048 transcripts corresponding to available microarray probes, over 2300 have shown significant changes over four generations of transgenerationally irradiated medaka with over 600 transcripts showing at least 2-fold changes at $p < 0.05$. Over 250 genes changed their expression between F0 and F1 generations; 137 transcripts from F0 to F2; 119 from F0 to F3; and 132 from F0 to F4. We have performed clustering and biological pathway analyses of these changes. We have also correlated these changes to the yields of DNA double-strand breaks (DSB) and oxidized base 8-hydroxyguanine (8-OHG) to postulate a hypothesis of adaptive organism response to chronic transgenerational low-dose irradiation. The authors are grateful to Dr. Ron Walter for kindly supplying the medaka microarrays for this study. This work was supported by DOE grant # DE-FG02-05ER64087 from the Low Dose Radiation Program.

(PS2.35) Low dose gamma-irradiation of C57Bl/6J mice *in vivo* does not modulate the rate of rejoining of DNA double strand breaks in splenocytes and thymocytes induced by subsequent high dose radiation. Rebecca R. Mantha¹, Melinda

S. J. Blimkie¹, Luke C. W. Fung², Dmitry K. Klovov¹, ¹AECL, Chalk River, ON, Canada, ²University of Waterloo, Waterloo, ON, Canada

Radioreistance induced by low dose ionizing radiation is known as radiation adaptive response. Enhancement of DNA repair processes is thought to be the main mechanism for radio-adaptation. In this study, we sought to determine whether low dose ionizing radiation, previously shown to induce a systemic adaptive response in mice, is capable of enhancing the rate of DNA double strand break repair. We used a phosphorylated form of histone H2AX (gammaH2AX), as a marker of DNA double strand breaks in chromatin. This marker is currently widely used due to its property to rapidly accumulate at sites of DNA double strand breaks and to disappear upon rejoining of a break. Female C57Bl/6J mice were sham- or gamma-irradiated with 2 or 10 cGy low dose radiation (⁶⁰Co) delivered at 1 mGy/min. Twenty four hours later, the mice were sacrificed and splenocytes and thymocytes were isolated and gamma-irradiated with 2 Gy. Expression of gammaH2AX was measured using Flow Cytometry and Immunoblotting at different time-points after the challenging irradiation up to 24 h. The resulting kinetics curves of formation and loss of gammaH2AX indicated that cells from low dose irradiated mice did not express more efficient DNA double strand break repair. These results indicate that radiation adaptive responses at systemic levels, such as increases in the tumour latency times in ageing mice previously demonstrated by our laboratory, are not necessarily mediated by modulated DNA repair, and that other mechanisms (e.g., modulation of the immune system) may be involved.

(PS2.36) Identification of DNA-PK phosphorylation targets in XRCC4 & XLF proteins and their physiological significance in the process of DNA double-strand break repair. Mukesh Kumar Sharma^{1,2}, Yoshihisa Matsumoto¹, ¹Tokyo Institute of Technology, Research Laboratory for Nuclear Reactors, Tokyo, Japan, ²Department of Zoology, R.L.S. Government (P.G.) College, Kaladera (Jaipur), India

DNA double strand break repair mechanism includes an error prone non homologous end joining repair pathway (NHEJ) and error free homologous recombination pathway (HR). In NHEJ repair DNA-PK is considered a pivotal enzyme and there are lines of evidence strikingly indicating that the catalytic activity to phosphorylate protein is essential for the repair function of DNA-PK. Nevertheless, it has remained to be elucidate which protein, and for what reason, should be phosphorylated by DNA-PK. In the present study, an attempt has been made to find the phosphorylation sites and the physiological significance of phosphorylation on XRCC4 and XLF proteins by DNA-PK. We identified four phosphorylation sites on XRCC4 and two phosphorylation sites on XLF. By the use of phosphorylation specific antibody we have observed that these phosphorylation sites in XRCC4 is found to be phosphorylated in living cells in response to ionizing radiation. To explore the biological significance we have mutated these phosphorylation sites into alanine and found that three of these phosphorylation sites might be important for DNA repair function, as loss of them lead to elevated radiosensitivity with deficient DNA repair capability. Altogether, these results would indicate that XRCC4 phosphorylation by DNA-PK is an essential event in NHEJ repair pathway of DNA double strand break. To analyze the biological importance of XLF phosphorylation further studies are currently under progress. These results are not only important to found a missing link in our understanding of DSB repair mechanism but also may provide us with a new therapeutic approach for the development of radiosensitizers in the cancer treatment and the prediction of radiosensitivity and cancer susceptibility, as will be discussed. Supported by Grant-in-Aid for Scientific Research from JSPS and MEXT, Japan. A part of this study is the result of "Study on Initiating Events in the Recognition and Repair of DNA Double-Strand Breaks" carried out under the Strategic Promotion Program for Basic Nuclear Research, MEXT, Japan.

(PS2.37) Plasma DNA reflects immediate tumor cell death after radiation. Lurong Zhang, Shaoqing Ju, Yansong Guo, Lei

Zhang, Mei Zhang, Bingrong Zhang, Shanmin Yang, Liangjie Yin, Steven Stwartz, Vidyasagar Sadasivan, Paul Okunieff, Department of Radiation Oncology, Gainesville, FL

Although radiation causes DNA strand breaks in a reliably dose-dependent manner, tumor cell killing is not easily measured. Hence the diversity of response and rate of cell kill can only be determined inaccurately by serial imaging studies. The problems associated with individualizing therapy therefore are significant. A major obstacle for realization of individualized radiotherapy is the lack of an appropriate biomarker to determine whether the cancer cells are responding in a fashion expected to lead to local control. In this study, the QuantiDNATM assay was used to determine whether plasma DNA from a finger stick collected at 9-12 hr intervals responded to irradiation. Plasma was collected before and after each fraction of IR (6 Gy X 11 fractions) in a patient with a localized malignant thymoma. The findings include: 1) at 24 hr (not 9 hr) after the 1st dose of IR, the plasma DNA was significantly increased from the basal level (3,183 vs 65 ng/ml). Previous results with total body exposure in rodents demonstrated a peak time in that system 9 hr after IR; 2) the elevated plasma DNA maintained or rose slightly 24 hr after 2nd dose of IR; 3) subsequently, despite continued irradiation, the plasma DNA level declined and returned again to basal level 24 hr after the 3rd IR dose; 4) subsequent doses of radiation did not again increase the circulating DNA. Serial imaging studies done using tomotherapy during the course of irradiation demonstrated tumor shrinkage. These results are consistent with early detection of tumor response to radiation and offer the potential of evaluation of tumor response at early time points in a course of therapy. The utility of measuring serial plasma DNA in patients undergoing irradiation include: a) monitoring tumor killing during treatment for the determination of tumor sensitivity; b) determine when the IR dose might be reduced, thereby reducing the risk of complication; and c) monitoring the tumor recurrence. All these deserve detailed studies.

(PS2.38) DNA damage checkpoint and DNA repair. Junjie Chen, The University of Texas M.D. Anderson Cancer Center, Houston, TX

The ability to sense DNA damage and activate responsive pathways that coordinate cell cycle progression and DNA repair is critically important for the maintenance of genomic stability and tumor suppression. A key component involved in this DNA damage response (DDR) is 53BP1. Studies from us and others have led to the conclusion that 53BP1 plays multiple roles in DNA damage checkpoint and DNA repair and contributes to tumor suppressor *in vivo*. However, the precise regulation and function of 53BP1 in DNA damage repair remains to be elucidated. We recently identified a PWWP domain-containing protein EXPAND1 as 53BP1-associated protein. EXPAND1 is an architectural component of the chromatin, which in response to DNA damage, serves as an accessory factor to promote cell survival. Depletion of EXPAND1 or inactivation of its PWWP domain resulted in chromatin compaction. Upon DNA damage, EXPAND1 rapidly concentrates at the vicinity of DNA damage sites via its direct interaction with 53BP1. Ablation of this interaction impaired damage-induced chromatin decondensation, which is accompanied by sustained DNA damage and hypersensitivity to genotoxic stress. Collectively, our study uncovers a chromatin bound factor that serves an accessory role in coupling damage signaling with chromatin changes in response to DNA damage.

(PS2.39) Interaction of PARP-1 and CDK5 in DNA damage response in neural cells following ionizing radiation. Xiaobing Tang¹, Minli Wang¹, Linlin Tian¹, Jackson R. Renegar², Chris K. Wang³, Huichen Wang¹, ¹Department of Radiation Oncology, Emory University School of Medicine, Winship Cancer Institute of Emory University, Atlanta, GA, ²George W. Woodruff School of Mechanical Engineering, Georgia Institute of Technology, Atlanta, GA, ³George W. Woodruff School of Mechanical Engineering, Georgia Institute of Technology, Atlanta, GA

Cyclin-dependent kinase 5 (CDK5) is a proline-directed serine/threonine cyclin-dependent kinase in postmitotic neuron and plays a critical role in neurogenesis. CDK5 also functions in proliferative neural cells and many tumor cells. Previous studies demonstrated that poly(ADP-ribose) polymerase 1 (PARP-1) is involved in repairing clustered DNA damage in neural cells exposed to high linear energy transfer radiation (LET) and low LET radiation. Here, we investigated the interaction of PARP-1 and CDK5 in radiation induced DNA damage response in an *in vitro* system based on cultures of mouse embryo neuronal progenitor cells (neurospheres) from PARP-1 knockout mice, mouse hippocampal neuronal cells and glioblastoma cells (U87 MG). We found that CDK5 inhibitor (roscovitine) can reverse the radiosensitivity of PARP inhibitor in neural cells exposed to X-ray, proton and iron radiation, but not in U87 MG cells using a clonogenic survival assay. Expression of dominant negative CDK5 significantly decreased radiosensitivity of hippocampal neurons and neural progenitors. PARP inhibitor increased radiation induced DNA damage and apoptosis in neural cells. These effects were abrogated when PARP inhibitor were combined with CDK 5 inhibitor or expression of dominant negative CDK5. CDK5 counteracted with PARP-1 in radiation induced p53 phosphorylation, ATM activation and glycogen synthase kinase-3 beta activity in neural cells, but not in glioblastoma cells. These suggest that CDK5 plays an opposite role in normal neural cells and glioblastoma cell, implicating a dual-edge sword in neural protection and tumor-killing. This work is supported by NASA space radiation program NNX08BA08G

(PS2.40) The dynamics of lymphocytes and p53 in the shortened lifespan by irradiation at a young age. Ryuji Okazaki¹, Yo Mabuchi², Yasuhiro Yoshida³, Sadafumi Suzuki², Ning Ding³, Yumi Matsuzaki², Akira Ootsuyama¹, Toshiyuki Norimura¹, ¹Department of Radiation Biology and Health, University of Occupational and Environmental Health, Kitakyushu, Japan, ²Department of Physiology, Keio University, Tokyo, Japan, ³Department of Immunology, University of Occupational and Environmental Health, Kitakyushu, Japan

Previously, we have been reported that irradiation at a young age induce delayed T-cell receptor mutation. In this study, we investigated the effect of exposure to radiation at a young age on lifespan, lymphocytes and p53 protein expression. At eight weeks of age, *p53^{+/+}* and *p53^{-/-}* mice were exposed a whole-body dose of 3Gy γ -rays. Kaplan-Meier survival analyses were used to test for significant differences. The cell numbers and cell cycle phases of bone marrow cells were determined by performing flow cytometric analysis. The proliferation of splenocytes was evaluated by modified MTT assay. Western blot analysis was performed to evaluate the expression of p53, p21 and MDM2. The lifespan of the irradiated mice was shorter than that of the non-irradiated mice. In the group of irradiated old mice, the number of lymphocytes in bone marrow decreased compared to that in the non-irradiated group. In old *p53^{+/+}* mice, the S and G2/M phases of lymphocytes in the irradiated mice were significantly increased compared to that in the non-irradiated mice. The proliferation of splenocytes in *p53^{+/+}* mice decreased with age, and the proliferation in the irradiated group was much lower than that in the non-irradiated group. In old *p53^{+/+}* mice after re-irradiation at 72 weeks of age, the protein expressions of p53, p21 and MDM2 in the irradiated group were delayed compared to those in the non-irradiated group. We suggest that the decrease of lymphocyte and the delayed response of p53 were related to shorten lifespan after irradiation at a young age.

(PS2.41) Tankyrase 1 influences telomeric recombination and stability of the NHEJ protein DNA-PKcs. Ryan C. Dregalla, Rupa R. Idate, Christine L. R. Battaglia, Junqing Zhou, Howard L. Liber, Susan M. Bailey, Colorado State University, Fort Collins, CO

Intrigued by the dynamics of the seemingly contradictory yet integrated cellular responses to the requisites of preserving telomere integrity while also efficiently repairing damaged DNA, we investigated roles of the telomeric PARP tankyrase 1 in telomere function and the DNA damage response. Utilizing siRNA

knockdown of tankyrase 1 in human cells, we found its reduction resulted in increased levels of telomeric recombination, specifically telomere sister chromatid exchange (T-SCE), in telomerase negative backgrounds. Consistent with defective DNA damage response, we also observed increased sensitivity to ionizing radiation-induced cell killing, mutagenesis and chromosome aberrations. Most unexpected however, was the finding that tankyrase 1 depletion also led to rapid reduction of DNA-PKcs protein levels, while Ku86 and ATM levels remained unchanged; DNA-PKcs mRNA levels were also unaffected. We demonstrate that depletion of tankyrase 1 results in rapid DNA-PKcs proteasome-mediated degradation, likely explaining the associated radiosensitivity phenotype. Our results also suggest that the requirement of tankyrase 1 for DNA-PKcs protein stability reflects the necessity of PARP enzymatic activity (PARsylation). While reciprocal interactions between PARP1 and DNA-PKcs have been reported, we provide the first evidence to our knowledge for tankyrase 1 - DNA-PKcs interaction, and in so doing reveal a novel aspect of DNA-PKcs regulation.

(PS2.42) The complexity of phosphorylated H2AX foci formation and DNA repair assembly at DNA double-strand breaks in mammalian cells. Asako Nakamura¹, Ashutosh V. Rao², Yves Pommier¹, William M. Bonner¹, ¹NIH/NCI/LMP, Bethesda, MD, ²FDA, Bethesda, MD

Upon DNA double-strand break (DSB) induction by ionizing radiation (IR), hundreds of molecules of multiple DNA damage response (DDR) protein species accumulate at DNA DSB sites forming foci known as ionizing radiation induced foci (IRIF). Phosphorylated H2AX (γ -H2AX) is a key component of numerous signaling pathways responsive to DNA DSBs. PI3 kinases, such as ATM, DNA-PKcs and ATR, phosphorylate H2AX rapidly after DNA DSB induction. The formation of hundreds of γ -H2AX molecules can be visualized as a large focus at the DNA DSB site. The γ -H2AX foci serve as sites of accumulation of DNA repair proteins and may also induce chromatin remodeling possibly to aid access of repair proteins to the DSB sites. Therefore the formation of γ -H2AX foci is critical for efficient DNA repair and for the maintenance of genome stability. Thus elucidating the structure of γ -H2AX foci is important in understanding the mechanism of DSB repair. To investigate the nature of γ -H2AX foci formation, we analyzed the distribution of γ -H2AX and other DNA repair proteins at DSB sites using a variety of techniques to visualize, expand and partially disrupt chromatin. Utilizing HeLa cells exposed to ionizing radiation, we examined the localization of γ -H2AX, 53BP1, NBS1, MDC1, and phosphorylated-BLM (pBLM). We showed that γ -H2AX foci change composition during the cell cycle, with proteins 53BP1, NBS1 and MRE11 dissociating from foci in G2 and mitosis to return at the beginning of the following G1. In contrast, MDC1 and pBLM remained colocalized with γ -H2AX during mitosis. In addition, when nuclei were swollen before fixation, γ -H2AX and MDC1 foci also became swollen, but 53BP1, MRE11, and NBS1 foci remained punctate. When metaphase chromosome spreads were prepared from HeLa cells after ionizing radiation exposure and immunostained for γ -H2AX and MDC1, MDC1 foci formed as doublets appearing to bracket the γ -H2AX foci. Interestingly, the MDC1 doublet foci appear to subdivide even further on swollen metaphase chromosomes. These observations agree with a model in which the 53BP1 and MRN complex concentrate near the DSB site, while MDC1 appears to be non-homogeneously distributed in the focus. Our data demonstrate that the DSB repair focus is a heterogeneous and dynamic structure containing internal complexity.

(PS2.43) Role of LATS1 in DNA damage signaling. Robert Latusek, Thomas Helleday, Eric O'Neill, University of Oxford, Oxford, United Kingdom

RASSF1A is a tumour suppressor epigenetically silenced in sporadic human malignancies. RASSF1A loss of function correlates with a decreased DNA-damaging therapy response. Re-expression of RASSF1A promotes cell cycle arrest and apoptosis. A key signaling pathway through which RASSF1A exerts DNA damage

response involves ATM dependent phosphorylation of on RASSF1A-Serine131 which leads to MST2 / LATS1 kinase activation resulting in subsequent stabilisation of a proapoptotic YAP1/p73 transcriptional complex. Additionally, as it was shown that a coding polymorphism in the ATM recognition site RASSF1A-A133S may result in greater chance of breast cancer development. LATS1 has been recently identified in a screen for factors regulating homologous recombination (HR) after DNA damage. LATS kinases are also documented regulators of cell cycle progression via restriction of cyclin dependent kinase (CDK) activity. Interestingly CDKs have also been observed to regulate the key HR proteins, BRCA2 and Rad51. Thus we wanted to investigate whether the finding of LATS1 in the HR screen is due to LATS-CDK binding and regulation of BRCA2-RAD51. Moreover, as RASSF1A regulates LATS1 in response to DNA damage, can RASSF1A regulate HR as a facet of its myriad of tumour suppressor effects. We have identified that activation of LATS1 in response to DNA damage promotes association with CDK2 which in turn prevents association with BRCA2. Preliminary evidence from cell based recombination assays suggests that RASSF1A and LATS1 indeed play a role in HR by restricting CDK function. References: • Esashi F, Christ N, Gannon J, Liu Y, Hunt T, Jasin M and West S (2005), CDK-dependent phosphorylation of BRCA2 as a regulatory mechanism for recombinational repair, Nature 434, 598-604 • Garth Hamilton, Karen Yee Simon Scrace and Eric O'Neil (2009), ATM regulates a RASSF1A-dependent DNA Damage Response, Current Biology 19, 2020-2025 • Matsuoka S, Ballif BA, Smogorzewska A, McDonald III R, Hurov KE, Luo J, Bakalarski CE, Zhao Z, Solimini N, Shiloh Y, Gygi SP, Elledge SJ (2007), ATM and ATR substrate analysis reveals extensive protein networks responsive to DNA damage, Science 316,1160-1166.

(PS2.44) A formulation of the multi-hit model with non-Poisson distribution of hits and an overview of its consistency with DNA strand break and cell survival data. Oleg N. Vassiliev, The University of Texas MD Anderson Cancer Center, Houston, TX

Recent advances in stereotactic radiotherapy have caused renewed interest in modeling of cell survival curves, especially at the relatively high radiation doses typically used for stereotactic radiotherapy. The multi-hit model has received little attention in this context, despite early work that found that the model was "adequate to explain most, if not all, experimental cell survival curves" [Fowler JF, Phys Med Biol 9:177-188, 1964]. We proposed a new formulation of the model with non-Poisson distribution of hits and tested this new formulation using DNA strand break and cell survival data. First, it was applied to calculate yields of DNA single and double strand breaks induced by protons and electrons as a function of particle energy. Parameters of the model were adjusted to match simulation data reported by Friedland et al. [Radiat Res 150:170-182, 1998; *ibid.* 159:401-410, 2003]. Then, survival curves generated with the model were compared with survival data for a range of lung cancer cell lines [Carmichael J, et al. Eur J Cancer Clin Oncol 25:527-534, 1989]. Finally, the model was tested for consistency with experimental data on variation of the initial slope of cell survival curves with radiation quality for a broad range of heavy-ion beams [Kase Y, et al. Radiat Res 168:629-638, 2006]. The new model performed well in all the tests. A better fit of survival curves was achieved with the new model than with the standard multi-hit model. The new model also correctly predicted, at least qualitatively, variation of radiation effects with radiation quality, such as reduction of the survival curve shoulder for high LET particles. Like the original multi-hit model, the proposed new model is conceptually very simple, and its parameters have a clear physical meaning.

(PS2.45) Recruitment of fanconi anemia and breast cancer proteins to DNA damage sites is differentially governed by replication. Lei Li, M. D. Anderson Cancer Center, Houston, TX

Fanconi anemia (FA) is a developmental and cancer-predisposition syndrome characterized by a cellular hypersensitivity

to DNA crosslinking agents. To date, it remains unclear how the Fanconi pathway protects cells from DNA crosslinking damage and whether Fanconi proteins act directly on crosslinks. In this report, we established a novel chromatin-IP strategy, termed eChIP, which may be broadly used to detect proteins at DNA lesions. Using this method, we detected the association of various FA proteins with DNA crosslink lesions in the context of DNA replication *in vivo*. Our results demonstrate that the FA core and FA I/D2 complexes are recruited to the sites of DNA crosslinks in a replication-independent fashion, while the recruitment of Brca-associated FA proteins, FANCD1/BRCA2, FANCI/BACH1/BRIP1, and FANCN/PALB2, relies on the ability of the crosslinked region to undergo DNA replication. Furthermore, the FA core complex is required for the recruitment of FANCD2 but not for that of FANCI and FANCN. The functional impact of the differential recruitment of FA proteins is reflected by the different levels of homologous recombination-independent repair of crosslinks between FANCD2 core and breast cancer-related FA mutants. These findings suggest that, in the face of DNA crosslink damage, components of the FA pathway may be involved in distinct response mechanisms governed by DNA replication status.

(PS2.46) Targeting BRCA1 localization to augment tumor cell susceptibility to poly (adp-ribose) polymerase-1 (PARP1) inhibition. Eddy S. Yang, Somaira Nowsheen, Fen Xia, Vanderbilt University, Nashville, TN

Purpose: Agents which target cancers deficient in DNA double strand break (DSB) repair, such as poly (ADP-ribose) polymerase-1 (PARP1) inhibitors, have gained recent attention due to their highly selective killing of BRCA-mutated familial breast and prostate tumors while maintaining minimal toxicity in normal tissues. However, the majority of sporadic breast and prostate cancers possess wild-type (WT) BRCA1 and maintain proficient DSB repair. In this study, we investigated whether the targeting of BRCA1 localization away from its nuclear repair substrates can transiently induce BRCA1 dysfunction in DSB repair, and thus subsequently augment sporadic breast and prostate tumor cell susceptibility to PARP1 inhibition. Methods: To generate a DSB repair defect, WT BRCA1 was targeted to the cytoplasm away from its nuclear repair substrates using irradiation (IR) or ectopic expression of the small peptide tr-BRCA1, a truncated form (1-301aa) of BRCA1 that can effectively shift BRCA1 to the cytosol. Immunohistochemistry for BRCA1 localization was performed following IR or tr-BRCA1 to confirm cytosolic BRCA1 redistribution. DSB repair capacity was assessed via a GFP-based repair assay. Cell survival as measured by colony formation assays was performed. The dependence on p53 was also investigated. Results: IR or ectopic tr-BRCA1 expression efficiently targeted BRCA1 to the cytosol and subsequently inhibited DSB repair by more than 3 fold compared to control in human breast and prostate cancer cells independent of cell cycle redistribution. Consequently, these cancer cells exhibited exquisite susceptibility to PARP1 inhibition (maximal 30 fold reduction in cell survival). Interestingly, the anti-tumor effects of PARP1 inhibition following IR were p53-dependent, while p53 was dispensable for PARP1 inhibition-mediated cell death following tr-BRCA1 expression. Conclusions: By transiently inducing a DSB repair defect via targeting BRCA1 localization away from its nuclear repair substrates, augmenting breast and prostate cancer cell susceptibility to PARP1 inhibitors can be an innovative strategy to enhance therapeutic index. Furthermore, this strategy may also be feasible for other tumor types, including lung, pancreas, and brain cancers.

(PS2.47) Role of *Mrad9b* in DNA repair. Corinne Leloup¹, Haiying Hang², Adayabalam Balajee¹, Kevin Hopkins¹, Howard Lieberman¹, ¹Columbia University, Center for Radiological Research, New York, NY, ²Chinese Academy of Sciences, Institute of Biophysics, Center for Computational and Systems Biology, Beijing, China

RAD9B was identified in our laboratory as a paralogue of the radiation resistance gene *RAD9*. To define *RAD9B* function, mice

and mouse embryonic stem (ES) cells with targeted *Mrad9b* deletion were constructed. *Mrad9b* is essential for embryonic development since *Mrad9b*^{-/-} embryos are resorbed after E7.5. Some of the *Mrad9b*^{+/-} embryos die between E12.5 and a few days after birth, and some display abnormal neural tube closure. *Mrad9b* is expressed primarily in the brain of WT mouse embryos. *Mrad9b*^{-/-} ES cells are sensitive to ionizing radiation, UV and mitomycin C treatment, as measured by clonogenic survival. Despite the observed sensitivity, cell cycle progression of *Mrad9b*^{-/-} cells was essentially similar to *Rad9b* proficient cells in response to gamma-rays exposure. We hypothesize that sensitivity of *Mrad9b*^{-/-} cells to the aforementioned DNA damaging agents is due to deficiencies in DNA repair. This supposition is strengthened by the fact that *RAD9* plays an active role in several DNA repair pathways, including base excision repair, homologous recombinational repair and mismatch repair. To test our hypothesis, we have begun experiments to evaluate the role of *Mrad9b* in several DNA repair pathways important for repair of DNA damage caused by exposure to gamma-rays, UV or mitomycin C, such as recombination repair, base excision repair and nucleotide excision repair. Results of our ongoing studies will be presented.

(PS2.48) The effects of acute dose charge particle radiation on expression of DNA repair genes in mouse. Nader Pourmand¹, Muhammad A. Tariq², Shishir Shishodia², Ayodotun Sodipe², Govindarajan Ramesh³, Honglu Wu⁴, Zhang Ye⁵, Olufisayo A. Jejelowo², ¹Dept. of Biomolecular Engineering, University of California Santa Cruz., Santa Cruz, CA, ²Center for Bionanotechnology and Environmental Research, Texas Southern University, Houston, TX, ³Department of Bioiogy, Norfolk State University, Norfolk, VA, ⁴NASA Johnson Space Center, Houston, TX, ⁵NASA Johnson Space Center, Houston, TX

The space radiation environment consists of trapped particle radiation, solar particle radiation and galactic cosmic radiation (GCR) in which protons are the most abundant particle type. During missions to the Moon or to Mars, the constant exposure to GCR and occasional exposure to particles emitted from solar particle events (SPE) are major health concerns for astronauts. Therefore, in order to determine health risks during space missions, an understanding of cellular response to proton exposure is of primary importance. The expression of DNA repair genes in response to ionizing radiation (x-rays and gamma-rays) has been studied, but data on DNA repair in response to protons is lacking. Using qPCR analysis, we investigate changes in gene expression induced by positively charged particles (protons) in four categories (0 Gy, 0.1 Gy, 1.0 Gy and 2.0 Gy) in nine different DNA repair genes isolated from the testes of irradiated mice. DNA repair genes were selected on the basis of their known functions. These genes include ERCC1 (5' incision subunit, DNA strand break repair), ERCC2/NER (opening DNA around the damage, Nucleotide Excision Repair), XRCC1 (5' incision subunit, DNA strand break repair), XRCC3 (DNA break and cross-link repair), XPA (binds damaged DNA in preincision complex), XPC (damage recognition), ATA or ATM (activates checkpoint signaling upon double strand breaks), MLH1 (post-replicative DNA mismatch repair) and PARP1 (base excision repair). Our results demonstrate that ERCC1, and PARP1 and XPA genes showed no change at 0.1 Gy radiation, up-regulation at 1.0 Gy radiation (1.09 fold, 7.32 fold, 0.75 fold respectively) and remarkable increase in gene expression at 2.0 Gy radiation (4.83 fold, 57.58 fold and 87.58 fold respectively). Expression of other genes, including ATM and XRCC3 was unchanged at 0.1 Gy and 1.0 Gy radiation but showed up-regulation at 2.0 Gy radiation (2.64 fold and 2.86 fold respectively). We were unable to detect gene expression for the remaining four genes (XPC, ERCC2, XRCC1 and MLH1) in either the experimental or control animals from 0.1 to 2.0 Gy proton radiation.

(PS2.49) High-throughput screens for small molecule inhibitors of DNA mismatch repair and novel repair-associated genes. Nicholas M. Pedley, Thomas Helleday, Gray Institute for Radiation Oncology & Biology, University of Oxford, Oxford, United Kingdom

The exploitation of tumour genetic abnormalities through the drugging of synthetic lethal targets has been shown to be an effective and selective new therapeutic strategy in the treatment of cancer. Defects in one or more DNA repair pathways have been shown to be a common feature of cancer, whilst loss of function mutations in 'stability' genes that normally maintain the integrity of the genome are likely a key rate-limiting step in carcinogenesis. Since even genetically unstable cells require some repair functionality to maintain viability, these cancers probably exhibit an over-reliance on other DNA repair pathways. An in-depth knowledge of the genetic basis of repair processes in combination with a suite of DNA repair inhibitors to knock out these backup pathways may therefore prove extremely useful tools in the development of the next generation of cancer chemotherapeutics. To this end, we present the results of a small molecule high-throughput screen to detect novel inhibitors of the DNA mismatch repair (MMR) pathway, together with results of a small interfering RNA (siRNA) screen for novel MMR-associated genes. Key to both screening strategies are the resistance of cells with a dysfunctional mismatch repair pathway to a range of cytotoxic drugs, including the alkylating agent N-methyl-N'-nitro-N-nitrosoguanidine (MNNG). By exploiting this MMR-dependent toxicity we have assayed for small molecules and siRNA that permit the survival of MNNG-treated MMR-proficient cells to levels comparable to MMR-deficient cells, and which therefore represent putative MMR modulating agents. Specific MMR activity assays that monitor the repair of a G:T mismatch in nuclear extracts and live cells were subsequently applied to verify our screen results. In summary, we are presenting small molecule structures that inhibit MMR activity in Human cells, together with the identification of novel genes that are involved in the MMR DNA repair pathway.

(PS2.50) Investigating the interplay between TGFbeta and ATM in the DNA damage response. Jennifer Anderson¹, Francis Cucinotta², Peter O'Neill¹, ¹University of Oxford, Oxford, United Kingdom, ²NASA Lyndon B. Johnson Space Center, Houston, TX

It is believed that crosstalk occurs between the ATM and TGFbeta signal transduction pathways. Both pathways are essential for cellular and tissue control responses to ionizing radiation (IR) and aberrant modifications to these pathways are extensive in cancer. We hypothesize that the ATM and TGFbeta signaling pathways are fully induced at high doses of acute low-LET radiation, whereas only partially induced at low doses. The aim is to investigate the effect of radiation quality on modulating the crosstalk between these pathways and the consequences for repair of DNA double strand breaks (DSB), the formation of which activates ATM. In rat fibroblast cells we have previously shown that addition of exogenous TGFbeta or low dose gamma- or alpha-radiation triggers intracellular signalling causing translocation of Smad1/2/3 from the cytoplasm to the nucleus. We now show using immunofluorescence that in human breast epithelial cells (MCF10A) irradiated with either high-LET 28Si heavy ions (150 MeV/n) or low-LET gamma-radiation the levels of nuclear Smad 1/2/3 increase up to 24 h after irradiation, consistent with perturbation of TGFbeta signaling in human cells. The percentage of MCF10A cells with nuclear Smad 1/2/3 is however decreased on inhibition of ATM, suggesting that cross-talk between the ATM and TGFbeta signal transduction pathways may be independent of radiation quality. Using gammaH2AX foci as a marker for DSB and RAD51 as a marker for homologous recombination, we observe that the levels of gammaH2AX and RAD51 foci numbers return to background levels by 24 h following irradiation with gamma-rays (2 Gy) or 28Si heavy ions (1 Gy) but interestingly they both remain high even 24 h after exposure to alpha-particles. These preliminary findings indicate that IR leads to perturbation of TGFbeta levels with potential crosstalk with ATM at the DNA damage level. The differences observed between 28Si ions/gamma-rays and alpha-particles will be explored in relation to DNA damage complexity and radiation dose.

(PS2.51) Functional relationship between Nbs1 and Ku70 in cellular responses to DNA damage. Hiroshi Tauchi¹, Maki

Ohara¹, Aya Tanaka¹, Kenta Iijima¹, Hiroko Abe¹, Kenshi Komatsu², Junya Kobayashi², ¹Ibaraki University, Mito, Ibaraki, Japan, ²Kyoto University, Kyoto, Japan

NBS1 is the protein responsible for the Nijmegen breakage syndrome in which patients display a predisposition for cancer, chromosomal instability, and hypersensitivity to ionizing radiation. NBS1 is known to form a complex with MRE11 and RAD50, and it regulates the precise and accurate repair of damaged DNA through homologous recombination. We reported that NBS1 regulates a p53-independent apoptotic pathway which responds to DNA damage induced by radiation. This p53-independent pathway is activated through the dissociation of the Ku70-Bax complex, which depends on the acetylation of Ku70 in the presence of NBS1. Phosphorylation of NBS1 at the 343-serine residue was essential for this function, whereas the FHA, MRE11-binding, or the ATM interacting domains were not essential for the activation of the apoptosis. The kinase responsible for this NBS1 phosphorylation step could conceivably be ATR because ATR inhibitors suppressed NBS1 phosphorylation at times when apoptosis was occurring, but an ATM inhibitor did not. This was further confirmed by our observation that ATR-Seckel syndrome cells display an apparent delay in apoptosis induction following DNA damage induced by radiation. Thus NBS1 and Ku70 competitively regulate DNA damage responses, not only DNA double strand break repair, but also the induction of apoptosis. To obtain insights into the nature of the functional link between NBS1 and Ku70 in responding to DNA damage, we tried to establish an Nbs1/Ku70 double knockout cell line in chicken DT40 cells. Surprisingly, Nbs1/Ku70 double knockout cells were viable, although they showed a significant delay in cell proliferation, and an extremely high incidence of chromosome aberrations. In this presentation, we will present a summary of the phenotypes of the Nbs1-Ku70 double knockout cells, and will discuss the functional link between NBS1 and Ku70 in DNA damage responses induced by ionizing radiation. Acknowledgements: We are grateful to Dr. Penny A. Jeggo for providing ATR-Seckel cells. This work was supported by the Ministry of Education, Science, Sports and Culture of Japan (HT).

(PS2.52) Search for novel inhibitors of homologous recombination. Sophia B. Chernikova, Rochelle B. L. Nguyen, Jessica T. Truong, J. Martin Brown, Stanford University, Stanford, CA

Homologous recombination (HR) is an important pathway of DNA double-strand break (DSB) repair. Due to the requirement for an identical copy of the broken DNA, most of HR repair occurs in the late phases of the cell cycle. Tumors usually have a high percentage of cycling cells and consequently higher fraction of cells in S/G2, therefore inhibition of HR would lead to a significant therapeutic gain, sparing the non-dividing or slowly dividing normal tissues responsible for the dose-limiting late effects following radiotherapy. We conducted a high-throughput screen of ~130,000 compounds to identify small-molecule inhibitors of HR. The screening strategy was as follows: we first looked for the small-molecule compounds that would potentiate the effect of chlorambucil, as this bifunctional alkylating agent produces lethal DNA interstrand crosslinks that require HR for their resolution. These compounds then were tested in gene conversion assay and we are currently testing the hits in radiation sensitivity and Rad51 foci formation assays.

(PS2.53) The role of protein phosphatase 6 catalytic subunit (PP6c) in regulating DNA-dependent protein kinase (DNA-PK) activity. Nicholas Valerie, Jaroslaw Dziegielewski, Amol Hosing, David L. Brautigan, James M. Larner, University of Virginia, Charlottesville, VA

A principal factor in human glioma radioresistance is the up-regulation of DNA double strand break (DSB) repair pathways. DNA-PKcs plays a key role in non-homologous end joining (NHEJ) and V(D)J recombination by binding to the ends of DSBs, thereby facilitating repair. DNA-PKcs contains numerous phosphorylation sites, which regulate DNA end processing (ABCDE and PQR clusters), as well as enzymatic activity (T2609, T3950). Phosphatases

are promiscuous enzymes which regulate many critical cellular functions, including the DNA damage response. Recently, our group has found that protein phosphatase 6 (PP6) interacts with DNA-PKcs. PP6 is a heterotrimeric protein composed of a catalytic subunit (PP6c), a regulatory subunit termed SAPS for Sit-4 associated protein (R1, R2, R3), and an ankyrin repeat subunit scaffold (ARS A, B, C). We have previously reported that PP6 interacts directly with DNA-PK and that PP6 is required for activation of DNA-PK post-IR. However, the mechanism by which PP6 regulates DNA-PK is still unknown. To determine whether PP6 catalytic activity and/or binding is necessary for radiation-induced activation of DNA-PK, we generated a catalytically inactive PP6c (H114N) mutant and several deletion mutants. HEK293 cells transiently transfected with mutant PP6c showed increase in radiosensitivity as compared to cells transfected with a wild-type PP6c construct. In addition, the catalytically inactive PP6c demonstrated decreased association with DNA-PKcs. Comparisons of IR-stimulated DNA-PK activity in glioma cells transfected with epitope-tagged PP6c (H114N) versus WT PP6c, as well as repair of DSBs measured using a unique fluorescence-based DNA repair assay in cells through FACS and qPCR analysis, will be presented.

(PS2.54) Low energy electron (LEE)-induced DNA damage: Formation of 5,6-dihydrothymine upon irradiation of TTT oligonucleotide trimer. Yeunsoo Park, Zejun Li, Pierre Cloutier, Léon Sanche, J. Richard Wagner, Université de Sherbrooke, Sherbrooke, QC, Canada

The interaction of low energy electrons (LEE, 0-20 eV) with elemental DNA components (e.g., nucleobases, deoxyribose, and phosphate), nucleosides, nucleotides, and oligonucleotides, leads to the stimulated desorption of several primary radicals and ions (<100 a.m.u.) from the surface of solid targets under ultra high vacuum (UHV). These studies have demonstrated that LEEs induce the formation of transient anions that dissociate into highly reactive neutral and anion radicals by dissociative electron attachment (DEA). To further understand the mechanism of LEE-induced DNA damage, our group has focused on the chemical analysis of products that remain on the surface of irradiated films of DNA model compounds. These studies reveal that LEEs induce cleavage of the N-glycosidic bond, leading to base release, and cleavage of the phosphodiester bond, leading to the release of fragments bearing an intact terminal phosphate group. These pathways, which are supported by theoretical studies, represent about 1/3 of the total damage remaining on the surface of irradiated targets. In the present study, we address the identification of the other products (2/3) consisting of unknown products. For these experiments, oligonucleotide trimer (TTT) was irradiated in the solid state under UHV with 10 eV electrons (constant electron beam flux $5.3 \mu\text{A} = 3.3 \times 10^{13}$ electrons/s). Post-irradiation of the films revealed several modifications of TTT that eluted between TT and TTT in reversed phase HPLC analysis. These products were subsequently identified as the sequence isomers of XTT, TXT, and TTX, where X=5,6-dihydrothymine, as inferred by HPLC coupled to tandem MS and comparison with synthetic standards. Presently, we are examining the mechanism of LEE-induced formation of 5,6-dihydrothymine using targets containing deuterium at specific positions of the target. These recent results point to novel pathways of damage in the mechanism of LEE-induced DNA damage.

(PS2.55) Spatio-temporal investigations of DNA damage repair following low LET radiation. Giuseppe Schettino¹, Kieran Savage¹, Luca Mariotti², Derek Richard³, Kevin Prise¹, ¹CCRCB, Belfast, United Kingdom, ²University of Pavia, Pavia, Italy, ³Queensland Institute of Medical Research, Brisbane, Australia

It is widely accepted that the biological effectiveness of ionizing radiation is determined by the ionization distribution (i.e. track structure) produced inside individual cells. However, the spatiotemporal organization of the repair proteins involved in the complex network and feedback loops of the DNA repair process to such damage distributions has still to be determined together with its relevance for the overall cellular response. Moreover, there is

significant debate concerning the possible short and long distance movement of damaged chromatin domains and its impact on the cell DNA repair efficiency. Single-cell approaches and high spatial resolution (such as those offered by microbeams) provide the perfect tool to study and quantify the dynamic processes associated with the induction and repair of DNA damage. We have followed the development of radiation induced foci for three DNA damage markers (i.e., γ -H2AX, 53BP1 and hSSB1) using normal fibroblasts (AG01522), human breast adenocarcinoma cells (MCF7) and human fibrosarcoma cells (HT1080) stably transfected with GFP fusion proteins. Samples have been irradiated with either conventional 225keV broad beam X-rays, the QUB X-ray microbeam (carbon X-rays $<2 \mu\text{m}$ spot) or single α -particles from an Am^{241} source. α -particle exposures were performed at a shallow incident angle allowing monitoring of the individual foci behaviour along the particle track. Position, size and intensity of the foci has been analysed as a function of dose and time post irradiation in order to investigate the dynamics of the above mentioned DNA repair processes and monitor the remodelling of chromatin structure that the cell undergoes to deal with DNA damage. Comparison of the spatiotemporal behaviour of the foci for the three different irradiation scenarios will also provide critical information on the effect of the LET and the clustering of ionizations.

(PS2.56) PTEN loss compromises homologous recombination repair in astrocytes: implications for GBM therapy with temozolomide or PARP inhibitors. Brian McEllin, Cristel Camacho, Nozomi Tomimatsu, Bipasha Mukherjee, Robert Bachoo, Sandeep Burma, UT Southwestern, Dallas, TX

Glioblastoma multiforme (GBM) are lethal brain tumors that are highly resistant to therapy. The only meaningful improvement in therapeutic response came from use of the $\text{S}_{\text{N}}1$ -type alkylating agent, temozolomide, in combination with ionizing radiation (IR). However, no genetic markers that might predict a better response to DNA alkylating agents have been identified in GBMs except for loss of MGMT *via* promoter methylation. In this study, using genetically defined primary murine astrocytes as well as human glioma lines, we show that loss of PTEN confers sensitivity to MNNG, an analog of temozolomide. We find that MNNG induces replication-associated DSBs that are poorly repaired in PTEN-null astrocytes and trigger apoptosis. Mechanistically, this is because PTEN-null cells are compromised in homologous recombination (HR) that is important for the repair of replication-associated DSBs. Our results suggest that reduced levels of Rad51 paralogs in PTEN-null astrocytes might underlie the HR deficiency of these cells. Importantly, the HR deficiency of PTEN-null cells renders them sensitive to the PARP inhibitor ABT-888 due to synthetic lethality. In sum, our results tentatively suggest that GBMs with PTEN loss (about 36%) might specifically benefit from treatment with DNA alkylating agents such as temozolomide. Significantly, these results also provide a rational basis for treating PTEN-deficient GBMs with novel PARP inhibitors that are currently in clinical trials for treating HR-deficient breast and ovarian cancers.

(PS2.57) Expression patterns of DSB repair-related genes in Arabidopsis seedlings after the irradiation. Masanori Hatashita, Keiichi Takagi, The Wakasa-wan Energy Research Center, Turuga, Japan

Double-strand breaks (DSBs) are one of the most serious forms of DNA damage that can occur in a cell's genome. DSBs in DNA, which can occur spontaneously in the cell or be induced experimentally by irradiation, represent one of the most serious threats to genomic integrity. There are two major pathways for DSB repair: homologous recombination (HR) uses an intact copy of the damaged region as a template for repair, whereas non-homologous end-joining (NHEJ) rejoins DNA ends independently of DNA sequence. NHEJ rather than HR is the major pathway for repair of DSBs in organisms with complex genomes, including plants. Rejoining of DSBs introduced in DNA damage is catalyzed by DNA ligase enzymes. A strong interaction between DNA ligase IV and XRCC4 was found in human cells. DNA ligase IV catalyses the

final step in the NHEJ pathway of DSB repair. In the present study, the transcript profiles of an Arabidopsis thaliana homologue (AtLIG4) of human DNA ligase IV and an Arabidopsis thaliana homologue (AtXRCC4) of human XRCC4 following irradiation were determined by RT-PCR.

(PS2.58) Inhibition of transforming growth factor β radiosensitizes 4T1 murine mammary tumors in vitro and in vivo. Sophie F. Bouquet, Karsten Pilones, Sandra Demaria, Mary Helen Barcellos-Hoff, NYU Medical Center, New York City, NY

Ionizing radiation (IR) triggers activation of transforming growth factor $\beta 1$ (TGF β), a cytokine implicated in regulation of cell cycle and apoptosis. Previously, our lab has shown that either genetic or pharmaceutical TGF β inhibition prior to IR inhibits the DNA damage response (DDR) in epithelial cells via blockade of ATM kinase activity (*Cancer Res* 62:5627, 2002; *Cancer Res* 66:10861, 2006). If cancer cells are similarly regulated, then TGF β inhibition could improve the therapeutic effect of radiotherapy (RT). We used the highly metastatic 4T1 mouse mammary carcinoma model to evaluate the impact of TGF β inhibition on the response to radiation in vitro and in vivo. In vitro, 4T1 cells were radiosensitized, as shown by clonogenic assay, following inhibition of TGF β type I receptor kinase with a small molecule inhibitor or with a monoclonal pan-specific TGF β neutralizing antibody, 1D11. For in vivo evaluation, 4T1 cells were injected s.c. in the flank of syngeneic mice and were treated when tumors became palpable 13 days later. Mice were randomly assigned to four groups receiving control isotype monoclonal antibody (mAb), 5 mg/kg 1D11, local RT and isotype mAb, or RT and 1D11. Antibodies were administered 24 h prior to the radiation treatment and 3 mice were sacrificed 1 h after RT of 8 Gy for $\gamma\text{H2A}\xi$ immunostaining, as an index of ATM kinase activity. $\gamma\text{H2A}\xi$ foci were reduced in irradiated tumors treated with 1D11 compared to irradiated tumors treated with isotype control mAb. Consistent with reduction of DDR, tumor growth delay was reduced in RT- and 1D11-treated mice (7 d) compared to mice unirradiated and compared to RT and isotype mAb (2 d). 1D11 alone had no significant impact on tumor weight at the time of experiment termination, which suggests that the TGF β inhibition and RT are synergistic. Increased radiosensitivity of 4T1 tumor cells in vitro and in vivo supports the use of TGF β inhibitors as means to increase the response to RT, in addition to potential benefit of promoting radiation-induced anti-tumor immunity (see abstract by Pilones et al, this meeting). Supported by funding from the NYU Cancer Center and 1D11 provided by Genzyme, Inc.

(PS2.59) DinB protein from the extremely radioresistant bacterium Deinococcus radiodurans. Sangyong Lim, Dusho Song, Minhjo Joe, Dongho Kim, Korea Atomic Energy Research Institute, Jeongeup, Republic of Korea

Deinococcus radiodurans is a bacterium best known for its extreme radioresistance to both acute and chronic exposure of high levels of ionizing radiation. The secret behind its incredible radioresistance lies in its ability to repair double strand breaks in its DNA. However, the molecular mechanisms underlying this phenotype are still poorly understood. In order to reveal proteins involved in the extreme radioresistance and DNA repair in *D. radiodurans*, we examined proteome changes in a wild type strain following γ -irradiation (10 kGy) using two-dimensional polyacrylamide gel electrophoresis. The expression levels of 13 protein spots showed significant changes under radiation stress. Among 8 up-regulated proteins, SSB (single-stranded DNA binding protein), PprA (DNA damage repair protein), DdrA (DNA damage response A), DdrD (DNA damage response D), and DinB (damage inducible protein) are presumably involved in the DNA repair process. Of these spots, we investigated the expression and function of DinB in detail. The expression of *dinB* promoter was activated by irradiation, which means that the radiation induction of DinB occurs at the transcriptional level primarily. Western blot analysis showed that the mutation in *ppr1* or *recA*, which encode regulatory proteins responsible for extreme radioresistance of *D. radiodurans*,

completely abolished the production of DinB, suggesting DinB is likely to be involved in DNA damage repair and protection pathways in response to DNA damage. A *dinB* null mutant was constructed using a deletion replacement method. As expected, the mutant exhibited higher sensitivity to other DNA damaging agents, such as UV and mitomycin C (MMC), as well as, irradiation with gamma rays. These results would be useful to progress in understanding of the mechanisms underlying radiation resistance of *D. radiodurans*.

(PS2.60) Intrinsic radiosensitivity correlated with radiation induced ROS and cell cycle regulation. Cha Soon KIM, Yong-Woo Jin, Ki Moon Seong, Seong Youg Nam, Kwang Hee Yang, Ji-Young Kim, Radiation Health Research Institute (KHNP), Seoul, Republic of Korea

Purpose: Ionizing radiation (IR) can induce multiple cellular responses which determine the fate of cells, including chromosomal aberrations, genetic mutations, cell cycle arrest, apoptosis, and cell differentiation. IR also enhances the production of reactive oxygen species (ROS) in a variety of cells, causing DNA damage and activating several proteins involved in the DNA repair system. The balance between DNA damage and repair is a key determinant of intrinsic radiation sensitivity. Method: We investigated the survival rate in different types of cell lines (HUVEC, Bud-8, CCD-18Lu and Jurkat) after irradiation at various doses of γ -radiation, and compared the radiation-induced ROS generation with cell viability. We also measured micronuclei frequency in the irradiated cells in order to verify the cytogenetic analysis by radiation. In addition, we analyzed the cellular level of several proteins related to the cell cycle in order to characterize the correlation between the intrinsic radiosensitivity and cell cycle regulation. Major findings: We found that the intrinsic viability of irradiated cells was correlated with the radiation-induced ROS production as well as the function of the organ of origination. We also observed increased cell cycle protein expression in radiation-sensitive cells compared to radiation-resistant cells. Conclusion: These results suggest that intrinsic cellular sensitivity to irradiation is dependent on ROS generation and cell cycle regulation.

(PS2.61) The comparison of bromodeoxyuridine (BrdU)-mediated sensitization effects between low-LET and high-LET ionizing radiation. Yoshihiro Fujii¹, Takamitsu Kato², Akira Fujimori³, Kiyoshi Miyagawa¹, Ryuichi Okayasu³, Ohtsura Niwa³, ¹The University of Tokyo, Tokyo, Japan, ²Colorado State University, Fort Collins, CO, ³National Institute of Radiological Sciences, Chiba, Japan

The exact mechanism of complex DNA damages produced after heavy charged particles is not known. The incorporation of halogenated pyrimidines such as bromo-, and iodo-deoxyridines (BrdU, IdU) into DNA as thymidine analogs enhances the cellular radiosensitivity. We studied radiosensitization effects of halogenated pyrimidines to high Linear Energy Transfer (LET) heavy-ions. Cells synchronized into G1-phase after unifilar (10h) and bifilar (20h) substitution with 10 μ M BrdU were exposed to various LET of heavy-ions and X-rays. We tested the colony formation assay to measure cell survival. DNA double strand break formation and repair were measured by γ -H2AX focus formation assay. Chromosome aberration formation for first post irradiation metaphase was also analyzed. For low-LET X-rays and carbon-ions (13keV/ μ m), BrdU incorporation led the impaired DNA repair kinetics, more initial number of DNA double strand breaks (DSBs), chromosome aberrations at first post-irradiated metaphase, and higher cellular radiosensitivity. The enhancement ratio was higher after bifilar substitution. In contrast, no such synergistic enhancements were observed after high-LET carbon-ions and iron-ions (70 and 200keV/ μ m, respectively) even after bifilar substitution. Our results suggested that incorporation of halogenated pyrimidines may lead to produce complex and clustered DNA damages along with radicals formed by low-LET ionizing radiations. On the other hand, the least radiosensitization effects for high-LET radiation may be explained that it has already produced such damages and no

synergistic biological effects were added. Elucidating the nature of complex DNA damages after high LET radiation should be very useful to produce better methods of radiotherapy for clinical and radioprotection for astronauts from galactic heavy-ions.

(PS2.62) Comparison of Liver Response After Proton Versus Electron Irradiation in a Mouse Model. Daila S. Gridley¹, Michael J. Pecaut¹, Erben J. M. Bayeta¹, Jian Tian¹, Andrew J. Wroe¹, Steve Rightnar¹, Ann R. Kennedy², James M. Slater¹, ¹Loma Linda University & Medical Center, Loma Linda, CA, ²University of Pennsylvania school of Medicine, Philadelphia, PA

Purpose: Protons and electrons are different forms of ionizing radiation particles which have low-linear energy transfer (low-LET). The purpose of this study was to determine whether protons and electrons differ in their effects on the liver when delivered to the same physical dose. Materials and Methods. Male ICR mice (n = 45) were used at 7-10 weeks of age. At the LLU Medical Center, non-anesthetized animals were placed individually into polystyrene aerated cubicles and irradiated to a total dose of 2 Gy in a single fraction at dose rates of 0.5 Gy/min (protons) and 3 Gy/min (electrons). Fully modulated 70 MeV protons and 21 MeV electrons were delivered with a field flatness of +/-7% and +/-2%, respectively, and a depth dose uniformity of +/-2%. Sham-irradiated controls were included. Euthanasia was performed in 100% CO2 approximately 36 hours post-exposure and a portion of livers were quick frozen to quantify expression of 84 oxidative/antioxidative stress genes using RT-PCR. Another portion of livers was used to determine oxidative burst capacity in response to a yeast preparation (Zymosan A). Immunohistochemistry is in progress. Results. Gene expression patterns were strikingly different for the proton and electron groups when compared to 0 Gy controls. The significantly modified genes (p<0.05) are summarized here. For the proton-irradiated group, there were 10 up-regulated genes (Ctsb, Dnm2, Gpx5, Il19, Il22, Kif9, Lpo, Ox4, Park7, Rag2) and 1 down-regulated gene (ApoE). For the electron-irradiated group, there were 16 up-regulated genes (Aass, Ctsb, Dnm2, Gpx1, Gpx4, Gpx5, Gpx6, Il22, Kif9, Lpo, Nox4, Park7, Prdx3, Prdx4, Prdx5, Rag2) and 1 down-regulated gene (Mpp4). There was a strong trend for a main effect of group on oxidative burst capacity (p = 0.055), likely due to slightly decreased levels for both irradiated groups versus 0 Gy. Post-hoc comparison of proton versus electron groups resulted in p = 0.055. Conclusions. The data show that oxidative stress-related gene expression profiles in liver were dependent on the form of radiation used and there was a strong trend for difference in oxidative burst capacity between the two irradiated groups. Although difference in dose rate cannot be ruled out, the data suggest that at least some biological effects induced by electrons cannot be extrapolated to protons.

(PS2.63) Normal human fibroblasts and keratinocytes are expressing distinct isoforms of the human Histone Acetyltransferase 1 (Hat1). Stefan T. Tafrov, Brookhaven National Laboratory, Upton, NY

Human Hat1 was isolated as an enzyme responsible for acetylating histone H4 molecules destined for deposition on newly synthesized DNA molecules during replication. Hat1 is known to participate in several other processes, including interactions with the origin recognition complex, transcriptional silencing, and DNA repair. Diverse protein isoforms seemingly support this breadth of Hat1's functions. The "AceView" annotation database (www.ncbi.nlm.nih.gov/IEB/Research/Acembly/index.html/ext-link) predicts the possible expression of four "very good" and six "good" human Hat1 protein variants. The alternative splicing databases (www.euraxnet.info/tools/asdatabases) identify at least nine possible alternative splicing mRNA isoforms originating from the human Hat1 gene. Some utilize alternative start and stop codons, and some result from skipping internal exons. To analyze these Hat1 protein isoforms, I undertook subcellular protein fractionation followed by western blotting analyses. The protein extracts from normal human keratinocytes (NHKs) and fibroblasts (NHFBs) were prepared according to protocol for nuclear matrix isolation. Briefly,

the cells were permeabilized with 0.5 % triton-X-100, and cytosolic- and soluble nuclear-proteins were collected. Digesting the cellular DNA with DNase I isolated the chromatin-associated proteins. The remnants of the cells first were extracted with 0.25 M ammonium acetate, and then with 2 M NaCl. The remaining insoluble nuclear-matrix proteins were solubilized in 8 M urea, the proteins of each sample separated by SDS-PAGE electrophoresis, and subjected to western blotting analysis. I used two anti-Hat1 antibodies to detect the Hat1 isoforms. The EK-14 antibody recognizes the N-terminal 8-21 amino acids of Hat1, and the EE-21 antibody recognizes its C-terminal twenty amino acids. In the same protein extracts from keratinocytes and fibroblasts, the EE-21 antibody detected three Hat1 isoforms, viz., a 64 kDa (isoform a), 52 kDa (isoform b), and 38 kDa, whilst the EK-14 antibody detected the 52 kDa isoform, along with the distinct novel isoforms - 50 kDa, 48 kDa, and 34 kDa. These protein isoforms show subcellular- and cell-type-specific variations in distribution that I discuss, along with the distribution of the Hat1 N- and C-terminal fusion proteins to GFP.

(PS2.64) Radiation induced chromatid-type aberrations after irradiation of late-S/G2 cells: roles of homologous recombination and non-homologous end joining. Hatsumi Nagasawa¹, John R. Brogan¹, Yuanlin Peng¹, John B. Little², Joel S. Bedford¹, ¹Colorado State University, Fort Collins, CO, ²Harvard School of Public Health, Boston, MA

We have compared the contributions of NHEJ and HRR in protecting cells from radiation- induced chromatid-type aberrations after irradiation of late S or G2 cells. This involved measurements in wild-type Chinese hamster cells and a variety of mutants defective in either the NHEJ or HRR. The wild-type cells were CHO K1, CHO AA8, V79B, or V79-4. Mutants were defective in either HRR [*irs-1(Xrcc2)*, *irs1SF(Xrcc3)*, *irs3(Rad51C)*, *CL-V4B(Rad51C)*, *V-8C (Brca2)*] or NHEJ [*Xrs-5(Ku70/80)*, *V3(DNA-PKcs)*, *irs-20 (DNA-PKcs)*, and *XR-1*]. Cultures were irradiated (0.0, 0.25, 0.5, or 1.0Gy) and then Colcemid collections were carried out at 0.5 to 2.5h (G2), or at 2.5 to 4.5h (late S). For gaps and breaks, the induced yields for both G2 and late S irradiations were appreciably higher for all the NHEJ mutants (presumably with intact HRR). This was especially striking for the *xrs-5 (Ku70/80)* mutant, indicating a large contribution to repair by the NHEJ system. There also was an increase in levels of induced gaps plus breaks for the HRR-deficient cells with (presumably) an intact NHEJ system. Regarding exchanges, one particularly interesting feature was the low level of increase in the exchanges for the NHEJ mutants, especially the *xrs-5 (Ku70/80-/-)* and *XR-1 (XRCC4/LIGASE4)*. Deficiency in dsb rejoining might be expected to result in a reduction in exchanges with a corresponding increase in unrejoined breaks and this is indeed what we observed. The exchange frequency was higher in V3 cells (DNA-PKcs null) than its wild-type parent. For the HRR deficient cells, we also saw a marked increase in exchanges indicating that the HRR system was also effective in repairing some breaks that interact to form exchanges. In summary, our results suggest that, along with NHEJ, HRR does contribute to repair of DNA damage leading to chromatid aberrations after irradiation of late S or G2 cells, and this is especially pertinent regarding the relative contributions from the two processes to exchange formation. HRR seems to function more effectively to repair damage in late S and G2 that would lead to exchange formation, with NHEJ less effective in this regard, but NHEJ seems much more effective in promoting the restitution of breaks that might otherwise lead to deletions. This research was supported by the Low Dose Radiation Research Program, DOE, Grant DE-FG-02-07ER64350.

(PS2.65) Investigating a potential chronology between the non-homologous end joining and base excision repair pathways during processing of complex DNA double strand breaks. Shubhadeep Purkayastha, Ronald D. Neumann, Thomas A. Winters, Radiology & Imaging Sciences Department, Nuclear Medicine Section, Warren Grant Magnuson Clinical Center, National Institutes of Health, Bethesda, MD

The molecular structure of a radiation-induced DNA double-strand break (DSB) is an important determining factor of DSB dependent cytotoxicity. In recent studies, we have investigated the differential effects of various individual and combined DSB associated lesion structures on the human non-homologous end joining (NHEJ) repair pathway by employing structurally defined synthetic duplex oligodeoxynucleotides as repair substrates and human whole cell extracts (WCE) as the source of repair proteins in *in vitro* NHEJ assays. We observe a strong positional effect for NHEJ inhibition by base damage (BD) situated 1 nucleotide (-1n) upstream from the DSB terminus, with $BD \geq -4n$ from the DSB end showing little or no inhibition. This inhibitory effect is conserved not only across multiple WCE (HeLa, WI38, MO59K, and M059J), but also for purified, human ligases (LigI, LigIII/XRCC1 and Ku/LigIV/XRCC4). Preliminary results also show that BD positioned within the putative footprint of the DSB repair complex (-22n or less) persisted in end joined product DNA suggesting these positions are blocked from base excision repair (BER) even after end joining. To investigate the chronology of BER and NHEJ during processing of such complex DSB damage, we use repair substrates that are refractory to end joining due to a complex multiple BD configuration. We established functional BER activity in our extracts and found evidence of a stalled repair complex non-productively bound at the DSB end. We found that in addition to precise cleavage at an internal 8-oxo-dG located outside the footprint of the DSB repair end-binding complex, ~25% of these substrates were refractory to cleavage by Fpg when concurrently incubated in the presence of dNTPs, indicating functional BER repair of the internal BD site. To confirm BER repair at positions outside the DSB repair complex and its absence at positions inside the complex footprint, we employed DSB repair substrates with dual 8-oxo-dG lesions, where one lesion is situated outside the footprint and the other is at various positions within the putative repair complex footprint. Preliminary results support the hypothesis that NHEJ and BER are independent processes in the context of complex DSB ends containing BD, and that under conditions where the DSB can support end joining, NHEJ is the dominant repair pathway.

(PS2.66) Differential role of DNA-PKcs phosphorylation and kinase activity in radiosensitivity and chromosomal instability in different cell cycle phases. Yu-Fen Lin¹, Hatsumi Nagasawa², John B. Little³, Joel S. Bedford², David J. Chen¹, Benjamin P. C. Chen¹, ¹Department of Radiation Oncology, University of Texas Southwestern Medical Center at Dallas, Dallas, TX, ²Department of Environmental and Radiological Health Sciences, Colorado State University, Fort Collins, CO, ³Center for Radiation Sciences and Environmental Health, Harvard School of Public Health, Boston, MA

Non-homologous end-joining (NHEJ) and Homologous recombination (HR) are the two major mechanisms for DNA double strand break (DSB) repair. While HR is active primarily in late S (LS) and G₂ phase, NHEJ is operational throughout all cell cycle phases. The catalytic subunit of DNA dependent protein kinase (DNA-PKcs) is the key factor of NHEJ pathway. In addition, recent evidence suggested that DNA-PKcs is involved in replication stress response and could modulate DSB repair through the HR pathway. It is likely that DNA-PKcs is engaged with HR mediated DSB repair during LS/G₂ but the detail remains largely unclear. We have previously reported that DNA-PKcs phosphorylation and kinase activity are critical for DSB repair and radiosensitivity when asynchronous cells were investigated. To further address the impact of DNA-PKcs activity on DSB repair during different cell cycle phases, we compared the relative radiosensitivity and chromosome instability of 13 DNA-PKcs site-directed mutant cell lines involving phosphorylatable residues of the T2609 cluster, the S2056 cluster, and the carboxyl-terminus PI3K domain of DNA-PKcs. These cells were synchronized with isoleucine-deficient protocol for G₀/G₁ or LS/G₂ phases prior to irradiation with Cs-137 γ -rays. In addition, we have examined the kinase activity of DNA-PKcs in different mutant cells after cell cycle synchrony. Our study revealed that DNA-PKcs mutant cells defective in phosphorylation at multiple sites within the T2609 cluster or within the PI3K domain displayed extreme radiosensitivity, whereas as DNA-PKcs mutant cells defective in phosphor-

ylation at the S2056 cluster displayed chromosome instability. Cells defective at the S2056 cluster or T2609 single site alone were only mildly radiosensitive, but cells defective at even one site in both the S2056 and T2609 clusters lead to maximal radiosensitivity, suggesting a synergism between phosphorylations at the S2056 and T2609 clusters is critical for induction of radiosensitivity.

(PS2.67) Mechanism of potentially lethal damage repair: consideration from chromosomal aberrations. Tetsuya Kawata¹, Cuihua Liu², Naoyuki Shigematsu¹, Junichi Fukada¹, Cucinotta Francis³, Kerry George⁴, Hisao Ito², ¹Keio University, Shinjuku, Tokyo, Japan, ²Chiba University, Chiba, Japan, ³NASA Johnson Space Center, Houston, TX, ⁴Wyle laboratories, Houston, TX

Potentially lethal damage (PLD) and its repair (PLDR) was studied in confluent human fibroblasts by analyzing the kinetics of chromosome break rejoining and misrejoining in X-ray irradiated cells that were either held in non-cycling G0 phase or forced to proliferate immediately after irradiation. Fusion premature chromosome condensation (PCC) methods were combined with fluorescence in situ hybridization (FISH) to study chromosomal aberrations in interphase. More than 95 percent of PCC breaks were rejoined within 15 hours and flow cytometry revealed that cycling cells were in G1 for more than 15 hours after exposure, indicating that most repair processes occurred during G1. The rejoining kinetics of PCC breaks was similar for each culture condition. However, under non cycling conditions misrepair peaked at 0.55 exchanges per cell 3 hours after exposure, and under cycling conditions a peak of 1.1 exchanges per cell occurred 6 hours after exposure. Complex-type exchanges were seven times more frequent under PLD conditions compared to PLDR conditions. Since the majority of repair in G0/G1 occurs via the Non Homologous End Joining process, increased PLDR may result from improved cell cycle specific rejoining fidelity of the NHEJ pathway.

(PS2.68) 2-Methoxyestradiol radiosensitizes prostate cancer cells irrespective of androgen dependence. Sukumar Sarkar, University of Virginia, Charlottesville, VA

2-Methoxyestradiol (2-ME2) is an endogenous estradiol metabolite which is known to inhibit microtubule polymerization. *In vivo*, 2-ME has been shown to inhibit both tumor growth and angiogenesis. However, the mechanism of action of this agent is not fully understood. Because radiation plays an important role in the therapy of prostate cancer and 2-ME2 has shown efficacy as a single agent against human prostate carcinoma, we evaluated 2-ME2 as a potential radiosensitizer in prostate cancer cells. Our data suggest that 2-ME2 radiosensitizes PC3 as well as LNCap (androgen dependent) and C4-2 (androgen independent) cells as measured by clonogenic assays. In response to IR, DNA-PK, a key protein for NHEJ is activated and autophosphorylates multiple serine residues including S2056. 2-ME2 abrogates IR induced phosphorylation of this site in all three cells suggesting that 2-ME's regulation of DNA-PK following IR does not depend on androgen dependence. 2-ME2 also attenuated the phosphorylation of Akt (at S743) a known target of DNA-PK in response to IR in all three cell lines. In contrast 2-ME-induced apoptosis in PC3 and C4-2 as measured by FACS analysis and by PARP cleavage but 2ME resulted in no PARP cleavage in LNCap cells. Our results suggest that 2-ME has both androgen dependent and well as androgen independent effects.

(PS2.69) Induction of DNA damage by positron emission tomography scans. Kristina Taylor, Mary Ellen Cybulski, Lisa Laframboise, Nicole McFarlane, Douglas R. Boreham, McMaster University, Hamilton, ON, Canada

This research is focused on assessing the radiation risk associated with positron emission tomography (PET) scans. PET

scans are an increasingly used nuclear medicine procedure that require the administration of ¹⁸F-fluorodeoxyglucose (¹⁸F-FDG) and result in a dose of 7-22 mSv. It has been suggested that low dose medical imaging poses a health risk from exposure to ionizing radiation. The short term biological effects following PET scans were evaluated in order to understand the modification of mechanisms that may influence cancer risk. A corresponding lifetime cancer study is in progress. Radiation induced DNA damage associated with PET scans was studied in 7-9 week old female wild type Trp53 +/- mice. Mice were scanned and the biological response was assessed in bone marrow using the micronucleated reticulocyte (MN-RET) formation assay. Mice were injected with 0, 20, 40, 100 or 400 µCi of ¹⁸F-FDG, corresponding to total body doses of 0, 12, 23, 58 and 233 mGy respectively. A significant dose response in the MN-RET frequency ≥ 100 µCi ¹⁸F-FDG was observed. A mouse given a 20µCi scan simulates the dose a patient receives during a PET exam and this was found to cause no measurable effect in mice. However, radiation exposure from a PET is non-uniform and some estimates report that a 20µCi injection could result in 400mGy to the bladder. Effects in the bladder are under investigation. It has also been hypothesized that oxidative stress, induced by exposure to low dose radiation from a PET scan, may stimulate an adaptive response. Mice were injected with 0, 20, 100 or 400 µCi of ¹⁸F-FDG and then challenged *in vivo* with 1 Gy, 24 hours post scan. No adaption was found. This was further examined in lymphocytes by assessing γ-H2A.X foci formation *in vitro*. Mice injected with 0, 20, 100 or 400 µCi of ¹⁸F-FDG were sacrificed and their bone marrow challenged *in vitro* with 0, 1, 2 or 4 Gy, 24 hours post scan. A single PET scan did not appear to modify the response of bone marrow to any of the challenge doses except at 400µCi where a reduced number of foci were observed. PET diagnostic exposures can induce effects in the bone marrow of mice. Depending on the endpoint, they may also induce an adaptive response that modifies the effects of larger radiation exposures but the timing and the magnitude of the challenge dose is important.

(PS2.70) Processing and biological consequences of clustered DNA damage containing a single strand break and an AP site. Naoya Shikazono¹, Miho Noguchi¹, Ayumi Urushibara¹, Peter O'Neill², Akinari Yokoya¹, ¹Japan Atomic Energy Agency, Tokai-mura, Japan, ²University of Oxford, Oxford, United Kingdom

Clustered DNA damage, defined as two or more lesions within one to two helical turns of DNA by a single radiation track, is a unique feature of ionizing radiation. Although extensive work has been carried out on how non-dsb type of clustered damage is processed *in vitro*, the processing of clustered damage *in vivo* still needs further investigation. Using a bacterial plasmid-based assay, we have studied the biological consequences of bistranded clustered damage sites which consist of a single strand break (SSB) and an apurinic/aprimidinic (AP) site. Plasmids were ligated with oligonucleotides containing clustered lesions. Following transformation of the ligated plasmids into the wild type strain of *Escherichia coli*, we found significantly lower transformation frequencies for the clustered SSB + AP lesions (separated by 1bp) than that for either a single SSB or a single AP site. When the two lesions were placed further apart (10-20bp), both transformation efficiency and mutation frequency are comparable to those of the single lesions. The lesion separation required for plasmid recovery is dependent on the relative orientation of the clustered SSB + AP lesions. The efficiency of plasmid recovery, in part, required PolI activity. We suggest that a double strand break or a replication block is formed during the processing of the SSB + AP clusters and that DNA synthesis plays a significant role in determining its biological consequences. These results indicate that the biological consequences of clustered DNA damage strongly depend on the separation and relative orientation of the lesions.

(PS2.71) Wip1 phosphatase, a replicative stress-induced short-lived oncogene, is specifically required for human prostate cancer cell proliferation. Hyeon U. Park¹, Simeng Suy¹, Heather Hanscom¹, HengHong Li¹, Brian T. Collins¹, Insoo Bae¹, Milton L. Brown¹, Anatoly Dritschilo¹, Hyukjin Cha², Albert J. Fornace¹,

Sean P. Collins¹, ¹Georgetown University, Washington, DC, ²CHA Stem Cell Institute, Seoul, Republic of Korea

The molecular mechanisms underlying the development of human prostate cancer are currently poorly understood. Wip1 (PP2Cgamma or PPM1D) is an oncogenic serine-threonine phosphatase that is up-regulated following DNA damage in a p53-dependent manner. Here, we report that Wip1 was highly expressed in proliferating androgen-dependent and androgen-independent human prostate cancer cells. In response to androgen-induced proliferation and replicative stress, Wip1 expression is increased and modifies the DNA damage response pathway to maintain cell proliferation. Wip1 expression was cell cycle-dependent with a short half life. We provide evidence that depletion of Wip1 leads specifically to decreased human prostate cancer proliferation and induces senescence. The evidence provided here is the first report that Wip1 is important in maintaining human prostate cancer proliferation in response to replicative stress and offers a new target for chemoprevention of human prostate cancer.

(PS2.72) Lucanthonone and its structural analogue hycanthonone, as direct inhibitors of Apurinic Endonuclease 1(APE1). Mamta D. Naidu¹, Rakhi Agarwal¹, Zina Sanchez², Min Shen³, Yuan Liu⁴, David Wilson III², Samuel Wilson⁴, ¹Brookhaven National Laboratory, Upton, NY, ²State University of New York, Stony Brook, NY, ³NIH Chemical Genomics Center, NIH, Rockville, MD, ⁴National Institute of Environmental Health Sciences, NIH, Research Triangle Park, NC, ⁵National Institute of Aging, NIH, Baltimore, MD

Lucanthonone and its active metabolite hycanthonone are both well known thioxanthone DNA intercalators used in the 1980s as antitumor agents. Lucanthonone is in Phase I clinical trial without any reports of drug-related death or lasting side effects, whereas hycanthonone was pulled out of Phase II clinical trials due to severe hepatotoxicity. Their potential mechanisms of action include DNA intercalation, inhibition of nucleic acid biosyntheses, generation of apurinic/ apyrimidinic/ abasic sites and inhibition of enzymes like Topoisomerases, MGMT, and the dual function DNA BER enzyme apurinic endonuclease 1 (APE1). Lucanthonone is a selective inhibitor of the endonuclease activity of APE1, without affecting the protein's redox activity. As the precise mechanism of its inhibition of APE1's endonuclease activity is presently unknown, our goal is to decipher this mechanism as a prerequisite to the development of improved therapeutic regimes that can counteract higher APE1 activity seen in GBM and other tumors. These proposed studies will elucidate whether the inhibition of APE1 is a result of balance between direct and/or indirect modulation of APE1. Our results show that lucanthonone is a good radiosensitizer for glioma cell lines, where we find that glioma cells show cleavage of APE1 in presence of increasing concentrations of lucanthonone. In addition, lucanthonone treated recombinant APE1 also showed cleavage and reduction in its endonuclease activity. APE1 structures report a hydrophobic pocket where hydrophobic small molecules like thioxanthenones can possibly bind. Binding and CD spectra studies indicate that hydrophobic sites, Phe266 and Trp280 play an important role in this direct binding. Molecular modeling showed that both lucanthonone and hycanthonone docked in hydrophobic site of APE1. Also, the DNA binding capacity of APE1 is only marginally altered by lucanthonone and hycanthonone. Thus, we hypothesize that thioxanthenones like lucanthonone and hycanthonone inhibit APE1 by direct protein binding. Preliminary data indicate that oxidative damage may be one of the mechanisms of lucanthonone induced direct inhibition of APE1. Finally, this research strongly emphasizes on future design of clinically efficacious thioxanthone analogues, which would bind and alter the hydrophobic site of APE1 protein.

(PS2.73) ATM-dependent de-repression of IGF-1 allows secretory clusterin (sCLU) expression after DNA damage and in genomic instability. David A. Boothman¹, Eva M. Goetz¹, Bhavani Shankar¹, Yonglong Zou¹, Julio Morales¹, Xiuquan Luo¹, Shinako Araki¹, Robert Bachoo¹, Lindsey Mayo², ¹UT Southwest-

ern Medical Center at Dallas, Dallas, TX, ²University of Indiana School of Medicine, Indianapolis, IN

Secretory clusterin (sCLU) is a stress-induced, pro-survival glycoprotein elevated in early stage cancers, in particular, APC/Min-defective colon cancers. Here, we show that activation of Ataxia telangiectasia-mutated kinase (ATM) by DNA damage is required to release the repression of IGF-1 by p53/NF-YA. Using cell lines that are genetically unstable due to loss of H2AX, MDC1, NBS1, mTR, or hMLH1, or in cells treated with DNA damaging agents, we observed elevated IGF-1 ligand, resulting in IGF-1R signaling and sCLU expression. Our results integrate DNA damage caused from genetic instability or in response to chemotherapeutic agents, to ATM activation and alleviation of p53/NF-YA mediated IGF-1 repression, resulting in IGF-1-sCLU expression. These key components are integrated into one pathway highlighting its importance in tumor progression, metastasis, and resistance to therapies. This work was supported by DOE grant, DE-FG02-06ER64186-17, to D.A.B. and a DOD breast cancer fellowship W81XWH-06-0748 to E.M.G. We are grateful to Robert and Virginia Payne for their support of this work.

(PS2.74) Evidence for the participation of DNA glycosylase NEIL1 in *in vivo* repair of radiation-induced (5'R)- and (5'S)-8,5'-cyclo-2'-deoxyadenosines and for the presence of these lesions in human urine. Pawel Jaruga, NIST, Gaithersburg, MD

(5'R)- and (5'S)-8,5'-cyclo-2'-deoxyadenosines (*R*-cdA and *S*-cdA) are among the major lesions formed in DNA by hydroxyl radical attack on 2'-deoxyadenosine. They accumulate in DNA and are detectable *in vivo* due to disease states and defects in DNA repair, pointing to their potential role in disease processes. We developed a methodology using liquid chromatography/tandem mass spectrometry with isotope-dilution (LC-MS/MS) to measure *R*-cdA and *S*-cdA in DNA *in vivo*, permitting a detection level of 0.1 fmol on-column. Using this methodology, we observed significant accumulation of *R*-cdA and *S*-cdA in liver DNA of *neil1*⁺ mice without exogenous oxidative stress, when compared to control or *ogg1*⁺ mice. NEIL1 is a DNA glycosylase that is involved in base excision repair (BER) of oxidatively induced DNA damage. It exhibits a strong preference for excision from DNA of 4,6-diamino-5-formamidopyrimidine and 2,6-diamino-4-hydroxy-5-formamidopyrimidine with no specificity for 8-hydroxyguanine. *R*-cdA and *S*-cdA are repaired by nucleotide excision repair (NER). Since the accumulation of *R*-cdA and *S*-cdA in *neil1*⁺ mice strongly points to the failure of their repair, these data suggest that NEIL1 is involved in NER of these compounds. We also applied the developed methodology to the measurement of *R*-cdA and *S*-cdA in human urine. These compounds had hitherto not been considered or investigated to be present in urine as possible biomarkers of DNA damage. We show that *R*-cdA and *S*-cdA exist in human urine and can be identified and quantified by LC-MS/MS. Our data strongly suggest that *R*-cdA and *S*-cdA may be well-suited biomarkers for disease processes such as carcinogenesis or used as markers of exposure to ionizing radiation, and can be accurately measured by LC-MS/MS *in vivo*.

(PS2.75) A role for the arginine methylation of Rad9 in checkpoint control and cellular sensitivity to DNA damage. Haiying Hang, Wei He, Xiaoyan Ma, Xiao Yang, Institute of Biophysics, Beijing, China

The genome stability is maintained by coordinated action of DNA repairs and checkpoints, which delay progression through the cell cycle in response to DNA damage. Rad9 is conserved from yeast to human and functions in cell cycle checkpoint controls. Here, a regulatory mechanism for Rad9 function is reported. In this study Rad9 has been found to interact with and be methylated by protein arginine methyltransferase 5 (PRMT5). Arginine methylation of Rad9 plays a critical role in S/M and G2/M cell cycle checkpoints. The activation of the Rad9 downstream checkpoint effector Chk1 is impaired in cells only expressing a mutant Rad9 that cannot be methylated. Additionally, Rad9 methylation is also required for cellular resistance to DNA damaging stresses. In

summary, we uncovered that arginine methylation is important for regulation of Rad9 function, and thus is a major element for maintaining genome integrity.

(PS2.76) The distribution of small ring products and associated deletions in human chromosomes as predicted by a generalized model of radiation-induced aberration formation.

Artem L. Ponomarev¹, Michael N. Cornforth², Brad Loucas², Francis Cucinotta³, ¹USRA, Houston, TX, ²UTMB, Galveston, TX, ³NASA JSC, Houston, TX

Recently it was reported that exposure to gamma-rays, a low-LET radiation, causes many small rings. This is contrary to previous experimental and theoretical work pointing to fewer smaller fragments, which can form deletions and associated rings, for low-LET radiation. Yet, the formation of very small ring products that, because of their size, are not directly detectable on a genome-wide scale by existing cytogenetic techniques (e.g., banding, mBAND, and various FISH approaches) has been hypothesized to occur at high frequency following ionizing radiation. Here we attempt to address this issue within the framework of a new model predicting chromosomal aberrations that is based on previously developed fragment-size distributions, a random walk polymer model of individual chromosomes, and stochastic track structure. Using this model, we performed Monte-Carlo simulations of radiation-induced chromosomal aberrations, particularly chromosomal rings and dicentrics, and calculated their relative frequencies and distributions. The model relies on previously simulated low- and high-LET patterns of radiation-induced DNA fragmentation, where an excess of smaller fragments was predicted for high-LET radiation. The model-driven prediction is one that favors the formation of very small rings (e.g., <20 kb) that underlie the formation of submicroscopic interstitial deletions. The hypothesized distribution of ring products is based on model fits to previously established experimental data for larger, microscopically visible, rings and dicentrics. Additional data are presented for complex chromosomal rearrangements, dicentrics, centric rings, and also for deletions, where the relationship between these cytogenetic lesions and small rings is also considered. Calculations pertain to multi-dose exposures to the following sources of ionizing radiation: gamma-rays, Fe ions, and protons. Further analyses for low energy, high-LET helium ions are also included. The theoretical analysis gives a roadmap for projecting available experimental data to chromosomal aberrations of smaller sizes.

(PS2.77) Genotoxic effects of low SAR 2.45 GHz microwave radiation exposures on sprague dawley rats. Mojisola Usikalu¹, Moses Aweda², Ding Nan³, Jian Wan³, Jiayun Zhu³, ¹Covenant University, Ogun State, Nigeria, ²University of Lagos teaching hospital, Lagos, Lagos, Nigeria, ³Institute of Modern Physics, Lanzhou, Lanzhou, China

Objective: The aim of the study is to investigate the genotoxic effects of 2.45 GHz microwave radiation exposure at low specific absorption rates. Materials and Methods: A microwave generator (ER6660E) was used for the irradiation and exposure was carried out under strictly controlled conditions of dosimetry and temperature. The induction of DNA damages was assessed in blood leucocytes, brain, lung and spleen using DNA direct amplification of length polymorphisms (DALP) Results: Results re-affirmed with single cell gel electrophoresis (SCGE) comet assay for same cells at SAR 2.39 W/kg. After exposure to 2.45 GHz radiation the band patterns of the exposed animals were distinctly altered in the range of 40 - 120 bp compared with the control and in their tail DNA before exposure, shown in the densitometric gel analysis. There is statistical significant difference in the Olive moment and % DNA in the tail of the exposed animals compared with control (p < 0.05). Conclusion: Exposures to low level of 2.45 GHz MW radiation may have potential genotoxic effects.

(PS2.78) New Computational Methods for Genome-wide analysis of Low Dose Radiation Reveals Regulators of Resonse. Bahram Parvin, Lawrence Berkeley National Laboratory, Berkeley, CA

We present a novel computational method for identifying molecular predictors of adaptive response and low dose effect from transcript data. The underlying concept is that a small subset of genes is activated for each treatment regime. The concept of a small subset of genes translates to the sparsity constraint, which is applied computationally. The advantages of this technique over traditional statistical methods are (i) simultaneous association of a subset of genes to a treatment regime, (ii) incorporating multi-class and multidimensional phenotypic profiles in one framework, and (iii) hypothesizing related genes simultaneously. We have applied our method to two data sets of mouse mammary gland and human derived fibroblast. We present the common regulator of response in mouse mammary gland at 5, 10, and 200 cGy.

(PS2.79) Recruitment and assembly of XRCC4-DNA LigaseIV complex on radiation damaged chromatin *in situ* revealed by biochemical fractionation analysis. Radhika P. Kamdar, Sicheng Liu, Yoshihisa Matsumoto, Tokyo Institute of Technology, Research Laboratory for Nuclear Reactors, Tokyo, Japan

Ionizing radiations cause DNA double strand breaks (DSBs), potentially the most lethal lesions if left unrepaired, causing genomic rearrangements and cancer. Homologous Recombination (HR) and Non-Homologous End-Joining (NHEJ) pathways are the major repair mechanisms observed in mammalian cells. HR is usually dominant in S and G2 phases of the cell cycle as it requires a pair of sister chromatids for error-free replication; whereas NHEJ is observed in all the stages. The core players of NHEJ are recognized as the Ku70/80 heterodimer as one of the initial sensors to bind the DSB site and recruit DNA dependent protein kinase catalytic subunit (DNA-PKcs) which brings the broken DNA ends in synapsis. The nucleases like Artemis and DNA polymerases like λ and μ process the DNA ends to attain adequate homology before the final end-joining step by XRCC4-DNA Ligase IV-XLF complex. The exact hierarchy and the complex dynamics of this repair machinery are yet to be clarified. We have been using a detergent fractionation method to capture the radiation induced chromatin bound complex. This revealed that a subpopulation of XRCC4 changed into an extraction resistant form that was liberated by micrococcal nuclease treatment, indicating that it had been tethered to chromatin DNA. Quantitative estimation revealed that a very small percentage of the XRCC4-Ligase IV complex was recruited to each DNA end. We further isolated the higher order chromatin bound complex associated with XRCC4 by immunoprecipitation. Western blotting and mass spectrometric analyses of this immunoprecipitate demonstrated the presence of DNA ligase IV, histone molecules and its interactor. Several ribonucleoproteins were also observed. Such striking associations of XRCC4 on the damaged chromatin site leads to a speculation that the NHEJ repair pathway is much more sophisticated and complex than hitherto comprehended.

(PS3.01) Simulation of secondary electron yields from thin metal foils after fast proton impact. Anderson Travia, Michael Dingfelder, East Carolina University, Greenville, NC

Accurate particle interaction cross sections are the fundamental input data of event-by-event Monte Carlo track structure codes used in the simulation of radiation effects on materials. The track structure simulation consists of recording the energy loss, interaction type, and classical path of the primary particle and all the induced secondaries from the first interaction to total stop. Tests on thin metal foils with well known physical properties are performed to assess the accuracy of these codes that can be used with complex targets such as water and biological tissues. We have simulated secondary electron yields from thin aluminum, copper, and gold foils after proton impact using the Monte Carlo track structure code PARTRAC. Energy- differential cross sections and total inverse mean free paths have been calculated using the first Born approximation and the dielectric response theory. The target is described by a generalized oscillator strength constructed with optical oscillator strengths obtained from photo-absorption data employing a delta oscillator dispersion algorithm. The shell

separation method has been applied to determine the inner atomic shells in which the ionization event originated. Electron exchange effects have also been incorporated. Comparisons with previous results will be presented. This work is supported in part by the National Institute of Health, National Cancer Institute Grant No. 2R01CA093351.

(PS3.02) Prototropic equilibria in dna containing one-electron oxidized gc: intra-duplex vs. duplex to solvent deprotonation. Amitava Adhikary, Anil Kumar, Shawn A. Munafo, Deepti Khanduri, Michael D. Sevilla, Oakland University, Rochester, MI

By use of ESR and UV-vis spectral studies, this work identifies the protonation states of one-electron oxidized G:C (viz. $G^{\cdot+}:C$, $G(N1-H):C(+H^+)$, $G(N1-H):C$, and $G(N2-H):C$) in a DNA oligomer $d[TGCGCGCA]_2$. Benchmark ESR and UV-vis spectra from one electron oxidized 1-Me-dGuo are employed to analyze the spectral data obtained in one-electron oxidized $d[TGCGCGCA]_2$ at various pHs. At $pH \geq 7$, the initial site of deprotonation of one-electron oxidized $d[TGCGCGCA]_2$ to the surrounding solvent is found to be at N1 forming $G(N1-H):C$ at 155 K. However, upon annealing to 175 K, the site of deprotonation to the solvent shifts to an equilibrium mixture of $G(N1-H):C$ and $G(N2-H):C$. For the first time, the presence of $G(N2-H):C$ in a ds DNA-oligomer is shown to be easily distinguished from the other prototropic forms, owing to its readily observable nitrogen hyperfine coupling ($A_{zz}(N2) = 16$ G). In addition, for the oligomer in H_2O , an additional 8 G N2-H proton HFCC is found. This ESR identification is supported by a UV-vis absorption at 630 nm which is characteristic for $G(N2-H)$ in model compounds and oligomers. We find that the extent of photo-conversion to the C1' sugar radical (C1'·) in the one-electron oxidized $d[TGCGCGCA]_2$ allows for a clear distinction among the various G:C protonation states which can not be easily distinguished by ESR or UV-vis spectroscopies with this order for the extent of photo-conversion: $G^{\cdot+}:C > G(N1-H):C(+H^+) \gg G(N1-H):C$. We propose that it is the $G^{\cdot+}:C$ form that undergoes deprotonation at the sugar and this requires reprotonation of G within the lifetime of excited state. Supported by the NIH Grant RO1 CA045424.

(PS3.03) Cross sections for bare and dressed carbon ions in water: a classical trajectory Monte Carlo calculation. Thiansin Liamsuwan, Hooshang Nikjoo, Karolinska Institutet, Stockholm, Sweden

We present a model calculation for the interaction cross sections for bare and dressed carbon ions 1keV/u - 1MeV/u in water. Cross sections are needed for the description of track, interaction by interaction, in irradiated media. At the investigated energies, the stopping power of ions exhibits a maximum. Therefore, understanding of energy-loss processes is of particular interest for the investigation of radiation effectiveness. When ion slows down under the Bragg peak, charge transfers give rise to the fraction of dressed projectiles in the ion track, and should be included for the precise determination of energy loss of track. We use the three-body Classical Trajectory Monte Carlo (CTMC) method to calculate the interaction cross sections. Two-center effect is automatically incorporated in the model. Two separated collision schemes were simulated: these are projectile-target electron-target core and; projectile core-projectile electron-target molecule. The radial and momentum distributions of the active electron to the core are determined from the binding energy, and used for sampling of the initial condition of the electron before the collision. Electron-electron interactions within a core are simplified using the model potential, taking into account the distance-dependent screening of the core. The total and differential cross sections for ionization, electron capture, and electron loss will be presented and compared to the existing experimental data. We aim to implement the calculated cross sections in a Monte Carlo track structure code for simulation of carbon ion tracks, and characterize radiation therapy beams using microdosimetry and biophysical modeling.

(PS3.04) Yields of oxidative damage produced in puc18 by the direct effects of 70kV x-rays at 4 K and room temperature. Anita R. Peoples¹, Jane Lee², Michael Weinfeld², Jamie R. Milligan³, William A. Bernhard¹, ¹University of Rochester, Rochester, NY, ²Cross Cancer Institute, Edmonton, AB, Canada, ³University of California at San Diego, La Jolla, CA

Our mechanistic understanding of damage formation in DNA by the direct effect relies on what is known of free radical intermediates studied by EPR spectroscopy. Bridging this information to stable product formation requires analytical methods with comparable detection sensitivities, a criterion met by the 32P-postlabelling assay developed by Weinfeld and Soderlind [Biochemistry 30, 1091(1991)]. When applied to the indirect effect, this technique detected thymine glycol (Tg) and phosphoglycolate (pg). Other base damage products were evident but not identified (called X). Importantly, X must be due to oxidation but is not 8-oxo-Gua, or 8-oxo-Ade. We used this assay to determine yields of products in pUC18 films with hydration levels (Γ) of 2.5, 15 or 22 waters per nucleotide and X-irradiated at either 4 K or RT. Results from the first set of experiments gave chemical yields of pg ($G(pg)$) close to zero; e.g., for $\Gamma = 2.5$, $G(pg) = 4 \pm 1$ nmol/J (RT) and 3 ± 1 nmol/J (4 K). Given that formation of pg requires O2 attack at the C4'-deoxyribose radical, this is evidence that the C4' radical contributes little to the total deoxyribose damage, which from the previously measured unaltered free base release is 134 ± 4 nmol/J. The yield of detectable base damage ($G(Tg+X)$) at $\Gamma = 2.5$ was found to be 35 ± 4 nmol/J (RT) and 19 ± 3 nmol/J (4 K). Given the paucity of water in these samples, formation of Tg appears unlikely, raising the possibility of other oxidation products similar to but different than Tg. Supported by PHS Grant 2-R01-CA32546 of the NCI.

(PS3.05) Comparative metabolomics reveals similarities and differences in the urine small molecule responses of rats and mice to gamma radiation exposure. John B. Tyburski¹, Evagelia C. Laiakis¹, Tytus D. Mak¹, Kristopher W. Krausz⁷, Frank J. Gonzalez², John F. Kalinich³, Albert J. Fornace Jr.^{4,1}, ¹Georgetown University, Washington, DC, ²National Cancer Institute, Bethesda, MD, ³Armed Forces Radiobiology Research Institute, Bethesda, MD, ⁴Lombardi Comprehensive Cancer Institute, Washington, DC

The threat of large-scale exposure to ionizing radiation has increased in the 21st Century. Rapid, minimally invasive biodosimetry is crucial to medical countermeasures against radiation yet is awaiting further discovery and validation. To address this gap, we recently described several urine small molecule biomarkers of gamma radiation exposure in adult male mice that exhibit both dose- and time-dependence. Here we extend these findings to the rat and offer comparative analyses that detail the similarities and differences among the responses of these species. Twenty-four hour urine samples were collected from adult male rats prior to and 24, 48, and 72 h post-exposure to single gamma radiation doses ranging from 0.5 to 10 Gy. Samples were analyzed by Ultra-Performance[®] Liquid Chromatography coupled to time-of-flight mass spectrometry operated in both positive and negative electrospray ionization modes and pre-processed with MarkerLynx[®] software (Waters, Inc.). Relative peak areas were normalized by corresponding creatinine peak areas and analyzed by Principal Components using SIMCA-P+[®] software (Umetrics, Inc.). Paired-group comparisons were made using Random Forests, and we also developed a novel method for comparing across more than 2 groups at a time. Analyses were compared as a function of top candidate biomarkers revealed. As shown previously in mice, rats exhibit dose-dependent elevation of urine thymidine and taurine excretion during the first 24 h post-exposure. In contrast, *N*-hexanoylglycine, 2'-deoxyuridine, 2'-deoxyxanthosine, and xanthine were not reliably detected in rat urine. Moreover, creatine excretion in mouse urine was not altered by radiation exposure, whereas rats exhibit a sustained elevation of creatine excretion post-exposure. Overall, the urine small molecule response to radiation exposure in rats is more dramatic and skews toward general attenuated ion excretion, contrasted with mice. These results demonstrate the power of comparative metabolomics in assessing species similarities and differences in exposure assessment. Cross-species validation of biomarkers warrants further investigation. Our findings give us insight into the mechanisms

underlying urine radiation responses and will likely guide and inform our ongoing efforts to develop human biodosimetry.

(PS3.06) Degradation of phospholipid molecules by low-energy electrons. Radmila Panajotovic¹, Mark Schnietz², Andrey Turchanin², Nigel Mason¹, Armin Götzhäuser², ¹The Open University, Milton Keynes, United Kingdom, ²University of Bielefeld, Bielefeld, Germany

In order to study the physico-chemical properties of a biological membrane, consisting of a variety of signalling and transporting molecules imbedded in the lipid matrix, it is necessary to start from a model membrane. DPPC (1,2-dipalmitoyl-sn-glycero-3-phosphocholine) molecule is used as a basic building block for a model lipid matrix, due to its relative ease for manipulation and its important role in the radiation-sensitive lung tissue. In our experiment, we are seeking information about the type and the extent of degradation of the DPPC, caused by electrons with energies from 5 to 200 eV, and representing the effects of the low-energy spectrum of secondary particles produced by the high-energy ionizing radiation. Our target was a thin DPPC film deposited on a solid substrate, transferred from a monolayer film formed at the air/water interface. We used the X-ray photoelectron spectroscopy (monochromatic Al K_α (1486.7 eV) source) to scan the samples before and after electron irradiation. The shifts and the intensity of the binding energies of C 1s, O 1s, P 2p, and N 1s atoms were observed, giving the information about the changes in the chemical bonds and in the molecular orientation. The results show that the electrons with energy between 20 and 100 eV have the largest effect on DPPC. However, there is no evidence of the selectivity in their fragmentation. Most damage to the polar head of the DPPC molecules is caused by cutting the methyl groups from nitrogen and phosphate group from the rest of the molecule. The least effect of electron irradiation is shown on the phosphate group itself, regardless of the incident energy. The effects are significantly smaller for 5 and 200 eV electrons, which is encouraging for the idea of using these phospholipids as a substrate for studying amino-acid, protein and DNA irradiation with electrons below 5 eV, where the dissociative electron attachment to these molecules have been previously observed [1, 2] to produce highly reactive chemical species. Main questions for further study are concerning the presence of water clusters trapped around polar head, as well as the effects of electron beam on mixed lipid bilayers. [1] Panajotovic R, Martin F, Cloutier P, Hunting D, and Sanche L, *Radiation Research*, 2006, 165, 452 [2] Panajotovic R, Michaud M, and Sanche L, *Phys. Chem. Chem. Phys.* 2007, 9,138.

(PS3.08) Studying the effects of temperature on the mechanism of iodine-125 decay induced DNA damage. Thabisile Ndlebe, Igor Panyutin, Ronald Neumann, National Institute of Health, Bethesda, MD

Targeted radiotherapy is an alternative cancer therapy that utilizes a tumor-localizing agent with a radioactive atom attached. This results in more localized damage primarily at the tumor cells. Gene targeted radiotherapy combines both gene manipulation and targeted radiotherapy. Our group has previously developed triplex-forming oligonucleotides, which target genes of interest and selectively cleave these genes by using an attached iodine-125 radionuclide. Understanding the DNA damaging mechanism of the Auger electron emitter, iodine-125, is relevant for the therapeutic potential of this method. Auger electron emitters produce highly localized damage in DNA. This highly localized damage primarily proceeds through three mechanisms; 1) direct damage by the emitted Auger electrons, 2) indirect damage by diffusible free radicals produced by Auger electrons in water, and 3) charge neutralization of the highly positively charged tellurium daughter atom. An additional intermediate charge transport mechanism has also been proposed as a factor in iodine-125 decay induced DNA damage. Charge transport is a mechanism that describes how charge travels along DNA and subsequently leads to damage in DNA. Our earlier work showed that charge transport was not a factor in iodine-125 induced DNA damage at 193K. The purpose of our current

work was to determine whether the charge transport mechanism along DNA contribute to iodine-125 decay produced damage at more elevated temperatures. This was achieved by using charge transport inhibitors, such as BrdU, 8-oxo-G, and GpG steps, to probe for charge transport in iodine-125 decay induced DNA damage. These charge transport inhibitors were each incorporated proximal to the iodine-125 in different DNA hairpins. Their effect on the distribution of DNA breaks produced by iodine-125 decay was analyzed by polyacrylamide gel electrophoresis. We found that the inhibitors had no measurable effect on the distribution of DNA breaks at the elevated temperatures of 253K, 277K and 298K. Our results, therefore, suggest that charge transport is not a factor in iodine-125 decay-induced DNA damage at these temperatures.

(PS3.09) Distribution of direct-type damage in DNA: the role of one-electron reduced cytosine. Paul J. Black, William A. Bernhard, University of Rochester, Rochester, NY

The overarching goal is to be able to predict, a priori, the yields and distribution of DNA damage produced by the direct effect. One-electron capture by cytosine is key to achieving this goal because it accounts for ~90% of the reductive damage initially formed in DNA. In doing so, Cyt strongly influences the yield and composition of clustered damage. Electron Paramagnetic Resonance (EPR) spectroscopy is used to study one-electron reduction of a series of oligodeoxynucleotides, e.g., d(GCGCGCGC)₂, d(GGCGGCC)₂, and d(GGGGCC)₂, suspended in a glass or in the form of film. In this report, we focus on the results obtained from glasses formed by cooling solutions of ~10mM oligomer, 8 M LiCl to 4 K. Irradiation with 70 KV x-rays generates holes trapped as Cl₂^{•-} and excess electrons trapped by Cyt. Because the Cl₂^{•-} spectrum is very broad it does not interfere with the relatively sharp doublet spectrum of one-electron reduced Cyt. In duplex DNA, the doublet is due to the N3 protonated radical anion, Cyt(N3+H)^{•-}, because proton transfer from N1 of Gua is coupled to electron trapping. We found that the resolution of the doublet assigned to Cyt(N3+H)^{•-} was markedly enhanced upon deuteration of the DNA's exchangeable hydrogens. This discovery offers an important new advantage in determining the distribution of electron attachment in DNA because it improves our ability to distinguish between electron trapping by Thy and Ade, which account for the remaining ~10% of the initial reductive damage. Supported by PHS Grant 2-R01-CA32546 of the NCI.

(PS3.10) One-electron oxidation of DNA by ionizing radiation: competition between base-to-base hole-transfer and hole-trapping. Kiran K. K. Sharma, Rahul Tyagi, Shubhadeep Purkayastha, William A. Bernhard, Univ. of Rochester, Rochester, NY

The distance of hole migration through DNA determines the degree to which radiation induced lesions are clustered. Migration distance is governed by a competition between hole transfer and irreversible trapping reactions. An important type of trapping is reactions that lead to formation of deoxyribose radicals, which are precursors to free base release (fbr). Using HPLC, fbr was measured in X-irradiated films of oligodeoxynucleotides and three genomic DNAs differing in GC/AT ratio. The chemical yields of each base, $G(\text{base})$, were measured and used to calculate the modification factor, $M(\text{base})$. This factor compensates for differences in the GC/AT ratio, providing a measure of the degree to which a given base influences its own release. In the highly polymerized genomic DNA, we found that $M(\text{Cyt}) > M(\text{Gua})$ and that $M(\text{Thy})$ is consistently the smallest of the M factors. For these same DNA films, the yields of total DNA trapped radicals, $G_{\text{tot}}(\text{fr})$, were measured using EPR spectroscopy. The yield of deoxyribose radicals was calculated using $G_{\text{dRib}}(\text{fr}) = \sim 0.11 \times G_{\text{tot}}(\text{fr})$. Comparing $G_{\text{dRib}}(\text{fr})$ with total free base release, we found that only about half of the fbr is accounted for by deoxyribose radical intermediates. We conclude that for a hole on cytosine, $\text{Cyt}^{•+}$, base-to-base hole transfer competes with irreversible trapping by the deoxyribose. In the case of a hole on thymine, $\text{Thy}^{•+}$, base-to-base hole transfer competes with irreversible trapping by methyl

deprotonation. Close proximity of Gua protects the deoxyribose of Cyt but sensitizes the deoxyribose of Thy. Supported by PHS Grant 2-R01-CA32546 of the NCI.

(PS3.11) Delayed formation of DNA double strand breaks within clustered-damage sites from thermally unstable deoxyribose adducts in irradiated cells. George Iliakis, Satyendra Singh, Minli Wang, Christian Staudt, University of Duisburg-Essen Medical School, Essen, Germany

Double strand breaks (DSBs) originate from sugar adducts (SA) induced within clustered-damage sites (CDS) in DNA exposed to ionizing radiation (IR). One form of SA (SA-1) immediately disrupts the sugar-phosphate backbone causing single strand breaks (SSBs) that contribute to the formation of prompt DSBs (p-DSBs). There is evidence for a form of SAs, which are not disrupting the sugar phosphate backbone but which display thermal instability, SA-2s. Such adducts convert to SSBs and cause DSBs when the postirradiation conditions promote their chemical processing. The conversion of SA-2s to DSBs was demonstrated during the 50°C lysis step employed in pulsed-field gel electrophoresis (PFGE) experiments. DSBs forming under such extreme conditions are considered artifactual devoid of biological relevance and confounding quantitative analysis. Whether SA-2s contribute to DSBs under physiological conditions remains unknown. Here, we show that irradiation of mammalian DNA, either as naked molecule or in the intact cell, induces SA-2s, and that these SA-2s are still converted to DSBs after incubation of the naked molecule at 50°C. However, we also show that the same subset of SA-2s is nearly completely converted to DSBs after incubation of the DNA at 37°C. Because the conversion of SA-2s to DSBs at 37°C occurs faster when DNA is bound to protein in a detergent inactivated cell, we infer that it will occur even faster in a biologically active cell engaged in repair under physiological conditions, thus generating delayed DSBs (d-DSBs). The number of DSBs estimated by calibrated PFGE after 50°C lysis is similar to the number of DSBs detected using the biological response of the cell in the form of γ -H2AX foci. We propose therefore that the biologically relevant load of DSBs in an irradiated cell approximates the sum of p-DSBs + d-DSBs and that this load is fully developed in a cell maintained at 37°C in less than 1h after IR. The ramifications of these observations for the kinetics of DSB repair in repair proficient and repair deficient cells will be discussed. Supported by grants from the BMBF, the DFG and the EU.

(PS3.12) Relative biological effectiveness for low energy electrons and photons. Jerome S. Puskin¹, Keith Eckerman², Michael Bellamy², Dudley Goodhead³, ¹U.S. EPA, Washington, DC, ²Oak Ridge National Laboratory, Oak Ridge, TN, ³Medical Research Council, Washington, United Kingdom

The risk from low dose, low-LET radiation appears to be mediated by the creation of clustered damage in DNA, also known as multiply damaged sites, which have a lower probability of being faithfully repaired. At low doses of low-LET radiation, this damage is believed to arise primarily from clusters of ionizations produced preferentially in the regions of higher ionization density near the ends of primary and secondary electron tracks. For example, it has been estimated that for electrons of initial energy greater than about 100 keV, or for ⁶⁰Co gamma rays, about 1/3 of the energy is deposited by electrons with energy less than 5 keV. The corresponding fraction is roughly 70% for beta particles emitted by ³H. This correlates well with the finding that, for a variety of biological end-points, ³H has an RBE of 2-3 compared with ⁶⁰Co gamma rays. Using Monte Carlo methods, it is possible, for a photon or electron of arbitrary initial energy, to estimate the fraction of energy deposited in tissue by electrons with energy below some cut-off. Based on these calculations, RBEs can be estimated for any beta/photon emitter deposited in tissue, and those results can then be used to refine risk estimates for internal emitters. The same methodology can be used to estimate the biological effectiveness of external X-ray sources, such as those employed in medical imaging.

(PS3.13) Electron transport in condensed media induced by fast ions. Jefferson L. Shinpaugh¹, Robert MacLawn¹, Steven MacLawn¹, Kevin D. Carnes², Michael Dingfelder¹, Larry H. Toburen¹, ¹East Carolina University, Greenville, NC, ²Kansas State University, Manhattan, KS

Monte Carlo track structure simulations are used to model the production and transport of secondary electrons in biologic media in order to predict chemical and biological response to ionizing radiation. To provide tests for the electron transport codes and to investigate the effect of chemical structure of the medium on low-energy electron transport, we have measured the electron emission from thin films of amorphous solid water and condensed hydrocarbons induced by the transmission of fast ions. Absolute doubly differential electron emission yields from thin films of amorphous solid water, butene, and propane following the transmission of 6-MeV protons and 1-MeV/u fluorine ions are presented. The thin films were produced by freezing the desired target vapor onto a cryogenic 1- μ m copper foil substrate held at 40 K. The absolute doubly differential yields as a function of electron energy and emission angle are compared for the various target materials and to the results from the PARTRAC track structure code for electron transport in liquid water. This work is supported in part by the National Institutes of Health, National Cancer Institute, and by the Chemical Sciences, Geosciences, and Biosciences Division, Office of Basic Energy Sciences, Office of Science, U.S. Department of Energy.

(PS3.14) The influence of amino acids on the fragmentation of oligonucleotides exposed to low energy electrons. Sylwia Ptasinska¹, Zejun Li², Nigel J. Mason¹, Leon Sanche², ¹The Open University, Milton Keynes, United Kingdom, ²University of Sherbrooke, Sherbrooke, QC, Canada

The majority of interactions between amino acids and nucleobases can be applied across all protein-DNA complexes [1]. Therefore investigating the effect of amino acids on DNA analogues can mimic the phenomena observed in the cell exposed to ionizing radiation and provide a better understanding of protein-DNA radiolysis at the molecular level. In our approach, we have studied tetramer oligonucleotides (GCAT) containing all four nucleobases: adenine (A), cytosine (C), guanine (G) and thymine (T) with glycine (Gly) and arginine (Arg), both amino acids can be found in natural proteins. The amino acid - GCAT pairs were irradiated with electrons of 1 eV. This electron energy was chosen to simplify the effects of multiple electron scattering in our samples. Moreover, one eV electrons can induce single strand breaks in DNA only via dissociative electron attachment [2]. Irradiated samples were analyzed by high performance liquid chromatography and the total fragmentation yields were measured for different molar ratios of Arg:GCAT and Gly:GCAT. Our experimental studies have shown that at higher molar ratios of glycine and arginine, both amino acids protect DNA from the direct action of electrons. Whilst at low ratios, mainly in the case of glycine, an increase in the total fragmentation yield was observed. This additional damage of oligonucleotides can be attributed to interaction of the H[•] radicals produced from glycine. As it has been shown in the gas phase studies on dissociative electron attachments to glycine the formation of dehydrogenated molecule and hydrogen radical appears with a huge cross section for this reaction [3]. In addition, the computational modelling has revealed binding energies and sites for particular amino acid-nucleobase/nucleotide pairs. Both amino acids interact relatively strongly with nucleotides via van der Waals and electrostatic interactions, however the average value for the binding energy for Arg-nucleotide (-1.633 kcal mol⁻¹) is higher than those for Gly-nucleotide pairs (-1.228 kcal mol⁻¹). Thus arginine interacts more strongly, which is in good agreement with our experimental results. [1] N.M. Luscombe et al., Nucl. Acids Res. 29, 2860 (2001) [2] F. Martin et al., Phys. Rev. Lett. 93, 068101 (2004) [3] S. Ptasinska et al., Anal. Bioanal. Chem. 377, 1115 (2003)

(PS3.15) The generalized oscillator strength of metallic calcium, and the mean free path of and the stopping power

for charged particles in calcium. Irakli G. Jorjishvili, Michael Dingfelder, Larry H. Toburen, East Carolina University, Greenville, NC

Exposure of astronauts to the galactic cosmic rays might cause leukemia, an abnormal proliferation of white blood cells. Development of leukemia might threaten lives of the affected astronauts, and jeopardize the success of the space flight mission. The laboratory equivalent to the galactic cosmic ray particles are high energy high charge (HZE) particles. Radiation impact of HZE particles on bone marrow can be evaluated by Monte Carlo computer simulations. Monte Carlo simulation codes need reliable sets of interaction cross sections between particles of a given type and given target media. The goal of current work is to calculate interaction cross sections of HZE particles with calcium, the heaviest element in the bone material. Updates will be provided on interaction cross sections, mean free passes, and stopping powers, calculated for different type particles, using slightly different models of the generalized oscillator strength of calcium. This research is supported in part by the Office of Biological and Physical Research, NASA, grant NNJ04HF39G.

(PS3.16) Effect of ionizing radiation on the differentiation responsible for transforming mouse iPS cells into the three germ layers. Naoki Hayashi¹, Kenji Takahashi¹, Satoru Monzen¹, Tsuyoshi Fujioka², Yukio Nakamura², Ikuo Kashiwakura¹, ¹Department of Radiological Life Sciences, Hirosaki University Graduate School of Health Sciences, Hirosaki, Japan, ²RIKEN BioResource Center, Tsukuba, Japan

Objective: iPS cells are generated by transfer of suitable genes such as *Nanog*, *Oct4*, *c-myc*, and *Klf4*. Although iPS cells have the potential to differentiate into various cells, detailed information with regard to their radiosensitivity is limited. This study aimed to examine the effects of ionizing radiation on the differentiation responsible for transforming mouse iPS cells into the three germ layers. Materials and Methods: Mouse iPS cells were purchased from RIKEN BioResource Center (Tsukuba, Japan). iPS cells were derived from mouse embryonic fibroblasts and cultured in DMEM containing 15% FBS and 1000 U/ml LIF. Embryoid body (EB) formation was performed in a conical tube with a loose cap in a culture medium of α -MEM containing 10% FBS. EB diameter was measured on culture day 5. The expression of various genes was analyzed by quantitative real-time RT-PCR. mRNA expression for the differentiation of the endoderm marker *Afp*, early mesoderm marker *brachyury*, and ectoderm marker *Nestin* was analyzed. X-irradiation was performed using an X-ray generator with 0.5-mm Al and 0.2-mm Cu filters at 150 kV, 20 mA, and a dose rate of 3.3-3.4 Gy/min in the range of 1-7.5 Gy. Results and Discussion: The surviving curve of mouse iPS cells showed D_0 and n values of 2.09 Gy and 1.02, respectively. The EB formation efficiency of nonirradiated and X-irradiated iPS cells was almost 100%, but EB diameter decreased in a dose-dependent manner. The mRNA expression of the pluripotent stem cell markers, *Nanog* and *Oct4*, detected in EBs derived from nonirradiated iPS cells was downregulated compared with iPS cells. No difference was observed in these markers detected in EBs derived from irradiated iPS cells. The expression of *Afp* was downregulated in EBs derived from irradiated iPS cells in a dose-dependent manner in comparison to that seen in nonirradiated control cells. Furthermore, no significant difference was observed in other two markers at 2-7.5 Gy irradiation. These results suggest the possibility that iPS cells are relatively radioresistant, but radiosensitive differences may be observed among differentiation pathways that transform iPS cells into the three germ layers.

(PS3.17) Radiation Biodosimetry in Patients Treated with Total Body Irradiation (TBI). Helen C. Turner¹, Barbara Szolc¹, Pratyush Narayan¹, Amanda McLane², Christopher A. Barker², Suzanne L. Wolden², Antonella Bertucci¹, Maria Taveras¹, Guy Garty¹, Sally A. Amundson¹, David J. Brenner¹, ¹Columbia University, New York, NY, ²Memorial Sloan-Kettering Cancer Center, New York, NY

Measurement of micronucleus (MN) frequency in peripheral blood lymphocytes is extensively used in molecular epidemiology and cytogenetics to evaluate the presence and the extent of chromosomal damage in human populations as a consequence of exposure to ionizing radiation. In the context for studies for high throughput biodosimetry, the goal of this study was to examine MN formation in peripheral lymphocytes after total body irradiation (TBI) exposure. Patients undergoing TBI at Memorial Sloan Kettering Cancer Center in preparation for hematopoietic stem cell transplant were recruited into this study. These patients were diagnosed with a variety of diseases including AML, ALL, CML, MCL, NHL, multiple myeloma and aplastic anemia. For this study, none of the patients had prior radiation treatment or had been treated with genotoxic drugs for at least 2 weeks before the start of radiation treatment, although diagnosis and differential white blood cell counts varied considerably. Blood samples were collected at three time points: 1) several hours before the initial radiation, 2) 4 hr after first 1.25-Gy fraction and 3) 24 hr after the first fraction. The 24 hr samples included exposure to three 1.25-Gy fractions with approximately 4 hr between fractions. Additionally, standard dose-response curves were established by *in vitro* irradiation of peripheral blood samples from healthy volunteers (aged 35 to 45 years) using a range of γ -ray doses between 0 and 8 Gy. Quantification of MN frequency in pre and post-irradiated blood samples from 9 TBI patients (aged 6 to 53 years) showed a significant ($p < 0.01$) induction of MN formation following first fraction. The results also show that the MN formation was accumulative observed by a further significant ($p < 0.01$) increase of MN measured 24 hours later. Generation of *in vitro* calibration curves from healthy volunteers was consistent with an equivalent whole body dose of approximately 3.5 to 4 Gy in the TBI patients. These findings indicate that measurements of MN as an index of radiation exposure, present a good correlation between the *ex vivo* and *in vivo* absorbed radiation dose. Further, these results suggest that the detection and quantification of MN formation represents a robust biomarker for whole body radiation dose prediction. Work supported by NIAID grant 5 U19-AI067773.

(PS3.18) Hypofractionated stereotactic body radiation therapy (SBRT) for the treatment of clinically localized prostate cancer: creation of a human specimen repository and initial analysis of potential radiation exposure biomarkers. Sean P. Collins¹, Hyeon U. Park¹, Christophe Redon², Asako Nakamura², Kathryn Sheikh¹, Heather Hanscom¹, Amrita Cheema¹, Albert J. Fornace¹, Anatoly Dritschilo¹, William M. Bonner², Simeng Suy¹, ¹Georgetown University, Washington, DC, ²National Cancer Institute, Bethesda, MD

Introduction: Recent data suggest that large radiation fractions are more effective than small fractions in prostate cancer radiotherapy. The CyberKnife is the ideal delivery system for hypofractionated radiation therapy due to its ability to deliver highly conformal radiation and to track and adjust for prostate motion. We report our early experience using the CyberKnife system to deliver hypofractionated radiotherapy to localized prostate cancer and the creation of a specimen repository to aid in the search for potential radiation exposure biomarkers. Methods: Patients were treated with SBRT (3625 cGy in five 725 cGy fractions over 1-2 weeks). Over 50 patients completed the planned treatment courses and sample collections. Human samples, including blood and urine, were collected one hour prior to irradiation, one hour and twenty four hours after the first fraction of radiation and at all follow-ups after the completion of radiation therapy. Aliquots of fixed blood samples were used for γ -H2AX foci measurements. Ultra-Performance Liquid Chromatography-Time of Flight Mass Spectroscopy (UPLC-TOFMS) was performed to measure changes in the serum and urine metabolome. Results: Prostate specific antigen (PSA) levels steadily decreased in all patients following treatment. Acute side effects associated with treatment included grade 1 and 2 urinary and gastrointestinal toxicity. DNA damage quantification by γ -H2AX detection revealed that a 725 cGy radiation fraction has a low impact on blood circulating lymphocytes. One hour after treatment, lymphocytes exhibit an average of 1.37 ± 0.46 γ -H2AX foci per cell with 6.4% of total lymphocytes exhibiting more than 4 γ -H2AX foci per cell as compared to 0.19 ± 0.18 and 0% for pre-treatment. In addition, γ -H2AX levels returned to pre-treatment values twenty

four hours after irradiation. Conclusion: Hypofractionated SBRT using the CyberKnife system appears to be a well tolerated by men with prostate cancer. Early PSA results suggest a biochemical response similar to other standard radiation therapy options. Limited side effects and γ -H2AX measurements imply a limited genotoxicity from the treatment. Preliminary analysis of human specimens suggests that SBRT treatment may be an adequate model system for acute radiation exposure and biomarker discovery.

(PS3.19) Early-response biological dosimetry using hematological profile - NHP dose response. William F. Blakely¹, Natalia Ossetrova¹, Arifur Rahman¹, Melanie V. Cohen², Ann Farese², David J. Sandgren¹, Thomas J. MacVittie², ¹AFRRI, Bethesda, MD, ²University of Maryland, School of Medicine, Baltimore, MD

Medical management of suspected radiation casualties necessitates use of multiple parameter biological dosimetry assessment. Radiation causes changes in peripheral blood (PB) counts that are useful for both dose- and acute radiation syndrome (ARS) - hematological system severity assessments. The ability to discriminate individuals exposed to radiation from controls by their hematological profile at an early time point is important in mass-casualty radiological incidents where repeated blood counts may not be possible. We are pursuing research activities to develop and enhance an integrated, multiple-parameter biodosimetric system for both triage and reference laboratory applications. We recently reported results from nonhuman primate (NHP) total-body irradiation (TBI) study demonstrating that combination of total lymphocytes with the neutrophil to lymphocyte ratio improved the discrimination index between 7.2 Gy and 8.4 Gy cohorts from 44% to 81% and 44% to 69% for 1 and 2 days post irradiation, respectively. Herein, we characterize the utility of changes in the hematological profiles for early (<4 days) radiation dose and injury assessment based on pooled data from NHP TBI studies over a broad dose range. Baseline and radiation time- and dose-dependent changes have been measured in the PB of NHP (males and females *Macaca mulata*) irradiated between the dose range of 1 to 13 Gy with ⁶⁰Co γ -rays (0.55 Gy/min) and 6 MV LINAC (0.8 Gy/min). A dose-dependent early-phase (1-3 d) demonstrated: a) decline in lymphocytes, b) abortive rise at 1d followed by a decline in neutrophils, c) increase in the neutrophil to lymphocyte ratio, and d) negligible changes in platelets. Lymphocyte depletion and increases in the neutrophil to lymphocyte ratios were most robust as diagnostic indices spanning the broad dose ranges from 1-3 d after irradiation, however, these two bioindicators plateau with progressive increases in radiation doses >6.5 Gy. These data support the development of an integrated and multiparameter biodosimetric software analysis system that provides diagnostic indices for medical management of radiation casualties. [Research was supported under AFRRI work units RBB4AR; DARPA under MIPR entitled: "Nonhuman Primate Testing for Biodosimetry", and NIAID contract number HHSN266200500043C.]

(PS3.20) Fast image analysis for the rapid automated biodosimetry tool. Oleksandra V. Lyulko, Guy Garty, Gerhard Randers-Pehrson, Helen Turner, David J. Brenner, Columbia University, Irvington, NY

The Rapid Automated Biodosimetry Tool (RABIT) has been developed at the Center for High-Throughput Minimally Invasive Radiation Biodosimetry for fast assessment of radiation doses received by many (tens to hundreds of thousands) individuals. The RABIT automates two well-known biodosimetric assays on isolated lymphocytes: γ -H2AX and Cytokinesis-Block Micronucleus (CBMN). Following the assays, the samples are robotically conveyed to the imaging unit where they are imaged and analyzed. High-throughput imaging in the RABIT is achieved through innovative imaging techniques such as the use of light steering instead of sample motion, parallel use of multiple high-speed cameras and single-step auto-focusing. In order to efficiently utilize these advanced techniques and to allow simultaneous image analysis we have developed scoring procedures which will be integrated into the imaging control software. In the case of γ -H2AX

analysis, we chose to measure the total fluorescence, per nucleus, of immunostained γ -H2AX in cell nuclei. The advantages of this approach over more traditional foci counting are its speed and the ability to provide rapid quantitative result even at high doses, when individual foci cannot be distinguished. During the processing of micronucleus assay results the images are analyzed for the presence and frequency of micronuclei in binucleated cells. Two different techniques have been developed: 1) an algorithm based on dual fluorescent labeling of lymphocytes and combined analysis of images of cytoplasm and nuclei and 2) an algorithm that requires only cell nucleus images, while the locations and extents of binucleated cells are estimated based on the proximity of two nuclei. Both γ -H2AX and micronuclei-scoring procedures were evaluated by generating dose-response curves in the range from 0 to 10 Gy. Correlation of the generated data with the dose was observed. Hence, the ability of the developed image analysis system to determine individual dose is consistent with the primary goal of RABIT; the system is specific and fast enough to provide the required high throughput. This work is supported by NIAID grant number U19 AI067773.

(PS3.21) Identification of protein markers in intestine and brain of irradiated mice by proteomic analysis. Young-Bin Lim, Bo-Jeong Pyun, Hae-June Lee, Sang-Rok Jeon, Yun-Sil Lee, KIRAMS, Seoul, Republic of Korea

There are increasing efforts in developing more sensitive and rapid molecular methodologies both at the genomic and proteomic levels for the identification of biomarkers of exposure to ionizing radiation (IR). However, until now, not specific biomarkers, especially with organ specificity were not identified. We analyzed altered protein expressions in various tissues including brain, lung, spleen, and intestine from the 1 Gy irradiated mice employing 2-DE analysis. MALDI-TOF MS and peptide mapping identified 30 proteins that showed greater than two-fold expression changes by IR. The total number of identified proteins for brain was 10, 5 for lung, 6 for spleen, and 5 for intestine. In order to confirm significant differences between the control and IR treated samples in 2-DE analysis, ten identified proteins with available commercial antibodies were selected for immunoblotting. Among them, only 5 proteins showed similar protein expression patterns with MS data in all three independent experiments. These were heat shock protein 5 (HSP5), heat shock protein 90kDa beta (HSP90-beta), heat shock protein 1 (HSP1), transaldolase 1 (TA1), and phosphoglycerate kinase 1 (PGK1). We excluded HSP5, HSP90-beta, and HSP1 as developing protein biomarkers, because they are belonging to the heat shock protein family. PGK1 was specifically upregulated in irradiated mouse intestine and TA1 was down-regulated in irradiated mouse brains without their alterations in other tissues. Based on these data, we suggest that TA1 and PGK1 might be candidates for tissue specific biomarkers of IR exposure.

(PS3.22) Metabolomic analysis of urine and serum from patients exposed to total body irradiation or hypofractionated radiosurgery for radiation biomarker discovery. Evagelia C. Laiakis¹, Simeng Suy¹, Kristopher W. Krausz², John B. Tyburski¹, Sally A. Amundson³, Christopher A. Barker⁴, Suzanne L. Wolden⁴, David J. Brenner³, Frank J. Gonzalez², Sean P. Collins¹, Albert J. Fornace Jr.¹, ¹Georgetown University, Washington, DC, ²National Cancer Institute, Bethesda, MD, ³Columbia University, New York, NY, ⁴Memorial Sloan-Kettering Cancer Center, New York, NY

The emergence of radiological terrorism as a real threat has led to the need for development of new fast, accurate, and non-invasive methods for detection of radiation exposure. Our studies have previously concentrated on identifying biomarkers in biofluids (urine, serum) from mice and rats. The purpose of this study was to extend the biomarker discovery to humans, which is the ideal experimental model. Two human cohort studies were utilized. The first included patients undergoing total body irradiation (TBI) at Memorial Sloan Kettering with a dose of 1.25-1.5 Gy prior to bone marrow transplantation. Urines from 35 patients and serum from 10 patients were collected just prior to irradiation, 6 h, and 24 h post

irradiation. The second cohort consisted of patients undergoing localized prostate hypofractionated robotic radiosurgery with the CyberKnife system at Georgetown University Hospital. Urine and serum were collected from 18 patients prior to irradiation and 48 h post irradiation with a localized fraction of 7.25 Gy to the planning target volume (PTV) and 8 Gy to the gross tumor volume (GTV). Global metabolic profiling was obtained through analysis with Ultra Performance Liquid Chromatography (UPLC) coupled to time-of-flight mass spectrometry. Peak alignment and deconvolution of the chromatographic data were conducted with MarkerLynx software (Waters, MA). Multivariate data analysis was performed through SIMCA-P+ (Umetrics, Sweden) and the machine-learning algorithm Random Forests. Correct classification into groups based on the top 100 metabolites varied from 70% to 100%. The top 50 metabolites were further evaluated for their identity and biomarker candidates were verified by tandem mass spectrometry (MS/MS) by comparison to pure chemicals. Quantitation of the markers was conducted with a triple quadrupole/linear ion trap mass spectrometer with a UPLC interface. Analysis revealed changes in amino acid levels, alterations in the purine metabolism pathway, and increases in inflammatory molecules, such as arachidonic acid. Recruitment of patients is ongoing for both studies and further analysis of biofluids will reveal additional information about the effects of radiation on human metabolism.

(PS3.23) Differential rank analysis: a rank-based algorithm for multiple comparisons across post-processed lc/ms radiation metabolomic data sets. Tytus D. Mak¹, John B. Tyburski¹, Evagelia C. Laiakis¹, John F. Kalinich², Albert J. Fornace¹, ¹Georgetown University Medical Center, Washington, DC, ²Armed Forces Radiobiology Research Institute, Uniformed Services University, Bethesda, MD

With the rise of metabolomics as a viable platform in radiation biodosimetry and biomarker discovery, there is an ever increasing need to develop methods and algorithms that adequately address both the strengths and deficiencies of the quantitative data produced. Metabolomics, the global study of small molecule complements, offers unprecedented quantitative insight into the metabolome via biofluid analysis. However non-experimental factors such as biofluid concentration, volume, seasonal fluctuations in animal metabolism, and diet all contribute to the exceptionally high variability of the measured metabolite levels from sample to sample. As such, a new algorithm, dubbed Differential Rank Analysis (DRA), has been developed for rapid and intuitive multiple comparisons across LC/MS post-processed metabolomic data sets acquired from biofluid samples. The general idea behind DRA is to rank the metabolites of a given sample from highest to lowest abundance. Metabolites are compared between samples strictly using these ranked lists, with their change quantified by the change in rank between the two lists. For this study, urine samples were collected at multiple time points from male adult rats before and after whole body exposures to doses of gamma radiation ranging from 0.5 to 10 Gy (n = 20 per dose). Urine metabolomics data were acquired by Ultra-Performance Liquid Chromatography coupled to time-of-flight mass spectrometry, operated in both positive and negative electrospray ionization modes, and pre-processed using MarkerLynx software (Waters, Inc.). The DRA algorithm was developed and tested using these data, from which lists of biomarker candidates were generated after analyzing across all pre-exposure data to factor for seasonal/temporal fluctuations, and across a varying range of doses and time points, depending on the classification of biomarker being searched for. Results from DRA were compared with results from more traditional methods for validation. In comparison to algorithms such as Random Forests, the strengths of DRA lie in its ability to analyze numerous, and often disjoint or dissimilar datasets in the same context, and in doing so, allow for a wide range of criteria to be considered during biomarker discovery.

(PS3.24) High-Throughput processing and analysis of micronucleus and γ -H2AX assays in ex vivo irradiated human samples. Antonella Bertucci, Helen C. Turner, Guy Garty,

Olekandra V. Lyulko, Maria Taveras, David J. Brenner, Columbia University, New York, NY

High-Throughput processing and analysis of micronucleus and γ -H2AX assays in *ex vivo* irradiated human samples At the Center for High-Throughput Minimally Invasive Radiation Biodosimetry we have developed the Rapid Automated Biodosimetry Tool (RABIT). The RABIT is a dedicated and ultra-high throughput robotically based biodosimetry system to quantify DNA damage and estimate individual past radiation exposures using a very small volume of blood. During the past year we have adapted established protocols for both γ -H2AX and cytokinesis-block micronucleus assays (CBMN) to be entirely performed in the RABIT. Histone H2AX phosphorylation on a serine four residues from the carboxyl terminus (producing γ H2AX foci) is a sensitive marker for DNA double-strand breaks (DSBs). The γ -H2AX assay measures DNA damage directly by immuno-staining the phosphorylated H2AX histones which localize DSBs. The *in vitro* micronucleus test is widely used to assess cytogenetic damage. In this system, chromosome fragments or whole chromosomes become detectable in the cytoplasm of cells that have undergone mitotic division as micronuclei (MN). Whole blood samples, from twelve healthy donors, were irradiated with γ -rays: 1, 2, 3, 4, 5, 7.5 and 10 Gy. After exposure, 30 μ l samples are placed into heparin-coated PVC capillaries containing 50 μ l of lymphocyte separation media. The separated lymphocyte bands are released into filter bottomed multi-well plates where the cells were either cultured for the MN assay or incubated for γ -H2AX assay. For the MN assay, isolated lymphocytes were cultured in complete RPMI 1640 medium containing phytohemagglutinin (PHA) to stimulate mitosis followed by the addition of cytochalasin B to block cytokinesis and obtain binucleate cells. Cells then were stained with DAPI. For the immunodetection of γ -H2AX foci, lymphocytes were incubated with an anti-human γ -H2AX monoclonal antibody and visualized using an Alexa Fluor 555 secondary antibody and nuclei were counterstained with Hoechst 33342. We will present dose response curves for both assays processed and imaged in the RABIT. Work supported by NIAID grant 5 U19-AI067773

(PS3.25) Protein biomarkers as a complementary approach to conventional biodosimetry for radiation injury and exposure dose assessment. Natalia I. Ossetrova, David J. Sandgren, Arifur Rahman, William F. Blakely, AFRRI/USUHS, Bethesda, MD

Terrorist attacks or nuclear accidents could expose large numbers of people to ionizing radiation. Optimal medical management of radiological terrorism and accidental irradiation situations would include use of validated biomarkers of radiation injury and exposure dose received by victims with an extremely high precision in order to distinguish non-exposed vs. exposed individuals, as well as to provide rapid diagnostic information for triaging of exposed individuals. We recently reported results from a murine total-body irradiation (TBI) model demonstrating for the first time that a protein expression profile (GADD45 α , IL-6, and SAA) measured in samples collected 1 and 2 d after exposure can predict mice exposed to radiation but also can distinguish the level of radiation exposure, ranging from 1 to 7 Gy ⁶⁰Co γ rays (0.1 Gy/min). The SAS-based algorithm was established for early (1 and 2 d) dose assessment and dose-dependent discrimination of study animal groups. Effect of combination of SAA and hematological biomarkers demonstrated: (1) an enhanced separation of 1-Gy irradiated animals from controls and also between different combinations of doses, and (2) an improvement of the threshold for γ -exposure detection compared to the selected protein profile only. Here in, we present similar results from the on-going nonhuman primate TBI radiation model using 30 rhesus macaques irradiated to a broad dose range of 1 to 8.5 Gy with ⁶⁰Co γ -rays (0.55 Gy/min) dose- and time-dependent changes in blood proteins CRP, Flt-3 ligand, IL-6, and GADD45 α measured by enzyme linked immunosorbent assay (ELISA). The combination of biomarkers provides greater accuracy than any one biomarker alone. The results also show that the dynamics and content of CRP and Flt-3 ligand levels reflect the course and severity of the acute radiation sickness (ARS) and may function as prognostic indicators of ARS outcome. These results demonstrate proof-in-concept that these radiation-responsive proteins show promise as a complimen-

tary approach to conventional biodosimetry for early assessment of radiation exposures and as may also contribute as diagnostic indices in the medical management of radiation accidents. [AFRRI supports this research under project RBB4AR; DARPA under MIPR entitled: "Nonhuman Primate Testing for Biodosimetry"].

(PS3.26) A broad energy range neutron target system. Yanping Xu, Gerhard Randers-Pehrson, Stephen A. Marino, David J. Brenner, Columbia University, Irvington, NY

Radiological Research Accelerator Facility (RARAF) at Columbia University has performed neutron irradiations for cells and mice for over 3 decades. Hundreds of flasks of cells and thousands of mice have been irradiated with monoenergetic neutrons having energies from 0.22 to 15 MeV. Currently we have designed a novel neutron target system to provide a broad-range energy spectrum from 100 keV to 10 MeV that will approximate the Hiroshima atomic bomb neutron spectrum. This highly innovative approach has never been tried previously. To generate a neutron beam with a broad range of energies up to 10 MeV, a mixed beam of deuterons and protons with an energy of 5 MeV will be incident on a thick beryllium target mounted on a beamline at zero degree to the accelerator axis. The Singletron RF ion source produces similar amounts of monatomic and diatomic ions and lesser amounts of triatomic ions, all of which will be incident on the target. The diatomic ions dissociate on impact with the target, producing two single ions, each with an energy of 2.5 MeV. The triatomic ions dissociate into three single ions, each with an energy of 1.67 MeV. The resultant neutron spectrum is the sum of the spectra from the ${}^9\text{Be}(d,n){}^{10}\text{B}$ reaction and ${}^9\text{Be}(p,n){}^9\text{B}$ reactions for all the incident ions. The shape of the spectrum can be modified by adjusting the ratio of protons to deuterons. The samples are placed at a 60 degree angle to the beam. The calculated neutron spectrum will be validated by measuring in-field microdosimetric spectra with a tissue-equivalent proportional counter. The measurements will be compared both with calculated microdosimetric spectra corresponding to the calculated neutron spectrum, as well as corresponding to the Hiroshima neutron spectra. Standard techniques will be used to calculate microdosimetric spectra from neutron energy spectra (ICRU microdosimetry, Zaider and Brenner 1985). This general approach is a well established one for validating calculated neutron spectra, and the well known relationships between the neutron energy spectrum and the microdosimetric spectrum will allow us to identify and quantify any energy regions where there are discrepancies.

(PS3.27) Radioecology at Savannah River National Laboratory: An integrative multidisciplinary research program for the assessment and risk reduction of exposure to radionuclides in the environment. Wendy W. Kuhne, Timothy G. Jannik, Eduardo B. Farfán, John B. Gladden, Savannah River National Laboratory, Aiken, SC

Radioecology is a multidisciplinary field incorporating several physical and biological disciplines to address radiological concerns in the environment. The history of the field of radioecology in the United States can be traced back to the early 1950s when research was directed towards understanding the fate and effects of natural and man-made radionuclides released to the environment from activities at nuclear production facilities or fallout from nuclear weapons tests. The research in those early years focused primarily on releases to local environments and effects arising from both internal and external pathways of exposure. Sixty years later radiation in the environment is a concern globally for both protection of human health as well as for non-human biota. Researchers and resource managers are challenged to identify pathways of exposure from acute and chronic sources through environmental media, non-human biota and ultimately to humans. The goal is to define the long-term consequences of exposure, which may include persistent sublethal DNA damage, genome instability and trans-generational effects arising in exposed and unexposed offspring and develop strategies to reduce the risk to human health. Recent advances in techniques for radionuclide

detection, remediation techniques, modeling as well as molecular and genetic techniques have provided the tools necessary for the field of radioecology to begin addressing the complex questions regarding the long term effects of exposure to low doses and low dose-rates of ionizing radiation and to develop innovative detection and remediation strategies. Savannah River National Laboratory is developing a research Center for Radioecology and Environmental Radiation Risk Reduction that will take an interdisciplinary approach to investigate this broad field by including; molecular and genetic level effects, individual and population level studies, ecosystem studies, contaminant sequestration, remediation and issues related to urban radioecology. A summary of the core research components of the program will be presented.

(PS3.28) β -catenin inhibitor SST-024 can sensitize breast cancer tumor initiation cells (TICs) to ionized radiotherapy. Wei Xu, UT MD Anderson Cancer Center, Houston, TX

Recent studies have shown that tumor initiation cells (TICs) are more resistant to ionized radiotherapy (IR) than differentiated cancer cells. In our lab, we have previously shown that aberrant Wnt signaling can contribute to radio-resistance of TICs in breast cancer. Herein, we use SST-024 (StemSynergy), an inhibitor of β -catenin and WNT signaling, to test if pharmacologic inhibition of β -catenin can sensitize breast cancer TICs to IR. Sum-149, an inflammatory breast cancer cell line, Sum-159, a non-inflammatory basal-type breast cancer cell line and MCF-12F, a non-tumorigenic breast cell line were used in these studies. We found that SST-024 inhibited Sum-149 mammosphere formation, a surrogate for TICs growth *in vitro*, at IC-50 1.5 nM while IC-50 for Sum-159 was 50 nM. On the other hand, the IC-50 for mammosphere formation inhibition in MCF-12F, a non-tumorigenic breast cancer cell line, was 100 nM. Similar efficacy against TICs was seen in assessments of alternative TIC surrogates including aldefluor staining by flow cytometry and CD44+CD24- marked cells. Moreover, standard monolayer and 3D mammospheres clonogenic assays demonstrate significant radiosensitization of SUM-149 TICs (mammospheres) as well as monolayer colony formation. In summary, SST-024 demonstrates significant efficacy against inflammatory breast cancer TICs and sensitize both TICs and non-TICs to IR implying targeting Wnt β -catenin signaling may be a feasible strategy to radiosensitize breast cancer TICs.

(PS3.29) CSCs enrichment and CSCs/Progeny phenotype plasticity are driven by Notch signaling pathway in breast cancer cells during radiation treatment. Chann Lagadec, Lorenza Della Donna, Erina Vlashi, Carmen Dekmezian, Frank Pajonk, UCLA, Los angeles, CA

Like in normal tissues, the self-renewal of cancer stem cells (CSCs) might be also under tight control of developmental pathway like the Notch, Wnt, Sonic Hedgehog or TGF β pathways. The Notch pathway plays an important role in normal breast development, cell fate, and normal stem cell self-renewal, and its deregulation has been shown to play a role in cancer. Aberrant Notch signaling has been implicated in the development and progression of both preinvasive ductal carcinomas *in situ* and invasive. Interestingly, in breast cancer, the Notch pathway plays major role for CSCs maintenance. While we previously published that BCSCs (Breast Cancer Stem Cells) are as more resistant to radiation, we demonstrated a link between BCSCs radio-resistance and the Notch pathway. We demonstrated that irradiation of MCF-7 cells increased the CSCs number in parallel with an induction of Notch signaling proteins expression in a dose and time specific manner. Jagged 1 was quickly (1h) increased 28-fold after 2Gy, DLL1 was increased 15-fold after 3 to 6h of 2 and 4 Gy irradiation, and Notch 2 was increased 16-fold 6h after 2, 4, 6 or 8 Gy, while DLL3 was increased 10-fold after the highest doses (6 to 12 Gy). Inhibition of Notch signaling pathway by the gamma-secretase inhibitor prevented enrichment for CSCs and reduced radiation-induced Notch proteins overexpressions. In another side, we demonstrated that radiation-induced Notch signaling contributes to the phenotype plasticity of BCSCs and their progeny via an

epithelial-to-mesenchymal induction. Thereby, while irradiation increase in a dose dependent manner the expression of Snail and Slug (Mesenchymal markers), E-cadherin (Epithelial marker) expression was downregulated. All together, our data produce a molecular explanation to the increase of breast cancer malignancy after radiation treatment.

(PS3.30) Validation of DCA QuickScan for emergency biodosimetry. Yvonne A. Devantier¹, Farrah Flegal¹, Ruth C. Wilkins², ¹Atomic Energy of Canada Ltd., Chalk River Laboratories, Chalk River, ON, Canada, ²Consumer and Clinical Radiation Protection Bureau, Health Canada, Ottawa, ON, Canada

It is widely accepted that the dicentric chromosome assay (DCA) is currently the most sensitive and radiation-specific assay for measuring biological damage due to exposure to ionizing radiation. However, the utility of this assay following radiological or nuclear accidents is limited due to the time- and expertise-intensive nature of the microscopic scoring. As a strategy to increase throughput for this assay, a new scoring technique (termed DCA QuickScan) has been validated as an alternative rapid scoring approach. Unlike conventional DCA scoring, the individual centromeres are not counted when scoring using DCA QuickScan criteria, rather the metaphase spread is quickly examined (< 10 seconds) to confirm that it appears to be complete. If no damage is obvious during that examination, then the spread is scored as normal. If damage is observed (i.e. fragments, visible rings and/or dicentrics), the scorer carefully enumerates the damage. Each dicentric must be accompanied by an acentric fragment to reduce the chance of mistaking overlapping chromatids with true dicentrics. Evaluating spread morphology is a useful parameter for QuickScan scoring, where round or oval spreads are most reliably found to contain a complete chromosome complement. As well, the use of an automated slide-maker has proven useful for providing spreads of consistent quality for use in DCA QuickScan scoring. In a previous study, triage-quality conventional DCA and DCA QuickScan analyses were compared based upon scoring a minimum of 50 metaphase cells or 30 dicentrics by 9-15 scorers across 4 laboratories. Results from this pilot study indicated that QuickScan scoring was as accurate, and much faster than, conventional DCA analysis (a 6-fold decrease in scoring time was realized using DCA QuickScan). As a follow-up study, and as validation of this scoring strategy, these scoring methods have been compared by generating full dose response curves with 1000 metaphases or 200 dicentrics scored for each dose point. Blood samples were exposed to 0-4 Gy of gamma radiation, cultured by standard methods and scored using either conventional DCA or DCA QuickScan criteria. The time required for construction of the dose response curves, and the sensitivity of DCA QuickScan scoring in comparison to conventional DCA scoring, will be reported.

(PS3.31) The development of stem cell therapy to reduce radiation-induced hyposalivation. Robert P. Coppes, Lalitha S. Y. Nanduri, Marianne van der Zwaag, Mirjam Baanstra, Jielin Feng, Monique A. Stokman, Ronald P. van Os, University Medical Center Groningen, Groningen, Netherlands

Salivary glands are often exposed to radiation, during radiotherapy for head and neck cancers. This may result in life-long salivary gland impairment severely reducing the post-treatment quality of life of the patients. In a culture of dissociated salivary glands both mice and human cells are able to form salispheres. In mice, we showed that transplantation of salisphere derived c-Kit⁺ stem/progenitor cells rescued the salivary glands from radiation-damage⁽¹⁾. In a similar manner c-Kit⁺ cells could be isolated from human salivary glands⁽¹⁾. Currently we are investigating the potency of these cells. To compare human and murine salisphere c-Kit⁺ cells we determined the co-expression of several adult tissue stem cell markers and their growth characteristics. Human salivary gland cells grow steadily and are able to generate new salispheres after digestion and further culturing in matrigel. Human and murine salispheres cultures were tested for the presence of several stem cells markers on c-Kit⁺ salisphere cells. Next, the differentiation potential of human

and murine salisphere cells was investigated in 3D culture and in a NODscid/beige kidney capsule transplantation model. Both human and murine salispheres contain CD133⁺ and CD24⁺/CD29⁺ cells. Transplantation of 10,000 mice CD133⁺ or CD24⁺/CD29⁺ cells could reduce radiation-induced hyposalivation. Within c-Kit⁺ cells between 50-85% also expressed CD133⁺. However, whereas mice c-Kit⁺ cells clearly co-expressed both CD24 and CD29, human c-Kit⁺ cells hardly expressed these markers. In 3D-differentiation culture a mixture of collagen and matrigel with medium containing R-Spondin, both human and murine salispheres gave rise to similar morphological structures, such as ducts and acinar cells. Moreover, human salivary gland cell like-structures were formed under the kidney capsule, most potently after implantation of c-Kit⁺ cells. In conclusion, human and murine salivary gland c-Kit⁺ co-express a different subset of stem cell markers but exhibit similar potencies. (1) Lombaert IM et al. *PLoS One* 2008;3(4):e2063. Supported by the Dutch Cancer Society and The Netherlands Organisation for Health Research and Development.

(PS3.32) Association of EGFRvIII and oxidative stress in glioblastoma stem cells following ionizing radiation. Yi Wang¹, Milota Kaluzova², Xiaobing Tang¹, Constantinos G. Hadjipanayis², Huichen Wang¹, ¹Department of Radiation Oncology, Emory University School of Medicine, Winship Cancer Institute of Emory University, Atlanta, GA, ²Department of Neurological Surgery, Emory University School of Medicine, Winship Cancer Institute of Emory University, Atlanta, GA

Glioblastoma multiforme (GBM) is the most lethal of primary adult brain tumors and intrinsically resistant to both chemotherapeutic and radiotherapeutic treatment. GBM stem cells (GSC) and the epidermal growth factor receptor deletion variants (EGFRvIII) are known to confer tumorigenicity and radioresistance. Here, we investigate the mechanisms underlying tumor radioresistance in glioblastoma stem cells derived from two separate patients with EGFR wild type and EGFRvIII expression. Neurospheres are sorted from xenograft tumors and cultured as four groups: EGFRCD133-, EGFRCD133+, EGFRvIII CD133- and EGFR CD133+ neurospheres. We found that radiation induces more reactive oxygen species (ROS) in EGFR wild type cells than in EGFRvIII cells, and more ROS in CD133- cells than in CD133+ cells. Over-expression of EGFRvIII in U87 cells also reduced the ROS level induced by radiation. Consistent with the ROS level, less DNA damage was detected in EGFRvIII neurospheres by a single cell electrophoresis assay. DNA double-strand breaks (DSB) were induced late and repaired fast in EGFRvIII neurospheres following radiation in the phosphorylated histone H2AX nuclear foci assay. Depletion of anti-oxidants enzyme increased DNA damage and radiosensitivity in EGFRvIII cells. Inhibition of EGFR kinase modulated anti-oxidant enzyme and DNA repair activity. These results suggest that the anti-oxidant system contributes to the radioresistance of EGFRvIII glioblastoma stem cell.

(PS3.33) Gene expression for practical biodosimetry: effects of smoking and gender. Sunirmal Paul¹, Sally A. Amundson^{1,2}, Frederic Zenhausern², Muriel Brengues², ¹Columbia University, New York, NY, ²University of Arizona, Center for Applied NanoBioscience and Medicine, Phoenix, AZ

In response to the perceived need for biodosimetry in the event of a radiological incident, we are developing radiation dosimetric signatures for gene expression profiling on a small volume of peripheral blood. Using Agilent's whole genome microarray platform with *ex vivo* irradiated blood from healthy individuals, we have previously identified a 74-gene set that can predict the radiation dose to which an individual sample was exposed with up to 98% accuracy across a long window of time (6 to 24 hr) and broad dose range (0.5 to 8 Gy). However, the utility of this approach also depends on the specificity of these signatures for radiation response. Factors like sex, age, body mass index, smoking habit and inter-individual genetic differences have been associated with variations in peripheral white blood cell basal gene expression profiles. However, the potential influence of these factors on the

accuracy of radiation dose measurement has not been thoroughly scrutinized. In the present study, we investigated the capacity of peripheral white blood cell gene expression profiles to distinguish radiation dose exposure, versus the impact of smoking or gender on the accuracy of these profiles. While broad differences in baseline gene expression were evident between smokers and non-smokers, and between males and females, hardly any of these genes intersected our previously defined radiation signatures. In a heterogeneous population with the same number of smokers and non-smokers of each gender, 289 genes were differentially expressed ($p < 0.001$ and $FDR < 4\%$) across four-radiation doses at 6 hr after irradiation, and multiple classifiers built from these genes correctly predicted samples as exposed to 0, 0.1, 0.5 or 2 Gy with up to 99% accuracy. The same samples were classified with 98% accuracy using the 74-gene *ex vivo* irradiation signature previously defined. Thus the 74-gene expression signature is robust across different sample sets, and neither smoking nor gender confounded the accuracy of radiation dose prediction. Translation of these signatures to a fully automated “lab-on-a-chip” device incorporating a quantitative nuclease protection assay is in progress, and will enable high-throughput screening for radiological emergencies, as well as making such tests practical for clinical uses.

(PS3.34) Radiation dose-response for induction of γ -H2AX foci in tissues: use of new automatic counting software. Alesia Ivashkevich¹, Olga A. Sedelnikova², Christophe E. Redon³, Andrea J. Smith¹, William M. Bonner², Roger F. Martin¹, Pavel N. Lobachevsky¹, ¹Peter MacCallum Cancer Centre, Melbourne, Australia, ²National Cancer Institute, Bethesda, MD, ³National Cancer Institute, Melbourne, MD

The γ -H2AX foci endpoint is extremely useful in many aspects of radiation biology, as well as other scenarios associated with oxidative damage to DNA. γ -H2AX foci are generally counted manually, but it is time consuming and fatiguing. One of us (PL) has developed a new computer program (TGR_IMG) for automatic counting of foci to address this problem. The software incorporates standard image analysis algorithms in sequences designated for focal analysis, while still allowing the flexibility in selecting or rejecting a particular algorithm and in optimizing the analysis parameters. It offers fast optimizing of focus identification and counting parameters based on test counts for a few images, and allows also user-independent parameter optimization. Automation requires minimum user input and allows batch processing of a range of images. The program also calculates focus area, total intensity, distribution of cells with respect to focus number etc. TGR_IMG has been initially validated using images of human lymphocytes collected from 4 different donors and irradiated *ex vivo* with various doses (0.02-1.5 Gy), in which γ -H2AX foci were also manually counted. In this validation exercise, which involved 50 images with an average of 30 cells per image, the respective times for manual and TGR_IMG analysis were 12-14 and 4 hrs. This study demonstrated a high degree of correlation between average values for each group (radiation dose/donor) obtained from manual and automatic counting ($R^2 = 0.973$). The automatic versus manual counting comparison was then extended to radiation dose response studies with various mouse tissues, by examination of touch prints (duodenum) or sections (oral mucosa, duodenum), after whole body irradiation (0.5-5 Gy). A correlation coefficient $R^2 = 0.773$ was obtained in the analysis of average numbers of foci per image comparing manual and automatic counting, and $R^2 = 0.952$ for average values per group (radiation dose). The results confirm the general utility of the automatic counting program coupled with significant time saving.

(PS3.35) Mesenchymal stem cells administered intravenously into mice ameliorate radiation combined injury. Nikolai V. Gorbunov, Wan Jiao, Thomas B. Elliott, G. David Ledney, Juliann G. Kiang, Armed Forces Radiobiology Research Institute, Bethesda, MD

Radiation combined injury (RCI) is a pathophysiological condition due to ionizing irradiation combined with trauma or other insults that complicate systemic responses and exacerbate the acute radiation syndrome. Considering the growing threat from potential

radiological and nuclear incidents, development of effective CI countermeasures is important to military and civilian personnel. This report focused on assessment of survival of mice engrafted with bone-marrow mesenchymal stem cells (BMMSCs) after RCI. RCI was induced in B6D2F1/J female mice by 9.75 Gy 60Co-photon followed within 1 hour by a 15% total-body-surface skin-wound trauma. Twenty-four hours later, animals received 0.4 ml Dulbecco's Modified Eagle Medium (DMEM) or 2x10⁶ BMMSCs in DMEM vehicle. BMMSCs were obtained from B6D2F1/J female syngeneic mice using a protocol adapted from STEMCELL Technologies Inc. The cells were expanded and cultivated in hypoxic conditions for 28 days in MESENCULT medium (STEMCELL Technologies Inc.). The phenotype and cell proliferative activity were analyzed with flow cytometry and immunofluorescence imaging; the cells were identified by BMMSC markers: CD44, STRO1, SCA1. BMMSCs were harvested at 80% confluency and transfused as mentioned above. Animal survival, body weight, water consumption, and wound closure were monitored for 30 days. Data were analyzed by a Kaplan-Meier survival curve. Statistical significance was determined using one-way ANOVA followed by post-hoc analysis with pairwise comparison by Tukey-Kramer test. The data support the contention that BMMSC transfusion can mitigate RCI-induced hematopoietic depression yielding a 20% increase in survival. (Supported by NIH/NIAID Y1-AI-5045-04).

(PS3.36) γ -H2AX quantification in plucked hairs to assess exposure to genotoxic agents – application to partial-body radiation biodosimetry. Christophe E. Redon¹, Asako J. Nakamura¹, Arifur Rahman², William F. Blakely², William M. Bonner¹, ¹NIH/NCI/CCR/LMP, Bethesda, MD, ²AFRRRI/USU, Bethesda, MD

One step towards more effective and personalized cancer treatments may be the ability to assess the effect of a particular drug or radiation treatment on individual patients. Since radiation exposure and many chemotherapeutic agents induce DNA double-strand breaks (DSBs) in a patient's cells, monitoring DSBs may be a useful tool for personalizing treatment. γ -H2AX is an attractive candidate for monitoring DSB levels, since it is formed upon DSB induction and is easily assayed by microscopy and immunoblotting with the appropriate antibody. One challenge in manifesting this idea is the choice of an appropriate surrogate tissue. Blood lymphocytes are commonly used to detect DSB following both exposures to drugs and ionizing radiation (IR). However, a good surrogate tissue should contain cells with high DNA metabolism since most cancer drugs target replication/transcription. Moreover, such a tissue should be obtainable by non-invasive means to minimize patient discomfort. Plucked hairs make an attractive candidate tissue because they fulfill both these criteria. In order to assess their suitability, we exposed human plucked hairs *ex vivo* to several DNA damaging agents including IR and chemotherapeutic drugs. Increased levels of γ -H2AX were detected after both treatments. To validate the use of plucked hairs, *in vivo* experiments were performed with Rhesus macaques against whole-body IR. Using microscopy, γ -H2AX response was linear 1 and 2 days after IR (with doses of 1, 3.5, 6.5 and 8.5 Gy). Moreover, persistent γ -H2AX signal was still detected 4 and 9 days after 8.5 Gy-IR. Results obtained using immunoblotting for hairs are also shown in this study. These findings suggest that plucked hair may be a suitable surrogate tissue for monitoring patient response to both IR and chemotherapy. Additional studies are required to evaluate the influence of potential confounders (i.e., inter-individuals variations, dose fractionation and response of special populations (i.e., elderly, etc.) for use of this assay. [Research supported by DARPA, NIAID and NIH]. The views, opinions, and/or findings contained in this article/presentation are those of the author/presenter and should not be interpreted as representing the official views or policies, either expressed or implied, of DARPA or the Department of Defense.

(PS3.37) Improvements in modelling external exposure to ionizing radiation for CERCLA risk and dose assessments. Fredrick G. Dolislager, The University of Tennessee, Oak Ridge, TN

To model the external exposure pathway in risk and dose assessments of radioactive contamination at Superfund sites, the U.S. Environmental Protection Agency (EPA) uses slope factors and dose conversion factors. Without any adjustment, this effectively assumes that an individual is exposed to a source geometry that is effectively infinite in vertical and horizontal extent. Increasingly complex adjustments, to account for the extent of contamination and corresponding radiation field, are presented to provide more accurate risk and dose assessment modelling when using various EPA web-based Preliminary Remediation Goal (PRG) calculators. New Area Correction Factors (ACFs) for adjusting slope factors were developed for 2-D exposure models. Eight different area sizes for 800 radionuclides are now available in the PRGs for Radionuclides calculator. (<http://epa-prgs.ornl.gov/radionuclides/>) For the PRGs in Buildings (BPRG) electronic calculator, two sets of further enhancements were developed. First, external ground plane SFs were determined for 800 radionuclides. Second, new surface factors (F_{SURF}) were developed to account for the varying radiation fields inside a contaminated room. 81 locations in 5 room sizes, ranging from 10 by 10 by 10 to 400 by 400 by 40 feet, were modeled to account for the dose contribution from multiple surfaces. The results show that only at very low photon energies is the position of the receptor in the room likely to be relevant. Also shown is that only at very low photon levels is the size of the room likely to be relevant. (<http://epa-bprg.ornl.gov/>) For the PRGs in Outdoor Surfaces (SPRG) electronic calculator, two sets of further enhancements were developed for 800 radionuclides. First, external 1, 5 and 15 centimeter soil volume SFs were developed. Second, new F_{SURF} values were developed based on exposure to 2 vertical surfaces (outside building surfaces on either side of a street) and a horizontal surface (road and sidewalk). Locations in the midpoint of the sidewalk, next to the buildings and in the middle of the street for building heights of 12.5, 30, 59 and 150 and 200 feet, were modeled to account for the dose contribution from multiple surfaces. Results show that building height doesn't effect the dose rate significantly after 150 feet. (<http://epa-sprg.ornl.gov/>).

(PS3.38) Tie2⁺ bone marrow endothelial cells regulate hematopoietic reconstitution following total body irradiation. Phuong L. Doan, J. Lauren Russell, Heather A. Himgburg, Sarah K. Meadows, Pamela Daher, Julie M. Sullivan, Nelson J. Chao, David G. Kirsch, John P. Chute, Duke University Medical Center, Durham, NC

Radiation causes myelosuppression via damage to bone marrow (BM) hematopoietic stem cells (HSCs). HSCs reside in association with BM endothelial cells (ECs), but the function of BM ECs in regulating HSC regeneration after injury is not well understood. We hypothesize that BM ECs regulate hematopoietic reconstitution following stress. To test this hypothesis, we compared the hematopoietic response to total body irradiation (TBI) of Tie2Cre;Bak^{-/-};BaxFl^{-/-} mice with Tie2Cre; Bak^{-/-};BaxFl^{+/+} mice which have constitutive *Bak* deletion but retain *Bax* in Tie2⁺ BM ECs. Two hours after 300 cGy TBI, Tie2Cre;Bak^{-/-};BaxFl^{-/-} mice displayed an increase in viable BM cells ($p=0.03$), total *ckit*+*sca*+*lineage*- (KSL) progenitor cells ($p=0.001$), CFU-Spleen day 12 ($p=0.005$), and a 2.5-fold increase in 12-week competitive repopulating units (CRUs, $p=0.009$) compared to Tie2Cre;Bak^{-/-}; BaxFl^{+/+} mice. Since Tie2 is expressed by BM ECs and, to a lesser extent, HSCs, we asked whether radioprotection of Tie2Cre;Bak^{-/-};BaxFl^{-/-} mice was caused by protection of Tie2⁺ BM ECs or Tie2⁺ HSCs. We transplanted 4×10^6 BM cells from Tie2Cre;Bak^{-/-};BaxFl^{-/-} mice into lethally irradiated wild type (WT) B6.SJL mice to generate mice that retained *Bak* and *Bax* deletions in HSCs while having a wild type BM ECs (HSC- BaxFl^{-/-};EC-WT), verified by qRT-PCR. At 16 weeks post-transplant, we exposed the chimeric mice to 300 cGy TBI and observed a significant decrease in total KSL cells ($p=0.02$), CFU-Spleen day 12 ($p=0.03$), and 12-week CRUs ($p=0.04$) in chimeric mice compared to Tie2Cre;Bak^{-/-}; BaxFl^{-/-} mice. After exposure to 750 cGy TBI, we observed 100% survival in Tie2Cre;Bak^{-/-};BaxFl^{-/-} mice compared to 10% survival in Tie2Cre;Bak^{-/-};BaxFl^{+/+} mice and wild type C57Bl6 mice at 30 days. Interestingly, the HSC-BaxFl^{-/-};EC-WT mice demonstrated 40% survival, which was significantly less than the Tie2Cre;Bak^{-/-}; BaxFl^{-/-} mice, indicating that BM ECs regulated the survival of mice

following high dose TBI ($p=0.005$). These results demonstrate that the hematopoietic response to ionizing radiation is governed by the function of BM ECs. BM ECs are a novel therapeutic target to facilitate hematopoietic reconstitution *in vivo* following radiation injury.

(PS3.39) An acellular comet assay as a portable test for DNA damage from ionizing radiation. Erin K. Redmond¹, James P. McNamee², Diana Wilkinson¹, ¹Defence Research and Development Canada, Ottawa, ON, Canada, ²Health Canada, Ottawa, ON, Canada

The comet assay (single cell gel electrophoresis) is a method used to measure the amount of DNA damage in a single cell based on the migration of DNA during electrophoresis. Whole cells are embedded in agarose and lysed, which results in the supercoiled structure of genomic DNA being maintained within the agarose. DNA strand breaks relax the supercoiled structure and allow loops and strands of DNA to migrate out of the nuclear region producing a comet-like tail; therefore, damage can be quantified by measuring the amount of DNA migrating into the tail region. Comet assays have been used in genotoxicity studies, clinical applications, DNA repair analysis, environmental biomonitoring, and various human studies including radiation dosimetry. Variations of the neutral comet assay include the alkaline comet assay, use of lesion-specific enzymes, comet-FISH, transcription-coupled DNA repair, and the acellular comet assay. Under alkaline conditions, DNA strands separate and there is a resulting increased loosening of the supercoiled structure because single strand breaks, double strand breaks, and alkali-labile sites permit loops of DNA to migrate further out of the comet head. This differentiates the comet assay from other dosimetric methods utilizing DNA, such as the dicentric and micronucleus assays, which only detect unrepaired double strand breaks. The acellular comet assay variation, when applied to Radiation Biology studies, provides many advantages not present in the standard alkaline comet assay. It allows for removal of free-radical scavengers and the potential to increase concentrations of reactive oxygen species, increasing the amount of DNA damage. The acellular comet assay does not require the use of live cells and consequently there is no DNA repair following damage, allowing for signal amplification in a portable assay. In addition, this assay does not account for additional DNA damage from experimental cytotoxicity and could allow the measurement of DNA damage that would kill live cells. Overall, we have validated a portable, versatile, reliable, and sensitive dosimetry protocol to measure direct genomic DNA damage, on a single cell level, from potentially multiple qualities of ionizing radiation.

(PS3.40) Localized irradiation disrupts the proliferation and migration of neural progenitor cells in the subventricular zone of the adult rodent brain. Pragathi Achanta, David Purger, Juvenal Reyes, Eric Ford, Alfredo Quinones, Johns Hopkins University, Baltimore, MD

Purpose: Neural stem cells (NSCs) and progenitor cells (NPCs) are being actively explored as means to control tumor growth and repair cognitive function in brain cancer patients. Little is known, however, about how radiation affects neurogenesis and the migration of NPCs. This is important since nearly all brain cancer patients receive radiation as part of their treatment. Here we employ a CT-guided localized radiation technique to study the effects of radiation on proliferation and migration of neuroblasts in a mouse model. Method and Materials: We delivered single 10 Gy doses of radiation selectively to the subventricular zone (SVZ), rostral migratory stream (RMS) and olfactory bulb (OB) of C57BL/6J mice using an in-house radiation device. Iodine was introduced intrathecally as a contrast agent to aid in visualization of targets on CT. Immunohistochemical staining for γ H2Ax was employed to validate the radiation beams and quantify targeting accuracy. Ki-67 and doublecortin (DCx) staining was used to evaluate the localized effects of the beam. A localized 10 Gy beam was also delivered to RMS and OB only, which leaves the SVZ (site of origin for NPCs) undisturbed. Pulse labeling with BrdU delivered

24 hours after radiation was used to track the migration of cells along this standard SVZ-RMS-OB pathway after irradiation. Results: Overall beam targeting accuracy was 0.18 mm as measured in gH2Ax stains. Quantification of Ki-67 positive cells demonstrated that the unirradiated regions of the brain showed undisturbed NPC proliferation relative to a sham mice. Immunohistochemistry with DCx showed a depletion of migrating neuroblasts in the irradiated region of the SVZ and RMS. A significant decrease in BrdU+ cells migrating through the irradiated RMS and OB region was observed. Conclusion: Localized irradiation can be achieved in the mouse with an accuracy needed to study local effects on neurogenesis and migration. Irradiation disrupts the migration of neural progenitor cells along an established pathway in the mouse. Further investigation of dose dependence and mechanisms are warranted.

(PS3.41) The RABIT - a Rapid Automated Biodosimetry Tool. Guy Garty¹, Youhua Chen², Helen C. Turner¹, Antonella Bertucci¹, Oleksandra V. Lyulko¹, Jian Zhang², Hongliang Wang², Nabil Simaan², Gerhard Randers-Pehrson¹, Y. Lawrence Yao², David J. Brenner¹, ¹Columbia University - Center for Radiological Research, New York, NY, ²Columbia University - Department of Mechanical Engineering, New York, NY

Over the past five years the Columbia Center for Minimally Invasive Radiation Biodosimetry has developed the RABIT, a completely automated, ultra-high throughput biodosimetry workstation. The RABIT analyzes fingerstick-derived blood samples, to estimate past radiation exposure or to identify individuals exposed above or below a cutoff dose. Through automated robotics, lymphocytes are extracted from small blood samples into filter bottomed multi-well plates. Depending on the time since exposure, either the cytokinesis-blocked micronucleus (CBMN) or the gamma-H2AX assay is then performed, in a fully automated robotic system. The use of filter-bottomed plates allows rapid washes without the need to pellet and re-suspend after each step, simplifying the liquid handling system and increasing throughput. The RABIT system is unique in the use of filter-bottomed multi-well plates, which greatly reduces the time required for processing the samples and greatly enhances the efficiency of lymphocyte retention. Following lymphocyte culturing (for the micronucleus assay), fixation and staining, the filter bottoms are removed from the multi-well plates and sealed prior to automated high-speed imaging. Analysis of the images obtained is performed online using dedicated image processing hardware. Both the sealed filters and the images are then archived. Parallel handling of multiple samples through the use of dedicated, purpose-built, robotics and high speed imaging allows throughputs of 6000-30,000 samples per day. In designing the RABIT we have taken a comprehensive approach. In addition to the robotic sample handling and analysis, we have developed and tested a sample collection kit and transport procedures that are compatible with high throughput collection in a disaster environment, while maintaining sample integrity. We will describe the sample processing in the RABIT and present sample dose-response curves from blood irradiated *ex-vivo*. This work is supported by NIAID grant number U19 AI067773.

(PS3.42) In-phantom determination of peripheral organ doses due to prostate radiation therapy using 18 MV photon beam and the associated risk of cancer induction. Eva Bezak¹, Rungdham Takam², Eric Yeoh³, ¹Department of Medical Physics, Royal Adelaide Hospital, Adelaide, Australia, ²Office of Atoms for Peace, Bangkok, Thailand, ³Department of Radiation Oncology, Royal Adelaide Hospital, Adelaide, Australia

Introduction. Peripheral photon and neutron doses in Rando phantom were measured and used to estimate the associated risks of second primary cancer in organs-at-risk located outside the target volume as a result of prostate carcinoma external beam radiotherapy using 18 MV X-ray beam from Varian iX medical linear accelerator. Methods. ⁶LiF:Mg,Cu,P and ⁷LiF:Mg,Cu,P glass-rod thermoluminescent dosimeters (TLDs) were inserted in slices of Rando phantom and followed by irradiation of the phantom to 80 Gy

radiation dose using 4-field 3D-CRT technique and 18 MV X-ray beam. ⁶LiF:Mg,Cu,P and ⁷LiF:Mg,Cu,P TLDs were calibrated using 6 and 18 MV X-ray beams. Neutron dose equivalents measured with CR-39 etch-track detectors were used to derive readout-to-neutron dose conversion factor for ⁶LiF:Mg,Cu,P TLDs. Results. The average total (photon + neutron) dose equivalents per 1 Gy isocentre dose range from 4.0 ± 0.9 mSv/Gy (thyroid) to 15.0 ± 13.9 mSv/Gy (colon). The associated risks of second primary cancer estimated using the competitive risk model were found to range from 1.5 ± 0.3% (thyroid) to 4.5 ± 4.2% (colon). Discussion: ⁶LiF:Mg,Cu,P and ⁷LiF:Mg,Cu,P glass-rod TLDs can be used in-pair to measure peripheral photon and neutron doses simultaneously in the Rando phantom which accordingly allow evaluation of the associated risks of second malignancy in organs-at-risk as a result of prostate radiotherapy using high-energy linear accelerator. Conclusion: Radiotherapy of prostate carcinoma using EBRT technique and high-energy linear accelerator is associated with elevated risk of second primary cancer in organs-at-risk.

(PS3.43) Gene expression study of irradiated blood samples from patients undergoing heterogeneous bone fracture. Muriel Brengues¹, Yoganand Balagurunathan², Michael Bittner², Ronald Korn³, Nicholas Flores³, David Liu³, Frederic Zenhausern¹, ¹University of Arizona, Phoenix, AZ, ²TGen, Phoenix, AZ, ³Scottsdale Healthcare, Scottsdale, AZ

In collaboration with our partners, we have developed an approach to measure the dose of radiation absorbed by the body that could be applied in public health situations such as the screening of potential victims of an act of radiological terrorism, as well as in clinical situations such as monitoring the dose of radiation received by patients undergoing radiotherapy. Our new platform technology comprises a low density microarray for rapid detection and triage containing less than 5 genes selected on the basis of their abundance and differential expression level in response to radiation (3 genes of interest, TNFRSF10B, AEN, CDKN1A, one housekeeping gene and one negative control). The platform performs gene expression analysis via direct signal amplification assays which simplify upfront sample preparation without the need for RNA extraction. We validated the assay platform with *ex-vivo* irradiated blood samples and the data demonstrated a good dose-response of gene expression in response to radiation. In order to accelerate the sample processing cycle time, while allowing higher multiplexing capacity, we have been exploring non enzymatic assay chemistries with fewer processing steps that are more suitable for rapid, cost effective and field deployable genomic tests. A clinical study is being initiated on patients undergoing radiotherapy treatment for validating our biodosimetry platforms and methodologies with *in-vivo* samples. As most of the cancer patients also undergo chemotherapy treatment which can create some changes in the gene expression signature, our study will be conducted with non cancer patients treated for heterotopic ossification prophylaxis. Large collection of samples will be used to develop classifier models that would predict the radiation levels, using gene expression signatures of potential markers. Our preliminary model studies reveal stringent quality control on the assay to achieve a 95% confidence in classification. These markers could also be used to predict other characteristics of the population paving way for new diagnostic applications.

(PS3.44) Urinary biomarkers identified by NMR spectroscopy for partial-body radiation exposure. Congju Chen, David J. Brenner, Truman R. Brown, Columbia University, New York, NY

In response to a radiological event, such as a nuclear accident or dirty bomb attack, tens or hundreds of thousands of people need to be rapidly screened for radiation exposure. Moreover, most exposures will not be homogeneous whole body, but will be inhomogeneous, either because of shielding, or because radioactive material was ingested. To develop a rapid automated high-throughput radiation biodosimetry which is both sensitive and specific to partial-body radiation exposure, we have employed Nuclear Magnetic Resonance (NMR) spectroscopy to identify quantitative metabolomics signatures (profiles of radiation-induced

small molecules) in urine (from irradiated mice) which are sensitive and specific to partial-body radiation exposure. The main advantages of NMR in this study are its nonselectivity, minimum sample preparation and reproducibility. Groups of C57BL/6 male mice were partially exposed to two doses of X-ray irradiation (8 Gy and 16 Gy). Four partial-body exposure scenarios were designed to include head, cardiac/pulmonary, gastro-intestinal and reproduction organs irradiations. Urine samples were collected from both irradiated and control mice when they were put in metabolic cages individually. NMR spectra of the urine samples were acquired on a Bruker Avance spectrometer operating at a proton frequency of 500M Hz. Principle Component Analysis (PCA) of the NMR spectra indicates that there are distinguishable biomarker patterns for different irradiation sceneries. For example, the irradiated mice with gastro-intestinal exposure to 16 Gy X-ray produced more creatine and less 2-oxoisocaproate in urine while those with cardiac/pulmonary exposure produced less taurine compared with the control group. More experiments for different exposure scenarios on various dosages are undergoing in our laboratory. We expect the metabolomic profile to provide information about radiation dose and the nature of the partial body exposure. This work is supported by grant HDTRA1-07-1-0025 from the Defense Threat Reduction Agency (DTRA).

(PS3.45) Notch-mediated radiation resistance in glioma stem cells. Jialiang Wang¹, Bruce A. Sullenger¹, Jeremy N. Rich², ¹Duke University, Durham, NC, ²Cleveland Clinic, Cleveland, OH

Malignant glioma is the most common and aggressive form of primary brain tumor. Radiotherapy represents the most effective nonsurgical treatment for gliomas, yet radioresistance is universal and recurrence is almost inevitable, suggesting insufficient killing of tumorigenic cells. Cancer cells with stem cell-like properties have been described in a wide range of human tumors, including gliomas. Recent studies in our laboratory and other groups suggest that cancer stem cells derived from glioma and breast tumors are more resistant to radiation than the matched non-stem cancer cells. The emerging role of cancer stem cells in tumor response to radiation suggests that these cells represent critical targets for radiotherapy and urges investigation on molecular mechanisms underlying radioresistance of these cells. The Notch developmental pathway plays an instructive role in normal stem cell biology. Aberrant activation of Notch has been documented in a wide range of human tumors. A growing body of evidence has found significant parallel between normal stem cells and cancer stem cells utilizing Notch to promote self-renewal and survival. Importantly, we recently show that Notch signaling regulates a core radioresistant mechanism in glioma stem cells. The key observations include: 1) Notch is activated by radiation in glioma stem cells; 2) Notch inhibition by gamma-secretase inhibitors (GSIs) or shRNA targeting Notch1 or Notch2 receptors significantly increased radiosensitivity of glioma stem cells; 3) expression of the constitutively activate intracellular domains of Notch1 or Notch2 (NICDs) protected glioma stem cells against radiation; 4) Notch does not regulate radiation response of the CD133-negative differentiated glioma cells; 5) the PI3K/Akt pathway critically mediates the radioprotective of Notch. This finding lays the groundwork to design novel adjunct to improve radiotherapy for glioma treatment. Such a strategy is anticipated to significantly improve long-term tumor control through effectively targeting the cancer stem cell subpopulation.

(PS3.46) Involvement of mitochondrial function in radiosensitivity of human hematopoietic stem cells. Yukiko Kaneyuki, Kenji Takahashi, Ikuo Kashiwakura, Department of Radiological Life Sciences, Hirosaki University Graduate School of Health Sciences, Hi, Hirosaki, Japan

Objective: Biological effects of ionizing irradiation are classified as direct and indirect actions. Low-LET irradiation, such as X-rays, mainly induces an indirect action by producing reactive oxygen species (ROS). Mitochondria act as a source as well as a target organ of ROS in this process. Although hematopoietic stem cells (HSCs) are highly radiosensitive, information with regard to

intracellular ROS production and the involvement of mitochondria remains to be largely elucidated. This study investigated these interactions in radiosensitive, human HSCs. Materials and Methods: Highly purified CD34⁺ cells prepared from human placental/umbilical cord blood were used as HSCs in this study. The clonogenic potential was assayed by the methylcellulose technique containing the optimal cytokine cocktails. The cells were treated with 2',7'-dichlorofluorescein diacetate and MitoTracker Green FM to estimate intracellular ROS production and fluorescence intensity of mitochondria, respectively. Each assay was analyzed by flow cytometry. X-irradiation was performed using an X-ray generator with 0.5-mm Al and 0.3-mm Cu filters at 150 kV, 20 mA, and a dose of 90-100 cGy/min. Results and Discussion: ROS was not detected in the CD34⁺ cells immediately after irradiation. Minimal ROS production was observed in cells cultured with cytokines at 3-6 h after irradiation. ROS production increased 5-10-fold in human monocytic U937 cells compared with CD34⁺ cells. The surviving fraction of CD34⁺ and U937 cells obtained at 2 Gy was 26.2 and 66.0, and that at 4 Gy irradiation was 5.1 and 21.0%, respectively. Differences between both cells were statistically significant. The intensity of mitochondrial luminescence observed in CD34⁺ cells was only half that observed in U937, which corresponds with the previous report, which indicated a lower number of mitochondria in HSCs compared with other cells. However, no significant relationship was observed between survival fraction and intensity of mitochondrial luminescence. These results suggest that HSCs are highly radiosensitive. However, their sensitivity against low-LET irradiation cannot be explained only by ROS production and mitochondrial function.

(PS3.47) Nf-kb-her2, a new biomarker to target radioresistant breast cancer stem cells. Nadire-Duru, Ming Fan, Jian Jian Li, UC Davis Medical Center, Radiation Oncology, Sacramento, CA

Acquired tumor resistance to chemo and radiation therapy, especially in recurrent and metastatic lesions, has been the challenge in improving the efficacy of tumor control and overall cancer patient survival. Cancer stem cells (CSCs), consisting less than 1% of total tumor cells, are defined as specific tumor cells with a unique capacity to self-renew and give rise to heterogeneous lineages of cancer cells within the tumor. Recent data show that CSCs are more radioresistant than cancer cells without the feature of CSCs. Therefore, identifying CSCs and their roles in tumor repopulation may generate valuable information for developing new therapeutics to control the aggressiveness of recurrent and metastatic tumors. In clinic, breast cancer patients with HER2/nue (a ErbB family member) over-expressing in a tumor are shown to live one-third shorter than HER2 negative patients due to the aggressive tumor growth, resistance to treatment and high risk of local relapse and recurrence. We reported that some cancer cell lines isolated from the survival fraction of cancer cells after exposure to multiple doses of therapeutic radiation show a resistant phenotype to radiation due to HER2 overexpression that is regulated by the transcription factor NF- κ B. HER2 protein levels, not gene copy number, are found to be elevated in the recurrent tumors compared with the primary breast cancer. Thus, radiation-induced repopulation of breast cancer cells appear to be related to activation of a specific pro-survival pathway with a novel set of radioresistant breast cancer stem cell marker, i.e., NF- κ B/HER2/CD44⁺/CD24^{-low}. The radioresistant MCF7 clones with high HER2 level or MCF7 cells overexpressing HER2 show a significant enhancement in cell invasiveness and aggressiveness compared with wild type MCF7 cells. Furthermore, with FACS live-sorted MCF7 cells we find that HER2⁺/CD44⁺/CD24^{-low} cells are more radioresistant, aggressive and invasive than the HER2/CD44⁺/CD24^{-low} cells. These results demonstrate a novel feature of tumor repopulation with radioresistant breast CSCs and a potentially effective therapeutic target for imaging and inhibiting radioresistant CSCs.

(PS3.48) Activation of hematopoietic stem cells attenuates radiation-induced genetic instability by stimulating the repair of DNA double-strand breaks. Senthil Kumar Pazhanisamy¹, Ningfei An², Yong Wang², Daynna J. Wolff², Daohong Zhou¹,

¹University of Arkansas for Medical Sciences, Little Rock, AR,²Medical University of South Carolina, Charleston, SC

Safeguarding the genomic integrity of hematopoietic stem cells (HSCs) is crucial for the maintenance of their function and prevention of genomic instability and leukemia. Unfortunately, little is known on why HSCs are highly susceptible to the induction of genomic instability by various genotoxic agents including ionizing radiation (IR). In the present study, we investigated the DNA damage and repair process in both HSCs and hematopoietic progenitor cells (HPCs) isolated from adult mouse bone marrow (BM) by using γ -H2AX immunofluorescent staining and neutral comet assay. The results from our study showed that HSCs repaired IR-induced DNA double-strand breaks (DSBs) less efficiently than HPCs. Intriguingly, this phenomenon is likely attributable to the quiescence of HSCs, because HSCs from both the embryonic day 14.5 (E14.5) mice fetal livers (FL) and adult mice BM 5 days after injection of 5-fluorouracil (5-FU) were proficient in repair of IR-induced DSBs. Further studies revealed that quiescent HSCs were deficient in repair of DSBs because they were unable to effectively activate the homologous recombination (HR) and non-homologous end joining DSB repair pathways even though they were capable of sensing and signaling the damage. However, activation of quiescent HSCs with stem cell factor (SCF) and thrombopoietin (TPO) in vitro and with polyinosinic:polycytidylic acid (PolyI:C) in vivo stimulated DSB repair function in HSCs. More importantly, it was found that a single iv injection of PolyI:C after total body irradiation (TBI) significantly attenuated IR-induced accumulation of DSBs in HSCs and increase in the number of unstable chromosomal aberrations in the progeny of HSCs. Taken together, these findings suggest that transient activation of HSCs may represent a novel mechanism-based approach for the prevention of genotoxic stress-induced hematopoietic genetic instability by stimulating the repair of DSBs in HSCs.

(PS3.49) Response of cancer stem cells to ionizing radiation and metformin alone and combined. Bo-hwa Choi¹, Hyemi Lee¹, Eun-Taeh Oh¹, Brent Williams², Moon-Taek Park¹, Min Jeong Song¹, Chang W. Song², Heon Joo Park¹, ¹Inha University College of Medicine, Incheon, Korea, Republic of, ²University of Minnesota Medical School, Mankato, MN

There is increasing evidence that the presence of small fractions of cancer stem cells (CSCs) in tumor is the limiting factor for the complete control of the tumors by radiotherapy because CSCs are radioresistant and, thus they induce recurrence after radiotherapy. A recent study demonstrated that metformin, the most widely used anti-type 2 diabetes drug, is able to selectively kill CSCs of human breast cancer cell lines. We hypothesize that metformin preferentially kills CSCs by suppressing the Akt/mTOR signaling pathway, which is hyperactivated in CSCs. We further hypothesize that suppression of mTOR, an important survival signal, may increase the radiosensitivity of CSCs. We first investigated the effect of metformin on the CSCs in MCF-7 human breast cancer cells by identifying CSCs based on the CD44+/CD24-/low surface marker and also based on the ability of CSCs to form non-adherent mammospheres. In the control MCF-7 cells, 3.40% of the total cell population was CD44+/CD24-/low cells, i.e. CSCs, and it decreased to about 2.29% and 0.71% upon incubation for 48 h with 0.1 mM and 10 mM metformin, respectively. Irradiation with 5 Gy, on the other hand, increased the CSCs population to about 5.5%. Such increases in % of CSCs by irradiation was apparently due to the preferential death of non-CSCs. Treating MCF-7 cells with 0.1 mM and 10 mM metformin decreased the mammosphere formation to 65% and 39%, respectively, of control. Irradiation of MCF-7 cells with 4 Gy decreased the mammosphere formation to 61% of control. Incubation with 1-5 mM metformin for 48 h markedly activated AMPK and suppressed mTOR in both monolayer MCF-7 cells and MCF-7 mammospheres. Combination of 4 Gy irradiation and metformin was significantly more effective than either of them alone to activate AMPK and suppress mTOR in both monolayer and mammosphere MCF-7 cells. Further insights into the mechanisms underlying the metformin-induced death and radiosensitization of CSCs would establish a theoretical base for the rational application of metformin to potentiate radiotherapy against cancer.

(PS3.50) Individual Differences in the Radiosensitivity of Hematopoietic Progenitor Cells Detected in Steady-State Human Peripheral Blood. Mikinori Kuwabara¹, Kengo Kato², Ikuo Kashiwakura², ¹Laboratory of Radiation Biology, Graduate School of Veterinary Medicine, Hokkaido University, Sapporo, Japan, ²Department of Radiological Life Sciences, Hirosaki University Graduate School of Health Sciences, Hirosaki, Japan

Steady-state hematopoiesis requires that a small fraction of stem cells circulate in the peripheral blood (PB), and they also play a decisive role in the homeostasis of blood cell production. The heterogeneity of hematopoietic stem/progenitor cells and their antioxidative capacities may result in a differential sensitivity to radiation. The aim of this study is to evaluate the individual differences in the radiosensitivity of lineage-committed myeloid hematopoietic progenitors, colony-forming cells (CFC), including colony-forming unit-granulocyte macrophage; burst-forming unit-erythroid; and colony-forming unit-granulocyte erythroid, macrophage, megakaryocyte, detected in steady-state human PB. Mononuclear cells (MNCs) were prepared from the buffy-coat of about 60 individuals PB specimens, and were assayed for CFC by semi-solid culture supplemented with cytokines. X irradiation of 0.5 Gy and 2 Gy was administered at a dose rate of about 80 cGy/min. The results showed the mean number of hematopoietic progenitor cells to be 55.3 ± 40.1 in 1×10^3 MNCs, thus indicating erythroid progenitor cells to be the major population of committed stem cells, and that large individual differences exist in the number of hematopoietic progenitor cells, especially regarding erythroid progenitor cells. The surviving fraction of total CFC observed in 0.5 Gy and 2 Gy was 0.70 ± 0.21 and 0.30 ± 0.12 , respectively. Furthermore, this study evaluated the relationship between individual radiosensitivity based on differences in sex and age. No statistically significant difference was observed in individual radiosensitivity between males and females at both radiation doses. In contrast, a statistically significant negative correlation was observed between the surviving fraction observed at a dosage of 0.5 Gy and the age of an individual. A similar correlation was also observed in the male population. However, none of these correlations were observed at a dosage of 2 Gy irradiation. The present study demonstrates that large individual differences exist in the radiosensitivity of hematopoietic progenitor cells in steady-state human PB. In addition, the present results also suggest that the individual responsiveness of hematopoietic progenitor cells to 0.5 Gy irradiation decreases with increasing age.

(PS3.51) Iodine uptake induction in human embryonic stem cells during differentiation into thyroid-like cells. Mykola Onyshchenko, Igor Panyutin, Ronald D. Neumann, National Institutes of Health, Clinical Center, Bethesda, MD

Radioactive iodine treatment (¹³¹I) is considered to be one of the promising strategies for cancer treatment as it implements local radiation delivery to the tumor while healthy tissues remain unharmed. Sodium-iodine symporter (NIS) is expressed on membrane of thyroid cells and is responsible for highly intensive iodine accumulation. It is known that treatment of anaplastic thyroid cancer with ¹³¹I is ineffective due to the low expression of sodium-iodine symporter (NIS) on its cell membranes. Cancers originating from other tissues lack sodium-iodine symporter except of few breast cancer types; numerous attempts have been undertaken to induce NIS expression, mostly via gene transfection. Human embryonic stem cells (hESC) among their traditional application as a source of substitutive cell therapy have a great potential to study differentiation patterns with respect to NIS maturation. This would provide a challenging model to study the mechanisms of NIS expression regulation during differentiation and propose alternative ideas of its induction in cancer cells. We designed a two step protocol for hESC differentiation into thyroid-like cells, which was previously done for mouse embryonic stem cells. First we obtained definitive endoderm from hESCs; various approaches have been used to get high yield of endoderm cells. Second step included directed differentiation of definitive endoderm cells into thyroid-like cells using defined factors including thyroid stimulating hormone as a main differentiating factor. Expression of pluripotency markers (OCT3, NANOG), early endodermal markers (SOX17, FOXA2) and thyroid markers (TSHR, TPO, TG, NIS) were

monitored during differentiation steps. ^{125}I uptake as a functional assay was used to measure NIS activity. Tested differentiation approaches did not result in efficient induction of thyroid-like cells. We may conclude that differentiation of hESCs into thyroid cells is a more complicated process compared to that of the mouse embryonic stem cells and might involve different developmental patterns that are yet to be studied. Study is supported from the Imaging Sciences Training Program sponsored by the Radiology and Imaging Sciences Department, Clinical Center and the Intramural Research Program of the National Institutes of Biomedical and Bioengineering.

(PS3.52) Effect of gamma radiation and ^{125}I IdU uptake on the survival, proliferation and differentiation of human embryonic stem cells. Irina V. Panyutin, Igor G. Panyutin, Ronald D. Neumann, NIH, Bethesda, MD

Pluripotent human embryonic stem cells (hESC) are precursors to all cell lineages in the human body. Due to their ability to differentiate to other cell types these cells carry great potential to regenerative cell replacement-based medicine. The full realization of the therapeutic potential of hESC in practice may require labeling these cells with radionuclides for in vivo analysis of their engrafting and subsequent tracking of their fate with imaging modalities like, for example, positron emission tomography (PET). However, the effect of ionizing radiation (IR) in general and radionuclide uptake in particular on the pluripotency and survival of hESC has not been extensively studied. In this study we irradiated cultured hESC with 0.2 Gy and 1 Gy of ^{60}Co gamma-radiation, or treated them with 5- ^{125}I iodo-2'-deoxyuridine (^{125}I IdU). Then we analyzed the expression of pluripotency markers (Oct-4, Nanog, SSEA4, TERT, TRA-1-60 and TRA-1-81), markers of apoptosis (cleaved Caspase 3 and Annexin-V) and early differentiation markers (Nestin, Brachyury and Sox7) by flow cytometry, immunocytochemistry and real-time PCR techniques. We showed that low doses of IR had little effect on pluripotency of the surviving fraction of hESC. On the other hand, uptake of ^{125}I IdU by hESC was considerably higher as compared with cultured cancer cell line HT1080 resulting in total death of the hESC population after treatment with 0.1 uCi/ml ^{125}I IdU for 24 hours, whereas HT1080 cells became quiescent but not detached after the same treatment. Treatment with lower dose of 0.01 uCi/ml resulted in colonies of hESC became less defined with numerous cells growing in monolayer outside colonies showing signs of differentiation. Our results provide important insights into sensitivity of hESC to ionizing radiation, in particular, that produced by decay of an internalized radionuclide.

(PS3.53) PTEN loss regulates the radiation resistance of glioma stem cells through an antioxidant response. Tiffany Phillips, Sarah Muradian, Harley Kornblum, University of California, Los Angeles, Los Angeles, CA

Radiation therapy is a powerful tool in the treatment of primary and metastatic brain tumors. However, normal tissue tolerance is limiting and radiation dosages must be tailored to minimize the deleterious effect on the nervous system (Fike et al, 1988). The late effects of radiation are of particular clinical relevance and manifest as cognitive impairment, for which there is currently no effective treatment (Roman et al, 1995). Cognitive functions are strongly influenced by the activity of neural stem cells (Broadbent et al, 2004), and it has been postulated that brain tumors may arise from transformed neural stem cells (Hemmati et al, 2003). The tumor suppressor PTEN has been implicated in the mutational disorder of brain tumors, as well as the maintenance of normal neural stem cells. Thus studying PTEN may lead to a better understanding of the molecular basis for the survival of both normal and cancer stem cells. PTEN and radiation response was examined in normal and cancer stem cells. Loss of PTEN in normal neural stem cells increases both self-renewal and radiation resistance. Knockdown of PTEN in glioma stem cells results in increased radiation resistance. This increase in radiation resistance is not a result of cell cycle kinetics. I hypothesized that modulation of the PTEN/P13K/Akt pathway may limit the induced radiation resistance

since PTEN loss results in pro-survival signaling via Akt phosphorylation. Pharmacological targeting of the pathway appears to lessen the induced resistance, however additional novel pAKT-dependent and independent mechanisms may further link PTEN and radiation response. PTEN status may influence antioxidant responses (Sakamoto et al, 2009), thus I hypothesized that a preferential antioxidant response in PTEN negative cells may contribute to increased survival following exposure to ionizing radiation. Knockdown of PTEN in glioma stem cells results in preferential stabilization of the transcriptional activator NRF2, and further results in transcription of ARE-driven antioxidant genes. Ionizing radiation preferentially increases expression of both NRF2 and downstream antioxidants in PTEN deficient cancer stem cells. Taken together, PTEN and NRF2 signaling may regulate each other in cancer stem cells and provide a survival mechanism following exposure to ionizing radiation.

(PS3.54) Regulating stem cell behavior under abnormal circumstances. Erich Giedzinski, Atefeh Izadi, Tatiana Suarez, Katherine Tran, Munjal Acharya, Bertrand Tseng, Charles Limoli, University of California, Irvine, Irvine, CA

Multipotent stem cells restore functionality to normal tissues damaged after radiotherapy or exposure to other cytotoxic agents. While beneficial under certain circumstances, multipotent cells with robust proliferative potential are predisposed to deleterious changes that pose risks to their host tissues. To address these issues, we compared the radioresponse of neural stem and precursor cells to other non-multipotent normal brain cells and to those derived from brain tumors. Acute exposure to low or high LET radiation increased oxidative stress in multipotent neural cells and glioma cells, but had the opposite effect or little impact on normal primary astrocytes. These trends in oxidative stress were not impacted significantly by perturbations in cell cycle progression, nor were they overly dependent on p53 status. Acute or fractionated irradiation of multipotent neural cells uncovered subpopulations of differing radiosensitivity. Based on sphere forming and proliferative assays, neural stem cells were found to be radioresistant (~2-fold) when compared to their immediate progeny precursor cells. Subjecting these multipotent (nestin positive) cells to low LET dose fractionation, revealed radioresistant subpopulations that were positive for CD133, a controversial cell surface marker for brain tumor stem cells. To determine whether high LET irradiation might provide an avenue for the ablation of radioresistant cells, normal multipotent cells and U87 gliomas were subjected to heavy ion fractionation. Data indicated that while normal and transformed cells were more sensitive to charged particle irradiation, radioresistant cells from each cell type survived and were enriched after our fractionated dosing paradigm. Irradiated multipotent neural cells were also found to express immature markers similar to gliomas, suggesting that normal neural stem and glioma cells possessed partially differentiated phenotypes with shared immature expression profiles. Our data indicates similarities between gliomas and normal multipotent cells in the brain, features that become more prominent after irradiation. Thus, while neural stem cells mediate the normal regeneration or repair of the irradiated brain, these benefits come at a cost, as these cells may ultimately incur changes that promote tumorigenesis.

(PS3.55) ^{56}Fe -irradiation predominantly down-regulates gene expression in human neural stem cells. Yongjia Yu, Ping Wu, University of Texas Medical Branch, Galveston, TX

Neural stem cells (NSCs) play a pivotal role in neurogenesis, which generates all the brain nerve cells as well as circuitry during embryonic development, and also persists in certain areas of adult brain. These neural stem cells in the brain of astronauts could be the target of space radiation damage during space explorations. Previously we have shown that both ^{56}Fe ions and gamma-rays inhibit neuronal differentiation of human fetal neural stem cells in a dose-dependent manner. To elucidate the molecular mechanisms underlying this effect, we have examined gene expression profiles in these cells following irradiation. RNA samples collected at 3 and

48 hour post irradiation (1 GeV/n at 1 Gy) were analyzed with Affymetrics HGU133+ 2.0 gene chips microarray assay. Using 2-fold change as the threshold, only 8 genes showed expression change at 3 hr post-IR, all of them up regulated. However, at 48 hr post-IR, a time point for plating cells for differentiation studies, more than 400 genes changed expression level. All but 25 genes were down regulated. Bioinformatics analysis of this data is currently underway. Initial examination indicates that most of these genes are involved in multiple signaling pathways or net-works of the cells, including DNA damage response, DNA repair, checkpoint control and cell proliferation.

(PS3.56) A quantitative assay for cancer stem cell fraction and sensitivity to treatment modalities. Christopher S. Lange, Shy'Ann Jie, Anna Groysman, Kaity Sanz Melo, Manuj Agarwal, Elliot Navo, Talal Syed, Angela Wortham, Bozidar Djordjevic, Ovadia Abulafia, Marvin Rotman, SUNY Downstate Medical Center, Brooklyn, NY

Methods: Hybrid Spheroids (HS) identify fresh tumor cells capable of extensive proliferation and self-renewal, hallmarks of stem cells. HS are formed by mixing cancer test cells and fibroblasts with overnight incubation under non-attachment conditions. Spheroid cell mixtures are the same as in the original single cell mixture. Spheroids of defined sizes are selected by filtration, distributed 1/well in 96-well ultralow attachment plates, treated (*e.g.*, irradiated), and then monitored for growth. As shown previously, HS growth is due to test cell, not fibroblast, growth. Using the fraction of HS that do not grow as the zero term of a Poisson distribution provides a measurement of clonogenicity and the putative Cancer Stem Cell (pCSC) fraction, for use with fresh tumor samples. Results: 1) Cervical carcinoma cells, from fresh surgical samples, produced no colonies from 40,000 cells plated in tissue culture dishes (Plating Efficiency, PE < 2.5x10⁻⁵). However, when mixed 5.5% tumor cells, 94.5% fibroblasts, to form HS, some cells were clonogenic (*i.e.*, producing 10 - 15 division spheroids). 2) There was at least one clonogen (a pCSC) in 3.7 ± 0.6% of small spheroids (88-105 μm) & 6.7 ± 0.6% of large spheroids (105-125 μm), yielding respective PEs or pCSC fractions of 0.50 ± 0.09% & 0.76 ± 0.15%. Ratios of the PEs for treated/control HS yield single cell survival curves. 3) Breast cancer cells, from fresh surgical samples, produced no colonies from 160,000 cells plated in tissue culture dishes (PE < 6.25x10⁻⁶). However, when mixed 20% tumor cells, 80% fibroblasts, to form HS, some cells were clonogenic. 4) Their respective PEs or pCSC fractions for small and large HS were (4.57 ± 3.95)x10⁻⁴ & (1.87 ± 0.40)x10⁻³. 5) Niche sites will be discussed as a function of HS size & geometry. 6) Due to their 4 to10-fold lower PEs, magnetic bead enrichment of the breast cancer pCSC fraction is being done for measurement of radio- and chemo-therapy pCSC survival curves. Conclusions: The measured PEs are consistent with expected CSC fractions. We are also testing cervical and breast cancer pCSC-containing spheroids for tumor production in NOD/SCID/Gamma mice, for CSC content in second generation HS, and measuring CSC survival curves. This assay could improve cure rates by individualizing cancer treatments to the sensitivities of each patient's CSCs.

(PS3.57) Metformin increases the response of tumors to radiotherapy by eliminating cancer stem cells. Chang W. Song¹, Brent Williams¹, Troy Dos Santos¹, John Powers¹, Chung K. Lee¹, Seymour H. Levitt¹, Heon J. Park², ¹University of Minnesota, Minneapolis, MN, ²Inha University, Incheon, Republic of Korea

Small fractions of cells in tumors are cancer stem cells (CSCs), which are radioresistant. CSCs are able to survive conventional radiotherapy, giving rise to relapse and metastasis after radiotherapy. Epidemiological and pre-clinical studies demonstrated that metformin, a widely used drug by more than 40 million type 2 diabetic patients in U.S. alone, has significant anti-cancer properties. A recent study indicated that metformin is able to selectively kill CSCs. The purpose of our study is to investigate whether metformin can increase the efficacy of radiotherapy by

eradicating the radioresistant CSCs in tumors. Using SP and Aldehyde Dehydrogenase activity methods, we observed that 1.92 % of FSAII tumor cells cultured in vitro are CSCs. An incubation of FSAII cells with 0.1 mM and 10 mM metformin for 48 h decreased the CSC population to 1.08 % and 0.36 %, respectively. However, the fraction (%) of CSC population significantly increased after 3-7 Gy irradiation as a result of selective death of non-CSCs. When about 150 mm³ of FSAII tumors growing *s.c.* in the hind legs of C3H mice were exposed to 20 Gy of X-rays, the tumor volume doubled in about 10 days. On the other hand, the tumor volume doubled in 22 days when the host mice received daily treatment with metformin solution at 50 mg/kg/day beginning 1 day before tumor irradiation. Metformin alone only slightly suppressed the tumor growth. Western blot analysis indicated that metformin significantly increased pAMPK expression and suppressed pmTOR expression indicating that metformin suppressed the AMPK/mTOR signaling pathway, thereby killing CSCs and markedly increasing the response of tumors to radiotherapy. It is concluded that the efficacy of radiotherapy can be markedly improved with non-toxic and inexpensive metformin. (This work was supported by Joseph Vargo Fund from the Minnesota Medical Foundation).

(PS3.58) Voluntary exercise enhances transplanted stem cell survival after irradiation to the young mouse brain. Andrew S. Naylor, Martina Hermansson, Klas Blomgren, Institute for Neuroscience and Physiology, Gothenburg, Sweden

Stem cells reside in important areas involved in cognition in the brain and these areas are severely injured by irradiation. We have previously demonstrated for the first time that voluntary exercise in mice is able to rescue endogenous stem cells, neurogenesis levels and alter the structural integration of immature neurons in the hippocampus that are injured after irradiation. Transplantation of stem cells to the irradiation-damaged brain allows healthy cells together with physical activity, to enhance the integration and increase the survival of the transplanted and endogenous stem cells. We irradiated mice with a moderate dose of irradiation (8 Gy) at P9 and injected 1.0 x 10⁵ mouse stem cells into the hippocampus at P22. Animals were then given free access to running wheels and were sacrificed after 30 days. There was no difference between the level of activity in the SHAM-running and Irradiated-running mice, indicating a comparable level of physical activity. Up to 50% of the injected stem cells in irradiated non-running animals were undifferentiated or showed an increased fate differentiation towards a glial lineage. However, many cells were differentiating into early-stage neurons (DCX). Preliminary results indicate that injection of stem cells after irradiation in combination with running enhances neuronal lineage differentiation, but further analysis is required. If we can mitigate the adverse side effects of radiotherapy in the increasing number of survivors of childhood cancer, we would improve their quality of life.

(PS4.01) Dcr3 blocks p53-dependent cell death upon ionizing radiation. Woong-Yang Park, Seoul National University, Seoul, Republic of Korea

In an effort to find radio-sensitivity related genes, we have investigated gene expression profiles of radio-resistant H1299 and radio-sensitive H460 cells. Among the differentially expressed genes, apoptosis-related genes were significantly up- and down-regulated in Gene Ontology analysis. Especially we focused on Dcr3 (Decoy receptor 3), which was expressed significantly higher in radio-resistant cell lines in comparison to radio-sensitive cell lines. Overexpression of Dcr3 increased the survival of γ -irradiated radio-sensitive cell lines (H460, MCF7, and U87MG cells) and knockdown of Dcr3 suppressed the radio-resistance of A549 cells. The survival rate of p53 (Tumor protein 53)-deficient H1299 after gamma-irradiation was not affected by the suppression of Dcr3 expression. However, when we introduced p53 into H1299 cells, siRNA of Dcr3 abolished the radio-resistance of H1299 cells by inducing p53-dependent Fas (Tumor necrosis factor receptor super family member 6)-mediated apoptosis pathway. These results

demonstrated that the genetic cooperation of Dcr3 and p53 can determine the radiation responses in lung cancer cell lines.

(PS4.02) The role of vascular damage in the development of radiation pneumonitis. Ghazaleh Ghobadi^{1,2}, Sonja J. van der Veen^{1,2}, Hette Faber^{1,2}, Michael G. Dickinson³, Beatrijs Bartelds³, Sytze Brandenburg⁴, Johannes A. Langendijk¹, Robert. P. Coppes^{1,2}, Peter van Luijk¹, ¹Department of Radiation Oncology, University Medical Center Groningen, University of Groningen, Groningen, Netherlands, ²Department of Cell Biology, Section of Radiation and Stress Cell Biology, University Medical Center Groningen, University of Groningen, Groningen, Netherlands, ³Department of Pediatrics, University of Groningen, Beatrix Children's Hospital, Groningen, Netherlands, ⁴University Kernfysisch Versneller Instituut, Groningen, Netherlands

The risk of radiation pneumonitis (RP) limits the treatment dose in thoracic tumors. Therefore treatment optimization requires more insight into the risk factors and mechanisms involved in the development of RP. Previously we found that, depending on dose and irradiated volume, early lung damage manifests in parenchymal and vascular inflammation¹. Since vascular damage occurs at lower doses and seems to precede parenchymal injury we hypothesize that the vascular damage is the primary determinant of early pulmonary function loss. Radiation-induced endothelial cell loss may initiate vascular damage leading to lung vascular remodeling which is known as a hallmark of pulmonary hypertension. In the present study the relation between early radiation-induced vascular damage, pulmonary hypertension and pulmonary function loss was investigated 8 weeks after radiation. Different combinations of vascular and parenchymal damage were induced by high-precision proton irradiation to 75, 50 and 33% of rat lungs with 17, 22 and 28 Gy respectively. To assess pulmonary function loss the increase of breathing rate (BR) was measured. Right ventricle (RV) and pulmonary artery (PA) pressures were measured directly by catheterization. Subsequently pulmonary vascular remodeling was assessed in tissue samples. Right ventricle hypertrophy (RVH) was assessed by FDG-PET and directly by the ratio of RV to left ventricular plus septal weight. In and out of field samples of the lung showed features of vascular remodeling such as endothelial cell loss, neointima, hypertrophy and proliferation of smooth muscle cells, which are common in pulmonary hypertension models. RV and PA pressures and RVH increased noticeably with irradiated volume. Increasing the irradiated volume led to more pronounced reduction of pulmonary function. A remarkable correlation ($r=0.999$) of BR increase and PA pressure indicates that early pulmonary function loss depends strongly on vascular damage. Early radiation-induced pulmonary function loss primarily results from vascular damage. Therapeutic interventions targeting early radiation-induced vascular damage by e.g. repairing endothelial cell injury may be a promising strategy for further optimization of thoracic radiotherapy. I. Novakova-Jiresova A et al. *Int J Radiat Oncol Biol Phys* 2007.

(PS4.03) A mouse model to study the skin complication following hypo-fractionation for SBRT. Juong G. Rhee, Jonathan Ha, Zhendong Whang, William F. Regine, Cedric X. Yu, University of Maryland at Baltimore, Baltimore, MD

Stereotactic body radiation therapy (SBRT) is a recent innovation that offers high tumor cure rates which are superior to the outcome of conventional radiotherapy. However, its toxicity to normal tissues appears to be clinically unacceptable in many cases; the nature of hypo-fractionation necessitates the use of high doses per fraction. We have established a mouse model to study the skin complication associated with hypo-fractionation. The dorsal skin of C3H/HeJ mice were sutured to a home-made metal chamber which has an open window (16 x 14 mm, oblique) for irradiation. NE cells (nullipotent embryonic teratocarcinoma) were implanted subcutaneously in the middle of the chamber. This chamber allowed us to secure the skin with or without tumor tissues at the same position for repeated irradiation, in a manner equivalent to stereotactic positioning. The skin and tumors were subjected to a hypo-fractionation (13 Gy, 4 times daily) or a grid-fractionation (52 Gy

each quarter, 4 times daily). The purpose of the former setup was to simulate SBRT while the intent of the latter was to integrate spatial fractionation through the use of a grid (20 x 20 mm), which has 25 openings (2 x 2 mm) that are aligned 2 mm apart in both the horizontal and vertical directions in order to expose 1/4th of the intended field to each exposure. There were 4 observation groups: 2 control groups (hypo-fractionation; 13 Gy x 4 days) for the skin or skin having tumor tissues and 2 variable groups (grid-fractionation; 52 Gy each quarter x 4 days for different quarter areas) for the skin or skin having tumor tissues. Our preliminary results from 12-14 mice for each group showed that the amount of hair re-growth (a late effect) in the grid-fractionation group was almost double the amount of hair re-growth in the hypo-fractionation group, suggesting a clear skin protection. In addition to this, tumor curability was reduced by only 1/5th (92% to 75%) due to the use of the grid. Our observation for the skin protection is stimulating and may implicate the possibility that migrating and repopulating skin stem cells are better saved when the skin is subjected to spatially fractionated radiation using a grid, and that skin complications in SBRT may be reduced to a clinically acceptable level by using the grid.

(PS4.04) Temporal expression signature of hypoxia associated genes in irradiated mouse lung. Isabel L. Jackson, Xiuwu Zhang, Zahed Rabbani, Yu Zhang, Zeljko Vujaskovic, Duke University Medical Center, Durham, NC

Tissue hypoxia in the irradiated lung is associated with the development of normal tissue injury. However, direct evidence of hypoxia-mediated signaling in irradiated tissue has not been fully investigated. C57BL/6J mice were sacrificed at 1-day, 3-day, 1-week, 3-week, 6-week, and 6-month after giving a single fraction of 15 Gy to the whole thorax. The mRNA expression of 113 hypoxia-associated genes was tested using the hypoxia signaling pathway specific Oligo DNA microarray and further verified by RT-PCR. In total, 44 hypoxia-related genes were found to be upregulated after radiation. These genes participate in a variety of physiological and pathological functions including cell signaling transduction, tissue regeneration and cell proliferation (Dr1, Dctn2, CdC42, Gap43) and apoptosis (DapK) as well as inflammation, oxidative stress (CygB) and extracellular matrix synthesis (Agtb1, Mmp14, Adm, Angpt14, CTGF, leptin, and Plod3). In this study, expression of genes involved in lipid, carbohydrate, and protein metabolism, such as Agpat2, Angpt4, Car12, Eef1a1, Fabp4, Lipe, Man2b1, Ppar α , Prka α 1, Rps7, Slc2a1, Slc2a8, Tub α 1, and Tub β 3 were upregulated at various time points post-radiation. The temporal expression of these genes suggest that following the initial ionizing event, genes are upregulated that result in sustained oxidative stress, cell apoptosis, and tissue repair. At later time points genes associated with inflammation and fibrogenesis begin to be expressed. During the period following radiation exposure and extending throughout the follow-up period, several genes involved in vascular function, lipid, protein, and carbohydrate metabolism, and angiogenesis remain upregulated. The expression profile provides insight into the hypoxia associated genes involved in lung injury beginning 24 hours after radiation exposure and extending throughout the time to disease progression. Although, the physiological processes highlighted by the genes identified herein are not novel, the transcriptome profile does provide a clear view of those genes involved in these processes and the timeline of events. Improved understanding of hypoxia-driven gene expression could lead to improved understanding of the pathophysiological mechanisms underlying radiation-induced lung injury.

(PS4.05) Cranial irradiation results in the delayed infiltration of peripheral immune cells into C57BL/6J mouse brain. Fiona A. Dubuss, Michael J. Moravan, Sean D. Hurley, Elizabeth W. Sorensen, Eric Hernady, Lee A. Trojanczyk, John A. Olschowka, Jacqueline Williams, M. Kerry O'Banion, University of Rochester, Rochester, NY

Cranial irradiation results in sequelae that are manifested as early as minutes after treatment and can continue to evolve for

years. Some of these effects respond to corticosteroid treatment, which suggests that neuroinflammatory processes may play a role in their etiology. To further evaluate this process, we characterized the radiation response in the male C57BL/6J mouse brain. Previously, our laboratory has reported early and late increases in mRNA levels of the proinflammatory cytokines TNF- α , IL-1 α , ICAM-1, and CCL2 that plateau between 15 and 25 Gy. We have also shown infiltration of peripherally derived cells starting at one month following doses of 15 Gy or greater. Recently, we found that cranial irradiation results in a delayed increase in the number of CD11c+/MHC+ cells in the brain. To further investigate cell infiltration, we quantified infiltrative cell types and explored possible mechanisms involved in their recruitment. Infiltrating cells stained positive for CD3, MHC II, CD11c, and Iba-1, suggesting that they consist of T cells, myeloid cells, and dendritic cells. We did not see an increase in the number of Iba-1 positive cells at 6 months post-irradiation. Mice transplanted with CCR2-deficient bone marrow demonstrated that cellular infiltration is dependent on CCR2 signaling. Conversely, it is not dependent on IL-1 signaling. Collectively, these findings indicate that cranial irradiation results in early glial and endothelial activation, as well as an infiltration of peripheral immune cells. Bystander effects do not appear to play a role in the process because infiltration and, more importantly, activation were limited to brain areas that were directly hit by the radiation beam. Understanding the role of these peripheral immune cells could facilitate novel methods for increasing CNS tolerance to radiation, new therapies to ameliorate radiation injury, or new applications for radiotherapy. This work was supported by NIH RO1 CA114587.

(PS4.06) Heavy ion beam irradiation regulates mRNA expression and cell surface antigens during maturation of megakaryocytes and thrombopoiesis. Satoru Monzen¹, Kenji Takahashi¹, Kiyomi Eguchi-Kasai², Ikuo Kashiwakura¹, ¹Department of Radiological Life Sciences, Hirosaki University Graduate School of Health Sciences, Hirosaki, Japan, ²Radiation Effect Mechanisms Research Group, Research Center for Radiation Protection, National Institute of Radiological Sciences, Chiba, Japan

Objective: Processes of the hematopoietic system, especially megakaryocytopoiesis and thrombopoiesis, are highly sensitive to low-LET irradiation, such as X-rays (*Radiat Res.* 153: 144-152, 2000). However, effects of high-LET irradiation, such as heavy ion beams which show greater biological effect on the hematopoiesis than low-LET, remain to be largely investigated. As these particles pose high risks for employees of nuclear facilities and those involved in space missions, its biological effect should be estimated in detail. This study examined the effect of heavy ion beams on mRNA expression and cell surface antigens during the maturation of megakaryocytes and thrombopoiesis. Materials and Methods: CD34⁺ cells from human placental/umbilical cord blood were highly purified using a magnetic beads selection kit (EasySep[®], Stem Cell technology Co. Ltd.) and used as human hematopoietic stem/progenitor cells in this study. The cells were exposed to monoenergetic carbon-ion beams at doses 0.5 and 2 Gy (290 MeV/nucleon, LET = 50 KeV/ μ m) generated by an accelerator (Heavy Ion Medical Accelerator in Chiba, Japan). The exposed cells were then cultured in a serum-free medium supplemented with thrombopoietin plus Interleukin 3. On days 7 and 14, the expression of cell surface antigens and various genes related to megakaryocytopoiesis were analyzed by flow cytometry and quantitative real-time RT-PCR. Results and Discussion: No significant difference was observed between non-irradiated control and irradiated cells with regard to megakaryocyte-specific markers. The expression of Tie-2, a receptor that acts in early hematopoiesis, showed a significant 1.31-fold increase after 2 Gy irradiation compared with control cells on day 7. With respect to its mRNA expression, a significant increase was observed on day 7. In addition, expression of other mRNAs, such as PECAM1, SELP, and CD44, was also significantly increased in cells exposed to heavy ion beam irradiation. The coagulation function of platelets derived from the culture of irradiated cells was decreased in comparison to the control. These results suggest that heavy ion beam irradiation affects the expression of cellular adhesion molecules during the process of megakaryocytopoiesis and thrombopoiesis.

(PS4.07) Effects of low-LET ionizing radiation on nutrient transport and survival of intestinal cells of human origin. Frank A. Portugal, John M. Akudugu, Ronaldo P. Ferraris, Roger W. Howell, UMDNJ-New Jersey Medical School, Newark, NJ

Recently, we showed that whole-body irradiation with Cs-137 gamma rays can cause marked dose-dependent reductions in intestinal sugar transport in mice (Am J Physiol Regulatory Integrative Comp Physiol 298:173-182, 2010). Fructose transport was most radiosensitive with the greatest reductions observed 8 days post-irradiation with 10 Gy. There were corresponding reductions in GLUT5 activity and mRNA abundance. While murine models offer the advantage of in vivo investigation, their tissues are not necessarily fully representative of their corresponding human counterparts. The Caco-2 cell line is a human colorectal adenocarcinoma that is used extensively to investigate many of the characteristics exhibited by the small intestine including, but not limited to, nutrient transport, digestion and absorption, ion transport, brush border enzymes, and gut-neuropeptide responsiveness. These cells remain undifferentiated up until they become confluent, whereupon they begin differentiating. The present study characterizes the radiation response of sugar transporters in this human cell line. Confluent undifferentiated and differentiated Caco-2 cells were exposed to varying doses (0-9 Gy) of low-LET ¹³⁷Cs γ -rays. The colony forming assay was used to generate survival curves and the data were fitted to the linear quadratic model. Differentiated Caco-2 cells are about 2-fold more sensitive to gamma radiation than undifferentiated Caco-2. Western blot analysis confirmed the increased presence of GLUT5 in differentiated cells while a functional transport assay was used to show that GLUT5 function is increased in differentiated cells. Flow cytometry showed that the differentiated cells were predominantly in the G₀/G₁ phase as opposed to the undifferentiated cells which had a larger G₂/M phase population. Therefore, the increased radiosensitivity of differentiated Caco-2 cells cannot be attributed to enrichment in the radiosensitive G₂/M phase population. Further studies will be carried out to quantify the effect of γ -rays on functional sugar transport and to elucidate the mechanisms underlying the increased radiosensitivity of the differentiated Caco-2 cells. This work was supported in part by Grant No. AI078518 from NIAID and R01 CA83838 from NCI.

(PS4.08) Stimulation type-dependent dendritic cells maturation from human monocytes after X-irradiation. Hironori Yoshino, Kenji Takahashi, Ikuo Kashiwakura, Department of Radiological Life Sciences, Hirosaki University Graduate School of Health Sciences, Hirosaki, Japan

Objective: Dendritic cells (DCs) play a crucial role in the immune system. Our recent reports indicate that X-irradiated monocytes, which are precursors of DCs, differentiate into immature DCs (iDCs). They then mature after tumor necrosis factor- α (TNF- α) stimulation in terms of surface antigens expression, while their functions, such as the ability to stimulate allogeneic T cells, are attenuated. Recent reports propose various types of maturation stimuli, including proinflammatory cytokines and pathogen-derived components on processing DCs for immunotherapies. This study investigated the influence of X-irradiation of monocytes on maturation of DCs in response to specific maturation stimuli. Materials and Methods: The use of human buffy coats was approved by the Medical Ethics Committee of Hirosaki University Graduate School of Medicine. Monocytes separated from buffy coat were exposed to X-rays at 0, 2, 5, and 10 Gy. iDCs were induced from the irradiated monocytes by rhGM-CSF and rhIL-4. iDCs were stimulated by LPS or a cytokine mixture (MIX; [rhTNF- α , interleukin-1 β , interleukin-6, prostaglandin E₂]) for 48 h. The surface antigens expression and intracellular reactive oxygen species (ROS) levels of the DCs was analyzed by flow cytometry. Intracellular ROS behavior after LPS stimulation was measured because ROS is involved in LPS-Toll-like receptor 4 signal transduction. Furthermore, the ability to stimulate allogeneic T cells was also investigated. Results: After LPS or MIX stimulation, the DCs expressed the maturation marker CD83 and higher levels of costimulatory molecules compared with iDCs. In LPS stimulation, the expression levels of CD80 and CD83 on the DCs from X-irradiated monocytes were lower than that of nonirradiated controls. However, no change was observed in the MIX stimulation. The

intracellular ROS level of DCs from X-irradiated monocytes was lower than that of nonirradiated controls. In terms of functional characteristic, the ability of DCs to stimulate T cells was lower in the irradiated-group despite the types of maturation stimuli. Discussion: These results suggest that the influence of X-irradiation of monocytes on maturation of DCs depends on the type of maturation stimulus and that X-irradiation impairs the response of DCs to pathogen-derived components.

(PS4.09) The utility of systems biology modeling in combined injury casualty predictions. Daniela Stricklin, Darren Oldson, Terry Pellmar, Kyle Millage, Applied Research Associates, Arlington, VA

Implementation of accurate and reliable tools in emergency planning is critical in preparing for and minimizing the impacts of radiological events. For example, mathematical models based on empirical data from case studies and radiobiological research have been developed to predict the severity of signs and symptoms after exposure to ionizing radiation. Such models have been implemented in software tools to provide estimates of the time course of symptom severity and incapacitation, as well as mortality probability and time to mortality. These tools can provide guidance to planners to understand material and medical personnel resource requirements and can help guide research by identifying critical treatment and therapy needs. Radiological or nuclear event scenarios will likely involve radiation exposure combined with other injuries such as burn and trauma. Although it is well accepted that combined injuries will exacerbate the severity of responses and worsen predicted outcomes, combined injuries have only been roughly modeled due to limitations in available data. A long-range effort to incorporate mechanistic modeling into our work, to increase the understanding of the pathogenesis of combined injury, and to ultimately improve current casualty estimation tools is described. Translational systems biology has provided valuable insight to understanding the underlying pathogenesis of several acute injury types such as sepsis and trauma. We are building on this modeling foundation to help understand and predict interactions leading to increased mortality in the case of radiation combined injuries. The focus of this initial effort is on modeling radiation combined with burn, but future development will include trauma and cutaneous injury. We will identify common target organ systems such as the hematopoietic and cutaneous systems and describe underlying mechanistic pathways of response to injury that pose potential synergistic effects. Such effects include escalated inflammation, impaired immune response, and overwhelmed repair mechanisms. Physiologically based modeling and incorporation of systems biology will enable us to enhance casualty prediction models. These efforts may also provide valuable insight into critical pathways for intervention and for targeting treatments.

(PS4.10) Late Effect of Ionizing Radiation on Mitochondrial Biogenesis. Steven B. Zhang, Mei Zhang, Yansong Guo, Shanmin Yang, Jun Ma, Chun Chen, Xiaohui Wang, Alexandra Litvinchuk, Steven Stwartz, Lurong Zhang, Paul Okunieff, UF Shands Cancer Center, Gainesville, FL

Ionizing radiation (IR)-induced late toxicity remains a significant obstacle to improving cancer therapy and health care. Mitochondria play multiple key roles in metabolic activity and fate of the cells. It is thought that higher mitochondrial copy number is protective for cells. In this study, alteration of mitochondrial copy number after IR was investigated. Balb/c and C57BL/6 mice were subjected to 5 Gy TBI at dose rate of 1.84 Gy per min and sacrificed 12 months later for tissue collection. Genomic DNA in brain, liver, gut, heart, and kidney was extracted using a standard proteolysis plus phenol-chloroform-isoamyl purification and ammonium acetate precipitation. Nuclear (18S rRNA) and mitochondrial (12S rRNA) DNA gene levels were analyzed by real-time PCR. Ratio of mtDNA to nDNA was used to present the mitochondrial biogenesis. The results showed that: 1) In adult mice (8 weeks), ratio of mtDNA to nDNA in C57BL/6 mice was higher (1.3 to 2.5 fold) than in Balb/c mice, suggesting that the

resistance to IR of C57BL/6 mice as compared to Balb/c mice might relate to its high copy of mtDNA; 2) ratio of mtDNA to nDNA decreased 0.29~0.69 fold between 8 week and 12 month old mice, independent of strains, suggesting that copy number of mtDNA might decrease with age; 3) In C57BL/6 mice, IR slightly increased the ratio of mtDNA to nDNA (1.25 folds) in liver and kidney. However, IR significantly decreased the ratio of mtDNA to nDNA (0.5 to 0.63 fold) in both gut and brain; while in heart there was a slight decrease (0.81 folds); and 4) in Balb/c mice, IR significantly decreased the ratio of mtDNA to nDNA (0.42 to 0.56 fold) in all the tissues examined. In conclusion, ratio of mtDNA to nDNA decreased with aging. IR changed the patterns of the ratio of mtDNA to nDNA, where it was lower in radio-sensitive Balb/c mice than in radio-resistant C57BL/6 mice. The molecular mechanism of IR-induced mtDNA to nDNA change remains to be investigated.

(PS4.11) Manganese superoxide dismutase 3'-untranslated region: sensor for cellular responses to environmental stress. Leena Chaudhuri, Amanda L. Kalen, Maneesh G. Kumar, Prabhat C. Goswami, The University of Iowa, Iowa City, IA

In recent years, there is a growing interest in understanding the role of 3'-untranslated region (UTR) in regulating mRNA turnover and translation. The 3'-UTR harbors the poly(A) signal and post-transcriptional regulatory sequences like miRNA and AU-rich elements. The presence of multiple poly(A) sites often results in multiple transcripts; shorter transcripts correlating with more protein abundance. Manganese superoxide dismutase (SOD2) is a nuclear encoded and mitochondrial localized antioxidant enzyme that converts mitochondrial generated superoxide to hydrogen peroxide. A decrease in SOD2 activity increases the steady state levels of superoxide leading to oxidative stress. Humans have two transcripts of SOD2, 1.5 and 4.2 kb. We hypothesize that the preferential abundance of SOD2 transcripts regulates its activity during quiescent and proliferative growth states, and in response to environmental stress. Results from a quantitative RT-PCR assay showed that the shorter transcript (1.5 kb) is more abundant in quiescent cultures of normal human skin fibroblasts, non-malignant (MCF-10A) and malignant (MB-231) human mammary epithelial cells. Conversely, the longer transcript (4.2 kb) was more abundant in the proliferative state of all three cell lines. MCF-10A cells exposed to 2-(4-chlorophenyl)benzo-1,4-quinone (4-Cl-BQ), a metabolite of the environmental pollutant polychlorinated biphenyl 3, showed a significant decrease in the abundance of the 4.2 kb transcript due to a faster mRNA turnover, 14 h compared to 20 h in untreated control cells. Interestingly, the same treatment did not result in any change in the abundance of the shorter transcript. The decrease in the 4.2 kb transcript levels was associated with a corresponding decrease in SOD2 protein levels and activity, which resulted in a significant inhibition of quiescent cells entry into the proliferative cycle. A preferential abundance of the SOD2 transcripts was also observed in irradiated cells compared to controls. A better understanding of the 3'-UTR regulating gene expression in irradiated cells could lead to the development of new molecular biology-based radiation therapy. (NIH RO1 CA111365 and NIEHS P42 ES 013661)

(PS4.12) The TGFβ/smad repressor TG-interacting protein (TGIF) plays a role in radiation-induced intestinal injury. Mohammad Hneino, Agnès François, Valérie Buard, Georges Tarlet, Marc Benderitter, Fabien Milliat, Institute for radiobiological protection and nuclear safety, Fontenay aux roses, France

TGFβ is a key mediator involved in radiation-induced normal tissue damage. The TGFβ signal is mediated through serine/threonine kinase receptors and activation of its downstream signaling mediators Smads. Smad signaling is controlled by various mechanisms including co-activators and co-repressors. Intestinal injury in patients treated with radiotherapy is associated with the activation of TGFβ mediators (Smad) and target genes (PAI-1) in vascular compartment. TGIF (TG-Interacting factor) is a transcriptional repressor that has been reported to repress expression of

TGF β /Smad target genes, antagonizing TGF β /Smad pathway. In this work, we hypothesized that TGIF could play a role in minimizing TGF β -dependent deleterious effects in irradiated tissues. Immunohistochemical labeling of TGIF was performed in patients treated with pre-operative radiotherapy for rectal adenocarcinoma. *In vitro*, influence of TGIF overexpression in transcriptional activation of TGF β /Smad pathway and target genes was investigated in endothelial cells. *In Vivo*, in a model of radiation enteropathy (19 Gy localized single dose), survival was monitored and intestinal radiation injury was assessed in wild-type, TGIF +/- and TGIF mice -/- mice (n=13 to 15 mice/group). In rectum from patients treated with radiotherapy TGIF immunoreactivity is observed in vascular compartment and especially in the endothelium. Using a gene reporter approach and after transfection of a TGF β /Smad responsive reporter (CAGA9 luciferase) in HUVECs, we demonstrate that overexpression of TGIF completely inhibits SMAD-dependent transcriptional activation showing that TGIF is a key regulator of TGF β signaling in endothelial cells. Interestingly, *in vivo*, TGIF genetic deficiency is associated with increased sensitivity to intestinal irradiation. At 10 days after irradiation, 64% of TGIF +/+ mice are alive compared with 35% for TGIF +/- and only 20% for TGIF -/- mice. Fifty days after irradiation, no TGIF -/- mice survive whereas 57 % of TGIF +/+ and 23 % of TGIF +/- are alive. This study demonstrates that TGIF plays a role in radiation-induced intestinal damage and suggests that strategies aimed to strengthen TGIF activity could be a powerful way to control TGF β -dependent damages observed in normal tissues after radiation therapy.

(PS4.13) Genetic analysis of tumors arising from un-irradiated *Trp53 null* mammary epithelium transplanted to low dose irradiated hosts reveals role of inflammation as a mechanism of non-targeted effects in cancer. David H. Nguyen^{1,2}, Jian-Hua Mao³, Mary Helen Barcellos-Hoff², ¹Univ. of California-Berkeley, Berkeley, CA, ²New York University, New York, NY, ³Lawrence Berkeley National Laboratory, Berkeley, CA

The classical view of radiation carcinogenesis focuses on mis-repaired DNA damage as the main driver of cancer, but it is increasingly clear that the non-targeted effects of ionizing radiation (IR) can promote cancers in tissues never exposed to IR. Few studies have documented the consequences of non-targeted effect on carcinogenesis. We have shown that exposure to a high (400 cGy) dose of IR solely to the host promotes mammary tumorigenesis of unirradiated epithelial cell injections (*Cancer Res* 60, 1254-1260, 2000). Using this radiation chimera model, un-irradiated Balb/c *Trp53 null* mammary fragments were orthotopically transplanted into syngeneic hosts previously irradiated with 10-100cGy of IR. Host irradiation increased tumor frequency and growth rate and unexpectedly decreased the frequency of estrogen receptor alpha positive tumors. Here we report that microarray analysis of 32 tumors from non-irradiated and irradiated hosts, using Significance of Microarray (SAM) analysis in conjunction with a permutation scheme, revealed a core transcriptional profile of 786 genes that define tumors specifically from irradiated hosts. Ingenuity Pathway Analysis of these core genes revealed biological processes that give insight into potential mechanisms of tumor promotion via the irradiated host: inflammatory response, hematological system development, cellular growth and proliferation, connective tissue development, and cell death and morphology. Many induced genes were of the CXCL-family cytokines involved in recruitment, maturation, and activation of T-lymphocytes, B-lymphocytes, and macrophages. This analysis implicates host immunity as a key mode of tumor promotion due to IR, and underscores non-targeted effects as an important mechanism of radiation carcinogenesis. This work was supported by funding from the DOD BCRP Pre-doctoral fellowship (DHHN), NASA Specialized Center of Research (MHBH; JHM) and the NIEHS Breast Cancer and the Environment Research Center (MHBH).

(PS4.14) Changes in calcium signaling following gamma irradiation. Martha C. Sanchez¹, Orlando X. Ramos², Charles E. Stout¹, Gregory A. Nelson¹, Lora M. Green¹, ¹Loma Linda

University, Loma Linda, CA, ²Claremont McKenna College, Claremont, CA

Calcium mediated signaling is one of the mechanisms by which cells of the central nervous system (CNS) communicate and modulate the activity of adjacent cells. Calcium waves can travel for millimeters and are believed to underlie the spatial transfer of information and coordination of distinct neuron-glia domains. We sought to examine the effect of ionizing gamma radiation on calcium wave propagation in human astrocytes. **METHODS:** Cultures of primary human astrocytes were established in 35 mm dishes at a minimum seeding density of 7500 cells/cm². Confluent cultures were irradiated with 10, 50, and 200 cGy cobalt-60 gamma rays. Propagation of calcium waves was measured with the fluorescent indicator fluo-4 AM. Cells were loaded with 4 μ M fluo-4 AM for 1 hr at 37°C, and de-esterification carried out for 25 min at room temperature. Calcium waves were elicited by point mechanical stimulation using a micromanipulator. Spatial changes in intercellular calcium were measured after mechanical stimulation 3 hrs, 2 days and 7 days following gamma irradiation. **RESULTS:** Gamma irradiation of astrocytes produced changes in calcium wave propagation measured as changes in wave area. Unirradiated control cultures displayed a wave area that was on average 1.4 x 10⁶ μ m². Irradiated cultures displayed variable differences in wave area compared to unirradiated controls. Cultures exposed to 10 cGy displayed a 36% increase in wave propagation. **CONCLUSIONS:** These results represent preliminary data of measurable changes in calcium signaling following exposure to gamma rays. The altered response following exposure could represent an early signaling change within the CNS. Such changes in calcium intercellular signaling could have vast consequences given the high degree of heterocellular crosstalk and coupling that exist in the CNS.

(PS4.15) Bone marrow derived cells are involved in the vascular formation in tumors growing in the pre-irradiated tissues. Sheng Yung Fu¹, Fang Hsin Chen^{1,2}, Chun Chieh Wang^{2,3}, Chi Shiu Chiang¹, Ji Hong Hong^{2,3}, ¹Dep. of Biomedical Engineering and Environmental Sciences, National Tsing Hua University, Hsinchu, Taiwan, ²Dep. of Radiation Oncology, Chang Gung Memorial Hospital, Taoyuan, Taiwan, ³Dep. of Medical Imaging and Radiological Science, Chang Gung University, Taoyuan, Taiwan

Tumors growing in pre-irradiated tissues (pre-IR tumors) had a prolonged latency period and retarded growth rate as compared with non-IR tumors, a phenomenon known as tumor bed effects (TBE). The aim of this study is to compare the structures, functions and involvement of bone marrow (BM) stem cells in the vasculatures of small pre-IR and non-IR tumors. Murine TRAMP-C1 prostate tumor cells transplanted into shank were used as a model and 25 Gy was given before tumor implantation for pre-IR tumors. For 3-4 mm size tumors, pre-IR tumors had decreases of microvascular density (MVD) and increases of hypoxic area than size-matched non-IR tumors. However, vasculatures in the pre-IR tumors were larger, and better perfused, as measured by Hoechst 33342 dye, than non-IR tumors. In the non-IR tumors, only 16.5% \pm 7.1% CD-31 positive endothelial cells were covered with α -SMA positive pericyte, significantly lower than 91% \pm 13% in pre-IR tumors. The behaviors of PDGFR- β positive cells are similar to those of α -SMA positive cells, with a tight coupling with endothelial cells and larger size in dilated vessels. These results suggested the vasculatures in small pre-IR tumors are more mature than those in control tumors. Three approaches were used to investigate if BM-derived cells are involved in the vascular formation in the pre-IR tumors; they are: 1. Co-injection of GFP-bone marrow derived cells (GFP-BMs) and TRAMP-C1 tumors. 2. Inoculation of tumors into GFP-BM-transplanted wide-type mice. 3. Continuous i.v injection of GFP-BMs during tumor growth. The results from these three approaches clearly showed CD31-positive endothelial cells were co-localized with GFP positive cells in pre-IR tumors but not in non-IR tumors, and the percentage was highest for the first approach and lowest for the third approach. The conclusions from this study are that vasculatures in the pre-IR tumors are more mature than non-IR tumors, and BM-derived cells are involved in the vascular formation in the small pre-IR tumors. Vasculogenesis plays an important role in the pre-IR tumors and

blockade of this pathway may decrease tumor relapse in the irradiated tissues. (This work is supported by grants NSC 98-2628-B-182-002-MY3 and CMRPG360991 to Ji-Hong Hong)

(PS4.16) Molecular basis for low-dose γ -radiation induced oxidative stress response in vivo. Jamunarani Veerarahavan¹, Mohan Natarajan², Rakesh Madhusoodhanan¹, Terence S. Herman¹, Natarajan Aravindan¹, ¹University of Oklahoma Health Sciences Center, Oklahoma City, OK, ²University of Texas Health Sciences Center at San Antonio, San Antonio, TX

Delineating radiation (IR) induced response in healthy tissues has momentous importance in predicting environmental genotoxicity. To that end, IR-induced amplification of ROS has been suggested to be a sensing mechanism for the activation of signaling cascades that influence cells' fate. However, low dose IR (LDIR)-regulated intrinsic mechanisms and downstream response targets are still unclear. Accordingly, we investigated the effects of LDIR on NF κ B signal transduction and SOD2 activity in mice brain and gut. Brain and gut tissues from C57BL/6 mice exposed to whole body LDIR (2, 10, 50cGy) were harvested after 1h through 8 days. LDIR resulted in both dose-dependent and persistent NF κ B activation in gut and brain. QPCR profiling displayed a dose and tissue specific differential modulation of 88 NF κ B signaling pathway molecules. Overall, LDIR induced 82, 55 and 51 genes and downregulated 1, 24 and 25 genes after 2, 10 and 50cGy, respectively in brain. In gut, LDIR induced 46, 81 and 59 genes and suppressed another 40, 6 and 27 genes after 2, 10 and 50cGy. With stringent criteria (≥ 2 -fold), LDIR induced 72, 49, 41 (brain) and 16, 74, 57 (gut) genes while, completely suppressing 1, 21, 25 (brain) and 35, 6, 24 (gut) genes after 2, 10 and 50cGy. A total of 15 (2cGy), 43 (10cGy) and 19 (50cGy) genes were commonly upregulated (≥ 2 -fold) between brain and gut. To that end, we observed a dose independent induction of 35 genes in brain and 11 genes in gut and a tissue independent induction of 44, 52 and 28 genes after 2, 10 and 50cGy. Interestingly, 14 genes overall and 3 genes that are more than 2-fold were induced in a dose and tissue independent manner. Coherently, LDIR induced a dose dependent SOD2 cellular localization and persistent SOD2 activity. Conversely, muting IR-induced NF κ B completely attenuated SOD2. Likewise, blocking IR-induced SOD2 alleviated p65 transactivation. These results clearly imply that exposure of healthy tissues to LDIR induced NF κ B and SOD2 activity and transcriptional activation of NF κ B signal transduction/target molecules. More importantly, the results suggest that NF κ B initiates a feedback response through SOD2 transactivation that may play a key role in LDIR induced oxidative stress response and thus control the switch that directs the cells fate.

(PS4.17) The role of p53 in hypoxia-induced apoptosis. Rachel Poole, Ester M. Hammond, Gray Institute for Radiation Oncology and Biology, Oxford, United Kingdom

Tumour hypoxia contributes to both chemo- and radio-resistance and is associated with poor prognosis. Severe hypoxia has been shown to select for the loss of the tumour suppressor p53, which induces apoptosis in these conditions. Despite this the mechanism by which p53 induces apoptosis in response to hypoxia remains unclear. In this study we have investigated the post translational modifications of p53 in hypoxic conditions. Previously, phosphorylation of p53 at serine 46 was shown to be important for apoptotic signalling in response to agents such as UV. We have shown that p53 is robustly phosphorylated at this residue in response to hypoxia but that this does not appear to contribute to hypoxia-induced apoptosis. We hypothesise that this relates to the lack of transactivation by p53 in hypoxia as serine 46 has been described as being essential for the induction of p53-regulated apoptosis inducing protein 1 (p53AIP1). Micro-array data suggest that in hypoxic conditions p53 acts primarily as a trans-repressor although few targets have been described. Recently p53 was shown to contribute to hypoxia-induced apoptosis through the repression of a specific miR. We have compared the effect of wild type and mutant (in the DNA binding region) p53 on miR expression using miR arrays. Expression arrays were also carried out in order to

identify potential targets of p53-regulated miRs in hypoxia. These results will be discussed.

(PS4.18) Regulation of 26S proteasome activity by radiation during the different phases of the cell cycle. Lorenza Della Donna, Chann Lagadec, Erina Vlashi, Carmen Dekmezian, Puneet Souda, Julian P. Whitelegge, Frank Pajonk, UCLA, Los Angeles, CA

The 26S proteasome is a multi-catalytic protein complex responsible for the degradation of many proteins. Aberrations of the ubiquitin/proteasome system contribute to many human diseases, including cancer. Remarkably, exposure of cells to ionizing radiation slows the rate at which proteasomes are able to degrade proteins, which may contribute to the effects of radiation on cancer cells. At present, the activity of the 26S proteasome is considered static throughout the cell cycle with protein degradation only depending on their ubiquitination status. We hypothesized that regulation of the activity of the proteasome complex itself could be an additional layer of regulation of cell cycle progression and we investigated the effect of radiation in the different phases of the cell cycle. Therefore, we synchronized two human cell lines, PC-3 prostate cancer cells and MDA-MB-231 breast cancer cells, and measured 26S proteasome activity in irradiated (2Gy) and un-irradiated cells in the presence of the drug and 3, 6, 12 and 24h after restarting the cell cycle. In parallel, using a proteomics approach we investigated changes of the expression levels and posttranslational modifications of proteasome subunits. Intact 26S proteasomes were pulled down from synchronized and untreated exposed or not to radiation. Proteasome subunits and proteasome interacting proteins were separated by 2-dimensional gel electrophoresis (2DE). Differences between synchronized and un-treated cells, irradiated and un-irradiated, were analyzed by specific staining for total protein and posttranslational modifications. Differentially expressed or post-translationally modified spots were identified by mass spectrometry. We observed that all three activities of the proteasome were regulated in a similar fashion with down regulation in cells arrested in the G1-phase of the cell cycle. After restarting the cell cycle, all activities increased with maximum values in cells in G2/M phase. Cell cycle synchronization caused specific changes in the phosphorylation pattern of 20S proteasome subunits. In conclusion, we demonstrated that protein degradation and accumulation throughout the cell cycle is not only controlled at the level of proteins involved in cell cycle progression but also by fine-tuning of the activity of the 26S proteasome.

(PS4.19) MKP1-mediated radioresistance in breast cancer cells. Demet Candas, Ming Fan, Jian Jian Li, University of California, Davis, Sacramento, CA

Mitochondria are considered the powerhouses of cells, essential for keeping the cells alive and functional. They play an additional and yet very crucial role in the regulation of cell death, namely apoptosis. Cancer specific mitochondrial alterations have gained more attention as cancer cells have been shown to have enhanced resistance to mitochondria-mediated apoptosis. The changes occurring in the mitochondrial membrane potential modulate vital functions including: ion transport, protein influx, biogenesis and energy conservation. Although many nuclear-encoded proteins have been identified in mammalian mitochondria, the exact mechanism underlying mitochondrial protein influx is unknown. We were able to show that mitogen activated protein kinase phosphatase 1 (MKP1), overexpressed upon radiation in a NF- κ B-mediated manner, translocates to mitochondria in response to radiation and potentially results in the inhibition of mitochondria-mediated apoptosis in breast cancer cells. Although the apoptosis inhibiting function of MKP1 is well-defined, its role in mitochondria has not been studied. We proposed that radiation-induced MKP1 mitochondrial localization is responsible for the inhibition of apoptosis, causing adaptive tumor radioresistance. The mechanisms of MKP1-mediated inhibition of apoptosis in radioresistant cells and the downstream molecules involved are of great interest as they might offer new therapeutic targets for breast cancer. Among the

MAPKs that are induced in response to radiation, JNK has been shown to be affected by MKP1 activation, indicating that radiation-induced MKP1 is likely to play an anti-apoptotic role via the inhibition of JNK-mediated apoptosis. Furthermore, JNK has been shown to localize to mitochondria upon radiation to initiate mitochondria-mediated apoptosis via the phosphorylation of Bcl-xL, suggesting that MKP1-mediated inactivation of JNK takes place in mitochondria and functions to block radiation-induced apoptosis, leading to increased cell survival. Therefore, suppression of MKP1 activity may enable the pro-apoptotic signals from JNK in radioresistant breast cancer cells. Elucidation of mechanisms of MKP1-mediated inhibition of apoptosis may provide novel drug targets to re-sensitize radioresistant tumors.

(PS4.20) Differential dose response kinetics of erythroblasts following sublethal total body irradiation. Scott A. Peslak¹, Jesse Wenger¹, Kathleen E. McGrath¹, Paul D. Kingsley¹, Ollivier Hyrien¹, Anne Koniski¹, Jeffrey Bemis², Jacqueline P. Williams¹, Yuhchayou Chen¹, Stephen Dertinger², James Palis¹, ¹University of Rochester, Rochester, NY, ²Litron Laboratories, Rochester, NY

The hematopoietic system is a sensitive target of radiation and the erythroid lineage has served as a marker of clastogenic activity with development of the micronucleated reticulocyte (MN-RET) assay. Micronuclei are formed following radiation-induced DNA damage and this process is believed to be directly proportional to dose; however, our recent studies in mice indicate that the MN-RET response is linear only up to 1.5-2 Gy total body irradiation (TBI; Dertinger et al. Mut. Res. 634:119, 2007). As the exposure is increased above 2 Gy, MN-RET frequency paradoxically decreases. We hypothesized that this downturn is due to the inability of erythroblasts to repair and survive following higher doses of radiation. Here, we examined the response of the erythroid lineage to 1 and 4 Gy (Cs-137, dose rate of 206 cGy/min) TBI in C57Bl/6 mice using a novel multispectral imaging flow cytometry (MIFC) assay (McGrath et al. J Immuno. Meth. 336:91, 2008) to quantify the kinetics and apoptotic loss of erythroblasts in the bone marrow. Following 1 Gy TBI, both immature and mature erythroblasts were partially depleted, with recovery already beginning by the second day post-radiation. In marked contrast, nearly all erythroblasts in the marrow were lost at two days post 4 Gy radiation. Examination of the erythroid response at 1-6 hours post-radiation indicated that immature erythroblasts were lost more rapidly than mature erythroblasts following both 1 Gy and 4 Gy TBI. In addition, MIFC analysis revealed that immature erythroblasts were lost by apoptosis following radiation exposure while mature erythroblasts were significantly more resistant to apoptotic induction. Importantly, apoptosis was induced at much higher rates in immature erythroblasts following 4 Gy TBI compared to 1 Gy TBI, indicating that higher sublethal radiation doses completely deplete the erythroid lineage and thus abrogate MN-RET formation. We conclude that the erythroid lineage is an extremely sensitive target of radiation injury and that increased radiation doses lead to progressive erythroblast cell death. In addition, near-complete apoptotic loss of erythroblasts following 4 Gy TBI is consistent with the hypothesis that MN-RET are not formed at higher sublethal radiation doses due to the inability of severely damaged erythroblasts to repair and survive.

(PS4.21) Detrimental role of mast cells in radiation proctitis: consequences on the acute inflammatory response in mice and human muscularis propria smooth muscle cells phenotype. Karl Blirando¹, Fabien Milliat¹, Isabelle Martelly², Jean-Christophe Sabourin³, Marc Benderitter¹, Agnès François¹, ¹IRSN, Fontenay-aux-roses, France, ²Laboratory of Tissue Growth Repair and Regeneration Université Paris 12, Creteil, France, ³Hôpital Charles Nicolle, Rouen, France

Radiation therapy, alone or in combination with chemotherapy and/or surgery, is used in a majority of cancer treatment. The intestine is one of the most radio-sensitive organs and particularly the rectum is at risk, since it is present in the irradiation field of prostate tumours treatment. About 80 % of patients will develop

acute complications mainly related to mucosal inflammation, and 5 to 10 % late complications such as chronic tissue fibrosis that may require surgical resection. Mast cells (MC) are immune cells able to release many pro-inflammatory and pro-fibrosing mediators, and MC hyperplasia is a characteristic of many inflammatory and fibrotic disorders among which asthma and Crohn's disease. MC staining of rectal tissues from patients treated with radiotherapy has revealed a correlation between tissue damage and MC numbers in the mucosa, the sub-mucosa and the external *muscularis propria*. To investigate the role of mast cells in rectal radiation damage, experimental radiation proctitis was induced in a mast cell-deficient (W^{sh}/W^{sh}) mouse model. The colo-rectum of W^{sh}/W^{sh} and wild type (Wt) mice was exposed to a 27Gy localized single dose irradiation and studied 2 and 14 weeks post-exposure. Irradiated rectum showed mast cell hyperplasia in the mucosa 2 weeks and in the serosa 14 weeks after irradiation. W^{sh}/W^{sh} mice developed less acute and chronic rectal radiation damages than their control littermates. In the hours following radiation exposure, tissue protection was associated with increased mRNA and protein level of several inflammatory mediators including MIP-2, and CXCL1 which are two chemokines with neutrophil chemoattractant activity. Indeed, neutrophil in blood and tissue were significantly more numerous in W^{sh}/W^{sh} mice than in WT. In addition, *in vitro* studies demonstrated that MC chymase, tryptase and histamine modified human smooth muscle cells of the *muscularis propria* towards a migrating/proliferating and pro-inflammatory phenotype. These data show that MC have deleterious effects on both acute and chronic radiation proctitis, possibly by limiting tissue acute neutrophil influx and by favouring a phenotypic orientation of smooth muscle cells making them active participants in the radiation-induced inflammatory process and dystrophy of the rectal wall.

(PS4.22) Ionizing radiation-triggered accelerated senescence is mediated by p53-dependent and -independent mechanisms in human solid tumor-derived cell lines: Evidence against a role for p16^{INK4A}. David Murray, Razmik Mirzayans, Cross Cancer Institute, Edmonton, AB, Canada

Human cells expressing wild-type p53 respond to moderate doses of ionizing radiation (e.g., 8 Gy) by exhibiting sustained nuclear accumulation of p21^{WAF1} (hereafter p21), which down regulates apoptosis and switches on the accelerated senescence program. Senescence is a growth-arrested state in which the cells acquire flattened and enlarged morphology, express the marker senescence-associated β -galactosidase, and remain viable and metabolically active for prolonged times following genotoxic insult. Recently, we reported that exposure of p53-deficient Li-Fraumeni syndrome fibroblasts to ionizing radiation also triggers accelerated senescence, and that this response correlates with upregulation of p16^{INK4A} (hereafter p16) but not of p21 (J Cell Physiol 223: 57-67, 2010). The objective of the present study was to determine the role of p16 in accelerated senescence induced by ionizing radiation in p53-proficient and -deficient human solid tumor-derived cell lines. Cancer cells that were either infected with oncogenic human papillomaviruses (HPV), or transfected with a vector carrying the E6 gene of HPV, expressed high levels of endogenous p16 and failed to undergo accelerated senescence post-irradiation. On the other hand, ionizing radiation exposure triggered accelerated senescence in HPV-free cancer cell lines expressing wild type p53, mutant p53, or no p53. Studies with isogenic cell lines revealed that p53-proficient cells were significantly (>2 fold) more sensitive than their p53-deficient counterparts to undergo accelerated senescence after exposure to a given dose of radiation. Somewhat surprisingly, immunofluorescence microscopy revealed that accelerated senescence in these cell lines was not associated with an increase in p16 expressing cells. We conclude that: (i) ionizing radiation-induced accelerated senescence in HPV-free human cancer cell lines is mediated by p53-dependent and -independent mechanisms; and (ii) p16 does not appear to play a role in the radiation-triggered accelerated senescence of cancer cells with differing p53 status. Thus, neither p53 nor p16 is a reliable marker of accelerated senescence in cancer cells grown *in vitro*. (Supported by the Canadian Breast Cancer Foundation - Prairies/NWT Chapter and the Alberta Cancer Research Institute.)

(PS4.23) Metabolomic changes in human skin induced by ionizing radiation. Huguette Albrecht¹, Dmitry Grapov², Theresa L. Pedersen², John W. Newman^{2,3}, David M. Rocke¹, ¹University of California Davis, School of Medicine, Sacramento, CA, ²Western Human Nutrition Research Center, United States Department of Agriculture, Davis, CA, ³University of California Davis, Department of Nutrition, Davis, CA

Effects of low dose ionizing radiation (LDIR), unlike the high IR dose effects, are not well defined. Yet, human exposure to LDIR occurs through a variety of sources, including natural, medical, occupational, and accidental. The effects of radiation in humans are best studied in humans, but irradiation of human subjects strictly for research purposes is understandably forbidden. To overcome this hurdle, our laboratory has pioneered the use of skin biopsies from patients undergoing radiation therapy for prostate cancer to study in vivo in human responses to LDIR at the transcriptional level (Goldberg et al, 2006). Skin is the most exposed tissue, as well as one of the most sensitive to IR. To complement analysis at the transcriptional level of in vivo irradiated human skin, and enable examination of responses at the proteomic and metabolomic levels, we use surgically excised human skin exposed ex vivo to IR. In comparison to the in vivo human skin model, this ex vivo human skin model has the following advantages: 1) it facilitates access frequency to human skin samples since they become available any time an abdominoplasty is performed on a consenting patient; and 2) it does not restrict sample size nor experimental design since large pieces of skin are usually obtained. The transcriptional response of in vivo human skin to LDIR includes the upregulation of inflammatory markers (Berglund et al, 2008). Cyclooxygenase-2 (COX2), is the key enzyme regulating the production of prostaglandins, the central mediators of inflammation. COX2 is induced in response to IR, and has also been shown to be a central player in mediating bystander signaling. Induction of COX2 in response to IR was observed in our ex vivo skin model, and thus demonstrated the relevance of this model for studying IR induced metabolomic changes in lipids. This study is underway, focusing on an array of arachidonic and eicosapentanoic acids and oxygenation products, known for their inflammatory and anti-inflammatory properties, and association with COX activation. Metabolomic changes induced in ex vivo skin irradiated with low and high IR doses will be presented. Analysis of metabolomic changes induced by low and high IR doses, is expected to contribute to a better definition of the biological effects of LDIR in humans, and thereby improve LDIR related risk assessment.

(PS4.24) Irradiation induces transcriptional up-regulation of Smad corepressors in a radiation-induced enteropathy model in mice. Mohammad Hneino, Agnès François, Valérie Buard, Georges Tarlet, Rym Abderrahmani, Karl Blirando, Marc Benderitter, Fabien Milliat, Institute for radiobiological protection and nuclear safety, Fontenay aux roses, France

Radiation fibrosis is a frequent side effect observed in patients treated with radiation therapy. Cytokines and growth factors play a central role in this process. Among them, transforming growth factor-beta1 (TGF- β 1) signaling activation is considered as a master switch for the initiation, development, and persistence of radiation fibrosis. TGF- β /smad pathway are tightly regulated by a family of corepressors (Ski, SnoN, Smurf, TGIF) and smad inhibitors (Smad6 and Smad7) which antagonize or repress TGF- β signaling effect on downstream target genes. The aim of this study was to investigate kinetics of mRNA levels of smad corepressors and inhibitors in a model of radiation-enteropathy in mice. Intestinal radiation injury was performed after exposure of an intestinal segment to 19 Gy radiation in C57B6J mice. Mice were sacrificed 5 hours, 1, 3, 14 and 42 days after irradiation. Irradiated intestinal fraction was isolated, RNA extracted, and real time pcr was performed on an array of interests genes (TGF- β 1, Smad3, PAI-1, Ski, SnoN, TGIF, Smad7 and Smurf). Activation of TGF- β signaling and downstream target gene is revealed by increased levels of transcripts for TGF- β 1 itself, Smad3 and PAI-1. No significant variations were detected for Ski and smad7 mRNA expression levels. Unexpectedly, TGIF, Smurf2 and SnoN up regulation were rapidly observed with a pick 14 days after irradiation. In a model of radiation enteropathy in mice, TGF- β /smad pathway activation is associated with an increased

expression of corepressors transcripts levels. These unexpected results require additional investigations to determine if levels of transcripts correlate with protein expression. Increased expression of corepressors could be a physiological response after radiation exposure to limit TGF β signaling activation. In case of post-translational regulation of Smad corepressor, a mechanism of ubiquitin proteasome degradation of corepressors is hypothesized.

(PS4.25) EGFR-inhibition and irradiation in human tumor xenografts; microenvironmental changes and growth delay. Hanneke Stegeman¹, Johannes H. Kaanders¹, Deric L. Wheeler², Paul N. Span¹, Albert J. van der Kogel¹, Jan Bussink¹, ¹Radboud University Nijmegen Medical Center, Nijmegen, Netherlands, ²University of Wisconsin School of Medicine and Public Health, Madison, WI

The EGFR signaling pathways are associated with major radiation resistance mechanisms. Blockage of EGFR improves the effect of radiotherapy in head and neck cancer, however at the cost of increased toxicity. Identification of biological tumor characteristics that affect treatment response allows better selection for these treatments. We treated two human larynx carcinoma xenograft models (SCCNij167 and 202) with different EGFR expression profiles with radiotherapy (10 or 20 Gy) and Cetuximab (C225, monoclonal against EGFR). Effects on EGFR signaling, hypoxia, proliferation and tumor growth delay were studied. SCCNij202 tumors showed extensive membranous EGFR and cytoplasmic pAKT expression. SCCNij167 showed low EGFR and pAKT expression. Both immunohistochemical and western blot analysis showed differences in basal expression of (p)EGFR and (p)AKT, but only minor changes after treatment. Growth delay experiments in SCCNij202 tumors showed only a marginal effect in response to radiotherapy, but the tumors were extremely sensitive to C225 treatment. In contrast, SCCNij167 tumors showed a strong response to radiotherapy, without any effect of C225. No synergism between C225 and radiotherapy was observed. Immunohistochemical analyses in SCCNij202 tumors revealed a decrease of both hypoxia and proliferation after C225 treatment. However, a single dose of radiotherapy alone did not affect these parameters. On the other hand, radiotherapy caused a clear decrease in proliferation in SCCNij167 tumors. Conclusion. We have identified two xenograft tumor models with clearly opposing responses to radiotherapy and C225. The high C225 sensitivity in combination with the radioresistance of SCCNij202 tumors suggests that these tumors are highly addicted to EGFR-signaling and that this EGFR-signaling is involved in radiation resistance. In contrast, EGFR signaling does not seem to be an important factor in the survival of SCCNij167 tumors and consequently EGFR-blockage has no effect in this xenograft line. The study of multiple tumor models with similar origin and histology will increase the understanding of the mechanisms involved in treatment response providing a tool to improve patient selection.

(PS4.26) The long term functional and genomic effect of tumor presence during radiation. Janice A. Zawaski¹, Omaira M. Sabek², Horatius X. Voicu¹, Eastwood X. Leung¹, Christy M. Wilson³, Thomas E. Merchant⁴, M. W. Gaber¹, ¹Baylor College of Medicine, Houston, TX, ²The Methodist Research Institute, Houston, TX, ³Duke University, Durham, NC, ⁴St. Jude Children's Research Hospital, Memphis, TN

Radiation (RT) has been shown to cause functional and genomic changes in the brain. However the majority of these studies have been carried out in normal rodent brains. In this study the long term effect of irradiation and tumor presence during radiation were investigated. Three experimental groups were studied; Sham implant, RT+sham implant, and RT+C6-GFP tumor (glioma). Rat brains were irradiated using hypofractionation (8Gy/d for 5 days) starting 5 days post implant resulting in complete regression of the tumor and prolonged survival. Tissue was biopsied in the area of the implant (80mm³) 65 days post implant and fluorescently imaged to ensure that there were no residual tumor cells. RNA was isolated and hybridized onto GeneChip Rat Exon 1.0 ST Array. Data was

analyzed using Significant Analysis of Microarray and Ingenuity Pathway Analysis. Whole brains were analyzed for changes in myelin and astrogliosis. Intravital microscopy also used to quantify blood brain-barrier (BBB) permeability and leukocyte activity. Functional changes at 65 days post implant resulted in a significant increase in astrogliosis and BBB permeability ($p < 0.05$) in the RT+tumor implant compared to sham but no change in leukocyte activity was measured. However, structural changes in myelination were observed. The heatmap of the groups shows a clear visual difference between sham implant, RT+sham implant, and RT+C6-tumor. A total of 84 genes had a false discovery rate of $< 3.5\%$ and no significant exon splicing was detected. The top functional networks for the RT+sham implant group was hematological system development and function/tissue morphology/cellular development and for the RT+C6-tumor group cell morphology/cellular development/inflammatory response. To find the effect of the tumor we compared RT+sham implant to RT+C6-tumor implant. The highest canonical pathway effected by the presence of the tumor was the acute phase response signaling ($p = 0.003$), an inflammatory response. The influence of the tumor also affected the networks associated with cell morphology/cancer/cell cycle. In conclusion, tumor presence during radiation significantly influenced function and genomic response following treatment. We have developed a clinically relevant rat brain tumor model that incorporates the effect of tumor on RT side effects.

(PS4.27) Barrier function of mouse small intestinal mucosa alters with irradiation dose. Kunzhong Zhang, Liangjie Yang, Mei Zhang, Pooja Vijaygopal, Pooja Vijaygopal, Jeevan Gurijala, Ayala Dvir, Paul Okunieff, Lurong Zhang, Vidyasagar Sadasivan, UF Shands Cancer Center, Gainesville, FL

Gastrointestinal (GI) mucosa performs the function of electrolyte and nutrient absorption and performing the barrier function. Loss of intestinal lining mucosa with irradiation (IR) leads to barrier defect, giving intestinal commensal bacteria and peptides easy access to systemic compartment leading to endotoxemia. We therefore hypothesize that IR dose dependent damages to the intestinal mucosa will have alterations at functional, systemic and structural levels. Functional loss of epithelial barrier were determined in Ussing chamber studies based the principle that mucosa will maintain the electrochemical potential gradient irrespective of the ionic strength of the bathing solution. Plasma endotoxin levels were measured using tachypleus ameocyte lysate kit. Changes in tight junction protein were determined in Western blot studies. These studies were done on small intestinal mucosa of BALB/c mouse on 3 or 6 days after exposure to 0, 3, or 7 Gy. Relative permeability of Cl^- and Na^+ (PCI/PNa) were determined using the modified GHK equation. The results showed that 1) Non-IR mice showed a membrane selectivity ratio of 0.52 with Na^+ ions more permeable than Cl^- ; 2) 3 Gy IR mice showed selectivity ratio of 0.32, suggesting increased selectivity; 3) 7 Gy IR mice showed decreased selectivity, with a ratio of 0.78; 4) Plasma endotoxin levels measured in 0, 3 or 7 Gy showed significant increase only at 7 Gy when compared to 0 Gy; 5) Conductance measured in Ussing chamber studies showed a significant decrease 3 Gy (13.2 ± 0.9 vs 8.3 ± 0.6 mS) and a significant increase at 7 Gy (13.2 ± 0.9 vs 23.7 ± 1.4 mS) when compared to non-IR mice. 6) the western blot analysis for tight junction proteins showed that the claudin-1, JAM-A were increased in 3 or 5 Gy mice while their protein levels showed significant decrease at 7 Gy. Conclusion: low dose IR shows increased selectivity and better preservation of paracellular structures. However, higher doses of IR were associated with both structural and functional loss of tight junction that was associated with increased plasma endotoxin level. Increased selectivity of paracellular spaces and tighter epithelium at low dose irradiation may be a protective mechanism resulting from increased proliferation of epithelial cells. Further studies are however essential to better understand these mechanisms.

(PS4.28) Overcoming cell adhesion mediated radiation resistance by altering A6B1 integrin function. Thomas C. Sroka,

Ryan Cameron, Raymond B. Nagle, Anne E. Cress, University of Arizona, Tucson, AZ

Previous work has documented the presence of cell adhesion mediated radiation resistance (CAM-RR) dependent upon integrin function. Prostatic Intraepithelial neoplasia (PIN) is resistant to the killing effects of ionizing radiation (IR) as compared to invasive cancer. We show that during human prostate cancer progression, a profound alteration of cell adhesion occurs during the transition of PIN to human invasive prostate cancer. PIN lesions retain focal expression of laminin 332 and its receptor (A6B4 integrin), whereas invasive prostate cancer has lost expression of A6B4 and the ligand, laminin 332. Invasive cancer switches to express A3B1 and A6B1, receptors for laminin 511. We investigated here whether an IR survival response (as measured by AKT activation) was modified by altering A6 integrin function or supplying laminin 332. Our results indicate that prostate cancer cells that reside on exogenously supplied laminin 332 or laminin 511 at the time of irradiation have an amplified phospho-AKT response as compared to cells residing on a tissue culture surface. Interestingly, IR given prior to adhesion of PC3N cells onto laminin 332 or 511 will suppress the ECM induced Akt signal. The suppression was time and dose dependent upon IR. These data suggest that IR delivered to prostate cancer cells prior to their engagement with a laminin 332 or 511 containing ECM (such as that found on vessels, nerves and within bone) will result in a suppression of a pro-survival and migration event. These data implicate the use of IR as an invasion or metastasis prevention strategy in addition to its traditional use as a lethal anti-cancer modality.

(PS4.29) Delayed wound healing after whole body irradiation can be reversed by bone marrow transplantation. Benny J. Chen, Divino Deoliveira, Kayla Corbin, Yiqun Jiao, Joel Ross, Nelson Chao, Duke University Medical Center, Durham, NC

Local and systemic radiation can cause skin lesion directly and delay the healing of surgical wound. In this study, we investigated specifically how whole body radiation affected the healing of surgical wound using a modified ear skin punch model. Surgical wounds were induced by a 2 mm surgical punch in the ear pinnae of MRL/MpJ mice. Pictures of the wounds were taken and the sizes of the ear punch wounds were quantified by using Photoshop software. Local radiation was delivered by X-ray using a special constructed jig. Using this model, we demonstrated that 10 Gy of local radiation significantly delayed the healing of ear punch wounds ($28 \pm 2.2\%$ vs. $66 \pm 2\%$ at day 7 and $76 \pm 5.6\%$ vs. $96 \pm 2.3\%$ at day 28; $P < 0.05$). Addition of sublethal whole body irradiation (7 Gy) further delayed the healing of ear punch wounds ($16 \pm 6.6\%$ at day 7 and $44 \pm 8.1\%$ at day 28; $P < 0.05$ compared with local irradiation alone). The delay in wound healing could be at least partly reversed by bone marrow transplantation (55 ± 6.7 vs. 44 ± 8.1 at day 28 and 97 ± 3.3 vs. $87 \pm 8.2\%$, $P < 0.05$). These data were further confirmed by histological analyses. Our data demonstrated that whole body irradiation has dramatic effect on the speed of wound healing and bone marrow transplantation could reverse this negative effect.

(PS4.30) Energy metabolism and radiosensitivity of two HNSCC tumor cell lines. Christian G. Fabian, Wolfgang Mueller-Klieser, Ulrike G. A. Sattler, Institute of Physiology and Pathophysiology, University Medical Center of the Johannes Gutenberg University Mainz, Mainz, Germany

Unlike normal tissue, most tumors show an increased glycolytic flux and an enhanced accumulation of lactate even in the presence of oxygen. This phenomenon, termed "aerobic glycolysis" or "Warburg effect", is mainly caused by an upregulation and/or transactivation of glycolysis-related enzymes and transporters. Previous studies showed that lactate accumulation in tumors is associated with a high incidence of distant metastases, local recurrence and poor survival of patients. Furthermore, lactate concentrations were positively correlated with radioresistance in human tumor xenografts. In the present experimental study, two HNSCC (head and neck squamous cell carcinoma) cell lines (UT-

SCC-8 and SAS) were characterized regarding metabolic, energetic and radiobiological properties. Lactate production was measured in medium supernatants with a commercial photometric test. Proton release and oxygen consumption were quantified with the Seahorse extracellular flux analyzer XF24. Colony forming assays were accomplished from cells irradiated with single doses of 0-8 Gy. The HNSCC tumor cell lines investigated showed significantly different ($p < 0.049$) lactate production rates, i.e., 0.24 and 0.34 mol lactate/liter cell volume/h for UT-SCC-8 and SAS, respectively. Accordingly, extracellular flux analyses revealed a significantly ($p < 0.0001$) lower acidification rate for UT-SCC-8 (27.7 ± 8.5 mpH/min) compared to SAS (54.9 ± 9.7 mpH/min). Oxygen consumption was significantly ($p < 0.01$) lower in UT-SCC-8 (81.8 ± 24.0 pmol/min) than in SAS (114.1 ± 18.8 pmol/min). Thus, SAS cells were characterized by an intensified glycolytic and oxidative metabolism compared to UT-SCC-8 cells. From dose response curves of UT-SCC-8 and SAS cells doses of 5.8 and 7.7 Gy, respectively, were obtained for a 10% clonogenic cell survival. The data presented support the hypothesis that enhanced lactate production may be associated with an intracellular accumulation of lactate and other glycolytic intermediary products. Due to the radical scavenger function of some of these products they may confer radioresistance to highly glycolytic cells. The results obtained encourage more research efforts to be directed towards targeting tumor glycolysis for radiosensitization. Supported by the DFG SA 1749/3-1.

(PS4.31) Phosphorylation of mitochondrial p53 by cyclin B1/Cdk1 inhibits mitochondria-mediated apoptosis. Danupon Nantajit, Zhaoqing Wang, Rui Liu, Cuihong Jin, Ming Fan, Jian Jian Li, The University of California Davis, Sacramento, CA

Mitochondria not only play a key role as the powerhouse in mammalian cells but also tightly involve in the regulation of cell death, i.e., mitochondria-regulated apoptosis. Although many nuclear-encoded proteins have been identified in mammalian mitochondria, the exact mechanism underlying mitochondrial protein influx is unknown. Mitochondria localization of p53 has been well-described as the activation of mitochondria-mediated apoptosis induced by exposure to ionizing radiation. However, recent reports have indicated that p53 may have protective functions to mitochondria and inhibit cellular apoptosis. The G2/M phase cell cycle regulators, cyclin B1 and Cdk1, have been found to co-translocate to mitochondria along with p53 especially after exposure to ionizing radiation. The mitochondria localized cyclin B1/Cdk1 functions as a kinase and phosphorylate mitochondrial p53 at ser-315 site. Altering mitochondrial localization of cyclin B1 or Cdk1 also affect the phosphorylation level of p53. The phosphorylation of mitochondrial p53 leads to enhanced mitochondrial functions and stability including ATP production, mitochondrial membrane potential and cell viability. These enhanced mitochondrial functions lead to less apoptotic cells induced by ionizing radiation. Conclusively, phosphorylation of mitochondrial p53 by cyclin B1/Cdk1 has pro-survival effect by suppressing p53 activation of mitochondria-mediated apoptosis.

(PS4.32) The effects of ionizing radiation and subsequent oxidative stress on endothelial gap junctions and vascular structure in radiation-induced pulmonary toxicity. Allison S. Betof, Caroline C. Hadley, Isabel L. Jackson, Mark W. Dewhirst, Zeljko Vujaskovic, Duke University, Durham, NC

Radiation (RT)-induced pulmonary toxicity limits patient quality of life and the maximum therapeutic radiation dosage. Vascular damage plays a role in acute and long-term normal tissue injury, but the mechanism of this damage is not well understood. Within days to weeks following radiation exposure, there is an observed decrease in perfusion followed by the development of tissue hypoxia. There is an increase in oxidative/nitroxidative stress that begins at the time of initial exposure, which continues to escalate during progression of tissue hypoxia and the period of decreasing perfusion. We hypothesize that there is a cyclical interaction between vascular dysfunction, development of hypoxia,

and oxidative/nitroxidative stress beginning at the time of the ionizing event and continuing throughout the time of disease progression. Endothelial cells communicate via gap junctions composed of transmembrane connexin (Cx) proteins. Of the four Cx isoforms in endothelial cells, Cx43 is likely the most important in vasomotor tone and myoendothelial junctions. Phosphorylation of Cx43 regulates its participation in gap junctions. Hypoxia and reactive oxygen species (ROS) have been observed to affect phosphorylation of Cx43 in hypoxic tumor environments, disrupting endothelial cell communication. We believe that changes in Cx phosphorylation also occur in irradiated lungs because of similar changes in the microenvironment. Protection of functional gap junctions could therefore preserve vascular function, minimizing pulmonary injury and widening the therapeutic window. We evaluate the hypothesis that ionizing radiation and subsequent oxidative stress alter Cx43 phosphorylation, resulting in vessel remodeling, changes in vascular networks, and angiogenesis. FVB/N mice expressing endothelial-cell specific GFP received 12.5 Gy whole thoracic irradiation. Mice were sacrificed and lungs were excised at two endpoints: 24 hours, when ROS levels first increase and 8 weeks, when pneumonitis is maximal. Changes in vessel perfusion, gap junction phosphorylation, and vascular remodeling will be presented. This work is supported by NIH CA40355, U19AI67798, RO1 098452, and The Gertrude Elion Medical Student Research Award.

(PS4.33) Chronic induction of senescence-like changes by single or fractionated irradiation in mice. Uhee Jung¹, Hyeon-Soo Eom¹, Seol Hwa Kim¹, Jong-Jin Kim², Sung-Tae Yee², Sung-Ho Kim³, Beom-Su Jang¹, Sung-Keo Jo¹, ¹Advanced Radiation Technology Institute (ARTI), Korea Atomic Energy Research Institute (KAERI), Jeonbuk, Republic of Korea, ²Sunchon National University, Sunchon, Republic of Korea, ³Chonnam National University, Jeonbuk, Republic of Korea

The mitochondrial DNA (mtDNA) common deletion, senescence-associated β -galactosidase (SA β -gal), increased p21 expression and FOXO3a phosphorylation are well-known biomarkers for oxidative stress and aging *in vitro* and *in vivo*. Although ionizing radiation (IR) is well known to induce cellular senescence *in vitro*, the long-term *in vivo* effects on senescence are not well defined. In this study, we observed the long-term inductions of senescence-associated biomarkers in mice irradiated with single or fractionated doses. The 2-months-old C57BL/6 female mice were exposed to 5Gy of γ -rays in a single (5Gy \times 1) or fractionated (1Gy \times 5, 0.5Gy \times 10, or 0.2Gy \times 25) doses, and their tissues (liver, lung, kidney) were analyzed for senescence biomarkers at 2, 4 and 6 months after IR. The increases of 3867 bp mtDNA common deletions were evident in liver, lung, and kidney of IR groups compared to the control group of same age. The mtDNA deletions were observed at all time points examined after IR. Also, the SA β -gal staining of kidney revealed that SA β -gal positive cells were increased in the IR groups. SA β -gal staining was more prominent in the fractionated IR groups than the single IR group. Next, the levels of senescence-associated proteins (p21, phosphorylated FOXO3a) in the tissues were examined. The expression of p21 and the phosphorylation of FOXO3 were increased in IR groups, with no evident differences between single or fractionated IR groups. As expected, similar changes in mtDNA common deletion, SA β -gal staining, and the levels of p21 and phosphorylated FOXO3a were also observed in 20-24 months-old aged mice. In conclusion, our results showed that ionizing radiation in single or fractionated doses induced the various senescence biomarkers *in vivo* that persisted at least 6 months after irradiation, which suggests that IR may be the inducer of chronic senescence in mice. [This study was supported by the Nuclear R&D Program of MEST(Grant No. 2007-00091).]

(PS4.34) Tumor educated macrophages suppress CD8+ CTL activity by the induction of arginase I and is regulated by TNF/TNFR signaling. Yuru Meng, Michael Beckett, Helena Mauceri, Ralph Weichselbaum, University of Chicago, Chicago, IL

Tumor educated macrophages suppress CD8+ CTL activity by the induction of arginase I and is regulated by TNF/TNFR signaling. Previous work demonstrated that some of the antitumor effects of ionizing radiation (IR) largely rely on the proliferation and infiltration of CD8+ T cells. Tumor-associated macrophages (TAM; M2) may contribute to tumor radioprotection through increased secretion of vascular endothelial growth factor (VEGF), cyclooxygenase-2, inducible NO synthase (iNOS), and arginase I (Arg-1). The altered Arg-1 and iNOS expression in TAM as a response to tumor-derived molecules or hypoxia in the tumor microenvironment has been explored as a major immunosuppressive mechanism. We tested the hypothesis that increased Arg-1 results in CD8+ T cell dysfunction and decreased TAM NO-dependent cytotoxicity due to depletion of L-arginine. We analyzed Arg-1 and iNOS expression in bone marrow derived macrophages (BMDM) in co-culture with B16 mouse melanoma tumor cells. We found Arg-1 induction 16 hours after co-culture of BMDM and B16 tumor cells, and this induction/upregulation of Arg-1 in BMDM can be blocked by irradiating BMDM with 5Gy. This suggests that irradiation may reduce the immunosuppressive activity of TAM. Arg-1 expression in mice with germline deletions in tumor necrosis factor receptors 1 and 2 (TNFR1,2^{-/-}) or TNF (TNF^{-/-}) were compared to wild-type (WT) mice. Moderate Arg-1 production in TNFR1,2^{-/-} BMDM and low levels in TNF^{-/-} BMDM were observed when compared to WT mice. This indicates there might be a less immunosuppressive microenvironment in tumors grown in TNF^{-/-} and TNFR1,2^{-/-} mice.

(PS4.35) Characterization of the effects of ionizing radiation on immune cells using genetic and metabolomics approaches. Henghong Li, Yiwen Wang, Bin Zhou, Habtom Ressom, Albert J. Fornace Jr, Georgetown University, Washington, DC

The objectives of this study are to investigate acute and persistent effects of ionizing radiation (IR) on immune cell subsets and function. The role(s) of p38 MAP kinase in such radiation responses is being investigated using a genetic approach where an engineered mouse line has had one wt p38 α gene replaced with a dominant-negative mutant (p38 α /DN). T cells are one of the most radiosensitive cell types in vivo and IR is known to impact CD4 T cells long term. T cells are normally activated by the antigen, which triggers differentiation to specific subsets involving various cytokines. In addition, T cells have a well-characterized cellular program upon activation by T-cell receptor (TCR) signaling that is reflected by major changes in metabolism. Our metabolomics approach is ideal to detect many of these IR responses and represents a global approach to assess changes in metabolism. We compared the sensitivity of subsets of immune cell to low-dose radiation with wild type mice (wt) and p38 α /DN model. The splenocytes were isolated from mice at one and two weeks after radiation. The subsets of splenic lymphocytes were determined by FACS analysis. The data for CD4 and CD8 staining on CD3+gated cells showed a significantly greater increase of CD4/CD8 ratio in p38 α /KI than wt at one week after IR. More interestingly NK1.1 staining on CD3-CD19- gated cells showed a dramatic enrichment of NK cell population in wt but not in p38 α /KI mice. Further studies are needed to elucidate the role of p38 in specific subset responses. We evaluated the effect of IR on T cell activation. In wild type mice the isolated T cells showed significantly compromised competence in responding to TCR mediated activation after IR. This effect was observed at two weeks after IR and recovered by four weeks. Interestingly T cells from p38 α /KI showed much milder changes compared to wt. In addition to measuring classical endpoints such as cell proliferation and cytokine production for evaluating T cell activation, we also applied our metabolomics approach. We observed a variety of metabolic changes during activation in unirradiated T cells, and observed changes in these profiles with T cells from irradiated mice. Taken together, our results indicate that even low-dose IR markedly affects T cell activation and that p38 has a major role in this modulation.

(PS4.36) Role of bradykinin in a rat model of radiation-induced heart disease. Marjan Boerma¹, Sunil Sharma¹, Eduardo

G. Moros¹, Peter M. Corry¹, Kerrey A. Roberto¹, Elena Kaschina², Thomas Unger², Martin Hauer-Jensen¹, ¹University of Arkansas for Medical Sciences, Little Rock, AR, ²Charite - University Medicine, Berlin, Germany

Background: Radiation-induced heart disease (RIHD) is a potentially severe side effect after radiation therapy of thoracic and chest wall tumors. We have previously shown that mast cells protect against cardiac function loss and adverse myocardial remodeling after local heart irradiation in the rat. Mast cells may play this protective role via bradykinin, a peptide hormone with cardioprotective effects. The current studies begin to address the role of bradykinin in a rat model of RIHD. Methods: Male Sprague-Dawley rats received localized fractionated heart irradiation with 9 Gy for 5 consecutive days. The effects of radiation on the expression of the bradykinin receptors B1 and B2 and on the cardiac *ex vivo* functional response to bradykinin perfusion were assessed. A breeding colony of Brown Norway Katholiek (BNK) rats, which are deficient in the precursor of bradykinin, was established. Kininogen-deficient BNK and wild-type BN rats received localized fractionated heart irradiation with 9 Gy on 5 consecutive days. At different time points after irradiation, *in vivo* cardiac function was assessed with small animal echocardiography. Results: Local heart irradiation resulted in a significant increase in the expression of both the B1 and B2 receptor in the rat heart. In addition, irradiated hearts showed a functional response to bradykinin similar to sham-irradiated hearts, as shown by a significant reduction in coronary pressure after *ex vivo* perfusion with bradykinin in the Langendorff apparatus. The effects of localized heart irradiation on echocardiographic parameters of cardiac function in BNK rats and BN rats are presented. Conclusions: These studies start to unravel the mechanistic role of bradykinin in functional and structural changes in the rat heart after localized irradiation.

(PS4.37) The effect of antiangiogenic therapy on tumor microenvironment: Good or bad? Gabi Hanna, Greg Palmer, Won Park, Yiting Cao, Pavel Yarmolenko, Kenneth Young, Joseph Herbert, Tina Taylor, Thies Schroeder, Gordana Gordana Vlahovic, Mark Dewhirst, Duke university, Durham, NC

Methods: We evaluated the effects of pazopanib (VEGFR1,2,3 & PDGFR α - β inhibitor), sunitinib (VEGFR1,2,3 & PDGFR α - β inhibitor), imatinib (PDGFR β inhibitor) & bevacizumab (anti-VEGF) on tumor microenvironment by examining effects on tumor oxygenation, Interstitial fluid pressure (IFP), hypoxia, vessel perfusion & vessel density. Nude mice were injected SQ with A-549 NSCLC cells. When the tumors reached 600-800 mm³ mice were randomized to 9 groups (n=10 mice/ group) treated daily with high and low doses of pazopanib, sunitinib, imatinib, bevacizumab or vehicle, respectively. Mice were sacrificed at 6, 9, & 14 days after start of treatment. Hoechst33342, EF-5 and Doxorubicin were delivered before sacrifice. A novel spectrofluorometer was used daily to non-invasively measure hemoglobin saturation & total Hb for each tumor; IFP was measured on the last day. Immunohistochemistry was used to determine microvessel density (CD31), Hypoxia (EF-5 + area) & smooth muscle actin for pericytes. Doxorubicin concentration was measured with HPLC. Quantitative western blots were used to measure the total VEGFR2, PDGFR β , & phosphorylated VEGFR2, PDGFR β . Results A significant increase in Hbsat was observed at day 8 for both pazopanib groups compared to controls (p=0.0109, p=0.0290). IFP in high dose pazopanib & sunitinib groups was significantly reduced; the remaining drugs demonstrated a strong trend towards reduction compared to controls. MVD and hypoxia were significantly reduced and increased, respectively, in all groups at day 14 compared to controls. No significant difference in doxorubicin concentration was seen between treated groups & controls. All drugs reduced the total PDGFRb, & total VEGFR2 with a relative increase in activated phosphorylated-VEGFR2. & PDGFR β for all groups. Conclusions All antiangiogenic drugs transiently improved tumor oxygenation, followed by a return to baseline levels. These antiangiogenic agents can increase the hypoxia at day 14 in this tumor model, despite decreases in MVD and IFP. Thus, IFP is a poor surrogate for the normalization window in this model. Work supported by a grant from GlaxoSmithKline.

(PS4.38) Variations in mast cell hyperplasia in the irradiated lungs of different mouse strains, rats and non-human primates. Zeljko Vujaskovic¹, Isabel L. Jackson¹, Hermina Borgerink², Mark Cline², Julian Down³, ¹Duke University Medical Center, Durham, NC, ²Wake Forest University School of Medicine, Winston Salem, NC, ³Harvard-Massachusetts Institute of Technology Division of Health Sciences and Technology, Cambridge, MA

The role of mast cell infiltrates in the pathology of radiation damage to the lung has been a subject of continuing investigation over the past four decades. This has been accompanied by a number of proposals as to how mast cells and the secretory products thereof participate in the generation of acute inflammation (pneumonitis) and the chronic process of collagen deposition (fibrosis). An additional pathophysiology regards the possible connection between mast cell hyperplasia and pulmonary hypertension through release of vasoactive mediators. As the timing and magnitude of pneumonitis and fibrosis are known to vary tremendously among different genetic mouse strains as well as animal species, we have systematically compared mast cell numbers on azure A or toluidine blue stained lung sections from nine mouse strains, rat and non-human primates (NHP) following whole thorax irradiation (WTI). Mice of the BALB/c strain stood out in having a dramatic increase in interstitial mast cell numbers similar to the August rat while a relatively low level of mast cell infiltrate was observed in other mouse strains (CBA, C3H, B6, C57L, WHT and TO mice) that entered respiratory distress after 10-15 Gy WTI. Enumeration of mast cell number in 6 NHP (rhesus macaque) exhibiting severe pneumonitis approximately 17 weeks after 10 Gy WTI also indicated a low response shared by the majority of mouse strains. There appeared to be no relationship between the mast cell response and the strain-dependent susceptibility towards pneumonitis or fibrosis. The participation of mast cells in mediating vascular responses is currently being investigated. It remains uncertain whether the marked mast cell hyperplasia observed in BALB/c mice or rats can be related to the radiation pathology experienced in humans.

(PS4.39) Effect of synthetic N-acyl-L-homoserine lactone analogs of *Pseudomonas aeruginosa* quorum sensing on the growth of human oral cavity carcinoma cells. Hongbo Chai¹, Jun Igarashi², Kenji Takahashi¹, Yoichiro Hosokawa¹, Ikuo Kashiwakura¹, ¹Department of Radiological Life Sciences, Hirosaki University Graduate School of Health Sciences, Hirosaki, Japan, ²Glycotecology Institute, Otsuka Chemical Co., Ltd., Japan, Tokushima, Japan

Objective: Quorum sensing has been recognized as a type of signal transduction that senses cell population density and responds to changes in cell number between bacteria cells. Its mechanism in gram negative bacteria is controlled by the hormone-like cell product N-acyl-L-homoserine lactone (AHL). Various synthetic AHL analogs have been investigated for use as regulators for bacterial growth. A growing interest in regulatory function of synthetic AHL analogs on the growth of carcinoma cells has been observed recently. This study investigated the effects of 96 synthetic AHL analogs of *Pseudomonas aeruginosa* 3-oxododecanoyl-L-homoserine lactone (OdDHL) on the growth of human oral cavity carcinoma cells. Materials and Methods: Ninety-six synthetic AHL analogs of *Pseudomonas aeruginosa* quorum sensing were provided by Otsuka Chemical. Suppressive and radiosensitizing effects were tested using human oral cavity carcinoma cell lines SAS and Ca9-22 derived from tongue cancer and gingival carcinoma, respectively. Each cell line was cultured in a liquid culture media containing 10 % FBS. Clonogenic potential was tested by the plasma clot technique using platelet-poor human plasma. X-irradiation was performed using an X-ray generator at 150 kV, 20 mA, and a dose of 90-100 cGy/min in the range of 1-8 Gy. Cell cycle distribution was analyzed using a flow cytometer. Results and Discussion: Some compounds showed significant suppressive effects on the growth of the SAS and Ca9-22 cell lines at 5 µg/ml. Fifty percent inhibition concentration (IC₅₀) was in the range of 0.3-3.6 µg/ml in Ca9-22. A significant radiosensitizing effect was observed in 1-8 Gy irradiation on Ca9-22 with compounds 5 and 87 at IC₅₀ values of 1.6 and 0.3 µg/ml, respectively. Moreover, compound 5 led to significant Sub G1

phase accumulation in the cell cycle distribution of Ca9-22, while compound 87 did not, indicating different mechanisms to suppress cell proliferation between the two compounds. No structural similarity was found in both compounds. These results demonstrate that some OdDHLs showed antiproliferative activity in human tumor cell lines. Furthermore, one of the compounds induced apoptosis. More detailed studies are currently underway to elucidate the structure-activity relationships and suppressive mechanisms.

(PS4.40) Hypoxia inhibits disulfide bond formation and protein folding in the endoplasmic reticulum. Marianne Koritzinsky^{1,2,3}, Twan van den Beucken^{1,2}, Kasper M. Rouschop², Ineke Braakman⁴, Bradley G. Wouters^{1,2,3}, ¹Ontario Cancer Institute, Toronto, ON, Canada, ²Maastricht University, Maastricht, Netherlands, ³University of Toronto, Toronto, ON, Canada, ⁴Utrecht University, Utrecht, Netherlands

Poor oxygenation (hypoxia) activates the unfolded protein response (UPR), a coordinated regulation of transcription and translation aimed to alleviate endoplasmic reticulum (ER) stress. The UPR is elicited by the three ER stress sensors PERK, IRE-1 and ATF6. Hypoxia has previously been shown to activate PERK and IRE-1, and here we show that ATF6 is also activated by hypoxia. Although the UPR represents an important adaptation to hypoxia, it remains unknown why the lack of oxygen activates it. The ER is a compartment where maturation of newly synthesized proteins destined for the extracellular space occurs. Other stresses that activate the UPR, such as lack of glycosylation, result in accumulation of misfolded or unfolded proteins in the ER that tend to aggregate. We hypothesized that one or more ER localized protein maturation steps depend on molecular oxygen, and hypoxia consequently activates the UPR due to the accumulation of immature improperly folded proteins in the ER. We hence monitored the maturation steps of several secreted or membrane-destined proteins during normoxic and anoxic conditions using a pulse-chase assay. We found that oligosaccharide modifications, including ER localized N-linked glycosylation and glycan trimming, Golgi-transport and Golgi-localized complex glycosylation, occurred independent of oxygen availability. In contrast, anoxic conditions prevented disulfide bond formation in all proteins investigated, including endogenous albumin and transferrin, as well as ectopically expressed influenza-hemagglutinin. This defect in disulfide bond formation was completely reversible upon reintroduction of oxygen. It has been previously shown that the yeast oxidoreductases ERO1 and PDI can use molecular oxygen as a terminal electron acceptor when catalyzing disulfide bonds in model proteins in vitro. Here we have demonstrated that oxygen is required in vivo for this process. We also show that the human Ero1- α , whose activity is regulated by the redox state of conformational disulfide bonds, is reduced under anoxic conditions. Although Ero1- α can be re-oxidized during anoxia by addition of an exogenous oxidizing agent, this cannot rescue disulfide bond formation. These results demonstrate that oxygen is the required oxidizing agent in vivo for disulfide bond formation.

(PS4.41) Comparison of radiation-induced tumor microenvironmental changes among five different murine tumor cell lines and two different mouse strains. Chi-Shiun Chiang¹, Sheng-Yung Fu¹, Chia-Chi Liu¹, Shu-Chi Wang¹, Fang-Hsin Chen¹, Ji-Hong Hong², ¹National Tsing Hua University, Hsinchu, Taiwan, ²Chang-Gung Memorial Hospital, Tao-Yuan, Taiwan

We have previously shown that 25 Gy irradiation (IR) to murine prostate cancer, TRAMP-C1, resulted in the decrease of microvascular density (MVD), increase of chronic hypoxia, and aggregation of CD68+ tumor-associated macrophages (TAMs) in chronic hypoxic regions. To further explore whether these changes in irradiated tumor microenvironments are mainly affected by tumor or host factors, five different murine tumors grown in 2 different mouse strains, TRAMP-C1 (adenocarcinoma/C57BL/6J), B16-F0 (melanoma/C57BL/6J), ALTS1C1 (astrocytoma/C57BL/6J), FSA (fibrosarcoma/C3H/HeN), and FSAN (fibrosarcoma/

C3H/HeN), were parallelly studied. Decreases of MVD were remarkable in 3 tumors, and were insignificant for the rest. Either vascular response could be observed in same strain mice bearing different tumors, suggesting the changes of MVD following IR are mainly affected by tumors rather than mouse strain. There was a negative association between MVD decrease and tumor growth delay, and the development of chronic hypoxic regions in where CD68+ TAMs aggregate. This negative association was only seen in tumors treated by irradiation, not in those treated with suten, an anti-angiogenic agent. This study suggests vascular responses following irradiation play an important role in the formation of chronic hypoxia and aggregation of TAMs. Even though the microvasculatures are derived from host cells, their responses to IR are determined by intrinsic characteristics of tumor cells. Tumor factors associated with vascular responses to IR are currently under investigation. (This work is supported by grants NHRI-EX99-9827BI and NTHU-99N2417E1 to Chi-Shiun Chiang).

(PS4.42) c-Abl function in TPA- and radiation-induced apoptosis in human prostate cancer cells. Akihisa Mino, Tuula Penate-Medina, Jean-Philip Truman, Judith Mesicek, Hyunmi Lee, Richard Kolesnick, Zvi Fuks, Adriana Haimovitz-Friedman, Memorial Sloan Kettering Cancer Center, New York, NY

We previously reported that 12-*O*-tetradecanoylphorbol 13-acetate (TPA) decreased transcription and protein levels of Ataxia-Telangiectasia Mutated (ATM) in human prostate cancer cell lines LNCaP and CWR22-Rv1, de-repressing the enzyme ceramide synthase (CerS) to promote apoptosis. Here we analyzed the expression and subcellular distribution of the six mammalian CerS isoforms and their specific ceramide species generated within mitochondrial-associated membranes (MAM) and within the mitochondria in these cells before and after TPA±radiation treatments. This analysis revealed that TPA±radiation induces *de novo* synthesis of ceramide by specifically activating CerS isoforms 5 and/or 6 generating pro-apoptotic C₁₆-ceramide species in mitochondrial membranes. In addition we demonstrate that LNCaP cells transfected with a c-Abl kinase dead (KD) mutant showed a significant decrease in both TPA and TPA + radiation-induced apoptosis compared with c-Abl (WT) transfected LNCaP cells. Thus, this result indicates that the kinase activity of c-Abl is necessary for TPA±radiation-induced apoptosis in LNCaP cells. In LNCaP cells transfected with WT-c-Abl, ceramide elevation was observed in response to TPA coupled to a synergistic increase of ceramide after TPA+radiation treatment. However, ceramide elevation was abolished in LNCaP transfected with the KD-c-Abl, for both TPA and TPA+radiation treatments. These findings identify kinase active c-Abl as a pro-apoptotic factor in these cells, which utilizes the activation of the CerS pathway to transduce this apoptotic response. Whether c-Abl directly or indirectly activates CerS5 and/or 6 activities, responsible for the generation of the pro-apoptotic ceramide species in response to TPA±radiation, remains to be elucidated.

(PS4.43) A further comparison of pathologies following thoracic irradiation among different rodent strains: finding the best preclinical model for evaluating mitigators. Julian Down¹, Isabel Jackson², Zeljko Vujaskovic², ¹Harvard-Massachusetts Institute of Technology Division of Health Sciences and Technology, Cambridge, MA, ²Duke University, Durham, NC

The human lung is among the most sensitive and critical tissues which determine survival following whole body radiation exposure. It is the subject of active preclinical research evaluating mitigating therapies within the radiation countermeasures program. The ability to accurately evaluate medical countermeasures is reliant on an accurate model of human radiation-induced lung injury. Our previous study comparing B6, CBA and C57L mice after whole thorax irradiation (WTI) pointed to the problems of late pleural effusions that prevented the full development of lung injury in B6 mice and rendered this strain unfavorable as a model of radiation injury in humans (Jackson et al. *Radiat Res* 173:10-20, 2010). We

have broadened these comparisons to include three additional mouse strains (BALB/c, A/J and C57BR/J) as well as one strain of rat (Wistar) receiving 10-16 Gy WTI. Most of these mice were unable to survive the first 6 months and presented with a mixture of lung injury and pleural effusions similar to earlier findings on WHT and TO mice. The independent and varying development of compressive pleural effusions of ill-defined etiology represents a concern for these strains in that they may not satisfy the requirements of the FDA "Animal Rule" prior to approval of products (radiation mitigators) for human use. While we are awaiting results from our study on Wistar rats, this species may share the same problem encountered in mice as the incidence of early pleural effusions have also been previously reported in certain rat strains (Brown Norway, August and WAG). Thus among nine different mouse strains so far studied for these pathologies, only three (CBA, C3H and C57L) appear to be desirable for further assessment of mitigating agents in exhibiting an early wave of pulmonary dysfunction attributed exclusively to radiation pneumonitis. C57L mice are particularly relevant in showing significant lung damage at lower radiation doses closer to that predicted for our own species.

(PS4.44) Cell-cycle dependent active thermal bystander effect (ATBE). Martin Purschke, R. R. Anderson, Dieter Manstein, Massachusetts General Hospital, Boston, MA

Recently we discovered the active thermal bystander effect (ATBE) in human fibroblasts, where heated fibroblasts can induce DNA damage and apoptosis in remote, non-heated, adjacent cells. The purpose of this study was to assess whether the ATBE is cell cycle dependant. We compared the ATBE, quantified by loss of cell viability, for dividing and non-dividing human fibroblasts, as well as for dividing human white preadipocytes (HWP) and non-dividing, mature differentiated human adipocytes. Dividing fibroblasts (< 30% are in cell cycle) and preadipocytes showed a significant ATBE ($p < 0.008$ and $p = 94\%$ are in G1) and mature adipocytes did not generate any ATBE within this temperature range. There was a statistically significant difference between dividing and nondividing cell subpopulations for fibroblasts ($p = 0.003$) and (preadipocytes ($p < 0.001$)). These results confirm that the ATBE is a cell cycle dependent process which requires actively dividing cells. In addition, the data suggest that the ATBE is a rather general phenomenon for dividing cells rather than a cell type specific process. The cell cycle dependency of the ATBE could have useful clinical applications in selectively targeting fast growing cells like tumor cells. Whether the yield of the ATBE can be amplified by synchronizing the exposure to the ATBE with specific phases of the cell cycle remains subject to further investigation.

(PS4.45) An *in vivo* hypoxic gene expression signature of gliomas. Constantinos Koumenis, Diane Marotta, Jayashree Karrar, Lori Hart, Timothy Jenkins, Cameron Koch, Amit Maity, University of Pennsylvania, Philadelphia, PA

Hypoxia is one of the primary determinants of tumor aggressiveness and radiation resistance, and yet little is known regarding the effects of hypoxia on gene expression *in vivo*. We have employed laser capture microdissection (LCM) and microarray gene expression profiling (MGEP) in the established 9L rat epigastric pedicle model of glioma following injection with the hypoxia-sensitive dye EF5 to enable the identification of hypoxic regions. Using LCM, viable hypoxic and normoxic regions of tumor tissue were isolated and RNA was purified. For comparison, RNA was also purified from 9L cells grown *in vitro* and exposed to hypoxia (0.2%, 6h and 16h). Validation of the microarray results was performed via qPCR on four mRNAs of interest: *Vegf*, *Pdk1*, *Glut1*, and *CA9*. Although MGEP identified a common set of genes that were upregulated both *in vitro* and *in vivo*, substantial differences were found between the *in vitro* and *in vivo* samples in the total number of differentially regulated genes and the fold-change in expression of downregulated genes. Interestingly, *in vivo* hypoxic regions contained more than twice as many upregulated and more than 70 times more downregulated genes than normoxic

regions when compared to corresponding *in vitro* conditions. Hypoxic regions exhibited higher levels of mRNAs involved in pathways with involvement in the hypoxic response, including angiogenesis (Vegf), glycolysis (Glut1), and ER stress response genes (ATF3), and the downregulation of genes involved in cell cycle progression (Cyclin B1) and DNA repair (Rad51). An unexpected and intriguing finding was the hypoxic-downregulation of a number of immune-related genes *in vivo* such as *CXCL9* and *Ly6C*, a finding we are currently exploring more in more detail. Immunohistochemical validation was performed by co-localization of Heme Oxygenase 1 and decreased levels of Rad51 in hypoxic regions. Gene ontology analysis of the top 200 altered mRNAs in the *in vivo* samples revealed glycolysis-related and immune-related processes as the primary up- and down-regulated pathways, respectively. To our knowledge, this is the first study analyzing the influence of hypoxia on gene expression *in vivo* and has uncovered some unanticipated differences between *in vitro* and *in vivo* conditions. We are extending these studies to miRNA expression and to human tumor samples.

(PS4.46) Endothelial cells modulate T cell survival after mixed field irradiation. Lynnette H. Cary, Margaret S. Williams, Therese Barber, Barbara F. Ngudiankama, Mark H. Whitnall, AFRRRI, Bethesda, MD

There is increasing concern about the potential danger of exposure to radiation, in the clinical setting as well as exposure due to nuclear attack. Nuclear detonations involve blast, thermal pulse, x-rays, gamma-rays, and neutrons, and the production of small modular neutron-producing devices heightens the importance of understanding the effects of mixed field radiation. There is increasing evidence that hematopoietic injury due to radiation exposure involves endothelial cells (EC) within hematopoietic organs, including the bone marrow. EC within the bone marrow vascular niche produce and respond to a number of cytokines and growth factors to help provide an environment that promotes proliferation and differentiation of hematopoietic stem and progenitor cells, as well as mobilization and homing of mature hematopoietic cells. Our hypothesis is that EC signals, both soluble and cell-surface, are important in promoting survival and recovery of hematopoietic cells within the bone marrow after radiation injury, and we are developing a co-culture *in vitro* model consisting of human umbilical vein endothelial cells (HUVEC) and Jurkat T cells to test this. After mixed field irradiation (6 or 8 Gy, 2:1 neutron/gamma), HUVEC exhibit MAPK phosphorylation and increased secretion of several growth factors, including IL-6, IL-8, G-CSF, platelet derived growth factor (PDGF)-BB, and Angiopoietin-2. Jurkat cells cocultured with non-irradiated HUVEC maintain similar or better rates of proliferation compared to non-cocultured Jurkat cells, suggesting HUVEC produce signals or factors which maintain hematopoietic cell growth. Interestingly, Jurkat cells cocultured with irradiated HUVEC or media from irradiated HUVEC show decreased proliferation, with no decrease in viability, compared to control Jurkat cells. This may be due to a decrease in pro-proliferative signals, or an increase in anti-proliferative signals. Preliminary data in the model suggest EC can modulate the proliferation of hematopoietic cells, and that mediators produced by EC may play important roles in recovery from mixed field radiation injury.

(PS4.47) Effect of UV irradiation on colorectal cancer cells with acquired TRAIL resistance. Yong J. Lee, University of Pittsburgh, Pittsburgh, PA

Tumor necrosis factor-related apoptosis-inducing ligand (TRAIL) is a member of the TNF superfamily. TRAIL shows strong cytotoxicity to many cancer cells but minimal cytotoxicity to most normal cells. Interestingly, our previous studies have demonstrated that pretreatment with TRAIL induces acquired resistance to TRAIL (Song et al., JBC, 282:319, 2007). Acquired TRAIL resistance develops within 1 day and gradually decays within 5 days after TRAIL treatment. In our current study, we examined whether human colorectal carcinoma CX-1 cells with

acquired TRAIL resistance are resistant to UV irradiation as well. CX-1 cells were treated with 200 ng/ml TRAIL for 6 h and incubated various times (0.25-5 days) and then challenged to UV irradiation. Unexpectedly, we observed an increase in apoptosis in acquired TRAIL resistant cells after UVC as well as UVB exposure. This was due to an increase in caspase activation which was mediated through cytochrome *c* release. These results suggest that cells with acquired TRAIL resistance are sensitive to UV irradiation.

(PS4.48) Alterations of Na⁺/H⁺ exchangers after ionizing radiation. Steven B. Zhang, Mei Zhang, Shanmin Yang, Liangjie Yin, Kunzhong Zhang, Alexandra Litvinchuk, Amy Zhang, Steven Stwartz, Vidyasagar Sadasivan, Lurong Zhang, Paul Okunieff, UF Shands Cancer Center, Gainesville, FL

Na⁺/H⁺ exchangers (NHE 1-3) play critical roles in multiple physiological processes, such as intracellular pH regulation and ion homeostasis. Ionizing radiation (IR)-induced abnormalities of NHE 1-3 might evolve into long-term cell dysfunction and manifest as a late toxicity after IR exposure. In this study, the effects of radiation on NHE 1-3 in brains and kidneys were measured in four strains of mice with varying radiation sensitivity characteristics (BALB/c ≈ NIH Swiss < C57BL/6 ≈ C3H/HeN). Four different strains of mice were exposed to different IR doses (0, 3, 5, 7, 9, and 11 Gy) at 1.84 Gy/min and sacrificed for tissue collection 9 hours later. Total RNAs of brain and kidney were extracted with Trizol. The RNA was reversely transcribed to cDNA. β-actin was used as sample loading control. The gene expression levels of NHE1-3 and β-actin were analyzed by Real-time PCR. For NHE1, the gene expression levels of BALB/c and NIH Swiss were significant lower than C57BL/6 and C3H/HeN in both brain (0.9 ± 0.14 vs 1.65 ± 0.07) and kidney (0.82 ± 0.15 vs. 1.48 ± 0.01). For NHE2, the more TBI sensitive strains were again lower in brain (1.74 ± 0.54 vs. 3.73 ± 0.49). In mouse brain, NHE1 gene expression levels were significant higher (3.0~9.3 folds) than NHE2, independent of strain; while in kidney both NHE2 and NHE3 were significantly higher (1.5 to 3.4 folds and 2.1 to 6.9 folds respectively) than NHE1. Upon IR (≥5 Gy), NHE1 levels in both brain and kidney decreased in all strains. In brain, IR significantly increased NHE2 transcription level (4.1 to 6.2 folds) only in C57BL/6; while in kidney, IR with ≥5 Gy decreased both NHE2 and NHE3 levels only in the more TBI sensitive strains. In C3H/HeN, both NHE2 and NHE3 levels increased after IR. In conclusion, the pattern of NHE1-3 depends on both strain and tissue type. The importance of NHE2 on radiation induced diarrhea and organ function deserves further investigation since more TBI-sensitive mice have a greater response to radiation.

(PS4.49) Decreased glucocorticoid receptor and increased signal regulatory protein α1 and small G protein RhoB induced by radiation in liver and duodenum of C57BL/6 mouse. Xiaohui Wang, Mei Zhang, Yansong Guo, Bingrong Zhang, Shanmin Yang, Alexandra Litvinchuk, Steven Stwartz, Vidyasagar Sadasivan, Lurong Zhang, Paul Okunieff, Paul Okunieff, Department of Radiation Oncology, UF Shands Cancer Center, Gainesville, FL

Although glucocorticoids (GC) suppress immunity and inhibit cytokine production in response to pro-inflammatory stimuli, the utility of GC for alleviation of radiation-induced inflammation is controversial. The effect of GC is mediated by the glucocorticoid receptor (GR) and a few target genes. RhoB is a low molecular weight GTPase belonging to the Ras superfamily, which regulates multiple physiological processes such as cell adhesion, motility, survival and proliferation. SIRPα1, a member of the signal regulatory protein (SIRP) family, is a plasma-membrane protein relatively ubiquitously expressed on myeloid cells including macrophages and plays important roles in immune regulation. Our previous work has confirms that the proliferation inhibitory effect of GR on murine macrophage RAW264.7 cells is mediated via RhoB and SIRPα1. We also demonstrated that radiation resulted in the increase of various cytokines, chemokines at multi-time points in

C57BL/6 mice, with remarkable changes at 6 hour, and 4 and 10 days after 5 or 9 Gy irradiation. In this study the pattern of protein levels of GR, SIRP α 1 and RhoB after mouse radiation were assessed with quantitative Western blot analysis to clarify the role of GR on radiation-induced inflammation and its possible signal pathway. It was found that the expression of GR was significantly decreased in hepatic cytosol at 6 hour, and 4 and 10 days after 5 or 9 Gy of radiation, with substantial inhibition at 4 days after 5Gy radiation (about 40% of control, $p < 0.05$). Concomitant with the decrease of GR, was a significant increase of RhoB and SIRP α 1 in the hepatic cytosol at these post-radiation time points, with the most obvious enhancement of RhoB and SIRP α 1 at 4 and 10 days after 5Gy radiation, respectively (about 1.9- and 1.3- fold of control, respectively, $p < 0.05$). A similar pattern was found in duodenum of C57BL/6 mice. In conclusion, our results indicate that radiation decreased the protein level of glucocorticoid receptor and increased the expression of RhoB and SIRP α 1 in liver and duodenum of C57BL/6 mice, and that these may play roles in radiation-induced inflammation.

(PS4.50) Alterations of plasma protein glycosylation after radiation. Mei Zhang, Yansong Guo, Steven B. Zhang, Shanmin Yang, Xiaohui Wang, Chun Chen, Jun Ma, Steven Stwartz, Vidyasagar Sadasivan, Paul Okunieff, Lurong Zhang, Department of Radiation Oncology, Gainesville, FL

Glycosylation is a major post-translational modification of proteins, and is often necessary for protein function. While great effort has been made to understand the alterations of DNA and protein synthesis/repair post-radiation, however very few studies have been undertaken for the effect of ionizing radiation (IR) on protein glycosylation. In this study, we have set up an ELISA-like assay to measure the plasma levels of glycoproteins with different sugars. The steps were: 1) 4 ug/ml of highly purified lectin were coated onto ELISA plates; 2) diluted (1:20) plasma was added to the plate; and 3) the bounded glycoproteins were detected by biotinylated lectin (0.5 ug/ml) followed by streptavidin conjugated HRP and substrate TMB as a signal amplification system. Results: A) in the Con A~biotin-WGA assay system, protein glycosylation with both mannose and N-Acetyl Glucosamine were reduced in an IR dose-dependent manner (0, 3, 6, 10 Gy) 7 days after total body IR (TBI) in C57BL/6 mice. In NIH Swiss mice, on day 2 after 8.6 Gy TBI, this type of glycoprotein appeared to increase compared with normal mice, and normalized when mitigated with FGF-P (a peptide derived from FGF-2); B) in the WGA~biotin-RCA assay system, glycosylation with both N-Acetyl Glucosamine and N-Acetyl galactosamine were increased 6 hr after 3-10 Gy TBI in C57BL/6 mice. In NIH Swiss mice it was decreased at day 9 after 8.6 Gy TBI, which again was increased by FGF-P; C) in the PNA~biotin-PHA-L assay system, the glycosylation with both galactose and sugar complex structures were unchanged in irradiated C57BL/6 mice. On day 2 after 8.6 Gy TBI in NIH Swiss mice, it was increased and normalized with FGF-P treatment; and D) in the PHA-L~biotin-UEAI assay system, glycosylation with both sugar complex structures and fucose were reduced 17 days after 15 Gy lung IR in C57BL/6 mice, which was increased by GA (an anti-inflammation agent extracted from medicinal herb). These studies indicate that the newly-established lectin-lectin ELISA assays are useful tools to study IR-induced alterations of protein glycosylation and vary with time after exposure and respond to mitigation agents.

(PS4.51) Molecular and histopathological changes in mouse intestinal tissue after proton exposure. Ashley Purgason¹, Ye Zhang², Ramesh Govindarajan³, Olufisayo Jejelowo⁴, Daila Gridley⁵, Stanley Hamilton⁶, Honglu Wu⁷, ¹NASA-Johnson Space center/UTMB, Houston, TX, ²NASA-Johnson Space center/Wyle, Houston, TX, ³Norfolk State University, Norfolk, VA, ⁴Texas Southern University, Houston, TX, ⁵Loma Linda University, Loma Linda, CA, ⁶The University of Texas MD Anderson Cancer Center, Houston, TX, ⁷NASA-Johnson Space center, Houston, TX

Radiation in space, especially energetic protons emitted from solar particle events (SPEs), poses serious health risks to

astronauts and is especially dangerous for long-duration missions. Protons are the most abundant particles in space and to date little is known about the details of the negative consequences crewmembers will face upon exposure to them. To elucidate some of the possible health effects induced by protons, we subjected BALB/C mice to 250 MeV of proton radiation at doses of 0 Gy, 0.1 Gy, 1 Gy, and 2 Gy. The gastrointestinal tract of each animal was dissected 4 hours after irradiation and tissue from the small intestine was isolated and fixed in formalin for histopathological examination or snap-frozen in liquid nitrogen for RNA isolation. Histopathologic observation of the tissue using standard hematoxylin and eosin staining methods to screen for morphologic changes showed a marked increase in apoptotic lesions for even the lowest dose of 0.1 Gy, and the dose response showed a possible higher sensitivity at low dose. Tissue of the small intestine was also homogenized and RNA was isolated for synthesis of complementary DNA and real-time polymerase chain reaction analysis for genes involved in apoptosis. The results of gene expression changes revealed consistent up or down regulation of a number of genes for all of the exposure doses, suggesting that these genes may play roles in proton-induced apoptosis. In addition, several genes (e.g., Bok and Casp1) were found to have significant changes in the RNA level after the lowest dose (0.1 Gy) but not the higher doses (1 and 2 Gy) of proton exposures, whereas other genes (e.g., Tsc22d3) had expression changes only after high-dose proton exposures. Changes of the proteins encoded by these genes whose expression was consistently altered by protons were further analyzed by immunostaining. These findings demonstrated that apoptosis may occur in the gastrointestinal tract after even low-dose proton exposures, and the different gene expression patterns of mice irradiated with low and high doses of protons may offer insight into molecular mechanisms that might explain the apparent high sensitivity of these mice to low doses of protons.

(PS4.52) Integrated experimental and computational strategy to develop a predictive understanding of radiation induced matrix remodeling in a human skin tissue model. Marianne B. Sowa, Adam J. Lewis, William B. Chrisler, Harish Shankaran, PNNL, Richland, WA

One of the early events following exposure to ionizing radiation is the activation of cell signaling pathways. These signaling pathways in turn elicit diverse proximal responses such as proliferation, apoptosis, activation of pro-survival programs and tissue remodeling. Radiation can in fact simultaneously activate several signaling pathways within cells leading to the induction of both protective effects as well as adverse consequences. However a key question is whether signaling cascades initiated by low doses are fundamentally different relative to high dose exposures. Understanding the link between radiation dose and dose rate to the pattern of cell signaling is an important prerequisite for developing a mechanistic understanding of radiation risk. We are investigating the mechanisms whereby radiation stimulates signaling cascades in a skin tissue culture model. We are currently pursuing an integrated experimental and computational strategy to develop a predictive understanding of the link between cell signaling, gene expression and proximal tissue responses to low dose/low dose rate radiation exposures. We are quantitatively measuring variables that represent these processes and using the experimental data to construct a mathematical model of the relationships between the measured variables. The constructed model will provide us with a mechanistic understanding of the effect of low dose radiation exposure on tissue responses. Experiments are specifically designed to obtain information on how low dose/low dose rate exposures modify radiation induced signaling pathways important to maintaining tissue homeostasis.

(PS4.53) Reduced oxygenation does not protect all prostate cancer cells from radiation: a new role for hypoxia in radiation therapy? Laure H. Marignol¹, Lynn M. Martin¹, Mark Lawler¹, Thomas H. Lynch², Donal Hollywood¹, ¹Trinity College Dublin, dublin, Ireland, ²St James's Hospital, dublin, Ireland

Introduction: Oxygen is essential for optimal cytotoxicity of radiation therapy. In the absence of oxygen at the time of radiation exposure, cell survival is commonly expected to increase by up to three-fold. We proposed that the proportion of cells completely deprived of oxygen within tumours may not be sufficiently large to be clinically significant and hypothesised that the surrounding hypoxic cells in fact may govern tumour response to radiotherapy. To test this hypothesis, this study proposed to re-examine the radioresponse of hypoxic prostate cancer cells and determine the consequences of these potentially clinically relevant oxygen levels. **Methods:** Prostate cancer cells (22Rv1, PC3, DU145) were exposed to hypoxia (0.5% O₂) for up to 48 hours prior to hypoxic irradiation with single radiation doses (0-20 Gy). Survival was assessed using clonogenic assays and radiation survival curves were generated. Radioresponses were compared to that of anoxic, fully oxygenated and CoCl₂ treated cells and correlated to cell cycle distribution, Hypoxia-Inducible-1 alpha (HIF-1 α) protein levels, γ -H2AX and Rad51 staining and . Split dose experiments were performed to investigate modification of the linear relationship between survival and radiation dose by these oxygen level. **Results:** Both anoxia and 0.5% O₂ resulted in increased survival following radiation exposure. Induction of radioresistance by 0.5% O₂ was however both time-dependent and cell type specific: 22Rv1 showed gradual increase (up to 2-fold) in survival with lengthening of pre-irradiation hypoxic exposure, whereas radiosensitivity was maintained in hypoxic DU145 and PC3 cells. Radioresistance induced by 0.5% O₂ was HIF-1 α independent and correlated with reduced recognition of double strand breaks. It did not appear to be dose-dependent and the relationship between survival and radiation dose appeared linear over the 0-10 Gy dose range. These levels of hypoxia progressively induced a G0/G1 arrest in all three cell lines tested, which did not correlate with radioresponse. **Conclusions:** These results confirm that hypoxia induces radioresistance in prostate cancer cells, however oxygen tension above anoxia levels do not affect all cancer cells. These preliminary data suggest potential expansion of clinical importance of hypoxia in prostate cancer.

(PS4.54) Low-dose radiation response in primary endothelial cells and cell lines and heart tissue studied by different proteomics approaches. Soile Tapio¹, Zarko Barjaktarovic¹, Omid Azimzadeh¹, Alena Shyla¹, Ramesh Yentrapalli^{1,2}, Arundhati Sriharshan¹, Hans Zischka³, Mats Harms-Ringdahl², Andrzej Wojcik², Siamak Haghdoost², Michael J. Atkinson¹, ¹Helmholtz Zentrum München, Institute of Radiation Biology, Neuherberg, Germany, ²Department of Genetics, Microbiology, and Toxicology, Stockholm University, Stockholm, Sweden, ³Helmholtz Zentrum München, Institute of Toxicology, Neuherberg, Germany

Recent epidemiological studies indicate that low-dose irradiation may enhance the risk of cardiovascular mortality in a moderate but significant manner. The aim of this study was to identify potential molecular targets or mechanisms involved in the pathogenesis of radiation-induced cardiovascular disease. Two main targets were chosen, namely the vascular endothelium playing a pivotal role in the regulation of cardiac function, and the heart tissue, in particular the cardiac mitochondria supplying the energy. As vascular endothelium models we used both human endothelial cell line (EA.hy926) and primary cells (HUVEC) that were irradiated with low doses of acute or chronic gamma radiation, respectively. In the case of EA.hy926 the cells were irradiated with Co-60 or Cs-137 gamma sources using different dose rates with a total dose of 0.2 Gy. The immediate radiation response 4 hours and 24 hours after exposure was analysed from cytosolic fractions with 2D-DIGE technology and from whole cell fractions with SILAC (Stable Isotope Labelling with Amino acids in Cell culture) approach. Several biological pathways involved in the low-dose response were identified. The HUVEC cells were grown under chronic low dose rate conditions (1.3 mGy/h and 4.1 mGy/h) and the proteomes were analysed using ICPL (Isotope Coded Protein Labelling) method at the time points of 2, 4, 6, and 8 weeks. The irradiated cells showed radiation-induced premature senescence compared to the sham-irradiated cells. Functional and proteomic changes in the murine cardiac mitochondria were studied four weeks after a heart-focussed exposure to X-ray irradiation using doses of 2 Gy and 0.2 Gy. Mitochondria isolated from ten sham-

irradiated and ten irradiated C57Bl/6 mice were tested using functional assays for respiratory coupling and ROS production. Succinate-driven respiration was significantly decreased by 13% in 2 Gy irradiated mitochondria. The decreased level of respiration was accompanied by a significant increase in the ROS production. Changes at the proteome level were analysed by 2-D DIGE and significantly differentially expressed proteins were identified by mass spectrometry. Cardiac mitochondria irradiated with 0.2 Gy showed no significant functional impairment but the expression of four proteins was significantly altered.

(PS4.55) Mek1-erk1/2 signaling pathway is required for radiation-induced c-jun activation. Zhiyong Deng¹, Paulo R. M. Rosa¹, Guangchao Sui², Weiling Zhao¹, ¹Department of Radiation Oncology, Neurosurgery and Brain Tumor Center of Excellence, Winston-Salem, NC, ²Department of Cancer Biology, Wake Forest University School of Medicine, Winston-Salem, NC

Radiation-induced normal brain injury has been a major concern and limitation of radiotherapy. A growing body of evidence supports the hypothesis that radiation-induced brain injury is driven in part by an acute and/or chronic inflammatory response. Recent studies suggest that microglia activation is a potential contributor to chronic inflammatory responses following irradiation. However, the molecular mechanism underlying the response of microglia to radiation is poorly understood. c-Jun, a component of the AP-1 transcription factors, has been suggested as an important regulator for neural cell death and neuroinflammation. We observed rapidly increased phosphorylation of c-Jun at Serine 63 and MAPK kinases Erk1/2, but not JNKs, in irradiated murine microglia BV2 cells. Radiation-induced c-Jun phosphorylation was markedly blocked by Erk1/2 inhibitor. Silencing of the ERK1 and ERK2 genes using lentiviral delivered shRNAs evidently attenuated radiation-induced c-Jun phosphorylation. Consistently, overexpression of Erk1/2 showed a dose dependent increase for c-Jun phosphorylation. Co-immunoprecipitation assay showed that c-Jun and phosphorylated Erk1/2 are endogenously associated and such association was increased by radiation. GST-pull experiment revealed the direct interaction between c-Jun and Erk1/2. Domain mapping study further indicated that Erk1 and Erk2 bind to a specific region of cjun, which does not overlap with the JNK binding domain, suggesting the distinct function of Erk1/2 and JNK on c-Jun. MEK1, an upstream kinase of Erk1/2, was found to be indispensable for radiation-induced c-Jun phosphorylation, as demonstrated by inhibition, knockdown and overexpression of this gene. We observed radiation-enhanced c-Jun transcriptional activity by the luciferase reporter assay. Blocking the activation of MEK1-ERK1/2 pathway led to an inhibition in radiation-induced upregulation of Cox-2 and cyclin-D1 proteins. Taken together, these findings reveal a novel radiation-mediated signaling pathway, which contributes to radiation-induced response in microglia.

(PS4.56) Studying the role of p53 in tumor stroma in lung cancer growth and response to radiation therapy. Paiman Ghafoori, Bradford Perez, Yifan Li, Chang-Lung Lee, Samuel Johnston, Cristian Badea, David G. Kirsch, Duke University, Durham, NC

Purpose/Objective: Stromal cells within the tumor microenvironment can influence cancer development and response to radiation therapy (RT), but the role that specific stromal cells play in regulating these processes remains to be fully defined. Although xenografts can be utilized to study the tumor microenvironment, differences between transplanted tumor cells and the stromal cells in the recipient mice may alter tumor growth and response to RT. To overcome this potential limitation, we have generated primary lung cancers in mice within a native microenvironment in which specific genes can selectively be deleted *in vivo* in tumor parenchymal cells or in the tumor stroma. **Material/Methods:** We generated genetically engineered mouse models (GEMMs) of primary non-small cell cancer (NSCLC) using the Cre-Lox recombination system by conditionally expressing oncogenic K-rasG12D in p53 deficient mice. Using the endothelial cell-specific Tie-2 promoter to drive Cre

expression, we selectively restored p53 expression in endothelial cells by deleting a transcription stop cassette (LSL) upstream of the p53 gene. We also utilized a second model with oncogenic K-rasG12D in p53 Flox mice. Using an adenovirus to deliver Cre to the lung epithelium, we deleted p53 specifically in lung cancer parenchymal cells, while tumor stromal cells retained wild-type p53. Both groups of mice were imaged with micro-CT to determine the 3-dimensional tumor volume for individual lung cancers over time. Mice were irradiated with RT (10 Gy) and the response of tumors to RT was assessed by micro-CT and immunohistochemistry. Results: Lung cancers with p53 deleted in tumor parenchymal cells grew at a similar rate as lung cancers with p53 deleted in both the tumor parenchymal cells and tumor stroma. Lung cancers lacking p53 demonstrated an impaired cell cycle arrest following RT. Restoring p53 in endothelial cells did not affect tumor growth. Conclusion: We have utilized a GEMM of primary lung cancer to selectively delete or restore p53 in vivo in parenchymal or stromal cells in mice. This model system will be useful to define the role of p53 and other genes in different cell types in regulating the response of lung cancer to RT.

(PS4.57) Characterisation of the increase of cancer cells migration caused by radiation on the syngeneic glioma model F98/fischer. Guillaume Desmarais, David Fortin, David Mathieu, Rachel Bujold, Benoit Paquette, Université de Sherbrooke, Sherbrooke, QC, Canada

Glioblastoma multiforme are known to be a highly radioresistant tumour subtype. Their migration properties decrease the effectiveness of radiotherapy treatment; the radiation dose needed to restrain all remaining cancer cells far exceeds normal brain tissue tolerance. Therefore, the radiation dose is established to optimize the "therapeutic ratio" which is obtained by maximum neoplastic cell kill with minimal adverse effects to normal tissue. Unfortunately, within this range of doses, tumour reappears in the previously irradiated brain volume. In this study, we have characterized the effects of radiations on the migration properties of the syngeneic F98 glioma cells implanted in the brain of Fischer rats. Looking at coronal hematoxylin/eosin microscopy slides of brain, the effects of radiation on the migration of F98 cancer cells were analysed by measuring the satellite formation of neoplastic cells away from the primary tumour. Our results show that irradiation (15 Gy) of brain prior to tumour implantation increased by 45% the invasive surface through the brain and doubled migration distances of these satellites formations. In these circumstances, the overall survival of rats implanted with a brain tumour has been decreased by 6 days. Moreover, irradiation enhanced the expression of matrix metalloproteinase (MMP-2, 2-fold) and prostaglandin E2 (3-fold) highlighting the implication of the inflammatory cascade in radiation-enhancement of cancer cells migration. We are currently investigating the possible use of a selective cyclooxygenase-2 inhibitor (Meloxicam) to diminish this adverse effect of radiations. The hypothesis of phenotypes sensitivity to radiations is examined using cell cycle specific fluorescent probe. These probes will carry out the spatiotemporal dynamics of tumour development affected by radiations. A better understanding of glioblastoma multiforme behaviour in the context of radiotherapy will help clinicians to improve this treatment modality.

(PS4.58) Detection of the radio-sensitivity of oxygenated cell fractions in quiescent cell populations within solid tumors. Shin-ichiro Masunaga¹, Hideko Nagasawa², Yong Liu¹, Yoshinori Sakurai¹, Hiroki Tanaka¹, Genro Kashino¹, Minoru Suzuki¹, Yuko Kinashi¹, Akira Maruhashi¹, Koji Ono¹, ¹Research Reactor Institute, Kyoto University, Osaka, Japan, ²Laboratory of Pharmaceutical Chemistry, Gifu Pharmaceutical University, Gifu, Japan

Purpose: To detect the radio-sensitivity of oxygenated tumor cells not labeled with pimonidazole among intratumor quiescent (Q) cells. Methods and Materials: C57BL mice bearing EL4 tumors received 5-bromo-2'-deoxyuridine (BrdU) continuously to label all proliferating (P) cells in the tumors. They received gamma-ray

irradiation at a high dose-rate (HDR) or reduced dose-rate (RDR) one hour after the administration of pimonidazole. The responses of Q and total (= P + Q) cell populations were assessed based on frequencies of micronucleation and apoptosis using immunofluorescence staining for BrdU. Meanwhile, the response of pimonidazole unlabeled tumor cell fractions was assessed by apoptosis frequency using immunofluorescence staining for pimonidazole. Results: The cell fraction not labeled with pimonidazole showed significantly greater radio-sensitivity than the whole tumor cell fraction more remarkably in the Q than total cell population. However, the pimonidazole unlabeled cells showed a significantly clearer decrease in radio-sensitivity through a delayed assay or decrease in irradiation dose-rate than the whole cell fraction, again more markedly in the Q than total cell population. Conclusion: Pimonidazole unlabeled, probably oxygenated, Q tumor cells are thought to be a critical target in the control of solid tumors as a whole, based on a significantly greater radio-resistance and capacity to recover from radiation-induced damage in the Q than total cell population within solid tumors.

(PS4.59) Targeting photodynamic therapy-initiated epidermal growth factor receptor signaling to enhance cancer cell cytotoxicity. Molly Peterlin, Christine Edmonds, Sarah Hagan, Keith A. Cengel, University of Pennsylvania, Philadelphia, PA

Patients with serosal (peritoneal or pleural) spread of malignancy have few definitive treatment options and consequently have a very poor prognosis. We have previously shown that photodynamic therapy (PDT) can be an effective treatment for these patients, but that the therapeutic index is relatively narrow. Therefore, we have studied the inhibition of PDT-initiated survival signals as a potential way to increase cytotoxicity of PDT in ovarian cancer (OvCa) and non-small cell lung cancer (NSCLC) cells. We found that PDT using benzoporphyrin derivative monoacid (BPD) leads to increased activation/tyrosine phosphorylation and nuclear accumulation of epidermal growth factor receptor (EGFR). In vitro clonogenic survival studies demonstrated that EGFR inhibition by either erlotinib or by EGFR-specific siRNA knockdown resulted in enhancement of direct PDT cytotoxicity in both OvCa and NSCLC cells. We are currently testing whether nuclear translocation of EGFR directly affects survival of cancer cells after PDT using a nuclear-targeted EGFR construct and inhibitors of EGFR nuclear translocation. The function(s) of nuclear EGFR remains incompletely understood, but may involve resistance to apoptosis induced by cytotoxic agents. Therefore, we hypothesized that EGFR inhibition would lead to increased apoptotic cell death following BPD-mediated PDT. Consistent with the hypothesis, erlotinib enhanced BPD-PDT showed accelerated kinetics and increased overall levels of apoptosis as compared to BPD-mediated PDT alone. Cancer cells have also been shown to use autophagy as a survival mechanism for low dose PDT. Since EGFR signaling has been implicated in survival of cancer cells by autophagy, we tested whether inhibiting autophagy using chloroquine might lead to increased cancer cell cytotoxicity following erlotinib-enhanced PDT. We found that the combination of erlotinib and chloroquine synergistically increased apoptosis in OvCa and NSCLC cells. Taken together, these studies suggest that PDT-mediated activation and nuclear translocation of EGFR increases cancer cell survival through mechanisms that involve autophagy. Conversely, targeting these specific survival pathways might increase the therapeutic index of PDT in patients with serosal spread of OvCa and NSCLC. Supported by P01-CA087971.

(PS4.60) Accelerated hematopoietic toxicity due to ablation of myeloid progenitors: A hallmark of heavy ion radiation. Kamal Datta, Daniela Trani, Bhaskar Kallakury, Michael Cole, Albert J. Fornace, Georgetown University Medical Center, Washington, NW, DC

Introduction: Research on biological effects of heavy ion radiation has implications in two very different fields - space exploration and radiotherapy. Here we have determined the relative biological effectiveness (RBE) for ⁵⁶Fe radiation, and used

biological parameters to evaluate differential effects of ^{56}Fe and g-irradiation in C57BL/6J mice on two radiosensitive tissues - hematopoietic and gastrointestinal (GI). Methods: 6 to 8 weeks old wild type female C57BL/6J mice were irradiated with 3 to 8 Gy of iron ion (^{56}Fe ; 1 GeV/nucleon) and 5 to 15 Gy of g radiation. All the mice except the three and a half day time point mice were monitored for survival and weight for 30 days. For partial body ^{56}Fe exposures hind limbs were shielded using tungsten bricks. For experiments at three and half day post-irradiation, mice were exposed to 7.25, 10, and 15 Gy of g radiation or 5 to 8 Gy of ^{56}Fe radiation. Results: With an average RBE of 1.25 for 30-day survival ^{56}Fe was not markedly more toxic than γ rays. Gamma radiation showed typical GI (15 Gy) and hematopoietic toxicity (7.25 & 10 Gy). With ^{56}Fe irradiation, all the lethality occurred earlier than 10 d, suggestive of GI toxicity. However, mice irradiated with hind limbs shielding, 100% survival was observed for 30 days even after 8 Gy of ^{56}Fe . GI toxicity in ^{56}Fe -irradiated mice was further excluded by bacterial colony count in blood culture. The number of surviving crypts at doses that caused lethality before 10 d post-radiation were significantly less in g irradiated samples. More TUNEL positive crypt cells were observed in small and large intestine of γ -compared to iron-exposed mice. In contrast, ^{56}Fe irradiated bone marrow showed higher TUNEL positive and lower number of progenitor cells per HPF. Body weight in mice irradiated with γ -rays, ^{56}Fe TBI and ^{56}Fe PBI showed marked differences. While there were dose dependent decreases in WBC counts after γ and ^{56}Fe radiation, significantly greater decreases were seen for the later at equitoxic or equal doses. Conclusions: We conclude from our results that ^{56}Fe , although with an RBE of 1.25 was not much more lethal than g-rays, showed greater hematopoietic toxicity than g-rays at equitoxic doses and suggests that ^{56}Fe -induced accelerated hematopoietic toxicity is due to preferentially greater ablation of myeloid progenitor cells in the bone marrow.

(PS4.61) Fat accumulation by ionizing radiation and its amelioration by anti-obestic drug. Sung-Kee Jo¹, Changhyun Roh¹, Hae-Ran Park¹, Namhee Choi¹, Uhee Jung¹, Sung-Tae Yee², Sung-Ho Kim³, ¹Advanced Radiation Technology Institute (ARTI), Korea Atomic Energy Research Institute (KAERI), Jeonbuk, Republic of Korea, ²Sunchon National University, Sunchon, Republic of Korea, ³Chonnam National University, Gwangju, Republic of Korea

Ionizing radiation has become a health concern emanating from natural sources like space travel and artificial sources like medical therapies. Although the risk of degenerative diseases by radiation has been reported, the detailed mechanisms are poorly understood. By revealing the underlying mechanisms, ionizing radiation can be used as a method to construct disease model systems. The regulation of adipocytes can be considered as a way to balance both glucose uptake and energy expenditure in order to derive the amount of fat stored. Thus, increases in glucose uptake or decreases in energy expenditure results in elevated fat deposition. In this study, we showed that γ -irradiation could trigger the biological response resulting in the fat accumulation of white adipose tissue in mice and that this can be a useful model for evaluation of anti-obestic drugs. To induce the fat accumulation by γ -irradiation, 2-months-old female C57BL/6 mice were irradiated at 5Gy and further raised for 6 months. Then, the mice were i.p. injected daily with orlistat (25 mg/kg) or vehicle for 3 weeks and analyzed for the adipose tissue weight and serum TG levels. The abdominal adipose tissue of the γ -irradiated mice weighed an average of 3.9g per 100g body weight, 1.7 fold higher than what was seen in the normal mice (2.3g per 100g body weight), indicating that γ -irradiation induced the fat accumulation in the adipose tissue. However, the administration of orlistat, a well-known anti-obestic drug, significantly reduced the adipose tissue weight to 1.7 g per 100g body weight in irradiated mice. Also, in these orlistat-treated mice, a significant reduction of serum triglyceride level by 14% was observed. The findings of this study that the fat accumulation is induced by radiation exposure and it can be ameliorated by an anti-obestic drug suggest that γ -irradiated mice can be applied as a useful model for the development of novel therapeutic approaches for obesity. [This study was supported by the Nuclear R&D Program of MEST (Grant No. 2007-00091)]

(PS4.62) Irradiation decreases SGLT1 mediated glucose absorption. Liangjie Yin, Kunzhong Zhang, Jacob Karimpil, Jeevan Gurijala, Pooja Vijaygopal, Mei Zhang, Paul Okunieff, Lurong Zhang, Vidyasagar Sadasivan, UF Shands Cancer Center, Gainesville, FL

Radiation affects rapidly dividing cells of the gastrointestinal (GI) tract causing epithelial dysfunction that leads to electrolyte and nutrient malabsorption. Treatment of dehydration and nutritional deprivation associated with secretagogue-induced diarrhea are derived from the resilience of the sodium dependent glucose transport system (SGLT1), which is the primary mechanism for glucose absorption across the brush-border membrane of enterocytes. There is little known information about the glucose transport following radiation induced secretory diarrhea. Our aim was to investigate the SGLT-1 function and consequently, its affect on glucose absorption following irradiation. These studies were done on small intestinal mucosa of Swiss mice on day 6 after exposure to 0, 1, 3, 5 or 7 Gy. Briefly, glucose-stimulated short circuit current (I_{sc}) measured in Ussing chamber was used to study SGLT1 transport function. Survival studies were carried out in 9 Gy TBI and 15.6 sub-TBI mice. The results showed that 1) glucose-stimulated I_{sc} decreased with increasing IR doses; 2) K_m values for glucose were (mM) 0.38 ± 0.04 , 0.49 ± 0.06 , 1.76 ± 0.16 , 1.91 ± 0.3 , 2.32 ± 0.4 in 0, 1, 3, 5 and 7 Gy respectively; 3) V_{max} values for glucose were 387.4 ± 16.2 , 306.6 ± 16.4 , 273.2 ± 14.9 , 212.9 ± 9.14 , 188.1 ± 9.12 in 0, 1, 3, 5 and 7 Gy respectively; 4) Changes in K_m and V_{max} measured with time since IR showed that their values returned to normal levels approximately 14 days after IR; 5) Survival studies showed that withholding glucose from supportive care for first 10 day showed increased survival; and 6) Western blot analysis for SGLT-1 brush border membrane showed increased protein levels with increasing IR dose. Conclusion: Increase in K_m with increasing IR dose suggestion decreased affinity for glucose. Decrease in V_{max} could suggest increasing loss of villus epithelial cells with increasing IR dose, which is supported by histopathology sections. Increased protein levels with IR in Western blot analysis suggest that the SGLT1 transporters are non-functional and further studies are essential to validate this observation. These studies suggest that inclusion of glucose in food may lead to osmotic diarrhea resulting from malabsorption of glucose and electrolytes, which further complicates IR-induced toxicity.

(PS4.63) Effects of ionizing radiation on stromal-epithelial communication in esophageal carcinogenesis. Zarana S. Patel¹, Katharine D. Grugan², Anil K. Rustgi², Francis A. Cucinotta³, Janice L. Huff¹, ¹NASA Johnson Space Center / USRA, Houston, TX, ²Division of Gastroenterology, University of Pennsylvania, Philadelphia, PA, ³NASA Johnson Space Center, Houston, TX

Esophageal cancer is the 6th leading cause of cancer mortality worldwide and is associated with a variety of risk factors including tobacco use, heavy alcohol consumption, obesity, and dietary factors. In addition, a link between esophageal cancer and radiation exposure is revealed by its high excess relative risk among the tumor types observed in survivors of the atomic bomb detonations in Japan. To better understand the role of radiation exposure in the development and progression of esophageal cancer, we are using hTERT-immortalized human esophageal epithelial cells and genetic variants grown in co-culture with esophageal stromal fibroblasts (Okawa et al. Genes & Development 2007). Because the stromal compartment plays an essential role in the maintenance and modulation of epithelial cell growth and differentiation and is implicated in cancer development, we examined how irradiation of stromal fibroblasts affected epithelial cell behavior. After exposure to conditioned media from irradiated fibroblasts, we quantified epithelial cell migration and invasion, both behaviors associated with cancer promotion and progression. These assays were conducted in modified Boyden chambers. Our results using low LET gamma radiation showed a dose-dependent increase in migration of epithelial cells when exposed to conditioned media from irradiated vs. non-irradiated fibroblasts. We also observed enhanced invasion through a basement membrane matrix in similarly treated cells. Antibody-capture arrays and ELISAs were used to identify increased secretion of hepatocyte growth factor

(HGF) and interleukin-8 (IL-8) in the conditioned media of irradiated fibroblasts. These factors are known to play a role in cancer progression and metastasis. Wound healing assays conducted with HGF and IL-8 showed a positive effect on epithelial cell migration, indicating that they may be responsible for motility after irradiation. To further characterize the biological role of these factors, we are conducting studies to analyze their influence on DNA repair using epithelial cells grown in 2-D monolayers and 3-D organotypic cultures, using both low and high-LET radiation. These results should further our understanding of the mechanisms by which radiation impacts the tissue microenvironment and its role in cancer development.

(PS4.64) In silico mammary gland: an agent-based systems biology model of mammary gland carcinogenesis following ionizing radiation. Jonathan Tang¹, Chen-Yi Chen¹, Mary Helen Barcellos-Hoff², Sylvain V. Costes¹, ¹Lawrence Berkeley National Laboratory, Berkeley, CA, ²New York University, New York, NY

There is a growing body of evidence suggesting that, in addition to induction of somatic mutations in irradiated cells as a result of DNA damage and misrepair, radiation exposure can also elicit non-targeted responses that can produce effects in non-irradiated cells or lead to a higher frequency of genomic instability in the progeny of irradiated cells. This evidence has brought awareness that carcinogenesis following exposure to radiation may be a culmination of many types of altered cell interactions and multicellular responses, and thus an emergent property of a perturbed system. Our prior work has shown that key aspects of irradiated mammary gland tissue include persistent activation of transforming growth factor β 1, loss of basement membrane integrity, genomic instability, and epithelial to mesenchymal transition. In order to explore this idea, we have constructed a computational systems model of the mouse mammary gland using an agent-based formalism. Agents are autonomous software objects that have defined rules or mathematical equations that determine how they behave and interact with each other and their local environment. Our *in silico* mammary gland consists of interacting agents simulating either mammary epithelial cells or stromal cells, in an environment with variables representing extracellular matrix properties. We have modeled normal murine mammary morphogenesis and maintenance by establishing a set of rules and parameters that led to cumulative agent behavior that match experimental data of the developing gland. Radiation can perturb each of the mammary gland compartments and lead to a disorganized morphogenesis, i.e. dysplasia, a hallmark of cancer. Our ultimate goal is to construct a tool for useful testing and visualizing the consequences of different assumptions about how mutant cells evolve in an irradiated tissue microenvironment. In combination with modeling microdosimetry of various radiation qualities in this system, we will have a tool that will allow us to test how geometrical properties of energy deposition can modify relative biological effectiveness. This exercise will help refine our hypothesis that radiation carcinogenesis is the result of a synergistic interaction between targeted damages and non-targeted effects. Supported by NASA Specialized Center of Research.

(PS4.65) Calsequestrin-1 upregulation at the cell surface in response to radiation in tumors and tumor vasculature. Arif N. Ali¹, Ralph J. Passarella², Margaret Willard¹, Lluís A. Lopez-Barcons¹, Roberto Diaz¹, ¹Emory University, Atlanta, GA, ²Vanderbilt University, Nashville, TN

Objectives: Calsequestrin-1 (CSQ-1) has been previously shown to be induced in some tumor histologies in response to ionizing radiation (XRT), though the exact mechanism of action and site of expression is unclear. In this work, we probe the mechanistic details of CSQ-1 upregulation and show that it is expressed primarily on the cell surface in both tumors and tumor vasculature post-XRT. Methods: GL261, LLC, and H460 cell lines were treated with 3 Gy of XRT for 3 fractions. Cells were harvested 4 hours later, separated into total protein or hydrophobic and hydrophilic protein, and electrophoresed and probed for CSQ-1. GL261 and

LLC tumors were also implanted into the hindlimbs of nude mice and treated with 3 Gy of XRT for 3 fractions, harvested and analyzed as previously described. Additionally, the GL261 implanted nude mice were injected with 40 mg/kg of anti-CSQ-1 antibody or an IgG serum control labeled with AlexaFluor 750. These *in vivo* tumors were removed and imaged 7 days after antibody injection. Finally, GL261 tumors were co-cultured with HUVECs and treated with 3 Gy of XRT for 3 days. HUVECs were harvested at sequential time points after XRT and total protein was extracted, electrophoresed, and probed with CSQ-1 antibody. Results: XRT treated *in vitro* GL261, LLC and H460 cell lines showed a decrease in the hydrophilic protein component in response to XRT and a corresponding increase in the hydrophobic protein proportion. XRT treated *in vivo* GL261 tumors analyzed with labeled CSQ-1 antibody demonstrated significantly enhanced fluorescence as compared to the labeled IgG serum control. GL261 tumors co-cultured with HUVECs demonstrated upregulation of CSQ-1 in response to radiation on western blot compared to controls. Conclusions: CSQ-1 is known to have a significant role in calcium homeostasis. This work uniquely demonstrates that CSQ-1 is preferentially expressed on the cell membrane in response to XRT as indicated by upregulation of the CSQ-1 hydrophobic protein component of *in vitro* tumor cells and the verified binding of CSQ-1 antibody to *in vivo* tumors compared to controls. Furthermore, co-cultured experiments with HUVECs show relevancy of CSQ-1 upregulation in tumor blood vessels. Taken as a whole, it appears that CSQ-1 plays an important role as a novel XRT-induced neoantigen in both tumors and tumor vasculature.

(PS4.66) Amplification of endothelial cells response to ionizing radiation by mast cells conditioned medium: an in vitro approach. Karl Bllirando¹, Fabien Milliat¹, Isabelle Martelly², Marc Benderitter¹, Agnès François¹, ¹IRSN, Fontenay-aux-roses, France, ²Laboratory of Tissue Growth Repair and Regeneration (CRRET) Université Paris 12, Creteil, France

Inflammation is a hallmark of tissue response to ionizing radiation (IR), in which the endothelium plays a pivotal role. Irradiated endothelium produces mediators and express adhesions molecules that stimulate inflammatory cells and facilitate their recruitment from the blood stream. During the course of radiotherapy for cancer treatment, normal tissues present in the irradiation field are irradiated and became inflamed contributing to development of side effects. Few studies have been made on the endothelium response to IR when confronted to an inflammatory environment. Using a human mast cells line (HMC-1) and two primary endothelial cells lines (HUVEC and HMVEC) we studied the influence of HMC-1 conditioned medium (MCCM) on endothelial cells response to a 10Gy IR. Our experiments have shown that several inflammatory genes expressed in response to IR and MCCM were synergistically increased at the RNA and protein levels. Whereas this increase was blocked by the Histamine H1 receptor antagonist mepyramine. Histamine (an important mast cell mediator) alone did not mimicked MCCM effect on endothelial cells response to IR suggesting implication of other HMC-1 mediators. To investigate the mechanisms underlying this synergy we used two inhibitors of the stress activated kinase P38 MAPK (P38) and an inhibitor of the transcription factor NFK-b which are both regulators of inflammatory gene expression. We found that NFK-b but also P38 activation were necessary for the synergy between IR and MCCM. Western Blot analysis have shown that MCCM and histamine increased P38, P65 (NFK-b) phosphorylation more rapidly and more strongly than IR, but no synergy in their phosphorylation rate have been observed. Downstream P38 we found that MAPKAP (MK2) phosphorylation was increased by IR and MCCM, and that its activation was abolished in presence of P38 inhibitors. Studies are ongoing to better understand which mast cells mediators are implicated and how IR and MCCM synergize in endothelial cells, by using siRNA against, P38alpha, P65, and MK2. Among P38 isoforms P38alpha is becoming a useful target for inflammatory bowel disease treatment, reinforcing the interest to dissect its downstream effectors and interactions in endothelial cells inflammatory gene expression after IR exposure.

(PS4.67) Oxidative stress mediated DNA damage and cell death in proton exposed mouse brain. Sudhakar Baluchamy¹, Ye Zhang², Vani Ramesh¹, Prabakaran Ravichandran¹, Joseph C. Hall¹, Olufisayo Jejelowo³, Daila Gridley⁴, Honglu Wu², Govindarajan T. Ramesh¹, ¹Norfolk State University, Norfolk, VA, ²NASA JSC, Houston, TX, ³Texas Southern University, Houston, TX, ⁴Loma Linda University, Loma Linda, CA

Exposure of living systems to radiation results in a wide assortment of lesions, the most significant of is damage to genomic DNA which alter cellular functions including cell proliferation. Although several radiation related research have been studied extensively, the molecular and cellular processes affected by proton exposure remain poorly understood. To directly assess the effect of protons, we exposed mice with different doses of protons (0.01, 1 and 2Gy) and investigated the effects on brain which controls the key functions such as physiology, memory and learning. A dose dependent increasing levels of Reactive Oxygen Species (ROS) and Lipid Peroxidase (LPO) and decreasing levels of antioxidants, Superoxide dismutase and Glutathione were detected in proton exposed mouse brain tissues compared with control brain. Oxidative stress induced tissue damage was also observed in these tissues. In addition, our real-time RT-PCR expression profiles showed differential gene expression pattern of DNA damage related genes in 2Gy proton exposed mouse brain tissues as compared to control brain tissues. Furthermore, we also show the significant increasing levels of apoptotic related genes, caspase-3 and 8 activities in 2Gy proton exposed brain, suggesting that in addition to induction of oxidative stress and differential expression of DNA damage genes, the alteration of apoptosis related genes may also contribute to the radiation induced DNA damage followed by programmed cell death. In summary, our findings suggest that proton exposed cells undergo severe DNA damage which in turn destabilize the chromatin stability.

(PS4.68) Comparison of acute photon and proton effects on lung profibrosis and tissue remodeling-related genes and protein expressions with low-dose photon pre-irradiation. Jian Tiian¹, Sisi Tian², James M. Slater¹, Daila S. Gridley¹, ¹Loma Linda University & Medical Center, Loma Linda, CA, ²Loma Linda University School of Medicine, Loma Linda, CA

Purpose: To compare expression of factors associated with profibrotic and tissue remodeling in mouse lung after whole-body exposure to photons or protons and evaluate modulating effects of pre-irradiation with low-dose/low-dose-rate photons (LDR). **Materials and Methods:** LDR radiation was delivered to C57BL/6 mice (0.01 Gy total, 0.03 cGy/min, ⁵⁷Co); additional groups received 2 Gy photons (0.8 Gy/min) or protons (0.9 Gy/min), alone or immediately after LDR. Eighty-four relevant genes were assessed utilizing RT-PCR, and expression and distribution of 14 tissue remodeling-related proteins were compared using immunohistochemistry on days 21 and 56 post-irradiation in lung tissue. Expression of genes with ≥ 2 fold difference and $p < 0.05$ compared to 0 Gy are presented. **Results:** More genes were modulated by all radiation regimens on day 56 than on day 21 as compared with the 0Gy group (4-6 vs. 1-2). Four members of MMP family with over 2-fold change were down-regulated by radiation; while their common inhibitor, timp3 was up-regulated by photons and LDR + photons on day 56 and by protons on both time points. All radiation regimens recruited inflammatory cells. When compared with 0 Gy, immunostaining revealed that TGF- β 1 and laminin intensity was enhanced on day 21, but remained unchanged on day 56 post-irradiation. Immunostaining intensity for CTGF was enhanced by photons, and LDR + protons while reduced by LDR + photons on both time points. The immunoreactivity for NCAM was slightly increased by radiation regimens but not by LDR + protons on day 56. Among 4 measured MMPs, MMP2, 7, 9 and 10, MMP 9 was affected least markedly by radiations. TIMP3 was significantly elevated by photons, protons, and LDR + photons on day 56 post-irradiation. In contrast, TIMP3 was slightly reduced by LDR + protons on both time points. Adamts13 activity was slightly attenuated by protons and LDR + protons. No difference in expression of α -smooth muscle actin and S100A4 was found in irradiation groups. **Conclusion:** The data show that profibrosis and tissue modeling-related gene expression profiles in lung were dependent on the form of radiation. The levels of gene transcription

were not entirely consistent with those of post-transcription. Priming with LDR prior to acute photons or protons exposure had some modifying effects on some measured parameters.

(PS4.69) Low dose ionizing radiation and HZE particle effects on adult hippocampal mRNA expression. M. Kerry O'Banion, Stephen L. Welle, Sean D. Hurley, John A. Olschowka, Jacqueline Williams, University of Rochester Medical Center, Rochester, NY

Adult hippocampal neurogenesis is postulated to play an important role in learning and memory. To explore low dose radiation effects on the neurogenic microenvironment, male C57BL/6J mice at 8-10 weeks of age were subjected to single-dose whole body radiation at BNL. Microdissected dentate gyrus RNA samples, representing 0, 3.06, 36.1 and 137 cGy gamma or 0, 3, 30, and 100 cGy HZE at each of 3 time points (8 h, 48 h, 30 d) and 6 mice per group (144 samples total) were submitted for microarray analysis using Illumina MouseRef-8 arrays (Asuragen). High-quality expression profiles were obtained from 141 samples. Data were analyzed with Partek software, including quantile normalization, principal components analysis, hierarchical clustering, ANOVA, and t-tests. There were 16,445 probes with signals above background noise in at least one condition. For 2,406 of these there was a "significant" (nominal $P < 0.01$, i.e. P not corrected for multiple comparisons) radiation type x dose x time interaction. A simpler set of ANOVAs (dose effects within each radiation type and time point condition) yielded the following numbers of differentially expressed genes at nominal $P < 0.01$: 1,187 for HZE at 8 h; 3,814 for HZE at 48 h; 1,824 for HZE at 30 d; 1,607 for gamma at 8 h; 2,265 for gamma at 48 h; 1,614 for gamma at 30 d. Even at the lowest dose of radiation (3 cGy) there were many differentially expressed genes: 93 for HZE at 8 h; 864 for HZE at 48 h; 947 for HZE at 30 d; 154 for gamma at 8 h; 200 for gamma at 48 h; 294 for gamma at 30 d. The majority of the largest effects (> 1.5 -fold) at 8 h were increased expression whereas most of the larger changes were decreased expression at 48 h. Preliminary analysis of functional relationships between differentially expressed genes reveals that many biological processes are affected by radiation, but that the lists are quite different for the various dose, time, and radiation conditions. Supported by Low Dose Radiation Research Program, NASA/DOE #DE-FG02-07ER64338.

(PS4.70) Synthetic peptides derived from cytokines mitigate BMC damages after radiation exposure. Alexandra Litvinchuk, Mei Zhang, Steven B. Zhang, Shanmin Yang, Liangjie Yin, Kunzhong Zhang, Yansong Guo, Vidyasagar Sadasivan, Steven Stwarts, Paul Okunieff, Lurong Zhang, UF Shands Cancer Center, Gainesville, FL

The stimulation of proliferation and differentiation of residual hematopoietic stem and progenitor cells (HSPC) is a major goal for medical treatment of acute radiation syndrome following exposures to ionizing radiation. Several cytokines play major roles in the repopulation of HSPC, from which several peptides derived from the receptor binding domains were synthesized. These small peptides were designed to: 1) possess little or no immunogenicity and no side toxicity; 2) high stable compared to parental intact proteins; and 3) linear structure to allow synthesis in large quality with very low cost. This study was to determine the bioactivity of the synthetic peptides on the irradiated HSPC. BALB/c mice were irradiated at 5Gy and at different time points (6hrs and 1, 2, 4,10, 21, 30 days after radiation, the BMC were flushed out from the two femur bones and cultured in UltraDoma media without serum. The cytokine peptides were added at a final concentration of 200 ng/ml as growth stimulators. The extent of BM proliferation was quantitatively measured using 3H-Thymidine incorporation during the 72 hour culture of HSPC. **Results:** in BALB/c the peptides had different capacities to stimulate the proliferation of HSPC: FGF-P (20-80%), TPO-P (20-80%), IL11-P (10-60%), IL3-P113 (10-60%), IL6-P196 (30%), IL11-P1 (60%), G-CSF-P147 (30%). In C57BL/6, the FGF-P and TPO-P stimulated the proliferation of HSPC up to 50-70% when the BM were harvested at 6 and 9 hours after mice were irradiated with 1 to 12 Gy. IL11-P seemed to have best effect for

HSPC exposed to 8-12Gy. The Annexin V/PI staining with flow cytometry analysis indicated that TPO-P and G-CSF-P147 reduced apoptosis. The data suggest that the synthetic cytokine peptides, using the receptor binding domain, have bioactivity and might be used as an alternative for cytokine treatment to rescue life after lethal dose irradiation.

(PS4.71) Cranial irradiation alters the expression of the behaviorally-induced immediate early gene Arc in the hippocampus. Susanna Rosi, Karim Belarbi, John R. Fike, University of California San Francisco, San Francisco, CA

Therapeutic irradiation of the brain is commonly used to treat brain tumors but can induce cognitive impairments that can severely affect quality of life. The underlying mechanisms responsible for radiation-induced cognitive deficits are unknown but likely involve alterations in synaptic plasticity. To gain some mechanistic insight into how irradiation may affect hippocampal neuronal networks known to be associated with learning and memory, we quantitatively assessed the molecular distribution of immediate early gene (IEG) Arc (activity-regulated cytoskeleton-associated protein) at the level of the mRNA and the protein in the hippocampal dentate gyrus, CA1 and CA3. Young adult C57BL/6J mice received whole brain irradiation with 0 or 10 Gy, two months after irradiation all animals were tested for the Morris water maze (Mwm). Two days after the Mwm training, the animals were allowed to explore for 5 min twice either the same or a different environment and euthanized immediately after the last exploration. The two explorations were separated by 25 min interval. The fractions of neurons expressing Arc mRNA and Arc protein were detected using fluorescence in situ hybridization (FISH) and immunocytochemistry, respectively. Our results showed that after brain irradiation there was a significant reduction in the percentage of neurons expressing both Arc mRNA and Arc protein in the dentate gyrus without neuronal cell loss. These changes were associated with a significant impairment for the Mwm task and with an increase in the number of activated microglia, supporting the idea that inflammation may contribute to neuronal dysfunction. We further investigated whether brain irradiation affected the accuracy of information processing in the CA1 and CA3 hippocampal regions using the immediate early gene-based brain imaging method called cellular analysis of temporal activity by fluorescence in situ hybridization (catFISH). With catFISH it is possible to detect primary transcripts at the genomic alleles, and to monitor the activity history of neurons after two given learning experiences separated by 30 minutes. catFISH provides exceptional temporal and cellular resolution and facilitate mapping of neuronal activity. Transcription and translation of Arc in the hippocampal CA areas is currently under analysis.

(PS4.72) Non invasive imaging of tissue oxygenation: a multivariate in vivo hemodynamic model (MiHMO2). Ning Cao¹, Ling Chen^{1,2}, Keith M. Stantz^{1,3}, ¹Purdue University, West Lafayette, IN, ²Jiao Tong University, Shanghai, China, ³Indiana University School of Medicine, Indianapolis, IN

Purpose: The objective is to develop a multivariate in vivo hemodynamic model of tissue oxygenation (MiHMO2) based on 3D photoacoustic spectroscopy and dynamic contrast enhanced CT measurements. Introduction: Low oxygen levels, or hypoxia, deprives cancer cells of oxygen and confers resistance to irradiation, some chemotherapeutic drugs, and oxygen-dependent therapies leading to treatment failure and poor disease-free and overall survival. Recent studies suggest that the type of hypoxia (acute, chronic, anemic) exposure to cancer cells influences their repair mechanisms and metastatic progression. Therefore, a non invasive method capable of monitoring local variations in tumor hypoxia due to the effects of perfusion diffusion, or anemia is devised. Photoacoustic CT spectroscopy (PCT-S) and dynamic contrast enhanced CT (DCE-CT) imaging measure the hemoglobin status (concentration and SaO₂) and vascular physiology (perfusion, f_{plasma}, f_{cell}). Fusion of these parameters as prescribed by a mathematical model provides a measure of tissue oxygen concentration and the physiological factors delineating the type of

hypoxia (MiHMO2). Material and Methods: Simulations of MiHMO2 model based on measured data and their effects on pO₂ and hypoxic fraction (HF) are performed. Next, breast and pancreatic xenograft tumors are non invasively imaged using PCT-S and DCE-CT to determine tumor hemodynamics, invasively imaged using bioluminescence lifetime imaging to determine dissolved oxygen (DO), and immunofluorescence imaged using immunofluorescence of pimonidazole stained tissue sections. Results. Presented will be simulated plots where pO₂ and HF are determined based on tumor perfusion (0.05-1.0 mL/min/g), average vascular diameter (7.5-30microm) blood volume, hemoglobin concentration (0.5-9g/dL) and SaO₂ (0-1.0) values. Preliminary results comparing intra-tumor variations in (normalized) DO measurements and hemodynamics demonstrate a spatial correlation between DO, SaO₂, and perfusion in many but not all instances, demonstrating a heterogeneous effect. These results in combination with pimonidazole IHC will be tested against MiHMO2 calculations. Conclusions: PCT-S provides a unique ability to monitor spatial and temporal changes in tumor hemodynamics and hypoxia

(PS4.73) Maintenance of type III TGF-β receptor by IM-1662 attenuates radiation-induced lung fibrotic process. Jie-Young Song, Ji-Yeon Ahn, Sarah Park, Mi-Hyoung Kim, Min-Jin Lim, Saeoom Lee, Yeon-Sook Yun, Korea Institute of Radiological and Medical Sciences, Seoul, Republic of Korea

Although pulmonary fibrosis occurs 5-20% of lung cancer patients who underwent radiotherapy, clinically standard treatment for fibrotic disease has not been developed yet. TGF-β is considered a critical mediator in normal wound healing as well as pathological fibrogenic processes. TGF-β transmits signals either directly or indirectly through types I, II and III (TβRI, II, and III) receptor complexes. The type III TGF-β (TβRIII or betaglycan) is a transmembrane proteoglycan without a functional kinase domain, and is regarded as a coreceptor to increase the affinity of ligand binding to TβRII. In contrast to a great number of studies about TGF-β ligand and TβRII signaling, the relationship between TGF-β and TβRIII (or betaglycan) remained largely unknown. In this study, considerable amount of TGF-β was generated by radiation that led to markedly increased expression of α-SMA, fibronectin and Procollagen Type I protein in human lung fibroblast. Phosphorylation of Smad 2 and 3 was increased by radiation. The expression level of TβRI and TβRII was also increased by radiation, suggesting that radiation-induced fibroblast differentiation is due to the activation of TGF-β dependent signaling. To search for novel compounds to inhibit TGF-β responses, we performed cell-based chemical screening and found a pyrazolopyrimidine compound IM-1662. IM-1662 significantly blocked TGF-β or radiation-induced fibroblast differentiation through the inhibition of TβRs and Smads. Interestingly, IM-1918 increased TβRIII expression which was downregulated by TGF-β treatment or radiation. These results suggest that TβRIII may act as a negative regulator of TGF-β signaling and provide a promising molecular target for pulmonary fibrotic disease.

(PS4.74) Manganese superoxide dismutase is not radioprotective in bovine pulmonary artery endothelial cells at systemic oxygen levels. Linda Pearce, Jim Peterson, Molly Stitt, Rachel Ungerman, University of Pittsburgh, Pittsburgh, PA

Bovine pulmonary artery endothelial cells (BPAEC) are extremely sensitive to oxygen, mediated by superoxide production. Ionizing radiation is known to generate superoxide in oxygenated aqueous media and yet, in this cell type, at systemic oxygen levels (3%), no oxygen enhancement is observed after irradiation. A number of markers (cell growth, alamarBlue, mitochondrial membrane polarization) for metabolic activity indicate that BPAEC under 20% oxygen grow and metabolize more slowly than cells maintained under 3% oxygen. BPAEC cultured in 20% oxygen grow better when they are transiently transfected with either manganese superoxide dismutase (MnSOD) or copper zinc superoxide dismutase (CuZnSOD) and exhibit improved survival following irradiation (0.5 - 10 Gy). Furthermore, x-ray irradiation of

BPAEC grown in 20% oxygen results in very diffuse colony formation, which is completely ameliorated by either growth in 3% oxygen or over-expression of MnSOD. However, MnSOD over-expression in BPAEC grown in 3% oxygen provides no further radioprotection, as judged by clonogenic survival curves. Irradiation does not increase apoptosis in BPAEC but induces cell-cycle arrest along with up-regulation of p53 and p21 at either 3% or 20% oxygen.

(PS4.75) *In vivo* global transcriptional response to hypoxia in human tumor xenografts. Akiko Minami, Fuqui He, C. Clifton Ling, Gloria C. Li, Memorial Sloan-Kettering Cancer Center, New York, NY

We have generated a human tumor (colorectal carcinoma) xenograft model (HT29-HRE) in which the dual reporter fusion gene (HSV1-TK and eGFP) was under the control of hypoxia-inducible promoter (HRE). One very promising aspect of this model is the ability to separate tumor cells of different hypoxia status, and then to examine their respective characteristics. We have previously demonstrated this in proof of concept by showing that the chronically hypoxic cells (eGFP^{high}) were much more radioresistant than aerobic cells (eGFP^{low}). In this study, we exploit this ability of the HRE model to investigate hypoxia-induced global transcriptional response *in vivo*. HRE tumors were grown subcutaneously in the limbs of 6-8 wk-old female nude mice. Tumors of ~ 10 mm diameter were excised, from which single cell suspensions were prepared and sorted by FACS based on the level of hypoxia-induced eGFP expression. The global transcriptional response to hypoxia of the sorted populations was then analyzed by DNA microarray analysis. In a pilot experiment with six individual tumors, cells were sorted into populations with eGFP^{high}, eGFP^{medium} and eGFP^{low} expression levels. DNA microarray analysis revealed clear differences in gene expression between the three groups, based on the hierarchical clustering of ~ 2200 genes ($p < 0.05$). Additional experiments and data analysis are in progress. Subsequently, we shall compare our results with the published hypoxia gene "signature" derived from the systematic analysis of *in vitro* primary epithelial cells by Chi et al. The above discussion pertains to eGFP-based FACS sorting of cells from air-breathing mice (tumors are surgically removed from live but anesthetized mice). We have also performed experiments in which the tumors were excised 30 min after animal sacrifice. In this case the eGFP^{low} cells would be acutely hypoxic cells, vis-à-vis chronically hypoxic cells with high eGFP level. Preliminary DNA microarray analysis showed that the global transcriptional responses to acute and chronic hypoxia are very different. Thus, our approach has the potential to derive hypoxia-induced gene expression signature(s) for both acute and chronic hypoxic cells. DNA microarray analysis was performed by the Genomic Core and bio-statistical support was provided by the Biostatistics Department at MSKCC.

(PS4.76) Differential expression of TNF receptor associated factors 1 and 3 (Traf-1 and Traf-3) as a possible mechanism for radioprotection by gamma-tocotrienol (GT3) in vivo. K. Sree Kumar¹, Sanchita P. Ghosh¹, Shilpa Kulkarni¹, Martin Hauer-Jensen², ¹AFRR, Bethesda, MD, ²UAMS, Little Rock, AR

GT3 is a naturally occurring tocol, which protects mice from radiation lethality not only due to its antioxidant activity but also due to the inhibition of hydroxymethyl glutaryl coenzyme A reductase (anti-inflammatory effects), and protection of hematopoietic stem cells (Ghosh et al., IJRB 85: 598-606, 2009; Berbee et al., Rad Res 171: 596-695, 2009; Kulkarni et al., Rad Res 173: in press, 2010). Since these studies also reported a Dose Reduction Factor of 1.29, which may indicate gastrointestinal protection, we studied the molecular aspects of apoptosis in jejunal sections. Mice were given 200 mg/kg of GT3 subcutaneously and irradiated (11 Gy @ 0.6 Gy/min) 20-24 hrs later. Jejunal sections were processed at 4 h and 24 h after irradiation using RT² profiler mouse apoptosis PCR Array System used to evaluate 84 key genes involved in apoptosis (SA Biosciences). Out of these, 9 genes were found to undergo significant differential expression. From these 9 genes, the

expression of Traf1 and Traf3 appears to be paradoxical. There was a 3.5-fold down regulation of Traf1 with vehicle and the same degree of up-regulation of Traf3, 24 hr after radiation. In contrast, GT3-treated mice showed down-regulation of Traf1 as well as Traf3 at the same time point. Heterodimers of Traf1 and Traf2 are known to interact with inhibitor-of-apoptosis proteins (IAPs) resulting in the inhibition of TNF receptor-mediated apoptosis. Down-regulation of Traf1 in the vehicle group may indicate enhanced apoptosis. Attenuation of the down-regulation by GT3 suggests reduction in TNF-induced apoptosis. The up-regulation of Traf3 by vehicle and down-regulation by GT3 at the same time point was intriguing. Traf3 and another member of the TNF family, CD40, participate in the activation of the immune responses. Traf3 down-regulation may be associated with the amelioration of radiation-induced immune response by GT3 as observed in the hematopoietic studies. Further studies are in progress to assess the mechanisms of radiation protection by GT3 as it relates to the association of Traf1 and Traf3 with IAPs and CD40 respectively. Supported by the U.S. Department of Defense Threat Reduction Agency grants H.10027_07_AR_R and H.10045_07_AR_R (KSK), and HDTRA 1-07-C- 0028 (MH-J).

(PS4.77) Survival response of normal cells vs cancer cells after "acute" and "chronic" lactate exposure. Kelly M. Kennedy, Thies Schroeder, Jonathan Dewey, Mark W. Dewhirst, Duke University, Durham, NC

Compared to normal tissue, the tumor microenvironment often experiences oxygen and nutrient depletion; dysregulated growth signaling, pH balance and metabolism; and pathophysiologic lactate levels (>4mM). Increased glycolysis via either the Pasteur (anaerobic) or Warburg Effect (aerobic) leads to lactate accumulation within tumors. Clinical studies in a many human solid tumors have found that high levels of lactate correspond to increased metastases, and poor disease-free, metastasis-free and overall survival for patients. Lactate affects redox status and can be taken up by cells for energetic purposes. It may also act as a signaling molecule, with involvement in specific cellular survival pathways. We tested twenty-five patient samples of locally advanced breast cancer (LABC) for lactate concentration using bioluminescence staining and imaging of frozen sections. When lactate concentrations were averaged over the entire area of the sample, we found that about 70% of samples tested showed lactate levels >4mM (high=7.16, low=0.42, median=4.7). Of these samples, 70% showed ≥75% invasive cancer. Cellular responses to lactate in normal vs. cancer human cell lines was performed using 3 cancer cell lines (two breast, one liver) and 2 normal cell lines (one breast, one liver). We assessed clonogenicity and gathered cell cycle information after cells were exposed to a range of lactate concentrations (+/-5mM glucose). All cell lines tested thus far show a downward trend of clonogenicity with lactate concentrations ≥20mM at all time points: 18hrs, 48hrs, and 1 week. However, in lactate concentration ranges from 0-20mM, cell lines show different clonogenic survival patterns dependent upon concentration, exposure duration and presence of glucose. Flow cytometry data indicates lactate may induce a G2/M block in cancer cells while increasing subG1 fraction in normal cells; however this is cell line dependent. Ongoing research suggests that survival signaling may occur through SIRT1, an NAD⁺-dependent histone deacetylase, in response to "acute" versus "chronic" lactate exposure. Results of these studies will also be presented.

(PS4.78) Radiomitigative signaling by lysophospholipid receptors. Gabor Tigyi¹, Gyongyi N. Kiss¹, Shuyu E¹, James Fells¹, Jianxiang Liu¹, Junming Yue¹, Abby L. Parrill², Karin Emmons-Thompson¹, Ryan Yates¹, Yun-Ju Lai³, Fang-Tsyr Lin³, ¹University of Tennessee Health Science Center Memphis, Memphis, TN, ²Department of Chemistry, The University of Memphis, Memphis, TN, ³University of Alabama School of Medicine, Birmingham, AL

Lysophosphatidic acid (LPA) and sphingosine-1-phosphate are growth factor-like lysophospholipids that protect and rescue apoptotically condemned cells. We have shown that LPA protects

IEC-6 embryonic crypt-like intestinal epithelial cells from gamma-radiation-induced cell death. LPA and its analogs also protect intestinal crypts from radiation-induced apoptosis and promote crypt regeneration *in vivo*. Using LPA receptor knockout mice and cell lines derived from knockout animals, we established that the LPA₂ receptor subtype plays an essential role in the antiapoptotic mechanism elicited by LPA and its analogs. Through its C-terminal PDZ and LIM-binding motifs the LPA₂ receptor forms agonist-dependent macromolecular signaling complexes. LPA₂ interacts with the proapoptotic protein Siva-1 and targets it for proteasomal degradation, which in turn arrests DNA-damage-activated apoptosis. Full activation of the NFκB and ERK1/2 prosurvival pathways requires formation of the LPA₂ receptor, NHERF2, and TRIP-6 ternary macromolecular complex. These signals inhibit the intrinsic mitochondrial apoptosis pathway as evidenced by reduced caspase 3/7/9 activation and DNA fragmentation. Furthermore, transfection of the LPA₂ receptor into mouse embryonic fibroblasts (MEFs) derived from LPA₁ and LPA₂ receptor double knockout (DKO) mice restores LPA-dependent radioprotection. Conditioned medium from 7 - 35 Gy gamma-irradiated U937 cells induces bystander apoptosis in non-irradiated IEC-6 cultures. Using a validated computational model of the LPA₂ receptor we developed a pharmacophore model and used it for *in silico* drug discovery of non-lipid LPA2 agonists. We found a novel LPA2 agonist GRI977143 which activates ERK1/2 and elicits an antiapoptotic effect in LPA₂-transfected DKO MEFs irradiated by 15 Gy and also protects IEC-6 cells from bystander apoptosis. Supported by AI 80405.

(PS4.79) Protection of super p53 mice from the radiation-induced gastrointestinal syndrome occurs through a p21-dependent mechanism. Julie M. Sullivan¹, Laura B. Jeffords¹, Rafaela Rodrigues¹, Yan Ma¹, David G. Kirsch^{1,2}. ¹Department of Radiation Oncology, Duke University Medical Center, Durham, NC, ²Department of Pharmacology and Cancer Biology, Duke University Medical Center, Durham, NC

Currently, no therapy exists to mitigate against the gastrointestinal (GI) syndrome. Identifying the mechanism behind the radiation-induced GI syndrome therefore remains an important area of investigation. The p53 signaling pathway has been implicated as an important player in the response to cellular damage that occurs after radiation exposure. The p53 protein is required for radiation-induced apoptosis and mediates cell cycle progression through p21, a cdk inhibitor. Mice deficient in p53 or p21 have been shown to be sensitized to the GI syndrome compared to wild type mice. Super p53 mice containing two additional copies of the wild-type p53 gene, (4 copies total), exhibit an enhanced DNA damage response, and have been shown to be protected from the radiation-induced GI syndrome. Here we test the hypothesis that Super p53 mice are protected from the GI syndrome through a p21-dependent mechanism. Transgenic Super p53 mice (Super p53; p21 +/+), Super p53 mice deficient in the p21 gene (Super p53; p21 -/-), p53 wild-type (p53 WT; p21 +/+) and p53 wild-type mice deficient in p21 (p53 WT; p21 -/-) were used to test this hypothesis. All mice and their littermate controls were irradiated with sub-total body irradiation at a dose that resulted in 50% reduction in survival between experimental groups. Immunohistochemistry of small intestinal tissue for phospho-histone H3 after radiation exposure showed that Super p53 mice exhibit a delayed entry into mitosis when compared to wild-type controls, consistent with a p53-mediated, p21-dependent cell-cycle arrest. Super p53; p21 -/- mice were sensitized to the GI syndrome after sub-total body irradiation when compared to Super p53; p21 +/- control mice. Additionally, no survival advantage was seen in Super p53; p21 -/- mice when compared to p53 WT; p21 -/- littermate controls. These results indicate that extra copies of p53 are unable to protect mice from the radiation-induced GI syndrome in the absence of p21, and are consistent with a model where a p21-dependent mechanism regulates the GI syndrome.

(PS4.80) Control of glycolytic flux by AMPK and p53-mediated signaling pathways in tumor cells grown at low pH. Dennis B. Leeper¹, Erin E. Mendoza², Jaime Caro¹, Randy M. Burd², ¹Thomas Jefferson University, Philadelphia, PA, ²University of Arizona, Tucson, AZ

Tumor cells in nutrient deprived microenvironments adapt by altering metabolic pathways. This adaptation process characteristically results in a tumor phenotype that displays upregulated Hif-1α, anaerobic glycolysis, chronic acidification, reduced rate of overall protein synthesis and aggressive invasive characteristics. We show that the critical glucose regulatory molecule, 6-Phosphofructo-2-Kinase/Fructose-2,6-Biphosphatase Isoform-3 (PFKFB3), a bifunctional enzyme central to glycolytic flux and downstream of the metabolic stress sensor AMP-activated protein kinase (AMPK), activates an isoform of phosphofructokinase, PFK-2, and drives lactate production. All methods including the growth of DB-1 human melanoma and U87 human glioma cells were standard and published. Results demonstrated that growth in air at pH 6.7 induced AMPK activation resulting in the upregulation of PFKFB3 and p53, and the downregulation of mammalian Target-Of-Rapamycin (mTOR) in both tumor cell lines. Conversely, inhibition of AMPK resulted in downregulation of PFKFB3 and inhibition of glycolysis. When PFKFB3 was over-expressed in DB-1 melanoma cells growing at pH 7.3 in air, it induced a high rate of glycolysis and reduced oxygen consumption. By contrast, cells growing at low pH did not display an increased rate of glycolysis after PFKFB3 expression because the level of the TP53-induced Glycolysis and Apoptosis Regulator (TIGAR) was increased. Cells growing at low pH also were resistant to radiation-induced apoptosis despite upregulation of p53. This could be partially explained by the expression of the anti-apoptotic proteins, Bcl-2 and Bax; TIGAR's ability to reduce lactate production; and downregulation of mTOR. Growth at low pH also blocked GSH production and reduced bioreduction. We conclude that growth at tumor-like low pH activates AMPK and PFKFB3 and induces a high glycolytic and apoptotic potential that is countered by TIGAR and anti-apoptotic proteins, respectively. Alterations of these pathways lead to predictable alterations in lactate and oxygen levels, mTOR, GSH and redox state, and response to radiation. These microenvironmental sensitive metabolic pathways are essential to understanding radiation treatment strategies. (Supported in part by NIH P01 CA36690 and K22 DE16096.)

(PS4.81) Genetically determined differential modulation of a mitotic cancer network after low doses of ionizing radiation in the mammary gland and its association with human breast cancer. Antoine M. Snijders, Francesco Marchetti, Sandhya Bhatnagar, Jian-Hua Mao, Joe W. Gray, Priscilla K. Cooper, Andrew J. Wyrobek, Lawrence Berkeley National Laboratory, Berkeley, CA

Our goal is to better understand the signaling pathways and mechanisms that control radiation induced breast cancer, the second leading cause of cancer death among U.S. women. Treatment usually includes exposing the tumor to high levels of ionizing radiation. However, this always involves irradiation of adjacent normal tissue with non-therapeutic low doses of radiation potentially increasing the risk of a second primary tumor. A mitotic gene network overexpressed in breast cancer and strongly associated with aggressive breast cancer was recently identified (Mao et al). SOX9 and to a lesser extent MYC were found to be master regulators of this network. Using a mouse model, we investigated whether low doses of radiation induce this mitotic cancer network and how the radioresponse varies with genetic background. We took advantage of the variation in sensitivity to radiation induced mammary gland (MG) cancer in two genetically defined inbred strains of mice (BALB/c: sensitive; C57BL/6: resistant). We investigated the *in vivo* low dose tissue response in the MG of female BALB/c and C57BL/6 mice by studying gene expression responses after repeat fractionated low-dose exposures (4 weekly doses of 7.5 cGy). Four weeks after the last exposure we processed the MG for global gene expression analysis. In the MG of both BALB/c and C57BL/6 mice, we observed a highly significant mitotic network. Genes in the BALB/c mitotic network were mostly upregulated whereas genes in the C57BL/6 mitotic network were mostly downregulated. A significant overlap was observed for both murine mitotic networks and the mitotic network previously associated with human breast cancer. We also found that Myc was upregulated in low dose exposed BALB/c MG and Sox9 downregulated in C57BL/6. Moreover, we observed upregulation of Serpine1 and inappropriate expression of epidermal differentiation

markers in MG of C57BL/6 mice. Serpine1 has been identified as a critical downstream target of p53 in the induction of replicative senescence. Our data suggests that non-therapeutic low dose radiation to normal breast tissue, such as those received during radiotherapy, can lead to persistent changes in mitosis-related pathways linked with human breast cancer and that differential responses of these pathways may provide an approach of identifying susceptible women.

(PS4.82) The Proteasome Activator, PA200, regulates radiation sensitivity through glutamine-glutamate metabolism and amino acid starvation. Jennifer Blickwedhl¹, Scott Olejniczak², Marion Schmidt³, Tej K. Pandita⁴, Craig B. Thompson², Naveen Bangia¹, ¹Roswell Park Cancer Institute, Buffalo, NY, ²University of Pennsylvania, Philadelphia, PA, ³Albert Einstein College of Medicine, Bronx, NY, ⁴University of Texas Southwestern, Dallas, TX

Radiation is a major therapeutic modality for multiple cancers with half of all cancers (i.e. representing 700,000 new cases/year and 265,000 deaths/year) treated with some form of radiation. However dose-limiting toxicity and resistance often results in suboptimal killing of tumor cells, which can lead to relapse of disease. The use of radiation sensitizers can improve tumor cell killing, but identification of suitable targets that modulate radiation sensitivity remains a significant challenge. We previously reported that inhibition of the proteasome activator, PA200, sensitizes tumor cells to ionizing radiation *in vitro*. New data suggests that PA200 is required for recovery of intracellular glutamine, a central metabolic hub for tumor cell survival, growth and proliferation. Although extracellular glutamine is considered essential for tumor cell growth, the impact of glutamine on survival from radiation has not been well studied. Furthermore, the physiological contribution of recovered or re-utilized intracellular glutamine to radiation sensitivity may be greatly underestimated because of the excess extracellular glutamine available in virtually all cell culture growth media. Here we show that ionizing radiation exposure causes intracellular amino acid starvation and a compensatory increase in uptake of extracellular glutamine from the growth media. Together, PA200 depletion AND radiation exposure severely depletes extracellular glutamine from the growth media leading to impaired long-term (clonogenic) survival. Additional extracellular glutamine or glutamate restores the radiation survival defect in PA200 knockdown cells. These observations highlight the importance of intracellular glutamine recovery through PA200 in determining long-term cell survival after damage induced by radiation.

(PS4.83) Analysis of low dose radiation-induced microRNAome changes in an animal model. Jody Filkowski, Olga Kovalchuk, University of Lethbridge, Lethbridge, AB, Canada

Epigenetic alterations, which, by definition, comprise mitotically and meiotically heritable changes in gene expression that are not caused by changes in the primary DNA sequence, are increasingly being recognized for their roles in health and disease. The major areas of epigenetics DNA methylation, histone modifications and small RNA-mediated silencing; are known to have profound effects on controlling gene expression. Yet, the exact nature of the epigenetic changes and their precise roles in radiation responses still need to be delineated. Understanding the radiation-induced epigenetic response to low dose exposures is a critical, but currently missing component, in the development of appropriate prognostic risk biomarkers and countermeasures and is a focus of our studies. We hypothesize that changes in epigenetic profiles (global and regional DNA methylation, chromatin status and regulatory microRNAs) play pivotal roles in radiation responses and radiation-induced genome instability. Here we tested the miR hypothesis by using an established *in vivo* mouse model to assay for microRNAome alterations in the radiation-target organ thymus after exposure to various doses of X-rays including low, mid, high, fractionated and adaptive doses.

(PS5.01) Human lung cancer risk from radon - Part II - Evidence of influence of combined bystander and adaptive response effects on radon case-control studies. Bobby E. Leonard¹, Richard E. Thompson², Georgia C. Beecher¹, ¹International Academy, Severna Park, MD, ²Johns Hopkins School of Public Health, Johns Hopkins Medical Center, Baltimore, MD

Since the publication of the BEIR VI report in 1999 on health risks from radon, a significant amount of new data has been published showing various mechanisms that may affect the ultimate assessment of radon as a carcinogen, in particular the potentially deleterious Bystander Effect (BE) and the potentially beneficial Adaptive Response radio-protection (AR). The case-control radon lung cancer risk data of the pooled 13 European countries radon study and the 8 North American pooled study have been evaluated. The large variation in the odds ratio radon lung cancer risk is reconciled, based on the large variation in geological and ecological conditions and variation in the degree of adaptive response radio-protection against the bystander effect induced lung damage. The analysis clearly shows Bystander Effect radon lung cancer induction and Adaptive Response reduction in lung cancer in some geographical regions. It is estimated that for radon levels up to about 400 Bq m⁻³ there is about a 30% probability that no human lung cancer risk from radon will be experienced and a 20% probability that the risk is below the zero-radon, endogenous spontaneous or perhaps even genetically inheritable lung cancer risk rate. The BEIR and EPA estimates of human lung cancer deaths from radon are most likely significantly excessive. The assumption of linearity of risk, by the Linear No-Threshold Model, with increasing radon exposure is invalid.

(PS5.02) *In vivo* Radiation Effects. Dulaney A. Wilson, William F. Morgan, Anthony C. James, Pacific Northwest National Laboratory, Richland, WA

Quantification of the risk of health effects in humans from exposure to radiation is limited by the observational nature of most studies. Life-span animal studies were designed to supplement the human data and assist in risk assessment. Beginning in the 1940s, various laboratories and universities conducted studies on incorporated radionuclides using beagle dogs. The National Radiobiology Archives, housed at the United States Transuranium and Uranium Registries (USTUR) in Richland, WA has been collecting, organizing, cataloging, and preserving these data and materials (including laboratory notebooks and archival tissue specimens), and making them available for future research or analyses. The data available includes documentation of the type and amount of exposure, dose and dose-rate, pedigree, housing conditions, detailed clinical health information from annual physicals with detailed blood chemistry, and extensive postmortem information. Radionuclides studied include plutonium, cesium, and strontium. Data on life-span studies have been used to estimate the risk of lung fibrosis and lung cancer in dogs after exposure to plutonium; currently, pedigree information is being used to evaluate a familial confounder of the risk of lung fibrosis or lung cancer. These data have also been used to explore lung, liver and bone cancer incidence with multistage modeling techniques. Materials available include tissue preserved in paraffin blocks and pathology slides. Modern methods of molecular biology and biochemistry can use these materials to investigate potential biomarkers of risk and exposure as a function of time after exposure. Immunohistochemistry can be done on samples to compare with *in vitro* studies. These archived materials are useful for identifying primary and secondary targets and providing essential information on the optimal time course of potential mitigation and decorporation strategies. This work was supported by Radiation Biology and Biophysics, U. S. Department of Energy, Pacific Northwest National Laboratory's Laboratory Directed Research and Development Program and funding from a pilot project awarded by the National Institutes of Health, National Institute for Allergy and Infectious Disease grant U19 AI 067770, Centers for Medical Countermeasures against Radiation.

(PS5.03) The dose-rate effect of exposure to ¹³⁷Cs in the beagle dog. Erika J. Peterson, Dulaney A. Wilson, William F. Morgan, Pacific Northwest National Laboratory, Richland, WA

Animal models have been used in radiation research in order to determine effects of radiation on living subjects which can then be used to establish probable effects on humans. Researchers have used animals as models for the human and have extrapolated from the resultant data to humans. Studies done in the 1960s and 1970s used the beagle dog as an animal model for radiation effects. These studies irradiated over 5000 beagle dogs with over 15 different radioactive isotopes at 150 locations worldwide. The focus of this study is to mine the databases and reports for the beagle dog data for those dogs irradiated with the isotope cesium-137 and to analyze it with regard to dose rate effects. Two studies were performed using cesium chloride to irradiate a total of 117 beagle dogs. The exposure to the cesium chloride was acute and spanned a range of initial dose rates of 0.1 Gy/day to 0.82 Gy/day. The studies were conducted at the Inhalation Toxicology Research Institute (ITRI) and at Argonne National Laboratory (ANL). The purpose of this study is to establish dose related effects of ^{137}Cs by determining if a threshold of exposure to the radionuclide exists for any adverse health effect. Survival analyses for all-cause mortality have been conducted and cause-specific survival analyses are in progress. By using current research on ^{137}Cs effects in man and the results that are given from this study, extrapolation of data from the beagle to man may be possible. Acknowledgement: This work was funded in part by a Pilot Project Award from the Fred Hutchinson Research Center CMCR grant U19 AI067770-05.

(PS5.04) Noncancer mortality (1950-1987) with respect to ionizing low-let radiation exposure in the Canadian Fluoroscopy Cohort study. Lydia Zablotzka¹, Geoffrey R. Howe², ¹UCSF, San Francisco, CA, ²Columbia University, New York, NY

Background: Ionizing radiation has been shown to be associated with several noncancer causes of death, particularly cardiovascular disease, in studies of atomic bomb survivors, patients treated with radiotherapy and studies of radiologists and radiological technicians. The associated risks are generally small compared to the cancer risks and can arise from unmeasured confounders and errors in dose estimates. Very low-dose studies, mainly of nuclear industry workers and the Chernobyl clean-up workers, have mixed results and are difficult to interpret. Methods: The Canadian fluoroscopy cohort includes 63,707 tuberculosis patients first admitted to an institution in Canada in 1930-1952. A substantial fraction (39%) was exposed to multiple chest fluoroscopies in association with artificial pneumothorax. Individual lung doses were estimated from the combination of sources and the cohort was linked with the Canadian National Mortality DataBase to ascertain mortality for 18 non-cancer outcomes in 1950-1987. Standardized mortality analysis, Poisson regression and proportional hazards modeling were used to analyze the data. Results: A total of 13,232 non-cancer deaths were observed. The majority of exposed subjects had a dose of under five centigray. The cohort experienced lower mortality from noncancer outcomes than the general population ($p < 0.01$). For all noncancer, the excess relative rate per gray (ERR/Gy) was -0.014 ($p = 0.22$). For cardiovascular disease as a whole, the ERR/Gy was -0.001 ($p = 0.91$). There was no consistent pattern of association between dose of ionizing radiation up to 10 Gy and risk of any of ischemic heart disease except for those first exposed under 10 years of age (ERR/Gy=8.43, $p = 0.13$) and for follow-up 30 years or more after first exposure (ERR/Gy=0.037, $p = 0.29$). Conclusion: The present study provided no meaningful evidence of any positive association between ionizing radiation and increased risk of noncancer mortality from moderately-fractionated ionizing radiation delivered at low to moderate dose-rates. The observation of increased risk for ischemic heart disease 30 years or more after first exposure, could be a chance effect or due to uncontrolled confounding by SES and smoking. Conduct of appropriate studies of radiation exposure and noncancer mortality is warranted.

(PS5.05) The effect of lifestyle factors on urothelial carcinoma radiation risk estimates among atomic bomb survivors. Eric J. Grant¹, Ritsu Sakata¹, Yukiko Shimizu¹, Fumiyo Kasagi¹, Hiromi Sugiyama¹, Midori Soda², Akihiko Suyama², Kotaro

Ozasa¹, ¹Radiation Effects Research Foundation, Hiroshima, Japan, ²Radiation Effects Research Foundation, Nagasaki, Japan

Background Urothelial carcinomas (UC, transitional carcinomas along the lumen of the urinary tract) occur in the bladder, ureter and renal pelvis. Known risk factors for UC include smoking and exposure to ionizing radiation in addition to the primary risk factors of age and male sex. In RERF's major incidence report published in 2007, bladder cancer had the highest sex-averaged excess relative risk (ERR) of any solid organ as well as the second highest female to male ERR ratio. However, these risk estimates were derived while ignoring smoking, dietary intake habits and other lifestyle data. The purpose of this study is to re-estimate the radiation-related risks of UC while accounting for lifestyle habits. Methods Life-Span Study (LSS) cohort members who were alive and cancer free in 1958 were followed for a first primary UC through 2001. Time-varying (including 'unknown') lifestyle data were collected from seven clinical or mailed surveys (1963-1991) and included smoking status, vegetable, fruit and alcohol consumption, and highest attained education. Other adjustment factors included sex, city, age, age in 1945 and distal survivor location. Excess relative risk (ERR) estimates were generated using Poisson regression of grouped survival data. A total of 549 incident cases of UC were observed among 105,406 persons during 2.88 million person-years of follow-up. Results Men were more likely to be 'ever smokers' than women (86% vs. 18%). Lifestyle factors significantly improved the model based on the likelihood ratio test. The lifestyle-adjusted sex-averaged ERR/Gy was 1.13 (95% CI: 0.36, 2.20) and the point estimate of the female-to-male ERR/Gy ratio was 3.31. Without adjustment for lifestyle factors, these values were 1.05 (95% CI: 0.45, 1.87) and 3.67, respectively. The cohort-based population attributable fraction of UC to smoking was estimated to be 46% (167/360) among men and 11% (21/189) among women. Conclusions The primary risk factor for UC is smoking, however adjustments for smoking and other lifestyle factors only modestly changed the radiation risk estimates for UC. This finding is important as many RERF studies do not adjust for lifestyle factors when estimating radiation-related risks. Concerns that lack of adjustments may lead to biased risk estimates, particularly due to smoking, may be unfounded.

(PS5.06) Understanding radiotherapy-induced second cancers. Igor Shuryak¹, Rainer K. Sachs², David J. Brenner¹, ¹Columbia University, New York, NY, ²University of California, Berkeley, CA

Mechanistic mathematical models of radiation carcinogenesis are important for understanding mechanisms and for predicting and interpreting the risks of radiotherapy-induced second cancers. There are two classes of such models: short- and long-term. We suggest that unifying both model types is needed, and present an example of this novel approach. Within this new formalism, we assume that radiation initiates, promotes, or kills pre-malignant cells; a pre-malignant cell generates a clone, which, if it survives, quickly reaches a size limitation; the clone subsequently grows more slowly and can eventually generate a malignant cell; the carcinogenic potential of pre-malignant cells decreases with age. We apply the model to nine solid cancer types (stomach, lung, colon, rectal, pancreatic, bladder, breast, central nervous system, and thyroid) using data on radiotherapy-induced second malignancies, on Japanese atomic bomb survivors, and on background US cancer incidence. The formalism provides an adequate description for all the selected data and can be incorporated into radiotherapy treatment planning algorithms, adding second cancer risk as an optimization criterion.

(PS5.07) Determination of relationship between radiation dose and age at menopause on female atomic bomb survivors. Ritsu Sakata¹, Yukiko Shimizu¹, Wan L. Hsu¹, Mikiko Hayashi¹, Midori Soda², Akihiko Suyama², Kotaro Ozasa¹, ¹Radiation Effects Research Foundation, Hiroshima, Japan, ²Radiation Effects Research Foundation, Nagasaki, Japan

[Purpose] Several reports have been made on premature ovarian failure and amenorrhea after radiation therapy. Early studies of female A-bomb survivors noted that the number of women experiencing menopause immediately after exposure was significantly higher in the proximally exposed group in comparison to the distally exposed group, with the average menopausal age tending to be significantly younger particularly among those suffering from acute radiation syndrome. However, it remains speculative whether the lowered menopausal age was caused by physical injury and mental shock immediately after A-bomb exposure, or a direct effect of radiation. In this study, we examined whether radiation dose was associated with a lowered age of menopause in women experiencing menopause several years after radiation exposure in the Life Span Study (LSS) population of the Radiation Effects Research Foundation (RERF). [Methods] Information on menopause was based on three mail surveys (1969, 1978, and 1991) that were conducted on female subjects of the LSS population by RERF. Women who reached menopause within 5 years after bombing were excluded from analyses in an effort to exclude the potential effects of physical injury and mental shock followed by the A-bomb. Subjects included 21,756 women with estimated radiation doses and that replied to a question about menopausal age in any of the three surveys. Poisson regression analyses were used for examining the relationships between age at menopause and ovarian dose after adjusting for birth cohort, parity, smoking history and age at menarche. [Results] Age at menopause was significantly younger with increased radiation dose for both natural and artificial menopause. The model with the best fit for natural menopause included a threshold dose at 0.39 Gy (95% confidence interval: 0.13-0.61); the model that have threshold dose at 0.2 Gy (95% confidence interval: 0.14-0.38) fit best for artificial menopause. The percentages of post-menopausal women before age 50 based on the estimated model were 38%, 52% and 66% for women who have 0 Gy, 1 Gy, and 2 Gy weighted ovarian doses, respectively.

(PS5.08) Human lung cancer risks from radon - Part I - Influence of bystander and adaptive response effects - A microdose analysis. Bobby E. Leonard¹, Richard E. Thompson², Georgia C. Beecher¹, ¹International Academy, Severna Park, MD, ²Johns Hopkins School of Public Health, Johns Hopkins Medical Center, Baltimore, MD

Since publication of the BEIR VI report in 1999 on health risks from radon, new data has been published showing various mechanisms that may affect the ultimate assessment of radon as a carcinogen, at low domestic radon levels, in particular potentially deleterious Bystander Effect (BE) and potentially beneficial Adaptive Response radio-protection (AR). A composite AR and BE Microdose Model has been developed and applied to published in vitro alpha particle and low LET radiation dose response data (International Journal of Radiation Biology 84:681-701:2008, Dose-Response Journal 6:115-183:2008). In a two part study, we have now conducted an analysis, using this Microdose Model, of what is presently known and what new research is needed to further evaluate human cancer risks from radon. We have analyzed the micro-beam and broad-beam alpha particle data of Zhou, Sawant, Miller, Hei, Nagasawa and Little and others and show that, in terms of alpha particle traversals, the shape of the cellular response to alphas is relatively independent of cell species and LET of the alphas in the range of radon progeny alpha energies. The result is that the same alpha particle traversal dose response behavior should be true for human lung tissue exposure to radon progeny alpha particles. At domestic radon levels, up to about 400 Bq/m³, the lung cell damage is from BE. Thus, extrapolation of underground miners lung cancer risks to human risks at domestic and workplace levels may not be valid. This is due to the non-monotonic, concave behavior for the residential radon level cell damage (Bystander) and linear behavior at the high underground miners radon level cell (Direct) damage from different mechanisms. With respect to AR influence primarily from low LET natural background and man-made human exposures, we find that, at the UNSCEAR worldwide average human exposures from natural background and man-made radiations, the human lung receives about a 25% adaptive response protection against the radon alpha bystander damage. At the UNSCEAR minimum range of background exposure levels, the lung receives minimal AR protection but at higher background

levels, in the high UNSCEAR range, the lung receives essentially 100% protection from both the radon alpha damage and also the spontaneously occurring, potentially carcinogenic, lung cellular damage.

(PS5.09) Increased lung tumorigenesis following low dose CT radiation. Michael Munley, Joseph Moore, John Olson, Scott Isom, Matthew Walb, J. G. Zora, Nancy Kock, Kenneth Wheeler, Mark Miller, Wake Forest U. School Med., Winston Salem, NC

Objective: Determine the carcinogenic potential of CT radiation exposure for individuals at high-risk for lung cancer. Introduction: The carcinogenic effects of CT lung procedures on smokers and ex-smokers are largely unknown. Presently there is a lack of experimental data to assess the carcinogenic potential of irradiation by CT. We present our updated findings using a sensitive rodent model of lung carcinogenesis that has been exposed to fractionated doses of whole-body CT radiation. Methods: We used standard whole-body CT screening protocols and a transgenic mouse model in which the mutant human *Ki-ras* gene was conditionally expressed in a doxycycline (DOX)-regulated, lung-specific manner. This model represents the earliest stages of lung tumorigenesis, where asymptomatic smokers or ex-smokers have smoke-induced genetic damage but have undetectable lesions. These studies involved acquiring radiation response data (≤ 160 mGy total) in mice+/-radiation+/-DOX. All mice in the radiation groups were irradiated once per week for four weeks starting one week after initiation of the DOX treatment using a clinical CT unit. Tumor induction and growth were followed using 7T magnetic resonance imaging (MRI) at 6 and 9 months post-irradiation. At 9 months post-irradiation mice were euthanized by CO₂ asphyxiation/exsanguination, and the number and size of lesions from both MRI data and histological examination were determined. Results: In mice expressing mutant *Ki-ras*, exposure to low dose CT radiation resulted in a significant increase in tumor incidence (24.1 ± 1.9 irradiated vs. 16.8 ± 1.3 unirradiated; $p=0.01$). A detectable dose response relationship was not found. Female mice had a significantly higher tumor incidence than male mice (25.8 ± 2.2 vs. 18.3 ± 1.7 ; $p<0.005$). In contrast, control mice (DOX naive mice) had tumor incidences of only 1 in 12, 0 in 13, 1 in 11, and 3 in 14 for the 0, 5, 15 and 25 mGy per fraction radiation groups, respectively. [Supported by NIH grant R01-CA136910 and a Partner Grant from the Comprehensive Cancer Center of Wake Forest University.]

(PS5.10) Localization of lens opacity and model fitting analysis by UV substitution in cataract of A-bomb survivors. Kazuo Neriishi¹, Eiji Nakashima¹, Atsushi Minamoto², ¹Radiation effects Research Foundation, Hiroshima, Japan, ²Minamoto Eye Clinic, Hiroshima, Japan

For evaluation of radiation-induced ocular lens damage, accurate assessment of risk factor characteristics is extremely important. Since a significant city difference was found to exist between Hiroshima and Nagasaki in terms of cataract prevalence in the previous study, we analyzed the localization of lens opacities and fit a model incorporating the variable impact of UV on the eye, assuming that the city difference in cataract prevalence was due to a difference in UV radiation between the two cities. The results suggest that cataracts among Nagasaki residents were more frequently located at the inferior nasal portion of the lens than among Hiroshima residents, with no radiation-specific localization observed. Based on incidence angles, UV was suggested as a possible cause of the city difference. We therefore analyzed the fit of the model by modeling city differences in terms of levels of UVA and UVB irradiation. The UVB model, compared with the UVA model, provided a better fit. The evidence suggests that UVB may be the cause of the city difference. The current study suggests that the location of residence and investigation period, as well as outdoor activities, are important as surrogate factors for UVB in evaluation of radiation-induced cataract, and that the superior temporal portion of the lens may be suitable for the evaluation of ionizing radiation effects because of the minor amount of interference at that site.

(PS5.11) Genome-wide profiling of histone acetylation in breast-cancer cells in response to histone deacetylase inhibitors. John H. Miller¹, Seema Verma¹, Julie Stanton², John Wyrick², Rajiv Prasad³, David Springer³, ¹Washington State University Tri-Cities, Richland, WA, ²Washington State University, Pullman, WA, ³Pacific Northwest National Laboratory, Richland, WA

Acetylation of lysine residues in core histones is a well characterized reversible posttranslational modification of chromatin that affects gene expression. Recent studies have suggested that histone deacetylase (HDAC) inhibitors de-repress genes involved in cell differentiation, growth arrest, and apoptosis of cancer cells and, because of these features, HDAC inhibitors are currently being used as anti-cancer agents. HDAC inhibitors have also been shown to enhance DNA repair. To gain more direct evidence of histone modification in the activities of HDAC inhibitors, genome-wide histone H3 acetylation patterns were measured in estrogen receptor positive MCF-7 breast cancer cells treated with 1 mM valproic acid (VPA) or 300 nM trichostatin-A (TSA) for 12 hours. ChIP-chip analysis was performed using affymetrix human promoter tiling arrays to identify genomic regions associated with acetylation of histone H3 at Lys 9 and Lys 14. Raw data was analyzed using the MAT algorithm and the affymetrix probes were mapped on the human assembly 18 to identify ChIP enriched peaks. Untreated control cells exhibited 1739 chromosome regions of significant antibody binding compared to 16,298 and 5822 significantly acetylated chromosome regions of VPA and TSA treated cells, respectively. These results clearly show that the HDAC-inhibitor properties of VPA and TSA led to extensive H3 acetylation in MCF-7 cells under our exposure conditions. MAT scores were used to compare treated and control cells at common acetylated regions. Analysis of hyperacetylated ChIP regions among significantly acetylated regions common to treated and control cells revealed 65 and 42 genes whose expression is likely to be up-regulated by VPA and TSA, respectively, due to chromatin remodeling. The MetaCore software was used to identify pathways significantly enriched in these genes. The top-ranked network included genes with functions in DNA replication, recombination and repair as well as regulation of cell-cycle, apoptosis and differentiation. These preliminary results suggest that HDAC inhibitors VPA and TSA up-regulate transcriptional targets of p53 that regulate DNA damage response, apoptosis, and cell differentiation.

(PS5.12) Separating toxic and leukemogenic functions of clastogenic agents. Andrew T. Vaughan^{1,2}, Shyh-Jen Shih¹, Sheetal Singh^{1,2}, To Uyen Do¹, ¹University of California, Davis, Sacramento, CA, ²Department of Veterans Affairs, Mather, CA

After radiation or drug treatment, DNA damage may facilitate leukemogenesis. The incidence of AML may be up to 1% per year of those exposed to chemotherapy. Current thinking indicates that secondary leukemia is inseparable from the tumoricidal potency of each treatment. To address this issue, DNA damage linked to tAML was studied using patient based and in-vitro methodology. Pro-leukemogenic DNA damage induced in the AML linked *MLL* gene was studied in patients undergoing chemotherapy for either non Hodgkin's Lymphoma or Breast cancer. In addition, an in-vitro model was established to screen the same *MLL* aberrations. Study volunteers donated blood before and 1, 3, 6 and 12 months after treatment. In addition, human lymphoblastoid (TK6) cells were treated with either a pro-apoptotic regimen (anti-CD95) antibody or estradiol (linked to Infant Acute Leukemia). Samples were then analyzed for chromosomal fusion breakpoints within the *MLL* gene using inverse PCR and conventional sequencing. Analysis focused on a location within the *MLL* gene known to be linked to tAML. Additionally, DNA fragmentation was assessed over the same region. Common to both in-vivo and in-vitro data, a specific 4bp hot spot for rearrangements was identified within exon 12 of *MLL* in 11/19 patient samples and 11/20 in-vitro samples. Further inspection showed the identified hot spot was restricted to the 5' base of a 101 bp stem-loop structure containing a Topoisomerase II binding site at its apex. DNA breaks identified in the in-vitro study were also concentrated at the stem base but evenly distributed over both the 5' and 3' side of the stem loop. The distribution observed may be due to the activity of a local Topoisomerase II enzyme, physically constraining DNA into a form that is a sensitive target for cleavage.

Additionally, the asymmetric (5' not 3') distribution of breakpoints suggests that leukemogenic aberrations require an additional contribution from a directional biological process, such as that provided by transcription. Creation of a treatment-linked leukemogenic fusion gene therefore requires specific processing, secondary to any DNA damage trigger, and thus may be a target for suppression without reduction of tumoricidal potency.

(PS5.13) Detecting changes in global DNA methylation levels in vivo following low dose ionizing radiation exposure. Michelle R. Newman¹, Benjamin J. Blyth¹, Pamela J. Sykes^{1,2}, Eva Bezak³, Rebecca J. Ormsby¹, ¹Flinders University and Medical Centre, Adelaide, Australia, ²SA Pathology, Adelaide, Australia, ³Royal Adelaide Hospital, Adelaide, Australia

Protective adaptive responses induced by exposure to low dose ionizing radiation (LDR) have been demonstrated for numerous endpoints, including tumour latency, DNA damage, and neoplastic transformation *in vitro*. High dose radiation (HDR) causes DNA damage, mutations and increases cancer risk and is associated with a significant and persistent reduction in DNA methylation, which is involved in the regulation of gene expression. Aberrant DNA methylation is an early event in cancer progression, silencing tumour suppressor genes and permitting the expression of normally silent genes, thereby promoting tumourigenesis. DNA methylation levels decline across the genome during ageing, and contribute to many age-related diseases, such as cancer. Given LDR exposure can reduce DNA damage, we hypothesise that LDR will induce a protective adaptive response that can prevent the global demethylation associated with either HDR exposure or ageing. DNA methylation changes could explain the persistent nature of the radioadaptive response. We have designed a high resolution melt curve assay to detect changes in mouse LINE1 (L1) repeat element methylation levels (considered to represent global DNA methylation levels). We have demonstrated that this assay is capable of detecting dose-dependant demethylation following 5-azacytidine treatment (a potent demethylating agent). We have observed that there are differences in L1 methylation between young, middle and old aged mice, as well as tissue differences, the spleen appearing more methylated at L1 repeat elements than the liver. These results are consistent with the literature regarding methylation of L1 repeat elements. Preliminary data has revealed no significant changes to DNA methylation of L1 7 hours following irradiation with 6 Gy in both liver and spleen tissues, compared to sham controls. These results were surprising, and indicate that the demethylation of DNA following HDR may not be as widespread as previously thought, with some sequences, such as L1 appearing to be radioresistant. We are now investigating L1 methylation levels in young, middle and old aged mice up to 12 months following LDR exposure. This research is funded by the Low Dose Radiation Research Program, Biological and Environmental Research, U.S. Department of Energy grant, DE-FG02-05ER64104.

(PS5.14) Transcriptional activity dictates susceptibility to stress-induced bystander DNA damage. Jennifer S. Dickey¹, Brandon J. Baird¹, Christophe E. Redon¹, Alexei Kondratyev², Valeriya Avdoshina², Guillermo Palchik², William M. Bonner¹, Olga A. Sedelnikova¹, ¹NIH, Bethesda, MD, ²Georgetown University, Washington, DC

The radiation-induced bystander effect (RIBE) is a well-known consequence of exposure to ionizing radiation (IR). An early event in this effect is the induction of DNA double-strand breaks (DSBs) in bystander cells that initiate downstream pathways leading to increased genomic instability and decreased viability. Measuring DNA DSB formation by monitoring γ -H2AX induction is an extremely sensitive way to detect this bystander damage. Similar to the RIBE, a distinct DNA DSB response is seen in bystander cell populations proximal to or when exposed to media from stressed, transformed, senescent, or damaged cells. Similar mechanistic pathways, involving NO, TGF- β , and other inflammatory cytokines seem to be responsible for bystander effects generated from all forms of stress. Bystander DNA damage seems to mainly be

induced in cells during S-phase. However it remains unclear whether cell cycle state alone confers bystander effect vulnerability. Therefore, primary human lymphocytes and primary rat neurons were examined. Bystander DNA damage induction was monitored in response to UVC, 0.2 Gy, and 20 Gy IR. Both media transfer and co-culture protocols were utilized. We found that while quiescent lymphocytes did not display a bystander response, activated lymphocytes were able to both transmit and respond to bystander signals. Lymphocytes one day post-activation were responsive to bystander signals though they have yet to reach S-phase. Additionally, while rat cortical and hippocampal neurons were unresponsive to bystander signaling, neurons derived from the cerebellum were susceptible, despite being non-replicating. Bystander effect vulnerability correlated with the ability of TGF- β and NO to induce DNA DSBs in these cell populations. Analysis also revealed that high transcription rates in cells conferred bystander signaling vulnerability regardless of cell cycle stage. Blocking transcription with α -amanitin eliminated bystander-induced DNA damage in both lymphocytes and neurons. Taken together, these results indicate for the first time that cellular signaling of stress to bystander populations is closely linked to transcriptional activity as well as cell cycle stage, and confirms that bystander effects are mediated through reactive oxygen species as well as inflammatory cytokines.

(PS5.15) Overexpression of RAD51 suppresses recombination defects: a possible mechanism to reverse genomic instability. David Schild¹, Claudia Wiese¹, Torsten Groesser¹, Alex Kuo¹, Jenny Flygare², ¹Lawrence Berkeley National Laboratory, Berkeley, CA, ²Karolinska Institute, Stockholm, Sweden

RAD51, a key protein in the homologous recombinational DNA repair (HRR) pathway, is the major strand-transferase required for mitotic recombination. An important early step in HRR is the formation of single-stranded DNA (ss-DNA) coated by RPA (a ss-DNA-binding protein). Displacement of RPA by RAD51 is highly regulated and facilitated by a number of different proteins known as the 'recombination mediators'. To assist these recombination mediators, a second group of proteins also is required and we are defining these proteins as 'recombination co-mediators'. Defects in either recombination mediators or co-mediators, including BRCA1 and BRCA2, lead to impaired HRR that can genetically be complemented for (i.e. suppressed) by overexpression of RAD51. Defects in HRR have long been known to contribute to genomic instability leading to tumor development. Since genomic instability also slows cell growth, precancerous cells presumably require re-stabilization of the genome to gain a growth advantage. RAD51 is overexpressed in many tumors, and therefore, we hypothesize that the complementing ability of elevated levels of RAD51 in tumors with initial HRR defects limits genomic instability during carcinogenic progression [1]. Experiments are underway to test if overexpression of RAD51 in human cells can suppress the phenotype of several different HRR defects. Initially, a derivative of HT1080 cells overexpressing RAD51 from a Tet-repressible promoter [2] will be used in conjunction with siRNA-mediated depletion of different HRR genes. These cells will then be assessed for their sensitivity to MMC, a DNA cross-linking agent, and their response to ionizing radiation. [1] Schild D. and Wiese C., NAR, 38: 1061-1070, 2010. [2] Flygare J. et al., Exper. Cell Res., 268: 61-69, 2001.

(PS5.16) *In vivo* non-targeted effect induced by photons versus heavy ions. Yunfei Chai¹, Nobuyuki Hamada², Shizuko Kakinuma³, Yukio Uchiyori³, Tom K. Hei¹, ¹Center for Radiological Research, Columbia University, New York, NY, ²Central Research Institute of Electric Power Industry, Tokyo, Japan, ³National Institute of Radiological Sciences, Chiba, Japan

Previous *in vitro* data have shown that bystander effects especially the signal generation process is dependent on the LET of radiation. Although we have shown that COX-2 and mutagenesis is induced in non-targeted lung tissues after 5 Gy X-rays irradiation of 1 cm² area (1 cm x 1 cm) in lower abdomen of *gpt* delta transgenic

mouse, we are not clear whether similar responses can be induced by high LET changed particle, which has been successfully used to treat many types of human cancers. A similar region of *gpt* delta transgenic mouse was irradiated with 1.5 Gy argon particles (LET=90.2 keV/um, 500MeV/u), accelerated at the Heavy Ion Medical Accelerator in Chiba (HIMAC) at the National Institute of Radiological Sciences in Japan. Comparing with a 20-fold increase of COX-2 expression in non-targeted lung tissues of all irradiated mice by X-rays, argon ions induced only a moderate increase in 2 of 5 irradiated animals. Similarly, there was a lower induction of 8-OHdG, an oxidative DNA damage marker, and an up-regulation of prostaglandin E2 in non-irradiated lung tissues within 24 hours after irradiation of argon ions when compared with an equivalent cytotoxic dose of X-rays. This is the first evidence showing that COX-2 related inflammatory response is related to non-targeted mutagenesis *in vivo* after heavy ion irradiation. Therefore, considering less energy is deposited in the normal tissues in the track of radiation for heavy ion irradiation comparing with low LET irradiation, the bystander effect in non-targeted tissues distant from the irradiation site will be a more significant concern in the argon particle irradiation, which has potential application in the radiotherapy treatment.

(PS5.17) Vitamin E and the active green tea agent EGCG suppress radiation-induced carcinogenesis by different molecular mechanisms. Marc S. Mendonca, Anthony Borgman, Ryan Dhaemers, Helen Chin-Sinex, Indiana University School of Medicine, Indianapolis, IN

Treatment induced secondary malignancies after successful radiation and/or chemotherapy cure of primary tumors is a growing area of concern. The identification of chemopreventive compounds that reduce radiation-induced secondary malignancy but are both nontoxic and tolerated with long-term use is a critical need. We investigated the chemopreventive potential and mechanism of action of Vitamin E and EGCG (the active agent in green tea) with the human CGL1 radiation neoplastic transformation assay. The molecularly characterized CGL1 assay allows both alterations of the quantitative neoplastic transformation as well the potential underlying molecular processes of the chemoprevention to be determined. We found long-term treatment with 15 microM EGCG or 50 microM Vitamin E beginning 72 hours after 7 Gy irradiation, significantly reduce radiation-induced neoplastic transformation frequency by a factor of 2.3. We determined that Vit E suppressed radiation-induced carcinogenesis by the induction of a p53 and pro-apoptotic Bax dependent apoptosis in the progeny of the irradiated cells. In addition, we demonstrated that EGCG does not reduce radiation-induced carcinogenesis by increased apoptosis, but rather by the onset of p16 dependent senescence in the irradiated CGL1 progeny. Vit E and EGCG are excellent candidate nontoxic chemopreventive agents for radiation-induced carcinogenesis that work by two distinct molecular mechanisms. We propose that this information should also aid in the development of next generation chemopreventive compounds. These studies were supported by a grant from the DOD awarded to MSM.

(PS5.18) Regulation of early signaling and gene expression in the alpha-particle and bystander response of IMR-90 human fibroblasts. Shanaz A. Ghandhi, Lihua Ming, Vladimir Ivanov, Tom Hei, Sally Amundson, Columbia University Medical Center, New York, NY

The existence of a radiation bystander effect, in which non-irradiated cells respond to signals from irradiated cells, is well established. To understand early signaling and gene regulation in bystander cells, we used a bio-informatics approach, measuring global gene expression at 30 minutes and signaling pathways within a few hours after exposure to alpha-particles in IMR-90 fibroblasts. Gene ontology suggested signal transduction and transcriptional regulation responding 30 minutes after treatment affected cell structure, motility and adhesion, and interleukin synthesis. Using quantitative PCR, we measured time-dependent expression of genes controlled by the NF-kappaB pathway; matrix metalloproteinases 1

and 3; chemokine ligands 2, 3 and 5; interleukins 1beta, 6 and 33 and growth differentiation factor 15. There was an increased response of this set of genes 30 minutes after treatment and another wave of induction between 4 and 6 hours. We investigated AKT-GSK3beta signaling and found both AKT and GSK3beta are hyperphosphorylated 30 minutes after irradiation and this effect is maintained through 4 hours. In bystander cells, a similar response was seen with a delay of 30 minutes. We proposed a network model where the observed decrease in phosphorylation of beta-catenin protein after GSK3beta dependent inactivation can trigger target gene expression at later times after radiation exposure. These results are the first to show that the radiation induced bystander signal induces a widespread gene expression response at 30 minutes after treatment and these changes are accompanied by modification of signaling proteins in the PI3K-AKT-GSK3beta pathway.

(PS5.19) Genetic dissection of the temporal role of p53 in regulating radiation-induced carcinogenesis. Chang-Lung Lee¹, Yongbaek Kim², Julie M. Sullivan³, Laura B. Jeffords³, Scott W. Lowe⁴, David G. Kirsch^{1,3}, ¹Department of Pharmacology and Cancer Biology, Duke University Medical Center, Durham, NC, ²Department of Population Health and Pathobiology, North Carolina State University, Raleigh, NC, ³Department of Radiation Oncology, Duke University Medical Center, Durham, NC, ⁴Cold Spring Harbor Laboratory, Cold Spring Harbor, NY

Suppression of p53 function during irradiation (IR) ameliorates short-term hematopoietic injury but may exacerbate long-term carcinogenesis as p53 heterozygous knockout mice show accelerated lymphomagenesis post-IR. By utilizing transgenic mice in which an shRNA to p53 can be induced temporally *in vivo* by doxycycline, we propose to 1) investigate if short-term inhibition of p53 during radiation promotes carcinogenesis and 2) elucidate the temporal role of p53 in eliminating damaged cells in hematopoietic tissues post-IR. Our results show that temporary induction of p53.shRNA prevented radiation-induced apoptosis in the thymus and protected mice from the hematopoietic syndrome caused by exposure to total body irradiation (TBI) of 7.5 Gy, indicating that short-term inhibition of p53 by RNA interference ameliorates acute radiation injury. To investigate the temporal role of p53 in regulating radiation-induced carcinogenesis, mice in which p53.shRNA were induced either short-term (during IR) or long-term (during and after IR) after exposure to a daily fraction of 1.8 Gy TBI every 24 hours for four days have been followed for tumor development. The mice in which p53.shRNA were induced permanently post-IR show significantly shorter latency of carcinogenesis compared to their littermate controls which did not express p53.shRNA. These results show that suppression of p53 expression permanently by RNA interference can recapitulate the tumor-prone phenotype of p53^{-/-} mice. We are utilizing this *in vivo* p53.shRNA model to investigate the effects of temporary inhibition of p53 during IR on long-term carcinogenesis.

(PS5.20) Quantifying the role of serotonin in generating radiation induced bystander effects. Jennifer M. Fazzari, Richard Smith, Colin Seymour, Carmel Mothersill, McMaster University, Hamilton, ON, Canada

Serotonin has been shown to be involved in the production of bystander signals by irradiated cells. In this study we examined levels of serotonin in 10 different batches of commercially available fetal bovine serum (FBS) and correlated the serotonin levels with the toxicity of medium harvested from irradiated cells (ICCM) using a standard medium transfer colony forming assay. Serotonin levels in the serum varied widely between batches and the levels correlated directly with the toxicity of the harvested ICCM. Three serum samples had levels of serotonin below 25ng/ml and these did not show medium transfer bystander effects. Exposure of serum samples to normal daylight reduced serotonin levels significantly. We suggest that serum batch variability may underlie much of the inter-laboratory variation in ability to produce bystander effects and further suggest that serum batches are protected from light and prescreened for ability to produce a bystander effect using a positive

control cell line. To answer the question of whether there is a limit to the amount of serotonin required to induce a bystander effect in naïve cells, the 5-HT₂ and 5-HT₃ receptors of the serotonin transport system will be competitively inhibited at varying intervals post medium transfer. Ketanserin and Granisetron (respective antagonists for the aforementioned receptors) will be used to inhibit serotonin transport. If a serotonin threshold does exist, then the variation in serotonin levels between batches of FBS would be insignificant as long as it is of a level that accommodates the threshold concentrations. Furthermore our preliminary data suggest, induction of the apoptotic cascade resulting from an intracellular influx of calcium may also be associated with a certain concentration of serotonin and this is currently being verified using a fluorometric calcium flux assay.

(PS5.21) Gene expression analysis of oxidative stress-initiated extracellular matrix remodeling in low-dose/low-dose-rate photon irradiated skin. Xiao Wen Mao¹, Tsehay Mekonnen¹, Ann R. Kennedy², Daila S. Gridley¹, Loma Linda University, Loma Linda, CA, ²University of Pennsylvania, Philadelphia, PA

Purpose: Examine the induction of oxidative stress and extracellular matrix (ECM)-associated gene expression profiles in mouse skin after exposure to low-dose/low-dose-rate (LDR) photon irradiation and compare these radiation-induced effects with those produced by high-dose-rate (HDR) exposure. Material and Methods: Whole bodies of ICR mice received gamma irradiation to total doses of 0, 0.25, 0.5 and 1 Gy at dose rates of 50cGy/hr or 50cGy/min. Skin tissues were harvested for characterization of gene expression profiles 4 hours after irradiation. Results: At LDR of 50cGy/hr, for oxidative stress, 0.25, 0.5 and 1 Gy significantly altered 28, 22, and 24 genes, respectively, among 84 genes assessed (P<0.05). At doses as low as 0.25 Gy, many genes responsible for inhibiting or reducing the production of ROS were significantly up-regulated with fold changes greater than 2.0 compared to controls, including aass, gpx1, gpx5, gpx6, prdx1, ptgs2 and sod1. In contrast, at doses of 0.5 and 1 Gy, most of these genes were significantly down-regulated. For ECM profile, 17 to 20 out of 84 genes were significantly up-/down-regulated following 0.25 to 1 Gy of irradiation. Among them, genes encoding collagen and ECM structural components, which included col2a1, col4a3 and col5a1, had the highest fold change at 1 Gy compared to controls. Genes encoding matrix metalloproteinases (MMP) were also significantly regulated following irradiation, including mmp2, mmp3, mmp10 and mmp15. Among them, the highest fold changes were detected at 0.25 Gy. Compared to LDR radiation, HDR induced different sets of gene expression profiles. At 0.25 Gy, of 84 genes associated with oxidative stress, 16 genes were significantly affected by irradiation, while at LDR, 28 genes were significantly regulated. Most interestingly, only 2 genes (exp and slc38a1) responded similarly for both LDR and HDR. Conclusion: These data revealed that exposure to low doses with LDR or HDR radiation induced oxidative stress-associated alterations in gene expression profiles of extracellular matrix and adhesion molecules. In response to physiological stress induced by ionizing radiation, the expression of genes involved in radiation-induced responses may be differentially regulated by different total dose and/or dose-rate regimens.

(PS5.22) Investigations into out-of-field cell survival and radiation induced bystander responses following exposure to intensity-modulated radiation fields. Karl T. Butterworth¹, Conor K. McGarry², Colman Trainor¹, Joe M. O'Sullivan², Alan R. Hounsell², Kevin M. Prise¹, ¹Queens University Belfast, Belfast, United Kingdom, ²Northern Ireland Cancer Centre, Belfast, United Kingdom

Intensity-modulated radiation therapy (IMRT) is an advanced radiotherapy approach in which highly modulated fields are used to achieve high dose conformity across a target tumor volume. Recent *in vitro* studies have suggested cell survival following exposure to modulated fields may not be accounted for using a traditional linear quadratic (LQ) model as non-local dose effects may have an important role in determining radiobiological response both within

and outside of the primary radiation field. Cell survival was determined by clonogenic assay in human prostate cancer (DU145) and transformed fibroblast (AGO1552) cells following exposure to different field configurations delivered using a 6 MV photon beam produced with a Varian clinical linear accelerator at the Northern Ireland Cancer Centre. Delivery of uniform dose distributions as modulated or non-modulated fields showed no significant difference in cell survival with the exception of DU-145 cells at 8 Gy ($p = 0.024$). Non-uniform dose distributions were delivered using a multileaf collimator (MLC) in which half of the cell population was shielded. Clonogenic survival in the shielded region was significantly lower than that predicted from the LQ model and for DU145 cells saturated at 40% survival at scattered radiation doses above 0.7 Gy. In contrast, cells in the exposed part of the field showed increased survival. These observations were abrogated by inhibition of cellular communication. Additional studies have shown the proportion of cells irradiated and dose delivered to the shielded and exposed regions of the field have an impact on response. These data demonstrate out of field effects as important determinants of cell survival following exposure to modulated irradiation fields with cellular communication between differentially irradiated cell populations playing an important role. This highlights the need for refinement of existing radiobiological models to incorporate non-targeted effects and modulated dose distributions. This work is supported by Cancer Research UK (Grant C1513 / A7047).

(PS5.23) Kinetics of propagation of bystander effects in human cells cultures exposed to low fluences of high LET radiations. Geraldine Gonon^{1,2}, Sonia M. de Toledo¹, Edouard I. Azzam¹, Michel Fromm², ¹Department of Radiology, New Jersey Medical School, Cancer Center, Newark, NJ, ²Laboratoire de Chimie-Physique et Rayonnements, Besançon, France

We and others have previously shown, in confluent cell cultures exposed to low fluences of α particles, that the proportion of cells that upregulate stress-inducible proteins is much higher than the number of cells irradiated. This phenomenon, called bystander effect, is now well accepted and is thought to impact the health risks of exposure to ionizing radiation. Here, we investigate the kinetics of propagation of signaling events that lead to induction of DNA damage in bystander cells in confluent normal human AG1522 fibroblasts exposed to a mean dose of 0.2 cGy from 3.2 MeV α particles (LET ~ 124 keV/ μ m) or 1 GeV/n iron ions (LET ~ 151 keV/ μ m). We evaluated the formation of 53BP1 foci (p53 binding protein 1), which localizes at sites of DNA double strand breaks, as a function of time after irradiation. The fraction of cells whose nuclei were traversed by an irradiating particle was derived from Poisson statistics and estimates of cell geometry, particle fluence and energy loss. At a mean dose of 0.2 cGy, only 1.4% and 1.2% of the cells are traversed through the nucleus by α particle or iron ion tracks, respectively. The number of 53BP1 foci in control cells was ~ 0.61 foci per cell. In α particle-irradiated cell cultures, the mean number of foci per cell was 0.73 ($p < 0.001$) at 15 min; it reached 0.90 by 3h ($p < 0.001$) after irradiation, following which a decrease was observed. The same trend was detected when the fraction of cells with foci was considered: it reached 61% at 3h which is higher than the expected 47.4% of the cells (46% in control + 1.4% traversed). The increase in foci formation over the expected value was eliminated when the cells were incubated with a specific inhibitor of ATM (Ataxia Telangiectasia Mutated protein). Analyses of bystander effects in iron ion-irradiated cell cultures and the effect of partial oxygen tension on the kinetic of 53BP1 foci formation in low fluences α particle-irradiated cell populations are in progress. Supported by Grant NNJ06HD91G from NASA.

(PS5.24) Radiation quality and the induction of non-targeted effects of ionizing radiation. Manuela Buonanno, Sonia de Toledo, Edouard Azzam, University of Medicine and Dentistry of New Jersey, Cancer Center, Newark, NJ

Radiation-induced phenomena such as genomic instability, bystander effects and adaptive responses have been suggested to impact the health risks of exposure to radiation. To evaluate the role

of linear energy transfer (LET) of radiation in induction of these phenomena, we examined the contribution of oxidative metabolism in the biological responses of irradiated normal human fibroblasts, their neighboring bystanders and their progeny. Twenty population doublings after exposure, progeny of cells exposed to mean doses as low as 10 cGy from 1 GeV/n iron ions (LET ~ 151 keV/ μ m) exhibited reduced ability to proliferate and harbored higher level of micronuclei than respective control. In contrast, progeny of cells exposed to 10 or 200 cGy from 1 GeV protons (LET ~ 0.2 keV/ μ m) had similar levels of micronuclei and cloning efficiency as control. Stressful effects persisted also in progeny of bystander cells that were contiguously co-cultured with cells exposed to low fluences of energetic iron ions. These cells had higher levels of micronuclei, reactive oxygen species, protein oxidation and lipid peroxidation than control, and showed decreased antioxidant enzymes' activities. A significant increase in the spontaneous neoplastic transformation frequency of bystander cells was also observed when mouse embryo fibroblasts were used. In contrast, progeny of bystander cells co-cultured with cells irradiated with energetic protons harbored similar levels of stress markers as control, and had increased antioxidant enzyme activity. Significantly, the latter bystander cells were protected from the clastogenic effect of a subsequent challenge dose from iron ions, and the induced mitigating effect persisted for ~ 24 h. Collectively, our data suggest that the nature of induced non targeted effects of ionizing radiation involves different levels of oxidizing species and greatly depends on intercellular communication and radiation quality and dose. Supported by Grant NNJ06HD91G from NASA

(PS5.25) Contribution of tissue level organization to genomic stability following low dose gamma irradiation. Cheryl Burrell¹, Linda Ritter¹, Brandon Bianski¹, Leticia Ortloff¹, Keigm Green¹, Munira Kadhim², Andrew Grosovsky³, Lora Green^{1,4}, ¹Loma Linda University, Loma Linda, CA, ²Oxford Brookes University, Oxford, United Kingdom, ³University of Massachusetts, Boston, Boston, MA, ⁴JL Pettis VAMC, Loma Linda, CA

Our study proposes that the level of tissue organization will affect the induction and persistence of low dose radiation-induced genomic instability. To investigate this hypothesis, we are using rat thyroid cells grown in vitro as three-dimensional (3D) tissue analogs in bioreactors and as traditional two-dimensional (2D) flask grown cultures. We postulated that cells grown as tissue analogs will exhibit a reduced expression of genomic instability as compared to aliquots of the same cells grown in two-dimensional tissue culture flasks. Analysis of reverse DAPI-banded and painted chromosomes have been performed using an Applied Spectral Imaging system. Aberrations have been scored and differences documented. Percentage active caspase 3 levels, indicating apoptosis, have also been determined from immunocytochemistry analysis. We have conducted replicate experiments of 2D and 3D cultures exposed to acute low dose (1, 5, 10 and 200 cGy) gamma rays with harvests taken at 2, 10 and 30 days post irradiation. Data assessing the percentage caspase 3 activity levels show that, initially, the 3D cultures display more immediate (2 days) genomic instability (as shown by the higher levels of apoptosis) compared to the 2D cultures. The intermediate time point of 10 days reveal little differences in apoptosis between the 2D and 3D cultures overall and by day 30, the 3D cultures have switched from being initially more unstable to becoming less unstable than the 2D cultures. Further analysis of chromosomal aberration among the dose and time points is currently underway and will be reported at the time of this meeting.

(PS5.26) Radio-adaptive response of hprt mutation in normal human fibroblasts induced by proton microbeams. Masao Suzuki, Chizuru Tsuruoka, Teruaki Konishi, Masakazu Oikawa, Cui H. Liu, Yumiko Kaneko, Yoshiya Furusawa, National Institute of Radiological Sciences, Chiba, Japan

Recently we have investigated that the mutation frequency at the hypoxanthine-guanine phosphoribosyltransferase (*hprt*) locus, which was detected with measuring 6-thioguanine resistant clones,

in normal human fibroblasts induced by the 200kVp X-ray challenging dose (1.5Gy) was reduced at 0.15 times in cells pre-treated with low-dose-rate neutrons (1mSv/8h) as a priming dose compared to unpre-treated cells. Furthermore, the reduced mutation frequency was returned to the control level, when using a specific inhibitor of gap-junction mediated cell-cell communication (40 μ M lindane). We set up a hypothesis that recoiled protons emitted by the interaction between primary neutrons and surroundings near irradiated cells induce radio-adaptive response in irradiated cell population via gap-junction mediated bystander effect. To examine the hypothesis around 1.5% of total cells were irradiated with single 3.4MeV proton before irradiating the X-ray challenging dose using the microbeam irradiation system, Single Particle Irradiation system to Cell (SPICE) in National Institute of Radiological Sciences, Japan. The result clearly showed that the X-ray induced mutation frequency of *hprt* locus was suppressed in cells pre-treated with proton microbeams and returned to the control level, when using a specific inhibitor of gap-junction mediated cell-cell communication. The result suggests that neutron-induced adaptive response is caused by recoiled protons and gap-junction mediated bystander effect plays an important role to induce such cellular response.

(PS5.27) Any apoptotic bystander effect induced by low dose radiation in spleen *in vivo* must fall within the homeostatic range. Alexander H. Staudacher¹, Benjamin J. Blyth¹, Rebecca J. Ormsby¹, Eva Bezak², Pamela J. Sykes^{3,1}, ¹Flinders University and Medical Centre, Adelaide, Australia, ²Royal Adelaide Hospital, Adelaide, Australia, ³SA Pathology, Adelaide, Australia

Adaptive responses and bystander effects contradict the current linear no-threshold (LNT) model of radiation risk assessment. There is evidence demonstrating that protective adaptive responses occur after low dose radiation exposure *in vivo* but evidence for the existence of bystander effects *in vivo* at low doses is very limited. In order to test whether bystander effects occur at low doses relevant to occupational and population exposure *in vivo*, we exposed mice to whole-body X-radiation doses where only a proportion of cells would receive an electron track, and then analysed the apoptosis frequency *in situ* in spleen tissue at 7 hours, 1, 3 or 7 days after irradiation and compared the results with that predicted from LNT. Apoptosis was induced above endogenous levels at a rate of 1.4%/Gy at 7 h after irradiation, and thus the LNT-predicted increases in apoptosis 7 h after a dose of 1 mGy and 0.01 mGy would be 1.4 in 10⁵ cells and 1.4 in 10⁷ apoptotic cells, respectively. Using a highly accurate method for apoptosis detection *in situ* analysing a minimum of 110,000 cells/mouse, Power calculations ($\alpha=0.05$, $1-\beta=0.8$) demonstrate that we would need $>10^4$ and $>10^8$ mice per group to detect the predicted increases in apoptosis described above, after 1 mGy and 0.01 mGy respectively. It is thus impractical to perform the experiments necessary to confirm such small increases in apoptosis frequency. In this study we used 10 mice/treatment group which would power a study to detect a >40 -fold bystander apoptosis effect. We did not observe any significant changes in the apoptosis frequency for either dose at any time-point. The 95% upper confidence limit on the apoptosis induced by 1 mGy was 1.4 extra apoptotic cells in 10³ cells for 1 mGy, and 1.7 in 10³ cells for 0.01 mGy. Even these small ranges only permit a potential bystander amplification of apoptosis of ≈ 100 -fold and $\approx 10,000$ -fold respectively. These data demonstrate that since the apoptosis expected from targeted effects at these low doses is only a fraction of the natural variation in unirradiated mice, even amplification of apoptosis due to a substantial bystander effect would be expected to fall within the homeostatic range. This research was funded by the Low Dose Radiation Research Program, Biological and Environmental Research (BER), U.S. Department of Energy, grant DE-FG02-05ER64104.

(PS5.28) Radiation dose dose-rate effectiveness factor (DDREF) and dose-rate effectiveness factor (DREF): How big should they be? Antone L. Brooks, Washington State University Tri-Cities, Richland, WA

The slope of the dose-response relationship for cancer induction from the A-bomb data is non-linear. To estimate the risk in the low dose and dose-rate region the slope in the high dose region is multiplied by a Dose, Dose-rate, Effectiveness Factor (DDREF). Currently the recommended values of this factor are from 1.5-2.0. This paper evaluates the molecular, cellular, animal and human data to evaluate the magnitude of the DDREF and the DREF. Molecular, cellular and animal data suggest that the Dose-Rate Effectiveness Factor (DREF) may be large and variable, due to observed adaptive responses following very low doses and dose-rate exposures. This paper evaluates data from dogs exposed to low LET radiation delivered over their life time and the influence of dose rate on the responses. This data show that following high doses to low dose-rate that the response is much lower than observed following high dose rate exposures. It was noted that the adaptive response is present following both high and low dose-rate exposures and that in many cases the response is decreased below the level seen in the control studies. The DREF for cancer in dogs with protracted exposures in the high dose region was high as 35, much higher than currently recommended. The data suggest a need to reevaluate the current values used for the DDREF and the fact that the DREF is very high following protracted exposure from internally-deposited radioactive materials.

(PS5.30) Elevated manganese superoxide dismutase (SOD2) activity as a mechanism for the low dose radiation- and thiol-induced adaptive responses in human RKO36 colon carcinoma cells and BFS2C mouse fibrosarcoma cells. Jeffrey S. Murley, Richard C. Miller, Kenneth L. Baker, Ralph R. Weichselbaum, David J. Grdina, The University of Chicago, Chicago, IL

Exposure of cells to low non-lethal doses of ionizing radiation (≤ 10 cGy) or WR1065, the active free thiol form of amifostine, can induce pro-survival pathways that result in protection against the damaging effects of a 2 Gy dose of ionizing radiation. One such signaling pathway involves the elevation of active manganese superoxide dismutase (SOD2). SOD2 is a mitochondrial matrix protein that serves as the primary mitochondrial defense against superoxide formation. Its primary function is to facilitate the dismutation of two molecules of superoxide anion (O_2^-) produced by normal respiratory processes or following exposure to ionizing radiation into water and hydrogen peroxide. To characterize the role of SOD2 in the radiation- and thiol-induced adaptive responses, RKO36 human colon carcinoma cells and BFS2C mouse fibrosarcoma cells were exposed to 10 cGy x-rays and 40 μ M or 4 mM WR1065 and SOD2 activity measured 24 h later. Significant increases in SOD2 activity in RKO36 cells (3.7-fold) and BFS2C cells (3.0-fold) were observed 24 h after exposure to 10 cGy. SOD2 activity was also observed to be significantly elevated in RKO36 cells (3.5-fold and 3.4-fold) and BFS2C cells (3.7-fold and 2.5 fold) 24 h after treatment with 40 μ M or 4 mM WR1065, respectively. The protective effect of the low dose radiation- and thiol-induced elevation in active SOD2 was examined using the endpoint of micronuclei formation as a measure of chromosomal damage. Exposure of RKO36 and BFS2C cells to 2 Gy resulted in a significant increase in the mean number of micronuclei observed relative to unirradiated control cells (8.8 versus 2.2; 5.4 versus 2.1, respectively). The frequency of micronuclei formation was significantly reduced in both RKO36 cells ($P = 0.003$) and BFS2C cells ($P = 0.011$) exposed to 10 cGy 24 h prior to the 2 Gy dose. A significant reduction in micronuclei formation was also observed in RKO36 and BFS2C cells treated with 40 μ M or 4 mM WR1065 30 min or 24 h prior to irradiation with 2 Gy. Treatment of both cell lines with SOD2 siRNA reduced SOD2 activity relative to mock-transfected control cells which resulted in the abrogation of both the radiation- and thiol-induced protective effect. This work was supported by NIH/NCI grant R01 CA132998 and DOE grant DE-SC0001271 (D.J.G.).

(PS5.31) X-ray and UVC-induced bystander effects in plants. Igor Kovalchuk, Viktor Titov, Youli Yao, Stephanie Wickersham, University of Lethbridge, Lethbridge, AB, Canada

Plants are capable of rapidly reprogramming patterns of gene expression, allowing fast acclimation and adaptation in response to specific environmental conditions. This ability depends on various signalling molecules operating within a plant and even between plants. Our previous experiments (Kovalchuk et al., Nature, 2003; Boyko et al., NAR, 2007; Boyko et al., 2010, PLoS ONE) showed that local exposure to stress results in systemic increase in homologous recombination frequency (HRF). We named this signal 'systemic recombination signal' or SRS. Although the nature of the signal was known, we hypothesized that plants are able to communicate this signal through phloem and through air. For the experiment, we used transgenic *Arabidopsis thaliana* plants carrying in the genome luciferase gene serving as a substrate for homologous recombination. Cells in which recombination events took place are visualized in CCD luciferase camera after application of luciferine. Recombination events then are scored and recombination frequency calculated. In the experimental set-up we planted two groups of plants in Petri dish and covered one group with either aluminium or lead cover and irradiated the second group with either UVC (7,000 ergs) or X-ray (5 Gy). To test whether signal is communicated through media or through air, we used Petri dish with 1/2 height dividers that separate the media but not the air exchange. In another set of experiments we placed two pots, one with irradiated and one with non-irradiated plants in sealed plastic bag for 4 days and scored recombination frequency in 7 days. We found that both groups of plants, irradiated and non-irradiated grown in Petri dish had higher recombination frequency. Moreover, we found that both groups of plants grown in divided Petri dish also had higher recombination frequency. This suggested that the signal leading to increase in HRF is indeed airborne. The experiment with plastic bags also showed the increase in HRF in both groups of plants. We conclude that irradiated plants exchange warning signals that could promote additional rearrangements in plant genome. This bystander effect could be one of the mechanisms of induced evolution, since increase frequency of rearrangements could potentially lead to diversification of genome composition in the progeny.

(PS5.32) A mathematical model for radiation bystander/abscopal effect based on the Gompertz tumor growth model and the kinetic reaction model of dose response. Seema Gupta, Xiaodong Wu, Kelin Wang, Mansoor M. Ahmed, University of Miami, Miami, FL

Radiation-induced bystander and abscopal effects have complex cellular mechanisms. Given the fact that the tumor dynamics is always associated with both the growth and decay components, the Gompertz growth model is proposed to quantify the bystander effect. According to this model, the tumor volume as a function of time $V(t)$ can be expressed by the differential equation: $V'(t) = aV(t) - bV(t) \ln V(t)$, where a is the tumor growth factor and b is the tumor decay factor. Theoretical analysis suggests that the ultimate state of the tumor growth is characterized by the ratio a/b . We proposed to quantify the bystander/abscopal effect by introducing a bystander enhancement index, $\eta = [a_c/b_c] / [a/b]$, where a and b are from the tumors subjected to the bystander effects, a_c and b_c are from the control group. A positive bystander effect would result in $\eta > 1$. When subsequent radiation is delivered to tumor cells that are subjected to bystander effect, sensitization is anticipated. The kinetic reaction model of dose response relations based on the repair and misrepair rates of DSBs, is further incorporated in to the analysis. The RMR (Repair and Misrepair) model analyses first-order DSB restitution competing kinetically with binary DSB misrepair. In this model, the viable DSB restitutions are presumably resulted from one-track DSB, while the restitutions from two-track DSBs are considered mostly lethal. We postulate that the enhanced radiation-induced apoptosis from the bystander effect is manifested by increasing the apoptosis rate of those viably restituted DNAs. This forms the quantitative base of bystander-induced radiation sensitization. To demonstrate the efficacy of the model, contra-lateral A549 lung xenograft tumors were used. Left tumor was irradiated by high dose spatially fractionated GRID radiation therapy (SFGRT; 15 Gy) or conventional open field radiation (CIR; 7.5 Gy) followed by 2 Gy CIR (5 days) to the same tumor or right tumor. The growth curves of the right tumors (abscopal effect) were analyzed using the model.

Abscopal effect was observed with all the radiation settings. Maximum η value was observed for 7.5 Gy CIR followed by 2 GyX 5 radiation setting indicating that abscopal effects were observed even with CIR. Model is now being used for fitting the bystander effects within the irradiated tumor.

(PS5.33) Comparison of space radiation-induced bystander signaling in 2D and 3D human skin model systems. Sarah Lumpkins^{1,2}, Chelvi Rajadurai², Hongying Yang², Nicole Magpayo², Kathryn Held², ¹Massachusetts Institute of Technology, Cambridge, MA, ²Massachusetts General Hospital, Boston, MA

The space radiation environment poses a significant hazard to astronauts on long duration missions, and the low particle fluences characteristic of this field implicate bystander effects as potentially significant contributors to overall cell damage. The purpose of this project is to investigate bystander effects due to signaling between mixed cell types under 2D and 3D tissue architectures. 2D bystander signaling was investigated using a transwell insert system in which AGO1522 fibroblasts (A) and keratinocytes (K) were irradiated with 1 GeV/n protons (0.1 and 2 Gy) or iron ions (0.1 and 1 Gy) at the NASA Space Radiation Laboratory. Medium-mediated bystander responses were investigated using the following cell signaling combinations (irradiated→bystander): K→K, A→K, K→A, and A→A. Bystander signaling was also investigated in a 3D model by developing tissue constructs consisting of fibroblasts embedded in a collagen matrix with a keratinocyte epidermal layer. Bystander experiments were conducted by splitting each construct in half and exposing half to radiation then placing the other half in direct contact with the irradiated tissue on a transwell insert. Cell damage was evaluated primarily by 53BP1 foci formation. In the 2D system, both protons and iron ions yielded a strong dose dependence for the induction of 53BP1 in irradiated cells, while the magnitudes and time courses of bystander responses were highly dependent on cell signaling combination. Results indicate that the bystander responses are least pronounced in K→A, while a 1.5-3 fold increase in cells positive for 53BP1 foci was found in the other 3 sets of bystander cells. These findings suggest that the bystander signal intensity and/or the susceptibility of a cell to be damaged by these signals is strongly dependent upon cell type. The 3D system resulted in a significant reduction (5-10-fold) in the percentages of both direct and bystander cells positive for 53BP1 foci, with a gradual increase in positive cells in the bystander population occurring in tandem with a gradual decrease in positive cells in the irradiated population from 1 to 72 hrs. Overall, these preliminary results provide evidence that the microenvironment significantly influences intercellular signaling and that a 3D tissue may be more resistant to radiation damage than 2D cell systems.

(PS5.34) Radiation exposure to protons delays the synaptic transmission decay during hypoxia in the mouse hippocampus. Roman Vlkolinsky¹, Alexander Shippee², Gregory A. Nelson¹, Andre Obenaus¹, ¹Loma Linda University, Loma Linda, CA, ²University of California, Los Angeles, Westwood, CA

Despite the advantageous spatial control of energy deposition by protons to malignant tissues, low radiation doses are still delivered to surrounding structures that often include the hippocampus. Radiation generates free radicals that at higher doses negatively impact synaptic transmission in the hippocampus. However, a moderate radiation exposure may trigger an adaptive response that can be unmasked during subsequent secondary oxidative challenges. While such adaptive response can be protective, we argue that it is the direct indicator of ongoing radiation-induced oxidative stress. The adaptive mechanisms can temporarily compensate for neuronal damage yet; the lasting shift in cell redox balance may have modulatory effects on synaptic functions and underlie later functional decrements. To unveil subtle, radiation-induced adaptive changes we exposed irradiated hippocampal tissue to *in vitro* hypoxia (HYP) and reoxygenation (ROX) used as a secondary stressor. Electrophysiological monitoring of synaptic responses in energy-deprived neurons enabled direct comparisons of the functional states of the irradiated and the

control tissue. We irradiated mice with protons (single exposure, 250 MeV/n, 4 Gy, head-only) and at 1 and 6 wks post-irradiation we prepared hippocampal slices to measure field excitatory postsynaptic potentials (fEPSP) and population spikes (PS) in CA1 neurons. Under normoxic conditions the synaptic responses were comparable between control and irradiated tissue. Thirty-two min of HYP led to the rapid decay of PS amplitudes and fEPSPs, followed by the transient appearance of anoxic spikes. Subsequent exposure to ROX returned these responses to normal albeit reduced in magnitude. In irradiated tissues at 1 wk we observed a tendency of delayed PS decay during HYP, while its recovery was not affected by ROX. However, at 6 wks the PS decay during HYP was significantly delayed from $t_{1/2}=7.0\pm 0.3$ min in controls to $t_{1/2}=13.9\pm 3.5$ min in irradiated animals ($p=0.04$) indicating lasting changes in adaptive, energy-saving mechanisms mediating resistance to HYP. Recovery of the PS amplitude during ROX was unaffected. These experiments demonstrate persistent functional changes of the neuronal tissue weeks after irradiation, suggesting a long-term sensitivity to subsequent injuries.

(PS5.35) DNA double strand break joinings as possible predictors of cancer induction. Fredric J. Burns, Moon-Shong (Eric) Tang, Wei Dai, Feng Wu, Krystyna Frenkel, NYU School of Medicine, Tuxedo, NY

Studies of cancer induction by single acute doses of various types of ionizing radiation in rat skin have been published piecemeal over a number of years. The published data together with additional unpublished data have been assembled and reanalyzed. The results obtained indicate a remarkable consistency and reproducibility of the cancer yields in relation to radiation dose for 2 diverse types of radiation, including minimally-effective low energy-density radiation (1.5 meV electron radiation and 100 keV x-rays) and maximally-effective high energy-density heavy ions (^{56}Fe and ^{40}Ar). DNA double strand breaks (DSBs) were quantified by the γ -H2Ax antibody technique in rat keratinocytes for the same radiations and for protons within the first 4 hr post-irradiation. The DSBs were scored either as in-track, i.e. in straight lines containing at least 4 γ -H2Ax-positive foci or not-in-track, i.e. no straight line apparent. Based on these approaches direct measurement of DSBs exhibited cancer-predictive capacity in spite of enormous quantitative differences between cancer yield relative to DSB yield. Not only were dose-response relationships predictable, but cancers arising from radiation lacking dense tracks, such as electrons, exhibited significant split dose repair as would be expected from initial lesions that arise independently at different times. Similarly cancers induced by dense track radiations exhibit no split dose repair as would be expected if initial lesions were simultaneous and dependent. Radiation carcinogenesis is still a complex multistage phenomenon that ultimately involves myriads of alterations, including genetic and epigenetic, to achieve the final malignant entity. However current findings imply that these known complexities fail to alter the effects of the DSB patterns induced in the first few hours after irradiation. An empirical calibration factor was derived from the data indicating that 100 DSB joinings per keratinocyte nucleus predicts a cancer yield of 1.0 carcinoma per rat @ 1 year post irradiation. The findings provide encouragement that cancer risk associated with complex radiation exposure scenarios might be predictable on the basis of a short-term *in vitro* biodosimetric assay.

(PS5.36) The progeny of a single cancer polyploid cell that had escaped radiation-induced mitotic catastrophe death acquires resistance to subsequent radiation exposure. Elizabeth A. Kosmacek, Michael A. Mackey, Eleonora Napoli, Elizabeth A. Colwell, Fiorenza Ianzini, University of Iowa, Iowa City, IA

We have previously demonstrated that a fraction of polyploid cells, formed *via* radiation-induced mitotic catastrophe (MC), are able to escape death and continue to divide normally after undergoing a depolyploidization process mediated by the activation of meiotic-like pathways. We now present data that demonstrate that the cell progeny derived from a single isolated polyploid cell that

escaped radiation-induced MC death is more resistant to subsequent radiation exposure than the naïve cells. At 14 days post-irradiation, we isolated a single large polyploid cell from a population of MDA-MB435 cells that had been irradiated with 5 Gy of γ -Rays. This single cell was cloned and expanded over 30 days at which time it was subjected to graded doses of γ -Rays and radiation sensitivity was determined using a clonogenic assay. The resultant surviving fraction was then compared with that obtained by irradiating the naïve cell population. Survival data analysis demonstrated that the surviving clone is resistant to radiation compared to the naïve cells presenting an overall higher survival and a decrease in both n and D0 survival curve parameters. Live cell imaging analyses demonstrate that the surviving clone presents both a higher yield of normal cell division, an overall lower yield of cell death, and an overall smaller cell size compared to the naïve cells. Moreover, the surviving clone cells are statistically significantly smaller than the untreated control cells (Mann-Whitney Rank test < 0.001). Thus, if we were not aware that the surviving clone derives from a MC event, we could infer that these cells had never been irradiated before. Conversely, they are well suited survivors of a multipolar division event occurred in a MC cell. These data further support the hypothesis that a progeny of cells morphologically indistinguishable from control cells, able to retain proliferative capacity, capable of binary divisions, and more resistant to subsequent radiation exposure can derive from cancer polyploid cells originated *via* radiation-induced MC. Understanding the fate of irradiated cancer cells and their potential for post-irradiation proliferation and survival will lend important insights into phenomena occurring during human tumor resistance to treatment and tumor progression. Support: NIH CA/GM94801; NIH/NCI 2P30CA086862; NASA NRA NNJ06HH68G.

(PS5.37) Model calculations on the release of and response to cell killing signals in bystander experiments with irradiated cell conditioned medium transfer. Werner Friedland, Pavel Kundrát, Helmholtz Zentrum Muenchen - Institute of Radiation Protection, Neuherberg, Germany

Experiments with the transfer of irradiated cell conditioned medium (ICCM) to unirradiated cells have demonstrated that low doses of radiation trigger the release of signals into medium that may reduce viability of unirradiated neighbouring bystander cells. Although there are indications for the involvement of mitochondria, cellular and mitochondrial membranes in the release of signals, the exact mechanism of signal release and the nature of signalling molecules are unclear. Modelling studies might help address these issues. Earlier models have been based on the assumptions of a cell autonomous release of signals and independent effects of individual signal molecules. However, recent data have shown that two-fold diluted medium harvested from twice higher donor cell number compared to the reference experiments fails to induce bystander effects at all (Ryan et al. 2008 Radiat Res 169:188), indicating the need for model refinements. A model will be presented that accounts for nonlinear effects of donor cell number and radiation dose on signal release as well as for nonlinear response of cells to the bystander signals. By comparing available experimental data with detailed Monte Carlo simulations of deposited energy in subcellular targets of varying size, multiplicities, and sensitivities, the possibility to derive detailed information on initiating targets responsible for the release of bystander signals will be discussed. Supported by NOTE IP 036465 (FI6R), Euratom, 6th FP of the EC.

(PS5.38) Hypersensitivity of human and rodent Fanconi anemia (FA) cells to bystander effect-induced DNA damage. Paul F. Wilson¹, Hatsumi Nagasawa², Ayano C. Kohlgruber¹, Salustra S. Ürbin¹, John R. Brogan², Matt A. Coleman¹, John M. Hinz³, ¹Lawrence Livermore National Laboratory, Livermore, CA, ²Colorado State University, Fort Collins, CO, ³Washington State University, Pullman, WA

Fanconi anemia (FA) is a chromosomal instability and cancer predisposition syndrome characterized by developmental defects, progressive bone marrow failure, and cellular hypersensitivity to

agents that induce DNA interstrand crosslinks and oxidative stress. Previously, we reported on the hypersensitivity of the isogenic *Fancg*-deficient CHO mutant KO40 for sister chromatid exchange (SCE) induction following low dose plutonium-238 α -particle irradiation where <1% of cell nuclei are hit. Compared to wild-type AA8 and *CgFancg*-complemented KO40 cells (40BP6) in which SCE frequencies increased ~30% over background levels in irradiated cultures, SCE frequencies in KO40 *fancg* cells increased ~50% over background levels in irradiated cultures. More recently, this hypersensitivity was also observed when KO40 cells were grown for two cell cycles in medium transferred from 2 Gy γ -irradiated AA8 cultures or medium to which a 1:10 dilution of Hank's balanced salt solution (HBSS) from 2 Gy γ -irradiated AA8 cultures was added (indicating bystander molecules can be released when cells are maintained and irradiated in simple isotonic buffers). Together, this data supports our hypothesis that DNA damage induced in non-irradiated bystander cells consists primarily of single-stranded oxidative lesions that interfere with replicative DNA polymerases and require FA proteins to direct repair using translesion polymerases or homologous recombinational repair (HRR). We are investigating bystander effect-mediated SCE induction in other CHO mutants, including UV40 and NM3 *fancg* cells and EM9 *xrcc1* cells, and *fanca*, *fance*, *fancd2*, and *fancg* primary human fibroblasts and their complemented controls. Bystander effect-mediated transcriptional responses in the human FA fibroblasts grown in bystander medium are being assessed by quantitative RT-PCR and microarray analyses following a recent report from our group demonstrating significant induction of Tp53-responsive genes in *fanca* lymphoblastoid lines following treatment with mitomycin C and hydroxyurea. The hypersensitivity of FA cells to bystander effect-mediated DNA damage makes them attractive candidates for identifying associated signaling mechanisms that are likely important factors modulating low dose IR cancer risk following low and high LET exposures.

(PS5.39) Enhanced intestinal tumor multiplicity and grade in vivo after HZE and proton exposure: mouse models for space radiation risk estimates. Daniela Trani, Kamal Datta, Bo-Hyun Moon, Elkhansa Sidahmed, Jiafang Sun, Bhaskar Kallakury, Albert J. Fornace Jr., Georgetown University, Washington, DC

Carcinogenesis induced by space radiation is considered a major risk in manned interplanetary and other extended missions. High-energy and charge (HZE) radiation, the main component of galactic cosmic rays (CGR), causes highly complex DNA damage, which may lead to increased frequency of chromosomal rearrangements and contribute to carcinogenic risk in astronauts. Gastrointestinal (GI) tumors are frequent in the U.S., and colorectal cancer (CRC) is the third most common cancer, accounting for 10% of all cancer deaths. In humans, mutations in the adenomatous polyposis coli (APC) gene occur early in the development of both sporadic and familial colon cancer (familial adenomatous polyposis, FAP). On the basis of epidemiological observations on the A-bomb survivors cohort and the frequency of spontaneous precancerous GI lesions in the general population, even a modest increase in incidence by space radiation exposure could have a significant effect on health risk estimates for future space flights. In the present study, we investigated in vivo effects of 1, 2 and 5 Gy of gamma rays, or equitoxic doses of HZE ions and high-energy protons, on intestinal tumor multiplicity and grade. We employed two different mouse models carrying a mutation in the adenomatous polyposis coli (APC) gene, the *Apc* mouse intestinal neoplasia (*ApcMin/+*) and the *Apc1638N/+* model. We showed that: 1) enhancement in intestinal tumor development and progression is dose, radiation-type and/or mutant-line specific; 2) radiation exposure elicits different responses along the GI tract in different mutants; 3) these different *Apc* models hold different suitability for risk estimates and countermeasure development studies. Our novel findings provide an understanding of quality factors in vivo for space radiation induced intestinal tumorigenesis effect. They clearly underscore the importance of selecting appropriate mouse models for studies of molecular pathways involved in initiation and/or progression of space radiation-induced intestinal cancer. Furthermore, considering the current emphasis on intestinal stem cells identity and the exquisite radiation sensitivity of a sub-population of cells in the crypt, our studies may contribute to elucidate tissue and molecular

mechanisms of both spontaneous and radiation-induced human CRC.

(PS5.40) Radiation enhanced antigen-specific immune response to mice melanoma. Mei Zhang, Hitoshi Ishikawa, Ayala Dvir, Liangjie Yin, Steven B. Zhang, Yeping Tian, Kunzhong Zhang, Shanmin Yang, Steven G. Stwarts, Paul Okunieff, Lurong Zhang, UF Shands Cancer Center, Gainesville, FL

The mechanisms by which radiotherapy (RT) controls tumor progression are likely to be two-fold: 1) to kill the irradiated tumor cells directly; and 2) to trigger the host immunity against tumor cells via altering the tumor antigen presentation and the tumor microenvironment. This study is to explore how localized radiation enhances anti-tumor immune response in a mouse melanoma model. Clone 62 mouse melanoma cells transfected with reporter luciferase gene were implanted into the right hind leg of syngeneic C3H/HeN mice. On day 24 after implantation, the tumors were irradiated with 15 Gy as tumor immune priming. After an additional 16 days, the mice were challenged with second injection of Clone 62 cells, either via s.c. to form a primary tumor or i.v. to form lung metastases and then sacrificed on either day 75 and day 90, respectively. The results showed: 1) a significantly higher tumor occurrence rate in no immune priming group compared with primary TR + 15 Gy IR group in both primary and metastasis models; 2) less secondary lung metastasis nodules and luciferase activity in the primary TR + 15 Gy IR group compared with no immune priming group when normalized to amount of lung lysate; 3) ELISA detection of anti-tumor IgG level was increased in both primary and metastasis models after RT immunization; 4) Western blot assay with lysate of Clone 62 as antigen and mouse plasma as antibody source showed that specific antibodies were generated against Clone 62 in 70% of the mice with RT immunization while only 50% in no immune priming group. A similar pattern was observed in the metastasis model, in which 60% of mice with RT immunization generated antibodies against tumor antigen while only 20% of no immune priming mice did so. Taken together, the local irradiation of primary tumor renders a beneficial effect on reducing the growth of new local tumor and lung metastases.

(PS5.41) Development of a low dose rate irradiation facility for long term animal exposures at Colorado State University. Paula C. Genik¹, Helle Bielefeldt-Ohmann², F. Andrew Ray¹, Christina M. Fallgren¹, Joel S. Bedford¹, Thomas B. Borak¹, Robert L. Ullrich³, Michael M. Weil¹, ¹Colorado State University, Fort Collins, CO, ²University of Queensland, Gatton, Australia, ³University of Texas Medical Branch, Galveston, TX

A low dose rate irradiation facility capable of accommodating up to 250 mice in Specific Pathogen Free conditions for hours to years at a time has been set up at Colorado State University. The basis of this facility is a panoramic irradiator room containing a JL Shepherd Model SS-070 600 Ci ¹³⁷Cs sealed source. The climate- and lighting-controlled room houses a large clear vinyl enclosure that is maintained at positive pressure with HEPA filtered air at greater than twenty room air changes per hour. Five movable custom designed cage racks each holding ten cages are positioned in an arc configuration in the enclosure according to dosimetrically-determined isodose lines. Standard ventilated Thoren caging system mouse cages without filter tops are held with their long axes perpendicular to the beam and water bottles distal to the irradiator. The dose-rate delivered can be varied by number and thickness of lead attenuators and by repositioning the cages and/or cage racks more distally or proximally to the source. We have used the facility to irradiate just over 230 male CBA/CAJ mice at a low dose rate of 10cGy/day over a period of 50 days. The actual dose-rate delivered was 0.5cGy/hour for 20 hours/day, for an overall total dose of 5Gy. The remaining 4 hours per day were used for animal health monitoring, cage and room maintenance, and weekly Institutional inspections. Mice were monitored until 800 days of age or moribund, and necropsied. Overall survival of these low dose rate irradiated mice was similar to that of unirradiated controls and better than that determined for sex-, strain- and age-matched mice

receiving acute 3Gy ^{137}Cs gamma exposures (0.85 Gy/minute). In contrast to the outcomes with high dose rate HZE ^{56}Fe or ^{137}Cs gamma irradiations for similar overall doses, few, if any low dose rate irradiated mice displayed overt signs of acute myeloid leukemia at the time of necropsy. Similar to observations made for ^{56}Fe HZE irradiated mice, we noted that a high proportion (60%) of the LDR mice developed hepatomegaly and/or liver tumors. Ongoing diagnostic histopathology studies and statistical analyses will enable this study to inform the relative biological effectiveness of dose, dose-rate and radiation quality relative to radiation leukemogenesis and/or hepatocarcinogenesis. Funded by the Department of Energy DE-F02-05ER63946.

(PS5.42) In vivo optical assessment of microbeam radiation therapy response. Andrew N. Fontanella¹, Greg Palmer¹, Jian Zhang², Larry Potter², Guoqing Zhang², Cassandra Fraser³, Sha Chang², Mark W. Dewhirst¹, ¹Duke University, Durham, NC, ²University of North Carolina - Chapel Hill, Chapel Hill, NC, ³University of Virginia, Charlottesville, VA

Microbeam Radiation Therapy (MRT) is a unique form of radiotherapy that has shown a marked tumor-specific effect. Compared to conventional radiation forms, MRT produces microscopic, spatially-discrete radiation patterns at an ultrahigh dose rate. The tissue-sparing property of this unique treatment modality is possibly facilitated by efficient normal-vessel repair mechanisms, contrary to the catastrophic disruption of poorly regulated tumor-associated vasculature. However, the non-local response characteristics associated with this treatment are not clearly understood. Therefore, we have applied a simulated MRT treatment (350micron single beam at 10Gy) to the murine window chamber model in order to observe and spatially quantify treatment response in terms of modulation of vascular structure and functionality. Over a week-long time course, we observed induced changes in tumor-associated vasculature after the MRT treatment. Structural data was gleaned from bright field microscopy. Simultaneous hyperspectral imaging was used to extract hemoglobin saturation values within each observable vessel segment, creating a map of oxygen gradients and allowing us to observe local and non-local changes in oxygen delivery in response to radiation. The recent development of non-toxic, oxygen-sensitive nanoparticles has further enabled us to measure oxygen tension within the tumor itself, correlating pO₂ values to spectrally-derived hemoglobin saturation values. Finally, all measurements were performed using a cell line genetically engineered to express GFP under an HRE promoter and RFP constitutively, allowing us to optically quantify tumor volume and HIF-1 response. Time course images and analysis presented here clearly show a treatment-induced modulation of the tumor vasculature with regard to both structure and function. Vasodilation is one of the most marked and immediate features of the post-treatment images, followed by increased saturation and decelerated growth, as compared to wide-field irradiation controls. These results indicate that modulation of vascular function at sites remote to the MRT beam plays an important role in determining overall tumor response to MRT treatment. This work is supported by NIH/NCI grant CA40355 and DoD grant BC083195.

(PS5.43) Cell stress responses in human 3D skin model after low dose exposure to ionizing radiation. Katrina Waters¹, Colette Sacksteder¹, Marianne Sowa¹, David Springer¹, David Stenoien¹, Susan Varnum¹, Thomas Weber¹, John Miller², Harish Shankaran¹, Qibin Zhang¹, William Morgan¹, ¹Pacific Northwest National Laboratory, Richland, WA, ²Washington State University-Tri-Cities, Richland, WA

We have applied a systems biology approach to identify molecular targets of cellular stress response in complex human tissue from low dose ionizing radiation exposure. Our goal is to distinguish between short-term transient effects and adaptive changes in homeostasis that could have either a positive or negative impact on human health. Using an *in vitro* 3-D human skin tissue model system, we have examined the temporal response of isolated

keratinocyte and fibroblast layers exposed to 10cGy of ionizing radiation using q-PCR, protein microarrays and global phosphoproteomics, as well as secreted effectors in the media using protein microarrays and metabolomics approaches. The use of integrated transcriptomic, proteomic, and metabolomic data is essential to fully capture multiple levels of molecular hierarchy and modes of regulation necessary to reconstruct the global response of a cell to perturbation. We found significant changes in gene expression for transcription factors and matrix modifying proteins, which reflected very early changes in the cell microenvironment. In addition, abundance levels for several receptor proteins were significantly altered with radiation exposure in the keratinocyte layer but not the fibroblast layer. Induced secretion of inflammatory effectors was also confirmed in the media of irradiated skin samples. We find that integrated data for RNA levels, protein abundance and phosphorylation status synergistically enhance network reconstruction beyond any single data type alone when developing computational models of cell stress response. Our data suggest that adaptive responses may occur in the skin after low dose ionizing radiation as a result of transcriptional dysregulation and inflammatory signaling in the surrounding tissue. Future experiments will determine if these changes result in a positive or negative long-term impact on the exposed system.

(PS5.44) Slow releasing long lived radicals are involved in the bystander mutagenesis response. Genro Kashino¹, Jun Kumagai², Hiroyuki Kugoh³, Mitsuo Oshimura³, Keizo Tano¹, Koji Ono¹, Masami Watanabe¹, ¹Research Reactor Institute, Kyoto University, Osaka, Japan, ²Nagoya University, Nagoya, Japan, ³Tottori University, Yonago, Japan

(Purpose) In order to know the mechanisms of bystander effects, we examined the involvement of slow releasing long lived radicals (SRLLRs) induced by the conditioned medium from the irradiated cells (IR-conditioned medium). (Method) Bystander effects were detected by the medium transfer method. Inductions of mutations at *HPRT* locus by bystander effects were examined in CHO cells or human immortalized mesenchymal stem cells (hMSC). The level of SRLLRs induced by conditioned medium in bystander cells were determined by ESR method. (Results) The results showed that the levels of SRLLRs were increased in the cells treated with IR-conditioned medium, suggesting that the IR-conditioned medium can induce SRLLRs in bystander cells. The irradiation to only medium could not induce the level of SRLLRs in cells. Also, the induced levels of SRLLRs by IR-conditioned medium were suppressed by the treatment of ascorbic acid which is specific scavenger of SRLLRs. Moreover, the mutation frequency at *HPRT* locus in cells treated with IR-conditioned medium were higher than those in control cells with non-IR-conditioned medium, and the induced mutation levels by IR-conditioned medium were completely suppressed by the treatment of ascorbic acid in bystander cells. (Conclusion) These results suggest that an indirect induction of SRLLR through the IR-conditioned medium play an important role for the inductions of bystander mutagenesis response in non-irradiated cells.

(PS5.45) Analysis of miRNA expression on irradiated lymphoblastoid cell lines that exhibit a radioadaptive response. Saipiroon Maksareekul, UC Davis, Davis, CA

MicroRNAs (miRNAs) are short 18-22 nucleotide RNA sequences that are involved in gene regulation by binding to mRNA and affecting its expression. Alterations in miRNA expression have been observed in response to DNA damage by radiation exposure and oxidative stress. In this study, our aims are to (1) determine whether low dose radiation sensitivity can be correlated with radioadaptive response using a phenotypic assay and (2) to profile global miRNA expression in irradiated human lymphoblastoid cell lines that exhibit a radioadaptive response. Currently, human lymphoblastoid cell lines are being screened for low dose radiation sensitivity by apoptosis, cellular proliferation, and colony forming assay. Low radiation dose will consist of 5 and 10cGy and multiple time points post-irradiation will be analyzed. In addition, these cells

will be challenged with high dose radiation of 5Gy six hours after low dose prime. Biological statistical analysis of cells during the priming response should reveal important miRNAs involved in low dose radiation sensitivity and its likelihood to develop high dose radiation resistance. These results will lead to a more focused examination of certain groups of miRNAs that may be directly involved in radioadaptive response.

(PS5.46) Bystander cell killing in normal human fibroblasts is induced by synchrotron X-ray microbeams. Masanori Tomita¹, Munetoshi Maeda¹, Hiroshi Maezawa², Noriko Usami², Katsumi Kobayashi³, ¹Central Research Institute of Electric Power Industry, Tokyo, Japan, ²University of Tokushima, Tokushima, Japan, ³High Energy Accelerator Research Organization, Ibaraki, Japan

Radiation-induced bystander response is defined as a response in cells that have not been directly targeted by radiation but have been in the neighborhood of cells that have been directly exposed. To elucidate the bystander response is important to evaluate the risk of low dose radiation. Many results of bystander response induced by charged particle radiations using microbeam irradiation systems have already reported. On the other hand, there are a few studies of detailed dose-responses for bystander cell killing induced by low-LET photons. Here we show the bystander cell killing effect showing a parabolic relationship to the irradiating dose. Monochromatic synchrotron X-ray microbeam irradiation was performed at the BL-27B station in the Photon Factory, High Energy Accelerator Research Organization (KEK, Ibaraki, Japan). Cell nucleus of confluent normal human lung fibroblast WI-38 cell was irradiated with a 5.35 keV monochromatic synchrotron X-ray microbeam of 5 μm x 5 μm square. All of the cells on dish were harvested and plated 24 h after irradiation. Surviving fractions were determined by colony formation assay. The surviving fraction decreased for doses above 0.09 Gy, and was 0.85 after a dose of 1.4 Gy. At doses above 1.9 Gy, the surviving fraction increased and approached to approximately 1.0, namely, no bystander killing effect above 1.9 Gy. This suggests that induction of the bystander cell killing effect may require some type of vital activity in the targeted cells, since the dose resulting in 37% cell survival was about 2.0 Gy. Cell death of the bystander cells were not observed when less than 5 cell nuclei were irradiated. On the other hand, if only 1 or 2 cell nuclei were irradiated, the decrease in cell survival levels was insignificant. Bystander effect was significantly suppressed by pretreatment with aminoguanidine (an inhibitor of inducible nitric oxide (NO) synthase), carboxy-PTIO (a scavenger of NO) or NS-398 (an inhibitor of COX-2), but not by DMSO (a scavenger of reactive oxygen species) or lindane (an inhibitor of gap junction). These results suggest that NO is the chief initiator/mediator of bystander response and COX-2 related pathway is important for the induction of cell killing in bystander cells.

(PS5.47) The European NOTE project: A commentary on current research in non-targeted effects of ionising radiation. Munira A. Kadhim, Oxford Brookes University, Oxford, United Kingdom

The discovery / elucidation of non-DNA targeted effects of ionising radiation, which include genomic instability (GI), and a variety of bystander effects (BE) including abscopal effects and bystander mediated adaptive response (BE/AR), has raised concerns for their implications in the radiation protection of the public, especially for quantification of human risk at low doses. Genomic instability, bystander effects and adaptive responses are defined by the experimental procedures used to study them. As such, they are not basic biological processes like transcription or DNA synthesis. Although these operational definitions serve a useful purpose, they constrain our thinking. Despite excellent research in this field from eminent research groups, there are still gaps in our understanding of the likely mechanisms associated with non-DNA targeted effects, particularly with respect to systemic (human health) consequences at low and intermediate doses of ionising radiation. Other outstanding questions include the direct / indirect cross mechanistic links between the different NOTE responses and if the variation in

non-targeted response observed between individuals and cell lines is linked to sex, genetic background, epigenetic effects or phenotype. This presentation is a contribution from a European Integrated Research Project on non-targeted effects (NOTE) which will aim to provide a commentary on the current state of the field. It will explore the background to the development of the concept of NOTE with respect to key radiobiological aspects, as well as critically examine how the evidence for non-targeted effects emerged from radiation biology research. It will also include discussion regarding terminology, some apparently contradictory results in the field and consider the implications of the effects for health effects, and therefore whether they would require revision of the approach to assessing radiation risk.

(PS5.48) Radiation-induced bystander effects after medical microbeam radiation treatment of rat brain. Cristian Fernandez¹, Elisabeth Schültke², Richard Smith¹, Elke Bräuer-Krisch³, Jean Laissue⁴, Hans Blattmann⁵, Jiayi Wang¹, Colin Seymour¹, Carmel Mothersill¹, ¹McMaster University, Hamilton, ON, Canada, ²University of Freiburg, Freiburg im Breisgau, Germany, ³European Synchrotron Radiation Facility, Grenoble, France, ⁴Universität Bern, Bern, Switzerland, ⁵Niederwiesstrasse 13C, Unterschönegg, Switzerland

Microbeam radiation therapy (MRT) is a new type of radiosurgery in the pre-clinical stage, developed for brain tumor treatment. MRT uses high-flux synchrotron light delivered as an array of parallel microbeams in high doses of irradiation to tumors in fractions of seconds. Some evidence suggests that MRT gives better clinical results than homogenous field radiotherapy but the mechanism of this effect is unknown. The aim of this study was to investigate the response and the potential adverse effects of MRT and homogenous field on non-irradiated tissue and to analyze the induction of bystander associated proteins, which were expected to occur under this controlled high-doses of irradiation in both brain tissue that is outside of the path of the irradiation array and in a distant organ (bladder). Healthy adult wistar rats were anaesthetised and exposed to either 35 or 350 Gy MRT or to homogenous field radiation to the right brain hemisphere. The rats were allowed to recover and were kept alive for 4, 8 or 12 hrs, without adverse effects being noticed. Sham controls and scatter dose controls were also included. The brain and bladder were then dissected and samples taken for proteomics and for the bystander reporter assay. The clonogenic survival of reporter HPVG cells fed with growth medium collected from explants showed that bystander effects occurred in both the non-irradiated left brain hemisphere and in the distant bladder tissue, confirming our hypothesis. Proteomic studies are in progress. The results suggest that systemic bystander or abscopal effects may be important to consider if this treatment is proposed for human brain glioma treatment.

(PS5.49) The use of whole body irradiation to reduce tumorigenicity in a murine prostate cancer model. Mark D. Lawrence¹, Pamela J. Sykes^{1,2}, Alexander H. Staudacher¹, Benjamin J. Blyth¹, Eva Bezac³, Rebecca J. Ormsby¹, ¹Flinders University, Adelaide, Australia, ²SA Pathology, Adelaide, Australia, ³Royal Adelaide Hospital, Adelaide, Australia

Prostate cancer represents a large health burden to society, particularly in Western countries where the prevalence is high and increasing. *In vivo* adaptive responses of increased tumour latency and reduced tumour frequency have been demonstrated in the literature, following single low dose or chronic low dose rate ionising radiation. Haematological malignancies are often studied, as they are particularly amenable to induction through whole body irradiation in mice. Few studies have investigated radiation influence over prostate cancer development. We aim to study the effect of radiation on epithelial carcinogenesis in mouse prostate, using the TRAMP (Transgenic Adenocarcinoma of the Mouse Prostate) model. We hypothesise that low dose radiation (10-100 mGy) will inhibit prostate tumourigenesis (initiation and/or progression), increasing tumour latency, and that high dose (2 Gy) exposures will accelerate tumour progression. Endpoints will

include time to palpable tumour, tumour size and weight, histopathology, serum PSP94 (a marker of tumour progression similar to PSA), proliferation, DNA damage/repair (gamma-H2AX) and apoptosis frequency. Initial studies have utilised immunofluorescent detection of the cell proliferation marker Ki-67, *in situ*, using image analysis software to score and distinguish between cell types. Preliminary data show no significant short-term proliferation changes associated with 50 mGy, when analysed 3 days after irradiation. Current and future experiments in irradiated versus unirradiated mice will investigate a range of radiation doses (both single and chronic) administered at various times during the staged progression of TRAMP prostate cancer, with analysis performed at a range of times post-irradiation. A greater understanding of the role of radiation on the tumorigenic process and evidence supporting low dose adaptive responses in prostate could potentially lead to novel prostate cancer treatment strategies. Research funded by The Cancer Council of South Australia and the Low Dose Radiation Research Program, Biological and Environmental Research, US Department of Energy, DE-FG02-05ER64104

(PS5.50) *In vivo* bystander effects induced by high charge and high energy particles. Min Li¹, Sonia de Toledo¹, Debkumar Pain¹, Edouard Azzam¹, Bernard Rabin², ¹University of Medical and Dentistry of New Jersey, Newark, NJ, ²An Honors University in Maryland, Baltimore, MD

Extensive data from tissue culture experiments have provided evidence for the expression of non-targeted stress responses in cell populations exposed to low fluences of high linear energy transfer (LET) radiations. However, there is limited evidence for such bystander effects *in vivo*. Here, we investigated redox-modulated responses in non-targeted organs of rats following cranial irradiation by energetic heavy ions. Relative to control, eighteen months after exposure, mitochondrial protein import was decreased in non-targeted liver of rats exposed to either 50 cGy from 500 MeV/n titanium ions (LET ~ 134 keV/μm) or 25 cGy from 600 MeV/n oxygen ions (LET ~ 16.4 keV/μm). These effects occurred in conjunction with increased protein carbonylation and activity of the antioxidant enzyme Mn-superoxide dismutase (Mn-SOD). A similar trend of increased protein oxidation also occurred in non-targeted heart and spleen tissues. The decrease in mitochondrial protein import was associated with increased level, in mitochondria of target and bystander tissues, of HSP60 and Tom20 (a translocase of outer mitochondrial membranes) that participate in the import process. The increase in the latter proteins, which were associated with increased activity of Mn-SOD, may be a compensatory but insufficient response to the decrease in protein import. Together, our data strongly implicate perturbations in oxidative metabolism in the expression of radiation-induced bystander responses, which may be expressed long after exposure to the high LET radiations found in deep space. Supported by grants from the US National Aeronautics and Space Administration

(PS5.51) Comparison of dose and dose rate effectiveness factors (DDREF) for intensity modulated and 3D conformal radiation therapy. Victor K. Yu¹, Patrick Meek¹, Wayne D. Newhauser², Robert D. Stewart¹, ¹Purdue University, West Lafayette, IN, ²MD Anderson Cancer Center, Houston, TX

Purpose: Estimates of the dose and dose rate effectiveness factor (DDREF) are needed to better quantify the risks of second cancer incidence following radiation therapy. A biologically motivated strategy to estimate the DDREF for fractionated radiation therapy treatments is developed and compared to data from the literature and to recommendations from the Biological Effects of Ionizing Radiation (BEIR) committee. Methods: Trends in cell death and neoplastic transformation are plausibly linked to the formation of small- and larger-scale DNA mutations. A linear-quadratic model for radiation mutagenesis is used to estimate trends in cell transformation and death with dose, dose rate and dose fractionation. We assume that excess cancer risk is proportional to the number of transformed cells and introduce a dimensionless factor, the DDREF, to modify ICRP risk estimates for excess cancer

mortality. Parameters for cell transformation and death in radiotherapy patients are estimated from *in vitro* experiments with the C3H10T1/2 mouse embryo cell line (M. Terzaghi and J. Little, *Cancer Research*, 36, 1367-1374, 1976). Effective DDREFs for the left- and right femoral heads, bladder, and rectum are estimated from dose-volume histograms (DVHs) for representative 3D conformal (3D-CRT) and intensity modulated (IMRT) prostate cancer treatments. Results: For the bladder, rectum and femoral heads, the DDREF increases with increasing fraction size. The DDREF for 44 fractions of 1.8 Gy delivered using IMRT ranges from 0.5 (right femoral head) to 0.8 (bladder). For 5 fractions of 7.25 Gy delivered using IMRT, the effective DDREF ranges from 2.3 (right femoral head) to 3.4 (left femoral head). For the rectum and bladder, the DDREFs are 2.3 and 2.8, respectively. For the same number of fractions, the DDREF is lower for 3D-CRT than for IMRT. Conclusion: For hypofractionated treatments, the maximum DDREF of 2.8 is comparable to the factor of 2 recommended by the BEIR VII committee. The DDREF for conventional fractionation (e.g., 44×1.8 Gy) may be as low as 0.5, which implies that excess cancer risks of some radiation therapy treatments may be substantially overestimated. Risk estimates that correct for tissue- and treatment-specific factors can help improve comparisons of second cancer risks for competing radiation treatments.

(PS5.52) The Search for Genes Regulating Bystander Signaling in the Nematode *C. elegans*. Tamako Jones, Leticia Orloff, Celso Perez, Gregory A. Nelson, Loma Linda University, Loma Linda, CA

We measure genotoxic damage in the *C. elegans* intestine by irradiating larvae and quantifying anaphase bridges in young adults. The endpoint is dose & LET dependent and analysis of individual intestinal (E) cells shows that they have unique radiosensitivities. We previously showed that germline signaling may modulate E cell radiosensitivity. A statistical analysis of responses for pairs of E cells shows that damage to one E cell substantially enhances the probability of damage in its neighbor. Precision irradiations of intestine cells with charged particles confirms that signals originating *in vivo* in the intestine spread longitudinally along the endothelium. A combination RNA interference and mutant screen is being used to identify genes required for the signaling and includes genes for: DNA repair, cell junctions, extracellular matrix and signal transduction. Analysis has been completed for approximately 50 genes. So far, genes in the NHEJ DNA repair pathway have been implicated in repairing damage leading to anaphase bridge whereas 9-1-1 response and homologous repair genes are not. Surprisingly, the *atm-1* and *atl-1* genes that serve as master regulators for DNA damage detection did not seem to be required. The biggest surprise was the observation that inhibiting *trt-1*, a telomerase reverse transcriptase, reduces bridge frequency. We expected the opposite: that improper telomere maintenance would lead to chromosome fusions in conjunction with the bridge-break-bridge cycle and result in higher frequencies bridges. Inhibition of gap junction genes expressed in the gut so far have not resulted in modification of the bridge frequency patterns. Inhibition of Notch (*lin-12*), MAP kinase (*sek-1*) and other signal transduction genes has increased overall bridge frequency but not altered the observed spatial patterns. We are currently testing several integrin mediated signaling components and genes regulating microRNA metabolism because as many as 19% of all worm genes may be under miRNA regulation. miRNA processing genes include argonaute genes *alg-1* and *alg-2* as well as *rde-1* & *rde-4* which are dsRNA binding proteins that act as accessories to the dsRNA ribonuclease Dicer (*dcr-1*). We will present a summary of the results from the genetic screens as well as more recent precision irradiation experiments.

(PS5.53) Microsatellite mutations in mouse tissues induced by low and high LET radiation. Jeanne Bourdeau-Heller¹, Rachel Leisemann Immel¹, Richard Halberg², Leta Steffen¹, Douglas Storts¹, Jeff Bacher¹, ¹Promega Corporation, Madison, WI, ²University of Wisconsin, Madison, WI

Mismatch repair (MMR) is important for maintaining genome integrity and loss of MMR gives rise to microsatellite instability (MSI) and a strong predisposition to cancer. Radiation exposure has been shown to increase mutations in coding and non-coding microsatellite repeats and may thus contribute to gene inactivation and carcinogenesis. To determine the effect of radiation on microsatellites in the presence and absence of MMR, we exposed a cohort of Msh2+/+ and Msh2-/- mice to 56Fe ions or γ -rays and calculated microsatellite mutation frequencies (MF) at different time points. Spontaneous MF was significantly higher in Msh2-/- mice as expected and varied for both genotypes by tissue type, corresponding to differences in cellular turnover rates (buccal>colon>spleen>blood>liver>brain). MF in 56Fe irradiated tissues 3 days after exposure increased in Msh2+/+ mice in all tissues, but increased only in colon of Msh2-/- mice. Previous data from our lab showed a dose dependent increase in MF in Msh2-/- mice after 10 weeks, thus mutation response might be time dependent. The kinetics of mutation induction revealed dramatic differences between low and high LET radiation in wildtype mice; although both types of radiation increased mutations over time, this increase was apparent 3 days following γ -rays but was not observed until 12 months following 56Fe exposure. This data suggests that although both types of radiation produce MSI, the effect is immediate and persistent following low LET radiation, but is latent subsequent to high LET exposure. In summary, these experiments reveal that radiation exposure causes a statistically significant increase in MF in MMR proficient cells that is tissue dependent. Further, the MF in irradiated Msh2+/+ tissues increased faster than background MF, suggesting ongoing MSI, which could increase carcinogenesis risk.

(PS5.54) SIRT3 regulates mitochondrial antioxidant enzyme activity following exposure to ionizing radiation. Mitchell C. Coleman¹, James A. Jacobus¹, David Gius², Douglas R. Spitz¹, ¹University of Iowa, Iowa City, IA, ²Vanderbilt University School of Medicine, Nashville, TN

Members of the sirtuin family of deacetylases can be found within many compartments of the cell and have been hypothesized to play critical roles in cell maintenance and repair. Recent work has demonstrated that the mitochondrially-located sirtuin 3 (SIRT3) is crucial in maintaining normal mitochondrial physiology and functions as a tumor suppressor in mouse embryonic fibroblasts (MEFs) as well as *in vivo*. SIRT3^{-/-} MEFs also demonstrate increased superoxide levels and increased genomic instability following exposure to ionizing radiation (*Cancer Cell* 17:41-52). Since the tumor-permissive phenotype seen in SIRT3^{-/-} MEFs was ameliorated by addition of superoxide dismutase and manganese superoxide dismutase (MnSOD) is a potential SIRT3 target, it was hypothesized that SIRT3^{-/-} mice may have deficiencies in mitochondrial MnSOD regulation in response to stress. When SIRT3^{-/-} mice were exposed to 2 x 2 Gy fractions of whole body ionizing radiation over 48 hours, SIRT3^{-/-} liver mitochondria showed no increase in MnSOD activity in contrast to a two-fold increase in control mice. Also, SIRT3^{-/-} heart mitochondria showed a 25-30% decrease in MnSOD activity following IR relative to control. In addition SIRT3^{-/-} heart and liver mitochondria demonstrated a slight 10-15% increase in glutathione peroxidase-1 (GPx-1) activity following IR while control mice showed a slight 15-20% decrease in GPx-1 activity following IR. These data support the hypothesis that SIRT3 may be a crucial factor in determining antioxidant enzyme responses in mouse mitochondria following exposure to ionizing radiation. (supported by a grant from DOE DE-SC0000830)

(PS5.55) Male rats are more sensitive than female rats to radiation-induced increases in risk factors for cardiovascular disease. John E. Baker¹, John Moulder¹, Brian Fish¹, John Hopewell², ¹Medical College of Wisconsin, Milwaukee, WI, ²Oxford University, Oxford, United Kingdom

Gender differences exist in susceptibility and progression of cardiovascular disease. However gender differences in response to

radiation are incompletely understood. We determined the effects of 10 Gy total body irradiation (TBI) from X-rays on risk factors for cardiovascular disease in adult male and female WAG/RijCmcr rats. Prior to radiation baseline values for total cholesterol, LDL-cholesterol and triglycerides were higher in females compared with males. Onset of TBI-induced hypercholesterolemia and hypertriglyceridemia was manifest 40 days after TBI in males and at 80 days in males. Add values for total cholesterol, LDL-cholesterol and triglycerides.

(PS5.56) How does radiation perturb cell communication? Luca G. Mariotti¹, Daniele Alloni², Andrea Ottolenghi¹, ¹Department of Nuclear and Theoretical Physics, PAVIA, Italy, ²LENA (Laboratorio di Energia Nucleare e applicata), PAVIA, Italy

Cellular communication is now considered of utmost importance in the radiation biology community. One of the main challenging puzzles where intercellular signaling plays a key role is the bystander effect phenomenon (damage observed in cells not hit by radiation) [1]. Other effects mediated by cellular communication are now being investigated, such as the induced apoptosis observed in transformed cells cultured with normal cells irradiated with low doses of alpha particles [2]. Aim of this work is to present possible methods to model the perturbation induced by radiation in intercellular signaling mediated by soluble factors (e.g. cytokines). Two complementary approaches are developed: a stochastic approach based on a Monte Carlo code, able to describe the local mechanisms involved in cell communication, and a deterministic approach based on a "systems radiation biology" fashioned model in which the signal molecules are treated as a population and their temporal behavior is described by differential equations. This model activity allowed us to question the use of *in vitro* models used to investigate bystander effects and, in general, biological effects mediated by extracellular signaling induced by low dose of radiation. In particular the results obtained thanks to this modeling activity allowed us to define the robustness of the *in vitro* systems ("a property that allows a system to maintain its functions against internal and external perturbations"[3]) and to compare/quantify some characteristics of the adopted experimental model respect to the *in vivo* conditions. Finally, quantification of signals has been investigated both theoretically and experimentally after the exposure to the same dose of low LET or high LET irradiation, in order to provide the dependence of cell signaling perturbation on the quality of radiation. 1. K. M. Prise and J. M. O'Sullivan, Radiation-induced bystander signalling in cancer therapy. *Nat. Rev. Cancer* 9, 351-360 (2009) 2. G Bauer, Low dose radiation and intercellular induction of apoptosis: potential implications for the control of oncogenesis. *Int J Radiat Biol.*, 83 873-88. (2007) 3. H. Kitano, Toward a theory of biological robustness. *Mol. Sys. Biol.* 3, 1371-7 (2007) This work was partially supported by the European Commission (EC Contract FP6-36465, "NOTE").

(PS5.57) Release of soluble/shed proteins from skin tissue following low dose irradiation exposure. Susan M. Varnum¹, Colette A. Sacksteder¹, Bobby-Jo M. Webb-Roberston¹, Katie Lien¹, John H. Miller², William F. Morgan¹, David L. Springer¹, ¹Pacific Northwest National Lab., Richland, WA, ²Washington State University-Tricity, Richland, WA

The purpose of this work is to determine how tissues respond to low dose radiation. This response includes complex interactions between cells that release specific proteins from the cell surface. It has been demonstrated that the bystander signal can travel up to 1 mm from human skin cells that were directly hit by radiation. This signal can be transmitted though gap junctions or through the release of soluble factors into the surrounding media by the directly hit cell. Our approach has been to irradiate 3D human skin samples with 10cGy of x-rays and collect the media at 24, 48 or 72 hrs following exposure. Using protein microarray approaches, the media was evaluated for changes in abundance against a panel of 120 inflammatory cytokines, chemokines, and growth factors. Using this approach, we determined that the concentration of a number of cytokines and chemokines are changed following

exposure of the skin samples to radiation. Our results indicate that seven of the inflammatory cytokines (G-CSF, GM-CSF, IL-11, IL-17, IL-8, MCP-1 and MIP1a) are all significantly increased. Several of these cytokines function to either stimulate the differentiation of hemopoietic stem cells to mature inflammatory cells (GM-CSF and G-CSF) or function as chemo-attractants to recruit inflammatory cells (MCP-1, IL-8, and MIP1a). Additionally, we identified five chemokines that are increased significantly in the skin cell model following exposure to irradiation (ENA-78, GCP-2, MCP-2, MCP-4 and NAP-2). These chemokines all act as chemoattractants for immune cells including neutrophils. These results are consistent with other studies showing that neutrophil infiltration occurs following exposure of hemopoietic tissue with a high dose, 4 Gy, of radiation. The other chemokines, MCP-2, MCP-4 and MIP-3alpha, chemoattract immune cells including monocytes and T-lymphocytes, are significantly increased in the cells following radiation exposure. These results indicate that inflammatory processes are activated early in the skin cell model following exposure with low doses of radiation.

(PS5.58) Radiation-induced changes in renal mitochondrial DNA. Marek Lenarczyk, Eric P. Cohen, Brian L. Fish, John E. Moulder, Medical College of Wisconsin, Milwaukee, WI

Radiation nephropathy is a well-defined late response with a poorly understood mechanism. We investigated mutagenic changes in renal mitochondrial DNA (mtDNA) as a mechanism. WAG/RijCmcr male rats 2 months old underwent total body irradiation (TBI) with a single dose of 10 Gy X-rays followed by a syngeneic bone marrow transplant. Control rats were sham-treated. Animals were sacrificed 1, 7, 21 and 49 days post-TBI and the kidneys were removed. Genomic DNA (gDNA) was isolated and subjected to quantitative PCR (qPCR) to detect mitochondrial DNA copy number and deletion frequency in gDNA samples pooled from 3-6 animals. PCR reactions were run with primers for mtDNA D-Loop (DL), or common deletion (CD) and nuclear DNA (beta actin-BA). Radiation nephropathy as measured by proteinuria and azotemia (standard physiological end-points) is not detectable up to 21 days but it begins by 49 days. All qPCR products showed correct size and were specific for the appropriate set of primers. TBI dramatically decreased the DL/BA ratio, suggesting directly-damaged mitochondria. This effect was seen at 7-49 days, but not at the 1 day. Age-matched sham-irradiated rats showed a continuous increase in DL/BA ratio over this time. The absolute mtDNA mutation frequency (CD/DL ratio), was ~3.5 times higher in irradiated than unirradiated rats at 1 day, decreased below the level in age-matched sham-irradiated rats at 7 and 21 days, then slightly increased again by 49 days. Results normalized to age-matched sham-irradiated controls showed a >3 fold increase of acute (1d) mtDNA mutagenic response which decreased by 7 days and then was elevated at 21 and 49 days. However, the mutagenic effect at 21-49 days was never as high as at day 1. A similar comparison for the DL/BA ratio showed a continuous decrease from 1 until 49 days. Results reported here may suggest a mechanism of radiation nephropathy. Our speculation is that mtDNA deletion may affect the oxidative stress response. Additional data on the mtDNA mutagenic response and related to pathway(s) of radiation nephropathy are expected from ongoing experiments including the entire transcribed rat genome (microarray). This work was funded by NIH cooperative agreement A1067734.

(PS5.59) Autosomal mutations in murine kidney epithelial cells exposed to energetic protons. Amy Kronenberg¹, Stacey Gauny¹, Ely Kwoh¹, Cristian Dan², Mitchell Turker¹, Lawrence Berkeley National Lab, Berkeley, CA, ²Oregon Health & Science University, Portland, OR

Humans are exposed to energetic protons in different settings. Protons are used in cancer therapy, where normal tissue can be exposed in the radiation field. Protons also represent the most abundant component of space radiation environments. Of particular concern is the risk of autosomal mutation, which represents the majority of cancer-associated mutations. An assessment of the

mutagenic risks of proton exposure would aid in our understanding of the potential carcinogenic risks. In this study, the first assessments of proton-induced autosomal mutations were obtained in epithelial cells. *Aprt* heterozygous kidney epithelial cells from C57BL/6 x DBA/2 mice were exposed to graded doses (0-5 Gy) of 1 GeV protons (LET=0.24 keV/um) at the NASA Space Radiation Laboratories at Brookhaven National Laboratory. *Aprt* mutations in this mouse strain and cell type can arise via mechanisms including small intragenic changes, interstitial deletions, mitotic recombination, discontinuous loss of heterozygosity, and whole chromosome loss. As such, this system provides a comprehensive assessment of mechanisms of proton-induced mutations. Mouse kidney epithelial cells were exposed in culture and seeded one week post-irradiation to determine mutant frequencies. Six replicate dose-response curves were performed. A marked dose-dependent increase in mutant frequency was found ($p < 0.001$) with a strong linear component and a very small quadratic component ($r^2 = 0.842$). In addition, eighty individual *Aprt*-deficient mutant colonies were picked from cultures exposed to 5 Gy of protons. DNA from each sample was subjected to a molecular analysis to determine alterations along mouse chromosome 8, where *Aprt* is situated. The proton mutant spectrum differed from the spontaneous mutant spectrum, with mitotic recombination and multilocus deletion strongly up-regulated in the proton spectrum ($p < 0.001$). The proton-induced mutant spectrum can also be differentiated from the spectrum of *Aprt* mutants arising in these kidney cells after *in vitro* exposure to 2 Gy of 1 GeV Fe ions (LET=151 keV/um, $p, 0.005$), demonstrating an effect of ionization density on autosomal mutation in an epithelial model. Supported by NASA grant NNN071HC721 to A. Kronenberg.

(PS5.60) Epigenetic responses of human cells exposed to chronic or acute low dose γ -rays. M. Ahmad Chaudhry¹, Romaica A. Omaruddin¹, Bridget Kreger¹, Sonia M. de Toledo², Edouard I. Azzam², ¹University of Vermont, Burlington, VT, ²UMDNJ-New Jersey Medical School Cancer Center, Newark, NJ

Human health risks of low dose ionizing radiation exposure remain ambiguous and are the subject of intense debate. To further understand the molecular mechanism(s) underlying the biological responses of normal human cells to low dose/low dose-rate ¹³⁷Cs γ -rays, we investigated epigenetic changes. We hypothesized that low dose γ -ray-induced effects are controlled by the modulation of gene expression involving micro RNA (miRNA). miRNAs participate in the control of gene expression at the posttranscriptional level, and are involved in many homeostatic cellular processes and carcinogenesis. To test our hypothesis, we monitored the expression of several miRNAs in AG1522 human fibroblasts exposed to acute or chronic 10 cGy γ -rays. We also examined the miRNA modulation following a moderate dose of 400 cGy. Dose and time dependent differences in the relative expression of several miRNA were observed. The expression patterns of many miRNA markedly differed after exposure to either chronic 10 cGy or acute 10 cGy. The expression of the negative regulator of RAS oncogene, miRNA *let-7e* and *c-MYC* miRNA cluster, was upregulated after chronic 10 cGy but was downregulated at 3 h after acute 10 cGy. The *miR-21* was upregulated in chronic or acute low dose- and moderate dose-treated cells, and its target genes *hPDCD4*, *hPTEN*, *hSPRY2*, and *hTPMI* were found to be downregulated. Taken together these results indicate the involvement of epigenetic mechanisms in the cellular responses to low dose radiation exposure. These results also show that dose-rate is a critical determinant of gene expression. Supported in part by Grant DE-FG02-07ER64344 from the U.S. Department of Energy, Low Dose Radiation Research Program.

(PS5.61) Nucleoside transport through gap junctions mediates long-range ionizing radiation oncogenic signals in vivo. Mariateresa Mancuso, Emanuela Pasquali, Simona Leonardi, Simonetta Rebesi, Mirella Tanori, Simonetta Pazzaglia, Vincenzo Di Majo, Anna Saran, ENEA, Agenzia nazionale per le nuove tecnologie, l'energia e lo sviluppo economico sostenibile, Rome, Italy

Ionizing radiation is a well-known genotoxic agent and human carcinogen. Recent work has questioned long-held dogmas by showing that cancer-associated effects of ionizing radiation can occur in cells and tissues that have not been directly exposed to radiation, raising questions on the robustness of the current system of radiation risk assessment. *In vitro* studies have shown that physical contacts through gap junction intercellular communication (GJIC) between irradiated and non-irradiated cells, and/or soluble factors released in the culture medium by irradiated cells are essential for the process. However, the mechanisms behind non-targeted radiation effects *in vivo* remain largely unknown. We investigated specifically the role of gap-junction intercellular communication (GJIC) in propagating radiation stress signals *in vivo* through the central nervous system (CNS), and the nature of factor(s) transmitted through GJICs in mouse CNS. We show that GJIC is critical for transmission of bystander radiation damage *in vivo*, and that damage is mediated by a mechanism involving purine nucleotide transmission. Altogether, our findings support a model whereby radiation generates long-range signaling responses that involve connexin channels and associated ATP release for transduction of damaging effects to non-exposed tissues. Moreover, they stress the importance of non-targeted effects in the assessment of cancer risks from environmental, diagnostic or therapeutic exposure to radiation.

(PS5.62) Intercellular induced apoptosis as a potential mechanism for low dose radiation-induced protection from cancer *in vivo*. Alexander H. Staudacher¹, Benjamin J. Blyth¹, Rebecca J. Ormsby¹, Georg Bauer², Pamela J. Sykes^{1,3}, ¹Flinders University and Medical Centre, Adelaide, Australia, ²Universitaets-klinikum Freiburg, Freiburg, Germany, ³SA Pathology, Adelaide, Australia

High doses of radiation ultimately increase cancer risk. The biological effects of low dose radiation are not as thoroughly understood and non-human and *in vitro* studies have indicated that low doses of radiation can protect from cancer. One likely mechanism involved in this protection is intercellular induced apoptosis. Intercellular induced apoptosis is initiated by normal cells which induce cancer-prone cells to undergo apoptosis and is upregulated by low dose radiation. This process has only been shown to occur *in vitro*. Our aim is to determine whether intercellular induced apoptosis occurs *in vivo*. The approach we are taking is to adoptively transfer normal and cancer-prone cells into mice, irradiate the mice with low dose radiation and then examine tissues from the recipient mice to identify the donor cells *in situ*. We can then determine whether the cancer-prone donor cells are preferentially removed via apoptosis. Splenic lymphocytes from *p53*^{-/-} mice were initially used as the cancer-prone donor cells. Irradiating recipient mice with low dose X-radiation (10 mGy) did not result in the preferential removal of *p53*^{-/-} donor cells compared to *p53*^{+/+} donor cells in the recipient mouse spleen 3 or 7 days after irradiation. Increasing the cancer potential of the *p53*^{-/-} donor cells by high dose irradiation prior to adoptive transfer did not make the cells any more susceptible to being preferentially removed *in vivo*. If intercellular induced apoptosis is occurring *in vivo*, the *p53*^{-/-} donor cells may not display the appropriate phenotype required to be targets for intercellular induced apoptosis. We are currently performing experiments which utilise siRNA technology to repress the expression of a key molecule which protects cancer cells from intercellular induced apoptosis *in vitro*. Cancer cells which have had this key molecule knocked down will be used for *in vivo* experimentation. Identifying intercellular induced apoptosis *in vivo* could explain the low dose radiation-induced protection from cancer observed in other *in vivo* studies and manipulation of the pathways involved in this process could be harnessed for cancer prevention. Research Funded by the Low Dose Radiation Research program, Biological and Environmental Research, U.S. Department of Energy, DE-FG02-05ER64104.

(PS5.63) Bystander effects involved in spatially fractionated radiation therapy. Rajalakshmi S. Asur, Sunil Sharma, Jose A. Penagaricano, Eduardo Moros, Peter Corry, Robert J. Griffin, University of Arkansas for Medical Sciences, Little Rock, AR

Radiation-induced bystander effects refer to damage in unirradiated cells. Two types of bystander effects are known: those requiring cell-cell contact and those that do not require physical contact in which the unexposed bystander cells respond to factors released by the irradiated cells. Here, we demonstrate the occurrence of bystander effects in murine mammary carcinoma (SCK) cells following spatially fractionated radiation fraction (GRID) as a single dose of 10 Gy. A small animal conformal radiation research system (SACRRS) was used to irradiate the cells. Confluent SCK cells were irradiated using a brass collimator to create a GRID pattern of 9 open circular areas, 12 mm in diameter with a center-center distance of 18 mm. The irradiated and bystander cells were separately isolated using a water-proof marker (pap pen) at 4, 24 and 48 h following irradiation. The cells were then incubated in fresh medium to determine the clonogenic survival. A traditional clonogenic radiation survival curve study was also performed with SCK cells, using a cabinet X-ray system. Dosimetry showed the valley dose, in the region where the bystander cells were collected, to be 0.9-1.2 Gy. These cells exhibited an 8% decrease in clonogenic survival following exposure to 1 Gy (approximately the valley dose in our GRID setup). However, the bystander cells exhibited a 40, 50 and 30% decrease in clonogenicity at 4, 24 and 48 h following GRID, respectively. Therefore, the net bystander effect was estimated to be a 20-40% decrease in cell survival. The slight increase in survival of bystander cells taken 48 h after radiation may be due to depletion of bystander factors and reactivation of cell cycle and growth processes. Very few studies have focused on bystander effects following exposure to clinically relevant doses of radiation or following high dose spatial fractionation. Our results suggest substantial bystander effects following spatially fractionated radiation therapy at clinically relevant doses. Ongoing studies in our laboratory are focused on understanding the physiological effects of spatially fractionated radiation in combination with the role of bystander effects to fully elucidate the mechanisms of action for this clinically effective technique in the control of advanced bulky tumors. Supported by NIH CA107160.

(PS5.64) The association of inbreeding with lung fibrosis incidence in beagle dogs that inhaled ²³⁸PuO₂ or ²³⁹PuO₂. Dulaney A. Wilson, Andrea Brigantic, William F. Morgan, Pacific Northwest National Laboratory, Richland, WA

Studies of the biological behavior and subsequent health effects from internally deposited plutonium in beagle dogs were intended to predict likely health effects in humans. Although care was taken to ensure 'random' mating, the beagle dog gene pool was limited compared with human populations. The relationship between plutonium inhalation and lung fibrosis was evaluated to determine if there was a genetic or familial component that would explain the relationship. The genetic or familial component is described by the inbreeding coefficient, the probability that a dog has two identical alleles for any gene. The inbreeding coefficient ranged from zero to 9.4 with a mean of 2.5 (SD 2.3). Dogs given plutonium-238 dioxide (²³⁸PuO₂) had lower inbreeding coefficients than dogs given plutonium-239 dioxide (²³⁹PuO₂) or control dogs. A previous analysis of data from life-span studies of beagle dogs given a single exposure to ²³⁸PuO₂ or ²³⁹PuO₂ generated estimates of the cumulative hazard of lung fibrosis. In dogs exposed to ²³⁸PuO₂ the addition of an inbreeding coefficient to the model did not improve the model fit. However, the inbreeding coefficient did affect the modeling in dogs given ²³⁹PuO₂. The best model of lung fibrosis after exposure to ²³⁹PuO₂ incorporated a linear dose-response function. When the inbreeding coefficient was added to the model, the best-fitting model included a linear dose-response function modified by the inbreeding coefficient, an interaction term between inbreeding coefficient and sex and the age at exposure. An increase in inbreeding coefficient was associated with decreased probability of lung fibrosis in females (RR 0.87; 95% CI 0.79-0.96) but a slightly increased probability in males (RR 1.14; 95% CI 1.04-1.25). These differences by sex probably reflect the make-up of the breeding population. However, the protective effect of increased inbreeding in dogs exposed to ²³⁹PuO₂ is surprising. This work was supported by Radiation Biology and Biophysics, U. S. Department of Energy, Pacific Northwest National Laboratory's Laboratory Directed Research and Development Program and funding from a pilot project awarded by the National Institutes of Health, National

Institute for Allergy and Infectious Disease grant U19 AI 067770, Centers for Medical Countermeasures against Radiation.

(PS5.65) Prostate cancer and hyperplasia in irradiated canines. Tatjana Paunesku¹, Ping Liu Yang², Amit Mittal¹, Benjamin Haley¹, Beau Wanzer¹, Lydia Finney², Stefan Vogt², Gayle Woloschak¹, ¹Northwestern University, Chicago, IL, ²Argonne National Laboratory, Argonne, IL

Very few studies to date analyzed radiation-induced prostate cancer in animals. In this work we investigate the effects of cobalt-60 gamma radiation on the incidence of prostate cancer and hyperplasia in a large cohort of beagle dogs. We retrospectively analyzed data from historic irradiation experiments conducted between 1952-1992 at Argonne National Laboratory on 347 beagles: 268 whole body gamma irradiated and 79 controls. Dogs in the cobalt-60 cohort were restricted to animals that lived at least 1000 days following first exposure to radiation. Total doses ranged from 218 to 14,745 cGy with dose delivered per day ranging from 0.3 to 26.3 cGy (0.14 - 1.20 cGy/hour for 22 hours per day) and first day of exposure starting from -62 days (*in utero* exposure) to 817 days. Because prostate cancer in dogs, as in humans, exhibits a strong age association, we first divided our control cohort into quartiles and then divided the cobalt-60 cohort into same groups based on the age at death. We analyzed each quartile/group using a chi-square test. In this analysis, beagles in the youngest quartile showed a significant difference in the incidence of prostate cancer and hyperplasia between control and cobalt-60 cohorts. As the age of the dogs increased, statistical significance of these differences steadily decreased. To investigate the nature of these "early" cases of prostate cancer and hyperplasia, we investigated pathological prostate tissues from irradiated dogs (especially from the first quartile) using histopathology and X-ray fluorescence microscopy. In the later studies, presence of high concentrations of zinc, associated with healthy prostate, was mapped and used for comparison between the samples.

(PS5.66) TNF α signaling of NF κ B and the elevation of manganese superoxide dismutase (SOD2) in the adaptive response. Richard C. Miller, Jeffrey S. Murley, Kenneth L. Baker, Ralph R. Weichselbaum, David J. Grdina, University of Chicago, Chicago, IL

Activation of the transcription factor NF κ B in response to stress including exposure to ionizing radiation propagates a cascade of complex signaling pathways. One of the pathways involves the elevation of manganese superoxide dismutase (SOD2) and the subsequent over expression of genes associated with the adaptive response. Wild type mouse embryo fibroblasts (wtMEF) and MEF tumor necrosis factor receptor 1 and 2 negative (double knockout cells, MEF_{TNFR1⁻/TNFR2⁻}) were exposed to 10 cGy x-rays or 40 μ M WR1065 followed 24 hr later by 2 Gy x-rays. Reproductive integrity ("cell survival") and micronuclei damage were used to evaluate the effectiveness of pretreatments with radiation and the thiol. Exposure of wtMEF and MEF_{TNFR1⁻/TNFR2⁻} cells to 2 Gy resulted in a significant increase in the mean number of micronuclei observed relative to unirradiated control cells. However, when wtMEF cells were treated 24 hr earlier with 10 cGy or WR1065 before the 2 Gy challenge dose, the frequencies of micronuclei formation were significantly reduced compared to wtMEF cells not pretreated and cell survival levels of wtMEF cells was significantly increased. The adaptive response for MEF_{TNFR1⁻/TNFR2⁻} cells stands in stark contrast to the results previously presented. The double knockout MEF cells showed no evidence of an adaptive response when exposed to 10 cGy of ionizing radiation 24 hr prior to a 2 Gy challenge. Interestingly, exposure of these cells to 40 μ M WR1065 resulted in an adaptive protective effect suggesting that the thiol effect is downstream of TNF α signaling. It is proposed that TNF α signaling plays an important role in the low dose radiation induced adaptive response and that TNFR mediated pathways play a role in whether cells exhibit either an enhanced or reduced resistance to ionizing radiation. An important downstream transcription factor affected by TNF α mediated signaling is nuclear transcription factor

κ B (NF κ B). It is further proposed that the thiol-induced adaptive response is mediated by direct activation of NF κ B which then leads to elevated SOD2 gene expression and subsequent elevated SOD2 enzymatic activity in the mitochondria. This work was supported by DOE grant DE-SC0001271 (D.J.G.) and NIH grant RO1-CA132998 (D.J.G.).

(PS5.67) The importance of radiation quality in the stimulation of intercellular induction of apoptosis in transformed cells at very low doses. Abdelrazek B. Abdelrazzak^{1,2}, Georg Bauer³, Peter O'Neill¹, Mark A. Hill¹, ¹Gray Institution for Radiation Oncology & Biology, University of Oxford, Oxford, United Kingdom, ²Physics Research Division, National Research Centre, Giza, Egypt, ³Abteilung Virologie, Institut für Medizinische Mikrobiologie und Hygiene, Universität Freiburg, Freiburg, Germany

An important stage in tumourgenesis is the ability of precancerous cells to escape natural anticancer signals. In order to characterise the underlying mechanism and how they are perturbed following exposure to ionising radiation, a well defined model system of intercellular induction of apoptosis was used where neighbouring normal cells are selectively eliminate transformed cells. We have characterised a system of intercellular induction of apoptosis (IIA) system in which non-transformed normal cells can induce apoptosis in co-cultured transformed cells through cytokine and ROS/RNS signalling. IIA was found to be enhanced after extremely low doses of both low and high-LET ionising radiation. Although a dose response is observed at low doses, the enhancement is independent of dose and radiation quality at medium to high doses. The use of ultrasoft x-rays (USX) with a range of irradiation masks has allowed us to not only vary the dose to the cells, but also the percentage of normal cells irradiated and compared results with those obtained for α -particles. The IIA response for USX was similar to that observed for γ -rays. Enhancement of IIA was observed when greater than 1% of the non-transformed cells were irradiated, with high-LET α -particle more effective for a given fraction of cells irradiated than low-LET USX. The enhancement increases with increasing percentage of cells irradiated until \sim 12 % where the response for both radiation qualities reached the plateau. The relative roles of the various signalling pathways, based on inhibitor studies, will also be presented along with the importance of levels of TGF- β . These results indicate that the stimulation of IIA by ionising radiation require both sufficient energy deposition within irradiated cells and fraction of cells irradiated, with the response dependent on radiation quality for when only a fraction of the cells are irradiated.

(PS5.68) Ying and Yang of radiation effects - molecular mechanisms of the sex differences in radiation responses. Olga Kovalchuk, University of Lethbridge, Lethbridge, AB, Canada

While being an important treatment modality, ionizing radiation (IR) is also a potent tumor- causing agent, and the risk of secondary IR treatment-related cancers is a growing clinical problem. Some studies link IR-induced secondary tumors to the enigmatic phenomenon of bystander effects. In bystander effects, exposed cells signal damage and distress to their naïve neighbors, which results in genome instability and carcinogenesis. Yet, the exact molecular etiology of IR-induced secondary tumors and IR-induced bystander effects remains unknown. Enigmatically, the IR-induced secondary cancer might occur at different frequencies in males and females. Overall, the area of sex-specificity of IR responses is rather unexplored. The long-term goal of my research program is to define the magnitude of toxic bystander effects and underlying epigenetic and molecular changes in males and females using an animal model. We aim to uncover the principal molecular basis of sex differences in bystander-induced responses by measuring the extent to which specific epigenetic changes correlate with the bystander effect in males and females. Using the experimental mouse and rat model, we have recently revealed that somatic IR-induced bystander effects are sex-specific, and the epigenetic mechanisms (*i.e.*, DNA methylation and microRNAs) are

involved in the generation and/or maintenance of IR-induced direct and bystander effects *in vivo* which are sex-specific. These analyses have yielded a novel molecular signature of the direct and bystander radiation effect in males and females. We will present and discuss the model describing the hierarchy and crosstalk between different constituents of epigenetic information as well as the maintenance and regulation of IR- and bystander effect-linked reprogramming events as a function of animal sex. In the long term, the understanding the molecular basis of bystander effects in males and females may contribute to the development of sex-specific diagnostic and treatment regimens and sex-specific radiation protection guidelines. The study was supported by the CIHR Operating Grant and the CIHR Chair in Gender and Health.

(PS5.69) Genetic Instability induced by tritium contamination. Yannick Saintigny¹, Fabio Di Giacomo², David Laurent¹, Jean-Baptiste Lahaye², Bernard S. Lopez², Paul-Henri Romeo², ¹CEA, Bruyere le Chatel, France, ²CEA, Fontenay aux Roses, France

Because of its low disintegration energy, tritium biological effects cannot come from external exposure but from integration of organically bound (OBT) tritium into tissue. Consequently, radioactive compounds incorporated in tissues can have biological effects resulting from energy deposition in subcellular compartments. We addressed the genetic consequences of 3H- or 14C-thymidine incorporation into mammalian DNA on cell survival, DNA double-strand breaks (DSB), cell cycle, mutagenesis and homologous recombination (HR). While γ -rays induced measurable DNA double strand breaks repair only at toxic doses and high dose rate, sublethal contamination with 3H-thymidine strongly induced DNA double strand breaks repair. Moreover, we found oxidative stress induced by low doses of 3H-thymidine responsible for mutagenesis induction. We then analyzed genetic instability induced by tritium contamination of haematopoietic stem cells. The hematopoietic tissue contains cells with long-term and short-term regeneration capacities and committed multipotent, oligopotent, and unipotent progenitors. One final goal is to compare the impact of an OBT, 3H-thymidine which target tritium to the DNA, with tritiated water. We evaluate in our animal models the haematopoietic consequences of contamination by tritium doses consistent with human accidental exposition. Our results emphasize that the biological impact of tritium is conversely proportional to the isotope emission energy but correlate to the energy transferred to the nucleus. Taking together, the data presented here show that cell contamination with non-toxic doses of tritium may be hazardous for genetic stability. Thus, the remarkable survival of these contaminated cells associated to genetics alterations may increase the risk of: 1 - transmission of genetic modifications to the next generation and 2 - increase the risk of cancer (cancer cell should accumulated mutations and be viable to generate a tumour). Our work emphasizes the strong differences between an external ionizing radiation exposure and an internal radioactive contamination on biological consequences.

(PS5.70) Tumorigenesis and normal tissue toxicity following single exposure gamma irradiation in mice. Haider A. Shirazi¹, Benjamin Haley¹, Mary Kwasny², Tatjana Paunesku¹, Gayle Woloschak¹, ¹Department of Radiation Oncology, Feinberg School of Medicine, Northwestern University, Chicago, IL, ²Department of Preventive Medicine, Feinberg School of Medicine, Northwestern University, Chicago, IL

The JANUS mouse (JM) program of Argonne National Laboratory studied acute and chronic radiation injuries in the B6CF1 mouse. JM-3 was a single-dose study run between April 1974 and June 1977. Here we analyze both tumorigenesis and normal tissue effects, both based on pathologic examination, following varying levels of total body gamma irradiation in these mice. We collected data on time of death, presence of tumors, and normal tissue toxicity. Six groups of mice were assessed, including a control group receiving sham irradiation, and five treatment groups receiving 90 cGy, 143 cGy, 206 cGy, 417 cGy, and 569 cGy, all

over 20 minute time periods. We excluded mice that received neutron irradiation, were removed to another experiment, died of accidental death, or were discarded. A total of 1495 mice were analyzed, and 64.1% of mice were male. The median survival was 1048 days for the control mice and 988 for irradiated mice. Median survival was decreased with irradiation on Kaplan-Meier (KM) ($p < 0.001$). On pairwise comparison with controls, only doses of 206 cGy or greater were associated with a statistically significantly decreased survival on KM ($p < 0.001$). Of the 1495 mice in the study, autopsy data were available on 1421 individuals. On Cochran-Armitage trend test, increasing levels of radiation were associated with an increased rate of development of angiosarcoma ($n = 25$, $p = 0.007$), hepatocarcinoma ($n = 60$, $p = 0.02$), and renal adenocarcinoma ($n = 20$, $P < 0.001$). Irradiation was associated with increased risk of developing granulosa cell tumor of the ovary ($n = 63$), angiosarcoma, luteoma ($n = 79$), renal adenocarcinoma, and tubular adenoma of the ovary ($n = 79$), all at a level $p < 0.01$. A similar analysis for normal tissue effects showed that increased radiation dose increased rates of anemia ($n = 178$, $p < 0.001$) and enteritis ($n = 26$, $p = 0.05$), while decreasing rates of hydronephrosis ($n = 142$, $p < 0.001$). This analysis suggests a minimum dose threshold of 206 cGy for tumorigenesis in this mouse cohort, as well as a predilection for development of female reproductive tract tumors with low-LET radiation exposure. Furthermore, in concordance with prior investigations, a life-shortening effect of radiation is redemonstrated in this study.

(PS5.71) Molecular events related to malignant conversion of normal human mammary epithelial cells. Ping Lu, Tom K. Hei, Yongliang Zhao, Columbia University, New York, NY

Breast cancer is a major cause of cancer death among female population. Therefore, development of appropriate model systems is critical for understanding the molecular basis of breast cancer progression. Telomerase is a RNA-dependent DNA polymerase containing a RNA template for telomere synthesis and a catalytic protein subunit with reverse transcriptase activity (hTERT). The hTERT is tightly suppressed in most type of normal human somatic cells and is upregulated in over 90% of cancerous cells including breast cancers. Ectopic expression of hTERT in telomerase-negative normal cells is sufficient to induce telomerase activity and immortalize a number of normal human cell types. In this study, introduction of human telomerase (hTERT) into normal human mammary epithelial cells (HMEC) renders them higher telomerase activity, elongated telomere length and an extended proliferative lifespan. Three independent lines of immortal HMEC-hTERT cells with stabilized telomere length have been established using hTERT transfection. The immortal cells show a near diploid complement of chromosomes albeit a few reciprocal and non-reciprocal translocations are identified. They are anchorage dependent and do not form tumors in immuno-suppressed host animals. The non-tumorigenic immortal HMEC cells were treated with a single dose of 60cGy of heavy ions. The irradiated cells were continuously cultured for 3-4 months and then inoculated subcutaneously into nude mice at 1×10^7 cells per site. The results showed that 7 out of 10 sites formed progressively-growing tumors in nude mice, and from these tumor nodules, six independent tumor cell lines were established. Gene expression profiles have demonstrated some gene clusters expression of which is uniquely altered in either hTERT-immortalized HMEC cells or heavy ion-induced malignant cells. Therefore, hTERT-immortalized human HMEC model provides a valuable tool for breast cancer research.

(PS6.01) Design and testing of compact tissue equivalent proportional counters for astronauts during extra vehicular activity and inside spacecraft. Thomas B. Borak¹, Leslie Braby², Lawrence Heilbronn³, Yoshi Iwata⁴, Terry Lusby⁵, Takeshi Murakami⁴, David Oertli¹, Tore Straume⁵, David Warner¹, ¹Colorado State University, Ft. Collins, CO, ²Texas A&M University, College Station, TX, ³University of Tennessee, Knoxville, TN, ⁴National Institute of Radiological Sciences, Chiba, Japan, ⁵NASA Ames Research Center, Moffett Field, CA

A compact real-time dosimeter will be required for astronauts during prolonged extra vehicular activities (EVA) and could be configured to serve as a portable radiation monitor inside transport spacecraft. It must be capable of measuring the dose rate and quality factor from galactic cosmic rays during ambient conditions. It must also record the dose and issue a warning to the astronaut during the initiation of a high intensity solar particle event (SPE). General specifications outlined by NASA are that the detectors should be tissue equivalent, omni-directional and capable of accurately measuring ambient dose rates on the order of 300 $\mu\text{Gy/d}$ for particles with LET ranging from 0.2 to 300 keV/ μm . At the onset of a solar particle event the system must be capable of signaling an alarm at 0.05 mGy/min and at 10 mGy/min. We have designed several prototype dosimeters to satisfy these requirements based on spherical tissue equivalent proportional counters. The directional response to HZE particles has been measured for several detector assemblies and electronic configurations. We are developing a version of the variance-covariance method, using a single detector, that can accommodate the large dynamic range of particles and dose rates. This work is supported by NSBRI-NASA, RE01301 (TB) and RE01302 (TS).

(PS6.02) Differences in cell inactivation between various ions of similar high LET in two different human cancer cell lines. Katarzyna Zielinska-Chomej¹, Chitralakha Mohanty¹, Margareta R. Edgren¹, Ryoichi Hirayama², Yoshitaka Matsumoto², Yoshiya Furusawa², Annelie E. Meijer^{1,2}, ¹Karolinska Institutet, Stockholm, Sweden, ²National Institute of Radiological Sciences, Chiba, Japan

Purpose. To investigate and compare the effects of four different accelerated ions with similar LET in two human cancer cell lines with different origin and gene status. Material and Methods. The two human cancer cell lines, AA (melanoma), and U-1690 (small cell lung cancer), were *in vitro* exposed to high LET accelerated boron, carbon, nitrogen and argon ions (60-90 keV/ μm) at the TSL (Uppsala, Sweden) and at the HIMAC/NIRS (Chiba, Japan). Low LET γ -rays were used as reference. Dose-response curves for clonogenic cell survival were established and the data were fitted to both the LQ and the RCR models. Cell samples were in parallel collected at different post-irradiation times (a few minutes up to several days) to analyse the induction of different types of cell inactivation using morphological and molecular biology techniques. Results. The four different ions induced different responses in cell inactivation in both the U-1690 and the AA exposed cells. Also, differences between U-1690 and AA cell lines were observed. A more pure apoptotic response was observed in the AA cells in comparison to the U-1690 cells. In the U-1690 cell line more necrotic like cell death was observed. Conclusions. Accelerated ions are significantly better to use than photons in treatment of radiation resistant tumours close to/in critical radiation sensitive organs because total higher level of cell kill could be achieved and the normal surrounding tissue can be saved from the damage. Also, depending on the type of ion, different responses can be induced. Apoptosis can be induced even in p53 mutated tumour cells that normally are resistant to low LET.

(PS6.03) The biological effectiveness of different radiation qualities for the induction of chromosome damage in human lymphocytes. Megumi Hada¹, Kerry George², Francis A. Cucinotta³, ¹NASA-JSC/USRA, Houston, TX, ²Wyle, Houston, TX, ³NASA-JSC, Houston, TX

Chromosome aberrations were measured in human peripheral blood lymphocytes after *in vitro* exposure to ²⁸Si-ions with energies ranging from 90 to 600 MeV/u, or to ⁵⁶Fe-ions with energies ranging from 200 to 5,000 MeV/u. The LET of the various Fe beams in this study ranged from 145 to 440 keV/ μm and the LET of the Si ions ranged from 48 to 158 keV/ μm . Doses delivered were in the 10- to 200-cGy range. Dose-response curves for chromosome exchanges in cells at first division after exposure, measured using fluorescence *in situ* hybridization (FISH) with whole-chromosome probes, were fitted with linear or linear-quadratic functions. The relative biological effectiveness (RBE) was estimated from the

initial slope of the dose-response curve for chromosome damage with respect to γ -rays. The estimates of RBE_{max} values for total chromosome exchanges ranged from 4.4 \pm 0.4 to 31.5 \pm 2.6 for Fe ions, and 11.8 \pm 1.0 to 42.2 \pm 3.3 for Si ions. The highest RBE_{max} value for Fe ions was obtained with the 600-Mev/u beam, and the highest RBE_{max} value for Si ions was obtained with the 170-MeV/u beam. For both ions the RBE_{max} values increased with LET, reaching a maximum at about 180 keV/ μm for Fe and about 100 keV/ μm for Si, and decreasing with further increase in LET. Additional studies for ⁴⁸Ti-ions and proton beams will be discussed.

(PS6.04) LET effect on DNA methylation in RKO and AG01522 cell lines. Michelle N. M. Morgan, Wilfried Goetz, Janet E. Baulch, University of Maryland, Baltimore, MD

Delayed non-targeted effects of irradiation can manifest in the progeny of irradiated cells multiple generations after the initial exposure. These deleterious effects are grouped together under the term radiation-induced genomic instability and are thought to be an early step in the carcinogenic process. The unexpectedly high frequency of transmission of non-targeted effects from the irradiated cell to its progeny suggests the possibility that epigenetics play a major role in the mechanism underlying radiation-induced genomic instability and carcinogenesis. DNA methylation is the most widely studied epigenetic mechanism and deregulation of DNA methylation is usually found to have deleterious effects. In this study, we compared the effect of x-ray, proton and iron ion radiation exposures to determine the effect of radiation linear energy transfer (LET) on methylation profiles of normal and cancer cell lines (AG01522 and RKO, respectively). For the RKO cell line the differences between populations and clonally expanded single cells surviving irradiation for DNA methylation profiles were also evaluated. An arbitrarily primed methylation sensitive PCR screen was used to evaluate changes in DNA methylation at random sites throughout the genome (AP-MSP). Alu and LINE-1 repeat element methylation was evaluated using combined bisulfite restriction analysis (COBRA) and methylation sensitive specific locus assays were used to evaluate MGMT and p16 promoter methylation. Together, these methods target specific coding sequences as well as repeat elements for analysis of DNA methylation. They provide a global, unbiased measure of genomic DNA methylation, as well as a link between changes in methylation and radiation induced genomic instability. [This work is supported by NASA grants NNX07AT42G and NNX06HD31G to JEB].

(PS6.05) On the use of the interaction density as a measure of the biological efficiency of ionizing radiation. Bengt K. Lind¹, Kristin Wiklund², Minna Wedenberg¹, Tommy Elfving³, ¹Karolinska Institutet, Stockholm, Sweden, ²Stockholm University, Stockholm, Sweden, ³University of Linköping, Linköping, Sweden

It is well known that the absorbed dose alone is not enough to quantify the biological effect from ionizing radiation. This is due to the varying spatial distributions of energy depositions on a microscopic scale. Historically, various approaches have been taken to characterize the differences seen in beam qualities, for example by the use of Specific Primary Ionization (SPI) or Linear Energy Transfer (LET). Most widespread today for this purpose is perhaps the use of LET, despite inherent shortcomings such as the fact that different charged particles, *i.e.* ions such as *p*+, *C* and *Li* etc, with the same LET can have different biological efficiency. Provided that the spatial distribution of energy deposits (disregarding the amount of energy per deposit) is the most important characteristic, a concept more in line with SPI than LET should be aimed at. Such a measure could be the average (and higher moments) nearest neighbor distance in 3D space. In order to account for both inter and intra track distances the particle fluence should also be included. Following this line of thoughts, the least biological efficiency would be expected for completely uniform density of energy deposits. An expression for the average nearest neighbor distance in *n* dimensions is thus needed. Assuming Poisson distributed interactions along parallel tracks with the density of energy deposits per unit *n*-volume, the average nearest neighbor distance *r* can be

expressed as $r = (n / (\rho k_n))^{1/n} \Gamma(1+1/n)$. Here Γ is the gamma function and k_n is a constant given by a closed-form expression and takes, e.g. the values 2 , 2π and 4π for the first three dimensions. Given the expression for the average nearest neighbor distance, one can for example calculate which fluence, Φ , is needed to achieve uniform density of energy deposits from charged particles with mean (inelastic) free path λ . The following expression for the fluence can be derived $\Phi = (2\Gamma(3/2) / \lambda)^2 / \pi = 1 / \lambda^2$. For absorbed doses used in therapeutic radiation therapy (some tens of Gray), high energy electrons, in the MeV range, have an almost uniform density of energy deposits. On the contrary high LET charged particles deviate largely from the purely random distribution. Different approaches to quantify this deviation from uniformity, and thus, the increases biological efficiency then seen will be shown and discussed.

(PS6.06) Biological Effects of Simulating the Whole Body Dose Distribution from a Solar Particle Event Using a Porcine Model. Keith Cengel, Jolaine Wilson, John Seykora, Jenine Sanzari, Casey Maks, Stephen Avery, Stephanie Yee, Eric Diffenderfer, James McDonough, Ann R. Kennedy, University of Pennsylvania, Philadelphia, PA

As a part of the near solar system exploration program, the whole body of an unshielded astronaut could receive significant proton radiation exposures during a solar particle event (SPE). SPE radiation is predicted to produce a highly inhomogeneous dose distribution (skin > internal organ dose) for which the dose-toxicity relationship is incompletely understood. To model the effects of such a superficial radiation dose distribution, Yucatan mini-pigs were exposed to 6MeV electrons using a linear accelerator and an opposed lateral beam arrangement. Dose distributions were determined using a pre-irradiation CT scan and a Monte Carlo-based simulation algorithm. External and internal dosimetry was confirmed using superficial and implanted MOSFET dosimeters, respectively. Overall, dose-dependent increases in skin toxicity were found, with grade 2 and grade 3 toxicity (CTAEv3.0) for doses up to 20Gy/3h and 25 Gy/3h, respectively. Skin histopathology of serial biopsies revealed increased deposition of pigment granules in the basal layer of the epidermis within 7 days after irradiation and evidence of cell shrinkage necrosis. Three animals developed symptomatic, radiation-associated pneumonopathy that radiographically involved all lung fields, but was worse in the pleura and apices. One animal received 12.5 Gy/3h and developed a non-productive cough 2 months after irradiation that did not respond to antibiotics, but improved on corticosteroid treatment. Two animals that received 25Gy/3h developed a similar pneumonopathy 2 weeks following irradiation. The mean lung doses were 3.5 Gy and 7 Gy while the V5Gy was 35% and 45% for the 12.5Gy and 25Gy groups, respectively. In conclusion, using total doses, patterns of dose distribution and dose rates that are compatible with astronauts' potential SPE exposure during an EVA, significant skin and lung toxicities were found. Moreover, at the 12.5Gy and 25Gy doses, animals experienced a radiation-associated pneumonopathy with a radiographic pattern that followed the pattern of dose deposition. Further research is necessary to determine the exact pathophysiology of the pneumonopathy and whether proton irradiation will cause similar effects. Acknowledgements: This research is supported by the NSBRI CARR grant; NSBRI is funded through NASA NCC 9-58.

(PS6.07) Optimization of Normal Tissue Sparing in Hadron Therapy through Ion Selection. Nicholas B. Remmes, Michael G. Herman, Jon J. Kruse, Mayo Clinic, Rochester, MN

Radiation therapy using ion beams is complicated by the substantial variability of the radiobiological effect (RBE) within these beams. This variable RBE makes it difficult to meaningfully compare the physical dose distribution of one ion beam with that of other ion beams. Instead, comparisons must be made between equivalent doses - the product of the physical dose with the RBE - which are tissue type and beam type specific. This research uses the microdosimetric kinetic model to quantitatively evaluate how the

dose given to different normal tissues varies as a function of ion species, while holding the effective dose to the target tissue constant. In order to calculate the saturation adjusted mean specific energy for use in calculating the RBEs, the microdosimetric probability density function described by T. Sato *et al** for use in the PHITS simulation code was translated from Fortran to C++ where it could be implemented with the GEANT4 toolkit. The treatment beams are taken to be two parallel opposed beams treating a 6cm deep volume centered in a 30 cm wide, rectangular phantom. The weighting of monoenergetic beams - simulated in GEANT4 - were optimized so that the effective dose of each of the two opposed beams and the effective dose of the sum was flat for the defined treatment dose within the target. Since the RBE is dependent on $(\alpha/\beta)_{T(\text{target})}$, the weightings had to be re-optimized for each new $(\alpha/\beta)_T$ value. Once optimized, the resulting physical dose distribution was used to find the effective dose distribution outside of the target for normal tissues having various $(\alpha/\beta)_{N(\text{normal})}$ values. Results are viewed as a 3D surface plot of effective dose to normal tissue at a specified depth with $(\alpha/\beta)_T$ and $(\alpha/\beta)_N$ on the horizontal axes. These plots show the regions where each ion type provides superior normal tissue sparing. This 3D surface is almost flat for protons and becomes steeper for heavier ions with the normal tissue dose slopping upwards from a minimum at higher $(\alpha/\beta)_N$ and lower $(\alpha/\beta)_T$ values to a maximum at lower $(\alpha/\beta)_N$ and higher $(\alpha/\beta)_T$ values. The results suggest that ions such as lithium may offer normal tissue sparing very similar to carbon for higher $(\alpha/\beta)_N$ and lower $(\alpha/\beta)_T$ values without the pronounced disadvantages of carbon at lower $(\alpha/\beta)_N$ and higher $(\alpha/\beta)_T$. *Rad Res, V.171, 107-117 (2009).

(PS6.08) Radiation-induced mucositis as a risk of extended space flights: Model studies using heavy ion-irradiated organotypic cultures. Ulrike G. A. Sattler, Wolfgang Mueller-Klieser, Institute of Physiology and Pathophysiology, University Medical Center of the Johannes Gutenberg University Mainz, Mainz, Germany

Radiation-induced mucositis is a severe complication of heavy ion radiotherapy, but may also be a health problem and a safety risk during extended space flights, such as missions of humans to moon and Mars. Men in exomagnetospheric space are exposed to highly energetic heavy ion radiation which can be hardly shielded. We present a new research project which will be focused on the homeostasis and physiology of human mucosa under the impact of densely ionizing radiation. The core intention of the project is the investigation of immediate and early mechanisms involved in the induction of mucositis by heavy ions. As a model system of oral mucosa, organotypic cell cultures are used. Thereby, oral mucosa is reconstituted from immortalized human keratinocytes, mesenchymal fibroblasts and vascular endothelial cells. We have developed a suitable system that allows for heavy ion irradiation with a horizontal particle beam. Space radiation will be mimicked by a spectrum of ions between protons and iron with high energies up to 1 GeV per microm, but in the low dose range of 0-4 Gy. Structural damages will be analyzed in cryosections immunohistologically stained for specific cytokeratin and collagen subtypes. The major focus with regard to endpoints is the expression and release of pro-inflammatory cytokines, such as TNF-alpha, IL-1 beta, IL-6 and IFN-gamma which will be assessed by ELISA assays. DNA damage will be characterized through gamma-H2AX staining. The elucidation of the respective mechanisms is expected to reveal ways of therapeutic intervention and prevention. This project is accomplished in cooperation with the Gesellschaft fuer Schwerionenfor-schung (GSI) Darmstadt and the European Space Agency (ESA); it is supported by the German Aerospace Center (DLR) and the Federal Ministry of Economics and Technology (BMWi), #50 WB 0926.

(PS6.09) Acute radiation effects resulting from exposure to solar particle event-like radiation. Ann R. Kennedy¹, Drew Weissman¹, Gregory King², Alexandra Miller², Gregory Freund³, Jeffrey Woods³, Erika Wagner⁴, James McDonough¹, Alan Gewirtz¹, Rosemarie Mick¹, Keith Cengel¹, ¹University of Pennsylvania School of Medicine, Philadelphia, PA, ²Armed Forces

Radiobiology Research Institute, Bethesda, MD, ³University of Illinois, Urbana-Champaign, IL, ⁴Massachusetts Institute of Technology, Cambridge, MA

A major solar particle event (SPE) may place astronauts at significant risk for the acute radiation syndrome (ARS), which may be exacerbated when combined with other space flight stressors such that the mission or crew health can be compromised. The National Space Biomedical Research Institute (NSBRI) has funded a Center of Acute Radiation Research (CARR), which is focused on the assessment of risks of adverse biological effects related to the ARS in animal models exposed to space flight stressors combined with the types of radiation expected during an SPE. As part of this program, FDA-approved drugs that can be used as countermeasures for the prevention and/or mitigation of the ARS symptoms will be evaluated, if warranted. The CARR has been established to determine whether there are adverse acute biological effects like those of the ARS which are likely to occur in astronauts exposed to the types of radiation, at the appropriate energies, doses and dose-rates, present during an SPE. The ARS is a phased syndrome which often includes vomiting and fatigue. Other acute adverse biologic effects of concern are the loss of hematopoietic cells, which can result in compromised bone marrow and immune cell functions. There is also concern for skin damage from high SPE radiation doses, including burns, and resulting immune system dysfunction. Using 3 separate animal model systems (ferrets, mice and pigs), the major biologic endpoints associated with the ARS being evaluated are: 1) vomiting/retching and fatigue, 2) hematologic changes (with focus on white blood cells) and immune system changes, resulting from SPE radiation with and without reduced weightbearing conditions, and 3) skin injury and related immune system functions. In all of these areas of CARR research, statistically significant adverse health effects have been observed in animals exposed to SPE-like radiation. Countermeasures for the management of ARS symptoms that are determined to require mitigation will be evaluated. The radiation facilities being used for these studies are in the Department of Radiation Oncology at Penn, the Loma Linda Medical Center, and the NASA Space Radiation Laboratory. Acknowledgements: This research is supported by the NSBRI CARR grant; the NSBRI is funded through NASA NCC 9-58.

(PS6.10) Distinct transcriptome profiles associated with HZE particle radiation of different energy and LETs. Lianghao Ding, Michael D. Story, UT Southwestern, Dallas, TX

The objective of this study is to characterize cell responses to HZE particle radiation of different energy and LETs. We used immortalized human bronchial epithelial cells (HBEC-3KT) to perform microarray analysis to study whole genome profiles of mRNA and miRNA expression. Radiation exposures were provided by the NASA Space Radiation Lab (NSRL) using 1GeV Fe, 1GeV Si, 1GeV O, 200MeV O and γ -rays. Experiments were carried out from 5 NSRL beam runs so that at least two independent radiations were received for each particle type. Cells were irradiated at 0.5 Gy and 1 Gy for HZE particles, 1 Gy and 3 Gy for γ -rays. Total RNA was isolated from cells that were harvested at 0hr (control), 1 hour, 4 hours, 12 hours and 24 hours after each irradiation. Whole genome expression Illumina BeadChips were used to perform microarray analysis. Raw signal intensities were background-subtracted and quantile-normalized using the MBCB algorithm. Results of principal component analysis showed segregation of gene expression profiles based on different particle types. Significantly changed genes after radiation were determined by applying a time course analysis model (maSigPro). A signature of 20 genes was used to build a model to predict Fe, Si and γ -ray exposures. The models were built using Support Vector Machine. The best model was chosen by repeatedly partitioning sample groups for building and cross-validation of the models. The cross-validating results showed 98% accuracy in predicting the three radiation types. An independent testing set was collected in the latest BNL run and the prediction results are being analyzed. We have now collected data from 200 MeV O exposures (LET equivalent to 1 GeV Si) as we intend to study whether LET is the dominant factor that defines the different expression profiles from different particles. This initial analysis is ongoing. Expression changes for miRNA are also being

investigated using the same cell samples. The preliminary data suggested that the most robust miRNA responses happen at 1 hour after radiation, which is earlier than mRNA responses. MiRNAs associated with the p53 pathway and cell cycle regulation were found significantly changed. More functional analysis of significantly changes mRNAs and miRNAs are underway and will be revealed at the time of the meeting.

(PS6.11) Prolonged lifespan, decreased thymic lymphoma incidence, and activated immune-regulated genes in low-dose-rate irradiated AKR/J mice. Hee-sun Kim, Suk-Chul Shin, Yu-Mi Kang, Kwang-Hee Yang, Cha-Soon Kim, Ji-Young Kim, Seon-Young Nam, Seung-Jin Choi, Young-Woo Jin, Radiation Health Research Institute, Seoul, Republic of Korea

To evaluate the effect of low-dose-rate radiation on cancer incidence, we reared AKR/J mice in a Long-term Low-dose-rate Irradiation Facility (¹³⁷Cs, 0.7 mGy/h). We compared the thymic lymphoma incidence and lifespan of high-dose-rate (¹³⁷Cs, 0.8 Gy/min, total dose of 4.5 Gy) irradiated mice with those of non-irradiated mice. Previously, we reported that the incidence of thymic lymphoma in low-dose-rate irradiated mice was decreased (15%, $P < 0.01$) and the average lifespan of low-dose-rate irradiated mice was extended (35 days, $P = 0.02$). We collected normal-sized thymuses at 130 days after irradiation and performed whole genome microarray analysis. In all, 17,625 genes were expressed. We classified expressed genes associated with the carcinogenesis pathways (DNA repair, DNA damage signaling, cell cycle, cancer pathway finder, p53 signaling, apoptosis, and T-cell and B-cell activation). In this study, we focused on the expression of immune-related genes. We found the expression of immune-regulated genes (*Lilrb3*, *Igh6*, *Fcgr2b*, *Fcgr3*, *MGC60843*, and *Jag 2*) in low-dose-rate irradiated mice. The results suggested that cells with incompletely repaired DNA and cancer cells are removed by the stimulation of apoptosis and activation of NK and T and B cells, which contribute to the decreased thymic lymphoma incidence and elongated lifespan. We also observed that the expressed down-regulated immune genes (*Il15*, *Cd3e*, *Sp3*, *Traf6*, *Ilra2*, *Rag2*, *CD28*, and *Cbfb*) in high-dose-rate irradiated mice. These data suggested that apoptotic pathway and immune related cells (NK cells and lymphocytes) and autoimmunity are suppressed by high-dose-rate radiation. Functional studies for identifying the role of the other genes associated with thymic lymphoma incidence that were expressed in low-dose-rate irradiated mice are currently in progress.

(PS6.13) Monte-Carlo simulation of radiation tracks and calculation of dose deposition in nanovolumes. Ianik Plante¹, Francis A. Cucinotta², ¹USRA/DSL, Houston, TX, ²NASA, Houston, TX

The radiation track structure is of crucial importance to understand radiation damage to molecules and subsequent biological effects. Of great importance in radiobiology is the induction of double-strand breaks (DSBs) by ionizing radiation, which are likely caused by clusters of lesions in DNA, and oxidative damage to cellular constituents leading to aberrant signaling cascades. DSB can be visualized in cell nuclei with immunofluorescence measurements of DNA repair proteins. The distribution of DSB is weakly dependent on the LET, however endpoints resulting from DSB misrepair such as chromosomal aberrations and mutations are strongly LET dependent. DSB produced by high-LET radiation are more difficult to repair than those resulting from low-LET radiation. To investigate DSB distributions and chromosomal aberrations, models of radiation tracks are used with chromosome geometry models. The DSB induction probability can be calculated by using the local dose obtained from the radial dose profile of a heavy ion track or by more CPU expensive models utilizing detailed Monte-Carlo scoring within atomistic representations of DNA structures. In the present work, a new approach is proposed to calculate the local dose deposited by ionizing radiation. The irradiated volume is divided in 3D pixels (voxels) of 20 nm x 20 nm x 20 nm. Then, tracks are simulated with the Monte-Carlo track structure code RITRACKS and the dose is calculated in each voxels. The number

of tracks is chosen such as the irradiated volume received 1 Gy. For high-LET ions, very high local dose is found in voxels corresponding to direct ion traversal. Voxels of high doses are also found distributed apparently as uncorrelated points around the path of the track, but corresponding, as expected, to electron track ends. In some cases, they may be found a few millimeters away from the track core. Voxels which receive very high dose are not found for low-LET ions. The appearance of the calculated dose distribution in 3D looks very similar to DSBs seen in γ -H2AX experiments, both for low and high-LET ions. This calculation also shows that very high dose voxels are found only in high-LET tracks and may explain the difference in the nature and reparability of DSBs induced by high and low-LET radiation.

(PS6.14) Apoptosis and cell cycle accumulation in p53 mutated small cell lung carcinoma differ after boron and nitrogen ion exposures. Annelie E. Meijer^{1,2}, Margareta R. Edgren¹, Woo-Chul Kim^{1,3}, Anders Brahme⁴, Karolinks Institutet, Stockholm, Sweden, ²National Institute of Radiological Sciences, Chiba, Japan, ³Inah University, Incheon, Democratic People's Republic of Korea

Purpose: To investigate the induction of apoptosis and change in cell cycle distribution in small-cell-lung-cancer (SCLC) cells after irradiations with boron and nitrogen ions. Materials and methods: The SCLC cell line U-1690, mutated in p53, was exposed in vitro to 2 Gy of low linear-energy-transfer (LET) photons (0.2 keV/ μ m) and high LET accelerated boron or nitrogen ions (40-140 keV/ μ m). The induction of apoptosis and other types of cell inactivation were measured using morphological scoring. In parallel, the cell cycle distributions were monitored by DNA-flow-cytometry. Results: Accelerated boron and nitrogen ions induced significantly elevated levels of post-mitotic apoptosis as compared to photons. Maximum levels of apoptosis of around 20-25 % were observed for medium LETs around 40 and 100 at 2 and 3 days after irradiation. Significantly increased levels of radiation-induced necrotic-apoptotic (60-80%) and ghost cells (5-27%) were found at 3-7 days after boron and nitrogen ion exposures, respectively. Conclusion: Light ion beams are suitable for treatment of tumours with defects in cell cycle arrest and apoptosis since elevated levels of apoptosis can be induced also in p53 mutated tumour cells that normally are insensitive to low LET induced apoptosis. More information on cell death inducing pathways in relation to tumour type, ion species and LET can be used to optimize the therapy outcome and quality of life for patients with resistant tumours difficult to treat with surgery, chemotherapy and/or conventional radiation therapy.

(PS6.15) Repair of DNA damage induced by high LET irradiation throughout the cell cycle: Survival and chromosomal aberration studies using synchronized CHO cells. Takamitsu A. Kato¹, Yoshihiro Fujii², Paul Wilson³, Akira Fujimori⁴, Penny Jeggo⁵, Ryuichi Okayasu⁴, ¹Colorado State University, Ft Collins, CO, ²University of Tokyo, Tokyo, Japan, ³Lawrence Livermore National Laboratory, Livermore, CA, ⁴National Institute of Radiological Sciences, Chiba, Japan, ⁵University of Sussex, Sussex, United Kingdom

In order to study the relative contribution of the two major DNA double-strand break (DSB) repair pathways, non-homologous end-joining (NHEJ) and homologous recombinational repair (HRR), to the repair of DSBs and non-DSB clustered DNA damage induced by high LET ionizing radiation through the cell cycle, we exposed wild type (WT), NHEJ-deficient, and HRR-deficient Chinese hamster ovary (CHO) cells synchronized by mitotic shake-off to accelerated heavy ions and X-rays. The cell cycle-dependent variation in survival observed in WT cells after X-irradiation was not observed after exposure to 500 MeV/amu iron ions. Non-homologous end joining (NHEJ) and homologous recombinational repair (HRR)-defective cells showed different patterns of cell cycle-dependent radiosensitivity after X-irradiation compared to WT cells, that were likewise significantly attenuated after iron ion exposures. Higher relative biological effectiveness for several other accelerated heavy ions (C, Ne, Si, Ar) of differing LETs was observed for cells exposed in S phase compared to cells

exposed in G1. We also observed that HRR deficiency, unlike NHEJ deficiency, did not affect the progression of irradiated G2 cells into mitosis, thus contributing to increased cell killing observed in G2-phase HRR-deficient cells. The HRR-deficient cells showed significantly increased levels of chromatid-type aberrations that correlated with their cell cycle pattern of survival after both X- and iron ion irradiation. Our results suggest that high LET radiation produces not only complex DSBs but also complex non-DSB clustered lesions that specifically require the HRR-mediated repair of these lesions if encountered during DNA replication.

(PS6.16) Water radiolysis with high-energy heavy ions: conversion of transient water radicals into stable product inside heavy-ion tracks. Shinichi Yamashita¹, Yosuke Katsumura², Jintana Meesungnoen³, Jean-Paul Jay-Gerin³, Mingzhang Lin¹, Yusa Muroya², Takeshi Murakami⁴, ¹Japan Atomic Energy Agency, Tokai-mura, Naka-gun, Ibaraki, Japan, ²School of Engineering, University of Tokyo, Bunkyo-ku, Tokyo, Japan, ³University of Sherbrooke, Sherbrooke, QC, Canada, ⁴National Institute of Radiological Sciences, Inage-ku, Chiba, Japan

Water radiolysis with high-energy heavy ions has been investigated through combination of yield measurement with scavenging method and track-structure simulation based on Monte-Carlo method. Deaerated aqueous solutions of 0.25 mM methyl viologen (MV) containing various concentration of sodium formate (HCOONa) were irradiated with He, C, Ne, Si, Ar and Fe ions of 135-500 MeV/u provided from HIMAC (Heavy Ion Medical Accelerator in Chiba) at NIRS, Japan. Water radicals such as hydrated electron (e_{aq}^-), hydroxyl radical (\cdot OH) and hydrogen atom (H) are scavenged by the solutes, leading to reduction of MV cation (MV^{2+}) into MV cation radical ($MV^{\cdot+}$), which is stable without oxygen and easily quantifiable by commonly-used off-line absorption spectroscopy. $HCOO^- + \cdot OH/H \rightarrow \cdot COO^- + H_2O/H_2$, $MV^{2+} + COO^- \rightarrow MV^{\cdot+} + CO_2$, $MV^{2+} + e_{aq}^- \rightarrow MV^{\cdot+}$. These scavenging reactions occur approximately at time scales estimated as the inverse of scavenging capacities, which are defined as the product of scavenger concentration and bimolecular rate constant for scavenging reaction. By changing formate concentration, yield of $MV^{\cdot+}$ was measured for the abovementioned heavy-ion beams. Then, the yield of $MV^{\cdot+}$ increased with decreasing LET and with increasing formate concentration. Specifically, $G(MV^{\cdot+})$ for He ions of 2.2 eV/nm in LET increased from 5.7 to 7.1 and that for Fe ions of 185 eV/nm in LET did from 2.2 to 4.1 (100 eV)⁻¹ with increasing formate concentration from 0.01 to 2 M. This fact shows that consumption of water radicals in intra-track reactions with time occurs and becomes more and more significant with increasing LET. In order to discuss more quantitatively, Monte-Carlo simulation code for water radiolysis with heavy ions named IONLYS-IRT, which has been developed by a group of University of Sherbrooke, was employed to reproduce our experimental results. Although a few reactions, which have not been reported yet, were needed to be added in the simulation, the experimentally measured $MV^{\cdot+}$ yields were well reproduced for wide ranges of ion-types, LET values and formate concentrations. Further, contribution of each elemental reaction in the simulation was separated from the others, and characteristics of intra-track dynamics were discussed, and possibility of non-negligible amount of "unexpected" reactions in heavy-ion tracks is indicated.

(PS6.17) Impact of sequential exposure to protons and iron ions in vivo. Polly Y. Chang, James Bakke, Abraham Wang, SRI International, Menlo Park, CA

As NASA's space exploration extends toward the moon and Mars, there is an increasing need to understand the potential risks of radiation exposure to humans in long-term manned space missions. In space, astronauts will likely be faced with exposure to a mixed field of radiation. The aim of our project is to examine the biological responses in the tissues after exposure to sequential exposure to particle radiations. Animals were exposed to a single dose of iron (Fe) ions, followed by a dose of protons (H). Another cohort of

animals was exposed to H, followed by Fe ions. Additional groups of animals were either sham treated or exposed to a single dose of either ions to serve as reference controls. Total reticulocytes (RET) and micronucleated reticulocytes (MN-RET) counts in peripheral blood were determined at 1 - 7 days post irradiation. Hippocampus and liver tissues were collected at 1 wk post irradiation to quantitatively probe for differential gene expression patterns. Our results indicate that there was a dose-dependent reduction in total circulating RET at 1 - 2 days after mixed H/Fe exposure, followed by a significant increase in RET counts at 3 - 7 days post irradiation. Similarly, a dose-dependent increase in MN-RET was evident at 1 day post irradiation. These values peaked at 2 days post irradiation. Gene expression in the hippocampus and liver tissues after mixed beams were compared to those obtained from animals that received either Fe or H alone. Results showed that gene expression profiles after mixed beams were significantly different from those that were exposed to either H or Fe ions. In addition, the sequence of ions appear to have a significant impact on targeted genes expressed in either tissues. These results show that, although sequential exposure to H or Fe ions induced transient genomic damage in the hematopoietic cellular compartment, such exposures altered the normal transcriptional regulation of genes involved in functionally important genes associated with neurotrophins and metabolism. These findings support our hypothesis that particle radiation effects are end-point- and tissue-specific. Information gathered from these studies will aid NASA in modeling human risks and setting standards for long term manned missions in space. The work is supported by NASA grant # NNX07AV20G.

(PS6.18) Adverse late HZE effects on marrow progenitors and recovery of bone from disuse. Ruth Globus¹, Joshua Alwood¹, Kenji Yumoto¹, Eduardo Almeida¹, Charles Limoli², ¹NASA Ames Research Center, Moffett Field, CA, ²University of California, Irvine, Irvine, CA

Therapeutic doses of radiation can cause bone loss that resembles age-related osteoporosis. The long-term effects of occupational radiation exposure to astronauts in space and radiation workers on earth are not known. We hypothesize that reduced mechanical loading that occurs in space due to microgravity and on earth due to inactivity or bedrest, renders skeletal tissue susceptible to damage from low dose radiation. We reported previously that total body irradiation of adult C57Bl6/J male mice with a relatively high dose of HZE (200 cGy, ⁵⁶Fe, 1GeV/amu), increases bone-resorbing osteoclasts leading to rapid bone loss and inhibits differentiation of bone-forming osteoblasts from marrow progenitors (osteoblastogenesis). However, a lower dose (50 cGy) inhibits osteoblastogenesis only if mice also are unloaded at the time of irradiation. To determine late effects of HZE, mice were irradiated with ⁵⁶Fe (1GeV/amu) then tissues harvested 6.5 mo. later; age-matched groups were hindlimb unloaded to cause musculoskeletal disuse for 10 days, irradiated, then released 3 days later to ambulate normally for 6.5 mo. Irradiation of normally loaded mice with 50 cGy did not affect fractional bone volume (an indicator of bone density), measured by 3D micro-computed tomography, relative to sham-irradiated controls; in contrast, if mice were hindlimb unloaded, irradiation with the same dose caused a 29-32% reduction in fractional bone volume compared to sham-irradiated controls either normally loaded or hindlimb unloaded (P<0.001, 1-factor ANOVA, Fisher PLSD). Detailed microarchitectural analysis revealed that transient unloading alone caused a loss of trabeculae (struts that comprise cancellous bone); irradiation of unloaded mice with 50cGy reduced fractional bone volume apparently by impairing adaptive thickening of residual trabeculae during the 6.5 month period of re-ambulation. Ex vivo marrow cultures revealed 50cGy profoundly inhibited osteoblastogenesis after 6.5 mo. We conclude that 50 cGy ⁵⁶Fe prevents skeletal recovery from disuse in the long term, which is likely to be caused by lasting damage to osteoprogenitors and stem cells in the marrow. Supported by NASA grant NNNH04ZUU005N/RAD2004-0000-0110 and by the Office of Science (BER), U.S. Department of Energy, Interagency Agreement No. DE-A02-09ER64784

(PS6.19) Techniques for whole body electron irradiation to simulate solar particle event dose distributions using a clinical

linear accelerator and dose verification with MOSFET dosimeters in conjunction with CT-based Monte Carlo dose calculations. Eric S. Diffenderfer, Stephen M. Avery, Jim McDonough, Ann R. Kennedy, Keith A. Cengel, University of Pennsylvania, Philadelphia, PA

In a solar particle event (SPE), the whole body of an unshielded astronaut could receive significant proton radiation exposures consisting mainly of protons with energies less than 50 MeV/n. This unique energy profile is predicted to produce a highly inhomogeneous dose distribution for which the dose-toxicity relationship is incompletely understood. Here, we present techniques for production of electron fields suitable for simultaneous whole-body irradiation of multiple animals to simulate the dose rate and dose distribution of an SPE using a Varian iX clinical linear accelerator. Electron fields with dose rates ranging from 54.5cGy/hr to 54.7cGy/min at the depth of maximum dose were obtained using a variety of beam scattering components and setup geometries. Systems for irradiation with nominal beam energies of 6MeV and a mixture of 80% 6MeV and 20% 12MeV were designed to simulate SPE dose distributions using a combination of Monte Carlo simulation of electron beam transport and experimental measurement. To approximate the dose rate expected in an SPE, scattering foils consisting of 2.37mm of aluminum were placed approximately 50cm from the beam source with the source to surface distance (SSD) set to 5m for the 54.5cGy/hr setup of the 6MeV beam. Under these conditions a field of 90cm x 90cm is achieved with variation from the central axis dose distribution of not more than 7%. Higher dose rates were obtained using no scattering foils for the 6MeV and 6+12MeV mixed beam with an SSD of 3.4 or 5m. Dose verification using both superficial and implantable MOSFET dosimeters were compared with Monte Carlo dose distribution and organ dose calculations based on the static animal CT images. These measurements showed significant deviation from predicted values, an effect attributed to animal motion during radiation exposures. In conclusion, we have simulated the dose distribution and dose rates that are compatible with astronauts' potential SPE exposure during an extra-vehicular activity (EVA). However, additional modeling to account for animal movement is necessary to reconcile measurement with calculation. Acknowledgement: This research was supported by the NSBRI Center of Acute Radiation Research (CARR) grant and NIH Training Grant 2T32CA009677. The NSBRI is funded through NASA NCC 9-58.

(PS6.20) Low dose and dose rate effects of proton irradiation on stem and precursor cells. Bertrand P. Tseng, Jennie Cho-Lim, Munjal M. Acharya, Erich Giedzinski, Katherine K. Tran, Mary L. Lan, Charles L. Limoli, Univ. of California, Irvine, Irvine, CA

Alterations in oxidative stress prime stem cell pools for the adaptation and remodeling of the irradiated tissues in which they reside. Throughout life these stem cells play critical roles in the development and maintenance of health. Their capability to continually regenerate proliferative, multipotent progeny provides the tissues of the body the means to counteract exposure to damaging agents, space radiation, disease and ageing. While the mechanisms regulating the responses of tissue-specific stem cells and their immediate progeny to stress are diverse, underlying themes are emerging that suggest changes in redox state are critical. Evidence from the musculoskeletal organ systems and CNS are highlighted that emphasize the importance of redox state to the stress response of their representative stem cells. We have examined the capability of low doses and dose rates of proton irradiation to modulate redox state in muscle and neural precursor cells. Radiation impairs the capability of muscle to undergo compensatory hypertrophy, and in mouse models deficient for antioxidant enzymes, elevated muscle wasting and impaired growth are evident. Our work demonstrates that low dose proton irradiation produces persistent oxidative stress in satellite cells. Our recent data also suggest that a fraction of radiation effects on muscle are mediated by pathways sensitive to changes in the level of nitric oxide thus altering proliferation. In the CNS, irradiation of multipotent neural stem and precursor cells has been shown to cause a persistent oxidative stress that impacts radiosensitivity. The nature, magnitude and duration of reactive species dictate whether these radiation-induced changes are harmful or beneficial to a variety of in vitro and

in vivo endpoints of viability and function. We believe that alterations found in oxidative stress are likely to underlie a portion of the radioadaptation elicited by low priming doses of protons to protect the precursors to a second higher challenge dose. Preliminary data suggests that the dose rate of the priming dose may have a key impact on the magnitude of the subsequent radioadaptation. Our results demonstrate the effects of irradiation on many stem cell compartments, and emphasize the importance of understanding the details of the redox microenvironment and stem cell niches.

(PS6.21) Space experiment “Rad Gene”-report: Analysis of DNA damage, p53-dependent gene expression and adaptive responses in human cells exposed to space radiations. Takeo Ohnishi, Akihisa Takahashi, Nara Medical University School of Medicine, Nara, Japan

The space environment contains two major biologically significant influences of microgravity and space radiations at low dose with low dose-rate containing high linear energy transfer particles. (1) To identify DNA damage induced by space radiations, phospho-H2AX (γ H2AX) foci formation was analyzed in two human cultured lymphoblastoid cell lines of TSCE5 (a wild-type *p53* gene) and WTK1 (a mutated *p53* gene) frozen in a freezer of International Space Station (ISS) for 133 days. Here, we show a track of the positive foci in them by immuno-cytochemical methods. We compared doses of space radiations between biological dosimetry by these frequencies and physical dosimetry by CR-39 and TLD. (2) To clarify the biological effects of space radiations and microgravity, gene and protein expression was analyzed from *p53*-dependent regulated manner by using DNA chips and protein chips, respectively. Under 1 gravity or microgravity condition, the cells were grown in a cell biology experimental facility of ISS for 8 days without the stresses during launching and landing. In addition, we analyzed the gene expression in the cells cultured on ground after space flight for 133 days with frozen condition. We report the results and discussion from the functions of the up-regulated and down-regulated genes after an exposure to space radiations and/or microgravity. (3) To clear the effect of space radiations on the radio-adaptive response, the cells kept at frozen state for 133 days in space were cultured for 6 h, and then exposed to challenging X-ray at 1.2 Gy or 2 Gy after landing. Cellular sensitivity, apoptosis, chromosome aberrations and mutation frequencies were scored. All of these radio-adaptive responses were found in *wtp53* cells, but not in the *mp53* cells. These results confirmed that the cells were exposed to space radiations with the specific low dose range (window; 20-100 mSv) which can lead to an adaptive response on ground-base experiments. The initial goal of “Rad Gene” space experiment was completely achieved. It is expected that data are useful in designing physical protection from the deleterious effects of space radiations during long term stays in space.

(PS6.22) Different modes of cell inactivation in prostate carcinoma exposed to high and low LET accelerated ions. Chitralakha Mohanty¹, Katarzyna Zielinska-Chomej¹, Margareta R. Edgren¹, Ryoichi Hirayama², Yoshitaka Matsumoto², Yoshiya Furusawa², Annelie E. Meijer^{1,2}, ¹Karolinska Institute, Stockholm, Sweden, ²National Institute of Radiological Sciences, Chiba, Japan

Purpose/Aim: To investigate and compare different modes of cell inactivation in two prostate cancer cell lines exposed to low and high LET carbon ions. Method: The prostate cancer cell lines PC-3 and DU-145 were *in vitro* exposed to low LET γ - and X-rays and high LET accelerated carbon ions (13-80 keV/ μ m) at the HIMAC, Chiba, Japan and the TSL, Uppsala, Sweden. The cells were irradiated with doses ranging from 0.25 Gy up to 8 Gy. Clonogenic cell survival assays were performed for establishment of dose response curves and to achieve the D_{10} dose. Cell samples were collected at different post-irradiation time points (a few minutes up to several days) for the D_{10} doses and for 2 Gy. These samples were analyzed for different modes of cell death (such as apoptosis, necrosis etc) using fluorescence microscopy and cell cycle alterations using flow cytometry. Also cell cycle arrest (senescence)

and autophagy were detected using molecular biology techniques. Results: Both the cell lines were more radiosensitive to accelerated ions as compared with photons. The PC-3 cell line was observed to be more radiosensitive than the DU-145. Low dose hypersensitivity was observed in the PC3 cells after low LET γ -ray. This was also observed in the Du145 cells after 13 keV/ μ m carbon ion exposure but not after low LET γ -rays. Different cell inactivation modes were observed in cells irradiated to either high or low LET carbon ions as compared with photon irradiations. Low LET carbon ion and photon irradiation showed cell killing through pure apoptosis where as high LET carbon ion irradiation resulted in giant cells with and without necrotic-apoptotic features and also higher levels of the total cell inactivation. Conclusion: High LET ion irradiations are considerably better than photons as higher total percentage of cell killing is achieved as compared to low LET ions and photons. Also, the differences in the modes of cell inactivation could suggest differences in the molecular signaling that occurs during irradiation with high and low LET accelerated ions.

(PS6.23) LET is a critical factor in accelerating development of lymphoma in irradiated Bax transgenic C57/B6 mice. James Jacobus, Chester Duda, Sean Martin, Mitchell Coleman, Kranti Mapuskar, Michael Knudson, Douglas Spitz, University of Iowa, Iowa City, IA

A major risk during exposure to both low and high linear energy transfer (LET) radiation is the development of lymphoma. Both occupationally and therapeutically exposed individuals are at risk for lymphoma development induced by low LET radiation, while deeply penetrating high LET radiation is a significant concern for those planning and undertaking long duration missions in space where a high degree of uncertainty on actual risk exists due to the lack of epidemiologically-based datasets. The C57/B6 transgenic mice used in this study have been genetically engineered to possess either one (Bax 1) or two (Bax 38/1) extra copies of the pro-apoptotic Bax gene under the T cell specific Lck promoter. Bax expression causes reduced cellularity of the thymus, increased relative cell proliferation, genomic instability, and development of T cell lymphoma, with an average age to death of 28 weeks in untreated Bax 38/1 animals and > 60 weeks for Bax 1 animals. Using these model systems we tested the hypothesis that overexpression of Bax would significantly affect lymphoma development in response to low (10 cGy) and high (100 cGy) dose radiation from either low LET or high LET sources. Mice were whole body irradiated using low LET radiation from a cesium-137 source or high LET irradiated with iron nuclei accelerated at Brookhaven National Laboratory, NASA Space Radiation Laboratory. Our results indicate that 100 cGy of 1 GeV iron in whole body irradiated double transgenic Bax 38/1 mice is significantly more potent at accelerating lymphoma development in the thymus than 100 cGy of low LET gamma rays. While this study is currently ongoing, at twenty-four weeks of age 80% (16/20) of 100 cGy high LET Bax 38/1 mice have died from lymphoma, versus 40% (5/12) of control Bax 38/1 mice. Low LET 10 and 100 cGy exposed Bax 38/1 and Bax 1 mice show a trend toward accelerated lymphoma development that is not dose-dependent nor statistically significant at this time. In contrast, there appears to be a dose response for accelerated lymphoma development using high LET radiation, with 10 cGy being less effective than 100 cGy in the Bax 38/1. These results suggest that the effects of high LET radiation on T cell lymphoma development may be greater than expected based on our low LET epidemiological data. (supported by a joint grant from DOE/NASA, DE-SC0000830).

(PS6.24) Response of Lymphocyte Populations in Different Strain Mice Irradiated with Iron Ions. Daila S. Gridley, Michael J. Pecaut, Loma Linda University & Medical Center, Loma Linda, CA

Purpose: Particle radiations could significantly impact astronaut health during space missions. However, crewmembers, like the human population in general, are likely to vary greatly in genetic background, and thus may also differ in immune responsiveness

after irradiation in the spaceflight environment. This study quantified the effects of iron ion radiation on various lymphocyte populations in two strains of mice differing in susceptibility to radiation-induced acute myeloid leukemia (AML) and thymic lymphoma (TL): C57BL/6 (AML resistant, TL susceptible) and CBA/Ca (AML sensitive, TL resistant). **Materials and Methods:** The animals (n = 60/strain) were irradiated with 56Fe26+ (1 GeV) to total doses of 0, 0.5, 2 and 3 Gy at a dose rate of 1 Gy/min and euthanized on days 4 and 30 thereafter; blood, spleen, and bone marrow were collected for flow cytometry analyses. Lymphocyte populations (CD4+ T, CD4+ Th, CD8+ Tc, B220+ B, NK1.1+ or panNK+ natural killer cells), and cells expressing CD25, CD71, CD34 and Sca1 molecules were quantified. **Results:** Exposure to radiation resulted in different distribution patterns in T, Th, Tc, B cells and leukocytes expressing activation (CD25, CD71) and progenitor (CD34, Sca1) markers in the two strains of mice. Significant main effects (p<0.05) were dependent upon strain, as well as radiation dose, body compartment, and time of assessment. Especially striking differences were noted between the two strains after 3 Gy, including differences in the CD4:CD8 ratio (day 4 blood; day 30 spleen), %CD25+ mononuclear cells in bone marrow (day 4) and %CD34+Sca1+ cells in the CD45lo gate in bone marrow (day 4). Numerous strain differences were also noted in the non-irradiated mice. **Conclusion:** The results show that genetic background, as well as radiation dose and time post-exposure, had a profound impact on lymphocyte populations, as well as other leukocytes, after exposure to iron ion radiation. It remains to be determined, however, whether any of the effects correlate with increased risk for neoplasia, as has been reported after exposure to photons.

(PS6.25) The combined effects of radiation and reduced weightbearing in a mouse model system. Jolaine M. Wilson¹, Jenine K. Sanzari¹, Gabriel S. Krigsfeld¹, Erika B. Wagner², Ann R. Kennedy¹, ¹University of Pennsylvania, Philadelphia, PA, ²MIT, Cambridge, MA

With the desire to further increase exploration of space, as well as a growing interest in space tourism, it is important to know the long- and short-term effects of space flight. The space environment, specifically psychological stress, radiation exposure, and hypogravity can impact many physiological and immunological systems. It has been found that reduced weightbearing and radiation both produce changes in white blood cell counts and have effects on immunologic function. As part of the Center for Radiation Research (CARR), we examined the effects of combined exposure to reduced weightbearing and radiation on hematopoietic cell loss, comparing the more traditionally used animal model of full loading, hindlimb suspension, with a recently developed system known as the Partial Weight Suspension (PWS) system. Six-week old female ICR mice were irradiated with 50, 100 and 200cGy with a Cs-137 irradiator and then either hindlimb suspended or placed in the PWS system at 16% quadrupedal weightbearing for 4 hours, 24 hours, 48 hours or 4 days at which point complete blood counts were obtained. Control animals were exposed to identical conditions without exposure to radiation, hypogravity or both. Comparing the hindlimb suspension system and the PWS systems alone, there were minimal differences observed in the total white blood cell (WBC), neutrophil or lymphocyte counts. To the 48 hour time point and with the addition of radiation, both radiation dose and PWS alone were significant factors affecting the WBC and lymphocyte counts. PWS was a significant factor affecting neutrophil count. The interaction between radiation dose and PWS for WBC count and lymphocyte count is significant, as is the interaction between radiation dose and time after irradiation. From our data, when assessing complete blood cell counts, the hindlimb suspension model is equivalent to the PWS system. When examining the combined effects of radiation and PWS, there appears to be a synergistic effect on WBC and lymphocytes counts. **Acknowledgements:** This research was funded by the NSBRI through NASA NCC 9-58.

(PS6.26) Spatial memory and attentional set shifting are significantly impaired following low hze doses. Richard A. Britten¹, Angela Johnson¹, Leslie Davis¹, Brian Parris¹, Gyorgy

Lonart¹, Shamina Green-Mitchell¹, Larry Sanford¹, Sylvia Singletary², Richard Drake¹, ¹Eastern Virginia Medical School, Norfolk, VA, ²Veterinary Consulting Services, Chesapeake, VA

Introduction. Current models predict that the astronauts will be exposed to ~25 cGy of HZE radiation on a deep space mission. Our studies are designed to define the HZE dose that will lead to defects in complex working memory, and also to elucidate the mechanisms whereby HZE radiation diminishes neurocognitive function. **Materials & Methods.** Four-week old male Wistar rats were exposed to either X-rays or 1 GeV 56Fe (Hze) particles. At 3, or 6, months post exposure the performance of the rats in the Barnes' Maze (Spatial memory) and the Attentional Set Shifting Test (Executive function) was established. The brain proteome of rats with good or bad spatial memory(SM) performance following Hze exposure was established using MALDI-MSI to identify the underlying cause of the Hze-induced cognitive impairment. **Results.** 11.5 Gy of X-rays led to impaired SM, in contrast, 20 cGy Hze was sufficient to impair SM at 3 months post exposure. Attentional set shifting (ASST) performance was also impacted following exposure to 20 cGy Hze. Eleven pairs of HZE irradiated (20 cGy) and control litter mates were assessed for ASST: 8/11 of the control rats were capable of working through all 7 paradigms of the test; only 3/11 of the irradiated rats managed to complete all the paradigms. Even with these numerical limitations we have shown that 20 cGy Hze results in a significant impairment of Simple Discrimination, Intra-Dimensional Shift and Extra Dimensional Shifts. Using MALDI-MSI, we have found that a peptide with a m/z of 14207 is differentially elevated in the Thalamus of irradiated rats that have good SM following HZE exposure. MALDI-MSI thus appears to be a powerful tool that can be used to identify HZE-induced changes in ancillary brain regions that correlate with neurocognitive impairment, and will ultimately be useful for identifying proteins whose expression changes in parallel with Hze-induced neurocognitive deficits. **Summary.** We have found that mission-relevant Hze doses (20 cGy) lead to significant neurocognitive defects. Clearly such low doses of Hze are unlikely to lead to a significant loss of neuronal cells, and have not been reported to lead to gliosis etc. We take this as further evidence that neurocognitive impairment is not solely dependent upon radiation-induced changes in neurogenesis and neuronal cell death.

(PS6.27) Effects of exposure to 56Fe particles on cognitive performance in male and ovariectomized female rats. Bernard M. Rabin¹, Kirsty L. Carrhill-Knoll¹, James A. Joseph^{2,2}, Barbara Shukitt-Hale², Katharine Luskin², Lauren V. Long¹, ¹Dept. of Psychology, Baltimore, MD, ²HNRCA/USDA, Boston, MA

On exploratory class missions astronauts will be exposed to types and doses of radiation (HZE particles) that are not experienced in low earth orbit. While it is likely that the crew will consist of both male and female astronauts, there has been little research on the effects of exposure to HZE particles on cognitive performance in female subjects. Ovariectomized (OVX) female rats were obtained from Taconic Farms. Thirty mm segments of silastic tubing containing either 180 pg 17β-estradiol/mL in sesame oil or vehicle alone were implanted subcutaneously in the neck. Three days following surgery the rats were exposed to 56Fe particles (1000 MeV/n, 0-200 cGy) at the NSRL. Following irradiation the rats were shipped to UMBC for behavioral testing using the elevated plus-maze, operant responding and novel object recognition tasks. The results indicated that the pattern of decrements in cognitive performance differed between estradiol- and vehicle-implanted subjects as well as between the specific tasks. On the plus-maze, the vehicle implanted subjects showed a dose-independent decrease in the amount of time spent exploring the anxiety-producing open arms of the maze; the estradiol implanted subjects showed a non-significant, but dose-dependent, decrease in exploration. Exposing the vehicle implanted subjects to 56Fe particles did not disrupt operant responding, but did cause a significant decrease in responding in the estradiol-implanted subjects exposed to the higher doses (150 and 200 cGy). Exposure to 56Fe particles did not affect responding on the novel object recognition task in either the estradiol or vehicle implanted subjects. These results suggest that estradiol may not be neuroprotective for the cognitive/ behavioral effects of exposure to HZE particles at the time of irradiation. Also,

the pattern of results suggests that females may respond to exposure to ^{56}Fe particles differently than do males. Additional research will be necessary to determine how estrogen affects behavioral responding following exposure to HZE particles and to define the differences in the patterns of performance decrements between males and females. This research was supported by Grant NNX08AM66G from NASA.

(PS6.28) Proton and Gamma-Ray Dose Rate Effects for Chromosome Aberration Induction. Yuanlin Peng, Hatsumi Nagasawa, Christy L. Warner, Joel S. Bedford, Colorado State University, Fort Collins, CO

During a solar particle event (SPE) astronauts on a mission may receive as much as 2 Gy over a 1 to 2 day period. This corresponds to a dose-rate of about 0.08 Gy/h at the high end of the low dose-rate range. Previous gamma-ray dose-rate effects for various damage endpoints indicate little change in effect per unit dose as dose-rates are reduced further below about 10 to 20 cGy/hour. The effect per unit dose does not increase much as dose rates are increased above about 20 cGy/minute. To limit the exposure time at a low dose-rate to a reasonable length in consideration of NSRL facilities limitations, we carried out our experiments using exposure times up to 10 hours and total doses up to 3 Gy. This would correspond to a "low dose rate" of 0.5 cGy/min and for the "high dose rate", about 70 cGy/minute. Three human cell lines were irradiated with either 1GeV protons or 150 MeV protons at NSRL at Brookhaven National Laboratory. We included the 1 GeV protons because of the possibility that production of neutrons by these higher energy protons may alter the effect per unit dose at the low dose rates more than it would from the high dose rate. Recently we have also carried out experiments using lower energy protons (50 MeV). Parallel samples were irradiated with gamma rays at the same dose rates. An appreciable dose rate effect was seen for both gamma rays and protons in this energy range. The total doses delivered were 1.0, 2.0, and 3.0 Gy at both high and low dose rates. The results so far indicate a significant dose rate effect for three the low passage human fibroblasts irradiated in the G₀/G₁ state. A dose rate effectiveness factor, DREF (rather than a DDREF) of about 1.9 was estimated, and was the same for both gamma-rays and protons in these energies and for these dose rates. This work is supported by grant # NN07AP85G from the National Aeronautics and Space Administration.

(PS6.29) Radiosensitization by inhibiting survivin in human hepatoma HepG2 cells to high-LET radiation. Xiaodong Jin, Qiang Li, Institute of Modern Physics., Lanzhou, China

In this study, we investigated whether survivin plays a direct role in mediating high-LET radiation resistance. We designed small interfering RNA (siRNA) targeting survivin mRNA and transfected into human hepatoma HepG2 cells. Real-time PCR and western blotting analysis revealed that survivin expression in HepG2 cells was decreased at both transcriptional and post-transcriptional levels after treatment with survivin-specific siRNA. Following exposure to high-LET carbon ions, a reduced clonogenic survival effect and an increased apoptotic rate were observed in the cells treated with the siRNA compared to those untreated with the siRNA. The cells with transfection of the survivin-specific siRNA also increased the level of G₂/M arrest. Moreover, in the intrinsic apoptotic pathway, caspase-9 expression and caspase-3 activity obviously increased in the siRNA-treated cells in relation to those of the other groups at 5Gy. These results suggest that survivin definitely plays a role in mediating the resistance of HepG2 cells to high-LET radiation and depressing survivin expression might be useful to improve the therapeutic efficacy of heavy ions for radioresistant solid tumors.

(PS6.30) The effects of space radiation on the prothrombin and partial thromboplastin times of irradiated ferrets. Gabriel Krigsfeld, Ann Kennedy, University of Pennsylvania, Philadelphia, PA

Future plans by NASA include manned space flights occurring over extended periods of time. These "exploration class" missions have augmented the risk of astronaut exposure to space radiation from a solar particle event (SPE). Of particular interest are the effects of space radiation on the cardiovascular system. Detrimental effects of ionizing radiation (IR) have been reported in atomic bomb survivors, those exposed to fall-out from the Chernobyl accident, radiological technicians, and cancer patients. Previous studies have shown that endothelial cell exposure to IR can alter the expression of genes/proteins in the coagulation cascade; these expression changes include: transcription of the von Willebrand Factor gene, increased levels of tissue factor, and a decrease of thrombomodulin levels. In these studies, ferrets have been exposed to SPE-like radiation, in vitro assays such as prothrombin time (pT) and activated partial thromboplastin time (aPTT) were employed to measure the intrinsic/extrinsic coagulation pathways. Upon arrival, ferrets were acclimated and pre-IR blood draws were performed. Ferrets were exposed to total body irradiation, using 110 MeV/n protons at doses of 25, 100, or 200 cGy, at a high dose rate (HDR) of 50 cGy/min or a low dose rate (LDR) of 50 cGy/hour. Ferrets were anesthetized 4h post-IR and blood was drawn. Isolated plasma was analyzed for pT/aPTT using START 4 instrumentation. Our results indicate that exposure to all proton doses led to increased pT clotting times ($p < 0.05$), with values increasing from 21.64 up to 28.40s. Further analysis showed LDR exposure enhanced this effect compared to HDR exposure. The intrinsic (aPTT) pathway was only affected by LDR exposures, which resulted in 20-30% elongation in clotting time from 31.95s to 36.62s ($p < 0.05$). HDR radiation exposure showed no effect on the aPTT pathway. In conclusion, clotting delays in pT/aPTT times could indicate deficiencies in proteins vital to the clotting cascade or could be a result of increased anti-coagulant inhibitors present in the circulation. Future studies will evaluate the molecular and cellular mechanisms of clotting prolongation. Ferret blood samples were obtained through the NSBRI CARR grant "tissue sharing" activities. The NSBRI is funded through NASA NCC 9-58. NIH Training Grant 2T32CAW9677.

(PS6.31) Cytokine profiles induced by exposure to low-dose radiation and simulated solar particle event protons. Asma rizvi, Xian Luo-Owen, Daila S. Gridley, Loma Linda University, Loma Linda, CA

Radiation/oxidative stress can alter the overall pattern of cytokine secretion, an integral part of host defense mechanisms. Studies of crewmembers on space missions have reported decreased production of interferon (IFN) α/β and other cytokines after return from flight, findings that may be at least partly related to radiation exposure. In the present study, C57BL/6 mice were low-dose/low-dose-rate (LDR) γ -irradiated (57Co) to a total dose of 0.05 Gy (0.024 cGy/h) and subsequently exposed to 2Gy simulated solar particle event (sSPE) protons over 36h. At 21 days post-irradiation, spleens were excised and leukocytes were evaluated for intracellular IFN- γ , IL-2 and TNF- α ; anti-CD3 monoclonal antibodies and PMA/I and were used to activate leukocytes for quantification of 22 secreted cytokines/chemokines. A significant increase was observed in the number of cells stained for intracellular IFN- γ after LDR+sSPE compared to 0Gy and LDR ($P < 0.05$), with a trend towards increase for LDR+sSPE versus sSPE ($P < 0.1$); cells with IL-2 and TNF- α showed no significant changes. After activation with anti-CD3, concentrations of IFN- γ , MIP-1 α , GM-CSF and RANTES were significantly increased in supernatants from all irradiated groups compared to control ($P < 0.001$), with a trend for high TNF- α when sSPE or LDR+sSPE groups were compared to 0Gy ($P < 0.1$). After PMA/I activation, concentration of MIP-1 α was significantly decreased in LDR+sSPE and LDR, but not sSPE, groups compared to control ($P < 0.001$). MCP-1 was increased after LDR+sSPE versus control ($P < 0.05$), while there was a trend towards increase versus sSPE ($P < 0.1$). RANTES was significantly decreased in all irradiated groups compared to LDR ($P < 0.05$). IL-7 and IL-9 after radiation were below the control level in supernatants activated by anti-CD3 and PMA/I. To conclude, we can say that anti-CD3 monoclonal antibodies and PMA/I shows different activation patterns in response to radiation, and cytokine patterns in response to sSPE were minimally affected by pre-exposure to LDR.

(PS6.32) Space radiation-induced cytogenetic damage in the blood lymphocytes of astronauts: persistence of damage after flight and the effects of repeated long-duration missions. Kerry George¹, Jordan Rhone², Lori Chappell³, Francis Cucinotta⁴, Wyle Labs, Houston, TX, ²U of H, Houston, TX, ³USRA, Houston, TX, ⁴NASA, Houston, TX

Cytogenetic damage was assessed in blood lymphocytes from astronauts before and after they participated in long-duration space missions of 3 months or more. The frequency of chromosome damage was measured by fluorescence *in situ* hybridization (FISH) chromosome painting before flight and at various intervals from a few days to many months after return from the mission. For all individuals, the frequency of chromosome exchanges measured within a month of return from space was higher than their preflight yield. However, some individuals showed a temporal decline in chromosome damage with time after flight. Statistical analysis using combined data for all astronauts indicated a significant overall decreasing trend in total chromosome exchanges with time after flight, although this trend was not seen for all individuals and the yield of chromosome damage in some actually increased with time after flight. The decreasing trend in total exchanges was slightly more significant when statistical analysis was restricted to data collected more than 220 days after return from flight. Limited data from astronauts who participated in multiple long-duration flights showed a lack of correlation between time in space and translocation yields. Data from three crewmembers who had participated in two separate long-duration space missions provided information on the effect of repeat flights and showed a possible adaptive response to space radiation exposure.

(PS6.33) Cytogenetic effects of chronic low-dose high-LET radiation on mice in vivo. Svetlana Sorokina¹, Svetlana Zaichkina¹, Olga Rozanova¹, Sergey Romanchenko¹, Helena Smirnova¹, Vladimir Peleshko², ¹ITEB RAS, Pushchino, Russian Federation, ²Institute of High Energy Physics, Protvino, Russian Federation

In the present work, we studied the effect of low-dose-rate high-LET radiation in the dose range of 0.005-0.16 Gy that simulates the spectral and component composition of radiation fields formed in the conditions of high-altitude flights on mice in vivo. The dose dependence, adaptive response (AR), and genomic instability (GI) in F1 and F2 generations born from irradiated males were examined in bone marrow cells using the micronucleus (MN) test. Irradiation of SHK mice was performed for 24 h a day in the radiation field behind the concrete shield of the accelerator of 70 GeV protons (Protvino) to accumulate doses of 0.005, 0.02, 0.05, 0.09 and 0.16 Gy (0.0043 Gy/day). For induction of AR, mice were exposed to radiation according to the following scheme: adapting doses of 0.005-0.16 Gy of high-LET radiation, followed after a day by a challenging dose of 1.5 Gy of X-rays (1 Gy/min). To reveal the GI, one group of males, offspring of chronically irradiated and unirradiated parents, were subjected to additional irradiation with a dose of 1.5 Gy of X-rays. Another group of males were exposed to X-irradiation by the standard scheme of AR (0.1 Gy+1.5 Gy). The experiments demonstrated that: 1) irradiation of mice with all doses leads to an increase in the level of cytogenetic damage compared with the level of spontaneous; 2) as opposite to X-rays, high-LET irradiation of mice with these doses induces no AR in polychromatic erythrocytes (PCE); 3) the levels of spontaneous PCE with MN in mice of the F1 and F2 generations born from males irradiated with doses of 0.005 and 0.16 Gy and in unirradiated animals are the same; 4) in mice of the F1 and F2 generations born from males irradiated with a dose of 0.005 Gy, the radiosensitivity to additional irradiation with a dose of 1.5 Gy of X-rays did not differ from that of the offspring of unirradiated males; 5) in mice of the F1 generation that were irradiated by the standard scheme of AR, AR is absent, whereas in mice of the F2 generation AR is induced; and 6) in mice of the F1 and F2 generations born from males irradiated with a dose of 0.16 Gy, the sensitivity to additional irradiation with a dose of 1.5 Gy of X-radiation increases and AR does not occur. These findings may be used to estimate radiation risks from long-term high-altitude aircraft and space flights and to elaborate the theoretical basis for adaptive medicine.

(PS6.34) Effects of radiation on blood cell numbers in mice exposed to whole body irradiation from gamma and electron radiation. Ana L. Romero-Weaver, Jeffrey H. Ware, Ann R. Kennedy, University of Pennsylvania, Philadelphia, PA

As part of the activities of the NSBRI Center of Acute Radiation Research (CARR), the effects of solar particle event (SPE) radiation on peripheral blood cell counts are being evaluated to determine the risks to astronauts from blood cell loss. From the data obtained, Relative Biological Effectiveness (RBE) values are being determined in which the results from SPE radiation are compared to those from a reference radiation. In these studies, both electrons and gamma radiation are being utilized in different experiments as the reference low Linear Energy Transfer (LET) radiations. Whole body irradiation can cause a decrease in the number of blood cells which can be due to killing of the circulating cells and/or loss of precursor cells and/or loss of cells from the circulation by hemorrhage. The doses of SPE (primarily proton) radiation that astronauts can be exposed to during extravehicular activity (EVA) include doses as high as 2 Gy (deep dose). The methods used for determining the numbers of blood cells in irradiated animals have been established. Two methods utilized to determine White Blood Cell (WBC) differential counts in mice (manual and automated cell counts) exposed to 0.25, 0.5, 1 and 2 Gy of 6-MeV electrons at a dose rate of 0.5 Gy/minute or 0.5 Gy/hour were compared. The results demonstrated a close correlation and a high degree of agreement between manual cell counts determined in our laboratory and those determined from automated counts at Antech Diagnostics. In experiments performed with gamma (2 Gy) or electron radiation (6 MeV, 1 Gy), the effects on whole body irradiation were evaluated utilizing a single high dose rate at numerous time points out to 30 days post-irradiation. At periods of time within the first day post-irradiation, WBC counts and lymphocyte counts were significantly reduced. Both neutrophil and lymphocyte counts reached their lowest numbers by day 2 post-irradiation. By 30 days post-irradiation the levels of these blood cells returned to normal levels. These results indicate that with a single acute dose as high as 2 Gy, blood cell numbers are significantly reduced for short time periods post-irradiation, but that there is no long-term effect on blood cell numbers for either electron or gamma radiation exposure.

(PS6.35) Boron neutron capture in prostate cancer cells. Linda S. Yasui¹, Samantha Gladden¹, Christine Andorf², Thomas Kroc³, Sajit Bux⁴, Narayan Hosmane¹, ¹Northern Illinois University, DeKalb, IL, ²Northern Illinois University Institute for Neutron Therapy at Fermilab, Batavia, IL, ³Fermi National Accelerator Laboratory, Batavia, IL, ⁴Kishwaukee Community Hospital, DeKalb, IL

A proof of principle study was designed to show that a cytotoxic boron neutron capture reaction is achievable using the modified enhanced thermal neutron beam irradiation set-up developed at Northern Illinois University Institute of Neutron Therapy (NIU INT) at Fermilab. The boron containing compound, p-boronophenylalanine (BPA) was used for these studies. Low solubility of BPA limited our ability to treat cells with a wide range of concentrations of BPA. The highest concentration of BPA that dissolved in medium was 6 mM. A higher concentration of (12 mM) of BPA could be dissolved in Hank's balanced salt solution (HBSS). No cellular toxicity (measured using the clonogenic assay) from continuous exposure of cells to 2, 4.9 and 6 mM BPA in medium was observed in human prostate cancer, DU 145, cells. In contrast, slight toxicity from a 3 hour treatment with 6 mM BPA in HBSS was detected. Statistically significant toxicity was observed for DU 145 cells treated with 12 mM BPA in HBSS for 3 hours. A non-toxic concentration of 4.9 mM was used for the boron neutron capture studies. Intracellular BPA concentration, quantitated by inductively coupled plasma mass spectroscopy (ICP MS), increased after depletion of amino acid pools in cells by a 1 hour pre-treatment with HBSS. Human prostate cancer cells, DU 145, were treated with 4.9 mM BPA for 3 hours to load a sufficient number of boron atoms into each cell. BPA loaded cells were transported to NIU INT at Fermilab and irradiated. After a 10 day colony formation time, colonies were fixed and stained. A clear increase in cell killing in the BPA loaded cells was observed. These data provide a proof-of-

principle showing an enhancement in cell killing from a boron neutron capture reaction.

(PS6.36) Investigation of proton and gamma radiation on white blood cell counts in mice. Casey J. Maks¹, Jeffrey H. Ware¹, Ana Romero-Weaver¹, Jenine K. Sanzari¹, Jolaine M. Wilson^{1,2}, Steven Rightnar³, Andrew J. Wroe³, Daila S. Gridley³, James M. Slater³, Ann R. Kennedy¹, ¹Department of Radiation Oncology, The University of Pennsylvania School of Medicine, Philadelphia, PA, ²University Laboratory Animal Resources, University of Pennsylvania, Philadelphia, PA, ³Department of Radiation Medicine, Loma Linda University, Loma Linda, CA

As NASA focuses space exploration beyond lower Earth orbit, thereby extending mission time, astronauts will be at a greater risk of exposure to solar particle event (SPE) radiation. In addition to the late effects seen due to space radiation exposure, including cancer, cataracts and neuronal disease, immediate effects after exposure are of prime importance due to potential mission threatening consequences. Protons are a major component of SPE radiation and are a primary focus of investigation of SPE-like radiation effects on white blood cells (WBCs) in mice. ICR mice aged 5-6 weeks were purchased from Harlan Laboratories (Livermore, CA) and total-body irradiated with gamma and proton radiation according to an approved Animal Care and Use Committee Protocol at Loma Linda University & Medical Center (LLUMC). Gamma irradiation was performed with a ⁶⁰Co source (LLUMC) at a dose rate of 50 cGy/min. Proton irradiation was completed at the same dose rate using 70 MeV protons (LLUMC) with a spread out Bragg peak (SOBP), which was determined to be a homogenous dose distribution for 4 cm (the width of the chamber in which the mice were irradiated). At 24 hours after the completion of the radiation exposure, six mice at each radiation dose were sacrificed and blood was collected for complete blood cell analysis in each experiment. Two separate experiments were performed with both 70 MeV protons and ⁶⁰Co gamma radiation at doses of 25, 50, 100 and 200 cGy. For gamma and proton radiation, at 24 hours post-irradiation, the mean WBC count for the mice irradiated with 50-200 cGy doses were statistically significant when compared to the sham-irradiated mice. For these experiments the relative biological effectiveness values were not significantly different from one. These data demonstrate a significant decrease in WBCs after SPE-like proton radiation even with relatively low doses, like those which could be experienced by astronauts from SPE radiation. These results do not rule out a potential effect from SPE radiation that may threaten mission performance or require treatment during space exploration. Acknowledgements: This research was supported by the NSBRI Center of Acute Radiation Research (CARR) grant, LLU/NASA Cooperative Agreement NNX08AP21G and NIH Training Grant 2T32CA009677. The NSBRI is funded through NASA NCC 9-58.

(PS6.37) Dependence on p53 status of in-vitro migration and invasion in human lung cancer H1299 cells irradiated with X-rays and carbon-ions. Hiroshi Maezawa¹, Atsushi Itami², Seikou Kim², Hiroyuki Sato², Ryoichi Hirayama³, Yoshiya Furusawa³, ¹Institute of Health Biosciences, University of Tokushima, Tokushima, Japan, ²Graduate School of Health Sciences, University of Tokushima, Tokushima, Japan, ³National Institute of Radiological Sciences, Heavy-Ion Radiobiology Research Group, Chiba, Japan

The present study examined whether radiation-induced migration and invasion activities depend on p53 gene status in p53-null human lung cancer H1299 cells which were transfected with a vector carrying a wild- or mutant-type p53 gene (H1299/wtp53, H1299/mtp53) or control vector (H1299/neo). Cells grown on T25 flasks or dish (60 mm) were exposed to carbon-ions (290MeV/n) at HIMAC or X-rays (150 kV). To obtain RBE of lethality of carbon-ions cell survivals were obtained from the colony formation assay immediately after irradiation. The migration and invasion activities in cells exposed to X-rays and carbon-ions were measured with a cell culture insert membrane (8 micron pore size) coated with Matrigel or fibronectin. The number of cells (Nt) moved

on lower side of membrane after 24h were counted under microscope after staining with crystal violet. Rate of migration or invasion of cells was calculated as the ratio of Nt to total number of viable (trypan blue-exclusion) cells plated in the culture insert membrane. Invasion rates increased slightly in H1299/wtp53, H1299/mtp53 and H1299/neo cells after X-ray irradiation at 1 and 2 Gy as compared with control (unirradiation). Invasion rate of H1299/neo, H1299/wtp53 and H1299/mtp53 irradiated with 100keV/μm carbon-ions decreased with increasing dose above 0.5Gy. Migration rate reduced in H1299/mtp53 and H1299/neo cells after X-ray irradiation at 1 and 2Gy, but did not in H1299/wtp53. In the case of carbon-ion irradiation at 100keV/μm and 40keV/μm, migration was also inhibited in three cell lines with dose dependent manner. Present results suggest that the migration activity depends on p53 gene status in cells exposed to X-rays, but carbon-ion irradiation causes the reduction of migration and invasion activities of cells independently of p53 status of cells.

(PS6.38) Biological risk of GCR determined using PHITS simulation. Brad Cox, Texas A&M University, College Station, TX

Galactic Cosmic Rays (GCR) pose a substantial cancer risk for humans in space. Uncertainties in risk estimates, caused by the interaction of GCR in human tissue, stem primarily from uncertainties in quality factors. Effective dose, calculated using a quality factor, is not specific enough to predict the differences in damaging ability of the components of the GCR spectrum. The ICRP notes the uncertainties involved by emphasizing that the quality factor and individual tissue weighting factors are designed for general radiation protection practices and serve only as rough indicators of risk, not actual risk assessment. Quality factor doesn't account for differences in particle tracks of different ions with equal LET. The Bethe-Bloch approximation to energy loss shows that ions of different atomic number and equal kinetic energy per nucleon deposit their energy at different rates since their stopping powers are based on the square of their charge. This approach doesn't account for processes other than Coulomb interactions, such as production of recoil particles and target and projectile fragmentation. The LET can be equal for different particle species with different velocities but radiobiological studies often indicate differing levels of damaging ability. To improve individual risk estimates, differences in damaging ability of different ions will be used to derive new weighting functions based on charge and velocity for particles in the GCR spectrum. Transport modelling that accounts for all processes along the path of the ion, rather than electromagnetic energy loss alone, will be used. This technique allows simulation of single particle traversals through individual cells as well as a macroscopic view of total energy deposition and particle fragmentation. Using the Particle and Heavy Ion Transport code System (PHITS), this poster presents the variations in particle traversals in tissue for ions of equal LET but different atomic number.

(PS6.39) Effects of fractionated irradiation with carbon ions on gut crypt survivals and tumors. Koichi Ando¹, Sachiko Koike², Akiko Uzawa³, Ryoichi Hirayama², Yoshitaka Matsumoto³, Yoshiya Furusawa³, Nobuhiko Takai⁴, Takeshi Fukawa⁵, Yukari Yoshida¹, ¹Gunma University, Maebashi, Japan, ²Natl Inst. Radiol. Sci., Chiba, Japan, ³Natl. Inst. Radiol. Sci., Chiba, Japan, ⁴Nagasaki International University, Sasebo, Japan, ⁵Josai International University, Togane, Japan

Effects of fractionated irradiation with carbon ions on gut crypt survivals and tumors Purpose: We have previously reported that RBE values of carbon-ion beams for skin reaction and tumors increases with an increase of fractionation in a different way so that therapeutic gain is maximally obtained at around 4 fractions. Purpose of present study is to compare survivals of crypts and tumor cells after multiple 1 Gy per fraction followed by top-up doses. Materials and Methods: C3H male and female mice at age 8-12 week old were used. NFSa fibrosarcoma was subcutaneously transplanted to ventral skin of male mice 10 days before irradiation. Carbon ions with 290 MeV/u were accelerated by HIMAC synchrotron, and LET of 20 keV/micrometer at entrance plateau of a Spread-Out Bragg peak (6 cm width) was used. Mice were immobilized by placing in Lucite holders without anesthesia, and

received horizontal beams every 4 hr. Tumors were removed shortly after final irradiation, and preceded to single cell preparation. Cell suspensions were intravenously injected to recipient mice that were pretreated with cyclophosphamide, and lung colony assay was conducted. Jejunum of female mice was removed 3.5 days after final irradiation and served for histology preparation. Results: Survival curves for crypts and tumor cells were obtained after single doses, 1 Gy x 5 fractions plus top-up doses and 1 Gy x 11 fractions plus top-up doses. The NFSa tumor showed biphasic curves after single doses, suggesting oxic and hypoxic cells included. Slopes of survival curves fit by single hit model were not significantly different between single doses and fractionated doses, even though single doses showed a lightly shallower curve than the fractionated doses. Crypt survivals plot against total doses clearly shifted to the right after fractionated doses: 1 Gy x 5 fractions moved survival curves parallel to single doses while 1 Gy x 11 fraction not only moved further to the right but also showed a shallower slopes that either single or 1 Gy x 5 fractions. Conclusion: Repair of damage caused by 1 Gy of low-LET carbon ions was different between the NFSa tumor and gut crypts. Therapeutic gain was apparently larger for 11 fractions than 5 fractions.

(PS6.40) Gap-junction communication and oxidative metabolism mediate the propagation of toxic effects between alpha-particle irradiated human cells. Narongchai Autsavaprom¹, Sonia M. de Toledo¹, John B. Little², Jean-Paul Jay-Gerin³, Andrew L. Harris⁴, Edouard I. Azzam¹, ¹New Jersey Medical School-Cancer Center, UMDNJ, Newark, NJ, ²Harvard School of Public Health, Boston, MA, ³University of Sherbrooke, Sherbrooke, QC, Canada, ⁴New Jersey Medical School, UMDNJ, Newark, NJ

Coordinated interactions of specific molecular and biochemical processes are likely involved in the cellular stress response to different types of ionizing radiation. Here, we investigated the roles of gap-junction intercellular communication and oxidative metabolism in modulating cell killing and repair of potentially lethal damage (PLDR) in confluent normal human fibroblasts exposed to ²⁴¹Am α particles or ¹³⁷Cs γ -rays at doses by which all cells in the exposed cultures are irradiated. As expected, α particles were more effective than γ -rays at inducing cell killing. Whereas PLDR occurred in γ -irradiated cells, holding α particle-irradiated cells in the confluent state for various times resulted in increased cell killing, which was associated with increased DNA damage, protein oxidation and lipid peroxidation. Inhibiting gap junction communication with 18- α -glycyrrhetic acid or knockdown of the level of connexin43, a constitutive protein of junctional channels, by siRNA, promoted protective effects in α particle-irradiated cell cultures; it decreased induced DNA damage and enhanced clonogenic survival. Using human adenocarcinoma cells in which specific connexins can be expressed in the absence of endogenous connexins, we found that permeability aspects of gap junctions affect the response to radiation. Whereas connexin26 and connexin43 channels mediated the propagation of toxic effects among irradiated cells, connexin32 channels conferred protective effects. We also investigated the role of oxidative metabolism: Up-regulation of antioxidant defense, by ectopic overexpression of glutathione peroxidase, protected against toxic effects expressed during the incubation period post α particle-irradiation. Together, these data show that the damaging effect of α particles, a high linear energy transfer radiation, is amplified by junctional communication among the irradiated cells and results in enhanced oxidative stress. Supported by Grant NNJ06HD91G from NASA.

(PS6.41) Blood cell counts in pigs are lowered by exposure to electron radiation that mimics SPE radiation dose distributions. Jeffrey H. Ware, Jolaine M. Wilson, Stephanie S. Yee, Casey Maks, Gabriel Krigsfeld, Jenine Sanzari, Eric Diffenderfer, Stephen Avery, James McDonough, Keith Cengel, Ann R. Kennedy, University of Pennsylvania, Philadelphia, PA

Astronauts may be exposed to solar particle event (SPE) radiation at relatively high doses during extravehicular activity (EVA). The major type of SPE radiation of particular concern

during an SPE is proton radiation involving protons of energies that will penetrate into tissues for short distances. In this program, electron radiation is being utilized to deliver radiation doses with a distribution that mimics the dose distribution produced by SPE protons. Yucatan minipigs have been utilized to study SPE-like proton radiation effects in the skin, as pig skin shows many similarities to human skin. We evaluated the effects of 6 MeV electrons or a mixture of 80% 6 MeV and 20% 12 MeV electrons on blood cell counts in minipigs. The dose from 6 MeV electrons is expected to irradiate primarily the skin of the minipigs, while the 6 + 12 MeV electron doses are expected to penetrate considerably deeper. Exposure to 6 + 12 MeV electrons is expected to closely mimic the SPE dose distribution curve predicted by Coutrakon, et al. (Coutrakon, G., et al., Nuclear Instruments & Methods in Physics Research Section B 261:791-794, 2007.) Exposure of Yucatan minipigs to a range of doses (up to 25Gy per side) of 6 MeV electrons did not produce consistent suppression of blood cell counts, and did not produce a dose-related response. Conversely, exposure to doses as small as 7.5 Gy per side of 6 + 12 MeV electrons did have statistically significant effects on the pig blood cell counts. Acknowledgement: This research was supported by the NSBRI-CARR (Center of Acute Radiation Research) Grant, funded through NASA NCC9-58.

(PS6.42) Irradiation of immortalized human fibroblasts with high energy protons at both high and low dose rates. Bradford D. Loucas, Richard L. Eberle, Michael N. Comforth, University of Texas Medical Branch, Galveston, TX

One characteristic of low LET radiations are dose rate effects. By lowering the dose rate, the magnitude of many radiation-induced effects is lessened. One such change is the flattening of chromosome aberration dose responses. These are thought to result from a reduction in the frequency of multi-track exchanges with decreasing dose rates. The rate below which no further reduction in effect is observed has been defined as the limiting low dose rate. When this is achieved, in theory, only single-track exchanges are formed which should produce linear dose responses. While this phenomenon has been well studied with X- and gamma-rays, it is unclear to what extent such an effect will be observed following irradiation with high energy, low LET protons which are of concern to NASA with regard to solar particle events. To test the presence and extent of dose rate effects for high energy protons, we irradiated plateau phase hTERT immortalized BJ-1 human fibroblasts at NSRL with 1 GeV, 150 MeV and 50 MeV protons at a low dose rate of about 0.5 cGy/min which is near the limiting low dose rate for gamma photons and at a high dose rate of about 100 cGy/min. Cells were subcultured 72-96 hours post-irradiation and mitotic cells were collected 32-36 hours later. These were fixed, spread onto slides and examined using mFISH to measure the frequency of chromosome aberrations. The scoring of cells irradiated with 1 GeV is nearing completion and results thus far indicate that the frequency of aberration break-points produced by 3 Gy at low dose rate is about 1/3 of that observed at the higher dose rate. Part of this difference seems to have resulted from a greater relative reduction in the frequency and size of complex exchanges forming from three or more chromosome breaks as compared to simple exchanges. The inspection of cells irradiated at the two lower energies is on going but preliminary evidence suggests that results will be similar to those of the 1 GeV experiments. The authors gratefully acknowledge support from the National Aeronautics and Space Administration, Office of Biological and Physical Research NASA/OBPR; NNJ07ZSA001N. Special thanks also to Adam Rusek and the NSRL support staff for their expertise during proton irradiations.

(PS6.43) Biological effects of exposure to mixed beams of radiation: alpha particles and X-rays. Elina Staa¹, Karl Brehwens¹, Siamak Haghdoost¹, Victor A. Nievaart², Joanna Czub³, Janusz Braziewicz³, Andrzej Wojcik¹, ¹Stockholm University, Stockholm, Sweden, ²Institute of Energy JRC, Petten, Netherlands, ³Jan Kochanowski University, Kielce, Poland

Introduction. Astronauts, aeroplane passenger and people living in areas of high background radiation are exposed to mixed beams of high and low LET radiation. From the perspective of radiation protection it is important to investigate the biological effects of mixed beams in relation to effects induced by a single radiation type. So far the investigations of mixed beams were not conclusive. We present results of experiments performed at a unique facility that allows exposing cells simultaneously to high and low LET radiation at constant temperature. **Materials and methods.** The exposure facility is composed of an alpha irradiator with a Am-241 alpha source operating at 37 °C. An X-ray tube is positioned underneath. Peripheral blood samples from one donor were exposed to X-ray doses of 0, 0.25, 0.5, 1.0, 1.5 and 2.0 Gy, alpha doses of 0.4, 0.8, 1.6, 2.8 and 4.0 Gy, and mixed beam doses of 0.25 + 0.4 Gy, 0.5 + 0.8 Gy and 1 + 1.6 Gy. After irradiation whole blood cultures were set up and micronuclei (Mn) were scored in lymphocytes. Three independent experiments were performed. Scoring included the frequency of Mn and their size. Results. There was no significant difference between the X-ray and alpha particle dose-response curves. For the mixed beams the observed dose-response curve was significantly different from the predicted curve ($p < 0.001$). The absolute size of Mn did not differ between the radiation types, but the relative size (in relation to the nuclei) was somewhat higher in cells exposed to alpha particles and mixed beams as compared to X-rays. **Conclusions.** Irradiation with mixed beams of radiation gave rise to significantly higher yields of Mn than predicted based on an additive response. This indicates that the health risk of exposure to mixed beams may be higher than estimated on the basis of high and low LET radiation alone. Exposure to mixed beam does not appear to have an impact on the size of Mn suggesting that exposure to mixed beams leads to a quantitative, but not a qualitative difference in the response of cells. Current research focuses on testing if this conclusion is true.

(PS6.44) Age/radiation parallels in the effects of ^{56}Fe particle irradiation: possible effects on autophagy and stress signaling.

James A. Joseph¹, Shibu Poullose¹, Donna F. Bielinski¹, Kirsty L. Carrihill-Knoll², Bernard M. Rabin², Marshall G. Miller³, Barbara Shukitt-Hale¹, ¹USDA, HNRCA at Tufts University, Boston, MA, ²UMBC, Baltimore, MD, ³Tufts University, Medford, MA

Research indicates that exposing young rats to HZE particles enhances indices of oxidative stress and inflammation, disrupts the functioning of the neuronal communication and alters cognitive behaviors in a manner similar to that seen in aged animals. However, these deficits can be antagonized by strawberry (SB) or blueberry (BB) supplementation given 8 wks prior the irradiation. Subsequent experiments in cell models have shown that stressors such as dopamine or A β 42 can increase numerous ROS-activated stress signals (e.g., p38 mitogen activated protein kinase) which subsequently enhance nuclear factor kappa B (NF κ B) and cytokines (e.g., tumor necrosis alpha). These signals are antagonized by pretreatment of the cells with the SB or BB extracts. Ionizing radiation appears to have similar effects on these signals. For example, research has shown that ionizing radiation can increase the NF κ B signaling cascade in neuroblastoma cells. Moreover, it also appears that NF κ B can repress autophagy, a dynamic process for intracellular degradation and recycling of toxic proteins as well as aging organelles in the brain. In the present study we assessed autophagy functions in the brains of five month old rats, exposed to 1.5 Gy and 2.5 Gy of ^{56}Fe radiation. The brains of these rats were stained for the accumulation of ubiquitin inclusion bodies and tyrosine hydroxylase in the striatum, hippocampus and substantia nigra (SN). Preliminary results indicate that exposure to HZE may decrease autophagy, in rat brain such that the SN dopaminergic neurons of the 2.5 Gy exposure rats exhibited a substantial accumulation of ubiquitin bodies, an early indicator of a dysfunctional autophagic process, that was not seen in control rats. We are now carrying out studies to determine if there are radiation-induced alterations in additional markers of autophagy. Markers such as LC3-I and LC3-II, p62/SQSTM1, mTOR and AMP activated protein kinase (AMPK) will be assessed. Since we have also shown that BB and SB can increase autophagy in stressed BV-2 cells, we will also assess whether BB or SB may produce their beneficial effects following irradiation through autophagy

increases. Supported by USDA Intramural and N.A.S.A. Grant NNX08AM66G

(PS6.45) The combined effects of reduced weightbearing and ionizing radiation on spleen lymphocyte population and function.

Jenine K. Sanzari¹, Jolaine M. Wilson², Erika Wagner³, Ann R. Kennedy¹, ¹University of Pennsylvania School of Medicine, Philadelphia, PA, ²University Laboratory Animal Resources, Philadelphia, PA, ³Massachusetts Institute of Technology, Cambridge, MA

The physiological effects of partial weight bearing, such as expected on the moon (16% of Earth's gravity), have yet to be quantified. As part of the NSBRI Center of Acute Radiation Research (CARR), the combined effects of ionizing radiation and reduced weightbearing on immunologic function are currently being investigated. To study the effects of reduced weightbearing, a new, validated model system has been utilized, the Partial Weight Suspension (PWS) Model. Six-week old ICR female mice were irradiated with a total body dose of 0.5, 1, and 2 Gy using a Cs-137 gamma irradiator and then immediately placed in the (PWS) System at 16% quadrupedal weightbearing for 4 hours, 24 hours, or 48 hours. Control animals were exposed to identical conditions without exposure to radiation, reduced weightbearing or both. Mouse spleens were excised at the time of sacrifice and white blood cells were prepared for flow cytometry and qRT-PCR analysis. The B lymphocyte population was significantly decreased while the T lymphocyte population was significantly increased by 24 hours after exposure to combined radiation (2 Gy dose) and PWS compared to radiation alone, PWS alone, and no treatment. T lymphocyte subpopulation distribution (CD4:CD8 ratio) was not affected in a statistically significant manner; however, T cell activation was significantly decreased at the 1 Gy dose + PWS and the 2 Gy dose + PWS, compared to mice exposed to PWS alone, suggesting that the combined effect of radiation and reduced weightbearing alters T cell function. These data indicate that moderate doses of gamma radiation in the presence of an acute reduced weightbearing environment can pose a deleterious effect on lymphocyte population and function. These changes may contribute to the immune compromise observed during space flight and should be explored in greater detail prior to human flights to the Moon or Mars. Acknowledgements: These studies were funded by the NSBRI through NASA NCC 9-58.

(PS6.46) Loss of p15/Ink4b accompanies tumorigenesis triggered by complex DNA double-strand breaks.

Cristel V. Camacho, Bipasha Mukherjee, Brian McEllin, Nozomi Tomimatsu, Liang-Hao Ding, Chaitanya Nirodi, Debabrata Saha, Michael Story, Adayabalam Balajee, Robert M. Bachoo, Sandeep Burma, University of Texas Southwestern Medical Center, Dallas, TX

DNA double-strand breaks (DSBs) are the most deleterious lesion inflicted by ionizing radiation. While DSBs are potentially carcinogenic, it is not clear whether complex DSBs that are refractory to repair are more potently tumorigenic compared to simple breaks that can be rapidly repaired, correctly or incorrectly, by mammalian cells. We previously demonstrated that complex DSBs induced by high LET Fe ions are repaired slowly and incompletely, while those induced by low LET gamma rays are repaired efficiently by mammalian cells. To determine whether Fe-induced DSBs are more potently tumorigenic than gamma ray-induced breaks, we irradiated sensitized murine astrocytes that were deficient in Ink4a and Arf tumor suppressors and injected the surviving cells sub-cutaneously into nude mice. Using this model system, we find that Fe ions are potently tumorigenic, generating tumors with significantly higher frequency and shorter latency compared to tumors generated by gamma rays. Tumor formation by Fe-irradiated cells is accompanied by rampant genomic instability and multiple genomic changes, the most significant of which is loss of the p15/Ink4b tumor suppressor due to deletion of a chromosomal region harboring the *CDKN2A* and *CDKN2B* loci. The additional loss of p15/Ink4b in tumors derived from cells that are already deficient in p16/Ink4a bolsters the hypothesis that p15

plays an important role in tumor suppression, especially in the absence of p16. Indeed, we find that re-expression of p15 in tumor-derived cells significantly attenuates the tumorigenic potential of these cells, indicating that p15 loss may be a critical event in tumorigenesis triggered by complex DSBs.

(PS6.47) The choroid plexus is a critical target of persistent CNS damage after space radiation in rats. Xiu Lowe^{1,2}, Bernard Rabin³, Francesco Marchetti¹, Sandhya Bhatnagar¹, Antoine Snijders¹, Andrew J. Wyrobek¹, ¹Lawrence Berkeley National Lab, Berkeley, CA, ²Kaiser Permanente® Medical Center, Hayward, CA, ³UMBC, Baltimore, MD

Forty years after the first astronauts landed on the Moon, we now have the ambitious endeavor to travel beyond the Moon and to reach Mars during the next two decades. While there is renewed enthusiasm of taking humans beyond the Earth's orbit into deep space, there are also concerns that space radiations (SR) from solar particle events and galactic cosmic radiation may pose significant hazards to space flight crews during extraterrestrial flights. Heavy nuclei such as ⁵⁶Fe and ¹²C are present in galactic cosmic radiation. We investigated rats at ~12 months after they received simulated SR exposure of ⁵⁶Fe or ¹²C and demonstrated that they had significant neurocognitive deficits (novel object recognition and operant responding). The brain tissues from these rats at ~21-month old were isolated and analyzed using molecular and cellular assays. Age-matched shams and young rats were used for reference. We found that transthyretin (Ttr), a key gene mainly synthesized by choroid plexus (CP) and involved in modulating β -amyloid aggregation, was consistently decreased in hippocampus of rats exposed to ⁵⁶Fe (100 cGy) and ¹²C (100 and 200 cGy), versus age-matched sham. The magnitude of down-regulation was significantly correlated with the severity of the behavioral deficit. In addition, the modulated transcriptomes in cortex of ⁵⁶Fe-exposed rats were significantly associated with a subnetwork of Huntington's disease, (>1.5 fold-change and $p < 0.0001$). We found that the CP of rats at ~21 months after exposed to ⁵⁶Fe (100 cGy) presented with: (a) decreased expression of Ttr protein ($p < 0.001$); (b) defects in epithelial morphology ($p < 0.004$), and (c) diminished expression of a mature neuron marker (NeuN). The significant CP damage that we observed after simulated SR is a novel finding and suggests that a damaged CP may alter the microenvironment that is important for neuronal survival, memory and cognitive behavior. (Supported by LBNL LDRD and NASA NNX08AM66G funding).

(PS6.48) Complexity of α -particle and γ -ray-induced chromosome aberrations in primary human bronchial epithelial cells. Matthew Themis¹, Elisa Garimberti¹, Andrew McVean¹, David Stevens², Mark Hill², Rhona Anderson¹, ¹Centre for Cell and Chromosome Biology, Brunel University, United Kingdom, ²Gray Institute for Radiation, Oncology and Biology, University of Oxford, United Kingdom

Previously we have exposed human peripheral blood lymphocytes (PBL) and human haemopoietic stem cells (HSC) to low doses of α -particles (~1 α -particle/nucleus) of variable linear energy transfer (LET) (110-152 keV/ μ m) and assayed for the induction of chromosome aberrations using the technique of M-FISH. We found complex chromosome aberrations (three or more breaks in two or more chromosomes) (CCA) to be the dominant exchange-type induced and proposed that the formation of these complexes was characteristic of the structure of the α -particle track and the geometry of the cell. We have now extended this study by exposing primary human bronchial epithelial (HBEp) cells *in vitro* to α -particles of LET 121 keV/ μ m (~1 α -particle/nucleus) and have assayed for chromosome aberrations in metaphase+G₂-prematurely condensed chromosomes (G₂-PCC) using M-FISH. HBEp cells were also exposed to 0.5 and 1.0 Gy low-LET γ -rays and assayed in the same manner. For α -particles, we observe simple aberrations (two breaks in two chromosomes) (S) and CCA to occur at frequencies of 0.141 and 0.067, respectively. Thus in contrast to PBL and HSC, CCA do not represent the dominant exchange type in HBEp cells. However we also observe an elevated frequency of

chromosome breaks (0.810) compared to sham (0.179) suggesting the reduced complexity of aberrations may be a consequence of incomplete repair at the time of PCC condensation. To assess this we are determining the complexity of aberration type observed in delayed 1st cell division metaphase+G₂-PCC spreads. For γ -rays, we observe frequencies of 0.053/0.009 and 0.146/0.021 for S and CCA, respectively, after exposure to 0.5 and 1.0 Gy γ -rays, respectively. These data will be discussed within the context of complex CCA formation. The work is supported by Department of Health Grant RRX115.

(PS6.49) Effects of ⁵⁶Fe Radiation on the development of Amyloid plaques in APP23 Transgenic Mice a model of Alzheimer's disease. Cecilia J. Favre, Roman Vlkokinsky, Mary Campbell-Beachler, Gregory Nelson, Loma Linda University, Loma Linda, CA

The damaging effects of high-energy, high charge (HZE) particles radiation on the central nervous system (CNS) are not limited to mitotic cells; it affects other cell types such as neuronal precursors or inflammatory cells, inducing long-term changes within the CNS. We investigated the effect of radiation in a model of neurodegenerative disease: the APP23tg mouse model of Alzheimer's disease, the most common dementing degenerative disease in aging human. Amyloidosis is usually associated with a significant increase in the number of activated microglia, supporting the idea that inflammation may contribute to neuronal dysfunction. Seven week old APP23tg males mice were exposed to brain-only ⁵⁶Fe radiation (600 MeV/n; 1, 2, 4 Gy). The plaque load of 9, 14 and 20 month old animals was scored. At 14 month, the amount of activated microglia was quantified in one hemisphere, measured by the difference in CD68 expression level. The other hemisphere was tested for changes in synaptic transmission and excitability in CA1 neurons measured as a function of plaque loads and radiation dose received. Lower doses of radiation (1 Gy) produced a more severe plaque load than at higher doses (4 Gy), and showed an earlier onset of the disease. At 14 month of age a lower dose (1 Gy) showed less microglial activity. Higher radiation exposure (4 Gy) reduced the development of amyloid deposits without significant change in microglial activity. Similarly, we show that the plaque load significantly enhanced the synaptic excitability in response to radiation, particularly at 2 Gy, and is unchanged at 4 Gy. We also provide evidences for differential microglial activity in two different regions of the brain. In the hippocampus there was a marked decrease in microglial activity at 1Gy, indicating a possible effect of inflammation on the synaptic efficacy response. These results combined with earlier results seen in irradiated brains for microvascular remodeling suggest an interesting biphasic relationship between radiation responses, inflammation and development of age related neurological diseases. The inflamed CNS presents multiple subpopulations of cells located in different region of the brain. These inflammatory cells have the dual property of destruction and protection of the CNS, and this dual role might be influenced by radiation.

(PS7.01) Suppression of medulloblastoma cell growth and migration by the PPAR α agonist fenofibrate. Paulo Richards Mottin Rosa, Zhiyong Deng, Weiling Zhao, Departments of Radiation Oncology and Neurosurgery and Brain Tumor Center of Excellence, Winston-Salem, NC

Childhood brain tumors are the second most common pediatric cancer, and of these, medulloblastoma is the most common primary malignant brain tumor. Despite improved treatment modalities, including radiation therapy, only 60-70% of the patients survive 5 years or more after diagnosis. These survivors are at considerable risk of developing radiation-induced late effects, including neurocognitive deficits and increased risk of secondary malignancies. Therefore, there is an urgent need to develop more effective drugs which have a dual role in preventing radiation-induced brain injury and inhibiting tumor growth. Peroxisomal proliferator-activated receptors (PPARs), members of the nuclear hormone receptor superfamily of ligand-activated transcription

factors, have been extensively studied to evaluate their anti-inflammation and anticancer effects. We have reported that administration of fenofibrate, a PPAR α agonist, inhibits radiation-induced inflammation and decline in neurogenesis in the normal mouse brain. In this study, we tested the anti-tumor effect of fenofibrate on human medulloblastoma cells. Incubating D283 and Daoy medulloblastoma cells with fenofibrate led to a dose-dependent reduction in cell viability and survival. No change in radiosensitivity was observed in cells treated with fenofibrate after irradiation. Western blotting results revealed that treating cells with fenofibrate inactivated STAT3 and increased synaptophysin protein level, a neuronal marker, in D283 cells. We also demonstrated that mitochondrial electron transport protein complex 1-4 levels were significantly up-regulated and MnSOD protein level was reduced following the treatment with fenofibrate. Furthermore, we examined Daoy cell migration using a scratch migration assay. Reduced wound healing and migration capacity were observed at 12 h post-treatment in cells with fenofibrate, compared with non-treated controls. These findings indicate that fenofibrate suppresses medulloblastoma cell growth, migration, and induces cell differentiation, suggesting that PPAR α might be a novel target for anti-medulloblastoma therapy (supported by the Matthew Larson Pediatric Brain Tumor Foundation).

(PS7.02) Dose-dependent changes in neurogenesis and microglial activation following single dose and fractionated irradiation of the young adult rat brain. Dana M. Greene-Schloesser, Valerie Payne, Mitra Kooshki, Mike E. Robbins, Wake Forest University Baptist Medical Center, Winston-Salem, NC

Partial or whole-brain irradiation (WBI) is routinely used for the treatment of primary and metastatic brain cancer. Animal models that investigate radiation-induced brain injury often use single dose regimens. However, fractionated regimens are likely more clinically relevant. To date, there has been a paucity of studies investigating putative histological and pathological differences between single and equivalent fractionated doses of WBI. This study investigates the neuro-inflammatory state of the brain using markers for activated microglia (ED1) and total microglia (Iba) as indices of neuro-inflammation in the dentate gyrus and hilus of the hippocampus. Additionally, neurogenesis (BrdU/NeuN) was assessed in the dentate gyrus of the hippocampus in rats. Young adult male Fischer 344 rats (n=4 per group) 12-14 weeks old, received WBI given as either a range of single doses of 11, 14 or 16.5 Gy of ^{137}Cs γ rays or a range of biologically equivalent fractionated doses of 20, 30, or 40 Gy administered in 5 Gy fractions twice/week for 2, 3, or 4 weeks, respectively. Control rats received sham-irradiation. Thirty days after the end of WBI, rats were injected IP with BrdU for 7 days (once daily) and euthanized 2 months post-irradiation. All brains were processed for immunohistochemistry using standard techniques. Sections were systematically, randomly sampled in a 1 in 12 interval and stained for ED1 or Iba and analyzed using StereoInvestigator software by MicroBrightField. Neurogenesis was assessed in 1 in 48 sections using BrdU/NeuN double-labeling and confocal microscopy. Preliminary results indicate that the number of activated microglia is increased in single dose irradiated groups as compared to the fractionated groups. Neurogenesis appears to be equally effected by either single or fractionated WBI. However, BrdU labeled cells, which reflect actively mitotic cells, are approximately 2 fold higher in fractionated groups as compared to single dose groups, indicating higher proliferation in the fractionated versus single dose groups. This study is currently ongoing and future data and analysis will aid in further characterization of histological differences between single dose and fractionated WBI. (Supported by CA112593 and CA113267).

(PS7.03) A Study of Biodistribution and Imaging of Radioiodinated HVGSSV in Irradiated Glioma-bearing Nude Mice. Charles A. Phillips¹, Dennis Hallahan², Jerry J. Jaboin¹, ¹Vanderbilt University, Nashville, TN, ²Washington University, St. Louis, MO

Background Utilizing biopanning with the T7 bacteriophage system, we previously demonstrated that among screened phage-

displayed peptides, the HVGSSV peptide binds with high sensitivity and specificity to irradiated allograft and xenograft glioma tumors. When bound to near infrared imaging agents, this peptide selectively binds to responding irradiated tumors differentiating responding from non-responding tumors. Our objective was to develop a system for imaging tumor response in humans. Methods We bioconjugated streptavidin-labeled HVGSSV to iodine radionuclides (^{123}I and ^{131}I) utilizing Iodogen[®] pre-coated tubes. Radiolabeling was obtained in 74-89% yield for ^{131}I and 37-52% yields for ^{123}I . Final radiochemical purity after gel chromatography was >98%. Constructs were injected via jugular catheters into mice 4 hours following irradiation of $\sim 1\text{ cm}^3$ GL261 (murine glioma) tumors grafted in the hind limb of nude mice. We used a SPECT/CT scanner to record localization of labeled constructs within the mice over time. For near infrared imaging experiments, cold iodide was bioconjugated to a streptavidin-labeled scrambled peptide and streptavidin-labeled HVGSSV. These constructs were subsequently labeled on tyrosine residues with Alex Fluor 750, and near infrared imaging was performed on a Xenogen IVIS scanner. Results ^{131}I -labeled HVGSSV had poor signal resolution with SPECT-CT imaging revealing diffuse uptake on day 0 followed by clearance within 24 hours with limited tumor binding. The ^{123}I -labeled HVGSSV had improved signal resolution over ^{131}I , but again rapidly cleared the mice. The streptavidin-labeled constructs had similar findings. In the near infrared imaging experiments, the streptavidin-HVGSSV (positive control) demonstrated robust tumor-specific uptake within 24 hours, which persisted through 142 hours. The streptavidin-HVGSSV conjugated to iodide, however, had mild tumor uptake similar to that of the negative control (streptavidin-labeled scrambled peptide). Conclusions Direct conjugation of iodide or its radionuclides abrogates tumor-specific targeting of HVGSSV, suggesting that peptide radioiodination is not a feasible approach for noninvasive monitoring of tumor response.

(PS7.04) Microarray analysis of mRNA and miRNA after single-dose and fractionated radiation in LNCAP human prostate carcinoma cells. Molykutty J. Aryankalayil, Sanjeevani T. Palayoor, Charles B. Simone, II, Adeola Y. Makinde, David Cerna, C. Norman Coleman, National Cancer Institute, Bethesda, MD

MicroRNAs (miRNAs) are an important class of non-coding small RNAs capable of regulating gene expression at the translation level. To explore the role of miRNAs in cellular response to ionizing radiation, in addition to the gene expression analysis by mRNA microarray, we examined radiation-induced changes in miRNAs. Methods: LNCAP cells were exposed to 5Gy and 10Gy either as a single-dose radiation or multi-fractionated (0.5Gy \times 10 and 1Gy \times 10) radiation. RNA was extracted at 24h after the final dose of radiation and miRNA and mRNA microarray analyses were done using Agilent human miRNA Microarray Kit (V2) and CodeLink whole genome bioarray (55,000 probes), respectively. Data were analyzed using GeneSpring software (Agilent technologies). Results: Of the total 723 miRNAs represented in the array, 91 miRNAs were differentially expressed (> 1.5 fold change) by the 4 radiation protocols and more than 70% of these miRNAs were induced by the 2 fractionated radiation protocols. mRNA microarray analysis revealed a total of 978 differentially expressed genes (> 2 fold change, p< 0.05) and 69% of these genes were altered by single-dose radiation. The most prominently altered genes were PIG3, SULF2, SERPINB5 and cyclin A2 (single dose radiation) and CES1, ANGPT2, NOS3 and CYP3A43 (fractionated radiation). Cell cycle regulatory genes AURKA, AURKB, CDKN2C, CCNB2, PLK4, E2F2 and E2F8 were significantly down regulated after single and fractionated radiation. Interestingly, the miRNA microarray analysis revealed significant upregulation of p53 inducible miR-34a, a known cell cycle regulator, after both single and fractionated radiation. Thus, the present data revealed an inverse correlation between miR-34a and cell cycle regulatory genes. This study also demonstrated significant changes in the let-7 family of miRNAs by radiation; 7 of the 9 let-7 miRNAs were significantly upregulated after fractionated radiation whereas none of them were altered after single dose radiation. Conclusion: We are currently in the process of evaluating radiation-induced differential gene expression changes by a combined approach of mRNA, miRNA

and protein array analysis to identify radiation induced molecular targets for cancer therapy. Modulation of miR-34a in cancers with mutated p53 may affect tumor radioresponsiveness.

(PS7.05) Lognormal shape parameter as a screening tool for design of patient-specific targeted radiochemotherapy cocktails. John M. Akudugu, Prasad V. S. Neti, Roger W. Howell, UMDNJ New Jersey Medical School Cancer Center, Newark, NJ

Radiopharmaceutical and chemotherapeutic drug uptake may appear uniform at the tissue level, however, there are invariably significant differences in uptake at the microscopic level (cellular and subcellular). The distributions of these agents are not only nonuniform, but also often lognormal. This suggests that failure in chemotherapy and targeted radionuclide therapy may be attributable to the character of this biologically ubiquitous type of distribution wherein some cells take up very little or no therapeutic agents while others accumulate large amounts. One approach toward overcoming this lognormal distribution problem that is often encountered in cancer therapy is to use cocktails of two or more agents, tailored such that at least one toxic agent is strongly incorporated by each cell in the target population. To achieve this, critically characterizing the cellular uptake of each cocktail component is warranted. Here, the distribution of cellular uptake of the α -particle emitting radiochemical (^{210}Po -citrate) and two anticancer drugs (daunomycin and doxorubicin) by Chinese hamster V79 cells was determined using flow cytometric techniques. The role of agent distribution among a clonal cell population, as described by the lognormal probability density function, was evaluated in terms of its impact on the surviving fraction of the population. The lognormal shape parameter σ correlated with both mean intracellular concentration of the agent and the surviving fraction. These data suggest that σ may be used as a tool for rapid screening and dosing of potential cytotoxic agents for their use in the informed design of patient-specific radiochemotherapy cocktails. Clinical implementation of this approach would constitute a major paradigm shift in the choice and dosing of chemotherapy drugs and complementary targeted radiotherapeutics. This work was supported in part by NIH/NCI 5 R01 CA083838-09.

(PS7.06) Functional FA pathway deficiency in HNSCC cell lines. Caroline V. M. Verhagen¹, Floor Hageman¹, Alfons Balm¹, Marcel Verheij¹, Reidar A. Grénman², Adrian C. Begg¹, Michiel W. M. van den Brekel¹, Volkert B. Wreessmann³, Conchita Vens¹, ¹The Netherlands Cancer Institute, Amsterdam, Netherlands, ²Turku University, Turku, Finland, ³Academic Medical Centre, Amsterdam, Netherlands

Chemoradiation, combining cisplatin with radiation, is the standard treatment for patients with advanced head and neck squamous cell carcinoma (HNSCC). Combined treatment increases the response rate, although local recurrences still occur in half of the patients. Cellular sensitivity to crosslinking agents such as cisplatin and mitomycin C (MMC) is determined by the Fanconi Anemia (FA) pathway, a replication-associated DNA repair process, and nucleotide excision repair. Patients with germline mutations in FA pathway genes (FA patients) and cells with a disrupted FA pathway are hypersensitive to crosslinking agents. Remarkably, FA patients have a 700-fold increased risk of suffering from HNSCC, indicating a role for the FA pathway in sporadic HNSCC development. This suggests that a fraction of the sporadic tumours is deficient in this particular DNA repair pathway. The objective of this study is to assess the FA pathway status in sporadic HNSCC. FA deficient cells display a prominent G2 block after exposure to MMC, due to their repair deficiency. We tested FA pathway function in a panel of 29 HNSCC cell lines derived from patients by MMC induced G2 block analysis and MMC sensitivity. Functional FA pathway disruption will be further confirmed by MMC induced chromosomal breakage, gene mutation and expression analyses and FANCD2 ubiquitination assays. We found a considerable variation in the MMC response of the HNSCC tumour cell panel as determined by G2 block analysis. The MMC dose response relationship was determined at different times after treatment. Four out of 29 HNSCC cell lines showed a G2

arrest comparable to FA-deficient control fibroblast cell lines with confirmed FANCA or FANCG mutations, thereby indicating MMC hypersensitivity. We further identified 5 cell lines that showed an intermediate phenotype, when compared to the FA-deficient and the control wildtype fibroblast cells, which suggests partial inactivation. The remaining 20 HNSCC tumour cell lines showed a similar response to wildtype cells. Our data suggest that FA-like deficiencies are prominent in sporadic HNSCC. Further analyses are underway to characterize the affected genes and the types of alteration.

(PS7.07) Effectiveness of the combined treatment of Hsp90 inhibitor 17AAG with gamma-rays or carbon ions in a tumor xenograft model. Ryuichi Okayasu¹, Dong Yu¹, Miho Noguchi², Momoko Takahashi¹, Akira Fujimori¹, ¹National Institute of Radiological Sciences, Chiba, Japan, ²Japan Atomic Energy Agency, Tokai-mura, Japan

Hsp 90 inhibitor 17AAG has been shown to be an effective radio-sensitizer *in vitro* using several tumor cell lines. One attractive point of using this chemical with radiation is its sensitizing effectiveness in normal cells being significantly smaller than that in tumor cells. We have shown that inhibition of DNA double strand break (DSB) repair by 17AAG is one of the causes for this sensitization in X-irradiated tumor cells. (Noguchi et al 2006). Inactivation of proteins associated with homologous recombination repair was also described in the publication. In this report, *in vivo* studies of 17AAG combined with radiation are presented using a mouse xenograft model with human tumor cells. SQ5 lung carcinoma cells were transplanted into the leg of nude mice, and the mice were treated with either 17AAG alone, radiation alone (gamma-rays or carbon ions), or the combined 17AAG and radiation treatment. 17AAG doses of 80 mg/kg body weight was given *i.p.* for 3 consecutive days. With 17AAG treatment or 10 Gy of gamma-ray alone, tumor growth was delayed in comparison to the control. The combination of 17AAG (pre-treatment for 3 days) and gamma-rays caused further delay in tumor growth. With 5 Gy dose of carbon ions, the combined treatment showed a significant delay in tumor growth, but by 25 days after irradiation, the tumor growth became similar in 5 Gy carbon treatment alone and in the combined treatment. These data indicate that 17AAG is effective in enhancing radiation response in gamma-irradiated tumors *in vivo*. Furthermore, carbon ion irradiation alone is very effective in controlling tumors *in vivo* even at low radiation doses.

(PS7.08) Targeted inhibition of MDM2 in prostate tumor cell with MDM2-siRNA tagged to near infrared nanoparticles (NIR). Thirupandiyur S. Udayakumar¹, Mohamed M. Shareef¹, Rao V. L. Papineni², Mansoor M. Ahmed¹, Alan Pollack^{1,2}, ¹University of Miami, Miami, FL, ²Carestream Health Inc., New Haven, CT

Our earlier studies show that AS-MDM2 and radiation therapy (RT) enhanced apoptosis and prostate tumor growth inhibition. These studies involved intraperitoneal delivery of AS-MDM2 and this type of delivery may not elicit specific targeting of the tumor cells. Since the use of AS-MDM2 is not specific and associated with toxicity, a targeted delivery system is warranted. An efficient *in vivo* gene silencing therapeutics system utilizing the siRNA technology requires the following criteria; (1) ability to deliver high volume siRNA molecules to the tissue of interest and efficiently transfer into the cells and (2) delivery vehicle should protect siRNA from the nucleases during systemic delivery. To address these, we have developed nanoparticles (NP)-based delivery of siRNA, which allows easy linking of siRNA and targeting antibodies. We have utilized the high affinity avidin-biotin interaction to modify NP. The biotinylated macromolecules in precise stoichiometric concentrations were linked to neutravidin decorated dye encapsulated polymeric NP designated as High affinity hooker NP (HAHNP). Such a system also facilitates the simultaneous NIR fluorescence imaging in a noninvasive manner along with targeted siRNA delivery. The HAH-NP linked with biotinylated anti-prostate specific membrane antigen (PSMA) antibody and biotinylated siRNA-MDM2 was prepared. *In-vitro* data revealed the specificity

of HAH NP binding to PSMA expressing prostate cancer cells (LNCaP), and no binding to PC3 cells and fibroblasts which are negative for PSMA. Further, the anti-PSMA linked HAH-NP significantly inhibited MDM2 in LNCaP-MST cells that have been stably transfected to overexpress MDM2 protein, suggesting the specificity of targeted inhibition. Further, *in-vivo* results showed that the anti-PSMA conjugated NP delivered through tail-vein injection targeted the LNCaP tumor, whereas the IgG conjugated NP did not target the tumor, indicating the specificity of the anti-PSMA-loaded NP to the PSMA expressing LNCaP tumor cells. In conclusion, utilizing biotin-avidin for the attachment of molecules that target specific tissues is possible and may be monitored by NIRF imaging. More studies are underway to analyze the targeted inhibition of MDM2 with or without radiation using *in-vitro* and *in-vivo* models.

(PS7.09) Down-regulation of human DAB2IP gene expression in prostate cancer cells results in resistance to ionizing radiation. Zhaolu Kong, Daxing Xie, Thomas Boike, Pavithra Raghavan, Sandeep Burma, David Chen, Jer-Tsong Hsieh, Debabrata Saha, UTSouthwestern Med Center, Dallas, TX

DAB2IP (DOC-2/DAB2 interactive protein) is a member of the RAS-GTPase activating protein family. In metastatic prostate cancer, DAB2IP is often down-regulated and has been reported as a possible prognostic marker to predict the risk of aggressive prostate cancer. We observed that a metastatic human prostate cancer PC3 cells deficient in DAB2IP (shDAB2IP) exhibit increased clonogenic survival in response to ionizing radiation (IR) compared to control cells expressing endogenous level of DAB2IP (shVector). Radio-resistance was also observed in normal prostate cells that are deficient in DAB2IP. This enhanced resistance to IR in DAB2IP-deficient PCa cells is primarily due to faster DNA double strand break (DSB) repair kinetics. More than 90% of DSBs were repaired in DAB2IP deficient cells by 8 hrs after 2 Gy radiation whereas only 60% of DSB repair was completed in DAB2IP proficient cells at the same time. Secondly, upon irradiation, DAB2IP-deficient cells enforced a robust G₂/M cell cycle checkpoint compared to control cells. Finally, DAB2IP deficient cells showed resistance to IR-induced apoptosis that could result from a striking decrease in the expression levels of pro-apoptotic proteins caspase 3, 8, and 9 and significantly higher levels of anti-apoptotic proteins Bcl-2 and STAT-3 than those in DAB2IP proficient cells. In order to radiosensitize the DAB2IP deficient prostate cancer cells we have used a microtubule stabilizing agent Epothilone B in cell culture and in animal study. We noticed significant radiation dose enhancement and tumor growth delay in response to the combined treatment of EpoB and radiation in DAB2IP deficient prostate cancer cells. This radiosensitization can be attributed to delayed DSB repair, prolonged G₂ block and increased apoptosis in cells entering the cell cycle after G₂/M arrest. In summary, DAB2IP plays a significant role in prostate cell survival following IR exposure due to enhanced DSB repair, robust G₂/M check-point control and resistance to IR-induced apoptosis. Therefore, it is important to identify patients with dysregulated DAB2IP for (i) assessing prostate cancer risk and (ii) alternative treatment regimens.

(PS7.10) Timing of, but not timely, antioxidant treatment is the key to survival in mice after lethal dose x-ray irradiation to the abdomen. Dan Jia, Katie Steed, Peter Corry, University of Arkansas for Medical Sciences, Little Rock, AR

We have shown that the acute death (5-10 days after exposure) in mice after lethal dose (20 Gy) abdominal irradiation (AI) is mediated by abscopal elevation of reactive oxygen species (ROS) in the un-irradiated bone marrow. In the present study, we examined the temporal changes in bone marrow oxidative stress after AI and identified an optimal antioxidant mitigation window. Ten-week-old male C57BL/6 mice were given a single dose 20 Gy x-rays to the abdomen. At post-AI 3h, 6h, 24h (1d), 2d, 3d, and 6d, bone marrow were harvested and the levels of ROS (e.g. H₂O₂), antioxidative defense components (e.g. total and reduced glutathione), and oxidation products (e.g. 8-OHdG) were measured. A rapid, 5-fold increase in bone marrow ROS was detected 3h after AI. The ROS

level, however, was back to that of the sham controls 24h after AI and remained low until 48h after AI, followed by a second, gradual increase in ROS that peaked at post-AI day 6 when most of the irradiated mice would have died shortly after. Bone marrow antioxidative defense components increased with time during the first 48h post-AI but dropped below the levels of the sham controls afterward. The levels of 8-OHdG did not change until 2 days after AI and increased steadily thereafter. Treatment of the irradiated mice with daily s.c. injection of the antioxidant N-acetyl-cysteine (NAC) had markedly diverse effects on both bone marrow oxidative stress as well as 10-day survival. When NAC was given concomitantly with AI, the elevation of antioxidative defense components was abolished while the accumulation of oxidation products was increased as compared with the vehicle-treated irradiated mice. When NAC was given 24-48h after AI, the increase in antioxidative defense components was prolonged whereas the second phase ROS elevation and the accumulation of 8-OHdG were diminished. Consequently, 10-day survival rate was 10% in mice treated with NAC immediately after AI but increased to 50% when NAC treatment started 24-48h after AI. Our results demonstrate a critical mitigation window for NAC rescue. When applied within this window, NAC prolongs the endogenous antioxidative defense responses without interfering with the initial activation of the defense process, which might be an essential element for successful antioxidant mitigation.

(PS7.11) Low-dose fractionated radiation as a potentiator of temozolomide in brain cancer cell lines. Seema Gupta¹, Nikita Nagpal², Mansoor M. Ahmed¹, ¹University of Miami, Miami, FL, ²Pennsylvania State University, University Park, PA

Our earlier studies in colorectal and head and neck cancer cell lines have shown the chemo-potentiating effects of low dose fractionated radiation therapy (LDFRT). Temozolomide (TMZ), an alkylating agent is an established regimen for treatment of brain neoplasias. Its cytotoxicity is thought to be primarily due to alkylation at the O⁶ position of guanine with additional alkylation occurring at the N⁷ position. During DNA replication, a futile cycle of repair by the mismatch repair pathway (MMR) is set up as thymine is repeatedly reincorporated (instead of cytosine) if O⁶-methylguanine persists on the parental strand triggering apoptosis. Cells exposed to TMZ are expected to be resistant if MMR was absent or deficient or due to O⁶-methylguanine-DNA methyl transferase (MGMT), a DNA repair protein that removes O⁶-methylguanine from DNA introduced by TMZ. Ionizing radiation (IR) has been shown to induce MGMT levels in various tissues of the rat and in some cell lines suggesting that MGMT plays a role in the cellular defense against IR. As LDFRT does not induce repair pathways, it is possible that MGMT is not induced by LDFRT and therefore will lead to increased effects with TMZ. In the present study, effects of TMZ and O⁶-benzylguanine (BG; a small molecule inhibitor of MGMT) in combination with LDFRT (4 fractions of 0.5 Gy with 8h interval) or 2 Gy were studied in U87 (human glioblastoma), H1915 (human lung cancer cells metastasized to the brain) and DAOY (human medullablastoma) cells. Based on the cell growth kinetics studied by real time cell electronic system (RT-CES), LDFRT mediated TMZ potentiation was more effective in both GBM and metastatic GBM compared to 2 Gy mediated TMZ potentiation. Flow cytometric analysis showed that at 48 and 72 h after irradiation, cells were arrested in G₂/M phase that corresponded with increased apoptosis as observed with both LDFRT and 2 Gy groups. Disturbances in cell cycle, specifically G₂/M arrest may be responsible for observed potentiation of TMZ by radiation. Even if both LDFRT and 2 Gy mediated TMZ potentiation are effective, clinically LDFRT can still be a better choice of treatment since 2 Gy fractions often result in normal brain tissue injury. Further molecular and cellular analysis is currently underway to ascertain that LDFRT can be a choice for potentiating the effect of TMZ.

(PS7.12) Radiation Suppresses Tumor Growth by Inducing Senescence in an Orthotopic Mouse Model of Human Lung Cancer. Caroline Yount, Aimin Yang, Hainan Lang, Kenneth N.

Vanek, Anand K. Sharma, Joseph M. Jenrette, Bradley A. Schulte, Yong Wang, Medical University of South Carolina, Charleston, SC

Although anticancer agent-induced apoptosis was thought to be a primary mechanism by which cytotoxic therapies suppress tumor growth, treatment with chemotherapy or radiation is not invariably cytotoxic to all tumor cells. Cellular senescence is characterized by an irreversible cell cycle arrest that can be triggered by many types of intrinsic and extrinsic stresses, including radiation. More importantly, senescence has been recognized as an indispensable cellular response to anticancer therapy and an important mechanism for anticancer agents to eliminate tumor cells. However, it is largely unknown if radiation-induced senescence contributes to the treatment outcome in lung cancer radiotherapy. In the present study, we established an orthotopic mouse model of human lung cancer using an H1299 lung cancer cell line bioengineered to stably express luciferase. We treated the tumor bearing mice with fractionated radiation (3.0 Gy/fraction) every other day for two weeks with a total dose of 18 Gy localized irradiation. Tumor size and location was measured and monitored using a Xenogen IVIS 200 bioluminescence imaging system. The results showed that 18 Gy of irradiation significantly suppresses tumor growth and results in a markedly better local control of lung tumors compared with those of sham control. Interestingly, the tumor suppression effect of radiation was associated with an increased senescence associated β -galactosidase (SA- β -gal) staining and reduced BrdU incorporation capacities of cancer cells in irradiated tumor tissues, which suggest that radiation can suppress tumor growth and prevent lung tumor metastasis most likely by inducing senescence. These results support the concept that senescence is a critical fate-determining factor for treatment outcome and suggest that novel therapeutic approaches of increasing senescence can be potentially exploited to improve the efficacy of lung cancer radiotherapy.

(PS7.13) The in vivo study on the effect of prolonged delivery time to tumor control in C57BL mice implanted with Lewis lung cancer. Xin Wang^{1,2}, Xiaopeng Xiong³, Shaoqin He², ¹Shanghai Huashan Hospital, Shanghai, China, ²Shanghai Cancer Hospital, Shanghai, China, ³Shanghai Cancer Hospital, Shanghai, China

Objective: Research the effect of different delivery time with same dose on the tumor growth delay and survival in C57BL mice implanted with Lewis lung cancer to determine whether prolonged delivery time would decrease the tumor response to radiation or not. Methods: 96 mice implanted with Lewis lung cancer in the back legs were involved and the experiment started when the transplanted tumor diameter reached about 0.8cm then randomized into 6 groups: control group, the single fraction with 18 Gy group, the two subfractions with 30min interval group, the seven subfractions with 5min interval group, the two subfractions with 60min interval group, the seven subfractions with 10min interval group. Seven days after irradiation, half of mice in each group were killed by cervical dislocation and the remaining ones were kept alive. Apoptosis was determined by TUNEL assay. Observe the tumor growth tendency, the tumor growth delay and the mice survival time. Results: The tumor grow delay of groups with prolonged delivery time was shorter than the group with single fraction of 18 Gy ($P < 0.05$). The tumor grow delay of groups with prolonged delivery time 30min was longer than that of groups with prolonged delivery time 60min ($P < 0.05$). There was no significant difference between groups with same delivery time ($P > 0.05$). The apoptotic rate decreased with the elongation of the total interfraction interval time ($p < 0.01$). When the rate of apoptotic cells of groups with the same total interfraction interval times was compared, there is no statistical significance ($p = 0.191, 0.216 > 0.05$). Compared to group with single fraction of 18 Gy, the groups with prolonged delivery time shorten the mice survival time while there was no significant difference between the group with prolonged delivery time 30min and the group with prolonged delivery time 60min. Conclusions: The prolonged delivery time with same radiation dose shorten the tumor growth delay and survival time in the mice implanted with Lewis lung cancer. Longer the delivery time prolonged, the effect on tumor control was more significant. However the different prolonged delivery time 30min and 60min had no significant difference of the effect on mice survival time.

(PS7.14) The small molecule inhibitor QLT0267 radiosensitizes human head and neck squamous cell carcinoma cells in an ILK independent manner. Iris Eke, Franziska Leonhardt, Katja Storch, Stephanie Hehlhans, Nils Cordes, OncoRay - Radiation Research in Oncology, Dresden, Germany

As cancer cell resistance to radio- and chemotherapy constantly increases, novel targeting approaches are required to improve patient survival. Integrin-Linked Kinase (ILK) has been reported as potent cancer target, which promotes survival and tumor growth. However, our previous findings using genetic models clearly showed that ILK transduces antisurvival signals in cells exposed to ionizing radiation. To evaluate the impact of the putative ILK inhibitor QLT0267 on the cellular radiation survival response, FaDu and UTSCC45 human head and neck squamous cell carcinoma (hNSCC) cells as well as ILKfloxed/floxed (fl/fl) and ILK-/- mouse fibroblasts growing either two-dimensionally (2D) on or three-dimensionally (3D) in laminin-rich extracellular matrix were treated with QLT0267 alone or in combination with irradiation (X-rays, 0-6 Gy single dose). Additionally, FaDu cells were stably transfected with a constitutively active ILK mutant (FaDu-IH) or empty vector. ILK knockdown was performed using small interfering RNA transfection. ILK kinase activity, clonogenic survival, number of residual DNA double strand breaks (rDSB; gammaH2AX/53BP1 foci assay), cell cycle distribution, protein expression and phosphorylation (e.g. Akt1, ERK1/2) were determined. Besides inhibition of ILK activity, treatment with QLT0267 resulted in dephosphorylation of several signaling molecules. Thus, QLT0267 seems to have a broad inhibitory spectrum. QLT0267 significantly reduced survival and radioresistance of all tested cell lines (including ILK-/- cells) independent of ILK status. In parallel, the number of gammaH2AX/53BP1 positive foci was increased. While in 2D treatment of QLT0267 led to an accumulation of cells in G2, the cell cycle distribution was not altered when cells grew in 3D. ILK knockdown had no effect on radiation survival of hNSCC cells. Our results clearly show that the small molecule inhibitor QLT0267 has potent cytotoxic and radiosensitizing capability in hNSCC cells, which could not be attributed to the effect on ILK. Further in vitro and in vivo studies are necessary to clarify the potential of QLT0267 as a novel approach in the clinic.

(PS7.15) Micro-CT evaluation of lung density and volume following unilateral lung irradiation of CBA, C57L and B6 mice. Julian Down, Matthew Davidson, Jacquelyn Yanch, Massachusetts Institute of Technology, Cambridge, MA

The majority of murine studies designed to investigate the pathogenesis, protection and mitigation of radiation-induced lung injury have so far been performed using whole thorax irradiation (WTI). This treatment often leads to a dose-dependent incidence of lethality that varies widely among different strains of mice. In addition to respiratory insufficiency due to development of widespread pneumonitis, there is also the complication of lethal pleural effusions, seen in rodents but not in humans, which prevent longer-term evaluation of lung pathology (Jackson et al. Radiat Res 173:10-20, 2010). Studies involving irradiation of the entire lung are also far removed from the routine clinical application of localized thoracic radiotherapy where the compensatory role of unirradiated lung tissue is expected to provide recovery from injury. We have therefore followed and compared the progression of lung damage among three diverse mouse strains (CBA, C57L and B6) receiving hemithoracic irradiation (HTI) whereby the dose is confined to the right lung. HTI was delivered at doses of 12.5-17.5 Gy to unanesthetized mice using 250 kVp X-rays. Micro-CT imaging at 4 months post-HTI revealed the development of marked increases in CT density in the irradiated lung corresponding to pneumonitis in CBA and C57L mice while the lungs of B6 mice remained normal at this time. Evaluation at the later time of 7 months, however, showed the emergence of increased lung density in B6 mice consistent with a prolonged latent period in this strain. All mice have survived in good health with no signs of pleural fluid accumulation and are being further assessed for later development of lung atrophy/fibrosis and accompanying hypertrophy of the contralateral lung as previously documented using low-resolution CT. These results indicate the promise of HTI and micro-CT in mice to (i) resolve the genetic strain-related differences in lung sensitivity

and latency and (ii) enable examination of chronic fibrosis or ischemic atrophy in the context of adaptation on the part of the unirradiated lung as expected in clinical radiotherapy.

(PS7.16) DCE-MRI assessment of tumor response to axitinib and radiation. Scott D. Kennedy, Scott F. Paoni, Bruce M. Fenton, University of Rochester Medical Center, Rochester, NY

Numerous antiangiogenic strategies have been shown effective over the past 10-20 years, both in experimental tumor models and in the clinic. A recurring issue with such agents, however, has been in defining therapeutic response in individual patients. Unlike chemotherapeutic agents, antiangiogenics may not produce tumor regression, but instead simply stabilize tumor volume. Thus, tumor size, as defined using standard RECIST criteria, may not optimally assess initial response. The current objective was to test whether dynamic contrast enhanced (DCE) MRI could monitor and/or predict the antiangiogenic effects of axitinib (Pfizer Global Research & Development), an inhibitor that predominantly targets vascular endothelial growth factor receptors. MCA-4 murine mammary carcinomas were implanted in the hind limbs of mice, and baseline DCE-MRI experiments were performed at 9.4 T to quantitate uptake of Gd-DTPA. Tumors were quantified in terms of initial area under the curve (IAUC) and K_{trans} at three timepoints (including pretreatment). Although IAUC decreased following combination therapy (25 mg/kg BID axitinib plus 6 Gy fractions), IAUC also decreased in controls, most likely due to rapid growth and accompanying blood flow reduction in these tumors. A second series of experiments utilized more slowly growing DU145 human prostate tumor xenografts, and focused specifically on pretreatment versus day two imaging to evaluate early response. Following two weeks of treatment, tumor volumes averaged 350 and 580 mm³ for treated and control tumors, respectively, indicating a significant, axitinib-induced growth delay ($p = 0.003$). At day two, however, volumes of control tumors were not yet substantially different from axitinib treated tumors. Over this initial period, preliminary DCE-MRI results already showed a trend towards a decreased IAUC_{day 2} / IAUC_{day 0} ratio (1.14 +/- 0.25 (mean +/- SEM) for control tumors and 0.66 +/- 0.10 for axitinib-treated tumors, N=5/group). For temporal MRI studies in which tumor volume-related hemodynamic alterations can play a primary role, the current work clearly demonstrates the advantages of utilizing more slowly growing xenograft tumor models as time-matched controls. Work in progress will confirm the significance of these preliminary results in a larger cohort of animals.

(PS7.17) Synergy of phytochemicals in tumor cell radiosensitization. Jamunarani Veeraraghavan¹, Rakesh Madhusoodhanan¹, Mohan Natarajan², Vibhudutta Awasthi¹, Hrushikesh Agashe¹, Terence S. Herman¹, Natarajan Aravindan¹, ¹University of Oklahoma Health Sciences Center, Oklahoma City, OK, ²University of Texas Health Sciences Center at San Antonio, San Antonio, TX

Accomplishing the desired anti-tumor efficacy with individual dietary phytochemicals requires doses not readily achievable *in vivo*. This along with the existence of complex, converging and diverging pathways spanning the metabolic networks in cancer cells demands the development of a multi-component approach with physiological doses of phytochemicals that could be used as a "deliverable" agent against tumors. To address this concern, we investigated the synergistic efficacy of Genistein (GEN), EGCG, Resveratrol (Res) and a synthetic analogue of curcumin (EF24) in mitigating breast cancer progression. Human breast adenocarcinoma cells (MCF-7 and MDA-MB-231) were exposed to radiation (2Gy; IR) alone, or treated with GEER (GEN, EGCG, EF24 and Res), or exposed to 2Gy after treating with GEER mixture and examined after 24h. IR significantly induced NFκB DNA-binding activity, and this induction was markedly inhibited by GEER. More importantly, IR-induced NFκB was completely and selectively (NFκB overexpression studies) suppressed by GEER. Consistently, GEER inhibited IR-induced NFκB-dependent transactivation and secreted TNFα. In addition, while IR transactivated NFκB-

dependent downstream targets, GEER completely blocked IR-induced NFκB-dependent *IAP1*, *IAP2*, *XIAP* and *survivin*. To that end, in contrast to the stand alone effect of phytochemicals, GEER significantly conferred IR-inhibited the survival of breast tumor cells. Consequently, forced activation of NFκB confirmed the synergistic effect of phytochemicals in regulating NFκB dependent cell survival. Also, GEER revealed a significant inhibitory effect on IR-induced MMPs (MMP 1, 2, 3, 7, 9, 11, 13, 14) and demonstrated a NFκB dependent regulation at least for MMP 2 and 9. Taken together, these data evidently exhibit the potential synergistic effect of EGCG, GEN, Res and EF24 in mitigating breast cancer progression as opposed to their stand alone effect. More importantly, these data strongly suggests that the GEER influenced synergistic cell killing may involve selective targeting of NFκB mediated survival advantage and tumor progression signaling.

(PS7.18) Gemcitabine and 5-fluorouracil as radiosensitizers of low dose rate radiation in the treatment of liver cancer. Theodore S. Lawrence, Mary A. Davis, University of Michigan, Ann Arbor, MI

Treatment options for diffuse hepatocellular carcinoma (HCC) are extremely limited; the only established therapy is sorafenib, which improves survival by only 2 months. Therefore, the use of low dose rate radiation delivered by ⁹⁰Yttrium labeled glass microspheres administered directly into the hepatic artery, from which HCC derives most of its blood supply, is being investigated as a treatment option. As we have successfully combined radiosensitizers with external beam radiation (Ben Josef, et al *J Clin Oncol*, 34:8735-8739, 2005), we hypothesized that sensitizers could improve the response of HCC to low dose rate radiation as delivered by ⁹⁰Yttrium microspheres. We used a custom built device which is housed in a cell culture incubator and which delivers gamma radiation (¹³⁷Cs) at a dose rate of 0.18 Gy/h. Exposing HepG2 or Hep3B cells for 16 h to low dose rate radiation resulted in surviving fractions of 0.35±0.06 and 0.22±0.06, respectively. We then examined the effects of gemcitabine, 5-fluorouracil (5-FU), and sorafenib on radiation sensitivity. Gemcitabine was added at nontoxic doses for 2 hours, 24h before the cells were placed in the low dose rate device. For 10 nM gemcitabine, the enhancement ratios were 1.99±0.39 in HepG2 cells, and in Hep3B cells, for 30 nM gemcitabine, was 1.52±0.31. Likewise, 5-FU was added 24 h prior to the start of radiation but was left on throughout the 16h of radiation treatment. Under these conditions, 1 μM 5-FU (nontoxic) treatment resulted in enhancement ratios of 1.91±0.04 in Hep G2 and 4.79±0.62 in Hep3B cells. At clinically achievable doses, sorafenib did not sensitize either cell line to low dose rate radiation. Experiments are underway to confirm these results in mice and at other, lower dose rates. These data suggest that radiosensitizers may be useful in combination with treatment with ⁹⁰Ymicrospheres and will form the preclinical rationale for a proposed clinical trial to treat HCC.

(PS7.19) Uptake mechanisms of tumor targeted TiO₂ nanoconjugates for radiosensitization. Ye Yuan¹, Tatjana Paunesku¹, Hans Arora¹, Jesse Ward², Sumita Raha¹, Stefan Vogt², Gayle E. Woloschak¹, ¹Northwestern University, Chicago, IL, ²Argonne National Laboratory, Argonne, IL

We are developing TiO₂ nanoconjugates (NCs) as therapeutic and diagnostic agents. Nanoscale TiO₂ can be surface conjugated with various molecules and has the unique ability to produce Reactive Oxygen Species (ROS) upon activation. The three major questions that we wish to answer are (1) how are NCs internalized by cells, (2) is targeting of NCs using a small peptide achievable, and (3) would targeted delivery of TiO₂ NCs lead to radiosensitization of cancer cells. To address these questions, we have created NCs targeted to Epidermal Growth Factor Receptor (EGFR) which is enriched in many cancers of epithelial origin. Since EGFR is rapidly endocytosed upon ligand binding, we predict that targeting NCs to EGFR will increase internalization by certain cancer cells. As a targeting peptide we selected an eleven amino acid region from Epidermal Growth Factor (EGF) that has been shown to bind

EGFR. Both FITC-labeled, and dopamine-conjugated peptides were used to treat HeLa cells as well as two isogenic colon cancer cell lines, one with high EGFR expression (SW480) and one with low EGFR expression (SW620). Immunofluorescent imaging of treated cells showed that FITC-labeled peptides colocalized with EGFR labeled with fluorescent antibodies on the cell surface and within the cytoplasm. The synthetic dopamine-conjugated EGF peptides were then attached to TiO₂ nanoparticles to create EGFR targeted NCs. These NCs also colocalized with EGFR in treated cells by immunofluorescence imaging. In addition, we used nano-gold labeled antibodies to target the cytoplasmic domain of EGFR and used X-ray Fluorescence Microscopy (XFM) to detect colocalization of gold and titanium in cells. These images showed overlap of titanium and gold nanoparticles thus further indicating that EGFR targeted NCs can bind cellular EGFR. Since EGFR is rapidly endocytosed upon ligand binding, EGFR targeted TiO₂ NCs will be enriched specifically in cancer cells. Treating these cells with radiation concurrent with the production of ROS by TiO₂ NCs will increase subsequent DNA damage. In this way, we expect that EGFR binding TiO₂ NCs will act as a targeted radiosensitizer.

(PS7.20) Metabolic disposition of Ex-RAD™ (ON 01210.Na), a novel radioprotectant. Chen Ren¹, Mitalee Tamhane², Glenn Fegley¹, David Taff², Manoj Maniar¹, ¹Onconova Therapeutics, Inc., Newtown, PA, ²Long Island University, Brooklyn, NY

Ex-RAD™ (ON 01210.Na), sodium salt of a benzyl styrylsulfone, is being developed by Onconova Therapeutics as a novel radiation protection agent. Ex-RAD™ has completed two Phase I clinical safety trials under an Investigational New Drug (IND) exemption. Initial development, in collaboration with the Armed Forces Radiobiology Research Institute (AFRRI), is focused on its use as a prophylactic agent. We have characterized the metabolic disposition of this drug in various species as part of the regulatory submission process for approval of this drug under the "Animal Rule," which applies to drugs that are developed without human efficacy studies. We investigated the metabolic fate of Ex-RAD™ in *in vitro* and *in vivo* systems. A major metabolite, glutathione conjugate (1210-GSH), was identified *in vitro* using hepatocytes from various species. In mice dosed subcutaneously with ¹⁴C-labelled ON 01210.Na, five additional metabolites were identified by HPLC/RAD and mass spectrometry, tentatively assigned as ON 01210-cysteine (1210-Cys), ON 01210-(N)-acetylcysteine (1210-NAC), ON 01210-thiol (1210-SH), ON 01210-unsaturated thiol (1210-uSH) and ON 01210-methylsulfide (1210-SCH₃). The formation of these metabolites potentially involves two pathways. Initially, ON 01210.Na undergoes Michael addition with glutathione, catalyzed by glutathione S-transferase. Subsequently, 1210-GSH is further metabolized to 1210-Cys via the mercapturic acid pathway; this key metabolite thus forms thiols and methyl sulfides through the cysteine s-conjugate β-lyase pathway. An LC/MS/MS method was optimized to monitor the levels of all six metabolites and ON 01210. The same set of metabolites was also monitored in the plasma of rats following oral and iv administration of Ex-RAD™ at various doses. All of these metabolites except 1210-SH were detected in rat plasma. ON 01210.Na follows nonlinear pharmacokinetics, especially at higher doses. The results indicate that the metabolic pathway of Ex-RAD™ is conserved from mouse to rat, and the same metabolic disposition pattern appears irrespective of the route of administration. These results and ongoing studies will help support the regulatory approval for this novel radioprotectant.

(PS7.21) Selective irradiation of the blood vessels differential suppress tumor growth. Koji Ono, Shin-ichiro Masunaga, Yuko Kinashi, Minoru Suzuki, Yong Liu, Hiroki Tanaka, Yoshinori Sakurai, Akira Maruhashi, Kyoto University Research Reactor Institute, Kumatori-cho, Osaka, Japan

We have proposed the following idea at ICRR 2003 in Brisbane and ISNCT 2004 in Boston. Liposome including ¹⁰B compound is injected into mice, and if size of the liposome is large enough it does not leak from blood vessels. Neutron capture cross

section of ¹⁰B nucleus is tremendously large compared with other elements in human body. The two particles emitted through ¹⁰B(α,n)⁷Li have extremely short tracks, 9μm and 4 μm, respectively. Then, slow neutron irradiation to the mice pre-injected with ¹⁰B compound liposome enables to deliver radiation dose to the blood vessel selectively. BSH (¹⁰B-enriched borocaptate sodium) is included in liposome with about 300 nm diameter. This size liposome dose not leak from blood vessels. Then, I have examined the effects of selective irradiation of blood vessels on tumor growth and on normal tissue reaction. C3H/He mice and tumor model SCCVII were used to examine the character and effect of this type liposome. Thermal neutron irradiation was performed by using heavy water facility in Kyoto University Reactor and ¹⁰B concentrations in the blood or tissues were measured by prompt gamma-ray spectrometry. The effects on tumors and normal tissues were examined by *in vitro* - *in vivo* colony formation assay, tumor growth delay assay and histopathology method, respectively. The ¹⁰B concentration ratio between blood and tumor 30 minutes after the liposome injection was 35-40, and this ratio was stable for several hours. The surviving cell fraction of the tumor treated by the liposome with neutron was very slightly suppressed in comparison with that of neutron irradiation alone, however, growth of the tumors was remarkably suppressed in the liposome neutron group. Irradiation of 60 Gy-eq selectively to tumor blood vessels completely suppressed the tumor growth. Normal tissues like skin did not show significant adverse effect like an epilation. Thermal neutron irradiation combined of BSH-liposome can irradiate the blood vessels selectively, and it suppressed tumor growth effectively but did not induce significant adverse effects on normal tissue.

(PS7.22) Microscopic peritoneal tumors in nude mice are resistant to radiation. Xiao-Feng Li^{1,2}, Yuanyuan Ma², John L. Humm², Clifton C. Ling², Joseph A. O'Donoghue², ¹University of Louisville School of Medicine, Louisville, KY, ²Memorial Sloan-Kettering Cancer Center, New York, NY

We previously reported intense hypoxia and poor perfusion in microscopic HT29 (human colorectal adenocarcinoma) tumors (<1 mm) in an animal model of disseminated peritoneal disease (Cancer Res, 2007; 67:7646). In contrast, larger tumors (1-4 mm) were well-perfused and not significantly hypoxic. We therefore hypothesized that microscopic tumors may be more resistant to radiation than larger ones. Methods: HT29 cell suspensions (10 × 10⁶ cells/0.2 ml) were injected intraperitoneally into 6-week-old NCr nu/nu female nude mice (8 mice) and experiments carried out 6 weeks later. Two groups, each of 4 mice, were either given 15 Gy X-ray whole body irradiation or sham-irradiated. Animals were sacrificed immediately after treatment. Microscopic ascites tumors from each group were collected and pooled separately. Larger tumors (2-4 mm) from each group were detached from serosa, cut into ~1mm fragments and pooled separately. Samples from each pool were assessed by carbonic anhydrase 9 (CA IX) staining. Volumes (~ 0.1 ml) of pooled tumor samples were re-implanted subcutaneously into the hind legs of 6-week-old NCr nu/nu female nude mice (5 mice per sample) and tumor growth over time was observed. Results: CA IX-positive fractions were ~95% for ascites tumors and ~2% for larger tumors. Following inoculation of either ascites or larger serosal tumor samples from sham-irradiated animals, tumor growth was rapid, reaching volumes (mean ± SD) of 1797 ± 384 mm³ and 1218 ± 458 mm³ respectively after 27 days. Following inoculation of larger serosal tumor samples from irradiated animals, only 1 in 5 implanted sites had a re-growing tumor (approximately 10 mm³) 27 days later. However following inoculation of ascites tumor samples from irradiated animals, tumor growth occurred at all sites reaching an average volume of 319 (± 185) mm³ by 27 days. Conclusion: The data support the hypothesis that microscopic tumors of sub-millimeter size are more resistant to radiation than larger ones from the same animals. If these findings are clinically applicable and micrometastatic disease can be radiation-resistant, this will be important in radiation oncology.

(PS7.23) Inhibition of hypoxia inducible factor-1 (HIF-1α) and monocarboxylate transporter-1 (MCT-1) results in hypoxic cell

kill and delays tumor growth in vivo. Satish K. Chitneni, Thies Schroeder, Diane R. Fels, Gregory M. Palmer, Michael R. Zalutsky, Mark W. Dewhirst, Duke University Medical Center, Durham, NC

Solid tumors adapt to the hypoxic environment by upregulation of hypoxia inducible factor-1 (HIF-1), a nuclear transcription factor that regulates >60 genes, thereby stimulating glycolytic energy production and promotion of hypoxic cell survival. Inhibition of HIF-1 suppresses the synthesis of glycolytic enzymes and prevents hypoxic tumor cells from using glucose which may lead to their death. On the other hand, normoxic fractions of cells in tumor are able to import lactate, which is a metabolic end product in hypoxic cells *via* the transporter MCT-1, and utilize it for ATP production. We recently showed that the inhibition of MCT-1 causes the switch-over of oxidative tumor cells from lactate utilization to glucose catabolism thus, resulting in the starvation and death of hypoxic cells. We hypothesized that the combination of HIF-1 inhibition and MCT-1 inhibition would maximize the hypoxic cell kill in vivo. To examine this, we used human prostate cancer cells (PC3) stably expressing tet-inducible dominant-negative HIF-1 α mutant as a model for HIF-1 inhibition. These cells showed good HIF-1 inhibition in vitro upon activation of the mutant with doxycycline (DOXY, 1 μ g/mL) under normoxia as well as with COCl₂ (200 μ M) as opposed to no-DOXY ($p < 0.01$). In vivo experiments were conducted using tumor xenografts where the animals received DOXY (in drinking water, 10 mg/mL) for HIF-1 inhibition and α -cyano-4-hydroxycinnamate (HCHC, 25 μ mol) for MCT-1 inhibition by daily i.p. injection for 13 days ($n=5$). Animals were injected with the hypoxia marker EF5 (80 mg/kg, i.p.) and the perfusion marker Hoechst 33342 (1 mg, i.v.) 180 min and 5 min prior to their sacrifice, respectively, on day 13. IHC analysis was performed on tumor sections to quantify hypoxic fraction (EF5 uptake area) in each tumor. The results showed that the combination therapy has inhibited the growth of tumors, almost, completely. The median value for hypoxic fraction in the treatment group was 7.8% vs. 22.1% in control group ($n=5$). As anticipated, EF5 binding was observed in (hypoxic) low perfusion areas of the tumor tissue. Qualitative examination of H&E stained sections from size matched tumors showed higher regions of necrosis in the treatment group than in control tumors, which corroborate our hypothesis. This work was supported by a grant from Varian Biosynergy.

(PS7.24) Curcumin-altered p53-response genes in neuroblastoma cells regulates radiosensitivity. Jamunarani Veeraghavan¹, Mohan Natarajan², Rakhesh Madhusoodhanan¹, Terence S. Herman¹, Natarajan Aravindan¹, ¹University of Oklahoma Health Sciences Center, Oklahoma City, OK, ²UT Health Science Center, San Antonio, TX

Tumor radio-resistance remains a critical obstacle in clinical radiotherapy. Curcumin, a dietary polyphenol, has been demonstrated to have anti-inflammatory, anti-proliferative, antitumor (including radio-sensitization) effects by modulating many molecular targets including p53. In this study, we investigated the effect of curcumin in radio-sensitizing p53 mutant human neuroblastoma cells (SK-N-MC). SK-N-MC cells treated with curcumin (10-100nM) and exposed to radiation (IR, 2Gy) were examined for p53, Bcl2, Mcl1, p21, BclXl, Bax, and Gadd45 genes activation at mRNA (by RPA and QPCR) and protein (immunoblotting) levels. Radio-sensitivity was measured by examining the induction of apoptosis (by Annexin V-FITC), DNA fragmentation (by Fluorescein Fragel), cell survival (by MTT assay) and clonal expansion. In contrast to mock-IR, 2Gy significantly induced Mcl1, p21, Bax, and BclXl. Curcumin pretreatment significantly conferred IR-induced p21, Bax and reverted IR-induced BclXl and Mcl1. Bcl2 protein levels remained constant in these cells after IR or curcumin plus IR treatments. However, the upregulation of Bax and no changes in Bcl2 protein levels in curcumin plus IR-treated cells, together, altered the Bcl2: Bax ratio and this caused the enhanced radio-sensitization. No significant alterations in p53 mRNA or protein levels were observed in response to IR with or without curcumin. Consistently, curcumin conferred IR-induced apoptosis and DNA fragmentation in a dose dependent fashion. Coherently, curcumin enhanced IR-induced cytotoxicity and clonal expansion. Together, these results firmly imply that curcumin is a potent radio-sensitizer, and it acts by regulating IR-modulated p53 response genes in p53

mutant human neuroblastoma cells. To that end, p53 independent mechanisms involved in curcumin regulated p53 response genes remains to be investigated.

(PS7.25) Dasatinib, an inhibitor of Src kinases, is a potent inhibitor of cancer cell invasion and metastatic spread. F. Matsumoto, U. Raju, D. Valdecanas, L. Wang, T. Sheu, K. Mason, K.K. Ang, L. Milas, M.D. Anderson Cancer Center, Houston, TX

cSrc, a member of a family of Src non-receptor kinases, is often over-expressed and constitutively active in many human cancers. It is implicated to promote cell survival and proliferation, tumor angiogenesis, and cell adhesion and motility. We recently reported that its inhibition of cSrc by dasatinib enhances in vitro cell radiosensitivity and in vivo radioresponse of head and neck tumor xenografts (PAAACR, 2010, Abstract #488). The present study tested whether dasatinib either alone or combined with radiation (IR) influences in vitro tumor cell migration and invasion of H460 human lung cell cancer cell line and FaDu head and neck cancer cell line, and in vivo tumor metastasis development from xenografts derived from these cell lines. Dasatinib at doses of 50 to 200 nM reduced the migration of H460 cells into the scratched area of culture plates by 20%, and reduced invasion through the Matrigel membrane of H460 cells by over 80% and of FaDu cells by 50%. IR of cells with 4 Gy had no significant effect on in vitro invasion of these cell lines, but the invasion was strongly inhibited by dasatinib treatment given before IR. H460 tumor xenografts in the leg of nude mice generate spontaneous lung metastases but this was inhibited by dasatinib (10 mg/kg) given daily for 27 days. Xenografts began to metastasize at about 8mm, and both the incidence and median number of metastases increased with tumor size. Tumor incidence and median number of metastases generated by 10 mm tumors were 7 of 8 (88%) and 14.5, respectively; this was reduced by dasatinib to 5 of 16 (31%) and 3.0, respectively. The experiments testing the antimetastatic effect of dasatinib when combined with fractionated local tumor irradiation using both H460 and FaDu tumor xenografts are ongoing. In conclusion, our results showed that dasatinib as a single agent strongly inhibited cell migration and invasion of cancer cells in vitro. Whereas IR only had no effect on H460 and FaDu in vitro cell invasion, the invasion was strongly inhibited when dasatinib was given before irradiation. Dasatinib also significantly blocked spontaneous metastatic spread of H460 tumor xenografts. Thus, in addition to being potent enhancer of local tumor radioresponse dasatinib offers a promising approach for controlling metastatic spread as well. (Supported by NIH PO-1 Grant CA-06294)

(PS7.26) Effect of γ -irradiation and angiogenesis inhibitor avastin treatment on distribution of blood flow and accumulation of boron compounds in murine tumors. Yong Liu¹, Kenji Nagata², Minoru Suzuki¹, Yi-Wei Chen³, Genro Kashino¹, Shin-ichiro Masunaga¹, Yuko Kinashi¹, Hiroki Tanaka¹, Yoshinori Sakurai¹, Mitsunori Kirihata⁴, Koji Ono¹, ¹Research Reactor Institute, Kyoto University, Osaka, Japan, ²Department of Radiology, Ishikiriseiki Hospital, Osaka, Japan, ³Department of Radiation Oncology, Taipei Veterans General Hospital, Taipei, Taiwan, ⁴Graduate School of Environment and Life Science, Osaka Prefectural University, Osaka, Japan

Previous studies have demonstrated that X-ray irradiation and angiogenesis inhibitor treatment can affect tumors vessels. Here, we studied the effects of γ -ray irradiation and angiogenesis inhibitor Avastin on tumor blood perfusion and boron-10 compound accumulation in murine tumor model. The mouse squamous cell carcinoma was irradiated with γ -ray before BSH (¹⁰B-enriched borocaptate sodium) administration. Then, the boron-10 concentrations in tumor and normal muscle tissues were measured by prompt γ -ray spectrometry (PGA). A tumor blood flow assay was performed, and cell killing effects of neutron irradiation with various combinations of BSH and γ -rays were also examined. BSH concentrations of tumor tissues were 16.1 \pm 0.6 μ g/g, 16.7 \pm 0.5 μ g/g at 72 hours after γ -ray irradiation at doses of 5 and 10 Gy, compared with 13.1 \pm 0.5 μ g/g in unirradiated tumor tissues

($p < 0.01$). The enhancing inhibition of colony formation by neutron irradiation with BSH was also found after γ -ray irradiation. In addition, increasing Hoechst 33342 perfusion was also observed after γ -irradiation or Avastin administration. In this study, we demonstrated that γ -ray irradiation or Avastin treatment enhances tumor blood perfusion and BSH accumulation in tumors. These results suggest that the combination of γ -irradiation or angiogenesis inhibitor treatment with boron compound administration may be useful to improve the efficacy of BNCT (boron neutron capture therapy), which is due to the changes in the extracellular microenvironment, including in tumor vessels. Next, we will study the micro-distribution of boron compound in tumor tissues using antibody of BPA (*p*-boronophenylalanine) or BSH, which has been demonstrated successfully in studying the boron compound distribution in cultured cells.

(PS7.27) Drug development of a novel radiosensitizing histone deacetylase inhibitor with fluorescent properties. Keith Unger, Thomas Walls, Scott Grindrod, Mira Jung, Milton Brown, Georgetown University, Washington, DC

Inhibitors of histone deacetylases (HDACs) are emerging as a new category of antitumor agents, with potential to sensitize cancers to radiation therapy. Using rational drug design, we have discovered a novel fluorescent HDAC inhibitor (THW-6-89) demonstrating radiosensitization of lung cancer cells. Recombinant purified HDAC protein isomers were used in screening Class I and II HDAC inhibitory activities and demonstrated selective inhibition of HDAC6. Growth inhibition was observed at nano- and micromolar drug concentrations in PC-3, LnCap, C42, SQ-20B, MCF-7, and MDA-MB-231 cancer cells. Twenty-four hours of exposure to THW-6-89 resulted in a G1 cell cycle arrest. THW-6-89 has a fluorescence moiety integral to its structure with a maximum wavelength of excitation at 500 nm and an emission maximum at 578 nm. Using multiphoton microscopy, THW-6-89 staining was observed in PC-3, LnCap, A549, MDA-MB-231, and MCF-7 cancer cell lines with drug localization in the cellular cytoplasm, suggesting a possible mechanism of action within the cytoplasm. The radiosensitizing properties of THW-6-89 were evaluated using clonogenic assays in A549 lung cancer cells. Following 24 hours of THW-6-89 treatment, the D_0 for untreated controls was 2.0 Gy and for THW-6-89 exposed cells was 1.7 Gy, showing radiosensitization with a ratio of 1.2. THW-6-89 is a potentially useful radiosensitizing HDAC inhibitor with novel fluorescent properties, offering diagnostic and therapeutic capabilities for further investigation.

(PS7.28) The impact of chromatin density and histone deacetylases for the radiation response of human tumor cells. Katja Storch¹, Iris Eke¹, Kerstin Borgmann², Mechthild Krause³, Kerstin Becker⁴, Evelin Schröck⁴, Nils Cordes¹, ¹OncoRay - Center for Radiation Research in Oncology, Dresden, Germany, ²Laboratory of Radiobiology Experimental Radiooncology, Hamburg, Germany, ³Department of Radiation Oncology, Dresden, Germany, ⁴Institut für Clinical Genetics, Dresden, Germany

Using three-dimensional (3D) cell culture models, cellular behaviour upon irradiation can be examined under more physiological conditions. As compared to a flat and spread cell morphology found when cells grow on culture plastic, 3D growth exhibits a round cell shape. Recent findings suggest these differences to substantially impact on nuclear structure and chromatin organization, which in turn strongly influence the regulation of cell survival and DNA repair. In 3D, the increased chromatin density is reflected by elevated heterochromatin protein (HP) 1-alpha and decreased histone H3 acetylation. Dynamic histone modifications like acetylation are mediated by the key regulators of chromatin architecture called histone acetyltransferases and histone deacetylases (HDAC). The aim of this study was to identify the relevance of HDACs in irradiated human A549 lung cancer cells by the means of siRNA knockdown (HDAC1+2+4) or pharmacological HDAC inhibition with LBH589 (Novartis). To further evaluate the role of chromatin condensation on radioresis-

tance, the number of eu- and heterochromatic foci were compared in A549 cells grown in 3D, as xenograft tumors and as monolayer cell culture. Clonogenic radiation survival (0-6 Gy), total number of radiogenic DNA double-strand breaks (foci assay), chromosomal aberrations (G0 assay, Spectral Karyotyping) and protein expression (acetyl-H3, HP1-alpha) were examined. These data show enhanced radioresistance in 3D cells in correlation with reduced numbers of DNA double-strand breaks (DSBs) and lethal chromosome aberrations. While the HDAC1+2+4 siRNA knockdown showed no effect on radiosensitivity, LBH589 significantly enhanced the radiosensitivity and the number of residual DBSs in a dose-dependent manner. Intriguingly, eu- to heterochromatin associated radiogenic DSBs were equally distributed in 3D and xenograft tumor cells while monolayer cells showed more DSBs in euchromatin. Taken together, these data show a relation between cell morphology and cellular radioresistance based on chromatin organization. Future studies will elucidate the underlying molecular mechanisms by which chromatin structure influences the radiation response. These results might be highly relevant for radiation cell survival and thus targeted therapies in radiation oncology.

(PS7.29) A small molecule screen to identify novel inhibitors of the Unfolded Protein Response and hypoxia tolerance in tumor cells. Lori S. Hart¹, Andrew T. Segan¹, Ioanna Papatheou², Albert Koong², Constantinos Koumenis¹, ¹University of Pennsylvania, Philadelphia, PA, ²Stanford University School of Medicine, Palo Alto, CA

Hypoxia arguably represents the most thoroughly characterized of microenvironmental factors in tumor pathogenesis. Clinical evidence identifies hypoxia as a contributor of therapeutic resistance, as well as an indicator of an aggressive tumor phenotype. The adaptation of tumor cells to hypoxia is largely due to activation of HIF1 and HIF2; however, other mechanisms also play a part. The Unfolded Protein Response (UPR) represents such a mechanism and contributes to tumor cell survival. Inactivation of the UPR results in reduced hypoxia tolerance and slower tumor growth in animal models. Our studies have focused on the role of PERK, a kinase that responds to unfolded proteins by phosphorylating eIF2 α , downregulating global protein synthesis, and specifically inducing the translation of ATF4. Loss of ATF4 sensitizes tumor cells to hypoxia, validating the importance of identifying ATF4 inhibitors. We have employed a small molecule screen to identify inhibitors of ATF4 via overexpression of a reporter construct with the 5'-UTR of ATF4 fused to the luciferase gene in HT1080 cells. When ATF4 reporter cells were treated with Thapsigargin, we observed more than a four-fold induction of luciferase over control cells in a PERK-dependent manner. Using the Stanford University chemical library of over 160,000 diverse small molecules and the NIH Molecular Libraries Small Molecule Repository at the University of Pennsylvania, we performed a primary screen on the HT1080 ATF4-luciferase cells. We identified 5 small molecules based on the inhibition of ATF4, with Z-values above 3 and low μ M or high nM IC50 values. The compounds are currently undergoing validation in secondary screens for the specific inhibition of ATF4 but not CMV-luciferase or XBP-1-luciferase reporters. We plan to identify structural families and perform structure-activity relationship (SAR) analysis to identify related compounds. Validated compounds will be assessed for the ability to reduce hypoxic tolerance through cell proliferation, cell survival, and *in vitro* and *in vivo* tumorigenicity assays. Tumor cells exploit normal cellular processes for their own survival and propagation. The identification of UPR inhibitors represents an opportunity to abolish one such process, and represents a novel therapeutic strategy for the treatment of solid tumors.

(PS7.30) Clinical feasibility of total body irradiation with helical tomotherapy. Jose A. Penagaricano, Ming Chao, Eduardo G. Moros, Vaneerat Ratanatharathorn, Peter M. Corry, University of Arkansas, Little Rock, AR

Purpose: This study details the use of Helical Tomotherapy (HT), for the first time, to conformally treat the clinical target

volume (CTV = whole body - [lungs + kidneys]) in total body irradiation (TBI) in AML patients as part of conditioning prior to allogeneic bone marrow transplantation (ABMT). Retrospective reconstruction of delivered region of interest (ROI) doses, details of treatment planning and delivery, and patient outcome are also described. Methods and Materials: Four AML patients received TBI with HT as part of a conditioning regime prior to ABMT: three with 100% matched donors and one refractory to induction therapy with unrelated donor. After TBI, patients received cyclophosphamide x 2 days followed by ABMT and then by graft vs. host disease (GVHD) prophylaxis. TBI prescribed dose was 12Gy in 6 fractions, to 80% of the CTV, BID, separated by 6 hours. With modulation factor 2.0, and pitch 0.287 or 0.43, beamlet calculation was 8 - 10 hours. With 5 cm jaw width, beam-on times were 19 - 23 minutes, comparable to the linac-based TBI. The means of the average doses to CTVs, lungs, and right and left kidneys were 12.2, 7.1, 7.8 and 7.8Gy, respectively. The mean standard deviation of the CTV dose was 0.65Gy whereas the CTV mean conformality index was 0.83. Pretreatment whole body MVCT was used for patient alignment. ROIs were contoured on each MVCT. The dose for each fraction was calculated based on the MVCT on the HT Planning Adaptive Station. Then, using B-Spline deformable registration, voxel-to-voxel correspondence between the MVCT and the planning CT was established thus obtaining voxel-to-voxel summed doses from all six fractions. The reconstructed dose plans were then compared to the original dose plans. Results: Two patients are alive without AML or GVHD at 11 and 12 months. Two died of GVHD at 5 and 6 months with no evidence of AML. All patients had faint skin erythema and one mild headache. Retrospective dose verification showed CTV doses to be < 1.5% to that of the original plan. For sensitive structures the differences were < 4.0%. Conclusion: This work demonstrates the feasibility and efficiency of HT to treat the CTV in clinical TBI with a superior degree of conformality and limited toxicities. In TBI with HT there is no need of compensators, beam spoilers, extended SSDs or lung blocks.

(PS7.31) Response of platinum-radiosensitizing agents in human colorectal cancer with true concomitant chemoradiotherapy. Thititip Tippayamontri, Rami Kotb, Leon Sanche, Benoit Paquette, University of Sherbrooke, Sherbrooke, QC, Canada

Responses to the combination of platinum drugs and radiation in experimental and clinical studies have been obviously recognized, but the best therapeutic schedule is yet to be determined. Understanding the cytotoxic mechanisms of platinum drugs and elucidating their underlying pharmacokinetics are crucial to improve their efficiency as radiosensitizers. We studied the cytotoxic effects on the human colorectal cancer HCT116 cells, the intracellular accumulation, and the DNA binding for four platinum drugs: cisplatin, oxaliplatin, and their respective liposomal formulation LipoplatinTM and LipoxalTM. Further, we examined the combined effect of platinum drugs with ionizing radiation in HCT116 cells with special attention to the timing of irradiation. At the inhibitory concentration (IC₅₀), their intracellular accumulation and DNA-binding levels were measured after 1, 4, 8, 24 and 48 h incubation using inductively coupled plasma mass spectrometry. The synergistic effect with radiation was tested after 8 h incubation which corresponded to the optimal drug uptake, and evaluated using a combination index. As control, the assays were repeated at a lower drug uptake (48 h). Although cisplatin was as efficient as oxaliplatin after a short exposure time, oxaliplatin either under its free form or transported in the liposome LipoxalTM became more efficient than cisplatin for treating the HCT116 cells after 24 h incubation. Our study supports that incorporation of oxaliplatin in the liposome LipoxalTM largely improved its accumulation in the HCT116 cells. The distribution cytoplasm/DNA of cisplatin and LipoplatinTM were similar. Conversely, LipoxalTM has largely modified the distribution cytoplasm/DNA of oxaliplatin. The concomitant treatment with radiation was found a clear synergistic effect at all the IC₅₀ values tested at 8 h incubation, where the maximum distribution ratio of DNA-Pt and cell-uptake were observed. The better concomitance effect was obtained with a LipoxalTM and LipoplatinTM, compared to their free analogs. Our finding on the nature of interaction of platinum drugs and radiation are that in order to reach an optimal cytotoxic effect of the combined therapy, the tumor cells should be

irradiated at the maximum distribution cytoplasm/DNA to better obtain the synergistic effect.

(PS7.32) LysoPLD and LPA receptors represent novel potential treatment targets for the radiosensitization of malignant glioma, largely through effects on the tumor microvasculature. Stephen M. Schleicher¹, Eugenia Yazlovitskaya¹, Amanda Linkous¹, Kathleen Leahy², Dennis Hallahan², Dinesh Thotala², ¹Vanderbilt University, Nashville, TN, ²Washington University in St. Louis, St. Louis, MO

Unresectable malignant glioma (MG) is uniformly fatal, partly because it exhibits disease progression and radioresistance despite wide margins and high dose. One potential mechanism for radiosensitization is targeting the tumor vasculature. The enzyme LysoPLD has been shown to play a role in the pathogenesis of multiple cancer phenotypes, and it is over-expressed in MG. LysoPLD converts lysophosphatidylcholine (LPC) to the lipid second messenger lysophosphatidic acid (LPA) which is believed to act on LPA receptors on cancer cells and vascular endothelial cells to induce pro-survival signaling pathways such as Akt. Cytosolic phospholipase A2 (CPLA₂), which is expressed in endothelial cells following irradiation and which produces LPC, the substrate for LysoPLD, has already been shown to be a molecular target for radiosensitization in other cancer cell lines and when inhibited induces cytotoxic and inhibitory effects on endothelial cells. In this study, BrP-LPA, an inhibitor of LysoPLD and LPA receptors, was used to investigate whether inhibition of these targets downstream of CPLA₂ leads to the radiosensitization of MG and its tumor microvasculature. Using bEnd.3 brain microvascular endothelial cells, we show that 5 μM BrP-LPA leads to reduced clonogenic survival, tubule formation, and migration in brain microvascular endothelial cells treated with 3 Gy. These results were confirmed in Human umbilical vein endothelial cells (HUVEC). Treatment with BrP-LPA also induced cell death at 2 Gy and reduced migration in GL261 mouse glioma cells. To investigate the relationship between endothelial and MG cells, bEnd.3 and GL261 cells were grown in co-culture. Immunoblotting of co-culture cell lysates showed that treatment with BrP-LPA 45 min prior to irradiation caused reduced phosphorylation of pro-survival Akt in irradiated bEnd.3 and GL261 cells. These findings suggest that LysoPLD and LPA receptors play a role in the radioresistance of MG cells, largely by effects on tumor vasculature, and should be studied further as a potential novel molecular target for radiosensitization.

(PS7.33) EF24 mitigates radiotherapy-orchestrated NFκB-mediated survival advantage. Jamunaranj Veeraraghavan¹, Mohan Natarajan², Rakesh Madhusoodhanan¹, Vibhudutta Awasthi¹, Hrushikesh Agashe¹, Terence S. Herman¹, Natarajan Aravindan¹, ¹University of Oklahoma Health Sciences Center, Oklahoma City, OK, ²University of Texas Health Science Center at San Antonio, San Antonio, TX

Recently, we reported that low LET radiation (IR) induces NFκB in neuroblastoma cells and curcumin impedes NFκB activation thereby enhancing IR-induced cell death. However, the full potential of curcumin is not apparent due to its poor bioavailability. Herein, we investigated the efficacy of a more potent synthetic analogue of curcumin, EF24 in regulating IR-orchestrated NFκB -dependent survival advantage. Human neuroblastoma (SH-SY5Y, IMR-32) cells either exposed to 2Gy or treated with EF24 prior to radiation exposure were examined after 1 through 72h. IR profoundly and persistently induced NFκB DNA binding activity at least for up to three days. Consistently, IR induced sustained transactivation and secretion of TNFα in these cells. Conversely, silencing NFκB with SN50 peptide or RelA siRNA completely suppressed IR-induced TNFα transactivation/secretion. Interestingly, blocking the binding of secreted TNFα by blocking TNF receptor inhibited IR-induced persistent activation of NFκB demonstrating the initiation and occurrence of IR-induced NFκB→TNFα→NFκB feedback mechanism (PFC). Furthermore, IR substantially induced NFκB dependent (silencing studies) downstream targets *Birc* (1, 2, 5) transactivation. Conversely,

EF24 completely and persistently inhibited IR-induced NF κ B and TNF α (transactivation/secretion) suggesting that EF24 disrupts IR-induced PFC and thereby inhibit persistent activation of NF κ B. In addition, EF24 inhibited IR-induced NF κ B dependent *Birc1*, 2 and 5. More importantly, EF24 profoundly conferred IR-induced inhibition of cell survival and clonal expansion in these cells. These results strongly suggest that neuroblastoma cells surviving a course of radiotherapy might develop survival advantage mediated by persistent NF κ B activation through NF κ B \rightarrow TNF α \rightarrow NF κ B PFC. More importantly; disruption of IR-initiated PFC by EF24 might significantly inhibit NF κ B-dependent survival advantage and could serve as a "deliverable" to mitigate neuroblastoma progression and relapse.

(PS7.34) Head-only radiation in adult mice and whole-body radiation in neonatal mice impair contextual fear memory. Amy M. Hein, Carl J. Johnston, Jack N. Finkelstein, Jackie P. Williams, John P. Olschowka, M. Kerry O'Banion, University of Rochester Medical Center, Rochester, NY

Cognitive deficits are commonly reported following ionizing radiation - both after targeted radiotherapy and following whole body radiation exposure. Often times these deficits are exacerbated in young children, revealing a particularly radiation susceptible population. Animal models in rodents have been developed to investigate the molecular bases of these radiation-induced cognitive impairments and have implicated oxidative damage, inflammation, and reduced neurogenesis as contributing factors. Here we corroborate previous studies and demonstrate a dose by time interaction for memory deficits following head only radiation. High (45 Gy) but not low (5-35 Gy) doses of head only gamma-radiation in adult mice impair contextual fear memory at 3 but not 1 month after exposure. Studies examining memory 6 months after radiation exposure are still ongoing. In separate experiments designed to examine potential radiation susceptibilities of young animals, mice received whole body gamma-irradiation (sham, 2.5, or 5 Gy) post natal day 4, and 2 months later underwent contextual fear conditioning. Mice receiving 5 Gy of radiation froze 50% less than sham-irradiated mice, indicating impaired hippocampal-dependent memory. Ongoing molecular analyses from this study will evaluate hippocampal neurogenesis, neuroinflammation, and systemic inflammation as potential correlates to memory dysfunction. While the central nervous system is often considered highly radiation resistant, these data clearly demonstrate functional neuro-sensitivities to head-only and whole-body irradiation. Therefore, further studies are needed to address potential therapeutic interventions to protect normal cognitive function following radiation exposure. This work was supported by RO1 CA114587 and U19 A1067733-05S1.

(PS7.35) Regulation of the metabolic network improves the response of human colon cancer cells to radiation. Ibraimoudi S. Ayene, Jie Li, Donglan Zhang, Lankenau Institute for Medical Research, Wynnewood, PA

Purpose: There is a recent upsurge of interest in regulating the metabolic network of adaptive mechanisms to improve the response of cancer cells to therapy. Arsenic trioxide (Trisenox) is a Food and Drug Administration (FDA) approved drug for treatment of acute promyelocytic leukemia in the US. This compound has shown significant improvement in the outcome of leukemia patients. Here, we investigated the use of arsenic trioxide to modulate the metabolic activity and radiation response of human colon cancer cells. Methods: We used HCT116 and HT29 human colon cancer cells obtained from ATCC. We have selected these two cells originated from colon because of the difference in the p53 status. The effects of Trisenox on the metabolic activity and radiation response of these cells were determined by glucose associated oxidative pentose phosphate cycle activity and cell growth respectively. Results: Much lower metabolic activity was found in both p53 wild type HCT116 and p53 mutant HT29 cells treated with trisenox as compared to the untreated cells. Trisenox by itself decreased the survival in both p53 wild type HCT116 and p53 mutant HT29 cells.

When exposed to gamma radiation in the presence of Trisenox, HCT116 exhibited a higher cell killing at clinically relevant low doses of gamma radiation. HT29 cells treated with trisenox also exhibited a better response to radiation but to a lesser extent as compared to HCT116. Conclusions: These results suggest that metabolic activity of human cancer cells can be inhibited by trisenox irrespective of the p53 status. Additionally, the results also demonstrated that trisenox is a novel sensitizer of both p53 wild type and mutant human cancer cells to gamma radiation. Potential mechanisms and clinical implications of this approach will be discussed. This work was supported by NCI, National Institute of Health Grant CA109604 (ISA).

(PS7.36) Role of YAP-1 in EGR-1 mediated radiosensitization of prostate carcinoma cells. Mohammed M. Shareef, Seema Gupta, Mansoor M. Ahmed, University of Miami, Miami, FL

Loss of the apoptotic response to ionizing irradiation (IR) by over-expression of pro-survival or down-regulation of pro-apoptotic genes has been linked to a radio-resistant phenotype. We selected the Early Growth Response-1 (Egr-1) gene to understand its role in radiation resistance, because (a) upon orchietomy Egr-1 is rapidly induced, leading to apoptosis of androgen-dependent prostate cells (b) IR upregulates EGR-1 expression and (c) EGR-1 protein upregulates pro-apoptotic gene expression. We previously demonstrated that EGR-1 transactivates the promoter of the Bcl2-associated X (Bax) gene and this is achieved by interaction of EGR-1 with WW domain of Yes-kinase Associated Protein 1 (YAP-1) with a PPxY motif (235YPPPAY240) in EGR-1. In this study, we analyzed the role of EGR1-YAP1 interaction in the regulation of radiation response of prostate cancer cells. In addition to the tyrosine residue at position 240, aromatic amino acid residue (Y235) present at the amino terminal of the PPxY motifs is crucial determinant of the WW domain binding activity. Using EGR-1 mutants defective in binding to YAP-1 (EGR-1Y235A; EGR-1Y240A) and YAP-1 ShRNA, we demonstrate that YAP-1 functions a suppressor of cell proliferation as assessed by clonogenic assay and real-time cell growth monitoring by RT-CES.

(PS7.37) The EGFR modulates DNA double strand break repair via MAPK pathway in bronchial carcinoma cell lines. Ekkehard Dikomey, Malte Kriegs, Ulla Kasten-Pisula, Jochen Dahm-Daphi, Laboratory of Radiobiology & Experimental Radiooncology, Hamburg, Germany

Purpose: The epidermal growth factor receptor (EGFR) seems to affect the outcome of radiotherapy presumably by regulating DNA double strand break (DSB) repair, but detailed mechanisms of this interaction are not yet clear. The aim of this study was to verify, if the activation status of EGFR modulates the DSB repair and which of the pathways downstream of EGFR (MAPK vs. Akt) are involved. Material & Methods: Experiments were performed using the bronchial carcinoma cell line A549 and H1299. DSB repair was studied either by measuring unrepaired DSBs 24 h after irradiation using γ H2AX foci technique or using a repair substrate (pEJ). This repair substrate was specifically designed to monitor non-homologous end joining (NHEJ) and was stably integrated into A549 and H1299 cells. EGFR was stimulated by EGF, Amphiregulin or TGF α ; EGFR signaling was inhibited using either a specific tyrosine-kinase inhibitor Erlotinib (Tarceva[®] Roche) or the monoclonal anti EGFR antibody Cetuximab (Erbix[®] Merck). MAPK and Akt signaling was inhibited using the specific MEK inhibitor PD98059 and the specific Akt inhibitor Akt VIII. Protein knock down was achieved using siRNA. Results: Stimulating the EGFR using EGF leads to a clear reduction of γ H2AX foci 24 h after irradiation indicating an enhanced DSB repair capacity. EGF was also found to stimulate NHEJ as detected by the specific repair substrate pEJ. This was also true for TGF α and Amphiregulin but in a lesser extent. Knock down of EGFR via siRNA prohibits EGF mediated increase of NHEJ. Additionally, stimulation of NHEJ could be inhibited by using either the monoclonal antibody Cetuximab or the small molecule inhibitor Erlotinib. Both substances caused also an increase of γ H2AX foci 24 h after

irradiation. Analyzing downstream pathways of EGFR in more detail, we discovered that the inhibition of MAPK signaling was sufficient to cause maximum inhibition of DSB repair. Conclusion: EGFR signal transduction stimulates DSB repair presumably by activating NHEJ. This regulation is mainly transmitted via the MAPK pathway. Project was supported by DFG project Di 457/8-1 which is part of PAK190.

(PS7.38) Inhibition of MGMT expression by Levetiracetam (Keppra®) Enhances Temozolomide-induced Radiosensitivity in Glioblastoma multiforme. Whoon Jong Kil, Kevin Camphausen, Elena Lita, Sharon Smith, Radiation Oncology Branch/National Cancer Institute, Bethesda, MD

Background: Glioblastoma multiforme (GBM) is among the most common and lethal brain cancers in adult. The maximum benefit from surgery + radiation therapy (RT) with temozolomide (TMZ) has been shown in patients with methylated MGMT gene. Levetiracetam (Keppra®), a new generation anticonvulsant, is reported as an inhibitor of cellular O⁶-methylguanine-DNA-methyltransferase (MGMT) expression. Here, we investigate the effect of Levetiracetam on RT with TMZ treatment *in vitro* and its clinical relevant. Patients and Methods: Four MGMT-positive cell lines (LN18, HCT116, H1299, MCF7) were used to evaluate Keppra® effects on MGMT expression. To find out optimal Levetiracetam treatment schedule *in vitro*, LN18 cell line was tested. The effects of Levetiracetam on the *in vitro* radiation enhancement of LN18 and U251 (MGMT-negative GBM) was evaluated using clonogenic assay. With data from 42 GBM patients, we then retrospectively assessed relations between Levetiracetam treatment and clinical outcome as a pilot study. Results: Levetiracetam (100µM for 16 hrs) showed a cellular inhibition of MGMT expression in all four MGMT-positive cell lines. Exposure of LN18 cell line to 50µM of Levetiracetam for 1 hr resulted in a decreased MGMT expression lasting 6 hrs. Enhanced radiation responses with dose enhancement factor at survival fraction of 0.1 were 1.28, 1.51 (TMZ alone, Levetiracetam +TMZ, respectively) with LN18, and were 1.34, 1.36 (TMZ alone, Levetiracetam +TMZ, respectively) with U251. Thirty-four patients received Levetiracetam during RT+TMZ treatment. The number of patients classified in RPA class III, IV, and V were 9, 24, and 9, respectively. Overall survival was 26 months with Levetiracetam along with RT+TMZ treatment and 18 months with RT+TMZ treatment (p=0.4349) after a median follow-up 16 months (range, 2~53 months). There was increased overall survival with patients in RPA class III and IV (27 months and 26 months, respectively) than class V (15 months) (p=0.0012). Conclusions: *In vitro* data indicate that Levetiracetam can enhance TMZ-induced radiosensitivity in MGMT-positive GBM cell line. Pilot clinical data suggest that Levetiracetam along with RT+TMZ could increase survival in GBM patients regardless of their MGMT-methylation status. Further investigation is needed to confirm this hypothesis.

(PS7.39) H6CAHA, a stable and potent hydroxamate-based histone deacetylase inhibitor, enhances the therapeutic efficacy in prostate cancer radiotherapy. Zacharoula Konsoula, Mira Jung, Georgetown University, Washington, DC

Structurally diverse histone deacetylase inhibitors (HDACIs) have emerged as an important class of anti-cancer agents and have shown to cause differentiation, cell cycle arrest and apoptosis. Here, we present evidence that a hydroxamate-based HDACI, H6CAHA, has favorable physicochemical properties, including lipophilicity, solubility and permeability. In addition, plasma pharmacokinetics in male nude mice revealed that the peak concentration (C_{max}) of H6CAHA was 6.88 ± 0.71 µM and the area under the curve (AUC) was 8.08 ± 0.91 µM x h, indicating good plasma distribution. Peak plasma levels were observed at 2 h post-administration of H6CAHA and the half-life was calculated to be 11.17 ± 0.87 h. Furthermore, H6CAHA was tested to determine whether it influences survival and DNA damage-repair in irradiated human prostate cancer and normal cells. *In vitro* clonogenic assays revealed that H6CAHA decreased the survival

in prostate cancer cells and promoted the survival in normal cells. Additionally, immunofluorescence analysis displayed that H6CAHA caused an accretion in the radiation induced phospho-H2AX (γH2AX) and RAD51 foci beyond 24 h in prostate cancer cells and a decline in normal cells. Taken together, H6CAHA has been shown to enhance the therapeutic potential in cancer radiotherapy by killing cancer cells and still protecting normal cells from radiation-induced damage. Thus, the results provide a rationale for clinical investigation of the therapeutic efficacy of H6CAHA in combination with radiotherapy.

(PS7.40) miRNA response in endothelium and tumors in response to angiogenesis inhibitors and radiation. Peter E. Huber¹, Ramon Lopez¹, Mechthild Wagner¹, Sebastian Schölich², Nuh Rabari², Moritz Koch², Ute Wirkner¹, ¹Radiation Oncology, dkfz and University Hospital, Heidelberg, Germany, ²Surgery, University Hospital, Heidelberg, Germany

The interdependencies between tumor and tumor microenvironment are critical for tumor therapy. Increasingly, for many tumors, combination therapy regimens that include new targeted biologicals e.g. angiogenesis inhibitors and radiotherapy are being pursued. Noncoding RNA has been shown to be important regulators for cancer and endothelial cells. Here we have systematically investigated the roles of noncoding RNA in response to cancer therapies including small molecule VEGF/PDGF RTKI (Sutent), TGF-beta RKI, integrin inhibitors (Cilengitide), and EGFR AB (Cetuximab) alone and in combination with ionizing radiation in human microvascular endothelial (HDMEC) and pancreatic carcinoma cells (BXP3) *in vitro* and *in vivo* using a balb c nude mouse model. RNA was isolated from 2 - 72 h after treatments, and the Exiqon V9.2 microarray expression profiling platform was used along with qRT-PCR to measure differentially regulated miRNA. To functionally analyze the roles of the differentially regulated miRNAs, cell proliferation, migration and clonogenic survival assays were performed after transfection with miRNA precursor or inhibitor constructs. We found that both drugs and radiation significantly regulated the expression of many miRNAs (~5-20 miRNA/modality) with distinct similarities between the *in vitro* and *in vivo* situation, e.g. Cetuximab and Cilengitide reduced miR-558 expression in BxPC3 which was further enhanced by their combination. In HDMEC, Cetuximab decreased e.g. miR-571, Cilengitide increased miR-335, and TGF-beta RKI increased let7g and miR-214 levels. Radiation up-regulated let-7g, miR-16, miR-20a, miR-21 and miR-29c, while miR-18a, miR-125a, miR-127, miR-148b, miR-189 and miR-503 were down-regulated. Overexpression of let-7g, miR-127, and miR-20a increased radiation-induced cell toxicity, while e.g. overexpression of miR-189 and miR-125a reduced radiosensitivity. The data show that microRNA in endothelium and tumor cells are regulated upon treatment with specific signaling inhibitors of VEGF/PDGF, TGF-beta, integrins and EGF. The data also suggest that miRNA are critically involved in a complex regulation of endothelial and tumor cell response to these specific drugs and radiation which may have important implications for choosing optimal tumor therapy combinations.

(PS7.41) Pharmacologic blockade of ribonucleotide reductase enhances human cervical cancer chemoradiosensitivity by inhibiting repair of dna damage. Charles Kunos, Tammy Stefan, Tomas Radivoyevitch, John Pink, Case Comprehensive Cancer Center, Cleveland, OH

Background Pharmacologic blockade of ribonucleotide reductase (RNR), the rate-limiting generator of deoxyribonucleotides (dNTPS) for DNA synthesis and repair, intensifies radiosensitivity by sustaining DNA damage. 3-aminopyridine-2-carboxaldehyde thiosemicarbazone (3-AP, NSC #663249) is a small molecule inhibitor of RNR, with greater clinical applicability than hydroxyurea, currently being tested in Phase 2 clinical trials as a potential radiosensitizer and chemosensitizer. Methods RNR was inactivated by clinically relevant doses of 3-AP (5µM) and resulting radiosensitization and chemosensitization was evaluated in CaSki

and C33-a human cervical cancer cell lines. DNA damage induced by IR (200cGy) or cisplatin (5 μ M) with or without 3-AP was measured by flow cytometry (γ H2AX signal), RNR enzyme activity by polymerase extension assay, survival by colony formation, and p53R2 and p21 protein levels by Western blot and laser scanning imaging cytometry. Results 3-AP treatment lead to sustained radiation- and cisplatin-induced DNA damage (i.e. increased γ H2AX signal) in both cell lines. 3-AP co-administration also caused significant lowering of RNR activity despite increased demand for dNTPs due to damage, resulting in a protracted G1/S-phase cell cycle arrest. Radiation and cisplatin plus 3-AP exposure resulted in significantly elevated and persistent presence of γ H2AX foci which was associated with reduced clonogenic survival. Elevated p53R2 levels correlated with DNA damage but p21 protein levels were unaltered 6-hours after radiation and/or cisplatin plus 3-AP treatment. Conclusions Pharmacologic blockade of RNR activity impairs DNA damage responses that rely on dNTP production, and thereby, substantially increase radiosensitivity and chemosensitivity of human cervical cancers.

(PS7.42) Combining HIF-1 inhibition with hyperthermia and chemotherapy as a new anti-tumor strategy for selectively targeting hypoxic cells in breast cancer. Yu-Chih Charleen Nien, Timothy Robinson, Mark W. Dewhirst, Duke University, Durham, NC

The proposed work aims to provide pre-clinical rationale for combining HIF-1 blockade with hyperthermia and chemotherapy in the setting of a novel doxorubicin containing thermally sensitive liposome (LTSL-Dox) for treating locally advanced breast cancer. Hyperthermia (HT) acts as a potent radio-sensitizer and enhances the antitumor effects of chemotherapy, suggesting the combined RT/CT+HT therapies as a very efficient adjuvant to treat cancer. However, one of the major hurdles for treating cancers is the adaptation of tumor cell subpopulations to selective environmental pressures, such as low pH, low glucose, and hypoxia. In response to hypoxic stress, through up-regulation of Hypoxia-Inducible Factor (HIF)-1 α , tumor cells become more aggressive and more treatment resistant. HIF-1 has also been found to control angiogenesis and cellular metabolism, thereby facilitating hypoxic tumor cell survival. The above findings underscore the need to eliminate hypoxic tumor cells for improving available therapeutic interventions. Our lab has previously demonstrated that HT increases HIF-1 α levels and its transcriptional activity due to increased ROS production. To identify whether HIF-1 contributes to resistance of tumor cells to heat, we observed that silencing HIF-1 decreases clonogenic survival of MDAMB 231 breast cancer cells after HT at 42 degrees rendering tumor cells more heat sensitive with a dose modifying factor of ~2. The data above suggests HIF-1 is a key regulator of HT sensitivity. Additional evidence from our group further supports the idea that HIF-1 targeted therapy can reverse hypoxia-related doxorubicin resistance. Thus, we hypothesize that selectively targeting the hypoxic tumor cell compartment by inhibiting HIF-1 α , combined with thermochemotherapy with the novel doxorubicin containing thermosensitive liposome will provide a synergistic therapeutic effect. Specific aim 1 will investigate whether combined HIF-1 blockade and thermochemotherapy achieves enhanced hypoxic cell cytotoxicity and whether it reverses treatment resistance by altering heat shock factor 1-mediated stress responses. Specific aim 2 will evaluate the therapeutic efficacy of this combined treatment as well as corresponding changes in tumor microenvironment in an orthotopic breast cancer xenograft model.

(PS7.43) DOCENT (Dynamic Oxygen Challenge Evaluated by NMR T₁ and T₂*): applications from rats to diverse tumors in man. Ralph P. Mason¹, Dawen Zhao¹, Jesús Pacheco-Torres², Rami Hallac¹, Yao Ding¹, Qing Yuan¹, Vikram D. Kodibagkar¹, Peter Peschke³, Robert D. Sims Jayanthi Lea¹, Ganesh Raj¹, Robert Timmerman Paul Weatherall¹, ¹UT Southwestern Medical Center, Dallas, TX, ²Instituto de Investigaciones Biomédicas "Alberto Sols" - CSIC, Madrid, Spain, ³DKFZ-German Cancer Center, Heidelberg, Germany

Tumor oxygenation influences response to radiation and plays important roles in malignant progression, angiogenesis, and metastasis. While methods are available to quantitatively map pO₂ dynamics in pre-clinical studies, methods are needed to non-invasively characterize tumor hypoxia and response to interventions in patients. Blood Oxygenation Level Dependent (BOLD) MRI based on T₂* contrast induced by [deoxyhemoglobin], is sensitive to tumor vascular oxygenation and blood flow. Meanwhile, TOLD (Tissue Oxygen Level Dependent) MRI is sensitive to tissue oxygenation based on the shortening of the tissue water T₁ due to oxygen. This prompted us to investigate the utility of BOLD and TOLD to evaluate tumor hypoxia in response to breathing hyperoxic gas in rats. Syngeneic Dunning prostate R3327 rat tumor sublines: anaplastic and poorly vascularized AT1 and moderately well differentiated and vascularized HI were investigated when small (<2 cm³) or large (>3.5 cm³). MR measurements were performed at 4.7 T. A series of interleaved T₁- and T₂*-weighted proton (water) images was acquired during transition from air to carbogen breathing to assess ability to detect tumor response. Small HI tumors showed large increases in SI in both T₁- and T₂*-weighted signal (mean maximum Δ SI (%) = 20.2 \pm 0.8 and 6.5 \pm 0.2, respectively), while large HI and small AT1 showed medium increase in signal intensity (mean maximum Δ SI (%) = 8.2 \pm 0.4 and 4.6 \pm 0.1 for big HI and 5.1 \pm 0.1 and 3.5 \pm 0.1 for small AT1, respectively). On the other hand, we found little response in T₁- or T₂*-weighted images in response to breathing carbogen in large AT1 (mean maximum Δ SI (%) = 0.0 \pm 0.1 and 1.17 \pm 0.05), which was significantly lower than the better vascularized small HI tumors (p<0.05). These results concur with quantitative ¹⁹F MRI oximetry suggesting that T₁ and T₂* weighted signal response to carbogen challenge reveals hypoxic tumors. Importantly, we now show the ability to perform oxygen-sensitive MRI in patients at 3 T and will present results in cervix, prostate and lung. We believe that *DOCENT* offers a new test for tumor hypoxia, which could allow the clinician to alter successfully expensive and debilitating patient treatments. Since *DOCENT* is entirely non-invasive they appear worthy of further exploration and correlation with response to therapy.

(PS7.44) Curcumin treatment and prediction of radiation dermatitis in breast cancer patients. Julie L. Ryan, Charles E. Heckler, Jacqueline Williams, Gary R. Morrow, Alice P. Pentland, University of Rochester Medical Center, Rochester, NY

Background: Radiation dermatitis occurs in nearly 95% of cancer patients receiving radiation therapy. Currently, there are no useful treatments or predictive markers for these skin reactions. We conducted a randomized, double-blind, placebo-controlled clinical pilot study to examine the use of curcumin for radiation dermatitis. Alterations in pro-inflammatory cytokines and chemokines may be a novel indicator for radiation-induced skin damage and curcumin activity. Methods: Female breast cancer patients prescribed radiation treatment without concurrent chemotherapy were eligible. After randomization, all patients took twelve 500mg capsules of curcumin or placebo daily (i.e., 6.0g daily) during their course of radiation treatment. Radiation dermatitis severity was measured weekly using Radiation Dermatitis Score (RDS) ranging from 0 to 4 with 0.5 increments. The Milliplex[®] MAP Human Panel I Assay was used to measure plasma levels (pg/ml) of 42 different cytokines and chemokines in blood collected from patients midway through radiation treatment. Results: Preliminary ANCOVA analyses performed on 21 patients who completed the clinical trial (95% White, mean age = 58) showed that radiation dermatitis severity was significantly lower in curcumin-treated patients compared to placebo (mean RDS = 2.46 and 3.33 respectively; p = 0.036). Correlative and regression analyses revealed that plasma levels of Eotaxin (p=0.007), IFN α 2 (p=0.010), IL-12/p40 (p=0.005), IL-12/p70 (p=0.006), and IP-10 (p=0.033) midway through radiation treatment were predictive of radiation dermatitis severity at the end of treatment. Eotaxin and IL-12/p40 negatively correlated with radiation dermatitis severity, while IFN α 2, IL-12/p70, and IP-10 positively correlated with radiation dermatitis severity. Tree-based modeling identified Eotaxin plasma levels \geq 119.4 pg/ml midway through radiation therapy as a marker for curcumin-treated patients. Conclusions: Curcumin significantly reduces the severity of radiation dermatitis in breast cancer patients. Plasma levels of

ectoxin, IFN α 2, IL-12, and IP-10 could be used to predict radiation dermatitis severity in breast cancer patients. Support: Dermatology Foundation Research Career Development Award, KL2 RR024136, and NCI PHS 1R25CA10618 grants.

(PS7.45) Enhancement of human lung cancer cell radiosensitivity by huachansu, an extract from toad skin. Li Wang, Luka Milas, Uma Raju, David Molkenline, Peiyong Yang, Lorenzo Cohen, Zhongxing Liao, UT M.D Anderson Cancer Center, Houston, TX

Huachansu (HCS), an extract from dried toad (*Bufo* sp.) skin, contains biologically active substances mainly steroidal cardiac glycosides and indole alkaloids. The agent possesses antitumor activity and is well tolerated by cancer patients. The present study tested whether HCS enhances radiosensitivity of cancer cells. HCS treatment of human lung cancer cell lines H460 and A549 (p53 wild type), and H1299 (p53 null) for 24 h resulted in a dose-dependent cytostatic and/or cytotoxic actions. IC50 was approximately 20 mg/ml, a dose we used in subsequent experiments in combination with irradiation (IR). The cells were treated with HCS for 24 h before or after 2-6 Gy single dose IR and clonogenic cell survival was determined 12-14 days after IR. HCS given before but not after IR strongly enhanced radiosensitivity of H460 and A549 cells with EFs of 1.91 and 1.94, respectively. However, HCS had no effect on radiosensitivity of H1299 cells. HCS significantly prolonged the presence of radiation-induced double-strand breaks in H460 and A549 cells, detected on the basis of γ H2AX foci beyond 24h. This suggests that inhibition of DNA repair may be an underlying mechanism of HCS-induced enhanced radiosensitivity. In addition, both H460 and A549 cells treated with HCS showed significant increase in radiation-induced apoptosis as assessed by TUNEL assay. Consistent with the induction of apoptosis are molecular changes showing increased expressions of cleaved caspase-3 and PARP as well as a decreased expression of Bcl-2. Therefore, increased susceptibility of cells to radiation-induced apoptosis may be another mechanism underlying HCS-induced enhancement of cell radiosensitivity. A possibility that cell cycle changes were also an underlying mechanism of the observed increase in cell radiosensitivity was dismissed since treatment with HCS had no significant effect on cell cycle distribution. In conclusion, our findings demonstrated that HCS strongly enhanced radiosensitivity of human lung cancer cell lines and that major underlying mechanisms included inhibition of DNA damage repair and increase in radiation-induced apoptosis. The observed radiosensitizing effect seems to be related to p53 status as only the p53 wt cell lines responded. These data suggest that HCS may have potential to improve the efficacy of radiotherapy.

(PS7.46) In vitro and in vivo radiosensitization of glioblastoma by the novel intercalating agent and topoisomerase inhibitor voreloxin. Ira Gordon, Tamalee Meushaw, Kevin Camphausen, National Cancer Institute, Bethesda, MD

Purpose: Voreloxin is a first in class anticancer quinolone derivative (AQD), structurally related to quinolone antibacterials, that intercalates DNA and inhibits topoisomerase II. Voreloxin is not a P-glycoprotein receptor substrate and its activity is independent of p53, thus evading common drug resistance mechanisms. To evaluate voreloxin as a clinically applicable radiation sensitizer, we investigated its effects on the radiosensitivity of the U251 human glioblastoma cell line. Methods: Voreloxin's effect on postirradiation sensitivity of U251 cells was assessed by clonogenic assay. DNA damage and repair was evaluated by comet assay and a high throughput γ H2AX assay. Cell cycle distribution and G2 checkpoint integrity was analyzed by flow cytometry. Mitotic catastrophe was based on microscopic evidence of fragmented nuclei by immunofluorescence. Apoptosis was assessed by flow cytometry. In vivo radiosensitization was measured by subcutaneous tumor growth delay assay. Results: 75 nM voreloxin treatment yielded a surviving fraction of 0.77 ± 0.16 . In irradiated cells at a surviving fraction of 0.10, the radiation

dose enhancement factor was 1.51. 16 hour drug treatment did not change cell cycle distribution, G2 checkpoint integrity or apoptotic fraction in control and irradiated cells. The number of cells in mitotic catastrophe was significantly greater in irradiated cells treated with voreloxin than cells receiving radiation only at 72 (p=0.009) and 96 (p=0.02) hr. Voreloxin alone did not significantly increase mitotic catastrophe over control (p=0.54). Cells treated with voreloxin and radiation maintained significantly higher γ H2AX levels than cells treated with vehicle control (p=0.014), voreloxin (p=0.042), or radiation alone (p=0.039) after 24 hr. In the comet assay, combination treated cells had significantly higher tail moments at 3, 6 and 24 hr than cells that were only irradiated (p=0.02) or drug treated (p<0.001). In vivo tumor growth delay was 1.5 days for voreloxin alone (IV 10 mg/kg), 0 days for radiation (3 Gy) alone, and 8.6 days for the group treated with voreloxin 4 hours prior to radiation. Conclusions: Voreloxin enhanced glioma cell radiosensitivity in vitro and in vivo. The mechanism appears to be related to inhibition of DNA repair and increased mitotic catastrophe.

(PS7.47) Enhanced radiobiological effects at distal-end of proton SOBP beam. Yoshitaka Matsumoto¹, Mami Wada¹, Taeko Matsuura², Teiji Nishio², Yoshiya Furusawa¹, ¹National Institute of Radiological Science, Chiba-shi, Japan, ²National Cancer Center Hospital East, Kashiwa, Japan

Purpose: Radiobiological efficiencies in distal-end part of proton SOBP beams may much higher than 1.1 that used as the RBE of SOBP beam in many proton therapy facilities. To confirm an actual biological efficiency in the position, we examine the efficiency with an in vitro cell system. Material and Method: We used HSG cells that obtained from human salivary gland tumor, and have been used as a standard cell-line for RBE measurements at therapeutic ion beam facilities in Japan. The cells were maintained in Eagle-MEM medium supplemented with 10% FBS and antibiotics, and incubated under 5% CO2 balanced with air at 37 °C. Cell samples were prepared two days before irradiation at NIRS (Nat'l. Inst. Radiol. Sci.), home laboratory in Chiba, brought them to NCC/HE (Nat'l Cancer Cen., Hosp. East) in Kashiwa under a warm condition, and brought back in a cool condition just before and after the irradiation. Cells were irradiated with proton beam (190 MeV, 5 cm-SOBP, 100 mm ϕ) at different depths in the distal-end part and the center of the SOBP beam at NCC/HE. Central position of the SOBP was fixed at the iso-center of the beam, and depths of each sample were adjusted by placing polyethylene plates. All biological assays were performed at home laboratory. Surviving fractions were obtained, and killing efficiencies at each depth to the center were obtained. Biological dose distribution was calculated with the efficiencies and the physical doses at each position, and was compared with the physical dose distribution. Results: Physical dose distribution was flat in the SOBP and decreased gradually at the distal-end of the SOBP. Biological efficiencies at the distal-end were higher than that at the center, and the efficiencies at all positions tested were approximately 1.48 to 1.75 compared to the center of the SOBP. This also means that the biological range of the beam is extended several millimeters to the down stream compared with physical dose distribution. Conclusion: Biological dose at distal-end of SOBP beam was higher than that at the center of SOBP beam. This higher radiobiological efficiency extends the biological efficient range of the beam than that for physically defined dose distribution. This may causes side effects to healthy tissues at the distal position of the beam.

(PS7.48) Mechanism of action of an imidopiperidine inhibitor of human polynucleotide kinase/phosphatase. Gary K. Freschauf, Rajam S. Mani, Todd R. Mereniuk, Mesfin Fanta, Dennis G. Hall, Michael Weinfeld, University of Alberta, Edmonton, AB, Canada

The small molecule, 2-(1-hydroxyundecyl)-1-(4-nitrophenylamino)-6-phenyl-6,7a-dihydro-1H-pyrido[3,4-b]pyridine-5,7(2H, 4aH)-dione (A12B4C3), is a potent inhibitor of the phosphatase activity of human polynucleotide kinase/phosphatase (PNKP) *in*

vitro. Cellular studies revealed that A12B4C3 sensitizes A549 human lung cancer cells to the topoisomerase I poison, camptothecin, but not the topoisomerase II poison, etoposide, in a manner similar to siRNA against PNKP. A12B4C3 also inhibits the repair of DNA single and double-strand breaks following exposure of cells to ionizing radiation, but does not inhibit two other key strand break repair enzymes, DNA polymerase beta or DNA ligase III, providing additional evidence that PNKP is the cellular target of the inhibitor. Kinetic analysis revealed that A12B4C3 acts as a non-competitive inhibitor, and this was confirmed by fluorescence quenching, which showed that the inhibitor can form a ternary complex with PNKP and a DNA substrate, i.e. A12B4C3 does not prevent DNA from binding to the phosphatase DNA binding site. Conformational analysis using circular dichroism, UV-difference spectroscopy and fluorescence resonance energy transfer all indicated that A12B4C3 disrupts the secondary structure of PNKP. Investigation of the potential site of binding of A12B4C3 to PNKP using site directed mutagenesis pointed to interaction between Trp⁴⁰² of PNKP and the inhibitor. A12B4C3 is thus a useful reagent for probing hPNKP cellular function and will serve as the lead compound for further development of PNKP-targeting drugs.

(PS7.49) Effect of cediranib combined with temozolamide and radiotherapy in U87 xenograft models of human glioblastoma expressing wtEGFR or EGFRvIII. Phyllis R. Wachsberger, Richard Y. Lawrence, Yi Liu, Barbara Andersen, Adam P. Dicker, Thomas Jefferson University, Philadelphia, PA

Introduction: Glioblastomas (GBM) frequently overexpress the epidermal growth factor receptor (wtEGFR) or its mutant, EGFRvIII contributing to radioresistance. New treatment strategies for GBM include blockade of EGFR signaling and angiogenesis. Cediranib (CD) is a highly potent VEGFR-2 RTKI that inhibits all three VEGF receptors. This study investigated the radiosensitizing potential of CD in combination with temozolamide (TMZ) in U87 GBM xenografts expressing wtEGFR or EGFRvIII. **Method:** U87 GBM cells transfected with wtEGFR or EGFRvIII were injected into the hind limbs of nude mice. CD was dosed at 3 mg/kg daily (days 0-9); TMZ at 10 mg/kg on day 0. Radiotherapy (RT) consisted of 3 fractions of 5 Gy (days 0-2). VEGF was assayed from culture media 48 hr after treatment. **Results:** In U87 EGFRvIII xenografts, RT, CD or TMZ alone significantly increased tumor doubling time (T_{2x}), when compared to control (4.6, 4.85 and 4.31 for CD, RT and TMZ respectively vs. 3.0 for control). TMZ + RT, but not CD+ RT, was significantly better than RT alone (T_{2x} = 6.22 vs. 4.85 respectively). However, CD + TMZ was significantly better than TMZ alone (T_{2x} = 6.3 for cediranib + TMZ vs. 4.3 for TMZ). The triple combination of CD, TMZ and RT was significantly better than RT alone. In U87 wtEGFR xenografts, single agent RT and TMZ were significantly better than control (T_{2x} = 7.84 and 6.72 for RT and TMZ respectively vs. 3.45 for control). Single agent CD marginally increased T_{2x} compared to control (4.69 vs. 3.45, NS). CD + TMZ was significantly better than TMZ alone (T_{2x} = 11.63 vs. 6.72 respectively). The triple combination of CD, TMZ and RT was marginally better than RT alone but did not reach significance. In cell culture, TMZ, stimulated VEGF secretion from both U87 wtEGFR and U87 EGFRvIII cells; however, VEGF levels were higher from U87 EGFR cells than U87 EGFRvIII cells. **Conclusions:** CD appears to be effective in GBM, both as a single agent and when combined with TMZ. Tumors expressing EGFRvIII were more sensitive than tumors expressing wtEGFR, possibly due to inability of CD to overcome excessive VEGF secretion by the latter. (Support: AstraZeneca Pharmaceuticals and the Radiation Therapy Oncology Group.)

(PS7.50) Long term alteration of cardiac structure and function induced by irradiation. Ingar Seemann¹, Saske Hoving¹, Nils Visser¹, Hans te Poele¹, Karen Gabriels², Fijs van Leeuwen¹, Ben Janssen², Sylvia Heeneman², Fiona Stewart¹. ¹The Netherlands Cancer Institute, Amsterdam, Netherlands, ²Cardiovascular Research Institute, Maastricht, Netherlands

Background: Radiotherapy is a common treatment for breast cancer and Hodgkin's lymphoma and it is associated with good long-term survival prognosis. However, it is now recognized that radiotherapy increases the long-term risk of microvascular damage and perfusion defects which are major underlying causes of heart failure after irradiation. In this study we will focus of the mechanism involved in radiation-induced cardiotoxicity. **Methods:** Single doses of 0, 2, 8 or 16 Gy was delivered to the heart of adult male C57BL/6J mice and mice were sacrificed after 20 and 40 weeks. Cardiovascular function was determined at 20 and 40 weeks after irradiation, by SPECT/CT or ultrasound imaging. Changes in cardiac function were correlated with structural and functional damage, assessed from histological specimens and from expression levels determined by Immunohistochemistry and RT-PCR. **Results:** Irradiation to the heart resulted in significant decreases in cardiac blood volume at 20 weeks after 2, 8 and 16 Gy (12-19%), with further decrease (12-30%) at 40 weeks after 2 and 16 Gy measured by SPECT/CT. Ultrasound measurements showed significant decrease in cardiac output (19%), end diastolic volume (25%), end systolic volume (52%) and a significant increase in fractional shortening and ejection fraction (22%) at 20 weeks after 16 Gy. Ultrasound parameters at 40 weeks after 16 Gy did not show significant changes relative to controls. CD 31 stained sections identified an increase in microvascular density (16-20%) 20 week after 2 - 8 Gy, with a trend for decreased microvascular density after 16 Gy. There was a further decrease in microvascular density (24%) at 40 weeks after 16 Gy. The epicardial thickness increased significantly at 20 weeks after 8-16 Gy and was still increased at 40 weeks after 16 Gy. This was associated with the presence of iron containing macrophages, indicative of previous hemorrhage. The number of vessels stained positive for alkaline phosphatase was reduced by 50% at 20 and 40 weeks after 8-16 Gy. **Conclusion:** Overall, these data suggest that 20 weeks after irradiation leads to an acute, inflammatory effect, which by 40 weeks has progressed to fibrotic damage to the heart. Funded by the Dutch Cancer Foundation, grant NKI 2008-3993 and European Atomic Energy Community's Seventh Framework Program, grant 211403.

(PS7.51) Radioresistant melanoma cells show defective G1 arrest in response to IR and are radiosensitized by inhibition of B-RAF. Janiel M. Shields, Craig C. Carson, Maria J. Sambade, Nancy E. Thomas, University of North Carolina, Chapel Hill, NC

While advanced melanoma is often reported to be relatively resistant to conventional radiotherapy, stereotactic radiosurgery (SRS) is increasingly used to treat melanoma brain metastases with 1-year local control rates ranging from 75-40% depending on tumor size. However, melanoma brain metastases tend to be multifocal with disparate SRS responses seen among brain metastases in individual patients resulting in high morbidity rates. Thus, there is a critical need to improve the therapeutic radioresponsiveness of melanoma. Mutational activation of the B-RAF oncogene occurs in approximately 50% of melanoma patients. B-RAF, a serine/threonine kinase, leads to constitutive activation of MEK1/2>ERK1/2. Activation of Raf>MEK1/2>ERK1/2 has previously been shown to promote radioresistance. Here, a large collection of melanoma cell lines (n=37) were treated with 0 - 8 Gy IR and clonogenic survival assays used to generate survival curves to rank relative radiosensitivities among the cell lines. Treatment of highly radioresistant *B-Raf*⁺ cells with the B-RAF inhibitor PLX-4032 in combination with radiation provided enhanced inhibition of proliferation in both colony formation (ER average 9.7; range 1.2 - 29.3) and invasion assays, and radiosensitized cells through an increase in G1 arrest. In addition, while p53 mutations are uncommon in melanoma, radioresistance in melanoma cell lines correlated with a defective G1 checkpoint and loss of p21 expression suggestive of loss of p53 function. Agilent 4 x 44k RNA microarrays were used to identify genes associated with radioresistance vs radiosensitivity by Quantitative Trait Analyses. Using the ranked radiation sensitivities of the cell lines and highly stringent filtering parameters 20/44,000 genes were found to be associated with either radioresistance or sensitivity (p<0.001) with increased expression of genes associated with DNA repair and regulation of histone acetylation in the radioresistant cell lines. These data suggest radioresistance in melanoma is mediated, in part, through loss of p53 function and increased DNA repair and that

pharmacologic inhibition of BRAF could provide improved radiotherapeutic response in B-Raf+ melanoma patients.

(PS7.52) Enhancement of cancer therapy using ketogenic diet.

Melissa A. Fath, Andrean L. Simons, Bryan Allen, Jeffery Erickson, Mark E. Anderson, Douglas R. Spitz, University of Iowa, Iowa City, IA

Ketogenic diets (KD; low in protein and carbohydrates and high in fats) force cells to rely more heavily on mitochondrial metabolism for energy production. Cancer cells have been hypothesized to exist in a condition of chronic oxidative stress with the site of pro-oxidant production being mitochondrial electron transport chains. If cancer cells have defective mitochondrial O_2 metabolism and KD force cancer cells to rely more heavily on mitochondrial metabolism, then KD would be expected to cause oxidative stress in cancer cells and would be expected to sensitize cancer cells to conventional cancer therapeutic agents that cause cell killing via oxidative stress. In the current study, FADU head and neck carcinoma cells were grown in the flank of nude mice and fed either KD (KetoCal® 4:1 ratio fat: carbohydrates + protein) or standard rodent chow (SD) ad libitum for 2 weeks during therapy. When mice bearing tumors were treated with cisplatin (CIS; 2mg/kg every other day) the mice treated with CIS + KD demonstrated longer tumor growth delay as well as longer median survival compared to mice on CIS + SD or KD however the mice in this combination group lost a significant amount of weight indicating systemic toxicity. When tumor bearing animals were given 6 x 2 Gy fractions of X-rays (IR) every other day for 2 weeks, the KD + IR group demonstrated significant tumor growth delays as well as greater median survival compared to IR + SD, SD or KD without significant weight loss. Furthermore when mice with MIA PaCa-2 pancreatic xenograft tumors were treated with 6 fractions of 2 Gy IR, animals given IR + KD also demonstrated a longer tumor growth delay as well as longer median survival compared to mice on SD + IR, KD or SD. Western blots of plasma harvested from animals fed ketogenic diets demonstrated increased levels of protein recognized by a polyclonal antibody with reactivity to an oxidized methionine epitope supporting the hypothesis that KD induces systemic oxidative stress. The current results support the hypothesis that feeding ketogenic diets to animals bearing human tumor xenografts can increase systemic oxidative stress as well as inducing radiosensitization. (Supported by CA139182 and CA133114).

(PS7.53) Using clonogenic survival curves and proteomic arrays to build a proteomic signature for predicting breast cancer cell radiation response. Diane R. Fels, John P. Kirkpatrick, Mark W. Dewhirst, Janet K. Horton, Duke University, Durham, NC

The purpose of our study is to generate protein activation patterns from breast tumor cells that may predict radiation sensitivity. Radiotherapy is commonly added to breast cancer regimens to improve local-regional control and enhanced overall survival. Therefore, potential knowledge of a tumor's intrinsic radiosensitivity could significantly alter clinical practice. However, tumor response to radiotherapy remains markedly heterogeneous and predicting tumor radiosensitivity is a challenge involving both intrinsic properties of the tumor cells and acquired resistance from treatment. Many molecular mechanisms affect radiosensitivity, including adaptive responses against tumor microenvironmental stresses such as hypoxia and intracellular alterations in key regulators of the cell cycle, DNA damage repair and apoptosis. These factors are affected, in part, by changes in protein function, expression or post-translational modification. Although gene expression profiles have been loosely correlated with radiation sensitivity, it is not clear if proteomic changes can be used to identify radiation sensitivity in breast cancer cells. We selected a panel of human breast cancer cell lines (SUM149, SUM159, ZR751, T47D) with disparate phenotypes to determine radiation sensitivity. Clonogenic survival assays and standard radiation response parameters, such as the surviving fraction at 2Gy (SF_{2Gy}) and α/β ratio, have been generated. Comparing SF_{2Gy} values, the SUM149 and ZR751 cells ($SF_{2Gy} = 0.28$) are more radiosensitive

than both the T47D ($SF_{2Gy} = 0.74$) and SUM159 ($SF_{2Gy} = 0.84$) cells. The calculated α/β ratios range from 5.8 - 7.3Gy, with the greatest changes seen in the α -values. For example, the more radioresistant SUM159 cells have $\alpha = 0.153$, $\beta = 0.022$ versus the more sensitive ZR751 cells with $\alpha = 0.471$, $\beta = 0.065$. In addition, total protein will be harvested from each cell line pre- and post-radiation and used to identify radiation-induced proteomic changes with reverse-phase protein microarrays. Together with the generated survival curves and the α/β ratios, these data will establish preliminary proteomic profiles of a radiation sensitivity pattern in breast cancer cells. Our long-term goal is to build a robust proteomic signature that may predict breast cancer clinical response to radiotherapy.

(PS7.54) Irradiating murine microglial cells leads to modulation of components of the renin-angiotensin system. Elizabeth D. Moore, Valerie Payne, Weiling Zhao, Mark Chappel, Michael E. Robbins, Wake Forest University, Winston-Salem, NC

Progressive cognitive impairment occurs in approximately 50% of primary and metastatic brain tumor patients who are long-term survivors after large field or whole brain irradiation (WBI). Currently there are no long term successful treatments or effective preventative strategies against radiation-induced late brain injury. Experimental work has indicated that late radiation-induced injury in the kidney and lung is treatable through blockade of the renin-angiotensin system (RAS). More recently we have demonstrated that administration of an angiotensin-converting enzyme inhibitor (ACEI) or an angiotensin II type 1 receptor antagonist (AT₁RA) to young adult male rats prevents/ameliorates radiation-induced cognitive impairment. These data suggest that radiation modulates the RAS, however the mechanism is unclear. We hypothesize that radiation modulates the intrinsic brain RAS resulting in increases in inflammation and reactive oxygen species and brain injury, including cognitive impairment. We have started to test this hypothesis in BV-2 murine microglial cells *in vitro*. Initial studies indicate that RAS components (angiotensinogen, angiotensin peptides, ACE1, ACE2 and renin) are present in these cells. Irradiating BV-2 cells with a range of single doses (0-10 Gy of ^{137}Cs γ rays) decreases angiotensinogen (parental substrate of the RAS) protein levels and increases levels of ACE1 and ACE2 in a dose-dependent manner; ACE2 levels increased 10 fold in response to 10 Gy γ rays. Irradiating BV-2 cells also lead to dose-dependent increases in reactive oxygen species (ROS) and inflammatory mediators including cyclooxygenase-2 (Cox-2). The addition of Angiotensin-(1-7) peptide (the main ACE2 cleavage product, 10 nm) ameliorated the radiation-induced increases in ROS and Cox-2. These findings support the hypothesis that radiation modulates the brain RAS. (Supported by CA122318).

(PS7.55) Pre-clinical evaluation of a novel combination therapy with BMS-354825 (dasatinib, an inhibitor of Src kinases) and radiation for human head and neck squamous cell carcinoma treatment. Uma Raju, Fumihiko Matsumoto, Li Wang, David Molkenkine, David Valdecanas, Luka Milas, K. Kian Ang, University of Texas M.D. Anderson Cancer Center, Houston, TX

cSrc is the earliest oncogene implicated in tumorigenesis, tumor progression, and metastasis. Many types of malignant cells over express cSrc, including head and neck squamous cell carcinomas (HNSCCs). The present study investigated the efficacy of dasatinib (BMS-354825), an inhibitor of Src kinases, in enhancing the tumor cell response to radiation in both *in vitro* and *in vivo* settings. The underlying mechanisms of dasatinib-induced radiosensitization were also investigated. HNSCC lines, HN-5, FaDu and UMSCC-1 were used for the study. Dasatinib (100 nM) inhibited the growth of HNSCC cells, assessed by cell viability assay. Exposure of cells to dasatinib before and after radiation enhanced the cell radiosensitivity, assessed by clonogenic cell survival and magnitudes of these effects were cell line specific. At the cellular level, dasatinib enhanced the radiation-induced apoptosis. Immuno-cytochemical analysis showed that dasatinib

prolonged the presence of γ -H2AX foci in the nucleus beyond 24 h post irradiation. Split-dose clonogenic survival experiments showed that dasatinib blocked sublethal DNA damage repair. Protein analyses revealed that dasatinib efficiently suppressed the phosphorylation of cSrc, cAbl and FAK. In addition, dasatinib blocked radiation-induced association of cSrc with EGFR and Her-2 proteins and radiation-induced activation of Nbs-1. These data suggest that dasatinib enhanced the cell radiosensitivity by increasing radiation-induced apoptosis and by blocking DNA repair. Dasatinib was found to significantly improve the response of FaDu tumors to radiation *in vivo*. Tumor growth delay studies revealed that dasatinib enhanced the radiation-induced tumor growth delay, which after the combined treatment was more than the sum of those induced by either treatment alone. Our results demonstrated that dasatinib potentially enhanced the radiosensitivity of select HNSCC lines *in vitro* and *in vivo*. Mechanisms of dasatinib-induced cell radiosensitivity included induction of apoptosis and inhibition of DNA repair. Our findings suggest that dasatinib has potential to increase tumor response to radiotherapy. Supported in part by Bristol-Myers Squibb Company (PI: U. Raju) and NIH PO-1 Grants CA-06294 (PI: K.K. Ang) supplemented by Gilbert H. Fletcher Distinguished Chair, K.K. Ang.

(PS7.56) Local radiation therapy inhibits tumor growth through the generation of tumor-specific CTL: Its potentiation by combination with Th1 cell therapy. Tsuguhide Takeshima¹, Kenji Chamoto², Hidemitsu Kitamura², Takashi Nishimura², Hiroki Shirato¹, ¹Department of Radiology, Graduate School of Medicine, Sapporo, Japan, ²Division of Immunoregulation Section of Disease Control, Institute for Genetic Medicine, Hokkaido University, Sapporo, Japan

Radiation therapy is one of the primary treatment modalities for cancer along with chemotherapy and surgical therapy. The main mechanism of the tumor reduction after irradiation has been considered to be damage to the tumor DNA. However, we found that tumor-specific cytotoxic T lymphocytes (CTL), which were induced in the draining lymph nodes (DLN) and tumor tissue of tumor-bearing mice, play a crucial role in the inhibition of tumor growth by radiation. Indeed, the therapeutic effect of irradiation was almost completely abolished in tumor-bearing mice by depleting CD8⁺ T cells by anti-CD8 mAb administration. In the mice whose DLN were surgically ablated or genetically defective (Aly/Aly mice), the generation of tetramer⁺ tumor-specific CTL at the tumor site was greatly reduced in parallel with the attenuation of the radiation-induced therapeutic effect against the tumor. This indicated that DLN are essential for the activation and accumulation of radiation-induced CTL, which are essential for inhibition of the tumor. A combined therapy of local radiation with Th1 cell therapy augmented the generation of tumor-specific CTL at the tumor site and induced a complete regression of the tumor, though radiation therapy alone did not exhibit such a pronounced therapeutic effect. Thus, we concluded that combination treatment of local radiation therapy and Th1 cell therapy is a rational strategy to augment antitumor activity mediated by tumor-specific CTL.

(PS7.57) Inhibition of radiation-induced recruitment of bone marrow-derived cells into tumors sensitizes glioblastomas in mice to irradiation. Mitomu Kioi, J. M. Brown, Stanford University School of Medicine, Palo Alto, CA

Despite the high doses of radiation delivered in the treatment of patients with glioblastoma multiforme (GBM), the tumors invariably recur within the irradiation field, resulting in the low cure rate of this malignancy. In order to grow these tumors stimulate the formation of new blood vessels either through sprouting of local vessels (angiogenesis) or colonization by circulating endothelial and other cells primarily derived from the bone marrow (vasculogenesis). We have proposed that the radiation doses given in radiotherapy will abrogate local angiogenesis and thereby force tumor regrowth to rely on vasculogenesis. Here we show using an intracranial U251 human GBM xenograft model in mice that

irradiation induces recruitment of bone marrow-derived cells (BMDCs) into the tumors, restoring the radiation-damaged vasculature by vasculogenesis, thereby allowing the growth of surviving tumor cells. We also show that tumor recurrence can be prevented by blocking the BMDC influx into the tumors, a process initiated by the induction of HIF-1 in the irradiated tumors due to increased tumor hypoxia post irradiation. Pharmacological inhibition of HIF-1, or of the interaction of the HIF-1-dependent stromal-cell derived factor-1 (SDF-1) with its receptor CXCR4 using the clinically approved drug AMD3100, or by neutralizing antibodies against CXCR4, prevents the influx of BMDCs, primarily CD11b⁺ myelomonocytes, and the post-irradiation development of functional tumor vasculature, resulting in abrogation of tumor regrowth. Our data therefore suggest a novel approach for the treatment of GBM: In addition to radiotherapy, the vasculogenesis pathway needs to be blocked, and can be done so using a clinically approved drug.

(PS7.58) Interplay between neurotensin receptor 1 (NTR1) and epidermal growth factor receptor (EGFR) in responses to ionizing radiation in prostate cells. Jaroslaw Dziegielewski, Nicholas C. K. Valerie, John O. Dasilva, Amol S. Hosing, Sarah J. Parsons, James M. Lamer, University of Virginia, Charlottesville, VA

Radiation is one of the most commonly used treatments for prostate cancer (PCa). However, even with recent advances in targeted radiotherapy, adverse effects on surrounding normal tissue remain a significant clinical problem. An agent that selectively sensitizes prostate tumor but not surrounding normal tissue should improve the therapeutic ratio of radiation. Our recent results demonstrate that SR48692, a specific small-molecule antagonist of NTR1, selectively sensitizes prostate cancer cells to ionizing radiation by blocking transactivation of the EGFR. To better understand the interplay between EGFR and NTR1 we studied SR48692 mediated radiosensitization in several PCa cell lines by varying expression of both NTR1 and EGFR, using shRNA-driven knock-down, chemical or antibody-based inhibition as well as protein over expression. The effects of NTR1/EGFR inhibition in PCa cells on their radiation sensitivity as well as the molecular interactions between NTR1 and EGFR signaling pathways were characterized. Our results indicate that the drug-induced radiosensitization of PCa but not normal prostate cells is due to differences in NTR1 expression. However, the degree of SR48692-induced radiosensitization depends on the level of EGFR expression. The combination of NTR1 inhibition plus EGFR inhibition significantly enhanced the cytotoxicity of radiation in PCa cells. Our study suggests that the NTR1 receptor together with EGFR, are viable targets for combined chemo/radiotherapy of prostate cancer. [This work is supported by DOD grant W81XWH-08-1-0114 and NASA grant NNX10AC13G].

(PS7.59) High level expression of Rad51 is an independent prognostic marker of survival in adenocarcinoma of the colon. Pierre Tennstedt¹, Robert Fresow², Ronald Simon¹, Guido Sauter¹, Luigi Terracciano³, Cordula Petersen⁴, Ekkehard Dikomey², Kerstin Borgmann², ¹Institute of Pathology, University Medical Center Hamburg, Germany, ²Lab of Radiobiology and Experimental Radiooncology, University Medical Center Hamburg, Germany, ³Institute of Pathology, University Medical Center Basel, Switzerland, ⁴Department of Radiotherapy, Center of Oncology, University Medical Center Hamburg, Germany

High-level expression of Rad51, a key factor in homologous recombination, has been observed in a variety of human malignancies. This study was aimed to evaluate Rad51 expression to serve as prognostic marker in adenocarcinoma of the colon. A total of 1209 adenocarcinomas of the colon were analysed immunohistochemically on Colon tissue microarrays. High-level Rad51 expression was observed in 1% (12), moderate in 11.5% (139), weak in 33.8% (409) and no Rad51 expression in 53.7% (649) of cases. Patients whose tumours displayed high-level Rad51 expression showed a significantly shorter median survival time of

10 vs 78 months ($P < 0.0013$, log-rank test). Similarly T status, N status, M status, clinical stage and histological tumour grade were significant prognostic markers in univariate Cox survival analysis. Importantly, Rad51 expression together with tumour differentiation, clinical stage and N status proved to be independent prognostic parameters in multivariate analysis ($p = 0.0105$). No significant correlation of Rad51 and p53 expression was observed ($p = 0.073$). Our results suggest that Rad51 expression provides additional prognostic information for surgically treated colon carcinoma patients. We hypothesise that the decreased survival of colon carcinoma patients with high-level expression of Rad51 is related to an enhanced propensity of tumour cells for genomic instability, chemo-/radioresistance, antiapoptosis and/or survival.

(PS7.60) PPAR δ -mediated modulation of radiation-induced inflammatory responses in microglia. Caroline Schnegg, Mitra Kooshki, Michael Robbins, Wake Forest, Winston Salem, NC

Approximately 200,000 patients a year receive partial or whole-brain irradiation (WBI) for primary or metastatic brain tumors. Radiation-induced cognitive impairment, which can progress to dementia and eventually death, will occur in up to 50% of these patients. There are no proven long-term treatments for radiation-induced cognitive impairment; therefore, it is imperative to investigate new therapeutic approaches. Although the exact mechanisms underlying radiation-induced late effects remain unclear, studies suggest that oxidative stress and inflammatory responses play a critical role. These observations provide the rationale for investigating anti-inflammatory-based approaches to prevent/ameliorate radiation-induced brain injury. Peroxisomal proliferator-activated receptors (PPAR α , δ , γ) have been shown to be potent mediators of anti-inflammatory responses. Microglia are one of the key mediators of neuroinflammation. Thus, we hypothesize that PPAR δ activation will modulate the radiation-induced inflammatory response in microglia. Irradiating BV-2 cells with single doses of 2.5-10.0 Gy of ^{137}Cs γ rays led to i) increased intracellular ROS generation 1 hour post-IR, ii) activation of pro-inflammatory transcription factors 1 hour post-IR and iii) a significant increase in Cox-2, iNOS and MCP-1 expression 7 hours post-IR; prior incubation with the PPAR δ agonist L165041 (5 μM) appeared to inhibit these radiation-induced changes. In contrast, incubating BV-2 cells with L165041 and a pharmacological inhibitor of PPAR δ , GSK0660 (10 μM), failed to prevent the radiation-induced increase in inflammatory mediators. Moreover, BV-2 cells transfected with a dominant negative (DN) PPAR δ construct, or in which PPAR δ expression was knocked down using shRNA, showed an increased inflammatory response following irradiation. Of interest, inhibiting PPAR δ also led to an increase in constitutive Cox-2 expression, suggesting that PPAR δ regulates the inflammatory environment in BV2 cells. These data support the hypothesis that PPAR δ can modulate the radiation-induced inflammatory response in microglia. (Supported by CA112593).

(PS7.61) Comparative evaluation of liposomal and nonliposomal platinum drugs combined or not with concomitant radiation to improve treatment of glioblastoma implanted in rat brain. Gabriel Charest, David Fortin, David Mathieu, Léon Sanche, Benoit Paquette, Université de Sherbrooke, Sherbrooke, QC, Canada

Despite recent advances, the radiotherapy and chemotherapy protocols only marginally improve the overall survival of patients bearing glioblastoma (GBM). In our study, the anticancer efficiency with and without radiation combination of five platinum compounds was tested: cisplatin, oxaliplatin, their liposomal formulation LipoplatinTM (cisplatin), LipoxalTM (oxaliplatin) and carboplatin. The liposomal formulations were included since they can potentially reduce the toxicity of cisplatin and oxaliplatin. The tumor F98 glioma implanted in the brain of Fischer rats was used as model to mimic the human glioblastoma. Although intra venous (i.v.) injection is the usual way to administrate the chemotherapeutic agents, the blood brain barrier (BBB) largely limits drug uptake to

brain tumor. To improve the efficiency of chemotherapeutic agents, the BBB was temporary disrupted (BBBD) and the drugs were injected via carotid artery (i.a.). The post-administration time corresponding to the maximal tumor drug uptake was determined to optimize the concomitant treatment with radiotherapy delivered by Gamma Knife. Up to now, only studies using the i.a. route of drug administration treatment were completed. The i.a. route allows preferential uptake (up to 30X) into the tumor volume compared to the healthy brain tissue. Our study confirms that the liposomal formulations allowed bypassing the toxicity and considerably improving the life span of the animals. The anticancer efficiency of oxaliplatin was increased when incorporated in LipoxalTM resulting in a considerable improvement of the life span of animals implanted with a GBM. The efficiency of LipoxalTM, LipoplatinTM and carboplatin were similar with a median survival times of 29-32 days, compared to 22 days for untreated rats. Concomitant treatment with radiotherapy further extend the median survival times with the highest efficiency obtained with LipoxalTM (37 days) and carboplatin (47 days), compared to 34 days with radiation only. We expect that i.v. administration should reduce the tumor uptake compare to i.a. whereas i.a. plus BBBD should increase the tumor uptake. The aim of this study is to find a better route of administration, a better chemotherapy formulation and a better post-administration time to combine ionizing radiation in clinical GBM therapy.

(PS7.62) Inhibition of SDF-1/CXCR7 radiosensitizes ENU-induced glioblastomas in the rat. Diane Tseng¹, Frederick Lartey¹, Shie-Chau Liu¹, Mitomu Kioi¹, Matthew Walters², Milton Merchant¹, Lawrence Recht¹, Martin Brown¹, ¹Stanford University, Stanford, CA, ²Chemocentryx, Mountain View, CA

Radiation therapy is the standard therapy for patients with glioblastoma (GBM) after maximal surgical excision. However, recurrences invariably occur within the radiation field. Recently we have shown that inhibition of the CXCR4-SDF-1 axis with AMD3100 can sensitize U251 glioblastomas to local irradiation in an orthotopic mouse xenotransplant model by preventing the influx into the irradiated tumor of proangiogenic CD11b+ bone marrow derived myelomonocytes. In the present study we tested the hypothesis that similar radiosensitization could be achieved by blocking post-irradiation endothelial cell influx by inhibiting the interaction of CXCR7, which is highly expressed on activated endothelial cells, with its ligand SDF-1. To test the hypothesis, we chose an extremely refractory tumor model that closely mimics human GBM. In this model pregnant rats are given a single dose of ENU on day 17 of gestation. The rats born to these mothers reliably die from brain tumors from day 120 - day 200. We monitored survival of rats following whole brain irradiation (WBI) in combination with blocking CXCR7 with CCX2066 (ChemoCentryx Inc., Mountain View, CA), or CXCR4 (with AMD3100) or the combination of the two after irradiation. Rats were irradiated with 15 or 20 Gy to the whole brain on day 112 and were randomized into 5 treatment groups: CCX2066 alone, WBI alone, WBI plus AMD 3100, WBI plus CCX2066, and WBI plus AMD 3100 + CCX2206. The drugs were administered for 4 weeks following irradiation. At 224 days the survival of rats given CCX2206 with WBI was significantly longer by > 50 days ($P_3 \times$ higher in the irradiated rats compared to the control rats at 10 days but had fallen to control levels by 17 days after irradiation. In conclusion, inhibition of SDF-1/CXCR7 in combination with local tumor irradiation significantly increased the survival of ENU-induced GBM in rats. In ongoing studies we are comparing the efficacy of inhibiting either SDF-1/CXCR4 or SDF-1/CXCR7 or the combination of the two with irradiation.

(PS7.63) Topical TLR-7 agonist imiquimod inhibits tumor growth and synergizes with local radiotherapy in a mouse model of breast cancer. M. Zahidunnabi Dewan¹, Tze-Chiang Meng², James S. Babb¹, Silvia C. Formenti¹, Sylvia Adams¹, Sandra Demaria¹, ¹New York University School of Medicine, New York, NY, ²Graceway Pharmaceuticals, Martin Luther King Jr Blvd Bristol, TN

Toll-like receptor (TLR) agonists are attractive agents for the active immunotherapy of cancer. TLR7 activation stimulates innate immune responses and directs the adaptive arm towards a Th1 profile. Local administration of TLR7 activator imiquimod (IMQ) creates an inflammatory environment suitable for tumor antigen cross-presentation and infiltration by effector T cells and dendritic cells (DC). Like IMQ, radiotherapy (RT) is a local modality that can alter the tumor microenvironment and enhance tumor immunogenicity, and we have previously shown its ability to synergize with immunotherapy. To test the therapeutic potential of topical IMQ alone or in combination with local RT for the treatment of subcutaneous (s.c.) breast cancer we employed the poorly immunogenic TLR7-negative TSA mouse breast carcinoma model injected into syngeneic immunocompetent mice. TSA cells (1x10⁵) were injected s.c. into Balb/c mice at the right flank. On day 10 when tumors became palpable, mice were randomly assigned to 4 groups (N=5-10/group): topical IMQ 5% or placebo cream 3x per week for up to 4 weeks with or without local RT (8 Gy x 3 fractions, days 12, 13 and 14). Treatment response was determined by measuring tumor growth and survival of mice. In some experiments, mice were injected in both flanks with TSA cells, and only one of the tumors was irradiated. Tumor-bearing mice treated with IMQ alone showed delayed tumor progression in comparison with control mice ($p < 0.0001$ on day 25) and increased infiltration by DC, CD4 and CD8 T cells. RT as single modality delayed tumor growth; however, neither treatment by itself was able to induce complete tumor regression. When IMQ was given in combination with RT, there was enhanced tumor inhibition ($p < 0.05$) and complete tumor regression in 4/6 mice at day 35. Analysis of regressing tumors at day 25 showed a marked enhancement over the baseline in untreated tumors in CD8 and CD4 T cell infiltration by IMQ + RT (5 to 10-fold) as compared to IMQ alone (2 to 3-fold). Remarkably, local treatment with RT + IMQ to one tumor resulted in significant inhibition of a second tumor outside of the radiation field only when the latter also received topical IMQ. Overall, results indicate that synergistic anti-tumor effects are obtained when local RT is administered coincident with TLR7 activation.

(PS7.64) Disposition of Ex-RADTM (ON 01210.Na), a new radioprotectant, in the isolated perfused rat liver model. Chen Ren¹, Mitalee Tamhane², David Taft², Manoj Maniar¹, Onconova Therapeutics, Inc., Newtown, PA, ²Long Island University, Brooklyn, NY

Ex-RADTM (ON 01210.Na) is a promising new radioprotective treatment being developed by Onconova Therapeutics, Inc. in collaboration with the Armed Forces Radiobiology Research Institute (AFRRI) for prophylactic or therapeutic use. The compound has been shown to be non-toxic and effective in increasing survival in cellular, tissue and animal radiation models by enhancing cell survival and DNA repair mechanisms. Ex-RADTM is currently in Phase I clinical development, and is targeted for use by emergency first responders. Ex-RADTM demonstrates rapid clearance from plasma in rats following IV dosing. A major metabolite, glutathione conjugate (1210-GSH), was identified *in vitro* using hepatocytes. In this study, the disposition of Ex-RADTM was evaluated in the isolated perfused rat liver (IPRL) model. The aim of the research was to assess the dose-linearity of Ex-RADTM disposition in the IPRL, and to evaluate the rate of formation of 1210-GSH in the model. Perfusion experiments (n=3/group) were performed at 4 doses (0.8, 4, 8, 20 mg), targeting a range of perfusate levels between 10 and 250 µg/ml. Perfusate binding was measured by ultrafiltration. Ex-RADTM was assayed in perfusate by HPLC and in bile using LC/MS/MS. Non-compartmental analysis was used to determine pharmacokinetic parameters. The protein binding results demonstrated high binding to perfusate proteins (88-95%) over the doses studied. Ex-RADTM displayed nonlinear disposition in the IPRL. The increase in AUC was disproportional at higher doses and consequently, the clearance decreased almost 2-fold at dose 20 mg. The half-life of ON 01210.Na was on an average 14 minutes at lower doses and increased to ~40 minutes at the high dose of 20 mg. The biliary clearance was found to be very low (0.01- 0.019 mL/min) and a very high abundance of the metabolite 1210-GSH was detected in the bile, which indicated a rapid degradation of Ex-RADTM. The results presented here demonstrate that IPRL model is a useful tool in studying the role

of the liver in the kinetics and metabolism of Ex-RADTM. A better understanding of how Ex-RADTM is taken up, metabolized and excreted by the liver will help to predict *in vivo* kinetics of the drug under various routes of drug administration.

(PS7.66) Inhibition of EGFR signaling induces metabolic oxidative stress and radiosensitization in head and neck cancer cells. Andrean L. Simons¹, Kevin P. Orcutt¹, Arlene D. Parsons¹, Arya Sobhakumari², Zita Sibenaller¹, Peter M. Scarbrough¹, Werner Wilke¹, Amanda Kalen¹, Prabhat Goswami¹, Douglas R. Spitz¹, ¹Free Radical and Radiation Biology Program, Iowa City, IA, ²Human Toxicology Program, Department of Radiation Oncology, Holden Comprehensive Cancer Center, The University of Iowa, Iowa City, IA

The epidermal growth factor receptor (EGFR) is believed to be an important molecular target in head and neck cancer (HNSCC) by activating pro-survival pathways. EGFR is up regulated in over 90% HNSCC tumors and is associated with poor clinical prognosis, and resistance to chemo-/radio-therapy. We hypothesized that EGFR inhibition with an EGFR tyrosine kinase inhibitor, Erlotinib, induces cytotoxicity and radiosensitization via oxidative stress in HNSCC cells. Erlotinib (10 µM) inhibited EGFR expression in FaDu, Cal-27, SCC-25 and SQ20B HNSCC cells and inhibited cell growth by inducing a G1 block over a 72 h period. Erlotinib induced significant clonogenic cell killing in all cell lines which was accompanied by significant increases in percent oxidized glutathione (%GSSG) and CDCFH2 oxidation. Additionally, EGFR knockdown using siRNA significantly increased %GSSG in SQ20B cells. Erlotinib-induced cytotoxicity was inhibited by the thiol antioxidant N-acetylcysteine (NAC) in all cell lines *in vitro*, and in a FaDu tumor xenograft model. NAC also suppressed Erlotinib-induced increases in %GSSG and CDCFH2 in FaDu cells. In addition, the NADPH oxidase inhibitors, diphenylene iodonium (DPI) and apocynin, significantly inhibited Erlotinib-induced cytotoxicity and increases in %GSSG. Radiosensitization and further increases in oxidative stress were induced in FaDu cells, only when Erlotinib was given 1 h after irradiation (2 Gy), and not 1 h before irradiation. These results support the hypothesis that oxidative stress mediated by NOX enzymes may be involved in the mechanism of Erlotinib-induced cytotoxicity. (Supported by KO1-CA134941, RO1-CA133114 and the Doris Duke Foundation).

(PS7.67) Predicted risk of a radiation-induced second malignant neoplasm for a 9-year-old girl with medulloblastoma after proton versus photon craniospinal irradiation. Phillip J. Taddei¹, Rui Zhang¹, Angelica Perez-Andujar¹, Rebecca M. Howell¹, Sarah B. Scarboro¹, Anita Mahajan¹, Fady Geara², Nabil Khater², Annelise Giebler¹, Dragan Mirkovic¹, Wayne D. Newhauser¹, ¹The University of Texas M. D. Anderson Cancer Center, Houston, TX, ²American University of Beirut, Beirut, Lebanon

Enhanced disease detection and treatment have led to improved survival rates of children with cancer. However, childhood cancer survivors who are treated with radiation face the prospect of radiation-induced late effects, including second malignant neoplasms (SMNs). Using proton beams rather than photon beams to treat regional cancers of the central nervous system, e.g., medulloblastoma, shows promise to reduce the frequency of SMNs and other late effects; however the potential amount of risk reduction has not been well quantified for boys and girls children of various ages. In this *in silico* study, we considered the case of a 9-year-old girl with medulloblastoma and compared her predicted risks of SMN incidence after proton and photon craniospinal irradiations. We determined the mean organ doses, including primary and stray (e.g., scatter and leakage) radiation, for proton and photon treatment plans using a combination of treatment planning system software, Monte Carlo simulations, and thermoluminescent dosimeter measurements. We then used those mean organ doses and age-, organ-, and sex-specific risk models from the literature to estimate the risks of SMN incidence from both radiation types. Preliminary results indicate that this patient's predicted risk of SMN incidence was reduced by half by treating her with

proton beams instead of photon beams. Thus, our findings contribute to the growing body of evidence supporting the use of protons rather than photons to improve long-term outcomes of children receiving craniospinal irradiation.

(PS7.68) Doxubicin conjugation to Fe₃O₄@TiO₂ core-shell nanoparticles show improved localization and cytotoxicity in drug-resistant ovarian carcinoma. Hans Arora, Aiguo Wu, Sumita Raha, John Boyle, Tatjana Paunesku, Gayle Woloschak, Northwestern University, Chicago, IL

Our laboratory investigates TiO₂ as a building material for nanoconjugates (NCs) for bionanotechnology. TiO₂ is particularly useful because of its semiconductor and nanocrystalline properties. TiO₂ molecules < 20nm develop surface "corner defects" allowing covalent binding of ligands to the surface. Excitation of TiO₂ nanomaterials by photons carrying energy greater than the 3.2 eV band gap results in a charge separation that can be transferred to a covalently-bound molecule, allowing the nanoparticle to act as a potential radiosensitizer. Addition of a Fe₃O₄ core allows imaging of such nanocomposites by magnetic resonance without affecting surface properties of TiO₂ molecules (Fe₃O₄@TiO₂). To such NCs we bound the chemotherapeutic doxorubicin (DOX) so that 35% of the 8 nm nanoparticle surface was bound with DOX (DOX-NP). Two ovarian carcinoma cell lines were used: A2780 and A2780/AD (isogenic cell line over-expressing multi-drug resistant (MDR) transporter p-glycoprotein). Cells in culture were treated with DOX-NPs or equimolar concentrations of DOX or NPs. Confocal microscopy of A2780 cells show time dependent uptake 1-18 hours post-treatment of both DOX and DOX-NPs, with DOX-NPs showing a predominantly cytoplasmic vesicular uptake pattern while DOX alone show a diffuse uptake pattern that localized to the nucleus. A2780/AD cells show no intracellular DOX signal 18 hours post-treatment, but cells treated with DOX-NPs show a similar fluorescent signal as DOX-NP-treated A2780 cells. In response to 2 Gy ionizing radiation A2780 and A2780/AD cells show remarkably different mRNA expression patterns for several genes involved in DNA repair and MDR transport. Previous experiments with DOX-sensitive and -resistant cells: OVCAR-8 and NCI/ADR-RES ovarian carcinoma cells show increased uptake and cytotoxicity of DOX-NPs relative to DOX in the resistant (NCI/ADR-RES) cell line, indicating the need for further study into the localization and cytotoxic effects of DOX-NPs relative to DOX in the A2780/AD resistant model, as well as further study into the radiosensitizing effects of DOX-NPs as compared to DOX or NPs alone. Additionally, flow cytometry was used to analyze proportions of dead and live cells after 5 Gy γ -ray exposure in HeLa cervical carcinoma cells pre-treated with CoFe₂O₄@TiO₂ nanocomposites.

(PS7.69) Gold nanoparticles sensitise cells to irradiation at clinically-relevant megavoltage energies. Jonathan A. Coulter¹, Suneil Jain², Karl Butterworth², Stephen McMahon¹, Mark Muir³, Wendy Hyland³, Alan Hounsell⁴, Joe O'Sullivan², Fred Currell³, Kevin Prise², David Hirst¹, ¹School of Pharmacy, QUB, Belfast, United Kingdom, ²CCRCB, QUB, Belfast, United Kingdom, ³School of Mathematics and Physics, Belfast, United Kingdom, ⁴Northern Ireland Cancer Centre, Belfast, United Kingdom

Background: Gold nanoparticles (GNPs) act as significant dose-modifying agents in several pre clinical studies. 1,2 Differences in the absorption coefficient between gold and soft tissue, as a function of photon energy, predict that maximum enhancement should occur in the low kilovoltage range (10 - 100 kV), with no enhancement at clinically-relevant megavoltage (MV) energies. We describe significant dose enhancement using 1.9 nm GNPs at MV energies generated by a linear accelerator. Methods: Normal L132, prostate cancer DU145 and breast cancer MDA-MB-231 cells were exposed to 1.9 nm GNPs (Aurovist, Nanoprobes, NY-USA) at a concentration of 500 μ g/ml for 24 h. Cellular uptake was measured by atomic emission spectroscopy and intracellular localisation by transmission electron microscopy. Nanoparticle-induced cytotoxicity was measured by flow cytometry and clonogenic assay.

Radiosensitisation by GNPs was determined by colony formation after irradiation at 160 kVp, 6 MV and 15 MV photon energies. Results: Nanoparticle localisation was restricted to the endosome, with uptake in the MDA-MB-231 cells peaking at 12 pg/cell compared with 0.6 pg/cell in L132 cells. Furthermore, cytotoxicity was observed when cells were exposed for 24 h to GNPs (100 μ g/ml) alone, resulting in a 27% loss of clonogenicity and a 2.2 fold increase in the sub G-0 fraction. In MDA-MB-231 cells, radiation dose enhancement factors of 1.4, 1.3 and 1.16 were achieved using 160 kVp, 6 MV and 15 MV X-ray energies respectively, suggesting that physical dose enhancement based on increased X-ray absorption is not the main mechanism of sensitization. In addition, 1.9 nm GNPs sensitized (SER = 1.38) MDA-MB-231 cells to the radiomimetic drug bleomycin. Conclusions: We have demonstrated a preferential uptake of 1.9 nm GNPs into tumour cells compared with normal cells in vitro. This resulted in significant radiosensitisation of MDA-MB-231 cells at both kV (p=0.004) and MV (p=0.002) X-ray energies and sensitization to bleomycin (p=0.0014) challenging the accepted dogma of physical radiation dose enhancement. The findings have the potential to improve the therapeutic index of radiotherapy, significantly reducing treatment-associated toxicity. 1. Regulla DF, et al. Radiat Res. 1998; 150:92-100. 2. Hainfeld JF, et al. Phys Med Biol. 2004;49:N309-15.

(PS7.70) Targeting DNA-PK and ATM with miR-101 sensitizes tumors to radiation. Ya Wang, Dan Yan, Wooi Loon Ng, Xiangming Zhang, Ping Wang, Zhaobin Zhang, Hui Mao, Chunhai Hao, Erwin G. Van Meir, Jeffrey J. Olson, Walter J. Curran, Emory University, Atlanta, GA

Ionizing radiation (IR) kills cells by inducing DNA double strand breaks (DSBs), which is one of the major cancer therapy approaches. However, the radioresistance of tumors frequently prevents successful treatment. Therefore, identifying new practical sensitizers is an essential step towards successful radiotherapy. MicroRNAs (miRNAs) represent a newly discovered class of small non-coding RNAs with ~22 nucleotides that bind to the 3' untranslated region (UTR) of multiple target mRNAs and either block the target translation or initiate the target degradation 1-3. Most mammalian mRNAs are conserved targets of miRNAs 4, and it is reasoned that identifying the miRNAs that target DNA DSB repair proteins could be a new way of sensitizing tumors to IR. Here we show that two proteins: DNA-PK (an essential factor for non-homologous end-joining (NHEJ) DNA DSB) and ATM (an important checkpoint regulator for promoting homologous recombination repair (HRR) DNA DSB) are predicted by a database search for the targets of miR-101. miR-101 binds to the 3'-UTR region of DNA-PKcs or ATM mRNA, up-regulating miR-101 in 95C or 95D cells (lung tumor cell lines) or U87MGD cells (glioblastoma (GBM) cell line) and decreases the levels of DNA-PK and ATM in these cells, resulting in these cells being more sensitive to IR. Mice xenograft derived from the human tumor cells with miR-101-up-regulation became more sensitive to IR than that without miR-101-up-regulation. More importantly, miR-101 packaged in a lentiviral vector could be delivered into the mice brain xenograft and dramatically sensitizes the tumors to IR. Taken together, these data open a new way to develop miRNA-sensitizers for improving radiotherapy.

(PS7.71) Modulation of E6 expression in HeLa cells by irradiation and nanoconjugates. Caroline B. Doty¹, Aiguo Wu², Tatjana Paunesku¹, Gayle E. Woloschak¹, Northwestern University, Chicago, IL, ²Ningbo University, Ningbo, China

Over half a million women worldwide are affected by cervical cancer each year. HPV, human papillomavirus, is the major causative agent of cervical cancer. Upon infection of host cells, HPV deregulates host cell cycle processes through the production of viral oncoproteins E6 and E7. The mechanism of action of these oncoproteins lies in the deregulation of tumor suppressor proteins p53 and Rb. Currently, our lab is evaluating the use of 6 nm Fe₃O₄@TiO₂ core-shell nanoparticles as a potential theranostic to target HPV oncogenes. Fe₃O₄@TiO₂ nanoparticles have a Fe₃O₄

core that can serve as MRI contrast agent. The Fe₃O₄ core is then coated with a shell of TiO₂ which creates reactive oxygen species, electrons and electropositive holes upon excitation with photons with energies above 3.2eV (e.g. white light, X-ray and gamma radiation). The production of electropositive holes by TiO₂ can be exploited to create DNA damage. TiO₂ also has the ability to bind bidentate ligands when nanoparticles are smaller than 20 nM. This allows conjugation of a short PNA (Peptide Nucleic Acid) leading to a sequence specific cleavage of targeted DNA. Since Fe₃O₄@-TiO₂ nanoparticles have a TiO₂ shell, we wanted to test the ability of Fe₃O₄@TiO₂ nanoparticles and Fe₃O₄@TiO₂-E6 PNA nanoconjugates to cleave viral DNA in vitro and in cells. We evaluated gamma radiation (2 Gy) alone or in the presence of nanoconjugates for its ability to cleave viral DNA in cells and modulate viral RNA expression. Western blots were done to determine changes of E6, p53 and Rb levels in treated HeLa cells. Upon light activation of nanoconjugates in HeLa cells we have found changes in E6, p53 and Rb protein levels. In gamma-ray irradiated HeLa cells treated with Fe₃O₄@TiO₂-E6/ORI PNA nanoconjugates we quantified E6 mRNA levels using RT-PCR. Results from this assay showed a dramatic decrease in E6 mRNA levels for irradiated nanoconjugate treated cells as compared to non-irradiated nanoconjugate treated cells.

(PS7.72) h-EsA reduces radiation-induced pneumonitis and lung fibrosis. Shanmin Yang, Mei Zhang, Chaomei Liu, Chun Chen, Steven B. Zhang, Xiaohui Wang, Yansong Guo, Amy Zhang, Steven G. Stwarts, Lurong Zhang, Paul Okunieff, UF Shands Cancer Center, Gainesville, FL

Esculentic acid (EsA) was chemically modified to produce h-EsA in order to reduce potential toxicity, and then tested for its bioactivity on radiation-induced pneumonitis and lung fibrosis. Effect of h-EsA on pro-inflammatory cytokines and cellular infiltrates were examined. The whole lung of C57BL/6 mice (10-12/group) was irradiated with 15 Gy at a dose rate of 1.84 Gy/min. The h-EsA (7.5-10 mg/kg) was delivered by gavage three times per week. Saline was used as vehicle control and Celebrex as positive drug control. The mice were sacrificed at different time points for assessment at the pneumonitis phase or lung fibrosis phase. The results showed that: 1) the extent of lung fibrosis was reduced as evidenced by a lower lung density measured using cone beam CT compared to that of saline control; 2) the respiratory rate, a measure of pulmonary function, was improved by h-EsA at both 7.5 and 10 mg/kg; 3) the lung compliance was also improved by h-EsA; 4) lung collagen measures in the h-EsA group were reduced compared to the saline control. These beneficial late effects might relate to the inhibitory effect of h-EsA on early IR pneumonitis as evidenced by: a) h-EsA reduced several key pro-inflammation cytokines, such as IL1 α , PF-4, p-selectin, TNF- α and VCAM-1, lymphotaxin and MIP- γ ; and b) on 2.5 and 17 days post-lung IR, h-EsA reduced the infiltrated lung macrophage in bronchial alveolar lavage. Finally, the therapeutic window (LD₅₀/ED₅₀ = 800 mg/kg / 10 mg/ml) for h-EsA was 80 as compared to only 20 for parental EsA. In conclusion, after modification, h-EsA remains an effective mitigator of early pneumonitis and late lung fibrosis. The mechanism likely includes inhibition of pro-inflammatory cytokine production and macrophages infiltration.

(PS7.74) Transforming growth factor β (TGF β) inhibition uncovers radiation-induced anti-tumor immunity in a mouse breast cancer model. Karsten A. Pilones, Sophie Bouquet, Mary Helen Barcellos-Hoff, Sandra Demaria, New York University, New York, NY

Prior studies have shown that radiation triggers the activation of transforming growth factor β 1 (TGF β 1) and that TGF β 1 is a potent inhibitor of effector functions of CD8 T cells. While testing the potential for TGF β neutralizing 1D11.16 monoclonal antibody (generously provided by Genzyme, Inc.) to block the DNA damage response (see abstract by Bouquet et al, this meeting), we examined

whether inhibition of TGF β 1 would also release immunosuppressive networks in the tumor microenvironment that prevent effective anti-tumor immunity. Employing the highly metastatic mouse breast cancer model 4T1, we have previously shown that local ionizing radiation therapy (RT) to the primary tumor induces tumor-specific CD8 T cells capable of inhibiting lung metastases as well as the irradiated tumor when combined with immunotherapy (*Clin Cancer Res* 11, 728, 2005, *Clin Cancer Res* 15, 597, 2009). Groups of 5 mice were treated with (1) isotype control monoclonal antibody (mAb), (2) RT, (3) 1D11.16, (4) RT + 1D11.16. Antibodies were given i.p. on day 13 post 4T1 tumor cell injection at 5mg/kg. RT was delivered exclusively to the primary tumor as a single non-ablative dose of 8 Gy on day 14. Mice were followed for tumor growth until day 22 or 30 when animals were euthanized for analysis of tumor-infiltrating T cells (TILs) and lung metastases, respectively. RT or 1D11.16 as single treatment did not significantly inhibit the growth of the primary tumor or lung metastases. In contrast, mice receiving 1D11.16 + RT had significantly smaller tumors ($p < 0.05$ on day 22), presumably due in part to increased radiation sensitivity, and concomitant with increased infiltration by CD8 but not CD4 T cells. The ratio of CD8+NKG2D+ effector to CD4+ T cells was significantly increased ($p = 0.04$), which suggests that TGF β inhibition also alters the immunological environment. Consistent with this, the number of pulmonary metastases evaluated on day 30 was significantly reduced only in mice given 1D11.16 + RT (median = 2, $p < 0.05$) compared to control (median = 8) or single agent RT or 1D11.16 (median = 7, $p > 0.05$) groups. These data suggest that inhibition of TGF β 1 is an effective strategy to improve radiation response by increasing both tumor radiation sensitivity and increased immunogenic response. Supported by NYU Cancer Center pilot funding.

(PS7.75) Application of human stem cell transplantation for the rescue of radiation-induced cognitive dysfunction. Munjal M. Acharya, Lori-Ann Christie, Mary L. Lan, Charles L. Limoli, University of California Irvine, Irvine, CA

Cranial irradiation remains a frontline therapy for primary and metastatic brain tumors. For many of these patients cognitive dysfunction is inevitable, a serious complication that may be caused by the radiation-induced depletion of neural stem and precursor cells. To explore the possibility of ameliorating radiation induced cognitive impairment, we transplanted human embryonic or neural stem cells (hESCs/hNSCs) into the hippocampal formation of rats after cranial irradiation. Athymic nude rats subjected to 10 Gy head only irradiation were grafted 2 days later with stem cells pre-labeled with BrdU at 4 distinct hippocampal-sites (100,000 cells/site, 8×10^5 cells/animal). Control (CON) and irradiated (IRR) rats receiving sterile media served as sham surgery groups. At 1 and 4 months postgrafting, rats were tested using a novel place recognition task (NPR). Compared to controls, irradiated rats showed significant cognitive decrements. In contrast, irradiated rats receiving either hESC or hNSC grafts did not differ from the CON group and spent more time than expected by chance exploring the novel place. To better understand these cognitive data, the total time spent exploring both objects during the familiarization phase of the task were analyzed. Significant differences between the groups were found; IRR animals spent less time exploring during familiarization compared to both CON and IRR+hESC/hNSC rats. These results suggested that hESC and hNSC transplantation attenuated radiation-induced cognitive impairment by preserving hippocampal-dependent spatial information processing when analyzed 1- and 4-months postirradiation. Immunocytochemical analysis revealed extensive migration of grafted stem cells throughout the host hippocampus and differentiation into neurons and astroglial cell types. Transplanted cells also exhibited significant homing to the neurogenic niche of the hippocampus. Unbiased stereology for the hESC group at 1 and 4 months postgrafting revealed 34 and 17% survival of transplanted cells respectively. These findings provide the first evidence that transplanted pluripotent (hESCs) and multipotent (hNSCs) human stem cells can survive, differentiate along neural lineages, and ameliorate cognitive impairments caused by cranial irradiation. [CIRM grant support CLL, MMA].

(PS7.76) Disruption of telomere equilibrium sensitises brain cancer cells to DNA repair inhibition and radiation. Resham L. Gurung, Swaminathan Sethu, Phoebe S. W. Lee, Esther S. H. Low, Shi N. Lim, Swapna Nandakumar, Shriram Venkatesan, Kalpana Gopalakrishnan, Prakash Hande, National University of Singapore, Singapore, Singapore

Primary malignant brain tumours are characterised by poor prognosis, recurrence and resistance to standard therapeutic strategies. Currently, chemotherapeutic agents are being tried in combination with the routine radiotherapy and surgical resection in the management of brain tumours with varying prognosis. Targeting telomere homeostasis has become one of the promising strategies in the therapeutic management of tumours. Recent investigations are beginning to indicate the potential of targeting telomerase in brain tumours. In this study, we show the anticancer potential of two different telomerase inhibitors, a cationic Porphyrin and a derivative from tea catechin, EGCG in brain tumour cells (medulloblastoma and glioblastoma). In addition to the disruption of telomere length maintenance, they decreased tumour cell viability, induced cell cycle arrest and DNA damage. Repair of EGCG induced DNA damage involved activation of DNA-PKcs protein with inhibition of DNA-PKcs activity causing delay in the repair of induced DNA damage. Additionally, telomere dysfunctional foci were more detectable in DNA-PKcs deficient glioblastoma cells as compared to DNA-PKcs proficient glioblastoma cells. The observed therapeutic potential in the brain tumour cells improved when they were combined with the inhibition of certain selective DNA repair factors (such as PARP-1 and DNA-PKcs). We have also observed the radio-sensitisation potential of these telomerase inhibitors in brain tumour cells. Therefore, targeting telomerase in addition to contemporary therapies and/or with inhibition of specific DNA repair pathways would improve the short and long term prognosis of malignant brain tumours. *This research is supported by Academic Research Fund, Ministry of Education, Singapore.

(PS7.77) Effect of GA on NF- κ B and JAK/STAT pathway after radiation. Xiaohui Wang, Mei Zhang, Yansong Guo, Steven B. Zhang, Shanmin Yang, Alexandra Litvinchuk, Chun Chen, Steven G. Stwartz, Paul Okunieff, Lurong Zhang, UF Shands Cancer Center, Gainesville, FL

Ionizing radiation (IR) triggers inflammation through the involvement of multiple immune and inflammation signal pathways such as nuclear factor kappa B (NF- κ B) and JAK/STAT pathway. The central role of NF- κ B in inflammation was well established both *in vitro* and *in vivo*. The activation of NF- κ B promotes the transcription of a panel of inflammatory genes, including cytokines such as TNF- α and IL-1 β , and enzymes associated with the synthesis of inflammatory mediators such as iNOS. JAK-STAT pathway was one of the important signaling pathways downstream of cytokine receptors. Indispensable functions of JAKs and STATs in cytokine signaling *in vivo* have been revealed through knockout mouse studies. Our goal is to explore the effect of GA (a natural anti-inflammatory agent) on blocking IR-induced inflammation via NF- κ B and JAK-STAT pathway. The levels of phosphorylated p65 (active subunit of NF- κ B), JAK2, stat3, stat4 and stat5 in murine macrophage RAW264.7 cells after 2, 4 and 6 Gy radiation with or without GA (5 and 10 μ g/ml) were assayed with in cell based ELISA using highly purified antibodies against phosphorylated proteins. Our results are: 1) compared with no radiation, macrophages exposed to 2, 4 and 6 Gy showed increased p65 phosphorylation, decreased phosphorylation of stat3 and stat5, and no observed change in phosphorylation of JAK2 and stat4; 2) GA significantly inhibited the level of basal p65 phosphorylation (about 85% of basal level at 5 μ g/ml GA, $p < 0.01$) and reversed the radiation-induced increase of Phosphorylated p65 in a dose dependent manner; 3) GA also reversed the radiation-induced decrease of phosphorylated stat5 in dose dependent in a manner dependent on oral dosage; and 4) GA had no influence on phosphorylated stat3. The results indicate that GA may act to reduce inflammation by significantly decreasing the basal and radiation-induced enhancement of phosphorylation of p65, while offsetting the radiation-induced inhibition of stat5 phosphorylation.

(PS7.78) Learning and activity after irradiation of the young mouse brain analyzed in adulthood using unbiased monitoring in a home cage environment. Niklas Karlsson, Marie Kalm, Klas Blomgren, University of Gothenburg, Göteborg, Sweden

Cranial radiotherapy in the treatment of pediatric malignancies may cause adverse so-called late effects. It is important to find methods to assess the functional effects of ionizing radiation in animal models, and to evaluate the possible ameliorating effects of preventive or reparative treatment strategies. We investigated the long-term effects of a single 8 Gy irradiation (IR) dose to the brains of 14-day-old mice. Activity and learning were evaluated in adulthood using open field and trace fear conditioning (TFC). These established methods were compared with the novel IntelliCage platform, which enables unbiased analysis of both activity and learning over time in a home cage environment. Neither activity, nor learning was changed after IR, as judged by the open field and TFC analyses. The IntelliCage, however, revealed both altered activity and learning impairment after IR. Place learning and reversal learning were both impaired in the IntelliCage three months after IR. These results indicate that activity and learning should be assessed using multiple methods and that unbiased analysis over time in a home cage environment may offer advantages in the detection of more subtle, IR-induced effects on the young brain.

(PS7.79) PARP-1 hyperactivation as a mechanism for radio-sensitization in prostate cancer by β -lapachone. David A. Boothman, Ying Dong, Erik A. Bey, Long-Shan Li, Wareef Kabbani, Jingsheng Yan, Xian-jin Xie, Jer-Tsong Hsieh, Jiming Gao, UT Southwestern Medical Center at Dallas, Dallas, TX

Beta-Lapachone (Arq 501, clinically) is a potent radiosensitizer *in vitro* by an unknown mechanism. Alone, the drug kills prostate cancer cells through NAD(P)H:quinone oxidoreductase 1 (NQO1) metabolism, inducing massive reactive oxygen species, irreversible single strand DNA breaks (SSBs), PARP-1 hyperactivation, NAD⁺/ATP depletion, and μ -calpain-induced programmed cell death. Since ~60% human prostate tumors expressed elevated endogenous NQO1 levels versus associated normal tissue, Beta-lapachone should be efficacious alone and in combination with radiation. Mechanistically, beta-lapachone radiosensitized ionizing radiation (IR)-exposed NQO1+ prostate cancer cells, wherein nontoxic doses of each agent reached threshold levels of SSBs required for PARP-1 hyperactivation. Significant SSBs and gamma-H2AX foci increases after combination therapy were accompanied by synergistic poly(ADP-ribosylated) (PAR)-modified PARP-1 formation, dramatic ATP loss and atypical PARP-1 cleavage in TUNEL+ cells, diagnostic of μ -calpain-mediated programmed necrosis. Along with dicoumarol (an NQO1 inhibitor), DPQ (a PARP-1 inhibitor) blocked radiosensitization. Synergistic antitumor efficacy *in vivo* was noted after IR + beta-lapachone therapy using PC-3 xenografts in athymic mice. Thus, radiotherapy using beta-lapachone (Arq501) is an efficacious, synergistic targeted strategy that exploits PARP-1 hyperactivation for cancers expressing elevated endogenous NQO1, as observed in prostate cancers. This work was funded by NCI/NIH grant # 2 R01 CA102792-07, and in part by DoD grant #W81XWH-06-1-0198 to DAB and DoD grant #W81XWH-08-1-0, a Prostate Cancer Postdoctoral fellowship to YD.

(PS7.80) Bioluminescence tomographic guided focal irradiation: the need for on-board integration. John W. Wong¹, Michael Armour¹, Richard Tuli¹, Juvenal Reyes¹, Eric Ford¹, Joseph Herman¹, Dmitri Artemov¹, Michael Patterson², ¹Johns Hopkins University School of Medicine, Baltimore, MD, ²Juravinski Cancer Centre and McMaster University, Hamilton, ON, Canada

New small animal radiation research platforms (SARRPs) employ on-board x-ray CT to guide focal irradiation. While CT is highly effective for positioning a target with high subject contrast, it is less apt for localizing small, soft tissue targets. Bioluminescent imaging (BLI) can detect small, even sub-palpable, tumors and is a powerful complement to x-ray CT. In this study, we examined the

utility of using BLI and BL tomography (BLT) for target localization in a mouse carcass on a SARRP. We employed a well defined target by depositing 5×10^5 luciferase-expressing human pancreatic cells in 20 μ l luciferin solution into a 5 mm glass bulb. The bulb was sealed and implanted in the vicinity of the pancreas of the open carcass. The carcass was then closed and placed in the Caliper IVIS 200 system for BLI and BLT. The procedure was repeated for 4 carcasses. The carcasses were then transported to a SARRP for bulb localization with CT. Three plausible off-line setup approaches on the SARRP were emulated: (A) using only surface BL images to align the perceived target to the beam axis without other imaging aid, (B) using CT on the SARRP to recapitulate the animal's position at time of BLI, and (C) registering the 3D torso contour from BLT with the corresponding contour from x-ray CT. For approach (A) and (B), CT was acquired of each animal after re-positioning. With no depth information, the 2D radial distances between the beam axis and the vertical axis through the centroid of the CT bulb were calculated, yielding 5.8 ± 1.4 (range: 3.0 - 7.3) mm for visual setup (A) and 3.5 ± 0.2 (range: 3.3 - 3.7) mm for CT assisted setup (B). For approach (C), the 3D distance between the centroids of BLT source and CT bulb after image registration was determined to be 2.9 ± 0.5 (range: 2.2 - 3.4) mm. Thus, all 3 off-line procedures would require appreciable margin expansion to ensure radiation coverage. For 2D setup with (A) and (B), the aperture of a vertical beam would need to be larger than 10 mm for even a small 3 mm target. For 3D setup (C), a margin expansion of 3 - 5 mm around a target volume would be required. As the uncertainties for BLT and off-line setup are both about 1-2 mm, a SARRP with integrated on-board x-ray/BL tomographic guidance would eliminate setup error, and allow margin expansion of < 2 mm for meaningful focal irradiation. The development of such system will be presented.

(PS7.81) Gender differences in neurogenesis and behaviour after irradiation to the developing mouse brain. Karolina Roughton, Klas Blomgren, University of Gothenburg, Gothenburg, Sweden

Radiation therapy to the brain used for the treatment of paediatric malignancies may lead to difficulties in learning and memory later in life. These late effects may be influenced by age at treatment and gender, where young girls suffer more from late effects compared to young boys. Unfortunately, most preclinical studies are performed on male animals, and no consideration of the gender is taken. Therefore we wanted to investigate possible long-term gender differences in the response to irradiation. The whole brain was irradiated with a single dose of 8 Gray in postnatal day 14 C57BL/6 mice of both genders. The behavioural effects were tested when the mice reached adulthood (3 months) by using the IntelliCage platform. We found a significant difference in learning and memory-related behaviour where irradiated male, but not female, mice performed worse than controls. To further investigate potential gender differences, the mice were injected with bromodeoxyuridine (BrdU), a thymidine analogue, one month prior to sacrifice. The brains were analysed by counting the number of newborn surviving cells in the hippocampus. This showed a significant gender difference in the granule cell layer, where the density of BrdU-positive cells after irradiation decreased more in female compared to male mice. In summary, our results reveal gender differences in the response to irradiation which need to be further investigated.

(PS7.82) GMX1777/1778 induces oxidative stress in solid tumor cell lines. David Cerna¹, Hongyun Li¹, Siobhan Flaherty¹, Donna J. Carter¹, Stephen Yoo², ¹SAIC-Frederick, Inc., Frederick, MD, ²Molecular Radiation Therapeutics Branch/Radiation Research Program, Rockville, MD

Targeting susceptible pathways in tumor metabolism can be an exploitable therapeutic strategy for the treatment of certain cancers while sparing normal tissues. The identification and characterization of these pathways are crucial for the success of these novel agents in the clinics. GMX1777/1778, a novel inhibitor

of NAD⁺ biosynthesis, is a potent and specific inhibitor of the nicotinamide adenine dinucleotide (NAD⁺) biosynthesis enzyme, phosphoribosyl transferase (NAMPT). Since cancer cells have a high rate of NAD⁺ turnover, modulation of NAD⁺ biosynthesis would be an attractive target for GMX 1777/1778. In addition to the depletion of NAD⁺ level, GMX 1777/1778 also induced oxidative stresses by specifically increasing the superoxide level in certain cancer cells. Addition of exogenous nicotinic acid (NA) restored NAD⁺ level via nicotinic acid phosphoribosyltransferase 1 (NAPRT1) in certain genotypes. Thus, the lack of NAPRT1 enzyme in certain cancers would provide additional cancer specific vulnerability. The results presented here shows that the oxidative stresses induced by GMX1777/1778 were maintained even in the presence of nicotinic acid (NA) when the NAPRT1 was lacking. Of critical importance, the induction of oxidative stresses in normal tissues are lacking, suggesting improved therapeutic index by GMX 1777/1778. We further investigated the role of p53 in the oxidative stress response to GMX 1777/1778 and have shown that combinations of NAPRT1 and p53 genotypes are responsible for cellular response and survival to GMX1777/1778 treatment. Since most of the glioblastomas lack the NAPRT1 and p53, the potential of GMX1777/1778 was investigated using an intracranial orthotopic brain tumor model in combination with radiation. The result presented here suggests clear clinical benefit of prolonged survival in mice treated with GMX1777/1778 and ionizing radiation with minimal toxicities to normal tissues.

(PS7.83) The novel radiolabelled benzamide solazed demonstrates melanoma specific retention in vitro as well as a cumulative inhibitory effect on tumour growth in vivo. Craig C. Joyce¹, Rob Mairs², John Babitch³, Annette Sorensen¹, Marie Boyd¹, ¹Strathclyde Institute of Pharmacy and Biomedical sciences, Glasgow, United Kingdom, ²Glasgow university, Glasgow, United Kingdom, ³Molecular Insight Pharmaceuticals, Boston, MA

Malignant melanoma (MM) accounts for 75% of skin cancer associated deaths, typically demonstrating a high resistance to conventional chemotherapeutic and radio-therapeutics, therefore novel strategies for targeting and treating MM are required. Selective irradiation of Melanoma tumour cells by target radionuclide therapy is one such approach. MM expresses varying degrees of melanin, the [¹³¹I] labelled benzamide 'Solazed' has demonstrated high melanin affinity. This study investigates the efficacy of [¹³¹I]Solazed treatment administered at 1.25 GBq/kg in combination with the melanoma benchmark drug, Dacarbazine (80mg/kg) on Sk-mel-3 nude mouse xenografts. Tumours treated with 3x 80mg/kg of Dacarbazine alone achieved a 3 fold increase in volume by day 50. Conversely, 3x 1.25 GBq/kg of Solazed achieved a static tumour volume by day 50. A combination dose of 3 x 80mg/kg Dacarbazine and 1.25Gqbq/kg Solazed achieved a static tumour volume by day 50. Single dose treatments of 1.25Gqbq/kg Solazed achieved reduced tumour growth by day 50 when compared to the saline control. Double dose treatments exhibited a static tumour volume by day 50. Between days 50 and 125 all Solazed treated groups achieved recurrent growth. 1.25 GBq/kg [¹³¹I]Solazed produces a cumulative inhibitory effect on tumour growth when administered at 7,14 and 21 days, with the combination of Dacarbazine and [¹³¹I]Solazed proving more effective than two doses of [¹³¹I]Solazed alone but less effective than three single doses of [¹³¹I]Solazed when compared to Dacarbazine alone. *In vitro* treatment of [¹³¹I]Solazed demonstrated melanin specific retention when compared to amelanotic cancer cell lines.

(PS7.84) Ciprofloxacin inhibits gamma radiation-induced increases in γ -H2AX, p53 phosphorylation in human tumor cells and p53 phosphorylation, Gadd45 α , bax, and Bcl-2 gene expression in human peripheral blood cells. Juliann G. Kiang, Bradley R. Garrison, Risaku Fukumoto, Thomas B. Elliott, David G. Ledney, Armed Forces Radiobiology Research Institute, Bethesda, MD

Background: Ionizing radiation increases cell mortality in a dose-dependent manner. Increases in DNA strand breaks, γ -H2AX,

phosphorylated p53, and protein concentrations of p53 and Bax also occur. We investigated the ability of ciprofloxacin (CIP), a topoisomerase II inhibitor, to inhibit DNA damage and its responsive gene expression induced by either ionizing radiation or the radiomimetic bleomycin. Methods: TK6, NH32, and human peripheral blood mononuclear cells (PBMCs) were irradiated with 1-8 Gy ^{60}Co -gamma-photon radiation or treated with 10-400 μM bleomycin. Flow cytometry measured $\gamma\text{-H2AX}$ (an indicator of DNA double-strand breaks) and phosphorylated p-53 (responsible for cell-cycle arrest); real-time PCR measured p21, Bax, Bcl-2, Gadd45 α , and DDB2 gene expression (regulated by p53 protein); and a clonogenic assay determined cell survival. Results: Both irradiation and bleomycin increased $\gamma\text{-H2AX}$ levels in TK6 cells in a dose-dependent manner within 1 h. CIP given 1 h prior to or 30 min after irradiation or bleomycin effectively inhibited the increase in $\gamma\text{-H2AX}$. In NH32 cells (p53 $^{-/-}$), CIP failed to inhibit the irradiation-induced $\gamma\text{-H2AX}$ increase, suggesting that CIP inhibition is mediated by p53. NH32 cells survived lethal irradiation significantly better than TK6 cells, suggesting p53 mediates the radiation-induced mortality. In human PBMCs, CIP effectively blocked the irradiation-induced $\gamma\text{-H2AX}$ increase but not the phosphorylated p53 increase. CIP inhibited radiation-induced increases in Gadd45 α , Bax, and Bcl-2 gene expression 24 h post-irradiation, but enhanced p21 and DDB2 expression 4 h post-irradiation, suggesting that CIP exerts its effect in PBMCs on steps of p53 activation. Conclusion: Results indicate gamma radiation activates both $\gamma\text{-H2AX}$ and p53 pathways within 1 h and subsequently upregulates p21, Bax, Bcl-2, Gadd45 α , and DDB2. CIP inhibits $\gamma\text{-H2AX}$ and p53 phosphorylation in cancer cells and p53 phosphorylation, Gadd45 α , Bax, and Bcl-2 in normal cells. These results suggest CIP may be used to treat irradiated tissues. (Supported by NIH/NIAID R21-AI080553).

(PS7.85) Early detection of radiation therapy response in non-Hodgkin's lymphoma xenografts by in vivo 1H magnetic resonance spectroscopy and imaging. Jerry D. Glickson¹, Seung-Cheol Lee¹, Harish Poptani¹, Stephen Pickup¹, Timothy Jenkins¹, Sunghoon Kim², Cameron J. Koch¹, E J. Delikatny¹, ¹University of Pennsylvania, Philadelphia, PA, ²New York University, New York, NY

The purpose of the study was to investigate the applicability of 1H MRS and MRI methods for the clinical detection of early response to radiation therapy in non-Hodgkin's lymphoma (NHL). Studies were performed on the WSU-DLCL2 xenograft model in nude mice of human diffuse large B-cell lymphoma, the most common form of human NHL. Radiation treatment was applied as a single 15 Gy dose to the tumor. Tumor lactate, lipids, total choline, T2 and apparent diffusion coefficients (ADC) were measured before treatment and at 24 h and 72 h after radiation. A Hadamard-encoded slice-selective multiple quantum coherence spectroscopy sequence was used for detecting lactate (Lac), while a stimulated echo acquisition mode sequence was used for detection of total choline (tCho) and lipids. T2- and diffusion-weighted imaging sequences were used for measuring T2 and ADC. Within 24 h after radiation, significant changes were observed in the normalized integrated resonance intensities of Lac and the methylenes of lipids; Lac/H₂O decreased by 38 \pm 15% (p=0.03) and lipid (1.3 ppm, CH₂)/H₂O increased by 57 \pm 14% (p=0.01). At 72 h after radiation, tCho/H₂O decreased by 45 \pm 14% (p=0.01) and lipid (2.8 ppm, polyunsaturated fatty acid)/H₂O increased by 97 \pm 36% (p=0.001). ADC increased by 14 \pm 2% (p=0.003), and T2 did not change significantly. Tumor growth delay and regression were observed thereafter. This study enabled comparison of the relative sensitivities of various clinically detectable 1H MRS and MRI indices to radiation, and suggests that 1H MRS/MRI measurements detect early responses to radiation that precede tumor volume changes.

(PS7.86) Temporal effects on hippocampal cell proliferation after irradiation to the young mouse brain. Martina J. M. Hermansson, Andrew S. Naylor, Klas Blomgren, Institute for Neuroscience and Physiology, Gothenburg, Sweden

Radiotherapy is commonly used in the treatment of brain tumors. However, there are several long-term debilitating effects after radiotherapy in children, including life-long cognitive decline. Areas in the brain where neurogenesis is present are particularly sensitive to radiotherapy and loss of these cells may contribute to cognitive deficits seen after radiotherapy. We investigated the temporal effects of irradiation on cell proliferation in the hippocampus, a region important in memory functions and one of the neurogenic areas in the brain. We irradiated mice on postnatal day (P) 14 and assessed cell proliferation and cell survival at different time points. We found a significant decrease in the number of bromodeoxyuridine- (BrdU) positive cells in mice injected at P16 and sacrificed at P22 (p=0.001). However, at P22, there was no decrease after irradiation in the number of dividing phospho-histone H3-positive cells. Furthermore, animals injected with BrdU at P23-P26 and sacrificed at P63 showed no significant difference in the number of labeled, surviving cells (BrdU-positive cells) after irradiation, but a significant difference in cell proliferation at P63 (phospho-histone H3-positive cells) (p<0.001). These results indicate that hippocampal cell proliferation initially decreases after irradiation, followed by a normalization compared to controls, eventually decreasing to a permanently low level. This may provide a window of opportunity to rescue proliferating cells and to encourage survival in order to prevent cognitive decline.

(PS7.87) Radiation-induced disruption of the glioblastoma (gbm)-associated blood:brain:barrier (bbb): multimodality imaging via a novel orthotopic model system. Jay F. Dorsey, Stephanie Yee, Sara Davis, Andrew Hollander, Andrew Zheng, Xiangsheng Xu, Gary Kao, University of Pennsylvania, Philadelphia, PA

Introduction: The prognosis of patients with glioblastoma (GBM) remains poor despite the addition of chemotherapy to the standard treatment of radiation therapy. The relative ineffectiveness of chemotherapy in treating GBM has been attributed in part to the low intra-tumoral drug concentrations due to the blood:brain:barrier (BBB). The development of animal models of the tumor:BBB would facilitate investigations of strategies to modulate the BBB, in hopes of increasing therapeutic efficacy. Methods: Human U251 GBM cells were established to stably express both GFP and luciferase and injected intracranially into nude mice to form orthotopic tumors. Luciferase expression enabled serial imaging of the growing tumors with the administration of luciferin. BBB integrity was assessed via the extravasation of Evans Blue (EB), which fluoresces under the red fluorescence channel, thereby allowing co-imaging with the GFP-expressing tumor. Results: Intracranial tumors were detected in the mice as soon as 5 days after orthotopic injection of human GBM cells by luminescence. The orthotopic tumors were also detected via GFP imaging with a lower signal to noise. Established GBM tumors showed high levels of EB extravasation, and correlated well with immunoglobulin (Ig) deposition, consistent with serum origin of EB extravasation. Mice without tumors but which were either mock-irradiated or irradiated with 20 Gy to the brain and subject to necropsy 24 hours later, served as additional controls. Unirradiated brains showed no EB extravasation, while irradiated brains showed 1.5-2.0-fold greater levels of EB signal (p < 0.05), consistent with disruption of the BBB by radiation. Results of computed (CT) and positron emission tomographic (PET) and magnetic resonance imaging of mice with GBM-derived brain tumors will be presented. Conclusions: The novel orthotopic intracranial system modeling human tumors we describe here should facilitate studies of new therapeutic strategies targeting GBM. We have furthermore developed techniques that allow the visualization and quantitation of BBB integrity, a potential determinant of chemotherapeutic efficacy in the treatment of GBM. Finally, studies testing sequencing of radiation to disrupt GBM-associated BBB integrity are planned and will be presented.

(PS7.88) Gene expressions profiles following single-dose and fractionated radiation in wild-type and mutant p53 prostate cancer cells. Charles B. Simone, II, Molykutty John-Aryankalayil, Sanjeevani T. Palayoor, Adeola Y. Makinde, David Cerna, C. N. Coleman, National Cancer Institute, National Institutes of Health, Bethesda, MD

Background: Malignant cells that survive repeated radiation (RT) fractions may undergo molecular changes and differ in treatment response to subsequent molecular-targeted therapy. We assess changes in cell lines of varying p53 status after various RT regimens to determine if fractionated RT can induced molecular pathways changes. Methods: LNCaP (p53 wild type), PC3 (p53 null) and DU145 (p53 mutant) prostate cancer cells were exposed to 5 Gy and 10 Gy as single-dose (SD) or multi-fractionated (MF: 0.5 Gy x 10, 1 Gy x 10, 2 Gy x 5) RT. RNA and protein were extracted at multiple time points 2-24 h after the final RT fraction. mRNA microarray analysis was via CodeLink Whole Genome Bioarray (55,000 probes). Validation of microarray data was via real-time RT-PCR or Western blot analysis. All samples were run in distinct biological triplicates. Results: Across RT regimens, mRNA analysis revealed 978 genes in LNCaP differentially expressed (>2 fold change, $p < 0.05$) after RT. Most were altered with SD (69%), with 90% downregulated. Fewer genes were induced in PC3 (343) and DU (116), with most upregulated (87% and 89%) and altered with MF. Gene ontology revealed immune response genes ($p = 2.76E-23$) most prominently expressed after RT in PC3 and DU but less significant in LNCaP ($p = 0.03$). Cell cycle regulatory ($p = 9.23E-73$) and DNA damage ($p = 3.82E-9$) and repair ($p = 6.86E-30$) genes were most prominently altered in LNCaP but less significant in DU and PC3. In LNCaP, among cell cycle genes (14% of altered genes), AURKA, AURKB, CDKN2C, CCNB2, PLK4, E2F2 and E2F8 were downregulated after all RT regimens. P53-activated genes were induced in LNCaP but not DU or PC3. Proapoptotic TP5313 and ANGPT2 were only upregulated in LNCaP and transcriptional activation of both was seen at the protein level. Selected genes in all cell lines were validated with real-time RT-PCR and 100% correlation was observed with microarray data. Conclusions: Differences in gene expression exist between cell lines and after varying RT regimens that are p53 dependent. Further study is underway to identify changes in molecular pathways (mRNA, miRNA, protein). As the duration of changes in surviving cells is ≥ 24 h, it may be possible to use RT-inducible targets for molecular-targeted therapy rather than depend on the presence of mutations, thus enhancing efficacy of targeted agents.

(PS7.89) Potentiation of the cytotoxic effects of metallated enediyne compounds by hyperthermia. Stefan Rott¹, Ju Zhu², Jeffrey M. Zaleski², Joseph R. Dynlacht¹, ¹Indiana Univ School of Medicine, Indianapolis, IN, ²Indiana University, Bloomington, IN

Enediynes are a class of chemotherapeutic agents that are potent inducers of DNA double-strand breaks. However, non-selectivity, control of thermodynamic activation (which often occurs at $< 37^\circ\text{C}$), the unspecific nature of their potent diradical intermediates, and a lack of resistance to biological radical quenchers has limited their clinical usefulness. Many investigators have attempted to overcome these challenges by selective recognition and targeted delivery, chemical- and/or photo-sensitive triggering mechanisms, or modulation of cycloaromatization through complexation with transition metals. Since enediyne activation is very sensitive to heat, hyperthermia treatment may provide a practical solution to selective drug activation *in vivo*. In this study, we describe the effects of two novel metalloenediynes [(Z)-N,N'-bis[1-quinolin-2-yl-meth-(E)-ylidene]oct-4-ene-2,6-diyne-1,8-diamine complexed with Zn(II), or QuinED-ZnCl₂, and (N,N'-bis-pyridin-2-ylmethyl-oct-4-ene-2,6-diyne-1,8-diamine, 4), or PyEd] on HeLa cells treated with the compounds at 37° or 42.5°C . HeLa cells, when exposed to concentrations of PyED (which forms a Mg(II) complex in growth medium) or QuinED-ZnCl₂ that were relatively non-toxic after a 1 h incubation at 37°C , were greatly sensitized when heated at 42.5°C for 1 h during treatment with the compounds. The enhanced cytotoxicity may be attributed to increased apoptosis or perturbation of normal patterns of cell cycle arrest. Cells exposed to heat only or to PyED only experienced significant G2/M blocks 18 h after treatment; however, interestingly, the cell cycle block was reduced when PyED and heat were administered simultaneously. Thus, heating during drug treatment resulted in an inhibition of cell cycle arrest that could be potentially necessary for repair of DNA damage induced by the drug. With ongoing improvements in site-specific heat delivery to tumors, the systemic administration of non-toxic concentrations of metalloenediynes coupled with localized hyperthermia treatment

may prove to be an attractive solution to selective enediyne activation and targeting in the clinical setting, which in turn could result in an enhancement of therapeutic gain.

(PS7.90) Development of an IVIS imaging-based murine combined Pseudomonas aeruginosa and radiation model. Chaela S. Presley, James Bina, Gabor Tigyi, Charles R. Yates, UTHSC, Memphis, TN

Purpose: Opportunistic infection involving translocated enteric flora is a major cause of mortality following high dose radiation exposure. The purpose of this study was to establish a model to characterize the kinetics of bacterial translocation from the gut following total body irradiation. Our objectives were: (1) Develop a lux-labeled P. aeruginosa strain suitable for live imaging in mice (2) Optimize inoculation route and schedule for colonization (3) Describe the kinetics of bacterial translocation and organ load, and (4) Evaluate the impact of combined injury on mortality. Methods: The lux labeled P. aeruginosa was generated with a plasmid containing a promoter from V. cholerae and a tetracycline resistance gene. Mice were treated with streptomycin (2 mg/mL in drinking water) to remove enteric flora prior to inoculation with lux labeled P. aeruginosa. Three different forms of oral inoculation strategies to achieve gut colonization were evaluated: single gavage of 1×10^7 cfu, serial gavage of 1×10^7 cfu, and ad libitum water containing 1×10^7 cfu/mL. Stool homogenates were plated from initial bacterial exposure through two days after exposure. Forty eight hours after colonization, mice were irradiated (TBI; 137Cs; 6 Gy) to determine the effect of bacterial colonization on mortality, thereby determining a window for imaging. A Xenogen IVIS imager was used to quantify bacteria in the intestine, liver, spleen, and lungs over time. Terminal counts were confirmed with *ex vivo* imaging of saline perfused organs. Results: Single and serial oral gavage of P. aeruginosa were insufficient to establish colonization post exposure as verified by fecal cultures. Sustained colonization occurred after four days of P. aeruginosa inoculated drinking water. Thus, this colonization strategy was used for imaging and mortality studies. Preliminary studies suggest that gut colonization does not affect mortality. Studies to determine systemic bacterial load are underway. Conclusion: We have developed a combined injury model which facilitates characterization of the kinetics of bacterial gut translocation via real-time imaging.

(PS7.91) Manipulation of body temperature as a novel treatment for augmenting hematopoiesis and neutrophil homeostasis following radiation-induced neutropenia. Maegan L. Capitano, Michael Nemeth, Thomas Mace, Phillip McCarthy, Elizabeth Repasky, Roswell Park Cancer Institute, Buffalo, NY

Cancer patients who are unable to receive the optimal dose of cytotoxic therapies such as chemotherapy and radiation have a significantly poorer prognosis than those who can receive the optimal treatment dose. For example, high dose total body irradiation (TBI) and/or chemotherapy are critical components of the myeloablative conditioning regimen for patients about to receive bone marrow transplantation. However these therapies result in a severe reduction of normal blood leukocytes, leaving transplant patients at high risk of opportunistic infections. We hypothesize that treating mice with mild (fever-range) thermal therapy, which is known to alter leukocyte numbers and migration patterns, following a non-myeloablative dose of TBI will enhance immune reconstitution through a thermally sensitive, cytokine driven bone marrow release of neutrophils to the peripheral blood. This hypothesis was generated from the following observations: C57BL/6 mice were given TBI (3Gy) followed 2 hours later by a 6 hour mild thermal therapy (MTT; body temperature maintained at 39.5°C). In mice treated with MTT following TBI, a significant increase in recovery of peripheral blood neutrophils was observed by day 8 compared to mice that received TBI alone or MTT alone. In addition, G-CSF concentration was increased two fold in the serum of TBI + MTT mice correlating with the increased rate of neutrophil recovery. Flow analysis of the bone marrow revealed comparable percentages of hematopoietic stem cells (HSCs) in the control and the TBI +

MTT groups; however there was a significantly lower percentage of HSCs in the bone marrow of the TBI-alone group. In addition a greater percentage of HSCs were undergoing proliferation when TBI was followed by MTT compared to TBI alone. Flow analysis also revealed that MTT following TBI increased the overall percentage of granulocyte-macrophage progenitors when compared to control and TBI-alone groups. This increase in progenitor cells seen in TBI + MTT mice is associated with an increase in overall number of CFUs when compared to radiation alone. These data reveal a previously unexplored role of body temperature in regulation of marrow output following stress and may help in the development of novel clinically applicable strategies to ameliorate the effects of TBI. NIH R01 CA71599 and CA135368.

(PS7.92) Stereotactic radiation therapy for spontaneously occurring canine osteosarcoma. Susan M. LaRue, Stewart D. Ryan, James T. Custis, Nicole E. Ehrhart, Deanna Worley, Joanne Tuohy, Joseph F. Harmon, Colorado State University, Fort Collins, CO

Introduction: Osteosarcoma (OSA) in human and canine patients is considered resistant to traditional fractionated radiation therapy. In a previous study using canine fibrosarcoma, we demonstrated acute endothelial cell apoptosis associated with large dose/fraction irradiation, implying an alternative mechanism for SRT as suggested by Kolesnick, Fuks and others. We hypothesized that delivering Stereotactic Radiation Therapy (SRT) in 3 fractions of 11-15 Gy would improve tumor control in spontaneously occurring canine OSA. Methods: A planning CT scan was acquired with the affected limb immobilized in an indexed frame. A treatment plan using 5-13 intensity modulated fields was developed using Varian EclipseTM. Fractions were administered 24-72 hours apart and carboplatin and pamidronate were administered to all patients. Patients were followed with lesion and thoracic radiography every 3 months to monitor for pathologic fracture and/or local tumor recurrence and metastatic disease, respectively. Results: 36 patients were treated. Lesions were located in the humerus, radius, ulna, femur and tibia. Mean dose to 95% of prescribed target volume was 36 Gy. Limb usage and durable pain palliation was good to excellent. Local tumor control was achieved in all tumors based on serial radiography, repeat scintigraphy in 3 dogs, and histology of retrieved limbs. At mean follow up time of 263 days, ten dogs are alive with 26 dead. All but one dog died from development of metastatic disease or decreased quality of life. Overall median survival time was 255 days, which is comparable to survival times achieved with amputation and chemotherapy. Moderate to severe acute skin effects were observed in the first three cases. The dose prescription was then modified to limit skin dose. Subsequently, only 0 or grade 1 skin effects were observed. Pathologic fractures occurred in 13 cases. With improved case selection criteria only three cases sustained fracture in the last 17 cases (18%) compared to 10 out the first 19 cases (53%). Conclusions: Control was achieved in a tumor known to be resistant to fractionated radiation therapy. Tumor control was higher than predicted based on linear quadratic formalism. Alternative mechanisms associated with improved response in bone tumors treated with SRT should be investigated.

(PS7.94) Radiosensibilization of gliomas for hadron therapy. Gianfranco Grossi¹, Daniela Bettega², Paola Calzolari³, Vittorio de Francischi⁴, Ilaria Improta⁵, Mario Lupi⁶, Lorenzo Manti⁷, Rita Massa⁸, Alessandra Pollice⁹, Paola Scamporrì⁷, Paolo Ubezio⁶, ¹Department of Physical Sciences & CRAFS - University Federico II & INFN, Napoli, Italy, ²Department of Physics - University & INFN, Milano, Italy, ³Department of Physics - University & INFN, Milano, Italy, ⁴CNR, Napoli, Italy, ⁵INFN, Napoli, Italy, ⁶Institute Mario Negri, Milano, Italy, ⁷Department of Physical Sciences - University Federico II & INFN, Napoli, Italy, ⁸Department of Physical Sciences - University Federico II & INFN, Napoli, Italy,

⁹Department of Structural and Functional Biology - University Federico II & INFN, Napoli, Italy

Glioblastoma (GB) is the most malignant primary brain tumour. It is associated with poor prognosis, low curability and is localized most frequently in the deep layers of gray matter, with intrinsic and hypoxia-induced radioresistance. In the last years, significant results have been obtained by radiotherapy (RT) new modalities allowing the tumour dose to increase up to 50-60 Gy, as well as using systemic agents (radiosensitizers), such as temozolomide (TMZ), an oral alkylating agent, which is clinically well tolerated. *In vitro* and preclinical studies in primary and recurrent gliomas have shown an additive or synergic activity of TMZ in combination with conventional RT. Because of the radiobiological (radioresistance, high percentage of hypoxic cells, localization, etc.) and clinical (low curability, incidence among young people) characteristics of GB, treatment of GB patients with carbon ion radiotherapy seems to be a promising alternative. In this *in vitro* study, four glioma cell lines (T98G, U87MG, LN229, U373) of different photon radiosensitivity and with different gene mutations, were exposed to graded doses (0.5 - 5.0 Gy) of photons and ¹²C mono-energetic beam (E = 6.7 MeV/amu, LET = 218 keV/μm and E = 19 MeV/amu, LET = 94 keV/μm) after treatment with 50 μM TMZ for 1 hr. Radio-induced cytotoxicity was measured by clonogenic survival assay, and apoptosis, as well as cell cycle progression, has been examined. Preliminary results show that high LET ¹²C-ions are very effective to inactivate glioma cell proliferative capacity, but it is not evident how TMZ interacts with low and high LET radiation (additive, synergistic or supra-additive).

(PS7.95) Aldo-Keto Reductase 1C3 as a novel target for the aerobic activation of the prodrug PR-104A in human hematopoietic cells. Julian Down¹, Kalindi Parmar², Alan D'Andrea², Fernando Doñate³, Adam Patterson⁴, William Wilson⁴, Massachusetts Institute of Technology, Cambridge, MA, ²Dana-Farber Cancer Institute, Boston, MA, ³Proacta Inc., San Diego, CA, ⁴University of Auckland, Auckland, New Zealand

Upon delivery *in vivo*, the pre-prodrug PR104 is hydrolyzed rapidly to the bioreductive dinitrobenzamide mustard prodrug PR-104A which then undergoes nitro reduction to DNA cross-linking and cytotoxic metabolites. PR-104 is currently in Phase I/II clinical trials and was initially developed to exploit tumor hypoxia through its one-electron reduction in the absence of oxygen. More recently, aldo-keto reductase 1C3 (AKR1C3) has been shown to be responsible for aerobic activation of PR-104A in human tumors (Guise et al., Cancer Res. 70: 1573-84, 2010). Clinical hematological toxicity has been observed as a consequence of PR-104 treatment in humans. Here, we ask whether hypoxia in the bone marrow stem cell niche (Parmar et al., PNAS 104: 5431-36, 2007) or AKR1C3 expression in myeloid progenitors might be responsible for this dose-limiting side-effect. PR-104 administration in C57BL/6J mice caused only moderate depletion of hematopoietic subsets and depression of peripheral blood cells at the maximum tolerated dose. Parallel experiments on human and mouse hematopoietic cells were therefore performed to evaluate whether *in vitro* treatment with PR104A affords species-specific cytotoxicity and to assess how this relates to the expression of AKR1C3, either through its inhibition by naproxen or by anti-AKR1C3 antibody staining and flow cytometry. The clonogenic survival of progenitors derived from hematopoietic cell lines or primary bone marrow showed a much higher sensitivity of human than mouse cells to PR-104A. The human leukemia cell line TF-1 appeared to be more sensitive than primary normal hematopoietic progenitors. The role of AKR1C3 in bioactivation of the drug is implicated by the ability of the AKR1C3 inhibitor naproxen to block PR-104A cytotoxicity and is further supported by expression of AKR1C3 in human bone marrow hematopoietic cells (CD34+). These findings provide an explanation as to why minimal myelosuppression has been seen following treatment of mice with PR104, in contrast to neutropenia observed in patients. The protection afforded by naproxen offers a method for ameliorating the hematological toxicity of PR-104 treatment while maintaining its therapeutic activity against hypoxic cells in tumors.

A

Abdelrazzak, Abdelrazek B. PS5.67
 Abderrahmani, Rym PS4.24
 Abe, Hiroko PS2.51
 Abergel, Rebecca J. PS1.92
 Abulafia, Ovadia PS3.56
 Achanta, Pragathi PS3.40
 Acharya, Munjal M. PS3.54, PS6.20, PS7.75, S303
 Adams, Sylvia MS801, PS7.63
 Adhikary, Amitava PS3.02, S102, S802
 Agarwal, Manuj PS3.56
 Agarwal, Rakhi PS2.72
 Agashe, Hrushikesh PS7.17, PS7.33
 Aguilera, Joseph A. S803
 Ahern, Charlotte H. PS1.87
 Ahmed, Mansoor M. PS5.32, PS7.08, PS7.11, PS7.36
 Ahn, G-one S504
 Ahn, Ji-Yeon PS4.73
 Akahane, Keiichi PS1.33
 Akudugu, John M. PS4.07, PS7.05
 Albanese, Joseph PS1.37
 Albrecht, Huguette PS4.23
 Alfieri, Alan MS702, PS1.51
 Ali, Arif N. PS4.65
 Allen, Bryan PS7.52
 Alloni, Daniele PS5.56
 Almasan, Alex PS2.03
 Almeida, Eduardo PS6.18
 Althouse, Bryan J. PS1.23, PS1.64
 Alwood, Joshua PS6.18
 Amoah-Buahin, Evelyn PS2.04
 Amundson, Sally A. PS2.23, PS3.17, PS3.22, PS3.33, PS5.18, S902
 An, Ningfei MS206, PS2.10, PS3.48
 An, You Sun PS1.47
 Andersen, Barbara PS7.49
 Anderson, Carl A. MS306, PS2.33
 Anderson, Jennifer PS2.50
 Anderson, Mark E. PS7.52
 Anderson, Rhona PS6.48
 Anderson, Robert F. S804
 Anderson, R. R. PS4.44
 Ando, Koichi MS407, PS6.39
 Andorf, Christine PS6.35
 Andreasson, Ulf PS1.80
 Andrews, David W. PS2.12
 Ang, K. K. PS7.25, PS7.55
 Anvari, Akbar PS1.79
 Anver, Miriam PS1.34
 Araki, Shinako PS2.73

Aravindan, Natarajan PS4.16, PS7.17, PS7.24, PS7.33
 Armour, Michael PS7.80
 Arora, Hans PS7.19, PS7.68
 Artemov, Dmitri PS7.80
 Aryankalayil, Molykutty J. MS101, PS7.04, PS7.88
 Asur, Rajalakshmi S. PS5.63
 Athar, Basit S. S704
 Atkinson, Jeffrey PS1.21
 Atkinson, Michael J. PS4.54
 Authier, Simon PS1.69
 Autsavapromporn, Narongchai MS408, PS6.40
 Avdoshina, Valeriya MS501, PS5.14
 Avery, Stephen PS6.06, PS6.19, PS6.41
 Awasthi, Vibhudutta PS7.17, PS7.33
 Aweda, Moses PS2.77
 Ayene, Iramoudi S. PS7.35
 Aygun-Sunar, Semra PS1.44
 Azimzadeh, Omid PS4.54
 Azzam, Edouard I. MS408, PS5.23, PS5.24, PS5.50, PS5.60, PS6.40

B

Baanstra, Mirjam MS205, PS3.31
 Babb, James S. MS801, PS7.63
 Babitch, John PS7.83
 Bacher, Jeff PS5.53
 Bachoo, Robert PS2.56, PS2.73, PS6.46
 Badea, Cristian PS4.56
 Bader, Judith PS1.78
 Bae, Insoo PS2.71
 Bailey, Susan M. PS2.41, S1504
 Baird, Brandon J. MS501, PS5.14
 Baker, John E. PS5.55
 Baker, Kenneth L. PS5.30, PS5.66
 Bakke, James PS6.17
 Balagurunathan, Yoganand PS3.43
 Balajee, Adayabalam PS2.47, PS6.46
 Balm, Alfons PS7.06
 Balmain, Alan P001
 Baluchamy, Sudhakar PS4.67
 Bangia, Naveen PS4.82
 Barber, Therese PS1.12, PS4.46
 Barcellos-Hoff, Mary Helen MS106, PS2.27, PS2.58, PS4.13, PS4.64, PS7.74, S503
 Barjaktarovic, Zarko PS4.54
 Barker, Christopher A. PS3.17, PS3.22
 Bartelds, Beatrijs PS4.02
 Basile, Lena MS707, PS1.20

Bateman, Ted A. MS704, PS1.16
 Batinic-Haberle, Ines PS1.05, PS1.46
 Battaglia, Christine L. R. PS2.41, S1504
 Bauer, Georg PS5.62, PS5.67, S1604
 Baulch, Janet E. PS6.04
 Bayachou, Mekki PS2.03
 Bayeta, Erben J. M. PS1.43, PS2.62
 Beaton, Lindsay A. MS304, PS2.31
 Becker, Kerstin PS7.28
 Beckett, Michael PS4.34
 Bedford, Joel S. PS2.64, PS2.66, PS5.41, PS6.28
 Beecher, Georgia C. PS5.01, PS5.08
 Begg, Adrian C. PS7.06
 Behjat, Joseph S302
 Bejugam, Naveen PS1.35
 Belarbi, Karim PS4.71
 Belikova, Natalia A. PS1.21
 Bellamy, Michael PS3.12
 Bemis, Jeffrey PS4.20
 Benderitter, Marc MS906, PS4.12, PS4.21, PS4.24, PS4.66
 Berbée, Maaïke PS1.45
 Bernhard, William A. MS605, PS3.04, PS3.09, PS3.10
 Bernstein, Jonine S604
 Bertucci, Antonella MS607, PS3.17, PS3.24, PS3.41
 Betof, Allison S. PS4.32
 Bettoga, Daniela PS7.94
 Beucher, Andrea P004
 Bey, Erik A. PS7.79
 Bezak, Eva MS706, PS1.54, PS3.42, PS5.13, PS5.27, PS5.49
 Bhanja, Payel MS702, PS1.22, PS1.51
 Bhatnagar, Sandhya PS4.81, PS6.47
 Bianski, Brandon PS5.25
 Bichsel, Hans S402
 Bielefeldt-Ohmann, Helle PS5.41
 Bielinski, Donna F. PS6.44
 Biggs, Peter PS1.40
 Biju, Prabath G. PS1.13, PS1.31
 Bina, James PS7.90
 Bittner, Michael PS3.43
 Björk- Eriksson, Thomas PS1.80
 Black, Paul J. PS3.09
 Blake, Eileen PS1.37
 Blakely, Eleanor A. PS1.92, S702
 Blakely, William F. MS608, PS3.19, PS3.25, PS3.36, S905
 Blattmann, Hans PS5.48
 Blennow, Kaj PS1.80
 Blickwedeh, Jennifer PS4.82
 Blimkie, Melinda S. J. PS2.35
 Bliorando, Karl PS4.21, PS4.24, PS4.66

Blomgren, Klas PS1.80, PS3.58, PS7.78, PS7.81, PS7.86
 Blyth, Benjamin J. MS706, PS1.54, PS5.13, PS5.27, PS5.49, PS5.62, S1004
 Boerma, Marjan MS901, PS1.13, PS4.36
 Bogdanova, Tetyana S1402
 Bohan, Michael PS1.37
 Boike, Thomas MS802, PS7.09
 Bone, Frederick PS1.72
 Bonner, William M. MS501, MS606, PS2.42, PS3.18, PS3.34, PS3.36, PS5.14, S1503
 Booth, Carmen J. PS1.07
 Boothman, David A. PS2.73, PS7.79
 Borak, Thomas B. MS401, PS5.41, PS6.01
 Boreham, Douglas R. PS2.12, PS2.19, PS2.69, TR005
 Borgerink, Hermina PS4.38
 Borgman, Anthony MS202, PS5.17
 Borgmann, Kerstin PS2.07, PS7.28, PS7.59
 Botchway, Stanley W. PS2.22
 Bouquet, Sophie F. MS106, PS2.58, PS7.74
 Bourdeau-Heller, Jeanne PS5.53
 Bourland, J. D. MS704, PS1.16
 Boutros, Jean PS2.03
 Boyd, Marie PS7.83
 Boyle, John PS7.68
 Braakman, Ineke PS4.40
 Braby, Leslie MS401, PS6.01, TR010
 Brahme, Anders PS6.14
 Brandenburg, Sytze PS4.02
 Bräuer-Krisch, Elke PS5.48
 Brautigan, David L. PS2.29, PS2.53
 Braziewicz, Janusz PS6.43
 Brehwens, Karl PS6.43
 Brengues, Muriel PS3.33, PS3.43
 Brenner, Alina V. S1402
 Brenner, David J. MS607, PS3.17, PS3.20, PS3.22, PS3.24, PS3.26, PS3.41, PS3.44, PS5.06
 Brigantic, Andrea MS507, PS5.64
 Britten, Richard A. PS6.26
 Brogan, John R. MS502, PS2.64, PS5.38
 Brooks, Antone L. PS5.28, S1003
 Brown, Darren S. PS1.65
 Brown, J. Martin MS108, PS2.52, PS7.57, PS7.62, S504
 Brown, Milton PS2.71, PS7.27

Brown, Stephen L. MS705, PS1.38, PS1.49
 Brown, Truman R. PS3.44
 Buard, Valérie MS906, PS4.12, PS4.24
 Buettner, Stefanie PS1.66
 Buglova, Elena PS1.78
 Bujold, Rachel PS4.57
 Buonanno, Manuela PS5.24
 Burd, Randy M. PS4.80
 Burdelya, Lyudmila PS1.44
 Burma, Sandeep MS802, PS2.56, PS6.46, PS7.09
 Burn, Trevor MS304, PS2.31
 Burnett, Alexander F. PS1.13
 Burns, Fredric J. PS5.35
 Burrell, Cheryl PS5.25
 Bussink, Jan PS4.25
 Butterworth, Karl T. MS503, PS5.22, PS7.69
 Bux, Sajit PS6.35

C

Callen, Elsa AL03, PS2.02
 Calzolari, Paola PS7.94
 Camacho, Cristel V. PS2.56, PS6.46
 Cameron, Ryan PS4.28
 Campbell-Beachler, Mary PS6.49
 Camphausen, Kevin PS7.38, PS7.46
 Candas, Demet MS902, PS4.19
 Cao, Ning PS4.72
 Cao, Yiting PS4.37
 Cao, Yongbing PS1.58
 Capitano, Maegan L. PS7.91
 Carlson, David J. S1304
 Carnes, Kevin D. PS3.13
 Caro, Jaime PS4.80
 Carr, Zhanat PS1.78
 Carrihill-Knoll, Kirsty L. PS6.27, PS6.44
 Carson, Craig C. MS808, PS7.51
 Carter, Donna J. PS7.82
 Cary, Lynnette H. PS1.19, PS4.46
 Case, Cullen PS1.04
 Casey, Rachael C. PS1.25, PS1.55
 Cengel, Keith A. PS4.59, PS6.06, PS6.09, PS6.19, PS6.41
 Cerna, David MS101, PS7.04, PS7.82, PS7.88
 Cha, Hyukjin PS2.71
 Chai, Hongbo PS4.39
 Chai, Yunfei PS5.16
 Chalmers, Anthony J. PS2.04
 Chamoto, Kenji PS7.56
 Chang, Jianhui PS1.14, PS1.15, PS1.70
 Chang, Polly Y. PS1.92, PS6.17
 Chang, Sha PS5.42
 Chao, Ming PS7.30

Chao, Nelson MS204, PS1.04, PS3.38, PS4.29
 Chappel, Mark PS7.54
 Chappell, Lori PS6.32
 Charest, Gabriel MS807, PS7.61
 Chaudhry, M. Ahmad PS5.60
 Chaudhuri, Leena MS907, PS4.11
 Chauhan, Vinita MS304, PS2.31
 Cheema, Amrita PS3.18
 Chen, Benjamin AL03, PS2.02, PS2.66
 Chen, Benny J. PS4.29
 Chen, Chen-Yi PS4.64
 Chen, Chun PS1.29, PS4.10, PS4.50, PS7.72, PS7.77
 Chen, Congju PS3.44
 Chen, David AL03, MS302, MS802, PS2.01, PS2.02, PS2.66, PS7.09, S1203, S1902
 Chen, Emily MS702, PS1.51
 Chen, Fang Hsin PS4.15, PS4.41
 Chen, Hua-Tang AL03, PS2.02
 Chen, James PS2.27
 Chen, Junjie PS2.38
 Chen, Ling PS4.72
 Chen, Yi-Wei PS7.26
 Chen, Youhua PS3.41
 Chen, Yuhchayau PS1.60, PS4.20
 Cheney, Alec PS1.72
 Cheng, Simon K. PS1.36
 Cheng, Yung-Chi PS1.07
 Chernikova, Sophia B. PS2.52
 Chiang, Chi Shiun PS4.15
 Chiang, Chi-Shiun PS4.41
 Chida, Koichi PS1.33
 Chin-Sinex, Helen MS202, PS5.17
 Chitneni, Satish K. PS7.23
 Cho-Lim, Jennie PS6.20
 Choi, Bo-hwa PS3.49
 Choi, Namhee PS4.61
 Choi, Seung-Jin MS404, PS6.11
 Choopan, Hosein PS1.81
 Choudhuri, Rajani PS1.74
 Chrisler, William B. PS4.52
 Christie, Lori-Ann PS7.75, S303
 Chute, John MS204, PS1.04, PS3.38
 Cline, Mark PS1.05, PS4.38
 Cloutier, Pierre PS2.54
 Coffey, Mary MS307, PS2.25
 Cohen, Eric P. PS1.64, PS5.58
 Cohen, Lorenzo PS7.45
 Cohen, Melanie V. MS608, PS3.19
 Cole, Michael PS4.60
 Cole, William C. PS1.55
 Coleman, C. Norman MS101, PS1.78, PS7.04, PS7.88

Coleman, Mitchell MS402, MS505, PS5.54, PS6.23
 Coleman, Matt A. MS502, PS2.30, PS5.38
 Collins, Brian T. PS2.71
 Collins, Sean P. PS2.71, PS3.18, PS3.22
 Cologne, John B. S601
 Colwell, Elizabeth A. PS5.36
 Conyers, Jodie PS1.25
 Cook, John A. PS1.34, PS1.74
 Coolbaugh, Thea PS1.52
 Cooper, Priscilla K. PS4.81
 Coppes, Robert P. MS205, PS3.31, PS4.02
 Corbin, Kayla PS4.29
 Cordes, Nils MS803, PS7.14, PS7.28
 Cornelissen, Bart S1704
 Cornforth, Michael N. MS405, PS2.76, PS6.42
 Corry, Peter MS703, MS901, PS1.42, PS4.36, PS5.63, PS7.10, PS7.30
 Cosenza, Stephen C. PS1.73
 Costes, Sylvain V. PS2.27, PS4.64
 Coulter, Jonathan A. PS7.69
 Cox, Brad PS6.38
 Cran, Jordan D. PS2.28
 Crapo, James D. PS1.27
 Cress, Anne E. PS4.28
 Cucinotta, Francis PS2.18, PS2.50, PS2.76, PS4.63, PS6.03, PS6.13, PS6.32, S1303
 Cui, Li PS1.06
 Curran, Walter J. PS7.70
 Currell, Fred PS7.69
 Custis, James T. PS7.92
 Cybulski, Mary-Ellen PS2.19, PS2.69
 Czub, Joanna PS6.43

D

D'Andrea, Alan PS7.95
 Daher, Pamela MS204, PS3.38
 Dahm-Daphi, Jochen PS7.37
 Dai, Wei PS5.35
 Dainiak, Nicholas PS1.37, PS1.78
 Damoiseaux, Robert S1803
 Dan, Cristian PS5.59
 Dasilva, John O. PS7.58
 Datta, Kamal PS4.60, PS5.39
 Davidson, Matthew PS7.15
 Davis, Anthony J. PS2.26, S1902
 Davis, Leslie PS6.26
 Davis, Mary A. MS103, PS7.18
 Davis, Sara PS7.87
 Davis, Thomas A. PS1.63
 de Franciscis, Vittorio PS7.94

de Toledo, Sonia MS408, PS5.23, PS5.24, PS5.50, PS5.60, PS6.40
 Dekmezian, Carmen PS3.29, PS4.18, S302
 Delikatny, E. J. PS7.85
 Della Donna, Lorenza PS3.29, PS4.18, S302
 Delli Carpini, Domenico PS1.37
 Demaria, Sandra MS106, MS801, PS2.58, PS7.63, PS7.74, TR012
 Deng, Zhiyong PS4.55, PS7.01
 Deoliveira, Divino PS4.29
 Derevyanko, Anna S1402
 Dertinger, Stephen PS4.20
 Desmarais, Guillaume PS4.57
 Devantier, Yvonne A. PS3.30
 Dewan, M. Zahidunnabi MS801, PS7.63
 Dewey, Jonathan PS4.77
 Dewhurst, Mark PS1.04, PS4.32, PS4.37, PS4.77, PS5.42, PS7.23, PS7.42, PS7.53
 Dhaemers, Ryan MS202, PS5.17
 Di Giacomo, Fabio PS5.69
 Di Majo, Vincenzo PS5.61
 Dianov, Grigory L. PS2.20, TR004
 Dianova, Irina I. PS2.20
 Diaz, Roberto PS4.65
 Dicker, Adam P. PS7.49
 Dickey, Jennifer S. MS501, PS5.14
 Dickinson, Michael G. PS4.02
 DiDonato, Joseph PS1.44
 Diffenderfer, Eric PS6.06, PS6.19, PS6.41
 Dikomey, Ekkehard PS2.07, PS7.37, PS7.59
 Ding, Lianghao MS403, PS6.10, PS6.46
 Ding, Ning PS2.40
 Ding, Yao PS7.43
 Dingfelder, Michael MS603, PS3.01, PS3.13, PS3.15
 Dixon, Tracy PS1.01, PS1.68, PS1.75
 Dizdaroglu, Miral S101
 diZerga, Gere S. PS1.83
 Djordjevic, Bozidar PS3.56
 Do, To Uyen T. PS2.16, PS5.12
 Do, Trinh T. S803
 Doan, Phuong L. MS204, PS3.38
 Dobbs, Tracey A. PS2.24
 Doctrow, Susan R. PS1.28, PS1.50, PS1.64
 Doemling, Alexander PS1.75
 Doerr, Wolfgang PS1.66
 Dolislager, Fredrick G. PS3.37
 Doñate, Fernando PS7.95
 Dong, Ruhong S903
 Dong, Ying PS7.79
 Dorsey, Jay F. PS7.87

- Dos Santos, Troy PS3.57
 Doty, Caroline B. PS7.71
 Douple, Evan B. S601
 Down, Julian PS1.77,
 PS4.38, PS4.43, PS7.15,
 PS7.95
 Downing, Laura PS1.24
 Doyle-Eisele, Melanie
 PS1.35
 Drake, Richard PS6.26
 Dray, Eloise PS2.06
 Dregalla, Ryan C. PS2.41,
 S1504
 Dritschilo, Anatoly
 PS2.71, PS3.18
 Du, Li-qing PS1.15
 Dubuss, Fiona A. PS4.05
 Duda, Chester MS402,
 PS6.23
 Dugan, Greg PS1.05
 Durante, Marco S701
 Duru, Nadire MS208,
 PS3.47
 Dvir, Ayala PS4.27,
 PS5.40
 Dynan, William S. S1204
 Dynlacht, Joseph R.
 PS7.89
 Dziegielelewski, Jaroslaw
 PS2.29, PS2.53,
 PS7.58
- E**
- E., Shuyu PS4.78
 Eberle, Richard L.
 MS405, PS6.42
 Eckerman, Keith PS3.12
 Edgren, Margareta R.
 PS6.02, PS6.14, PS6.22
 Edmonds, Christine
 PS4.59
 Eguchi-Kasai, Kiyomi
 PS4.06
 Ehrhart, Nicole E. PS7.92
 Eke, Iris MS803, PS7.14,
 PS7.28
 Elena Feinstein, Elena
 PS1.72
 Elfving, Tommy PS6.05
 Ellefson, Dolph D.
 MS707, PS1.20
 Elliott, Thomas B.
 PS1.19, PS3.35, PS7.84
 Elmore, Eugene S1001
 Emmons-Thompson, Karin
 PS4.78
 Eom, Hyeon-Soo PS4.33
 Epperly, Michael PS1.01,
 PS1.21, PS1.68,
 PS1.75
 Erickson, Jeffery PS7.52
 Espinoza, Theresa
 PS1.82, PS1.83
 Essers, Jeroen MS302,
 PS2.01
 Evers, Patrick S302
- F**
- Faber, Hette PS4.02
 Fabian, Christian G.
 PS4.30
 Fabre, Kristin PS1.34,
 PS1.74
 Fallgren, Christina M.
 PS5.41
- Fan, Ming MS208,
 MS902, PS3.47, PS4.19,
 PS4.31
 Fang, Shujuan MS305,
 PS2.17
 Fanta, Mesfin MS104,
 PS7.48
 Farese, Ann MS608,
 PS3.19
 Farfán, Eduardo B.
 PS3.27
 Fath, Melissa A. PS7.52
 Favre, Cecilia J. PS6.49
 Fazzari, Jennifer M.
 PS5.20
 Fedorenko, Zoya S1402
 Fegley, Glenn PS7.20
 Feinstein, Elena PS1.03,
 PS1.12
 Feiveson, Alan PS2.18
 Fells, James PS4.78
 Fels, Diane R. PS7.23,
 PS7.53
 Feng, Jielin MS205,
 PS3.31
 Fenton, Bruce M. PS7.16
 Fernandez, Cristian
 PS5.48
 Ferraris, Ronaldo P.
 PS4.07
 Figueroa, Maria PS1.34
 Fike, John R. PS4.71
 Filkowski, Jody PS4.83
 Fink, Louis PS1.76
 Finkelstein, Jacob N.
 PS1.08, PS1.24, PS1.48,
 PS1.61
 Finkelstein, Jack N.
 PS7.34
 Finney, Lydia PS5.65
 Fish, Brian PS1.02,
 PS1.23, PS1.28, PS1.41,
 PS1.50, PS1.64, PS1.71,
 PS5.55, PS5.58
 Flaherty, Siobhan PS7.82
 Flegal, Farrah PS3.30
 Flood, Ann B. S901
 Flores, Nicholas PS3.43
 Flygare, Jenny PS5.15
 Fontanella, Andrew N.
 PS5.42
 Ford, Eric PS3.40, PS7.80
 Formenti, Silvia MS801,
 PS1.36, PS7.63
 Fornace Jr., Albert J.
 PS2.71, PS3.05, PS3.18,
 PS3.22, PS3.23, PS4.35,
 PS4.60, PS5.39
 Fortin, David MS807,
 PS4.57, PS7.61
 Francis, Cucinotta PS2.67
 François, Agnès MS906,
 PS4.12, PS4.21, PS4.24,
 PS4.66
 Francicola, Darcy PS1.01,
 PS1.75
 Fraser, Cassandra PS5.42
 Freeman, Tanya L.
 PS1.27
 Frenkel, Krystyna PS5.35
 Freschauf, Gary K.
 MS104, PS7.48
 Fresow, Robert PS7.59
 Freund, Gregory PS6.09
 Friedland, Werner
 PS5.37, S401
 Fromm, Michel PS5.23
 Fu, Dadin PS1.26
 Fu, Hanjiang PS2.32
- Fu, Qiang PS1.06,
 PS1.31, PS1.45, PS1.76
 Fu, Sheng Yung PS4.15,
 PS4.41
 Fujii, Yoshihiro PS2.61,
 PS6.15
 Fujimori, Akira MS107,
 PS2.61, PS6.15, PS7.07
 Fujioka, Tsuyoshi MS207,
 PS3.16
 Fukada, Junichi PS2.67
 Fukawa, Takeshi MS407,
 PS6.39
 Fuks, Zvi PS4.42
 Fukumoto, Risaku
 PS1.85, PS7.84
 Fukushima, Masakazu
 PS2.15
 Fung, Luke C. W. PS2.35
 Furusawa, Yoshiya
 MS407, MS504,
 PS5.26, PS6.02, PS6.22,
 PS6.37, PS6.39, PS7.47
- G**
- Gaber, M. Waleed
 PS1.57, PS1.87, PS4.26
 Gabriels, Karen PS7.50
 Gallaher, Tim MS707,
 PS1.20
 Gallant, Noelle PS1.37
 Gambles, Kristen PS1.10
 Gao, Feng PS1.02,
 PS1.50, PS1.71
 Gao, Jinming PS7.79
 Gao, Ying PS1.02
 Garg, Sarita PS1.13,
 PS1.31, PS1.59
 Garimberti, Elisa PS6.48
 Garrison, Bradley R.
 PS7.84
 Garty, Guy MS607,
 PS3.17, PS3.20, PS3.24,
 PS3.41
 Gauny, Stacey PS5.59
 Gaynutdinov, Timur
 S1701
 Geara, Fady PS7.67
 Genik, Paula C. PS5.41
 Gent, Robert N. PS1.78
 Georgakilas, Alexandros G.
 PS2.05
 George, Kerry PS2.67,
 PS6.03, PS6.32
 Gervais, Julie PS1.69
 Gerweck, Leo E. PS1.40
 Gewirtz, Alan PS6.09
 Ghafoori, Paiman PS4.56
 Ghandhi, Shanaz PS2.23,
 PS5.18, S1801
 Ghobadi, Ghazaleh
 PS4.02
 Ghosh, Sanchita PS1.10,
 PS1.17, PS4.76
 Ghosh, Swarajit N.
 PS1.02, PS1.50, PS1.71
 Giaccia, Amato J. S204
 Giebeler, Annelise
 PS7.67
 Giedzinski, Erich PS3.54,
 PS6.20
 Gilbert, Ethel S. S1403
 Girard, Peter TR011
 Gius, David MS505,
 PS5.54, S202
 Gladden, John B. PS3.27
- Gladden, Samantha
 PS6.35
 Gleiberman, Anatoli
 PS1.03
 Glickson, Jerry D. PS7.85
 Globus, Ruth PS6.18
 Goetz, Eva M. PS2.73
 Goetz, Wilfried PS6.04
 Golding, Sarah E. PS2.11
 Golightly, Marc MS306,
 PS2.33
 Götzhäuser, Armin
 PS3.06
 Gonon, Geraldine PS5.23
 Gonzalez, Frank J.
 PS3.05, PS3.22
 Goodarzi, Aaron P004
 Goodhead, Dudley
 PS3.12
 Gopalakrishnan, Kalpana
 PS7.76
 Gorbunov, Nikolai V.
 PS3.35
 Gordana Vlahovic, Gordana
 PS4.37
 Gordon, Ira PS7.46
 Gorin, Claude PS1.78
 Gorokh, Evgeniy S1402
 Goswami, Prabhat
 MS907, PS4.11, PS7.66
 Govindarajan, Ramesh
 PS4.51
 Grant, Eric J. PS5.05
 Grapov, Dmitry PS4.23
 Graves III, John MS708,
 PS1.11
 Gray, Joe W. PS4.81
 Grdina, David J. MS706,
 PS1.54, PS5.30, PS5.66
 Green, Keigm PS5.25
 Green, Lora PS4.14,
 PS5.25
 Green-Mitchell, Shamina
 PS6.26
 Greenberg, Marc M.
 S104
 Greenberger, Joel
 PS1.01, PS1.21, PS1.68,
 PS1.75
 Greene-Schloesser, Dana
 M. PS7.02
 Grénman, Reidar A.
 PS7.06
 Gridley, Daila S. PS1.27,
 PS1.43, PS2.62, PS4.51,
 PS4.67, PS4.68, PS5.21,
 PS6.24, PS6.31, PS6.36,
 S1103
 Griffin, Robert J. PS5.63
 Grinberg, Oleg S903
 Grindrod, Scott PS7.27
 Groesser, Torsten
 PS5.15
 Grosovsky, Andrew
 PS5.25
 Grossi, Gianfranco
 PS7.94
 Groysman, Anna PS3.56
 Gruenloh, Stephanie
 PS1.02
 Grugan, Katharine D.
 PS4.63
 Grygoryev, Dmytro
 PS2.34
 Gudkov, Andrei PS1.03,
 PS1.44
 Gududuru, Veeresa
 PS1.91

Guha, Chandan MS702,
PS1.51
Guilmette, Raymond A.
PS1.35
Guo, Yansong PS1.29,
PS2.37, PS4.10, PS4.49,
PS4.50, PS4.70, PS7.72,
PS7.77, S904
Gupta, Arun PS2.21
Gupta, Prem K. PS1.13
Gupta, Seema PS5.32,
PS7.11, PS7.36
Gurijala, Jeevan PS4.27,
PS4.62
Gurung, Resham L.
PS7.76

H

Ha, Cam T. PS1.26
Ha, Jonathan MS905,
PS4.03
Ha, Kyungsoo S1204
Haase, Gerald M. PS1.55
Hada, Megumi PS2.18,
PS6.03
Haderski, Gary PS1.44
Hadjipanayis, Constantinos
G. PS3.32
Hadley, Caroline C.
PS4.32
Hagan, Sarah PS4.59
Hageman, Floor PS7.06
Haghdooost, Siamak
PS4.54, PS6.43
Haimovitz-Friedman,
Adriana PS4.42
Hair, Jessica M. PS2.05
Halberg, Richard PS5.53
Haley, Benjamin PS5.65,
PS5.70
Hall, Dennis G. MS104,
PS7.48
Hall, Joseph C. PS4.67
Hallac, Rami PS7.43
Hallahan, Dennis MS804,
PS1.67, PS7.03, PS7.32,
TR008
Hamada, Nobuyuki
PS5.16
Hamilton, Stanley PS4.51
Hammond, Ester M.
MS908, PS4.17, S502
Hande, Prakash PS7.76
Hang, Haiying PS2.47,
PS2.75
Hanna, Gabi PS4.37
Hanscom, Heather
PS2.71, PS3.18
Hao, Chunhai PS7.70
Harbo, Sam PS1.86
Hareyama, Masato
PS2.15
Harmon, Joseph F.
PS7.92
Harms-Ringdahl, Mats
PS4.54
Harper, Jane V. PS2.22
Harris, Andrew L.
MS408, PS6.40
Harrison, London MS708,
PS1.11
Hart, Lori S. MS805,
PS4.45, PS7.29
Hasegawa, Azusa S705
Haston, Christina PS1.61
Hatashita, Masanori
PS2.57, S1603

Hatch, Maureen S1402
Hatzi, Vasiliki I. PS2.05
Hauer-Jensen, Martin
MS901, PS1.06, PS1.13,
PS1.17, PS1.31, PS1.45,
PS1.59, PS1.62, PS1.76,
PS1.78, PS4.36, PS4.76
Hayakawa, Mikito PS1.33
Hayashi, Mikiko PS5.07
Hayashi, Naoki MS207,
PS3.16
Hayashi, Tomonori S601
He, Fuqui PS4.75
He, Hui PS1.91
He, Shaoqin PS7.13
He, Wei PS2.75
He, Xiaoming S904
Head, Jennifer L. PS1.08
Heckler, Charles E.
PS7.44
Heeneman, Sylvia
PS7.50
Hehlgans, Stephanie
MS803, PS7.14
Hei, Tom K. PS5.16,
PS5.18, PS5.71, S1602
Heilbronn, Lawrence
MS401, PS6.01
Hein, Amy M. PS7.34
Held, Kathryn D. PS1.40,
PS5.33, S1601
Helleday, Thomas
MS301, PS2.43, PS2.49
Hendrickson, Eric A.
S1501
Hennings, Leah MS703,
PS1.42
Herbert, Joseph PS4.37
Herman, Joseph PS7.80
Herman, Michael G.
PS6.07
Herman, Terence S.
PS4.16, PS7.17, PS7.24,
PS7.33
Hermansson, Martina
PS3.58, PS7.86
Hernady, Eric PS1.48,
PS1.61, PS4.05
Hieber, Kevin PS1.10,
PS1.17
Higgins, Susan A. PS1.07
Hill, Colin K. PS1.82,
PS1.83
Hill, Mark A. PS2.22,
PS5.67, PS6.48
Hill, Richard P. PS1.61,
PS1.84, S1101
Himborg, Heather A.
MS204, PS3.38
Hinton, Thomas PS2.34
Hinz, John M. MS502,
PS5.38
Hirayama, Ryoichi
MS407, PS6.02, PS6.22,
PS6.37, PS6.39
Hirst, David PS7.69
Hneino, Mohammad
MS906, PS4.12, PS4.24
Hollander, Andrew
PS7.87
Hollywood, Donal
MS307, PS2.25, PS4.53
Hong, Hyun Sook PS1.47
Hong, Ji Hong PS4.15,
PS4.41
Honikel, Louise MS306,
PS2.33
Hopewell, John PS5.55
Hopkins, Kevin PS2.47

Horton, Janet K. PS7.53
Hosing, Amol PS2.29,
PS2.53, PS7.58
Hosmane, Narayan
PS6.35
Hosokawa, Yoichiro
PS4.39
Hounsell, Alan MS503,
PS5.22, PS7.69
Hoving, Saske PS7.50
Howe, Geoffrey R.
PS5.04
Howell, Rebecca M.
PS7.67
Howell, Roger W.
PS4.07, PS7.05
Howland, Matthew
MS304, PS2.31
Hsieh, Jer-Tsong MS802,
PS7.09, PS7.79
Hsu, Wan L. PS5.07
Huang, Zhenhai PS1.21
Huber, Peter E. MS105,
PS7.40
Huff, Janice L. PS4.63
Humar, K. Sree PS1.06
Humm, John L. PS7.22
Hunter, Jeffrey MS708,
PS1.11
Hurley, Sean D. PS4.05,
PS4.69
Huynh, HoangDinh AL03,
PS2.02
Hyde, James S903
Hyland, Wendy PS7.69
Hyrien, Ollivier PS4.20

I

Ianzini, Fiorenza PS5.36
Idate, Rupa R. PS2.41,
S1504
Igarashi, Jun PS4.39
Iijima, Kenta PS2.51
Ikura, Tsuyoshi S1904
Iliakis, George PS3.11
Imai, Kazue S601
Imaizumi, Misa S1401
Improta, Ilaria PS7.94
Ishikawa, Hitoshi PS5.40
Isom, Scott PS5.09
Itami, Atsushi PS6.37
Ito, Hisao PS2.67
Ivanov, Vladimir PS5.18,
S1602
Ivashkevich, Alesia
MS606, PS3.34
Iwamoto, Keisuke S.
S1102
Iwata, Yoshi MS401,
PS6.01
Izadi, Atefeh PS3.54

J

Jaboin, Jerry J. MS804,
PS7.03
Jackson, Isabel L.
MS904, PS4.04, PS4.32,
PS4.38, PS4.43
Jacob, Peter S401
Jacobs, Elizabeth R.
PS1.02, PS1.28, PS1.71
Jacobus, James MS402,
MS505, PS5.54, PS6.23
Jadhev, Sachin PS1.82
Jafari, Hamid PS1.81
Jain, Suneil PS7.69

Jakob, Burkhard S701
James, Anthony C.
PS5.02
Jang, Beom-Su PS4.33
Jannik, Timothy G.
PS3.27
Janssen, Ben PS7.50
Jaruga, Pawel PS2.74
Jay-Gerin, Jean-Paul
MS408, PS6.16, PS6.40,
S1302
Jayanthi Lea, Robert D.
Sims PS7.43
Jean, Juan MS108
Jeffords, Laura B.
MS201, PS4.79, PS5.19
Jeggio, Penny P004,
PS6.15
Jejelowo, Olufisayo
PS2.48, PS4.51, PS4.67
Jelveh, Salomeh PS1.84
Jenkins, Timothy PS4.45,
PS7.85
Jenrette, Joseph M.
PS7.12
Jenrow, Kenneth A.
MS705, PS1.38, PS1.49
Jeon, Sang-Rok PS3.21
Jia, Dan MS703, PS1.42,
PS7.10
Jiang, Jianfei PS1.21
Jiao, Wan PS1.19,
PS3.35
Jiao, Yiqun PS4.29
Jie, Shy'Ann PS3.56
Jin, Cuihong PS4.31
Jin, Xiaodong PS6.29
Jin, Yeung Bae PS1.30
Jin, Yong-Woo PS2.60
Jin, Young-Woo MS404,
PS6.11
Jo, Sung-Kee PS4.33,
PS4.61
Joe, Minho PS2.59
Johnson, Angela PS6.26
Johnson, Krista MS708,
PS1.11
Johnston, Carl J. PS1.08,
PS1.48, PS1.61, PS7.34
Johnston, Samuel
PS4.56
Jones, Jeffrey A. PS1.55,
PS1.68
Jones, Tamako PS5.52
Jorjishvili, Irakli G. PS3.15
Joseph, James A.
PS6.27, PS6.44
Joyce, Craig C. PS7.83
Ju, Shaoqing PS2.37
Jung, Mira MS102,
PS7.27, PS7.39
Jung, Uhee PS4.33,
PS4.61

K

Kaanders, Johannes H.
PS4.25
Kabarriti, Rafi MS702,
PS1.51
Kabbani, Wareef PS7.79
Kachikwu, Evelyn L.
S1102
Kadhim, Munira A.
MS506, PS5.25, PS5.47
Kagan, Valerian E.
PS1.21, S1802

- Kakinuma, Shizuko PS5.16
 Kalen, Amanda L. MS907, PS4.11, PS7.66
 Kalinich, John F. PS3.05, PS3.23
 Kallakury, Bhaskar PS4.60, PS5.39
 Kalm, Marie PS1.80, PS7.78
 Kaluzova, Milota PS3.32
 Kamdar, Radhika P. PS2.79
 Kanaar, Roland MS302, PS2.01
 Kaneko, Yumiko MS504, PS5.26
 Kaneyuki, Yukiko PS3.46
 Kang, Anthony D. PS1.73
 Kang, Mi-Hyun PS1.47
 Kang, Yu-Mi MS404, PS6.11
 Kao, Gary PS7.87
 Kapralov, Alexandr PS1.21
 Karimpil, Jacob PS4.62
 Karlsson, Niklas PS7.78
 Karrar, Jayashree PS4.45
 Kasagi, Fumiyoshi PS5.05, S1401
 Kaschina, Elena MS901, PS4.36
 Kashino, Genro MS903, PS4.58, PS5.44, PS7.26
 Kashiwakura, Ikuo MS207, PS3.16, PS3.46, PS3.50, PS4.06, PS4.08, PS4.39
 Kasten-Pisula, Ulla PS7.37
 Kato, Kengo PS3.50
 Kato, Takamitsu A. PS2.61, PS6.15
 Katsumura, Yosuke PS6.16, S1302
 Kawata, Tetsuya PS2.67
 Kennedy, Ann R. MS406, PS2.62, PS5.21, PS6.06, PS6.09, PS6.19, PS6.25, PS6.30, PS6.34, PS6.36, PS6.41, PS6.45
 Kennedy, Kelly M. PS4.77
 Kennedy, Scott D. PS7.16
 Khanduri, Deepti PS3.02, S802
 Khater, Nabil PS7.67
 Khoronenkova, Svetlana V. PS2.20
 Kiang, Juliann G. PS1.19, PS1.85, PS3.35, PS7.84
 Kil, Whoon Jong PS7.38
 Kim, Cha-Soon MS404, PS2.60, PS6.11
 Kim, Dongho PS2.59
 Kim, Hee-sun MS404, PS6.11
 Kim, Jae Ho MS705, PS1.38, PS1.49
 Kim, Ji-Young MS404, PS2.60, PS6.11
 Kim, Jong-Jin PS4.33
 Kim, Kwanghee S1803
 Kim, Mi-Ra PS1.47
 Kim, Mi-Hyoung PS4.73
 Kim, Seol Hwa PS4.33
 Kim, Sung-Ho PS4.33, PS4.61
 Kim, Seikou PS6.37
 Kim, Sungheon PS7.85
 Kim, Tae-Hee PS1.30
 Kim, Woo-Chul PS6.14
 Kim, Yongbaek MS201, PS5.19
 Kinashi, Yuko MS903, PS4.58, PS7.21, PS7.26
 King, Gregory PS6.09
 Kingham, Guy L. PS2.13
 Kingsley, Paul D. PS4.20
 Kioi, Mitomu MS108, PS7.57, PS7.62, S504
 Kirihata, Mitsunori PS7.26
 Kirkpatrick, John P. PS7.53
 Kirsch, David G. AL02, MS201, MS204, PS3.38, PS4.56, PS4.79, PS5.19
 Kiss, Gyongyi N. PS4.78
 Kitamura, Hidemitsu PS7.56
 Klein-Seetharaman, Judith PS1.21
 Klovov, Dmitry K. PS2.35
 Kma, Lakhan PS1.02, PS1.50, PS1.71
 Knudson, Michael MS402, PS6.23
 Kobayashi, Junya PS2.51
 Kobayashi, Katsumi PS5.46
 Koch, Cameron PS4.45, PS7.85
 Koch, Moritz MS105, PS7.40
 Kock, Nancy PS5.09
 Kodama, Yoshiaki S1404
 Kodibagkar, Vikram D. PS7.43
 Koguchi, Yasuhiro PS1.33
 Kohlgruber, Ayano C. MS502, PS5.38
 Koike, Sachiko MS407, PS6.39
 Kojouharov, Bojidar PS1.44
 Kolesnick, Richard PS4.42
 Kolozsvary, Andrew MS705, PS1.38, PS1.49
 Komatsu, Kenshi PS2.51
 Kondratyev, Alexei MS501, PS5.14
 Kong, Zhaolu MS802, PS7.09
 Konishi, Teruaki MS504, PS5.26
 Koniski, Anne PS4.20
 Kononov, Eugene PS1.72
 Konsoula, Zacharoula MS102, PS7.39
 Koong, Albert MS805, PS7.29
 Kooshki, Mitra PS7.02, PS7.60
 Koritzinsky, Marianne PS4.40, TR003
 Korn, Ronald PS3.43
 Kornblum, Harley PS3.53
 Koshurnikova, Nina A. S1403
 Kosmacek, Elizabeth A. PS5.36
 Kotb, Rami PS7.31
 Koumenis, Constantinos MS805, PS4.45, PS7.29, S1804
 Kovalchuk, Igor PS5.31
 Kovalchuk, Olga PS4.83, PS5.68
 Krasnov, Peter PS1.72
 Krause, Mechthild PS7.28
 Krausz, Kristopher W. PS3.05, PS3.22
 Kreger, Bridget PS5.60
 Kriegs, Malte PS7.37
 Kriehuber, Ralf S1702
 Krigsfeld, Gabriel PS6.25, PS6.30, PS6.41
 Krishna, Murali C. PS1.34
 Krivokrysenko, Vadim PS1.03
 Kroc, Thomas PS6.35
 Kronenberg, Amy PS5.59
 Kruse, Jon J. PS6.07
 Kugoh, Hiroyuki PS5.44
 Kuhne, Wendy PS3.27, TR015
 Kulkarni, Ashwini PS1.62
 Kulkarni, Shilpa PS1.10, PS1.17, PS4.76
 Kumagai, Jun PS5.44
 Kumar, Anil PS3.02, S802
 Kumar, K. Sree PS1.10, PS1.17, PS1.45, PS4.76
 Kumar, Maneesh G. MS907, PS4.11
 Kumar, Rakesh PS2.21
 Kumar, Ramesh MS701, PS1.56
 Kümmerle, Eberhard S1702
 Kundrát, Pavel PS5.37, S401
 Kunos, Charles PS7.41
 Kuo, Alex PS2.06, PS5.15
 Kusunoki, Yoichiro S601
 Kuwabara, Mikinori PS3.50
 Kwasny, Mary PS5.70
 Kwoh, Ely PS5.59
 Kyoizumi, Seishi S601
- L**
- Laframboise, Lisa PS2.19, PS2.69
 Lagadec, Chann PS3.29, PS4.18, S302
 Lahaye, Jean-Baptiste PS5.69
 Lai, Yun-Ju PS4.78
 Laiakis, Evagelia C. PS3.05, PS3.22, PS3.23
 Laissue, Jean PS5.48
 Lan, Mary L. PS6.20, PS7.75, S303
 Landauer, Michael R. PS1.63
 Lang, Hainan PS7.12
 Lange, Christopher S. PS3.56
 Langendijk, Johannes A. PS4.02
 Lapanowski, Karen MS705, PS1.38
 Larnar, James M. PS2.29, PS2.53, PS7.58
 Lartey, Frederick MS108, PS7.62
 LaRue, Susan M. PS7.92
 Latif, Nabil H. PS1.26
 Latusek, Robert PS2.43
 Laurent, David PS5.69
 LaVerne, Jay A. S1301
 Lawler, Mark MS307, PS2.25, PS4.53
 Lawrence, B. Paige PS1.08
 Lawrence, Mark D. MS706, PS1.54, PS5.49
 Lawrence, Richard Y. PS7.49
 Lawrence, Theodore S. MS103, PS7.18
 Lazar, J. PS1.23
 Lazarova, Zelmira PS1.23
 Leahy, Kathleen PS7.32
 Leblanc, Pierre PS1.40
 Ledney, G. D. PS1.19, PS3.35, PS7.84
 Lee, Byong Won PS1.30
 Lee, Chang-Lung MS201, PS4.56, PS5.19
 Lee, Chung K. PS3.57
 Lee, EunAh PS1.47
 Lee, Hae-June PS3.21
 Lee, Hyemi PS3.49
 Lee, Hyunmi PS4.42
 Lee, Jane MS605, PS3.04
 Lee, Phoebe S. W. PS7.76
 Lee, Saeloom PS4.73
 Lee, Seung-Cheol PS7.85
 Lee, Yong-J. PS4.47
 Lee, Yun-Sil PS1.30, PS3.21
 Leeper, Dennis B. PS4.80
 Lees-Miller, Susan P. MS305, PS2.17, PS2.24, S1202
 Lehockey, Katie A. PS2.05
 Leisemann Immel, Rachel PS5.53
 Leloup, Corinne PS2.47
 Lenarczyk, Marek PS5.58
 Leonard, Bobby E. PS5.01, PS5.08
 Leonardi, Simona PS5.61
 Leonhardt, Franziska MS803, PS7.14
 Lesniewski, Piotr S903
 Leung, Eastwood X. PS4.26
 Levitt, Seymour H. PS3.57
 Lewis, Adam J. PS4.52
 Li, Deguan PS1.14, PS1.70
 Li, Gloria C. PS4.75
 Li, HengHong PS2.71, PS4.35
 Li, Hongliang PS1.46
 Li, Hongyun PS7.82
 Li, Jian Jian MS208, MS902, PS3.47, PS4.19, PS4.31
 Li, Jie PS7.35
 Li, Lei PS2.45
 Li, Long-Shan PS7.79
 Li, Min PS5.50
 Li, Qiang PS6.29
 Li, Shuyi S1204
 Li, Xiang Hong PS1.26
 Li, Xiao-Feng PS7.22
 Li, Yifan PS4.56
 Li, Zejun MS602, PS2.54, PS3.14

Liamsuwan, Thiansin
MS601, PS3.03, TR011
Liao, Yu-Pei S1102
Liao, Zhongxing PS7.45
Liber, Howard L. PS2.41,
S1504
Lieberman, Howard
PS2.47
Lien, Katie PS5.57
Lillis-Hearne, Patricia
PS1.78
Lim, Min-Jin PS4.73
Lim, Sangyong PS2.59
Lim, Shi N. PS7.76
Lim, Young-Bin PS3.21
Limoli, Charles L. PS3.54,
PS6.18, PS6.20, PS7.75,
S303
Lin, Fang-Tsyr PS4.78
Lin, Mingzhang PS6.16,
S1302
Lin, Yu-Fen AL03,
PS2.02, PS2.66
Lin, Zi-Wei S403
Lind, Bengt K. PS6.05
Lindquist, Kirstin E.
PS2.28
Lines, Lynette PS1.37
Ling, C. Clifton PS4.75,
PS7.22
Linkous, Amanda PS7.32
Lita, Elena PS7.38
Little, John B. MS408,
PS2.64, PS2.66, PS6.40
Litvinchuk, Alexandra
PS1.29, PS4.10, PS4.48,
PS4.49, PS4.70, PS7.77
Liu, Chia-Chi PS4.41
Liu, Chaomei PS7.72
Liu, Cui H. MS504,
PS5.26
Liu, Cuihua PS2.67
Liu, David PS3.43
Liu, Jianxiong PS4.78
Liu, Laibin MS702,
PS1.51
Liu, Rui PS4.31
Liu, Shie-Chau MS108,
PS7.62
Liu, Sicheng PS2.79
Liu, Yanfeng PS1.07
Liu, Yi PS7.49
Liu, Yong MS903,
PS4.58, PS7.21, PS7.26
Liu, Yuan PS2.72
Lobachevsky, Pavel N.
MS606, PS3.34, S1703
Lobrich, Markus P004
Lombardini, Eric MS708,
PS1.11, PS1.52
Lonart, Gyorgy PS6.26
Long, Lauren V. PS6.27
Lopez, A. PS1.23
Lopez, Bernard S. PS5.69
Lopez, Ramon MS105,
PS7.40
Lopez-Barcons, Lluís A.
PS4.65
Loucas, Bradford D.
MS405, PS2.76, PS6.42
Louie, Stan L. PS1.82,
PS1.83
Lovaglio, Jamie PS1.86
Low, Esther S. H. PS7.76
Lowe, Scott W. MS201,
PS5.19
Lowe, Xiu PS6.47
Lowery, Lynette J.
PS1.63

Lu, Lu PS1.14, PS1.15,
PS1.70
Lu, Ping PS5.71
Ludwig, Thomas PS2.21
Lumpkins, Sarah PS5.33
Luo, Xiuquan PS2.73
Luo-Owen, Xian PS1.27,
PS6.31, S1103
Lupi, Mario PS7.94
Lusby, Terry MS401,
PS6.01
Luskin, Katharine PS6.27
Lynch, Thomas MS307,
PS2.25, PS4.53
Lyulko, Oleksandra V.
MS607, PS3.20, PS3.24,
PS3.41

M

Ma, Jun PS1.29, PS4.10,
PS4.50
Ma, Xiaoyan PS2.75
Ma, Yan PS4.79
Ma, Yuanyuan PS7.22
Mabery, Shalini PS2.30
Mabuchi, Kiyohiko S1402
Mabuchi, Yo PS2.40
Mace, Thomas PS7.91
Mackey, Michael A.
PS5.36
MacLawhorn, Robert
PS3.13
MacLawhorn, Steven
PS3.13
MacVittie, Thomas J.
MS608, PS3.19
Mader, Marylou PS1.23,
PS1.41, PS1.64
Madhusoodhanan, Rakesh
PS4.16, PS7.17, PS7.24,
PS7.33
Maeda, Munetoshi
PS5.46
Maezawa, Hiroshi
PS5.46, PS6.37
Magpayo, Nicole PS5.33,
S1601
Mahajan, Anita PS7.67
Mahaney, Brandi L.
MS305, PS2.17
Mahmood, Javed PS1.84
Mairs, Rob PS7.83
Maity, Amit PS4.45
Mak, Tytus D. PS3.05,
PS3.23
Makinde, Adeola Y.
MS101, PS7.04, PS7.88,
S1103
Maks, Casey PS6.06,
PS6.36, PS6.41
Maksaereekul, Saipiroon
PS5.45
Mancuso, Mariateresa
PS5.61
Mani, Rajam S. MS104,
PS7.48
Maniar, Manoj PS1.10,
PS7.20, PS7.64
Manning, Casey M.
PS1.08
Mannino, Mariella PS2.04
Manstein, Dieter PS4.44
Mantha, Rebecca R.
PS2.35
Manti, Lorenzo PS7.94
Mao, Hui PS7.70
Mao, Jian-Hua PS4.13,
PS4.81

Mao, Xiao Wen PS5.21,
S1103
Mapuskar, Kranti MS402,
PS6.23
Marchetti, Francesco
PS4.81, PS6.47
Marignol, Laure MS307,
PS2.25, PS4.53
Marino, Stephen A.
PS3.26
Mariotti, Luca G. PS2.55,
PS5.56
Marotta, Diane PS4.45
Maroz, Andrej S804
Marples, Brian MS307,
PS1.24, PS2.25
Marsala, Martin S304
Martelly, Isabelle PS4.21,
PS4.66
Martin, Lynn M. MS307,
PS2.25, PS4.53
Martin, Roger MS606,
PS3.34, S804, S1703
Martin, Sean MS402,
PS6.23
Maruhashi, Akira MS903,
PS4.58, PS7.21
Mason, K. PS7.25
Mason, Nigel J. MS602,
PS3.06, PS3.14
Mason, Ralph P. PS7.43
Massa, Rita PS7.94
Masunaga, Shin-ichiro
MS903, PS4.58, PS7.21,
PS7.26
Mathias, Askale PS1.74
Mathieu, David MS807,
PS4.57, PS7.61
Matsumaru, Yuji PS1.33
Matsumoto, Fumihiko
PS7.25, PS7.55
Matsumoto, Hideki
S1603
Matsumoto, Yoshihisa
PS2.15, PS2.36, PS2.79,
S1201
Matsumoto, Yoshitaka
MS407, PS6.02, PS6.22,
PS6.39, PS7.47
Matsuura, Taeko PS7.47
Matsuzaki, Yumi PS2.40
Mauceri, Helena PS4.34
Mayo, Lindsey PS2.73
Mazumder, Suparna
PS2.03
McBride, William H.
S1102, S1803
McCarthy, Phillip PS7.91
McDonough, James
PS6.06, PS6.09, PS6.19,
PS6.41
McEllin, Brian PS2.56,
PS6.46
McFarlane, Nicole
PS2.19, PS2.69
McGarry, Conor K.
MS503, PS5.22
McGrath, Kathleen E.
PS4.20
McGurk, Ross PS1.32
McLane, Amanda PS3.17
McMahon, Stephen
PS7.69
McNamee, James P.
MS304, PS2.31, PS3.39
McVean, Andrew PS6.48
Meador, Jarah PS2.23
Meadows, Sarah K.
MS204, PS3.38

Medhora, Meetha
PS1.02, PS1.28, PS1.41,
PS1.50, PS1.64, PS1.71
Meek, Patrick PS5.51
Meeks, Christopher
PS1.82, PS1.83
Meesungnoen, Jintana
PS6.16, S1302
Meijer, Annelie E.
PS6.02, PS6.14, PS6.22
Meineke, Viktor PS1.78
Mekonnen, Tsehay
PS5.21
Mendonca, Marc S.
MS202, PS5.17
Mendoza, Erin E. PS4.80
Meng, Aimin PS1.14,
PS1.15, PS1.46, PS1.70
Meng, Tze-Chiang
MS801, PS7.63
Meng, Yuru PS4.34
Menzel, Hans TR010
Merchant, Milton
MS108, PS7.62
Merchant, Thomas E.
PS4.26
Mereniuk, Todd R.
MS104, PS7.48
Mesicek, Judith PS4.42
Meushaw, Tamalee
PS7.46
Mick, Rosemarie PS6.09
Milas, L. PS7.25
Milas, Luka PS7.45,
PS7.55
Millage, Kyle PS4.09
Miller, Alexandra PS1.53,
PS6.09
Miller, Duane D. PS1.57,
PS1.91
Miller, Jen-nie PS1.61
Miller, John H. MS203,
PS5.11, PS5.43, PS5.57
Miller, Joseph MS707,
PS1.20
Miller, Mark PS5.09
Miller, Marshall G.
PS6.44
Miller, Richard C. PS5.30,
PS5.66
Milliat, Fabien MS906,
PS4.12, PS4.21, PS4.24,
PS4.66
Milligan, Jamie R.
MS605, PS3.04, S803
Mills, Caitlin E. PS2.12
Minami, Akiko PS4.75
Minamoto, Atsushi
MS508, PS5.10
Minchinton, Andrew I.
PS2.28
Ming, Lihua PS5.18
Mino, Akihisa PS4.42
Mirkovic, Dragan PS7.67
Mirzayans, Razmik
PS4.22
Mitchel, Ron E. S1002
Mitchell, Jennifer PS1.52
Mitchell, James B. AL01,
PS1.34, PS1.74, S202
Mittal, Amit PS5.65
Miyagawa, Kiyoshi
PS2.61
Miyamoto, Yuka PS1.33
Mizoe, Jun-etsu S705
Mizuno, Yusuke PS1.33
Mo, Yin-Yuan PS1.18
Moccia, Krinon PS1.52

Mohanty, Chitralkha PS6.02, PS6.22
 Molkentine, David PS7.45, PS7.55
 Molthen, Robert C. PS1.28, PS1.50
 Montesinos, Carlos PS1.68
 Monzen, Satoru MS207, PS3.16, PS4.06
 Moon, Bo-Hyun PS5.39
 Moore, Elizabeth D. PS7.54
 Moore, Joseph PS5.09
 Morales, Julio PS2.73
 Moravan, Michael J. PS4.05
 Morgan, Michelle N. M. PS6.04
 Morgan, William F. MS507, PS5.02, PS5.03, PS5.43, PS5.57, PS5.64
 Moritake, Takashi PS1.33
 Moroni, Maria PS1.52
 Moros, Eduardo G. MS901, PS4.36, PS5.63, PS7.30
 Morotomi-Yano, Keiko S1203
 Morrow, Gary R. PS7.44
 Moskalenko, Oleksandr PS2.34
 Mothersill, Carmel PS5.20, PS5.48
 Mottin Rosa, Paulo Richards PS7.01
 Moulder, John E. PS1.02, PS1.23, PS1.28, PS1.41, PS1.50, PS1.64, PS1.71, PS5.55, PS5.58
 Mueller-Klieser, Wolfgang PS4.30, PS6.08
 Muir, Mark PS7.69
 Mukherjee, Bipasha PS2.56, PS6.46
 Mullaney, Conor MS708, PS1.11
 Munafa, Shawn A. PS3.02
 Munger, John PS1.36
 Munley, Michael PS5.09
 Muradian, Sarah PS3.53
 Murakami, Takeshi MS401, PS6.01, PS6.16, S1302
 Murley, Jeffrey S. PS5.30, PS5.66
 Murnane, John P. S301
 Muroya, Yusa PS6.16, S1302
 Murphy, Mark K. PS1.86, PS1.89, PS1.90
 Murray, David PS4.22
 Mutyam, Shravan PS1.35

N

Nagasawa, Hatsumi MS502, PS2.64, PS2.66, PS5.38, PS6.28
 Nagasawa, Hideko MS903, PS4.58
 Nagata, Kenji PS7.26
 Nagle, Raymond B. PS4.28
 Nagpal, Nikita PS7.11
 Nagy, Vitaly PS1.52

Naidu, Mamta D. PS2.72
 Nakachi, Kei S601
 Nakamura, Asako J. PS2.42, PS3.18, PS3.36, S1503
 Nakamura, Nori S1404
 Nakamura, Yukio MS207, PS3.16
 Nakano, Mimako S1404
 Nakashima, Eiji MS508, PS5.10
 Nam, Seon Young MS404, PS2.60, PS6.11
 Nan, Ding PS2.77
 Nandakumar, Swapna PS7.76
 Nanduri, Lalitha S. Y. MS205, PS3.31
 Nantajit, Danupon PS4.31
 Napoli, Eleonora PS5.36
 Narayan, Pratyush PS3.17
 Narayanan, Jayashree PS1.02, PS1.71
 Natarajan, Mohan PS4.16, PS7.17, PS7.24, PS7.33
 Navo, Elliot PS3.56
 Naylor, Andrew S. PS3.58, PS7.86
 Ndllebe, Thabisile MS604, PS3.08
 Nelson, Gregory A. PS4.14, PS5.34, PS5.52, PS6.49
 Nemeth, Michael PS7.91
 Neriishi, Kazuo MS508, PS5.10
 Neti, Prasad V. S. V. PS7.05
 Neumaier, Teresa PS2.27
 Neumann, Ronald D. MS604, PS2.65, PS3.08, PS3.51, PS3.52, S1701
 Newhauser, Wayne D. PS5.51, PS7.67
 Newman, John W. PS4.23
 Newman, Michelle R. PS5.13
 Ng, Wooi Loon PS1.18, PS7.70
 Ngudiankama, Barbara F. PS1.19, PS4.46
 Nguyen, David H. PS4.13
 Nguyen, Rochelle B. L. PS2.52
 Nicolalde, Roberto J. S903
 Nien, Yu-Chih Charleen PS7.42
 Nievaart, Victor A. PS6.43
 Nikjoo, Hooshang MS601, PS1.39, PS3.03, TR011
 Nirodi, Chaitanya PS6.46
 Nishimura, Takashi PS7.56
 Nishio, Teiji PS7.47
 Niwa, Ohtsura PS2.61
 Noguchi, Miho MS107, MS308, PS2.70, PS7.07
 Norimura, Toshiyuki PS2.40
 Norris, Andrew S1803
 Nowak, Irena PS1.60
 Nowsheen, Somaira MS303, PS2.46

Nussenzweig, Andre AL03, PS2.02

O

O'Banion, M. Kerry PS4.05, PS4.69, PS7.34
 O'Connor, Mark J. PS2.11
 O'Donoghue, Joseph A. PS7.22
 O'Neill, Eric PS2.43
 O'Neill, Peter MS308, PS2.22, PS2.50, PS2.70, PS5.67
 O'Sullivan, Joe M. MS503, PS5.22, PS7.69
 Obenaus, Andre PS5.34
 Oertli, David MS401, PS6.01
 Oh, Eun-Taex PS3.49
 Ohara, Maki PS2.51
 Ohnishi, Takeo PS6.21, TR006
 Ohtaki, Kazuo S1404
 Oikawa, Masakazu MS504, PS5.26
 Okatenko, Pavel V. S1403
 Okayasu, Ryuichi MS107, PS2.61, PS6.15, PS7.07
 Okazaki, Ryuji PS2.40
 Okunieff, Paul PS1.29, PS1.58, PS2.37, PS4.10, PS4.27, PS4.48, PS4.49, PS4.49, PS4.50, PS4.62, PS4.70, PS5.40, PS7.72, PS7.77, S904
 Olasz, E. B. PS1.23
 Oldson, Darren PS4.09
 Olejniczak, Scott PS4.82
 Olschowka, John PS4.05, PS4.69, PS7.34
 Olson, Jeffrey J. PS7.70
 Olson, John PS5.09
 Omaruddin, Romaica A. PS5.60
 Ono, Koji MS903, PS4.58, PS5.44, PS7.21, PS7.26
 Onyshchenko, Mykola PS3.51
 Ootsuyama, Akira PS2.40
 Orcutt, Kevin P. PS7.66
 Orecchia, Roberto S705
 Ormsby, Rebecca J. MS706, PS1.54, PS5.13, PS5.27, PS5.49, PS5.62
 Orloff, Leticia PS5.25, PS5.52
 Osborne, J. W. HCP001
 Oshimura, Mitsuo PS5.44
 Ossetrova, Natalia MS608, PS3.19, PS3.25, S905
 Ostvold, Anne Carine PS2.06
 Otsuka, Kensuke S1603
 Ottolenghi, Andrea PS5.56
 Ozasa, Kotaro PS5.05, PS5.07, S1401

P

Pacheco-Torres, Jesús PS7.43
 Paganetti, Harald S704
 Pain, Debkumar PS5.50
 Pajonk, Frank PS3.29, PS4.18, S302
 Palayoor, Sanjeevani T. MS101, PS7.04, PS7.88
 Palchik, Guillermo MS501, PS5.14
 Palis, James PS4.20
 Palmer, Gregory M. PS4.37, PS5.42, PS7.23
 Pan, Cory PS1.43
 Panajotovic, Radmila PS3.06
 Pandita, Tej K. PS2.21, PS4.82
 Pantani, Bruce PS1.37
 Pantelias, Gabriel E. PS2.05
 Panyutin, Igor MS604, PS3.08, PS3.51, PS3.52, S1701
 Panyutin, Irina V. PS3.52
 Paoni, Scott F. PS7.16
 Papandreou, Ioanna MS805, PS7.29
 Papineni, Rao V. L. PS7.08
 Paquette, Benoit MS807, PS4.57, PS7.31, PS7.61
 Paretzke, Herwig G. TR010
 Park, Hae-Ran PS4.61
 Park, Heon Joo PS3.49, PS3.57
 Park, Hyeon U. PS2.71, PS3.18
 Park, Ki Hun PS1.30
 Park, Moon-Taek PS3.49
 Park, Sarah PS4.73
 Park, Won PS4.37
 Park, Woong-Yang PS4.01
 Park, Yeunsoo PS2.54
 Parker, Anthony W. PS2.22
 Parmar, Kalindi PS7.95
 Parpys, Ann C. PS2.07
 Parrill, Abby L. PS4.78
 Parris, Brian PS6.26
 Parsons, Arlene D. PS7.66
 Parsons, Jason L. PS2.20
 Parsons, Sarah J. PS7.58
 Parvin, Bahram PS2.78
 Pasquali, Emanuela PS5.61
 Passarella, Ralph J. PS4.65
 Patel, Zarana S. PS4.63
 Pathak, Rupak PS1.12
 Patterson, Adam PS7.95
 Patterson, Michael PS7.80
 Paturas, James PS1.37
 Paul, Sunirmal PS3.33
 Paunesku, Tatjana PS2.08, PS5.65, PS5.70, PS7.19, PS7.68, PS7.71
 Pawar, Snehalata A. PS1.76
 Payne, Valerie PS7.02, PS7.54
 Pazhanisamy, Senthil Kumar MS206, PS1.46, PS2.10, PS3.48
 Pazzaglia, Simonetta PS5.61
 Pearce, Linda PS4.74

Pecaut, Michael J. PS1.27, PS1.43, PS2.62, PS6.24, S1103
 Pedersen, Theresa L. PS4.23
 Pedley, Nicholas M. MS301, PS2.49
 Pekna, Marcela PS1.80
 Pekny, Milos PS1.80
 Peleshko, Vladimir PS6.33
 Pellmar, Terry PS4.09
 Penagaricano, Jose A. PS5.63, PS7.30
 Penate-Medina, Tuula PS4.42
 Peng, Yuanlin PS2.64, PS6.28
 Pentland, Alice P. PS7.44
 Peoples, Anita R. MS605, PS3.04
 Perez, Bradford PS4.56
 Perez, Celso PS1.27, PS1.43, PS5.52
 Perez-Andujar, Angelica PS7.67
 Perkins, Michael W. PS1.10
 Perry, Donna PS1.05
 Peschke, Peter PS7.43
 Peslak, Scott A. PS4.20
 Peterlin, Molly PS4.59
 Petermann, Eva PS2.07
 Petersen, Cordula PS7.59
 Petersen, Karl-Uwe PS1.76
 Peterson, Erika J. PS5.03
 Peterson, Jim PS4.74
 Peterson, Leif E. PS2.30
 Phan, Nghi PS2.19
 Phillips, Charles A. MS804, PS7.03
 Phillips, Roger PS2.04
 Phillips, Tiffany PS3.53
 Pickup, Stephen PS7.85
 Pietrusz, Jennifer PS1.60
 Pilonas, Karsten A. MS106, PS2.58, PS7.74
 Pimblott, Simon M. S1301
 Pink, John PS7.41
 Piper, Roman K. PS1.89, PS1.90
 Plante, Ianik PS6.13, S1303
 Plesca, Dragos PS2.03
 Pogozelski, Wendy K. TR001
 Pollack, Alan PS7.08
 Pollice, Alessandra PS7.94
 Polyzos, Aris PS2.27
 Pommier, Yves PS2.42
 Pomplun, Ekkehard S1702
 Ponomarev, Artem L. PS2.76
 Poole, Rachel MS908, PS4.17
 Poptani, Harish PS7.85
 Portugal, Frank A. PS4.07
 Potter, Larry PS5.42
 Poulouse, Shibu PS6.44
 Pourmand, Nader PS2.48
 Powell, Simon TR013
 Powers, John PS3.57
 Poznansky, Mark C. PS1.40
 Prasad, Kedar N. PS1.55

Prasad, Rajiv MS203, PS5.11
 Presley, Chaela S. PS7.90
 Preston, Dale L. S1403
 Price, Brendan S1803
 Prise, Kevin MS503, PS2.55, PS5.22, PS7.69
 Ptasinska, Sylwia MS602, PS3.14
 Purgason, Ashley PS4.51
 Purger, David PS3.40
 Purkayastha, Shubhadeep PS2.65, PS3.10
 Purschke, Martin PS4.44
 Puskin, Jerome S. PS3.12
 Pyun, Bo-Jeong PS3.21

Q

Quinones, Alfredo PS3.40

R

Rabari, Nuh MS105, PS7.40
 Rabbani, Zahid MS904, PS4.04
 Rabin, Bernard PS5.50, PS6.27, PS6.44, PS6.47
 Radivoyevitch, Tomas PS7.41
 Raghavan, Pavithra MS802, PS7.09
 Raha, Sumita PS2.08, PS7.19, PS7.68
 Rahman, Arifur MS608, PS3.19, PS3.25, PS3.36, S905
 Rahnama, Ruyan PS2.06
 Raj, Ganesh PS7.43
 Rajadurai, Chelvi PS5.33
 Raju, Uma PS7.25, PS7.45, PS7.55
 Ramesh, Govindarajan PS2.48, PS4.67
 Ramesh, Vani PS4.67
 Ramos, Orlando X. PS4.14
 Randers-Pehrson, Gerhard PS3.20, PS3.26, PS3.41
 Rao, Ashutosh V. PS2.42
 Ratanatharathorn, Vaneerat PS7.30
 Ratikan, Josephine A. S1102
 Ravichandran, Prabakaran PS4.67
 Ray, F. Andrew PS5.41
 Raymond, Kenneth N. PS1.92
 Reynolds, Tim S903
 Rebessi, Simonetta PS5.61
 Recht, Lawrence MS108, PS7.62
 Reddy, E. Premkumar PS1.73
 Reddy, M. V. Ramana PS1.73
 Redmond, Erin K. PS3.39
 Redon, Christophe MS501, MS606, PS3.18, PS3.34, PS3.36, PS5.14
 Redpath, J. Leslie S1001

Reed, Christina PS1.08, PS1.61
 Regine, William F. MS905, PS4.03
 Remmes, Nicholas B. PS6.07
 Ren, Chen PS7.20, PS7.64
 Renegar, Jackson R. PS2.39
 Repasky, Elizabeth PS7.91
 Resson, Habtom PS4.35
 Reungpatthanaphong, Paiboon MS306, PS2.33
 Reyes, Juvenal PS3.40, PS7.80
 Reynolds, Pamela PS2.22
 Rhee, Juong G. MS905, PS4.03
 Rhone, Jordan PS6.32
 Rich, Jeremy N. PS3.45
 Richard, Derek PS2.55
 Rightnar, Steven PS2.62, 6.36
 Rithidech, Kanokporn MS306, PS2.33
 Ritter, Linda PS5.25
 Rivina, Yelena O. PS1.88
 Rizvi, Asma PS6.31, S1103
 Robbins, Michael E. MS704, PS1.16, PS7.02, PS7.54, PS7.60
 Roberto, Kerrey A. MS901, PS4.36
 Robinson, Timothy PS7.42
 Rocke, David M. PS4.23
 Rockwell, Sara PS1.07, PS1.37
 Roda, Norma PS1.82, PS1.83
 Rodgers, Kathleen E. PS1.82, PS1.83
 Rodrigues, Rafaela PS4.79
 Roh, Changhyun PS4.61
 Romanchenko, Sergey PS6.33
 Romanyukha, Lyudmila PS1.17
 Romeo, Paul-Henri PS5.69
 Romero-Weaver, Ana L. MS406, PS6.34, PS6.36
 Ron, Elaine S1403, TR009
 Rosa, Paulo R. Mottin. PS4.55
 Rosenberg, Elizabeth A. PS2.11
 Rosi, Susanna PS4.71
 Ross, Joel R. PS1.04, PS4.29
 Rotman, Marvin PS3.56
 Roughton, Karolina PS7.81
 Rouschop, Kasper M. PS4.40
 Routt, Stefan PS7.89
 Rozanova, Olga PS6.33
 Rusek, Adam S404
 Russell, J. Lauren MS204, PS3.38
 Rustgi, Anil K. PS4.63
 Rwigema, Jean-Claude PS1.75

Ryan, Julie L. PS7.44
 Ryan, Stewart D. PS7.92

S

Sabatier, Laure M. S1502
 Sabek, Omaima M. PS1.57, PS1.87, PS4.26
 Sabourin, Jean-Christophe PS4.21
 Sachs, Rainer K. PS5.06
 Sacksteder, Colette PS5.43, PS5.57
 Sadasivan, Vidyasagar PS2.37, PS4.27, PS4.48, PS4.49, PS4.50, PS4.62, PS4.70
 Saha, Debabrata MS802, PS6.46, PS7.09
 Saha, Subhrajit MS702, PS1.51
 Saintigny, Yannick PS5.69
 Sakae, Takeji PS1.33
 Sakata, Koh-ichi PS2.15
 Sakata, Ritsu PS5.05, PS5.07
 Sakurai, Hideyuki PS1.33
 Sakurai, Yoshinori MS903, PS4.58, PS7.21, PS7.26
 Saleh, Anthony S202
 Sambade, Maria J. MS808, PS7.51
 Sanche, Leon MS602, MS807, PS2.54, PS3.14, PS7.31, PS7.61, TR014
 Sanchez, Martha C. PS4.14
 Sanchez, Zina PS2.72
 Sandgren, David J. MS608, PS3.19, PS3.25, S905
 Sanford, Larry PS6.26
 Sankaranarayanan, K PS1.39
 Sanz Melo, Kaity PS3.56
 Sanzari, Jenine PS6.06, PS6.41, PS6.25, PS6.36, PS6.45
 Saran, Anna PS5.61
 Sarkar, Sukumar PS2.68
 Sato, Hiroyuki PS6.37
 Sattler, Ulrike G. A. PS4.30, PS6.08
 Satyamitra, Merriline M. MS708, PS1.11
 Sauter, Guido PS7.59
 Savage, Jason S202
 Savage, Kienan PS2.55
 Sawarynski, Kara PS1.24
 Sayre, James S1803
 Scampoli, Paola PS7.94
 Scarboro, Sarah B. PS7.67
 Scarbrough, Peter M. PS7.66
 Schall, Tom MS108
 Schaeue, Dörthe S1102
 Schettino, Giuseppe PS2.55
 Schiestl, Robert H. PS1.88
 Schild, David PS2.06, PS5.15
 Schleicher, Stephen M. PS7.32
 Schmid, Herbert PS1.31

Schmidt, Margret PS1.66
 Schmidt, Marion PS4.82
 Schnegg, Caroline PS7.60
 Schnietz, Mark PS3.06
 Schock, Ashley M. PS1.23, PS1.41
 Schölch, Sebastian MS105, PS7.40
 Schonfeld, Sara J. S1403
 Schröck, Evelin PS7.28
 Schroeder, Thies PS4.37, PS4.77, PS7.23
 Schulte, Bradley A. PS7.12
 Schültke, Elisabeth PS5.48
 Sedelnikova, Olga A. MS501, MS606, PS3.34, PS5.14, S1503
 Seed, Thomas M. PS1.10, PS1.65
 Seemann, Ingar PS7.50
 Segan, Andrew T. MS805, PS7.29
 Sells, R. PS1.23
 Seo, Haeng Ran PS1.30
 Seo, Woo Duck PS1.30
 Seong, Ki Moon PS2.60
 Sethu, Swaminathan PS7.76
 Sevilla, Michael D. PS3.02, S802
 Seykora, John PS6.06
 Seymour, Colin PS5.20, PS5.48
 Shakhov, Alexander PS1.12, PS1.72
 Shakhova, Vera PS1.72
 Shankar, Bhavani PS2.73
 Shankar, Gita N. PS1.35
 Shankaran, Harish PS4.52, PS5.43
 Shao, Lijian PS1.46, PS2.10
 Shareef, Mohammed M. PS7.08, 7.36
 Sharma, Anand K. PS7.12
 Sharma, Kiran K. K. PS3.10
 Sharma, Mukesh Kumar PS2.36
 Sharma, Sunil MS901, PS4.36, PS5.63
 Shay, Jerry W. S703
 Sheikh, Kathryn PS3.18
 Shelton, Larry PS1.52
 Shen, Min PS2.72
 Sheu, T. PS7.25
 Shibata, Atsushi P004
 Shields, Donna PS1.75
 Shields, Janiel M. MS808, PS7.51
 Shigematsu, Naoyuki PS2.67
 Shih, Shyh-Jen PS5.12
 Shikazono, Naoya MS308, PS2.70
 Shimada, Yoshiya S1404
 Shimizu, Yukiko PS5.05, PS5.07
 Shin, Suk-Chul MS404, PS6.11
 Shinde, Sujata S. S804
 Shinpaugh, Jefferson L. PS3.13
 Shippee, Alexander PS5.34
 Shirato, Hiroki PS7.56
 Shirazi, Haider A. PS5.70
 Shishodia, Shishir PS2.48
 Shore, Roy E. S601, S1401
 Shpak, Victor S1402
 Shuh, David K. PS1.92
 Shukitt-Hale, Barbara PS6.27, PS6.44
 Shuryak, Igor PS5.06
 Shyh, Shyh-Jen PS2.16
 Shyla, Alena PS4.54
 Sibenaller, Zita PS7.66
 Sidabras, Jason S903
 Sidahmed, Elkhansa PS5.39
 Sigurdson, Alice S602
 Simaan, Nabil PS3.41
 Simon, Ronald PS7.59
 Simone, Nicole S202
 Simone, Il, Charles B. MS101, PS7.04, PS7.88
 Simons, Andree L. PS7.52, PS7.66
 Sims, Matthew PS1.24
 Singh, Kamini PS2.03
 Singh, Satyendra PS3.11
 Singh, Sheetal PS2.16, PS5.12
 Singh, Vijay K. PS1.12, PS1.65, PS1.72
 Singletary, Sylvia PS6.26
 Slack, Frank S201
 Slater, James M. PS1.27, PS2.62, PS4.68, PS6.36, S1103
 Smilenov, Lubomir S203
 Smirnova, Helena PS6.33
 Smith, Andrea J. MS606, PS3.34
 Smith, Richard PS5.20, PS5.48
 Smith, Sharon PS7.38
 Snijders, Antoine M. PS4.81, PS6.47
 Sobhakumari, Arya PS7.66
 Soda, Midori PS5.05, PS5.07
 Sodipe, Ayodotun PS2.48
 Sokolnikov, Mikhail E. S1403
 Someya, Masanori PS2.15
 Son, Youngsook PS1.47
 Song, Chang W. PS3.49, PS3.57
 Song, Dusub PS2.59
 Song, Jie-Young PS4.73
 Song, Min Jeong PS3.49
 Sorensen, Annette PS7.83
 Sorensen, Elizabeth W. PS4.05
 Sorokina, Svetlana PS6.33
 Souda, Puneet PS4.18
 Sowa, Marianne B. PS4.52, PS5.43
 Sowers, Anastasia PS1.34, PS1.74
 Span, Paul N. PS4.25
 Spitz, Douglas R. MS402, MS505, PS5.54, PS6.23, PS7.52, PS7.66
 Splinter, Joern S701
 Springer, David MS203, PS5.11, PS5.43, PS5.57
 Springhorn, Jeremy P. MS708, PS1.11
 Sprung, Carl N. PS2.09
 Sree Kumar, K. PS1.59
 Sriharshan, Arundhathi PS4.54
 Srinivasan, Venkataraman MS708, PS1.11
 Srivastava, Devika PS2.05
 Sroka, Thomas C. PS4.28
 Staaf, Elina PS6.43
 Stanton, Julie MS203, PS5.11
 Stantz, Keith M. PS4.72
 Staska, Laurie PS1.86
 Staudacher, Alexander H. PS5.27, PS5.49, PS5.62
 Staudt, Christian PS3.11
 Steed, Katie MS703, PS1.42, PS7.10
 Stefan, Tammy PS7.41
 Steffen, Leta PS5.53
 Stegeman, Hanneke PS4.25
 Stenoien, David PS5.43
 Stevens, David PS6.48
 Stewart, Fiona A. PS7.50, TR007
 Stewart, Robert D. PS5.51, S1304
 Stitt, Molly PS4.74
 Stocki, Trevor J. MS304, PS2.31
 Stokman, Monique A. MS205, PS3.31
 Storch, Katja MS803, PS7.14, PS7.28
 Storts, Douglas PS5.53
 Story, Michael D. MS403, PS6.10, PS6.46
 Stout, Charles E. PS4.14
 Stoyanovsky, Detcho A. PS1.21
 Stram, Daniel S603
 Stratford, Ian J. TR016
 Straume, Tore MS401, PS6.01
 Stricklin, Daniela PS4.09
 Stuerzbecher, Horst-Werner PS2.07
 Stwarts, Steven G. PS1.29, PS2.37, PS4.10, PS4.48, PS4.49, PS4.50, PS4.70, PS5.40, PS7.72, PS7.77
 Suarez, Tatiana PS3.54
 Sugiyama, Hiromi PS5.05
 Sugiyama, Hiroshi S103
 Sui, Guangchao PS4.55
 Sullenger, Bruce A. PS3.45
 Sullivan, Julie M. MS201, MS204, PS3.38, PS4.79, PS5.19
 Sun, Hongliang PS1.60
 Sun, Jiafang PS5.39
 Sun, Yingli S1803
 Sung, Patrick PS2.06
 Suy, Simeng PS2.71, PS3.18, PS3.22
 Suyama, Akihiko PS5.05, PS5.07
 Suzuki, Keiji S1903
 Suzuki, Masao MS504, PS5.26
 Suzuki, Minoru MS903, PS4.58, PS7.21, PS7.26
 Suzuki, Sadafumi PS2.40
 Swartz, Steven G. S904
 Swartz, Harold M. S901, S903, S904
 Syed, Talal PS3.56
 Sykes, Pamela J. MS706, PS1.54, PS5.13, PS5.27, PS5.49, PS5.62
 Szolc, Barbara PS3.17

T

Taddei, Phillip J. PS7.67
 Tafrov, Stefan T. PS2.63
 Taft, David PS7.20, PS7.64
 Tailor, Tina PS4.37
 Takagi, Keiichi PS2.57
 Takagi, Masaru PS2.15
 Takahashi, Akihisa PS6.21
 Takahashi, Kenji MS207, PS3.16, PS3.46, PS4.06, PS4.08, PS4.39
 Takahashi, Momoko MS107, PS7.07
 Takai, Nobuhiko MS407, PS6.39
 Takam, Rungdham PS3.42
 Takeda, Shunichi MS302, PS2.01
 Takeshima, Tsuguhide PS7.56
 Taleei, Reza PS1.81, TR011
 Tallant, Tomas PS1.44
 Tamburini, Paul MS708, PS1.11
 Tamhane, Mitalee PS7.20, PS7.64
 Tanaka, Aya PS2.51
 Tanaka, Hiroki MS903, PS4.58, PS7.21, PS7.26
 Tang, Jonathan PS4.64
 Tang, Moon-Shong (Eric) PS5.35
 Tang, Vicky J. S803
 Tang, Xiaobing PS2.14, PS2.39, PS3.32
 Tano, Keizo PS5.44
 Tanori, Mirella PS5.61
 Tapio, Soile PS4.54
 Tariq, Muhammad A. PS2.48
 Tarlet, Georges MS906, PS4.12, PS4.24
 Tashiro, Satoshi S1901
 Tatsukawa, Yoshimi S1401
 Taucher-Scholz, Gisela S701
 Tauchi, Hiroshi PS2.15, PS2.51
 Taveras, Maria MS607, PS3.17, PS3.24
 Taylor, Kristina PS2.69
 te Poelle, Hans PS7.50
 Tennstedt, Pierre PS7.59
 Tereshchenko, Valeriy S1402
 Terracciano, Luigi PS7.59
 Terzoudi, Georgia I. PS2.05
 Themis, Matthew PS6.48
 Theriot, Corey A. PS1.25
 Thetford, Angela PS1.34
 Theus, Sue MS703, PS1.42
 Thomas, Cindy PS2.30

Thomas, Nancy E. MS808, PS7.51
 Thompson, Craig B. PS4.82
 Thompson, Karin E. PS1.91
 Thompson, Richard E. PS5.01, PS5.08
 Thotala, Dinesh PS1.67, PS7.32
 Thrall, Karla D. PS1.86
 Tian, Jian PS2.62, PS4.68, S1103
 Tian, Linlin PS2.14, PS2.39
 Tian, Sisi PS4.68
 Tian, Yeping PS1.58, PS5.40
 Tigyi, Gabor PS1.91, PS4.78, PS7.90
 Timmerman, Robert PS7.43
 Tippayamontri, Thititip PS7.31
 Titov, Viktor PS5.31
 Toburen, Larry H. PS3.13, PS3.15
 Tomimatsu, Nozomi PS2.56, PS6.46
 Tomita, Masanori PS5.46, S1603
 Toshkov, Ilya PS1.03
 Toshkova, Troitzta PS1.72
 Trainor, Colman MS503, PS5.22
 Tran, Katherine PS3.54, PS6.20
 Trani, Daniela PS4.60, PS5.39
 Travia, Anderson MS603, PS3.01
 Trojanczyk, Lee A. PS4.05
 Troncy, Eric PS1.69
 Tronko, Mykola S1402
 Truman, Jean-Philip PS4.42
 Truong, Jessica T. PS2.52
 Tsai, Ying PS1.60
 Tsareva, Yulia V. S1403
 Tseng, Bertrand PS3.54, PS6.20
 Tseng, Diane MS108, PS7.62
 Tsuboi, Koji PS1.33
 Tsujii, Hirohiko S705
 Tsuruoka, Chizuru MS504, PS5.26
 Tuli, Richard PS7.80
 Tullius, Tom P002
 Tuohy, Joanne PS7.92
 Turchanin, Andrey PS3.06
 Turker, Mitchell PS5.59
 Turner, Helen C. MS607, PS3.17, PS3.20, PS3.24, PS3.41
 Tyagi, Rahul PS3.10
 Tyburski, John B. PS3.05, PS3.22, PS3.23

U

Ubezio, Paolo PS7.94
 Uchihori, Yukio PS5.16
 Udayakumar, Durga S1204

Udayakumar, Thirupandiyur S. PS7.08
 Ullrich, Robert L. PS5.41
 Unger, Keith PS7.27
 Unger, Thomas MS901, PS4.36
 Ungerman, Rachel PS4.74
 Unverricht, Marcus S1702
 Urbin, Salustra S. MS502, PS5.38
 Urushibara, Ayumi MS308, PS2.70
 Usami, Noriko PS5.46
 Usikalu, Mojisola PS2.77
 Uzawa, Akiko MS407, PS6.39

V

Valdecanas, David PS7.25, PS7.55
 Valerie, Kristoffer PS2.11
 Valerie, Nicholas PS2.29, PS2.53, PS7.58
 Vallis, Katherine S1704
 van den Beucken, Twan PS4.40
 van den Brekel, Michiel W. M. PS7.06
 van der Kogel, Albert J. PS4.25
 van der Veen, Sonja J. PS4.02
 van der Zwaag, Marianne MS205, PS3.31
 van Leeuwen, Fijis PS7.50
 van Luijk, Peter PS4.02
 Van Meir, Erwin G. PS7.70
 van Meter, Timothy PS2.11
 van Os, Ronald P. MS205, PS3.31
 Vanek, Kenneth N. PS7.12
 VanRompay, Koen PS1.91
 Varnum, Susan PS5.43, PS5.57
 Vassiliev, Oleg N. PS2.44
 Vaughan, Andrew PS2.16, PS5.12
 Veeraraghavan, Jamunarani PS4.16, PS7.17, PS7.24, PS7.33
 Venkatesan, Shriram PS7.76
 Vens, Conchita PS7.06
 Verhagen, Caroline V. M. PS7.06
 Verheij, Marcel PS7.06
 Verma, Seema MS203, PS5.11
 Vijaygopal, Pooja PS4.27, PS4.27, PS4.62
 Visser, Nils PS7.50
 Vlashi, Erina PS3.29, PS4.18, S302
 Vlkolinsky, Roman PS5.34, PS6.49
 Vogt, Stefan PS5.65, PS7.19
 Voicu, Horatiu X. PS4.26
 Voss, Kay-Obbe S701

Vujaskovic, Zeljko MS904, PS1.05, PS1.32, PS4.04, PS4.32, PS4.38, PS4.43

W

Wachsberger, Phyllis R. PS7.49
 Wada, Mami PS7.47
 Wagner, Erika PS6.09, PS6.25, PS6.45
 Wagner, J. Richard PS2.54, TR014
 Wagner, Mechthild MS105, PS7.40
 Walb, Matthew PS5.09
 Walls, Thomas PS7.27
 Walters, Matthew MS108, PS7.62
 Wan, Jian PS2.77
 Wang, Abraham PS6.17
 Wang, Chris K. PS2.39
 Wang, Chun Chieh PS4.15
 Wang, Hong PS1.68
 Wang, Hongliang PS3.41
 Wang, Hongyan MS302, PS2.01, PS2.32
 Wang, Huichen PS2.14, PS2.39, PS3.32
 Wang, Jialiang PS3.45
 Wang, Jiaxi PS5.48
 Wang, Junru PS1.59, PS1.62, PS1.76
 Wang, Kelin PS5.32
 Wang, Li PS7.25, PS7.45, PS7.55
 Wang, Minli PS2.14, PS2.39, PS3.11
 Wang, Ping MS302, PS2.01, PS2.32, PS7.70
 Wang, Qiong PS2.08
 Wang, Shu-Chi PS4.41
 Wang, Weixin PS2.05
 Wang, Wenze PS1.13, PS1.31
 Wang, Xiao-Chun PS1.15
 Wang, Xiaohui PS1.29, PS4.10, PS4.49, PS4.50, PS7.72, PS7.77
 Wang, Xin PS7.13
 Wang, Ya MS302, PS1.18, PS2.01, PS2.32, PS7.70
 Wang, Yan PS1.14
 Wang, Yi MS708, PS1.11
 Wang, Yi PS3.32
 Wang, Yiwon PS4.35
 Wang, Yong MS206, PS1.46, PS1.70, PS3.48, PS7.12
 Wang, Yong PS1.14
 Wang, Yongbao S1501
 Wang, Yueying PS1.14, PS1.15, PS1.70
 Wang, Zhaoqing PS4.31
 Wanzer, Beau PS2.08, PS5.65
 Ward, Jesse PS7.19
 Ware, Jeffrey H. MS406, PS6.34, PS6.36, PS6.41
 Warner, Christy L. PS6.28
 Warner, David MS401, PS6.01
 Watanabe, Masami PS5.44

Waters, Katrina PS5.43
 Watts, Colin PS2.04
 Weatherall, Paul PS7.43
 Webb-Roberston, Bobby-Jo M. PS5.57
 Weber, Thomas PS5.43
 Weber, Waylon PS1.35
 Wedenberg, Minna PS6.05
 Weichselbaum, Ralph R. PS4.34, PS5.30, PS5.66
 Weil, Michael M. PS5.41
 Weiler, Hartmut PS1.76
 Weinfeld, Michael MS104, MS605, PS3.04, PS7.48
 Weinstock, David PS1.78
 Weissman, Drew PS6.09
 Welle, Stephen L. PS4.69
 Wenger, Jesse PS4.20
 Whang, Zhendong MS905, PS4.03
 Wheeler, Deric L. PS4.25
 Wheeler, Kenneth PS5.09
 Whitelegge, Julian P. PS4.18
 Whitnall, Mark H. PS1.52, PS4.46
 Wicha, Max S. P003
 Wickersham, Stephanie PS5.31
 Wiese, Claudia PS2.06, PS5.15
 Wignarajah, Shayalini PS2.11
 Wiklund, Kristin PS6.05
 Wilcox, Dean S904
 Wildermuth, Caroline PS1.66
 Wilds, Edward PS1.37
 Wilke, Werner PS7.66
 Wilkins, Ruth MS304, PS2.31, PS3.30
 Wilkinson, Diana PS3.39
 Willard, Margaret PS4.65
 Willey, Jeffrey S. MS704, PS1.16
 Williams, Benjamin B. S901, S903
 Williams, Brent PS3.49, PS3.57
 Williams, Jacqueline PS1.08, PS1.24, PS1.48, PS1.61, PS4.05, PS4.20, PS4.69, PS7.34, PS7.44
 Williams, Margaret S. PS4.46
 Wilson, Christy M. PS4.26
 Wilson, Dulaney A. MS507, PS5.02, PS5.03, PS5.64
 Wilson, Jolaine M. PS6.06, PS6.25, PS6.36, PS6.41, PS6.45
 Wilson, Paul F. MS502, PS2.30, PS5.38, PS6.15
 Wilson, Samuel PS2.72
 Wilson, William PS7.95
 Wilson III, David PS2.72
 Winters, Thomas A. PS2.65
 Wipf, Peter PS1.01
 Wirkner, Ute MS105, PS7.40
 Wojzik, Andrzej PS4.54, PS6.43

Wolden, Suzanne L. PS3.17, PS3.22
 Wolff, Daynna J. MS206, PS3.48
 Woloschak, Gayle PS2.08, PS5.65, PS5.70, PS7.19, PS7.68, PS7.71
 Wong, John W. PS7.80
 Woods, Jeffrey PS6.09
 Worley, Deanna PS7.92
 Wortham, Angela PS3.56
 Wouters, Bradly G. PS4.40, S501
 Wreesmann, Volkert B. PS7.06
 Wright, Eric S1104
 Wroe, Andrew J. PS2.62, PS6.36
 Wu, Aiguo PS7.68, PS7.71
 Wu, Feng PS5.35
 Wu, Honglu PS1.25, PS2.18, PS2.48, PS4.51, PS4.67
 Wu, Hongying PS1.14, PS1.15, PS1.70
 Wu, J. H. David PS1.60
 Wu, Lixian PS2.10
 Wu, Ping PS3.55
 Wu, QingPing PS1.28, PS1.50
 Wu, X. PS1.23
 Wu, Xiaodong PS5.32
 Wyrick, John MS203, PS5.11
 Wyrobek, Andrew J. PS4.81, PS6.47

X

Xia, Fen MS303, PS2.46
 Xiao, Mang PS1.26
 Xie, Daxing MS802, PS7.09
 Xie, Xian-jin PS7.79
 Xiong, Hairong S1204
 Xiong, Xiaopeng PS7.13
 Xu, Puting PS1.32
 Xu, Wei PS3.28
 Xu, Xiangsheng PS7.87
 Xu, Yanping PS3.26

Y

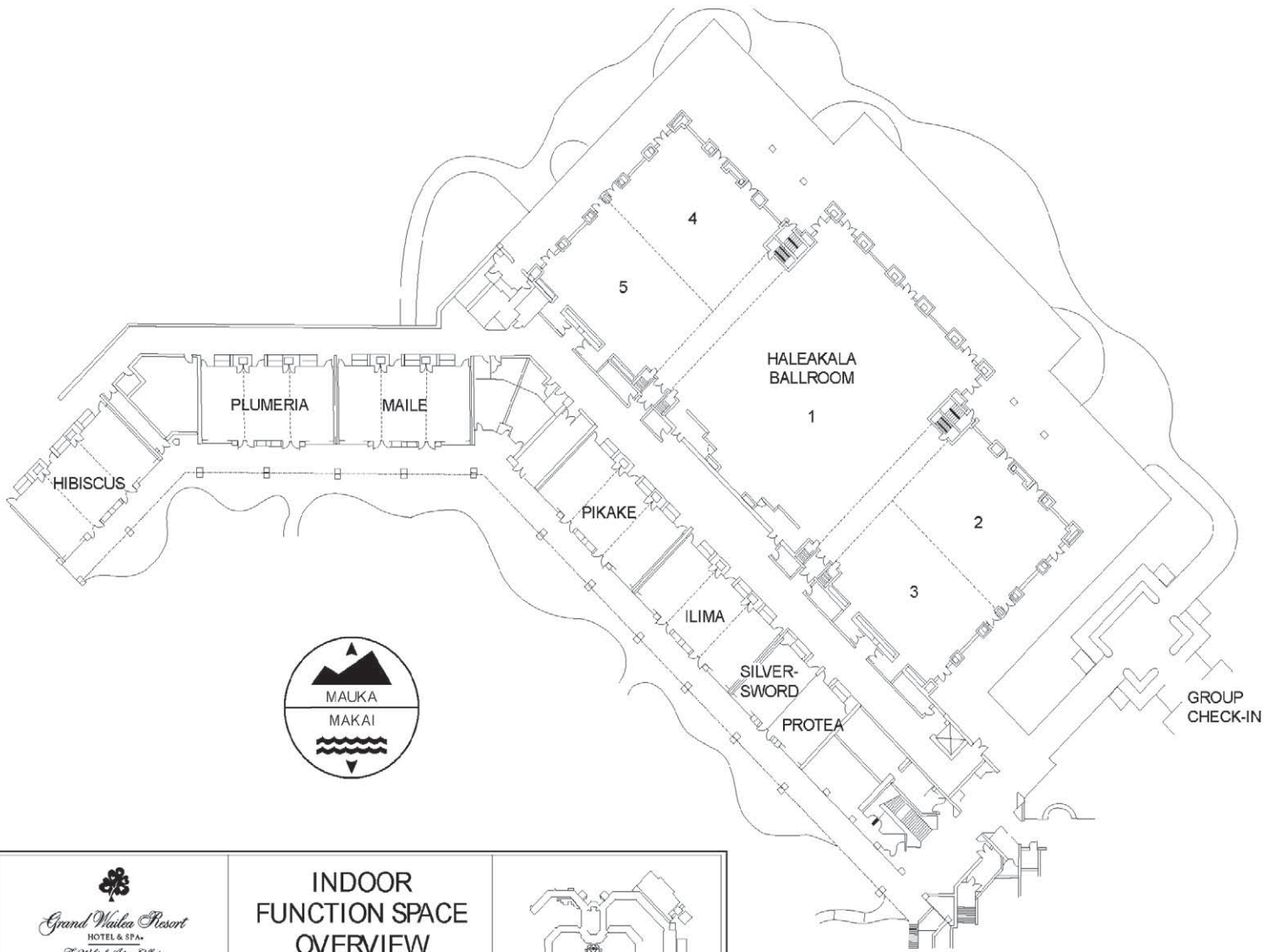
Yajima, Hirohiko AL03, PS2.02


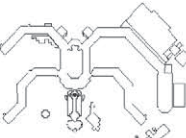
Yamashita, Shinichi PS6.16, S1302
 Yan, Dan PS1.18, PS7.70
 Yan, Jingsheng PS7.79
 Yanamala, Naveena PS1.21
 Yanch, Jacquelyn PS7.15
 Yang, Aimin PS7.12
 Yang, Brian PS2.27
 Yang, Eddy S. MS303, PS2.46
 Yang, Hongying PS5.33, S1601
 Yang, Kwang-Hee MS404, PS2.60, PS6.11
 Yang, Liangjie PS4.27, PS4.27
 Yang, Ping Liu PS5.65
 Yang, Peiyong PS7.45
 Yang, Shanmin PS1.29, PS1.58, PS2.37, PS4.10, PS4.48, PS4.49, PS4.50, PS4.70, PS5.40, PS7.72, PS7.77
 Yang, Xiao PS2.75
 Yang, Yunzhi PS1.57
 Yano, Ken-ichi S1203
 Yao, Y. Lawrence PS3.41
 Yao, Youli PS5.31
 Yarmolenko, Pavel PS4.37
 Yasui, Linda S. PS6.35
 Yates, Charles R. PS1.57, PS1.91, PS7.90
 Yates, Ryan PS4.78
 Yazlovitskaya, Eugenia PS1.67, PS7.32
 Ye, Ruiqiong PS2.24
 Ye, Zhang PS2.48
 Yee, Sung-Tae PS4.33, PS4.61
 Yee, Stephanie PS6.06, PS6.41, PS7.87
 Yentrapalli, Ramesh PS4.54
 Yeoh, Eric PS3.42
 Yi, Jae Youn PS1.47
 Yin, Liangjie PS1.58, PS2.37, PS4.48, PS4.62, PS4.70, PS5.40
 Yokoya, Akinari MS308, PS2.70, S801
 Yoo, Stephen PS7.82
 Yoshida, Kengo S601
 Yoshida, Yukari MS407, PS6.39
 Yoshida, Yasuhiro PS2.40

Yoshino, Hironori PS4.08
 Young, Kenneth PS4.37
 Yount, Caroline PS7.12
 Yu, Cedric X. MS905, PS4.03
 Yu, Dong MS107, PS7.07
 Yu, Victor K. PS5.51, S1304
 Yu, Xiaoyan MS302, PS2.01, PS2.32
 Yu, Yaping MS305, PS2.17
 Yu, Yongjia PS3.55
 Yuan, Qing PS7.43
 Yuan, Ye PS7.19
 Yue, Junming PS4.78
 Yumoto, Kenji PS6.18
 Yun, Yeon-Sook PS4.73

Z

Zablotska, Lydia PS5.04
 Zaichkina, Svetlana PS6.33
 Zaleski, Jeffrey M. PS7.89
 Zalutsky, Michael R. PS7.23
 Zawaski, Janice A. PS1.57, PS1.87, PS4.26
 Zenhausen, Frederic PS3.33, PS3.43
 Zhai, Zhibin PS1.14, PS1.15, PS1.70
 Zhang, Amy PS4.48, PS7.72
 Zhang, Bingrong PS1.58, PS2.37, PS4.49
 Zhang, Cheng Cheng AL03, PS2.02
 Zhang, Donglan PS7.35
 Zhang, Guoqing PS5.42
 Zhang, Heng PS1.14, PS1.15, PS1.70
 Zhang, Jian PS3.41, PS5.42
 Zhang, Junling PS1.70
 Zhang, Kunzhong PS4.27, PS4.48, PS4.62, PS4.70, PS5.40
 Zhang, Lei PS1.58
 Zhang, Lei PS2.37
 Zhang, Lurong PS1.58
 Zhang, Lurong PS1.29, PS2.37, PS4.10, PS4.27, PS4.48, PS4.49, PS4.50, PS4.62, PS4.70, PS5.40, PS7.72, PS7.77, S904
 Zhang, Mei PS1.29, PS1.58, PS2.37, PS4.10, PS4.27, PS4.48, PS4.49, PS4.50, PS4.62, PS4.70, PS5.40, PS7.72, PS7.77
 Zhang, Qibin PS5.43
 Zhang, Rui PS7.67
 Zhang, Shichuan AL03, PS2.02
 Zhang, Steven B. PS1.29, PS4.10, PS4.48, PS4.50, PS4.70, PS5.40, PS7.72, PS7.77, S904
 Zhang, Xiangming MS302, PS1.18, PS2.01, PS7.70
 Zhang, Xichen PS1.01
 Zhang, Xiuwu MS904, PS4.04
 Zhang, Yu MS904, PS4.04
 Zhang, Ye PS2.18, PS4.51, PS4.67
 Zhang, Zhaobin PS7.70
 Zhao, Dawen PS7.43
 Zhao, Weiling PS4.55, PS7.01, PS7.54
 Zhao, Yongliang PS5.71
 Zheng, Andrew PS7.87
 Zheng, Junke AL03, PS2.02
 Zheng, Xiaofei PS2.32
 Zhou, Bin PS4.35
 Zhou, Dao-hong PS1.15
 Zhou, Daohong MS206, PS1.14, PS1.46, PS1.70, PS2.10, PS3.48
 Zhou, Hongning S1602
 Zhou, Junqing PS2.41, S1504
 Zhu, Jiayun PS2.77
 Zhu, Ju PS7.89
 Zhu, Yun PS2.32
 Zielinska-Chomej, Katarzyna PS6.02, PS6.22
 Zimbrick, John D. PS2.34
 Zimmermann, Cathy PS1.61
 Zischka, Hans PS4.54
 Zora, J. G. PS5.09
 Zou, Yonglong PS2.73
 Zvinchuk, Olexandr S1402



 <p>Grand Wailea Resort HOTEL & SPA <i>The Wailea Collection</i> TEL (808) 875-1234 FAX (808) 874-2411</p>	<p>INDOOR FUNCTION SPACE OVERVIEW</p> <p>1" = 60'</p>	
--	--	---



Radiation Research Society
810 E. 10th St.
Lawrence, KS 66044

Telephone (800) 627-0326
Fax (785) 843-6153
E-mail: info@radres.org
Website: www.radres.org